



Publicly Accessible Penn Dissertations

1-1-2016

The Design, Synthesis, and Biological Evaluation of Dimeric B-Carbolines Based on the Structure of Neokauluamine and the Study of Manzamine A Dimerization Toward Neokauluamine

Jaruwan Chatwichien

University of Pennsylvania, jchatwichien@gmail.com

Follow this and additional works at: <http://repository.upenn.edu/edissertations>

 Part of the [Organic Chemistry Commons](#)

Recommended Citation

Chatwichien, Jaruwan, "The Design, Synthesis, and Biological Evaluation of Dimeric B-Carbolines Based on the Structure of Neokauluamine and the Study of Manzamine A Dimerization Toward Neokauluamine" (2016). *Publicly Accessible Penn Dissertations*. 1643.

<http://repository.upenn.edu/edissertations/1643>

This paper is posted at ScholarlyCommons. <http://repository.upenn.edu/edissertations/1643>

For more information, please contact libraryrepository@pobox.upenn.edu.

The Design, Synthesis, and Biological Evaluation of Dimeric β -Carbolines Based on the Structure of Neokauluamine and the Study of Manzamine A Dimerization Toward Neokauluamine

Abstract

Neokauluamine, a naturally occurring dimeric β -carboline alkaloid, was isolated from an Indo-Pacific sponge (family Petrosiidae, order Haplosclerida) by Hamann et.al. in 2001. Neokauluamine exhibited improved antimalarial activity in vitro and in vivo relative to currently available drugs artemisinin and chloroquine. Moreover, neokauluamine showed potent cytotoxicity against many types of human cancers including lung, colon and cervical cancers. Bases on the structure of neokauluamine, we designed, synthesized and evaluated simple dimeric β -carbolines as lead structures for the development of biologically active compounds. Interestingly, the synthesized dimeric β -carbolines exhibited antimicrobial activity and cytotoxicity against melanoma and lung cancer cell lines comparable to neokauluamine and its monomer, manzamine A. The cellular mechanism by which the dimeric β -carbolines induce cell death in H1299 lung cancer cells was studied and it was found that the β -carboline dimer accumulated in lysosomes and mediated apoptosis by upregulating a pro-apoptotic protein, PUMA (p53 upregulated modulator of apoptosis). The abundance of manzamine A relative to neokauluamine in Nature makes manzamine A an attractive starting material for the synthesis of neokauluamine. Recently, Tsukamoto et.al. discovered a novel manzamine alkaloid, pre-neokauluamine, as the key intermediate in the conversion of manzamine A to neokauluamine. Thus, we designed and synthesized a pre-neokauluamine-based model system to study optimal reaction conditions and selectivity of the key dimerization step.

Degree Type

Dissertation

Degree Name

Doctor of Philosophy (PhD)

Graduate Group

Chemistry

First Advisor

Jeffrey D. Winkler

Keywords

dimeric β -carbolines, neokauluamine

Subject Categories

Organic Chemistry

THE DESIGN, SYNTHESIS, AND BIOLOGICAL EVALUATION OF DIMERIC β -CARBOLINES
BASED ON THE STRUCTURE OF NEOKAULUAMINE AND THE STUDY OF MANZAMINE A
DIMERIZATION TOWARD NEOKAULUAMINE

Jaruwan Chatwichien

A DISSERTATION

in

Chemistry

Presented to the Faculties of the University of Pennsylvania

in

Partial Fulfillment of the Requirements for the

Degree of Doctor of Philosophy

2016

Supervisor of Dissertation

Jeffrey D. Winkler, Merriam Professor of Chemistry

Graduate Group Chairperson

Gary A. Molander, Hirschmann-Makineni Professor of Chemistry

Dissertation Committee

Gary A. Molander, Hirschmann-Makineni Professor of Chemistry

Madeleine M. Joullié, Professor of Chemistry

Donna M. Hury, Professor of Chemistry

THE DESIGN, SYNTHESIS, AND BIOLOGICAL EVALUATION OF DIMERIC β -CARBOLINES
BASED ON THE STRUCTURE OF NEOKAULUAMINE AND THE STUDY OF MANZAMINE A
DIMERIZATION TOWARD NEOKAULUAMINE

COPYRIGHT

2016

Jaruwan Chatwichien

*For my Grandfather.
In Loving Memory of Khun Chatwichien*

ACKNOWLEDGMENT

I would not be able to write this doctoral dissertation without the support and help from all of the kind people around me.

First of all, I would like to thank my research advisor, Professor Jeffrey Winkler, for the great support on both an academic and a personal level. I have learned how to be a good chemist as well as a good mentor from him throughout my past years in the lab and the group meetings. I also would like to thank him for always having faith in me more than what I have in myself. Thanks for giving me the opportunity to work on this interesting project that makes me gain so much knowledge in organic synthesis, medicinal chemistry and biology. This will be greatly useful in my future career as a researcher and lecturer.

I would like to thank my committee, Professor Gary Molander, Professor Madeleine Joullie' and Professor Donna Huryn for their advice in annual committee meetings. All of their suggestions not only helped me with my research but also guided me to think more thoughtfully as a researcher.

I would not have a great opportunity to expand my knowledge in biology without the great help and support from Professor Maureen Murphy and the lab members at The Wistar Institute. Especially, I thank Dr. Subhasree Basu for the great training and help with all the biology work described in this dissertation. I could not have made it without her. Above all, thanks for the friendship that everyone in the lab gave to me. I cannot say enough how much I truly appreciate.

I also thank our collaborators, Professor Garret A. FitzGerald, Dr. Soon Yew Tang and Dr. Tatsunori Suzuki for all the great work and kind help.

Thanks to all the former and current lab members in the Winkler lab. It has been a great time to work with them all. Thanks for all the support and friendship that made my time in the lab go by so quickly.

Without the great facilities in the Department of Chemistry and the Wistar Institute, I would not be able to finish all the work here. I would like to thank Dr. George Furst and Dr. Jun Gu for all the NMR help. Thanks to Dr. Rakesh Kohli for mass spectrometry. Thanks to James Hayden and Frederick Keeney for all the help with the imaging experiments.

I would like to acknowledge the Royal Thai Government Scholarship for the financial support throughout my master's and Ph.D. study.

Lastly, I would like to thank my family and friends for all of their support, inspiration and encouragement. I would not have finished my Ph.D. study without them. Words cannot describe how much I am thankful to have them all in my life.

ABSTRACT

THE DESIGN, SYNTHESIS, AND BIOLOGICAL EVALUATION OF DIMERIC β -CARBOLINES BASED ON THE STRUCTURE OF NEOKAULUAMINE AND THE STUDY OF MANZAMINE A DIMERIZATION TOWARD NEOKAULUAMINE

Jaruwan Chatwichien

Jeffrey D. Winkler

Neokauluamine, a naturally occurring dimeric β -carboline alkaloid, was isolated from an Indo-Pacific sponge (family Petrosiidae, order Hapsclerida) by Hamann et.al. in 2001. Neokauluamine exhibited improved antimarial activity in vitro and in vivo relative to currently available drugs artemisinin and chloroquine. Moreover, neokauluamine showed potent cytotoxicity against many types of human cancers including lung, colon and cervical cancers. Bases on the structure of neokauluamine, we designed, synthesized and evaluated simple dimeric β -carbolines as lead structures for the development of biologically active compounds. Interestingly, the synthesized dimeric β -carbolines exhibited antimicrobial activity and cytotoxicity against melanoma and lung cancer cell lines comparable to neokauluamine and its monomer, manzamine A. The cellular mechanism by which the dimeric β -carbolines induce cell death in H1299 lung cancer cells was studied and it was found that the β -carboline dimer accumulated in lysosomes and mediated apoptosis by upregulating a pro-apoptotic protein, PUMA (p53 upregulated modulator of apoptosis). The abundance of manzamine A relative to neokauluamine in Nature makes manzamine A an attractive starting material for the synthesis of neokauluamine. Recently, Tsukamoto et.al. discovered a novel manzamine alkaloid, pre-neokauluamine, as the key intermediate in the conversion of manzamine A to neokauluamine. Thus, we designed and synthesized a pre-neokauluamine-based model system to study optimal reaction conditions and selectivity of the key dimerization step.

TABLE OF CONTENTS

ABSTRACT.....	VI
LIST OF TABLES	IX
LIST OF FIGURES.....	X
LIST OF SCHEMES	XI
LIST OF ABBREVIATIONS	XII
CHAPTER 1. DESIGN, SYNTHESIS AND BIOLOGICAL EVALUATION OF DIMERIC β- CARBOLINES BASED ON THE STRUCTURE OF NEOKAULUAMINE.....	1
Section 1.1 Introduction	1
Section 1.2 Design and synthesis of dimeric β -carboline analogs	5
Section 1.3 Biological evaluation of dimeric β -carbolines	8
Section 1.4 Cellular mechanism of dimeric β -carboline induced cell death in H1299 cells.....	14
Section 1.5 Discussion	23
Section 1.6 Conclusions.....	25
Section 1.7 General methods and experimental procedures	25
CHAPTER 2. MODEL STUDY FOR THE DIMERIZATION OF MANZAMINE A TOWARD NEOKAULUAMINE.....	41
Section 2.1 Introduction	41
Section 2.2 Total synthesis and structural modification of manzamine A	41
Section 2.3 Synthetic analysis for the conversion of manzamine A toward neokauluamine	48
Section 2.4 Model study for the key dimerization step	51
Section 2.5 Model study for the key oxidation step	59

Section 2.6 Conclusions.....	65
Section 2.7 General methods and experimental procedures	66
CHAPTER 3. ANTAGONISTS OF THE F PROSTANOID (FP) RECEPTER AS A NOVEL DRUG TARGET FOR THE TREATMENT OF HYPERTENSION	94
Section 3.1 Causes and treatments of hypertension	94
Section 3.2 FP receptor inhibition as a novel target for treatment of hypertension.....	95
Section 3.3 Lead compound and previous efforts for FP antagonists.....	95
Section 3.4 Structural design and synthetic plans for PGF _{2α} antagonist analogs.....	97
Section 3.5 Synthesis of the designed PGF _{2α} antagonist analogs	100
Section 3.6 Biological evaluations of PGF _{2α} antagonist analogs	103
Section 3.7 Conclusions.....	107
Section 3.8 General methods and experimental procedures	108
REFERENCES.....	138
APPENDIX	145
BIBLIOGRAPHY	372

LIST OF TABLES

CHAPTER 1

Table 1.1 Antituberculosis activity of manzamine A and β -carboline analogs.	9
Table 1.2 Antibacterial activity of manzamine A and β -carboline analogs.	9
Table 1.3 Cytotoxicity and selectivity index (SI) for manzamine A, neokauluamine, and dimeric and monomeric β -carboline analogs against H1299, A375 and IMR90	11
Table 1.4 Cytotoxicity for β -carboline compounds against NSCLC.	13

CHAPTER 2

Table 2.1 Relative natural abundance of neokauluamine compared to other manzamine alkaloids.	42
Table 2.2 ^1H - and ^{13}C NMR data for neokauluamine and dimer 96	58
Table 2.3 Calculated distances in space between H-atoms in isomer 96	59

CHAPTER 3

Table 3.1 Structures and $\text{PGF}_{2\alpha}$ antagonist activities of the lead compound, AS604872, and previous thiazolidine analogs	96
Table 3.2 Structures and $\text{PGF}_{2\alpha}$ antagonist activities of the previous proline analogs	97
Table 3.3 FP antagonist activity (IC_{50}) of biaryl thiazolidine derivatives.	103
Table 3.4 FP antagonist activity (IC_{50}) of biaryl proline derivatives.	105

LIST OF FIGURES

CHAPTER 1

Figure 1.1 Examples of β -carboline alkaloids.	2
Figure 1.2 Linkers varied in length and rigidity.	6
Figure 1.3 Cytotoxicity (IC_{50}) substituted β -carboline analogs against H1299.	12
Figure 1.4 Colocalization study of the β -carboline compounds in H1299.	16
Figure 1.5 Study of autophagy inhibition for H1299 treated with β -carboline analogs	17
Figure 1.6 Annexin positive cells for H1299 treated with β -carboline compounds	19
Figure 1.7 Western blot and confocal analysis of apoptotic proteins in H1299 cells treated with β -carboline compounds	20
Figure 1.8 Analysis of PUMA levels in H1299 cells treated with β -carboline compounds	22
Figure 1.9 Proposed mechanism for dimeric β -carboline induced cell death	24

CHAPTER 2

Figure 2.1 X-ray crystal structure of manzamine A hydrochloride.	42
Figure 2.2 Key HMBC and NOESY correlations of neokauluamine	48

CHAPTER 3

Figure 3.1 Blood pressure regulation through the renin-angiotensin system (RAS)	94
Figure 3.2 Structure analysis of AS604872.	98
Figure 3.3 Synthetic strategy for the variation at the sulfonamide moiety	98
Figure 3.4 FP antagonist activity (IC_{50}) of the amino acid derivatives	106
Figure 3.5 FP antagonist activity (IC_{50}) for derivatives with variation of the amide branch.	107

LISTS OF SCHEMES

CHAPTER 1

Scheme 1.1 Formation of β -carboline from Pictet-Splengler condensation.....	1
Scheme 1.2 Proposed biosynthesis of manzamine alkaloids by Baldwin and Whitehead.	3
Scheme 1.3 Synthesis of monomeric and dimeric β -carboline analogs.	7

CHAPTER 2

Scheme 2. 1 Key steps for the first total synthesis of manzamine A by Winkler <i>et.al.</i>	43
Scheme 2. 2 Key steps for the total synthesis of manzamine A by Martin <i>et.al.</i>	44
Scheme 2. 3 Key steps for the total synthesis of manzamine A by Fukuyama <i>et.al.</i>	45
Scheme 2. 4 Key steps for the total synthesis of manzamine A by Dixon <i>et.al.</i>	46
Scheme 2. 5 Ring-opening metathesis of manzamine A.	47
Scheme 2. 6 Regioselective ring-opening of the azocine ring of manzamine A.	47
Scheme 2. 7 Proposed mechanism for the dimerization of pre-neokauluamine toward neokauluamine.	49
Scheme 2. 8 Key steps for the dimerization of manzamine A toward neokauluamine.	50
Scheme 2. 9 Model system for the study of the dimerization step.	51
Scheme 2. 10 Possible isomers from the dimerization of the model system 94	53
Scheme 2. 11 Previous effort to study the dimerization of the model system 94	54
Scheme 2. 12 Initial effort to prepare model system 94	55
Scheme 2. 13 Stereoselective synthesis of the model system for the study of the dimerization of pre-neokauluamine.	57
Scheme 2. 14 Model study for the dimerization of compounds 123 and 124	57
Scheme 2. 15 Model system for the study of the key oxidation step.	60
Scheme 2. 16 Synthesis of the model system 125	61
Scheme 2. 17 Proposed mechanism for C-H activation of tertiary amine.	62

Scheme 2. 18 Examples of selective oxidation of tertiary amines in natural product synthesis. ...	62
Scheme 2. 19 Polonovski-Potier reaction of model 125	63
Scheme 2. 20 Synthesis of model system 159	64
Scheme 2. 21 Polonovski-Potier reaction of model 159	65

CHAPTER 3

Scheme 3.1 Synthetic plan for the variation at the thiazolidine core (B).....	99
Scheme 3.2 Synthetic plan for the variation at the amide portion (C).....	99
Scheme 3.3 Synthesis of the chiral amine (180) by using Ellman's chiral ulfonamide.	100
Scheme 3.4 Initial efforts for the synthesis of the enantiopure N-protected thiazolidine carboxylic core (191).....	101
Scheme 3.5 Propose mechanism for epimerization of the thiazolidine carboxylic acid.....	101
Scheme 3.6 Synthesis of the the enantiopure thiazolidine carboxylic core (191).....	101
Scheme 3.7 Synthesis of the lead compound, AS604872, and its derivatives.	102

LIST OF ABBREVIATIONS

Ac	acetyl
AcCl	acetyl chloride
Ac ₂ O	acetic anhydride
Ar	aryl
atm	1 atmosphere
BINAP	2,2'-bis(diphenylphosphino)-1,1'-binaphthyl
Boc	tert-butoxycarbonyl
cat.	catalytic
d	doublet
δ	chemical shift in parts per million
dd	doublet of doublets
DMF	dimethylformamide
DMSO	dimethyl sulfoxide
Et	ethyl
Et ₂ O	diethyl ether
EtOAc	ethyl acetate
EtOH	ethanol
h	hour(s)
H ₂ O	water
HRMS	high resolution mass spectrometry
Hz	Hertz (S ⁻¹)
IR	infrared spectroscopy
<i>J</i>	coupling constant in Hertz
LCMS	liquid chromatography–mass spectrometry
m	multiplet
M	molar (mol. L ⁻¹)

<i>m</i> CPBA	<i>meta</i> -chloroperoxybenzoic acid
Me	methyl
MeOH	methanol
MHz	megahertz
Min	minutes
mL	milliliter(s)
mmol	millimole(s)
Ms ₂ O	methanesulfonic anhydride
<i>m/z</i>	mass to charge ratio
NaH	sodium hydride
NMR	nuclear magnetic resonance
Pd(OAc) ₂	palladium acetate
Ph	Phenyl
PPh ₃	triphenylphosphine
ppm	parts per million
PPTS	pyridinium <i>p</i> -toluenesulfonate
q	quartet
s	singlet
t	triplet
TBAF	tetra- <i>n</i> -butylammonium fluoride
TBS	<i>tert</i> -butyldimethylsilyl
TBDPS	<i>tert</i> -butyldiphenylsilyl
TFA	trifluoroacetic acid
TFAA	trifluoroacetic anhydride
Tf ₂ O	trifluoromethanesulfonic anhydride
THF	tetrahydrofuran
TLC	thin-layer chromatography

TMSOTf

trimethylsilyl trifluoromethanesulfonate

TsOH

p-toluenesulfonic acid

CHAPTER 1. DESIGN, SYNTHESIS AND BIOLOGICAL EVALUATION OF DIMERIC β -CARBOLINES BASED ON THE STRUCTURE OF NEOKAULUAMINE

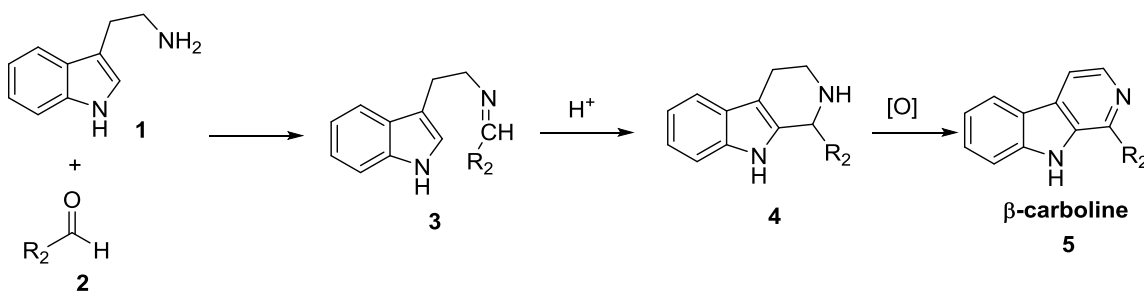
(Adapted with permission from Chatwchien, J., Basu, S., Murphy, M. E., Hamann, M. T. & Winkler, J. D.

Design, synthesis, and biological evaluation of β -carboline dimers based on the structure of neokauluamine.

Tetrahedron Lett. **56**, 3515–3517 (2015), License number 3854361042387)

1.1. Introduction

β -carboline alkaloids are a group of natural product that possess a tricyclic pyrido [3,4-b]indole ring moiety.¹ β -carbolines can be prepared by Pictet-Spengler reaction of tryptamine (1) and aldehyde precursors (2), as shown in **Scheme 1.1**.¹ To date, more than one hundred β -carboline alkaloids have been isolated from a variety of terrestrial plants and marine sponges² and exhibit a diverse range of biological activities including antitumor, antiviral and antimicrobial properties. For instance, Harman (7) and norharman (6) (**Figure 1.1**) are the two most simple β -carboline alkaloids. Both are cytotoxic against several human tumor cell lines due to their ability to intercalate DNA and to disrupt enzymatic function.¹



Scheme 1.1 Formation of β -carbolines from Pictet-Spengler condensation.

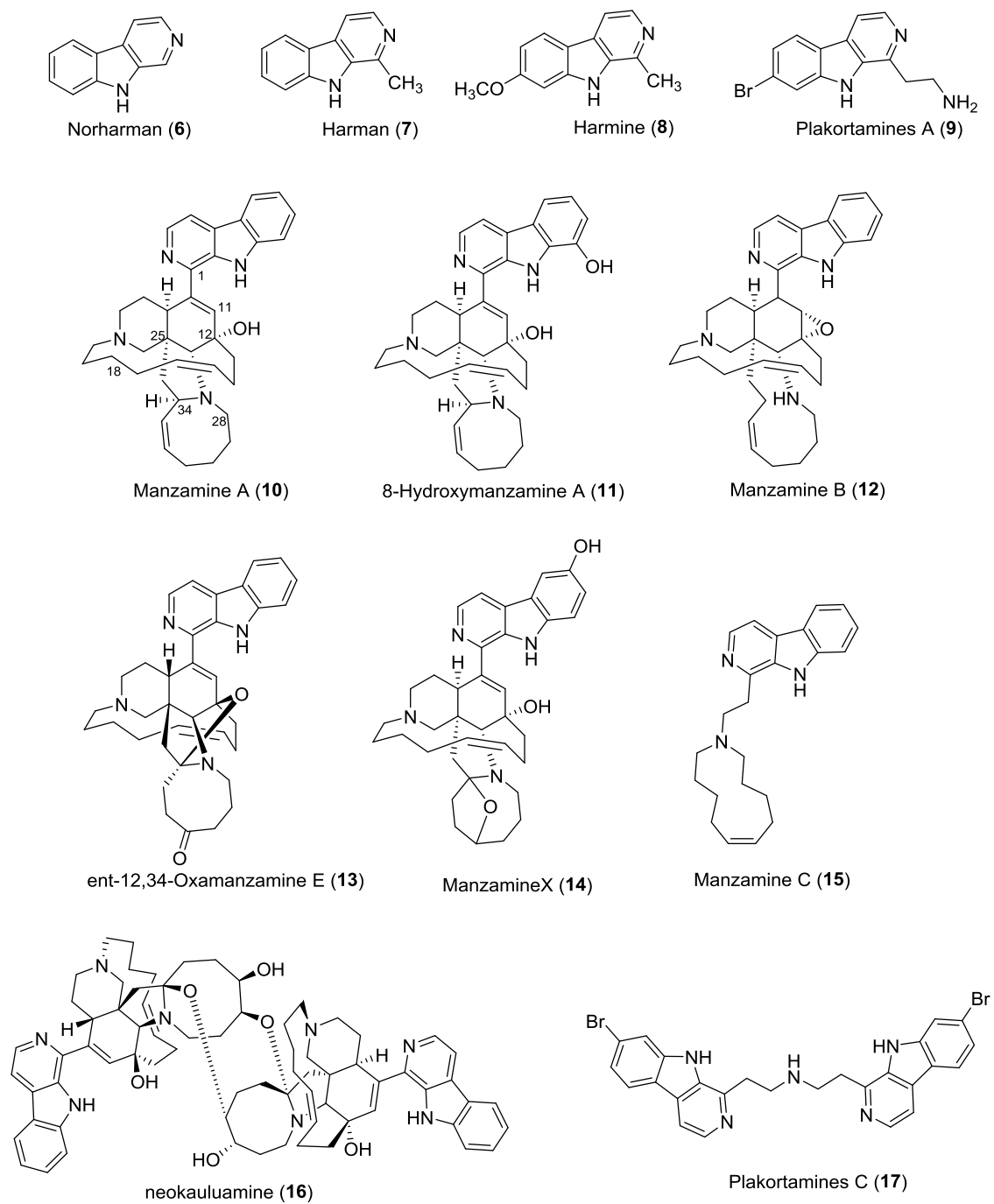
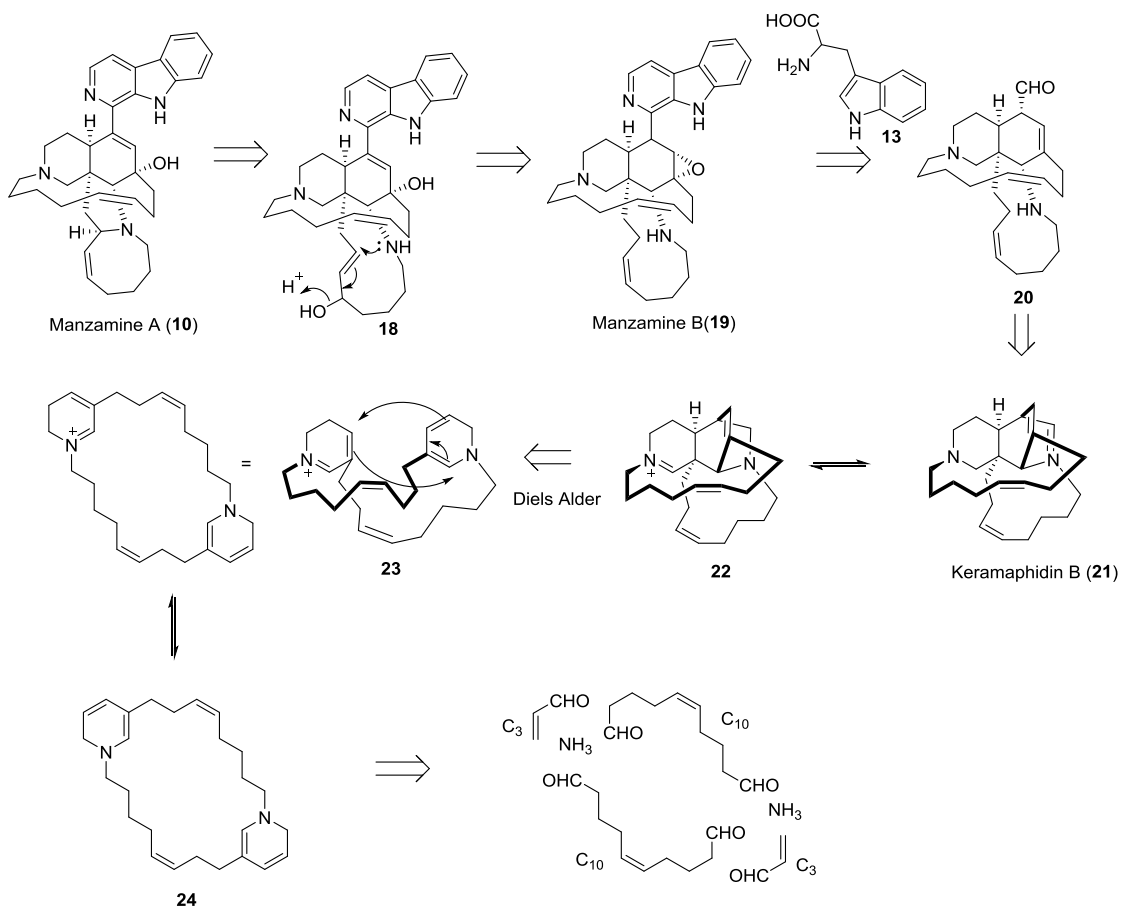


Figure 1.1 Examples of β -carboline alkaloids.

Manzamines are a class of marine β -carboline alkaloids that possess a fused and bridged tetra- or pentacyclic system attached to β -carboline moiety.² Over the last decades, more than 80 manzamine alkaloids have been isolated. They exhibit a broad range of biological activities including antitumor, antimalarial, antimicrobial, anti-Alzheimer, insecticidal, anti-inflammatory and anti-HIV/AIDS opportunistic infections.³ Baldwin and Whitehead proposed the biosynthesis of manzamine alkaloids via the key intramolecular Diels-Alder cyclization of the bis-dihydropyridine (**23**), derived from the simple building blocks; ammonia, C10 and C3 units, shown in **Scheme 1.2**.⁴ This hypothesis was later verified by the isolation of many manzamine-related alkaloids, such as ircinal A and keramaphidin B (**21**) that have similar structures to the proposed intermediates, and the biomimetic synthesis of keramaphidin B (**21**).⁵



Scheme 1.2 Proposed biosynthesis of manzamine alkaloids by Baldwin and Whitehead.

Manzamine A (**10**) is a representative member of the family of manzamine alkaloids. It was first isolated from marine sponges of the genus *Haliclona* by Higa *et.al.* in 1986, as a novel alkaloid that exhibited the growth inhibition of P388 mouse leukemia cells with an IC₅₀ of 0.07 µg/mL.⁶ Due to the uniquely complex structure and interesting biological activity, manzamine A has been an attractive and challenging target for total synthesis^{7,8,9} and shows intriguing biological activity.¹ Manzamine A displayed *in vitro* cytotoxicity to a variety of human cancer cell lines including colon, lung and breast carcinoma cells. Moreover, manzamine A showed improvement in antimalarial activity both *in vitro* and *in vivo* over the clinically used drugs chloroquine and artemisinin.^{10,11} The structure-activity relationship (SAR) of manzamine A for antimalarial activity has been studied from its naturally occurring manzamine A-related alkaloids¹² and its synthetic analogs³ and showed that the C-12 hydroxyl, the conformation of the eight-membered ring and the orientation of β-carboline are crucial for the activity.

Neokauluamine (**16**)¹⁰, a naturally occurring dimer of manzamine A, was isolated from an Indo-Pacific sponge (family *Petrosiidae*, order *Hapsclerida*) by Hamann *et.al* in 2001. Unlike the previously reported manzamine dimer, kauluamine, neokauluamine exhibited potent antimalarial activity *in vitro* and *in vivo* comparable to that of manzamine A. Moreover neokauluamine displayed two times greater cytotoxic against Hela cells and ca. 10 times more proteasome inhibitory activity than manzamine A.¹³ Since neokauluamine is relatively less abundant than manzamine A and other manzamines in Nature, we wanted to design and synthesize simple analogs of neokauluamine that retain the potent biological activity of the natural product.

1.2. Design and synthesis of dimeric β-carboline analogs

The concept of polyvalency offers an attractive strategy for enhanced selectivity and binding affinity of polyvalent ligands to receptors relatively to their corresponding monomers.¹⁴ Whitesides *et.al.* reported that a trivalent binding system of vancomycin and D-Ala-

D-Ala (DADA) has binding constant 25 times higher than biotin-avidin interaction, one of the strongest interaction in biological systems.¹⁵ Recently, our group has also reported that dimeric chloroquines exhibit higher autophagy inhibitor over a known monomeric antimalarial drug, hydroxychloroquine (HCQ).¹⁶

Inspired by the dimeric structure of neokauluamine, we reasoned that the replacement of the complex central portion of the structure with linkers that could tether the two β -carboline moieties in the relative orientation as in neokauluamine might retain the bioactivity of the natural product. While the published structure of neokauluamine, determined through NMR analysis, did not assign the stereochemistry at C-30', C-31', and C-34',¹⁰ molecular modeling at the level of MMFF (SPARTAN v. 10.0, Wavefunction, Inc.) of each of the possible diastereomers revealed that the distance between the two β -carboline moieties is ca. 13.8 Å for each of the possible diastereomers. The appropriate linker lengths were established using ChemBio3 Pro 13.0 by calculating the lengths of the extended conformations of commercially available or easily prepared diamines, the structures of which are shown in **Figure 1.2**.

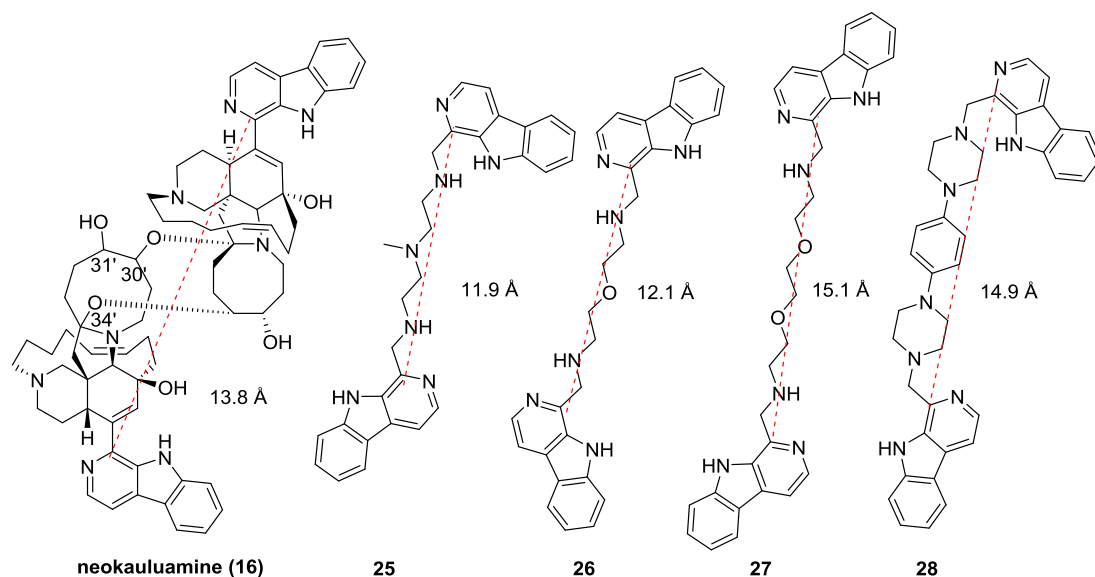
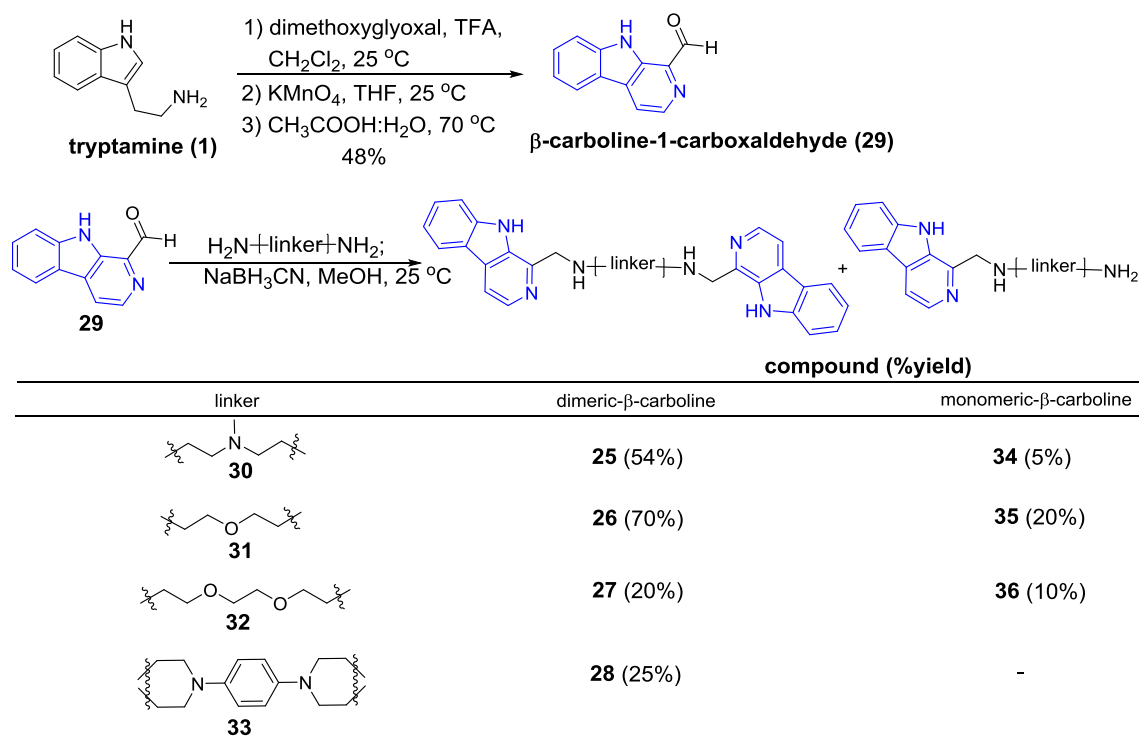


Figure 1.2 Linkers varied in length and rigidity.

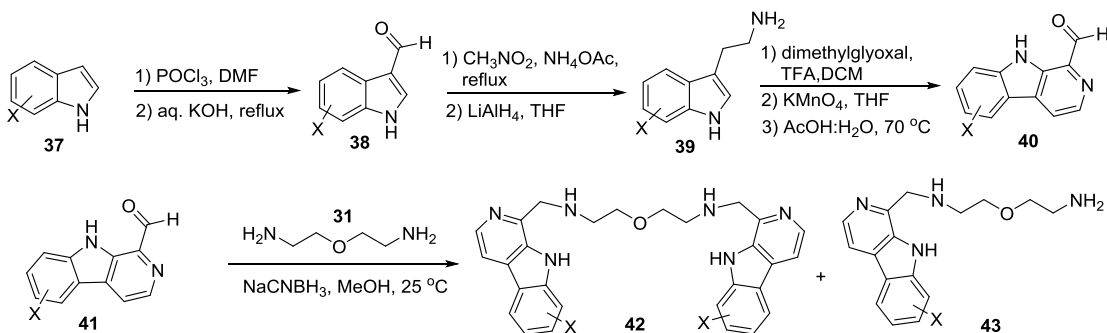
As shown in **Scheme 1.3**, we envisioned that reductive aminations of β -carboline-1-carbaldehyde (**29**) with diamine linkers would be an efficient way to put β -carbolines onto the diamine linkers to prepare the desired analogs. β -carboline-1-carbaldehyde (**29**) was prepared from tryptamine (**1**) in three steps according to a known procedure.¹⁷ The aldehyde **29** was then condensed with diamines **30-33** to form the corresponding Schiff base followed by reduction with sodium cyanoborohydride. Partial conversion to the dimers **25-28** resulted in the concomitant formation of corresponding monomeric β -carbolines **34-36**, which serve as important control compounds to test the importance of the dimeric structures for biological activity.



Scheme 1.3 Synthesis of monomeric and dimeric β -carboline analogs.

Substitutions on β -carboline have shown to have a significant impact on its biological activity.¹ To screen for improved bioactive compounds, we prepared substituted dimeric β -carboline analogs from a variety of substituted β -carbolines (**41**) coupling with 2,2'-oxybis(ethylamine) (**31**)

which is one of the optimal linkers at the time, based on its antimicrobial activity and cytotoxicity. The substituted dimeric β -carboline aldehydes were prepared from commercially available substituted indoles, following a precedent literature.¹⁸ They then were tethered onto the diamine **31** by reductive amination reaction, shown in **Scheme1.4**.



Scheme1.4. Synthesis of substituted dimeric β -carboline analogs

1.3. Biological evaluation of dimeric β -carbolines

1.3.1. Antimicrobial activities

Infectious diseases such as HIV/AIDS, malaria and tuberculosis (TB) are a major cause of death worldwide.¹⁹ Most of the existing therapies for these diseases are either inefficient or yield severe side effects. The discovery of novel therapeutic agents is therefore urgently needed.

Most of manzamine alkaloids have been reported to induce 98-99% inhibition of Mycobacterium tuberculosis (H37Rv) with MIC <12.5 μ g/ml.¹⁰ Collaborating with Professor Hamann's group at the University of Mississippi, we therefore evaluated the dimeric β -carboline analogs for the inhibition activity against H37Rv and found that dimeric compounds **25-27** are comparable in their potency to manzamine A and significantly more active than the corresponding monomeric ligands. Interestingly, the rigid structure in dimeric β -carboline **28** led to loss of biological activity. This suggests that the orientation of the two β -carbolines is crucial for biological potency, and that the more rigid linker excludes the necessary orientation between the two heterocycles.

Compound	H37Rv
	MIC [$\mu\text{g/ml}$] (%Inh)
25	3
26	1.3
27	2.3
28	>50 (23%)
35	24
36	17.8
manzamine A (10)	1.5

Table 1.1 Antituberculosis activity of manzamine A and β -carboline analogs.

We further evaluated antibacterial activity of the prepared dimeric β -carbolines and found that similar differences in the activity were observed between dimeric and monomeric β -carbolines against *S. aureus*, MRS, *E. coli*, *P. aeruginosa* and *M. intracellulare*. The only system that we examined for which this trend did not hold was *P. aeruginosa*.

Compound	IC ₅₀ (μM)				
	<i>S. aureus</i>	MRS	<i>E. coli</i>	<i>P. aeruginosa</i>	<i>M. intracellulare</i>
25	1.5	2.14	10.27	12.11	5.99
26	1.4	1.4	4.86	>20	3.15
27	2.02	3.74	11.28	>20	9.1
35	>20	>20	>20	>20	>20
36	>20	>20	>20	>20	>20
manzamine A (10)	0.9	1.3	-	-	0.6

Table 1.2 Antibacterial activity of manzamine A and β -carboline analogs.

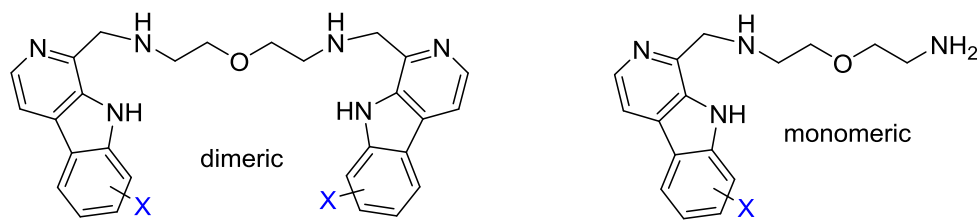
1.3.2. Cytotoxicity against cancer cell lines

To study the biological activities of the prepared dimeric β -carboline analogs compared to the corresponding monomers and the natural products, neokauluamine and manzamine A, we examined their cytotoxicity against carcinoma cells which were sensitive to other β -carboline-containing structures.²⁰ In collaboration with Professor Murphy at the Wistar Institute, we tested the dimeric analogs against H1299 (lung) and A375 (melanoma) cancer cell lines as well as IMR90 (normal lung fibroblast). The results are summarized in **Table 1.3**. We find that the dimeric β -carbolines **25-27** are comparable in potency to both neokauluamine and manzamine A, and ca. 10x more potent than the corresponding monomeric β -carbolines **34-36** and the more rigid linker analog, **28**. The loss in potency of compound **28** again supported the importance of the orientation of the two β -carbolines in the dimers. A significant difference was also observed in the selectivity of these dimeric compounds for cancer vs. non-cancer cells. As indicated in **Table 1.3**, the selectivity index (SI) was ca. 10x greater for the dimeric compounds vs. the monomeric ligands against both cell lines.

Cell lines	IC ₅₀ (μM)			SI	
	H1299	A375	IMR90	IMR90/H1299	IMR90/A375
neokauluamine	1.7	N/A	N/A		
manzamine A	1.9	4.9	79	41.2	16
25	1.6	N/A	N/A		
26	1.6	3	200.6	123.5	67
27	1.8	2.2	127.7	69.1	58
28	17.0	N/A	N/A		
34	15.1	N/A	N/A		
35	12.6	14.1	117.5	9.4	8
36	14.5	24.1	181.3	12.5	8

Table 1.3 Cytotoxicity (IC₅₀) and selectivity index (SI) for manzamine A, neokauluamine, and dimeric and monomeric β-carboline analogs against H1299 (human non-small cell lung carcinoma cell line), A375 (human malignant melanoma) and IMR90 (human Caucasian fetal lung fibroblast).

To screen for more potent biologically active compounds, we prepared dimeric substituted β-carboline compounds in which the linker is 2, 2'-oxybis (ethylamine) (**31**) (**Figure1.3**). The cytotoxicity against H1299 cells was evaluated and the results are summarized in **Figure1.3**. Unfortunately, most of them showed similar activities to the corresponding dimeric unsubstituted β-carboline, **26**, with no significant improvement in potency.



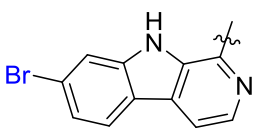
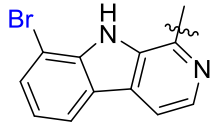
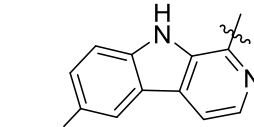
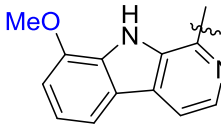
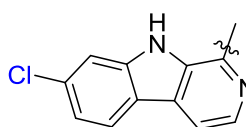
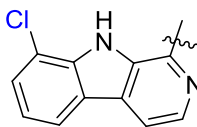
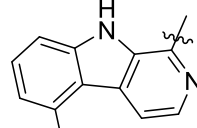
	Compound	IC₅₀ H1299(μM)
	dimeric(monomeric)	dimeric(monomeric)
	44 (45)	2.8 (4.6)
	46 (47)	1.8 (20.3)
	48 (49)	0.8 (4.9)
	50 (51)	1.6 (12.0)
	52	1.6
	53 (54)	1.6 (31.0)
	55 (56)	1.5 (2.3)

Figure 1.3 Cytotoxicity (IC₅₀) for dimeric and monomeric substituted β-carboline analogs against H1299 (human non-small cell lung carcinoma cell line).

According to the World Health Organization (WHO), lung cancer is one of the most 5 common types of cancer in both men and women and the leading cause of cancer deaths worldwide.²¹ Lung cancer is traditionally categorized into two major types; small cell (SCLC) and non-small cell (NSCLC) lung cancer. Most lung cancers are NSCLC (85%) and very challenging to treat due to acquired resistance. With currently available drugs for the treatment of NSCLC, the 5-year survival rate is still less than 15%. The development of novel and more effective chemotherapeutic agents is therefore necessary.

Since the dimeric β -carboline analogs **25-27** displayed potent cytotoxicity against H1299 (human non-small cell lung carcinoma cell line), we decided to study the cytotoxicity of the dimeric β -carbolines against other NSCLC cell lines. Compound **25** was evaluated for cytotoxicity against another five NSCLC cell lines (A549, H441, H1373, H1993 and H2009). As observed previously, dimeric β -carboline **25** exhibited comparable potency to manzamine A and was significantly more potent than its monomer **34** in all indicated NSCLC cell lines. This result supports the importance of the dimeric β -carbolines, and their potential utility as the starting point for the development of antitumor agents.

compound	IC ₅₀ (μ M)				
	A549	H441	H1373	H1993	H2009
manzamineA	2.3 \pm 0.5	1.1 \pm 0.1	2.1 \pm 0.1	3.9 \pm 1.7	1.6 \pm 0.2
25	2.9 \pm 0.8	0.7 \pm 0.3	3.3 \pm 2.1	1.2 \pm 1.1	1.4 \pm 0.2
34	20.5 \pm 9.2	4.3 \pm 2.8	13.2 \pm 0.3	9.3 \pm 7.1	8.9 \pm 0.1

Table 1.4 Cytotoxicity (IC₅₀) for manzamine A, dimeric β -carboline (**25**) and monomeric (**34**) β -carboline against NSCLC.

1.4. Cellular mechanism of dimeric β -carboline (**25**) induced cell death in H1299 cells

Due to the striking activity of the simple synthetic dimeric β -carboline structures that exhibited similar cytotoxicity against cancer cells to the natural products manzamine A and neokaulamine, we were motivated to investigate the mechanism of dimeric β -carbolines to induction of cell death. As a preliminary study, we studied the mechanism of cell death with compound **25** (one of the most potent dimeric β -carboline analogs) along with manzamine A and its monomer (**34**), served as the controls, in H1299 cells.

Lysosome, a membrane-bound organelle that contains different types of acidic hydrolases, has emerged as an interesting target to induce cancer cell death.²² Lysosome is a key component in autophagy. When fuse with autophagosomes, lysosome dispenses its enzymes into the autophagic vesicles to digest cellular unwanted materials.²³ The environment inside is usually maintained acidic by a vacuolar ATPase as a proton pump transferring protons from cytosol into lysosomal lumen.²⁴ Lysosomal dysfunction due to vacuolar ATPase inhibition and interior pH elevation impairs autophagy and consequently activates apoptosis.²⁵ Moreover, losing lysosomal membrane integrity renders lysosomal membrane permeabilization (LMP). In case of moderate lysosomal destruction, LMP mediates caspase-dependent apoptosis via the leakage of cathepsins into cytosol. Moreover, when massive lysosomal damage occurs, necrotic cell death is induced.²⁶

Manzamine A²⁵, chloroquine^{27,28} and Lys05¹⁶ have been reported as lysosome-targeting anticancer agents. Due to their weakly basic property (pKa = 9.2, 10.1 and 8.4, respectively), they are protonated and trapped in the acidic interior of lysosomes. The accumulation of these weak bases enhances the interior pH, causing inhibition of hydrolase activities and consequently autophagy inhibition.

To study the cellular mechanism of dimeric β -carboline **25** induced cell death, we first determined the localization of the compound at the subcellular level. Taking advantage of the

inherent fluorescent properties of the β -carboline moiety (Ex/Em: 358/461 nm), we treated H1299 cells with compound **25**, **34** and manzamine A for 1h before staining mitochondria with MitoTracker® Green FM (Invitrogen) and lysosomes with LysoTracker® Red DND-99 (Invitrogen). As expected by the weakly basic property of the compounds (**25**; pKa= 8.2 and **34**; pKa = 8.1), live confocal microscopy demonstrated that each of the compounds predominantly localized in lysosomes. These observations are similar to the finding seen previously for manzamine A that is known to target vacuolar ATPases in lysosomes and inhibits autophagy by preventing autophagosome turnover in pancreatic cancer cells.²⁵ To investigate whether compounds **25** and **34** lead to the same effect as was observed with manzamine A, we performed western blot analysis, probing for autophagy markers (LC3 and p62/SQSTM1). H1299 cells treated with dimeric β -carboline **25** showed an increase in autophagy adaptor protein, p62/SQSTM1, and a dose-dependent increase in LC3II levels, compared to the control DMSO. To further confirm these findings, we examined LC3II puncta by immunofluorescence studies for GFP-LC3 in H1299 cells transfected with GFP-LC3. Similar to western blot analysis, the transfected cells treated with β -carbolines and manzamine A showed an increase in LC3II puncta, indicating a decrease in autophagosome clearance.

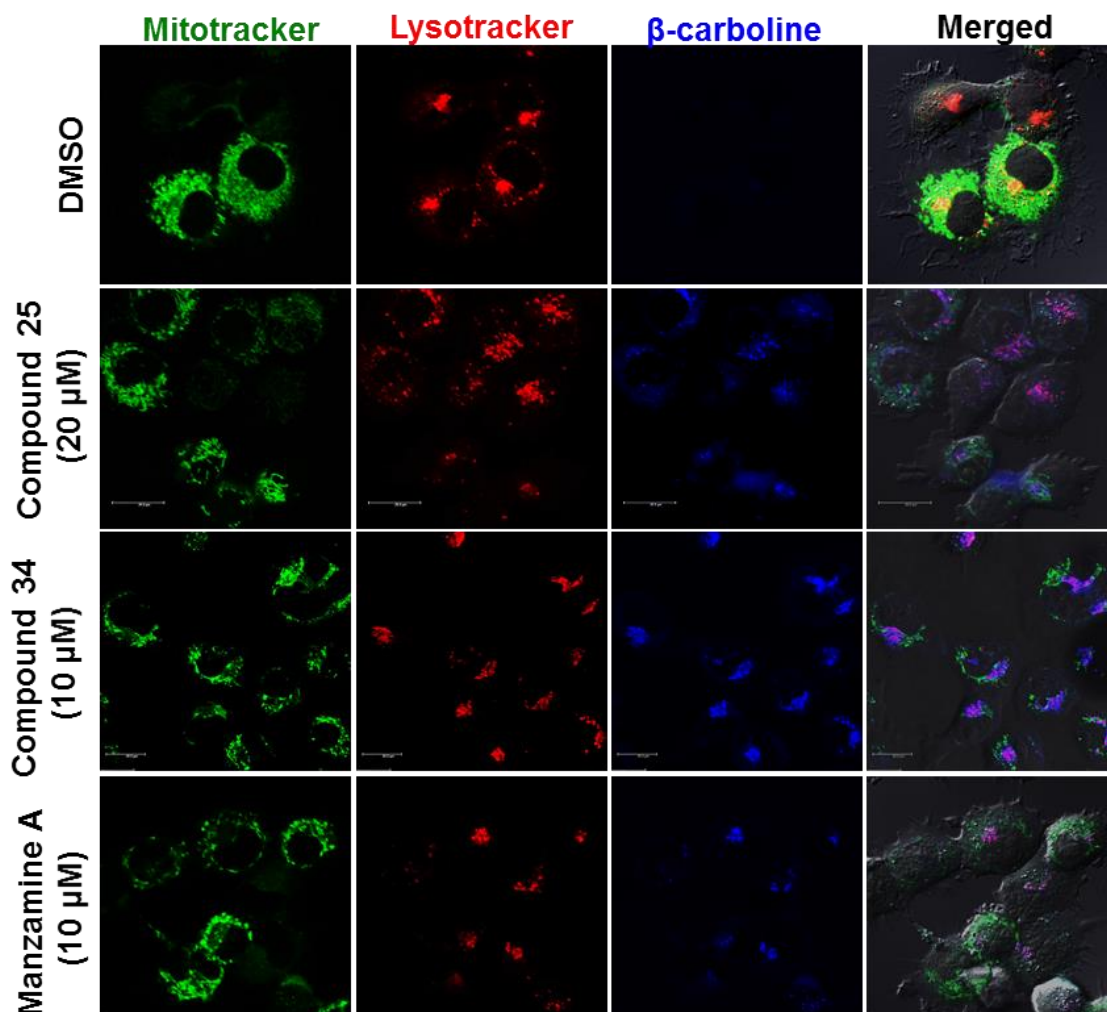


Figure 1.4 H1299 cells were treated with compound **25**, **34** or manzamine A for 1h before staining mitochondria with MitoTracker® Green FM (Invitrogen) and lysosomes with LysoTracker® Red DND-99 (Invitrogen). Confocal analysis showed localization of the β -carboline compounds in lysosomes.

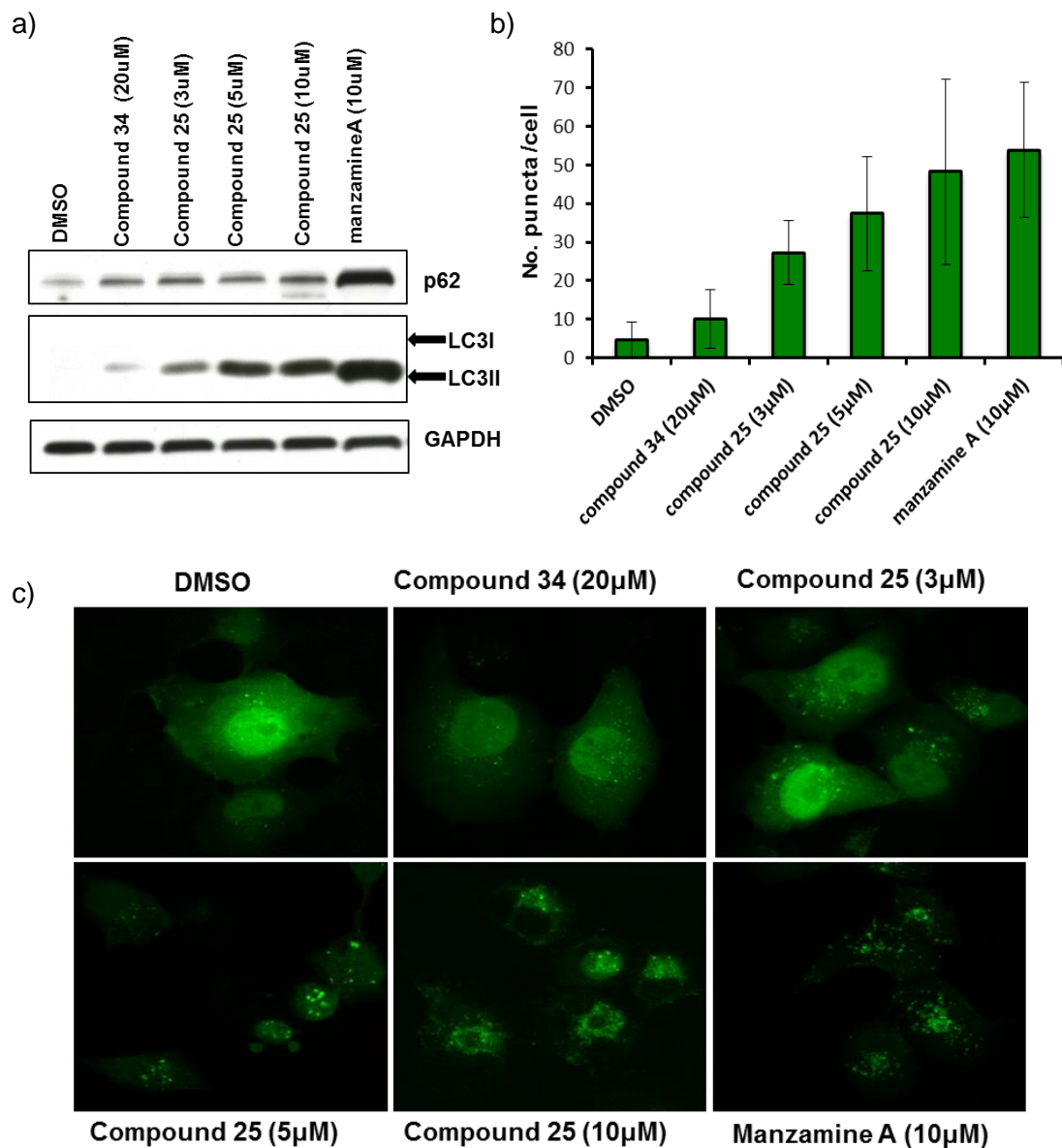


Figure 1. 5 a) Western blot analysis of LC3 and p62 in H1299 cells treated with DMSO, compound **34** (20 μ M), compound **25** (3, 5 and 10 μ M) or manzamineA (10 μ M) for 24 h incubation. b) GFP-LC3 transfected H1299 cells were treated with DMSO, compound **34** (20 μ M), compound **25** (3, 5 and 10 μ M) or manzamineA (10 μ M) for 24h. The GFP-LC3 puncta were analyzed by confocal microscope. c) Number of punta/cell was scored by ImageJ software. n=30; error bars, s.d.

Apoptosis and autophagy cross-regulate each other.^{29,30,31} Autophagy inhibition was reported to induce apoptotic cell death.^{32,33,34} To determine if the dimeric β -carboline (**25**) induces cell death in H1299 cells through apoptosis, we examined Annexin positive cells using the Guava Nexin reagent. H1299 cells were treated with either compound **25** or compound **34** for 48h before staining with Annexin V-PE and 7-AAD. Flow data analysis for the number of apoptotic cells showed that the dimeric β -carboline (3 μ M) induced significant increase in apoptotic cell death compared to the monomer (15 μ M), (**Figure 1.6**). Similarly, dimeric β -carboline (**25**) induced significant increase in cleaved caspase 3 expression in a dose-dependent manner as seen by western blot analysis (**Figure 1.7a**) and immunofluorescence (**Figure 1.7b**). Other apoptotic markers such as cleaved lamin A and cleaved PARP levels were upregulated with dimeric β -carboline (**25**) compared to the monomer (**Figure 1.7a**). These results suggest that the dimeric β -carboline (**25**) induces cell death through caspase-dependent apoptosis more efficiently than its monomer.

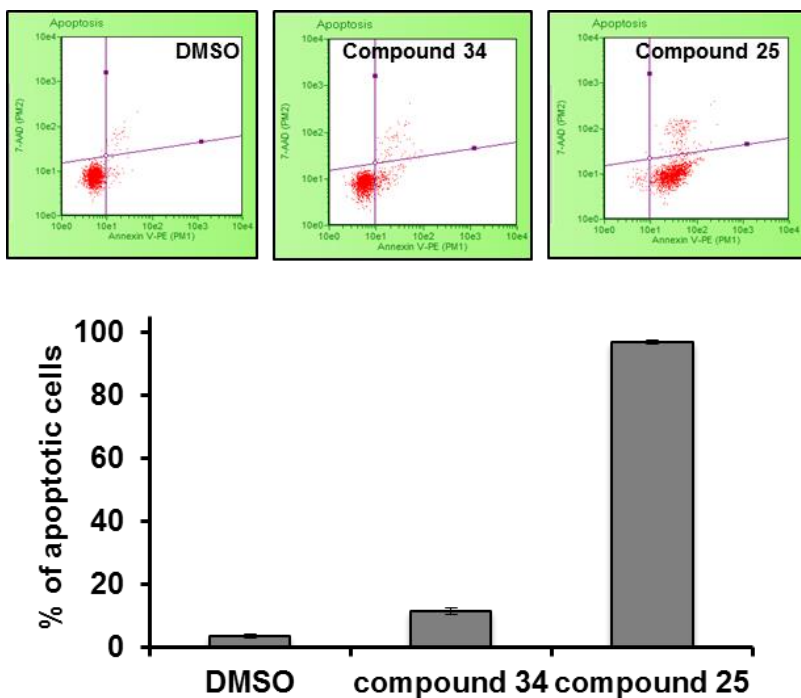


Figure 1. 6 H1299 cells were induced to undergo apoptosis by incubation with DMSO (control experiment), compound **34** (15 μ M) and compound **25** (3 μ M) for 48 h. After incubation, cells were stained with Guava Nexin Reagent, and data acquired on the PCA-96 System. The results showed 4%, 11% and 97% apoptotic cells, respectively. n=3; error bars, s.d.

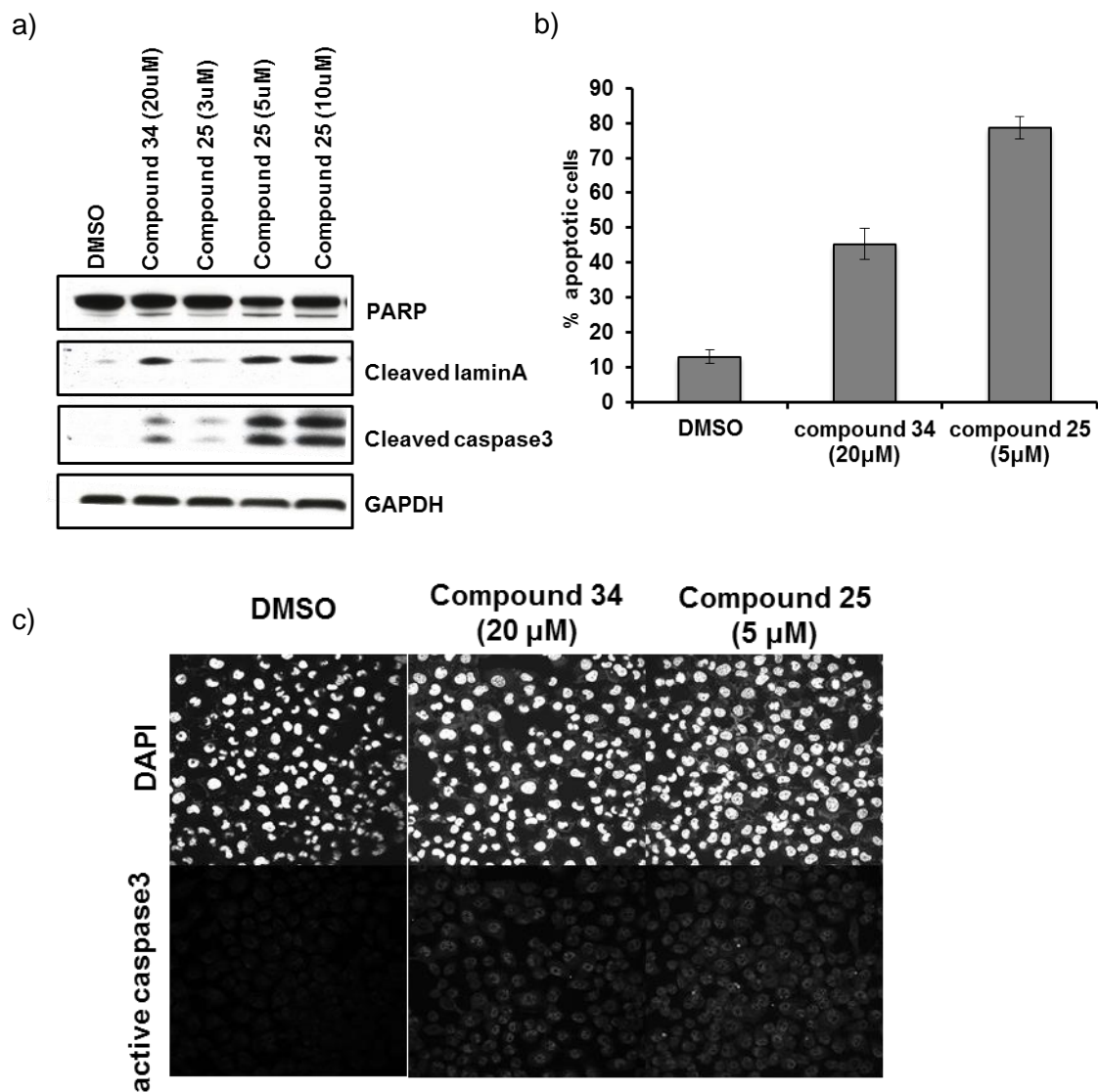
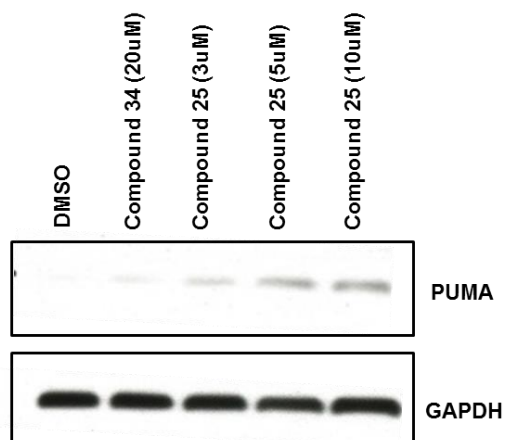


Figure 1. 7 a) Western blot analysis of apoptotic proteins in H1299 cells treated with DMSO, compound **34** (20 μ M) and compound **25** (3, 5 and 10 μ M) for 24 h incubation. b) Confocal immunofluorescent analysis for active caspase 3 of H1299 cells treated with DMSO, compound **34** (20 μ M), compound **25** (5 μ M) for 24 h incubation. c) Apoptotic cells were quantified from the ratio of number of cell expressing active caspase to total cell number, n=3; error bars, s.d.

To further investigate the mechanism of induced cell death with dimeric β -carboline (**25**), we performed western blot analysis to detect proteins that are involved in the apoptotic pathway. Our previous experiments suggested that dimeric β -carboline (**25**) accumulated in lysosomes and mediated caspase-dependent apoptotic cell death. We therefore elected to further investigate the relationship between lysosomal dysfunction and caspase-mediated cell death. Many recent studies have demonstrated the crosstalk between autophagic and apoptotic pathways.³¹ Several BH3-only proteins are known to play dual roles in the regulation of these pathways. PUMA (p53 upregulated modulator of apoptosis), in particular, mediates caspase cleavage by either activation of Bax/Bak or inhibition of antiapoptotic proteins.³⁵ Recent studies have shown that autophagy inhibition upregulates PUMA expression.³² Interestingly, western blot analysis of H1299 cells treated with different concentrations of dimeric β -carboline (**25**) showed a dose-dependent increase in PUMA level, corresponding to the cleaved caspase 3 level observed previously. To determine whether dimeric β -carboline (**25**) induced PUMA expression at the transcription level, we performed qRT-PCR analysis and found that the PUMA mRNA levels in H1299 treated with dimeric β -carboline increased in a dose- and time-dependent manner, consistent with PUMA protein levels. Besides p53, PUMA expression can be regulated by other transcription factors (e.g. p73 and E2F1) depending on stimuli and cell lines.³⁵ Since H1299 is a p53 null cell line, these data suggests that dimeric β -carboline (**25**), by accumulation in lysosomes, may be involved in a mechanism that affects p53-independent regulation of PUMA expression and consequently mediates caspase-dependent apoptosis.

a)



b)

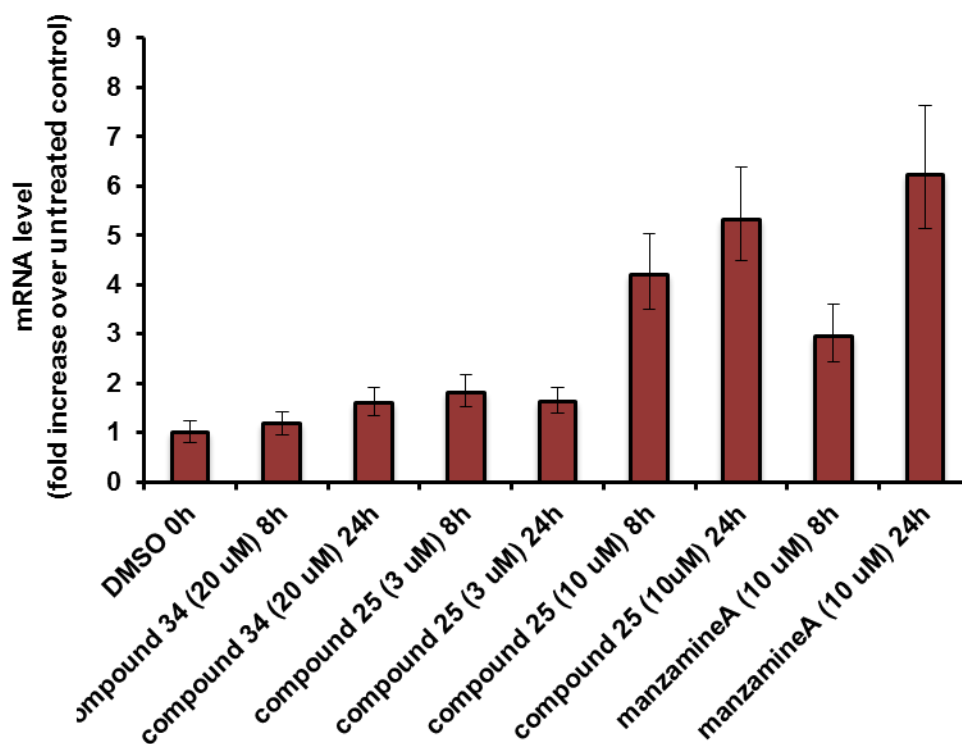


Figure 1.8 a) Western blot analysis of PUMA in H1299 cells treated with DMSO, compound **34** (20 μM) or compound **25** (3, 5 or 10 μM) for 24 h incubation. b) RNA was harvested after 8 and 24 hours after treatment with DMSO, compound **34** (20 μM) or compound **25** (3 or 10 μM). PUMA expression was analyzed by qRT-PCR. Expression was normalized to 18S levels and is reported as fold increase over untreated control.

1.5. Discussion

Inspired by the naturally occurring dimeric β -carboline, neokauluamine, the dimeric β -carboline analogs were prepared and demonstrated interesting biological activities including antimicrobial and anticancer properties. The dimeric compounds **25-27** exhibited comparable potency to the natural products manzamine A and neokauluamine and were significantly more potent than their corresponding monomers. The more rigid molecule (**28**) showed decreased potency compared to the flexible dimeric analogs, suggesting that the activity is dependent on the orientation of the two β -carboline moieties.

Substitutions have shown to affect biological activities of β -carboline compounds.¹ However, in our experiments, the substituents on dimeric β -carboline demonstrated no effect on its cytotoxicity against a human lung cancer cell line (H1299).

The interesting biological activities of dimeric β -carboline (**25**) against various NSCLC cell lines led us to further study its cellular mechanism to induce cell death in H1299 cells. Apoptosis is one of the most common cell death mechanisms. Our study showed that dimeric β -carboline (**25**) significantly induced apoptosis in H1299 cells more efficiently than its monomer. This observation correlated with the increase in levels of caspase-dependent apoptosis markers and the proapoptotic protein, PUMA. These data support our hypothesis that dimeric β -carboline (**25**) induces cell death through caspase-dependent apoptosis mediated by PUMA.

H1299 cells treated with dimeric β -carboline (**25**) showed a dose-dependent increase in PUMA mRNA levels. Although PUMA expression is usually regulated by p53, a transcription factor that is not present in H1299, it is also be controlled by other transcription factors such as p73 and E2F1.³⁵ However, western blot analysis showed no alteration of these proteins, compared to the DMSO control (data not shown). Our data support a mechanism whereby dimeric β -carboline (**25**) may indirectly modulate PUMA expression and thus contribute to cell death.³²

The subcellular co-localization analysis demonstrated that both dimeric (**25**) and monomeric (**34**) β -carboline predominantly localized in lysosomes. This action is similar to many weakly basic agents such as chloroquine, Lys05¹⁶ and manzamine A²⁵, which were reported to target lysosomes causing lysosomal dysfunction and consequently autophagy inhibition. H1299 cells treated with dimeric- β -carboline (**25**) showed a dose-dependent increase in LC3II levels, indicating increased autophagosome accumulation. Many studies have shown that autophagy and apoptosis regulate each other.^{30, 31, 36} In particular, autophagy was reported to regulate apoptosis via modulation of constitutive PUMA expression, which controls the rate of mitochondrial outer membrane permeabilization (MOMP).³² These findings support the hypothesis that dimeric β -carboline (**25**) accumulates in lysosomes and inhibits autophagy, thereby inducing PUMA expression and caspase-dependent apoptosis.

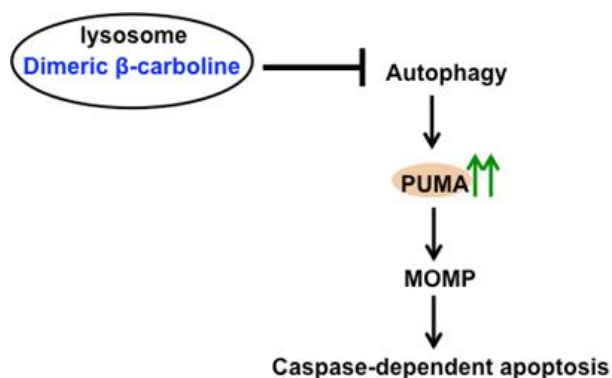


Figure 1.9 Proposed mechanism.

1.6. Conclusions

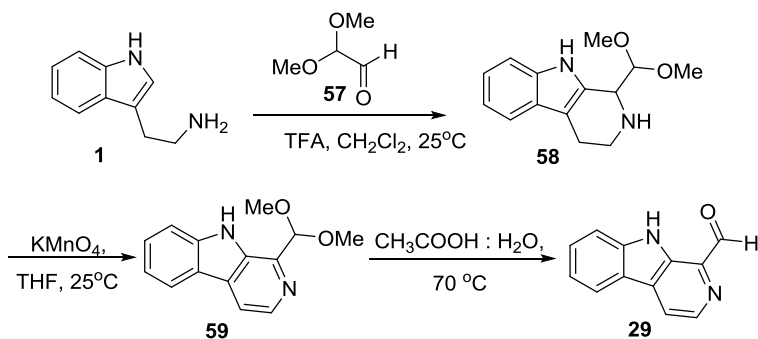
Inspired by the unique structure and interesting biological activities of neo-kauluamine, we have prepared simple dimeric β -carbolines that are significantly more active in both antimicrobial and anticancer activities than the corresponding monomeric ligands. Our results are consistent with the importance of multivalency in biological systems. In particular, dimeric β -carboline (**25**) has been shown to be a potential lead compound for the treatment of NSCLC. Our mechanistic studies suggest that dimeric β -carboline (**25**) targets lysosomes in H1299 cells and mediates caspase-dependent apoptosis through a PUMA induction process. However, the detailed mechanism still remains to be established.

1.7. General method and experimental procedures

1.7.1. General information

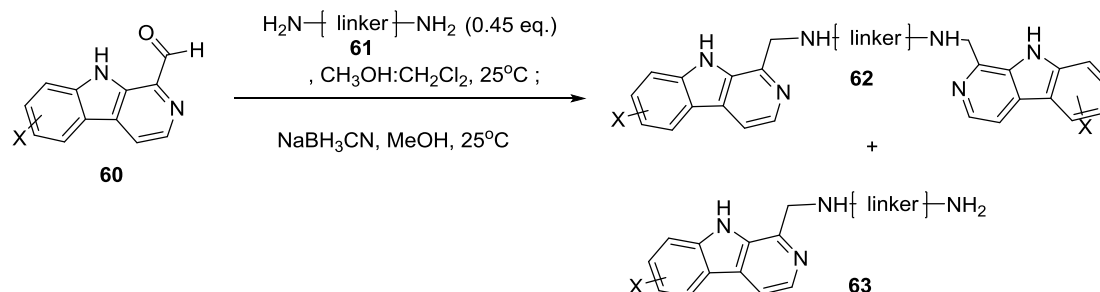
Unless otherwise stated, all reagents were purchased from Sigma Aldrich, Alfa Aesar, Acros Organic or TCI America and used without further purification. Manzamine A and neokauluamine were kindly provided by Professor Hamann at the University of Mississippi. ^1H and ^{13}C NMR spectra were recorded on Bruker AVII500B (500 MHz) and DRX-500 (500 MHz) spectrometers. Chemical shifts are reported relative to the solvent resonance peak δ 7.26 (CDCl_3) for ^1H NMR and δ 77.16 (CDCl_3) for ^{13}C NMR. Infrared spectra were recorded on a NaCl plate using a Perkin-Elmer 1600 series Fourier transform spectrometer. High-resolution mass spectra were obtained by Dr. Rakesh Kohli at the University of Pennsylvania Mass Spectrometry Service Center.

1.7.2. Synthesis of 9H-pyrido [3,4-b]indole-1-carbaldehyde (**29**)



9H-pyrido [3,4-b]indole-1-carbaldehyde (**29**) was prepared by following the previously reported procedure with some modification.¹⁷ Tryptophan (1g, 6.24 mmol, 1 eq.) in CH₂Cl₂ (20 mL) was added to dimethoxyglyoxal (60% solution in water) (1.13 mL, 7.49 mmol, 1.2 eq.) and TFA (1 mL). The mixture was stirred at 25°C for 16 h, then poured into 10% NaHCO₃ (20 mL). The reaction mixture was extracted three times with CH₂Cl₂ (5 mL). The combined organic layer was washed with brine, dried over Na₂SO₄ and concentrated under reduced pressure to yield 1.5 g of dark brown oil. The crude product was oxidized using KMnO₄ (2.96 g, 18.72 mmol, 3 eq.) in THF (70 mL) at 25°C for 20 h, and then filtered through a thin pad of Celite, washed with THF (50 mL) and EtOAc (20 mL). The organic solvent was removed under reduced pressure and the crude product was purified by flash column chromatography on silica gel (30% ethyl acetate/hexane) and gave the corresponding acetal as yellow oil (1.1 g). The acetal was heated with a mixture of acetic acid:water (2:3) at 70°C for 1 h. The reaction was cooled down to 25°C and the solvent was then removed under reduced pressure. The residue was treated with 10% NaHCO₃ (50 mL) then extracted three times with ethyl acetate (15 mL). The crude product was purified by flash column chromatography on silica gel (30% EtOAc/Hexane) and gave the desired aldehyde (587.7 mg, 2.99 mmol, 48% overall yield) as yellow solid. ¹H- and ¹³C NMR were identical to those previously reported.¹⁷

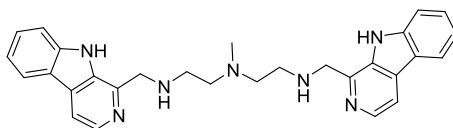
1.7.3. General procedure for the synthesis of dimeric- and monomeric- β - carboline analogs.



A mixture of 9H-pyrido [3,4-b]indole-1-carbaldehyde (**60**) (1 eq.) and diamine (**61**)(0.45 eq.) in a mixed solvent ($\text{CH}_3\text{OH}:\text{CH}_2\text{Cl}_2$ (2:1)) (0.1M) was stirred at 25°C for 16 h. The solvent was evaporated under reduced pressure to give the crude Schiff base, which was used directly in the next step without further purification. The solution of the crude product in anhydrous CH_3OH (0.1 M) was added NaBH_3CN (10 eq.) at 0°C . The mixture was stirred at 25°C for 16h and then concentrated under reduced pressure. The residue was dissolved in CH_2Cl_2 (15 mL) and washed three times with sat. Na_2CO_3 (aq.) (5 mL). The organic layer was dried over anhydrous Na_2SO_4 and concentrated under reduced pressure. The crude product was purified by flash chromatography on silica gel ($\text{NH}_4\text{OH}:\text{CH}_3\text{OH}:\text{CH}_2\text{Cl}_2$, 1:10:90) to give the corresponding dimeric (**62**) and monomeric β - carbolines (**63**).

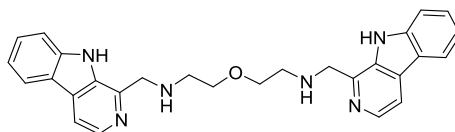
1.7.4. Characterization data for dimeric- and monomeric β -carboline analogs

N1-((9H-pyrido[3,4-b]indol-1-yl)methyl)-N2-(2-(((9H-pyrido[3,4-b]indol-1-yl)methyl)amino)ethyl)-N2-methylethane-1,2-diamine (25)



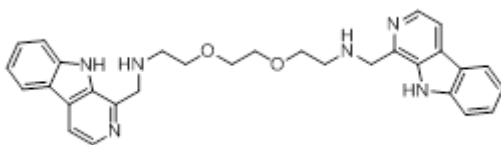
^1H NMR (500 MHz, Chloroform-*d*) δ 10.63 (s, 2H), 8.28 (d, J = 5.2 Hz, 2H), 8.06 (d, J = 7.9 Hz, 2H), 7.79 (d, J = 5.3 Hz, 2H), 7.52 – 7.39 (m, 4H), 7.22 (t, J = 7.4 Hz, 2H), 4.33 (s, 4H), 2.85 (t, J = 5.7 Hz, 4H), 2.59 (t, J = 5.7 Hz, 4H), 2.25 (s, 3H). ^{13}C NMR (126 MHz, Chloroform-*d*) δ 143.37, 140.49, 137.89, 135.04, 129.05, 128.25, 121.73, 121.51, 119.67, 113.83, 111.81, 56.57, 54.28, 46.72, 42.63. FTIR (CHCl_3 film): 3062.41, 2847.38, 1625.7, 1430.92, 1323.89 cm^{-1} . HRMS: $[\text{M}-\text{H}]^-$ calc. 476.2563, found 476.2565.

2,2'-oxybis(N-((9H-pyrido[3,4-b]indol-1-yl)methyl)ethan-1-amine) (26)



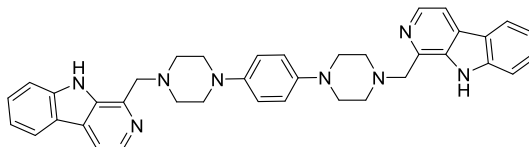
^1H NMR (500 MHz, Chloroform-*d*) δ 10.44 (s, 2H), 8.33 (d, J = 5.3 Hz, 2H), 8.08 (dt, J = 7.9, 1.0 Hz, 2H), 7.82 (d, J = 5.3 Hz, 2H), 7.46 (dddd, J = 14.8, 8.2, 7.0, 1.1 Hz, 4H), 7.22 (ddd, J = 8.0, 6.8, 1.3 Hz, 2H), 4.39 (s, 4H), 3.54 (t, J = 5.2 Hz, 4H), 2.85 (t, J = 5.2 Hz, 4H). ^{13}C NMR (126 MHz, Chloroform-*d*) δ 143.38, 140.34, 137.96, 135.02, 129.03, 128.25, 121.71, 121.44, 119.69, 113.76, 111.74, 70.21, 54.51, 48.88. FTIR (CHCl_3 film): 3223.43, 2892.7, 1626.66, 1431.89, 1324.86, 1123.33 cm^{-1} . HRMS: $[\text{M}+\text{H}]^+$ calc. 465.2403, found 465.2393.

2,2'-(ethane-1,2-diylbis(oxy))bis(N-((9H-pyrido[3,4-b]indol-1-yl)methyl)ethan-1-amine) (**27**)



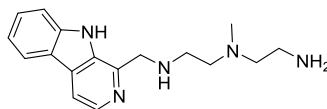
^1H NMR (500 MHz, Chloroform- d) δ 10.26 (s, 2H), 8.29 (d, J = 5.3 Hz, 2H), 8.08 (d, J = 7.9 Hz, 2H), 7.80 (d, J = 5.2 Hz, 2H), 7.49 (dd, J = 6.2, 1.4 Hz, 4H), 7.23 (ddd, J = 8.0, 6.0, 2.1 Hz, 2H), 4.35 (s, 4H), 3.66 (t, J = 4.9 Hz, 4H), 2.87 (t, J = 4.9 Hz, 4H), 2.60 (m, 4H). ^{13}C NMR (126 MHz, Chloroform- d) δ 143.59, 138.10, 135.10, 129.00, 128.19, 121.77, 121.55, 119.68, 113.69, 111.85, 70.45, 54.90, 48.86, 46.40. FTIR (CHCl_3 film): 3151.11, 2886.91, 1625.7, 1430.92, 1240.97, 1124.3 cm^{-1} . HRMS: $[\text{M}+\text{H}]^+$ calc. 509.2665, found 509.2662. $[\text{M}+\text{Na}]^+$ calc. 531.2484, found, 531.2483.

1,4-bis(4-((9H-pyrido[3,4-b]indol-1-yl)methyl)piperazin-1-yl)benzene (**28**)



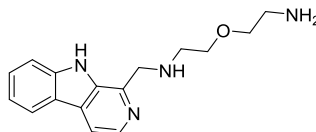
^1H NMR (500 MHz, Chloroform- d) δ 9.94 (s, 2H), 8.37 (d, J = 5.3 Hz, 2H), 8.14 (d, J = 7.8 Hz, 2H), 7.89 (d, J = 5.3 Hz, 2H), 7.58 – 7.50 (m, 4H), 7.29 (ddd, J = 8.0, 6.6, 1.4 Hz, 2H), 6.93 (s, 4H), 4.21 (s, 4H), 3.21 (t, J = 4.9 Hz, 8H), 2.80 (t, J = 4.8 Hz, 8H). ^{13}C NMR (126 MHz, Chloroform- d) δ 145.37, 140.06, 138.53, 134.93, 129.05, 128.47, 121.89, 121.65, 120.01, 117.80, 114.01, 111.84, 64.52, 53.74, 50.64. FTIR (CHCl_3 film): 3626.48, 3355.53, 2814.6, 1626.66, 1514.81, 1428.99 cm^{-1} . HRMS: $[\text{M}+\text{H}]^+$ calc. 607.3298, found 607.3302.

N1-((9H-pyrido[3,4-b]indol-1-yl)methyl)-N2-(2-aminoethyl)-N2-methylethane-1,2-diamine (34)



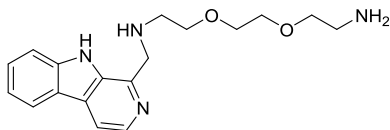
^1H NMR (500 MHz, Chloroform-*d*) δ 8.16 (dd, $J = 5.3, 1.1$ Hz, 1H), 8.01 (d, $J = 7.9$ Hz, 1H), 7.81 (d, $J = 5.3$ Hz, 1H), 7.53 – 7.41 (m, 2H), 7.16 (t, $J = 7.4$ Hz, 1H), 4.21 (s, 2H), 2.74 (t, $J = 5.8$ Hz, 2H), 2.65 (t, $J = 5.7$ Hz, 2H), 2.44 (q, $J = 5.5$ Hz, 4H), 2.11 – 2.03 (m, 3H). ^{13}C NMR (126 MHz, Chloroform-*d*) δ 140.60, 137.90, 135.22, 129.00, 128.19, 121.77, 121.54, 119.55, 113.77, 111.85, 56.94, 54.52, 46.64, 42.52, 39.48. FTIR (CHCl₃ film): 3061.52, 2857.39, 1624.7, 1321.54 cm⁻¹. HRMS: [M+H]⁺ calc. 298.2032, found 298.2035.

N-((9H-pyrido[3,4-b]indol-1-yl)methyl)-2-(2-aminoethoxy)ethan-1-amine (35)



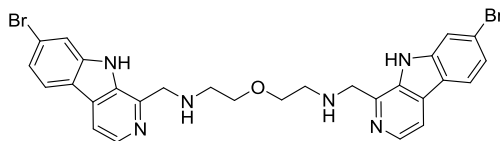
^1H NMR (500 MHz, Chloroform-*d*) δ 10.54 (s, 1H), 8.32 (d, $J = 5.3$ Hz, 1H), 8.10 (d, $J = 7.9$ Hz, 1H), 7.84 (d, $J = 5.3$ Hz, 1H), 7.56 – 7.47 (m, 2H), 7.27 – 7.21 (m, 1H), 4.41 (s, 2H), 3.58 (d, $J = 4.5$ Hz, 2H), 3.48 (t, $J = 5.2$ Hz, 2H), 2.87 (dt, $J = 7.0, 4.9$ Hz, 4H). ^{13}C NMR (126 MHz, Chloroform-*d*) δ 143.44, 140.43, 138.02, 135.09, 129.03, 128.25, 121.73, 121.48, 119.67, 113.74, 111.85, 72.76, 70.17, 54.58, 48.93, 41.69. FTIR (CHCl₃ film): 3158.83, 1626.66, 1567.84, 1324.86, 1121.4 cm⁻¹. HRMS: [M+H]⁺ calc. 285.1715, found 285.1714.

N-((9*H*-pyrido[3,4-*b*]indol-1-yl)methyl)-2-(2-(2-aminoethoxy)ethoxy)ethan-1-amine (**36**)



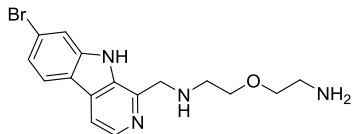
^1H NMR (500 MHz, Chloroform-*d*) δ 10.50 (s, 1H), 8.32 (d, *J* = 5.3 Hz, 1H), 8.11 (d, *J* = 7.9 Hz, 1H), 7.85 (d, *J* = 5.2 Hz, 1H), 7.56 – 7.49 (m, 2H), 7.27 – 7.21 (m, 1H), 4.42 (s, 2H), 3.70 – 3.61 (m, 6H), 3.51 (t, *J* = 5.2 Hz, 2H), 2.91 (t, *J* = 6.2, 4.9 Hz, 2H), 2.84 (t, *J* = 5.2 Hz, 2H). ^{13}C NMR (126 MHz, Chloroform-*d*) δ 143.68, 140.46, 138.07, 135.13, 128.99, 128.16, 121.73, 121.54, 119.63, 113.68, 111.90, 73.29, 70.64, 70.39, 70.35, 54.79, 48.87, 41.73. FTIR (CHCl₃ film): 2919.7, 1625.7, 1566.88, 1455.99, 1122.37 cm⁻¹. HRMS: [M+H]⁺ calc. 329.1978, found 329.1981. [M-H]⁻ calc. 327.1821, found 327.1824. [M+Na]⁺ calc. 351.1797, found 351.1786.

2,2'-oxybis(*N*-((7-bromo-9*H*-pyrido[3,4-*b*]indol-1-yl)methyl)ethan-1-amine) (**44**)



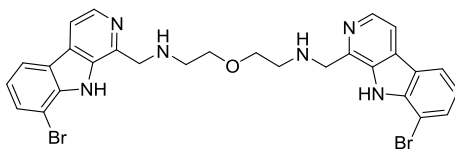
^1H NMR (500 MHz, Chloroform-*d*) δ 10.65 (s, 2H), 8.30 (d, *J* = 5.3 Hz, 2H), 7.84 (d, *J* = 8.3 Hz, 2H), 7.73 (d, *J* = 5.3 Hz, 2H), 7.51 (d, *J* = 1.6 Hz, 2H), 7.28 (dd, *J* = 8.4, 1.6 Hz, 2H), 4.36 (s, 4H), 3.52 (t, *J* = 4.9 Hz, 4H), 2.84 (t, *J* = 4.9 Hz, 4H). ^{13}C NMR (126 MHz, Chloroform-*d*) δ 143.31, 141.03, 138.39, 135.02, 128.55, 123.02, 122.79, 121.91, 120.30, 114.76, 113.71, 70.09, 54.04, 48.90. FTIR (CHCl₃ film): 2854.13, 1622.8, 1568.81, 1420.32, 1317.14 cm⁻¹. HRMS: [M+H]⁺ calc. 621.0613, found 621.0608.

2-(2-aminoethoxy)-N-((7-bromo-9H-pyrido[3,4-b]indol-1-yl)methyl)ethan-1-amine (45)



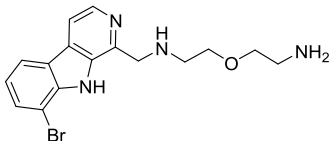
^1H NMR (500 MHz, Chloroform- d) δ 8.31 (d, J = 5.3 Hz, 1H), 7.90 (d, J = 8.4 Hz, 1H), 7.77 (d, J = 5.3 Hz, 1H), 7.73 (d, J = 1.7 Hz, 1H), 7.32 (dd, J = 8.4, 1.7 Hz, 1H), 4.40 (s, 2H), 3.52 (t, J = 4.6, 2.9 Hz, 2H), 3.46 (dd, J = 6.2, 3.8 Hz, 2H), 2.88 – 2.80 (m, 4H). ^{13}C NMR (126 MHz, Chloroform- d) δ 143.17, 141.37, 138.39, 135.05, 128.59, 123.05, 122.78, 121.98, 120.33, 115.10, 113.75, 71.29, 69.84, 53.37, 48.70, 41.06. FTIR (CHCl_3 film): 2856.06, 1621.84, 1567.84, 1420.32, 1319.07 cm^{-1} . HRMS: $[\text{M}+\text{H}]^+$ calc. 363.0820, found 363.0819.

2,2'-oxybis(N-((8-bromo-9H-pyrido[3,4-b]indol-1-yl)methyl)ethan-1-amine) (46)



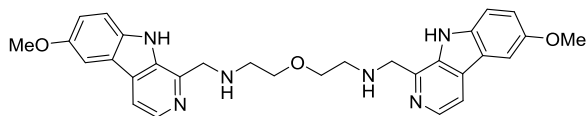
^1H NMR (500 MHz, Chloroform- d) δ 10.33 (s, 2H), 8.34 (d, J = 5.3 Hz, 2H), 8.10 (dd, J = 7.9, 1.0 Hz, 2H), 7.85 (d, J = 5.3 Hz, 2H), 7.54 – 7.45 (m, 4H), 7.26 – 7.22 (m, 2H), 4.43 (s, 4H), 3.58 (t, J = 4.9 Hz, 4H), 2.88 (t, J = 4.9 Hz, 4H). ^{13}C NMR (126 MHz, Chloroform- d) δ 143.42, 140.29, 138.13, 135.09, 129.06, 128.33, 121.80, 121.50, 119.78, 113.82, 111.80, 70.26, 54.85, 48.96. FTIR (CHCl_3 film): 3062.41, 1625.7, 1565.92, 1430.92 cm^{-1} . HRMS: $[\text{M}+\text{H}]^+$ calc. 621.0613, found 621.0612.

2-(2-aminoethoxy)-N-((8-bromo-9H-pyrido[3,4-b]indol-1-yl)methyl)ethan-1-amine (47)



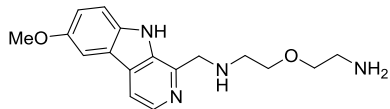
^1H NMR (500 MHz, Chloroform- d) δ 10.84 (s, 1H), 8.32 (d, J = 5.3 Hz, 1H), 8.10 (dt, J = 7.9, 1.0 Hz, 1H), 7.85 (d, J = 5.3 Hz, 1H), 7.60 (dt, J = 8.2, 0.9 Hz, 1H), 7.51 (ddd, J = 8.2, 7.0, 1.2 Hz, 1H), 7.26 – 7.22 (m, 1H), 4.44 (s, 2H), 3.52 (t, J = 4.8 Hz, 2H), 3.45 (t, J = 5.0 Hz, 2H), 2.84 (dt, J = 11.7, 5.0 Hz, 4H). ^{13}C NMR (126 MHz, Chloroform- d) δ 142.72, 140.66, 137.98, 135.03, 129.17, 128.40, 121.69, 121.42, 119.75, 113.95, 112.17, 71.44, 69.76, 53.57, 48.71, 41.16. FTIR (CHCl_3 film): 3369.03, 2917.77, 1627.63, 1563.99, 1430.92 cm^{-1} . HRMS: $[\text{M}+\text{H}]^+$ calc. 363.0820, found 363.0819.

2,2'-oxybis(N-((6-methoxy-9H-pyrido[3,4-b]indol-1-yl)methyl)ethan-1-amine) (48)



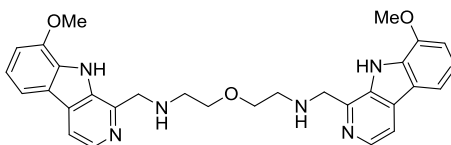
^1H NMR (500 MHz, Chloroform- d) δ 11.29 (s, 2H), 8.30 (d, J = 5.3 Hz, 2H), 7.80 (d, J = 5.2 Hz, 2H), 7.51 – 7.44 (m, 4H), 7.13 (dd, J = 8.8, 2.5 Hz, 2H), 4.36 (s, 4H), 3.90 (d, J = 1.5 Hz, 6H), 3.16 (t, J = 4.6 Hz, 4H), 2.56 (t, J = 4.7 Hz, 4H). ^{13}C NMR (126 MHz, Chloroform- d) δ 154.07, 141.72, 137.20, 135.95, 135.65, 129.12, 121.55, 118.72, 114.20, 113.15, 103.36, 68.82, 56.08, 52.19, 48.42. FTIR (CHCl_3 film): 3136.65, 1567.84, 1496.49, 1290.14, 1214.93 cm^{-1} . HRMS: $[\text{M}-\text{H}]^-$ calc. 523.2458, found 523.2449.

2-(2-aminoethoxy)-N-((6-methoxy-9H-pyrido[3,4-b]indol-1-yl)methyl)ethan-1-amine (49)



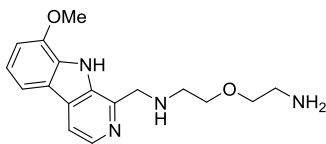
^1H NMR (500 MHz, Chloroform- d) δ 10.90 (s, 1H), 8.26 (d, J = 5.2 Hz, 1H), 7.77 (d, J = 5.4 Hz, 1H), 7.49 (dd, J = 5.7, 3.1 Hz, 2H), 7.14 (dd, J = 8.9, 2.5 Hz, 1H), 4.37 (s, 2H), 3.89 (s, 3H), 3.44 (dd, J = 6.5, 3.2 Hz, 2H), 3.38 (t, J = 5.0 Hz, 2H), 2.82 – 2.72 (m, 4H). ^{13}C NMR (126 MHz, Chloroform- d) δ 154.04, 143.12, 137.39, 135.80, 135.62, 128.92, 121.69, 118.54, 113.85, 113.10, 103.42, 71.18, 69.83, 56.16, 53.39, 48.79, 41.02. FTIR (CHCl_3 film): 2939.95, 1566.88, 1496.49, 1290.14, 1214.93 cm^{-1} . HRMS: $[\text{M}+\text{H}]^+$ calc. 315.1821, found 315.1815.

2,2'-oxybis(N-((8-methoxy-9H-pyrido[3,4-b]indol-1-yl)methyl)ethan-1-amine) (50)



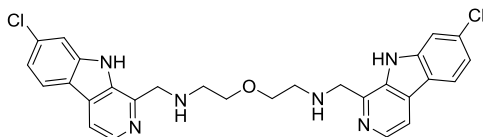
^1H NMR (500 MHz, Chloroform- d) δ 10.25 (s, 2H), 8.28 (d, J = 5.3 Hz, 2H), 7.76 (d, J = 5.3 Hz, 2H), 7.63 (dd, J = 7.9, 0.9 Hz, 2H), 7.12 (t, J = 7.9 Hz, 2H), 6.89 (dd, J = 7.9, 0.8 Hz, 2H), 4.41 (s, 4H), 3.93 (s, 6H), 3.63 (t, J = 4.4 Hz, 4H), 2.89 (t, J = 5.0 Hz, 4H). ^{13}C NMR (126 MHz, Chloroform- d) δ 146.33, 143.76, 137.94, 134.66, 130.77, 129.10, 122.46, 120.10, 113.94, 113.81, 107.56, 70.26, 55.55, 54.67, 48.78. FTIR (CHCl_3 film): 3065.3, 2836.77, 1631.48, 1578.45, 1480.1, 1428.99, 1260.25 cm^{-1} . HRMS: $[\text{M}+\text{H}]^+$ calc. 525.2614, found 525.2611.

2-(2-aminoethoxy)-N-((8-methoxy-9H-pyrido[3,4-b]indol-1-yl)methyl)ethan-1-amine (51)



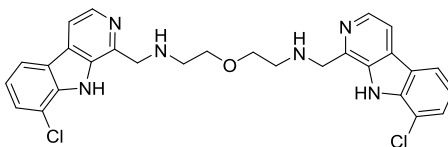
^1H NMR (500 MHz, Chloroform-d) δ 8.28 (dd, $J = 5.3, 1.3$ Hz, 1H), 7.78 (d, $J = 5.1$ Hz, 1H), 7.65 (dd, $J = 8.1, 2.1$ Hz, 1H), 7.15 (tt, $J = 7.8, 1.6$ Hz, 1H), 6.93 (d, $J = 7.7$ Hz, 1H), 4.47 (s, 2H), 3.97 (d, $J = 1.3$ Hz, 3H), 3.59 (t, $J = 4.7$ Hz, 2H), 3.55 (t, $J = 4.9$ Hz, 2H), 2.95 (t, $J = 5.0$ Hz, 2H), 2.87 (t, $J = 4.7$ Hz, 2H). ^{13}C NMR (126 MHz, Chloroform-d) δ 142.83, 137.84, 120.25, 114.16, 113.83, 107.82, 70.77, 69.80, 55.71, 48.32, 40.99, 32.75. FTIR (CHCl_3 film): 2933.2, 1577.49, 1508.06, 1428.99, 1326.79, 1261.22 cm^{-1} . HRMS: $[\text{M}+\text{H}]^+$ calc. 315.1821, found 315.1821.

2,2'-oxybis(N-((7-chloro-9H-pyrido[3,4-b]indol-1-yl)methyl)ethan-1-amine) (52)



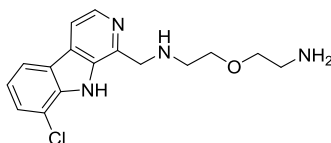
^1H NMR (500 MHz, Chloroform-d) δ 10.75 (s, 1H), 8.32 (d, $J = 5.4$ Hz, 1H), 7.94 (d, $J = 8.3$ Hz, 1H), 7.76 (d, $J = 5.3$ Hz, 1H), 7.42 (d, $J = 1.8$ Hz, 1H), 7.17 (dd, $J = 8.4, 1.9$ Hz, 1H), 4.38 (s, 2H), 3.53 – 3.45 (m, 2H), 2.86 – 2.78 (m, 2H). ^{13}C NMR (126 MHz, Chloroform-d) δ 143.11, 140.85, 138.46, 135.29, 134.03, 128.62, 122.58, 120.49, 120.00, 113.77, 111.84, 69.90, 53.97, 48.83. FTIR (CHCl_3 film): 3142.44, 1625.7, 1425.14 cm^{-1} . HRMS: $[\text{M}-\text{H}]^-$ calc. 531.1467, found 531.1418.

2,2'-oxybis(*N*-((8-chloro-9*H*-pyrido[3,4-*b*]indol-1-yl)methyl)ethan-1-amine) (**53**)



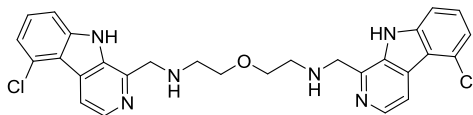
¹H NMR (500 MHz, Chloroform-*d*) δ 10.47 (s, 2H), 8.31 (d, *J* = 5.3 Hz, 2H), 7.93 (d, *J* = 7.8 Hz, 2H), 7.75 (d, *J* = 5.3 Hz, 2H), 7.47 (d, *J* = 7.6 Hz, 2H), 7.15 (t, *J* = 7.8 Hz, 2H), 4.44 (s, 4H), 3.66 (t, *J* = 4.9 Hz, 4H), 2.91 (t, *J* = 5.0 Hz, 4H). ¹³C NMR (126 MHz, Chloroform-*d*) δ 143.76, 138.69, 137.54, 134.82, 129.23, 127.41, 123.01, 120.42, 120.13, 117.21, 113.95, 70.34, 54.71, 48.96. FTIR (CHCl₃ film): 2861.84, 1625.7, 1566.88, 1427.07, 1304.61 cm⁻¹. HRMS: [M+H]⁺ calc. 533.1623, found 533.1632.

2-(2-aminoethoxy)-*N*-((8-chloro-9*H*-pyrido[3,4-*b*]indol-1-yl)methyl)ethan-1-amine (**54**)



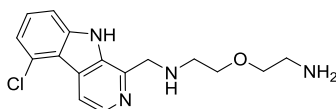
¹H NMR (500 MHz, Chloroform-*d*) δ 8.33 (d, *J* = 5.3 Hz, 1H), 7.96 (dd, *J* = 7.8, 1.0 Hz, 1H), 7.78 (d, *J* = 5.3 Hz, 1H), 7.49 (dd, *J* = 7.8, 0.9 Hz, 1H), 7.16 (t, *J* = 7.8 Hz, 1H), 4.44 (s, 2H), 3.62 (dd, *J* = 5.5, 4.5 Hz, 2H), 3.49 (t, *J* = 5.2 Hz, 2H), 2.87 (t, *J* = 5.1 Hz, 4H). ¹³C NMR (126 MHz, Chloroform-*d*) δ 144.29, 138.79, 137.57, 134.90, 129.19, 127.42, 123.10, 120.43, 120.25, 117.20, 113.95, 73.22, 70.44, 55.03, 49.04, 41.86. FTIR (CHCl₃ film): 2871.49, 1625.7, 1558.2, 1496.49, 1428.99, 1317.14 cm⁻¹. HRMS: [M+H]⁺ calc. 319.1326, found 319.1319.

2,2'-oxybis(N-((5-chloro-9H-pyrido[3,4-b]indol-1-yl)methyl)ethan-1-amine) (55)



^1H NMR (500 MHz, Chloroform- d) δ 10.70 (s, 2H), 8.35 (d, J = 5.4 Hz, 2H), 8.25 (d, J = 5.4 Hz, 2H), 7.38 – 7.28 (m, 4H), 7.18 (dd, J = 7.5, 1.0 Hz, 2H), 4.39 (s, 4H), 3.53 (t, J = 4.9 Hz, 4H), 2.84 (t, J = 4.8 Hz, 4H). ^{13}C NMR (126 MHz, Chloroform- d) δ 143.09, 141.24, 138.35, 134.90, 130.02, 128.51, 127.97, 120.38, 119.15, 116.00, 110.12, 70.10, 54.44, 48.88. FTIR (CHCl_3 film): 2866.67, 1620.88, 1560.13, 1420.32 cm^{-1} . HRMS: $[\text{M}-\text{H}]^-$ calc. 531.1467, found 531.1476.

2-(2-aminoethoxy)-N-((5-chloro-9H-pyrido[3,4-b]indol-1-yl)methyl)ethan-1-amine (56)



^1H NMR (500 MHz, Chloroform- d) δ 10.83 (s, 1H), 8.36 (d, J = 5.4 Hz, 1H), 8.28 (d, J = 5.4 Hz, 1H), 7.47 – 7.37 (m, 2H), 7.21 (dd, J = 7.2, 1.2 Hz, 1H), 4.42 (s, 2H), 3.58 (dd, J = 5.5, 4.3 Hz, 2H), 3.51 – 3.44 (m, 2H), 2.87 (td, J = 5.2, 2.3 Hz, 4H). ^{13}C NMR (126 MHz, Chloroform- d) δ 143.41, 141.35, 138.42, 134.97, 130.00, 128.46, 127.91, 120.29, 119.20, 115.89, 110.28, 72.79, 70.12, 54.62, 48.92, 41.70. FTIR (CHCl_3 film): 2869.56, 1620.88, 1563.99, 1421.28, 1321 cm^{-1} . HRMS: $[\text{M}-\text{H}]^-$ calc. 317.1169, found 317.1158.

1.7.5. Biological evaluations

Cell culture: H1299 cells were cultured and maintained in DMEM medium with 10% fetal bovine serum (FBS) and 1% penicillin/streptomycin. A549, H441, H1373, H1993 and H2009 were kindly provided by Professor Lewis Cantley's lab, Weill Cornell Medical College, Cornell University. These cell lines were maintained in PRMI medium with 10% fetal bovine serum (FBS) and 1% penicillin/streptomycin. All cell lines were maintained in standard tissue culture incubators at 37°C and 5% CO_2 .

Cell viability assay: For cell viability assays, Cells were plated in 96-well plates (5000cells/well) in triplicate and cultured overnight before treating with compound **25**, **34** or manzamine A for 48h. Cells were then incubated with Alamar blue (Life Technologies, DAL1025) for 2 h at 37°C and viability was read out according to manufacturer's protocol on a SynergyHT plate reader (BioTek), Fluorescence intensity was determined at ex/em: 545/600. Percent viability was calculated and normalized to a no treatment control. Data analysis (including logarithmic transformation, graphical analysis, and IC₅₀ calculation) was conducted using Prism (GraphPad) software.

Western blot analysis: For western blot analysis, cells were treated with indicated compounds at indicated concentrations for 24h and lysed in RIPA buffer containing protease/phosphatase inhibitors. 50 µg of protein lysate was loaded in each lane and separated by Novex™ 10% Tris-Glycine Mini Denaturing Protein Gel (Invitrogen) using MES buffer. Proteins were next transferred onto a polyvinylidene fluoride (PVDF) membrane (Millipore, USA) and blocked in 5% milk made in TBS-Tween buffer for 1h at 25°C. Membranes were next incubated with the indicated primary antibodies at 4°C overnight. Membranes were then washed sequentially three times (10 mins interval) with TBS-Tween buffer before incubating with the corresponding HRP secondary antibodies at 25°C for 1h. After, secondary antibody incubation, membranes were then washed again three times with TBS-Tween buffer before analyzing using chemiluminescence with ECL.

LC3 immunofluorescence analysis: H1299 were transfected with GFP-LC3 using Lipofectamine® 3000 Reagent (Invitrogen) according to the manufacturer's protocol and incubated at 37°C for 24h. The medium was replaced before treatments with DMSO, compound **34** (20 µM), compound **25** (3, 5 and 10 µM) or manzamine A (10 µM) for 24h. Cells were then washed with PBS, fixed with freshly prepared 4% paraformaldehyde in PBS buffer for 10 min at 37°C and mounted onto slides in medium containing DAPI (Prolong Gold Antifade, Molecular Probes,

Eugene) and analyzed by confocal microscopy. Thirty cells per treatment were scored for GFP-puncta using ImageJ software.

Quantitative real-time PCR: H1299 cells were treated with DMSO, compound **25** and **34** at the indicated concentrations for 24 h. Cells were lysed using QIAshredder columns. Total RNA was isolated using RNeasy Mini Kit (Qiagen) and on-column DNase digestions (Qiagen) following the manufacturer's protocol. Equal amounts of RNA from these samples were then used to make cDNA using a High Capacity Reverse Transcription Kit (Applied Biosciences, 4368814). Quantitative PCR (qPCR) was performed using Brilliant III UltraFast SYBR Green QPCR Mix kits (Agilent Technologies) on a Stratagene Mx3005P device (Agilent Technologies). Data analysis of fold changes in gene transcription levels was done using the MxPro program (Stratagene). RNA expression levels were normalized to the housekeeping gene 18S. Primer sequences used are human PUMA; Forward: 5'-ACCTCAACGCACAGTACGAG-3', Reverse: 5'-CCCATGATGAGATTGTACAGGA-3'.

Confocal microscopy: H1299 cells were plated on Poly-L-Lysine-coated slips and cultured for 24h, then treated with DMSO, compound **25** or compound **34** at the indicated concentrations. After 24 h, cells were washed in PBS and fixed with 4% paraformaldehyde in PBS at room temperature for 15 min, followed by permeabilization in 0.25% Triton-X-100 for 15 mins. Cells were next blocked with 10% normal goat serum (NGS) for 1h. The cells then were incubated with a rabbit polyclonal antibody against cleaved caspase 3 for 2h at room temperature. The cover slips then were washed three times with PBS before incubation with a secondary antibody using the same procedure as for the primary antibody. The cover slips were then mounted on slides with mounting media (VECTASHIELD Antifade Mounting Medium, Vector Laboratories) and were examined with confocal microscopy.

Guava Nexin Assay: H1299 cells were treated with DMSO, compound **25** or compound **34** at the indicated concentrations for 48h and performed the assay according to the manufacture's protocol.

Live image analysis: H1299 cells were treated with DMSO and the β -carboline compounds for for 1h. The culture medium was removed. The cells were stained with MitoTracker® Green FM (Invitrogen) and LysoTracker® Red DND-99 (Invitrogen) according to the manufacture's protocol and analyzed using confocal microscope.

CHAPTER 2. MODEL STUDY FOR THE DIMERIZATION OF MANZAMINE A TOWARD NEOKAULUAMINE

2.1. Introduction

Neokauluamine is a marine β -carboline alkaloid isolated from an Indo-Pacific sponge (family *Petrosiidae*, order *Haplosclerida*) in 2001 by Hamann *et.al.*¹⁰ Its complex structure was elucidated as a dimeric form of manzamine A, the first isolated manzamine alkaloid.⁶ Neokauluamine exhibited interesting antimalarial and anticancer activities. However, because of the limited supply (**Table 2.1**) and the complex structure of neokauluamine, its stereochemistry was not completely assigned and its biological activity was not widely studied. Manzamine A is more relatively abundant in Nature compared to other manzamine alkaloids. We therefore elected to study the use of manzamine A as a starting material for the total synthesis of neokauluamine.

2.2. Total synthesis and structural modification of manzamine A

Manzamine A was isolated from an Okinawa sponge in 1986 by Higa *et.al.* as a hydrochloric salt.⁶ Its X-ray crystal structure (**Figure 2.1**) showed that it possessed a β -carboline moiety attached to the pentacyclic core comprising two six-membered rings, as well as 5-, 13- and 8- membered rings. The total synthesis and structural modifications of manzamine A have been reported and provide precedent for the synthetic methods that could be employed for the dimerization of manzamine A to neokauluamine.

The lipophilic extract contents from Indo-Pacific sponge (family *Petrosiidae*, order *Haplosclerida*).¹⁰

Manzamine A	0.66%
Manzamine E	0.003%
Manzamine J	0.0017%
Ircinal A	0.008%
6-deoxymanzamine X	0.0021%
<i>ent</i> -8-hydroxymanzamine A	1.24%
<i>ent</i> -manzamine F	0.055%
neokauluamine	0.0048%

Table 2.1 Relative natural abundance of neokauluamine compared to other manzamine alkaloids.

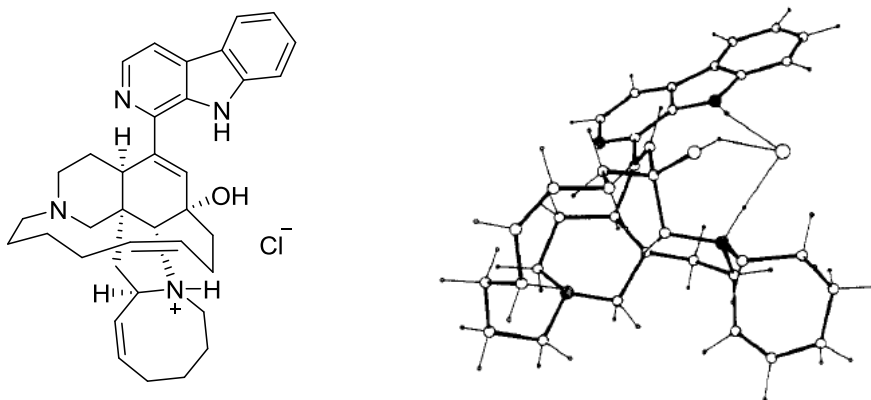
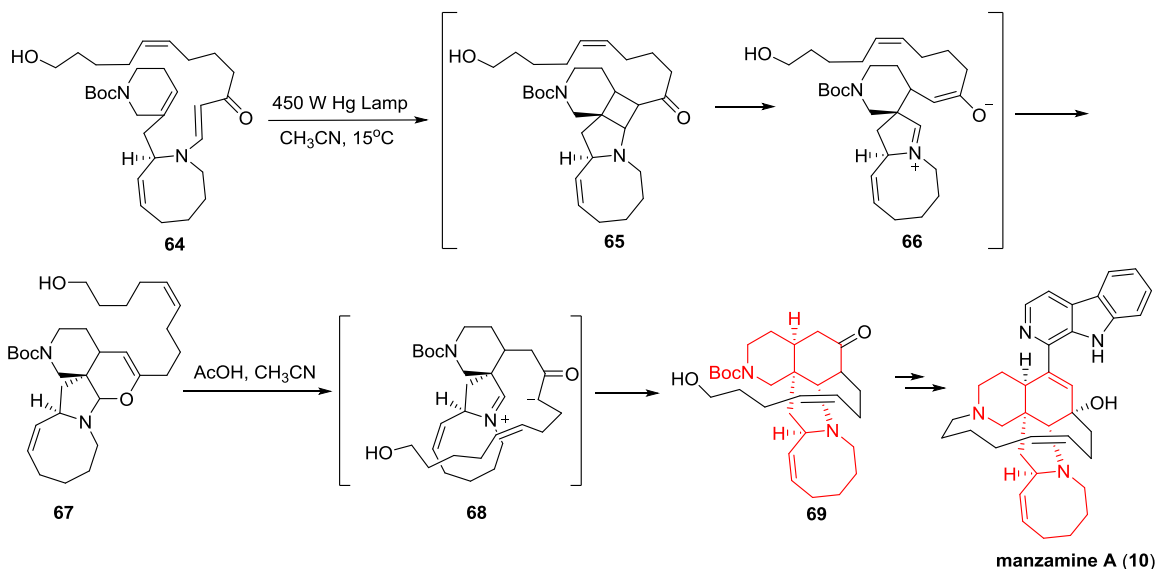


Figure2. 1 X-ray crystal structure of manzamine A hydrochloride.

2.2.1. Total synthesis of manzamine A

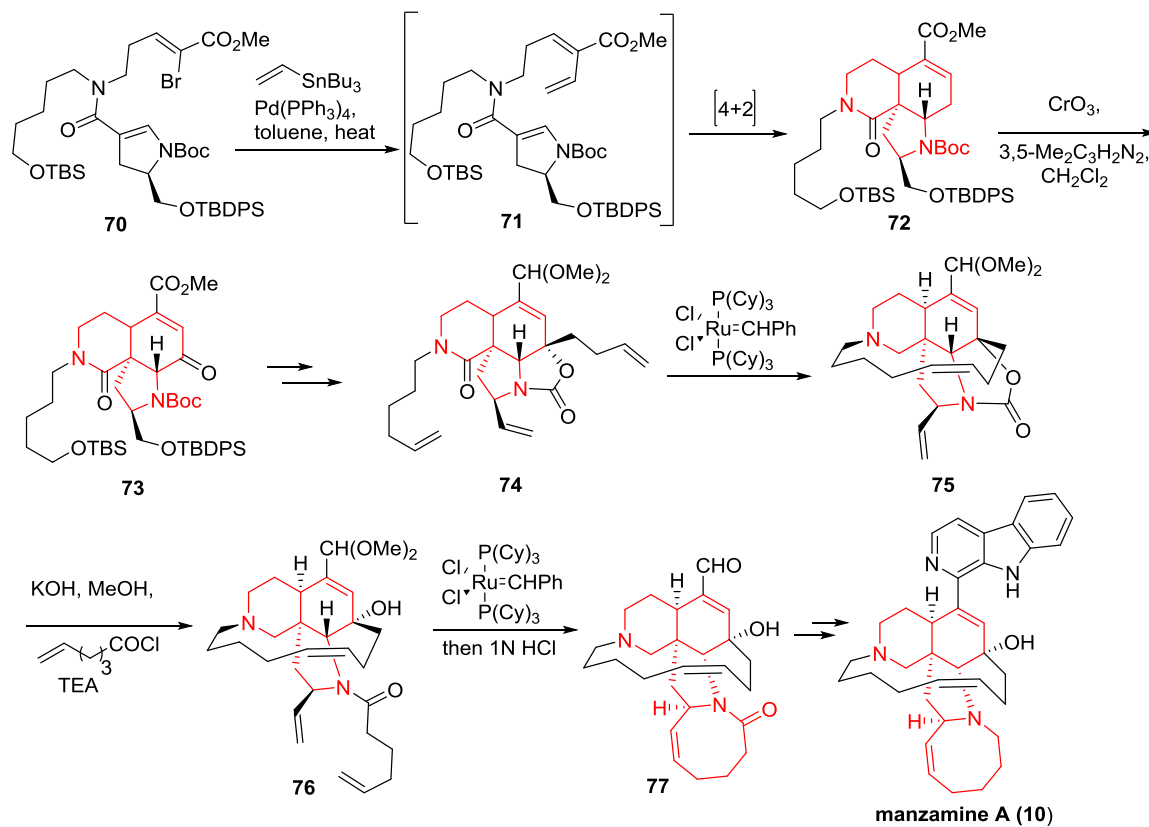
Manzamine A has attracted much interest as a complex target for total synthesis.^{7,8,9} Since the first total synthesis by our group⁹ in 1998 until now, multiple synthetic approaches toward manzamine A have been reported. The following are highlights for the successfully enantioselective total synthesis of manzamine A.

The first total synthesis of manzamine A was reported by our group in 1998, shown in **Scheme 2.1**.⁹ The key step involved a stereoselective intramolecular photoaddition of the vinylogous amide **64**, followed by retro-Mannich fragmentation and Mannich ring closure, respectively, to form the tetracyclic system (labeled in red) in **69**. Steps were then performed to complete the synthesis of manzamine A in 31 total steps.



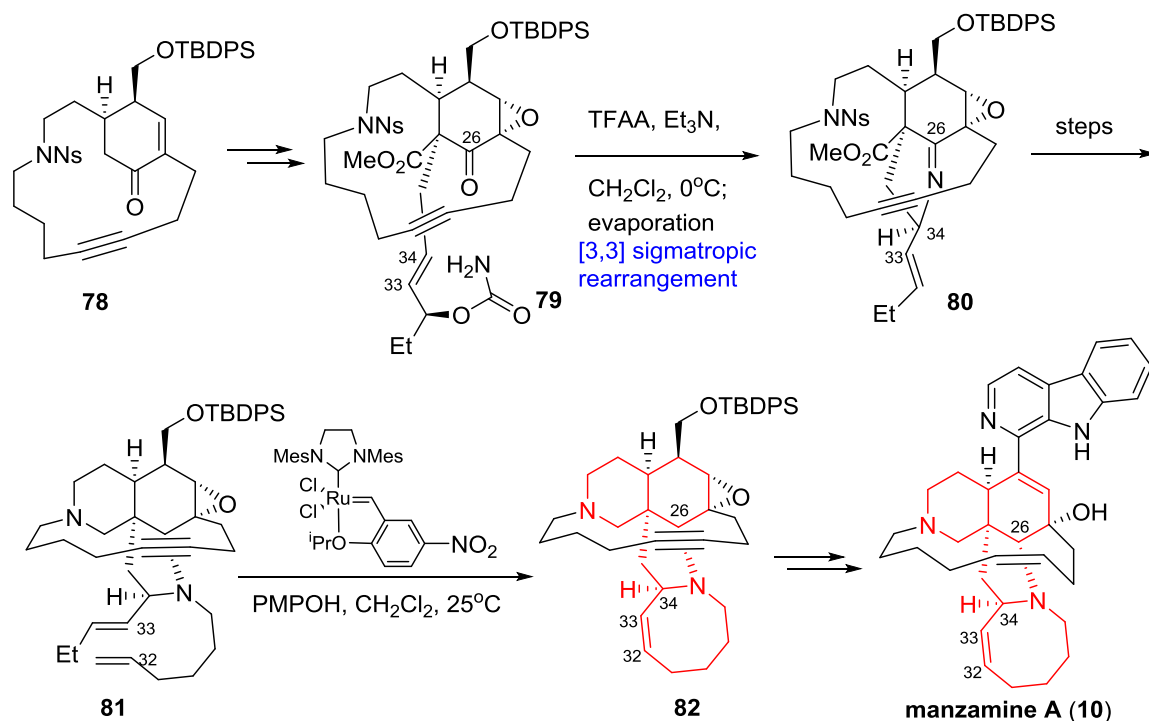
Scheme 2. 1 Key steps for the first total synthesis of manzamine A reported by Winkler *et.al*.

In 2002, Martin *et al.* (**Scheme 2.2**) reported a stereoselective total synthesis of manzamine A (23 steps).³⁷ The tricyclic ring system in **72** was constructed *via* the intramolecular Diels-Alder reaction of the vinylogous amide **71**. Two ring closing metathesis were later used to form the 13-membered ring in **75** and the 8-membered ring in **77**, respectively.



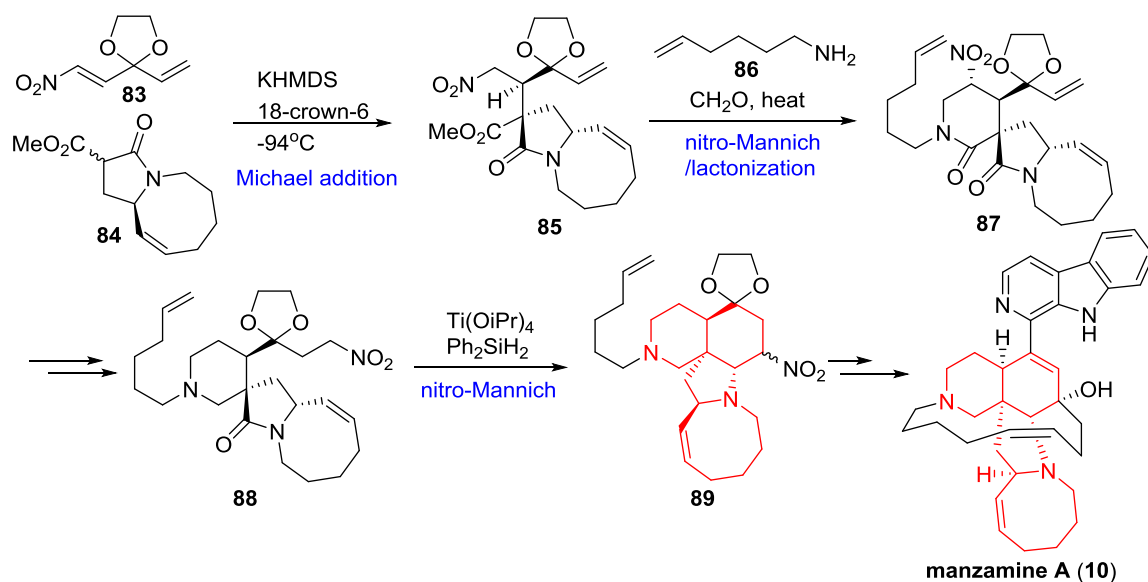
Scheme 2.2 Key steps for the total synthesis of manzamine A by Martin *et al.*

Fukuyama *et.al.* reported the synthesis of manzamine A (29 steps) involving the highly strained 15-membered ring precursor **78**.⁷ [3, 3]-sigmatropic rearrangement of the allyl cyanate **79** was performed to stereoselectively introduce the nitrogen functionality at the sterically hindered C-34 position in **80**. Similarly to Martin's approach, the 8-membered ring in **82** was formed by ring closing metathesis of the diene **81**.



Scheme 2. 3 Key steps for the total synthesis of manzamine A by Fukuyama *et.al.*

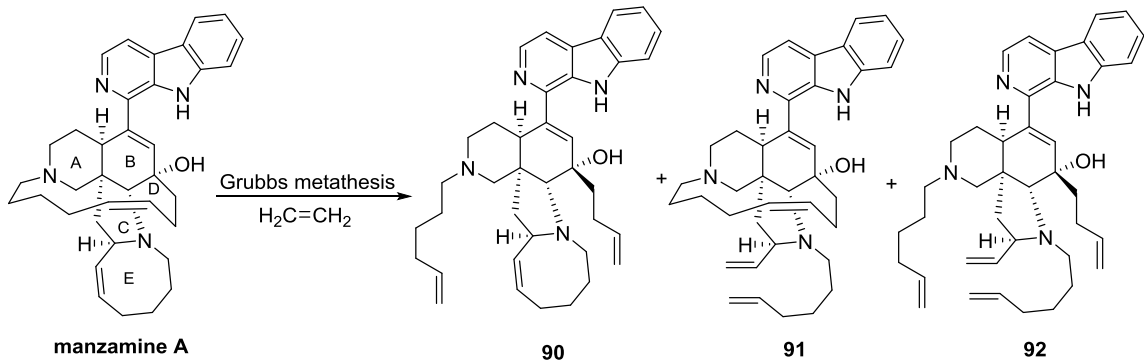
Recently, Dixon *et.al.* reported the shortest (18 steps) stereoselective synthesis of manzamine A.³⁸ Michael addition of the lactam **84** into the nitro alkene **83** yielded **85** as a major diastereomer. Nitro-Mannich/lactonization reaction of the nitro alkane **85**, the amine **86** and formaldehyde gave the lactam **87**. Another intramolecular nitro-Mannich reaction was performed to transform the lactam **88** to the desired ring system in **89**.



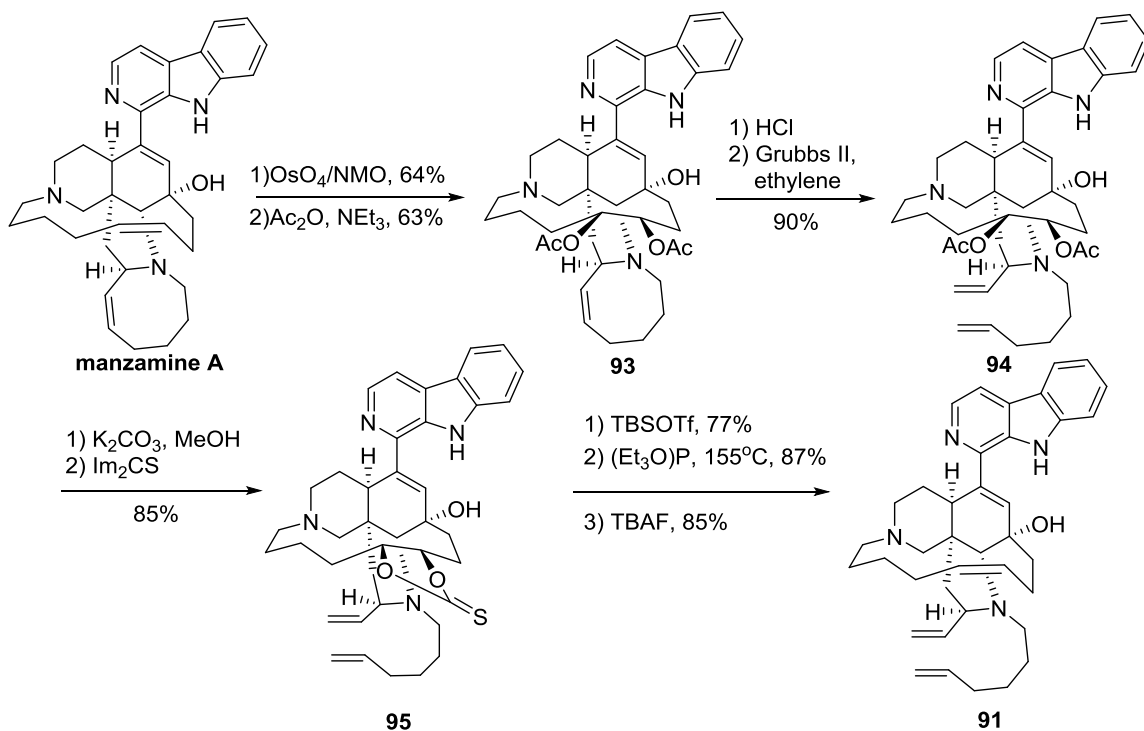
Scheme 2. 4 Key steps for the total synthesis of manzamine A by Dixon *et.al*.

2.2.2. Structural modification of manzamine A

To study structure-activity relationship (SAR) of manzamine A, derivatives of manzamine A were prepared and evaluated for biological activities. For example, the importance of the pentacyclic ring system in manzamine A for antibacterial and antiprotozoal properties was determined by the analog **90**, **91** and **92** (**Scheme 2.5**),³⁹ prepared by ring opening metathesis of manzamine A with ethylene. The hydrochloric acid salt of manzamine A was treated with the second generation Grubbs catalyst under ethylene atmosphere to afford a mixture of **90** and **92** (4:1) in 73% yield. No formation of **91** was observed under these conditions. This result suggested that the alkene in the D ring is more reactive than the one in the E ring, a result that could be attributed to steric hindrance. However the analog **91** could be selectively prepared as shown in **Scheme 2.6**. Selective dihydroxylation of the D ring and subsequently acylation led to the protected diol compound **93**. Ring-opening metathesis of the azocine ring was then performed to yield **94** in 90% yield. The transformation of the diacetate back to the desired alkene in **91** was successfully done *via* Corey–Winter olefin synthesis.⁴⁰



Scheme 2. 5 Ring-opening metathesis of manzamine A for the study of the importance of its pentacyclic system to antibacterial and antiprotozoal properties.



Scheme 2. 6 Regioselective ring-opening of the azocine ring of manzamine A.

2.3. Synthetic analysis for the conversion of manzamine A toward neokauluamine.

Neokauluamine was first isolated in 2001 by Hamann *et.al.*⁴¹ Its ¹H- and ¹³C-NMR spectra showed two set of nonidentical peaks that closely correlated to those of manzamine A (1-25C and 1'-25'C). Besides other extensive NMR experiments, the key HMBC and NOESY correlations of the molecule suggested the structure shown in **Figure 2.2**. However, since NOE correlation between 26'-H and 31'-H was not observed, the stereochemistries of C-30', C-31'- and C-34' were not assigned.

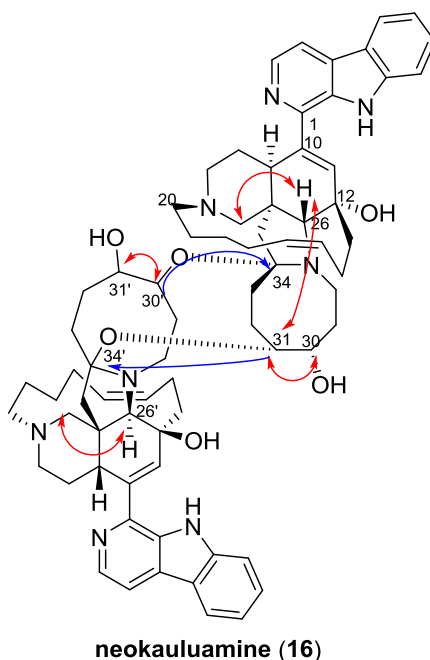
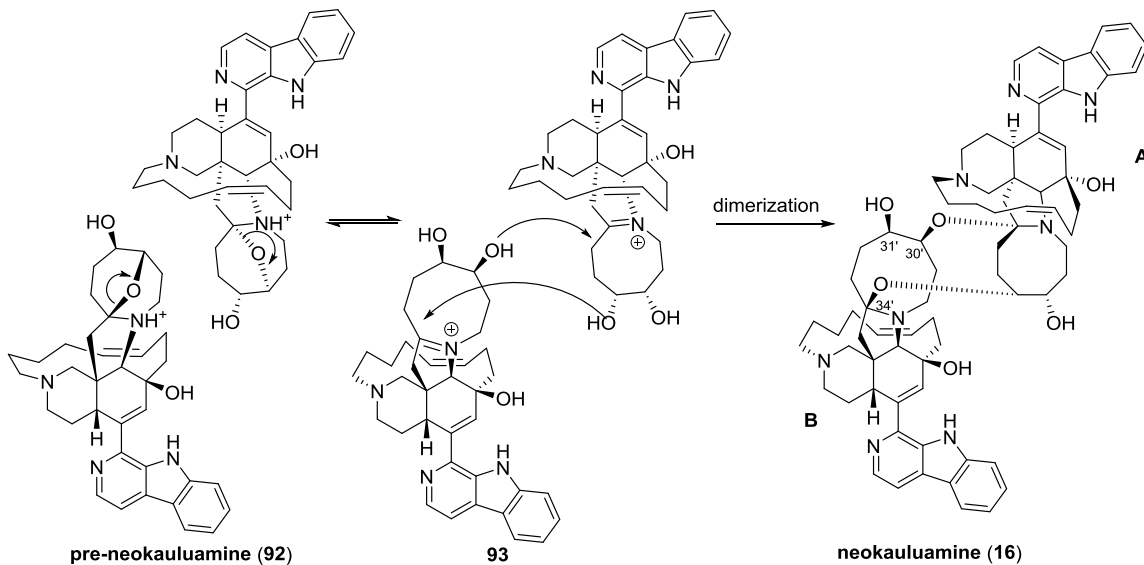


Figure2. 2 Key HMBC (blue) and NOESY (red) correlations of neokauluamine reported by Hamann *et.al.*

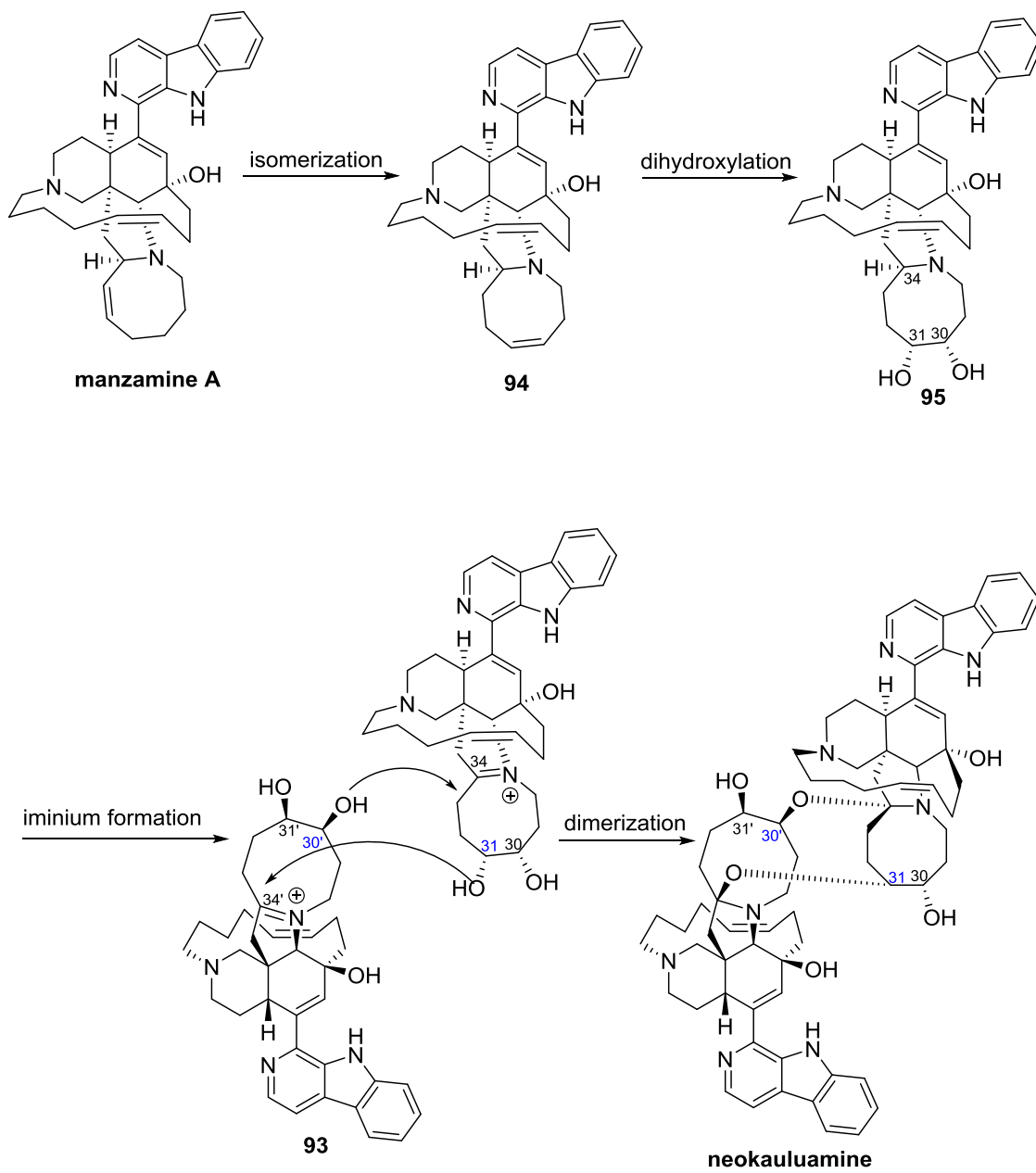
Recently, Tsukamoto *et.al* discovered a novel manzamine alkaloid called pre-neokauluamine (**Scheme 2.7**) and found that pre-neokauluamine converts to the structure of the dimeric structure of neokauluamine upon storage at -20°C for two months.¹³ This observation clearly indicated that the units A and B in neokauluamine were derived from the same molecule (pre-neokauluamine) and revealed the missing stereochemistries at 30', 31'- and 34'-C. The dimerization mechanism was proposed to occur through the ring-opening of pre-neokauluamine to

form the corresponding reactive iminium diol which then underwent reaction as shown in **Scheme 2.7**.



Scheme 2.7 Proposed mechanism for the dimerization of pre-neokauluamine toward neokauluamine.

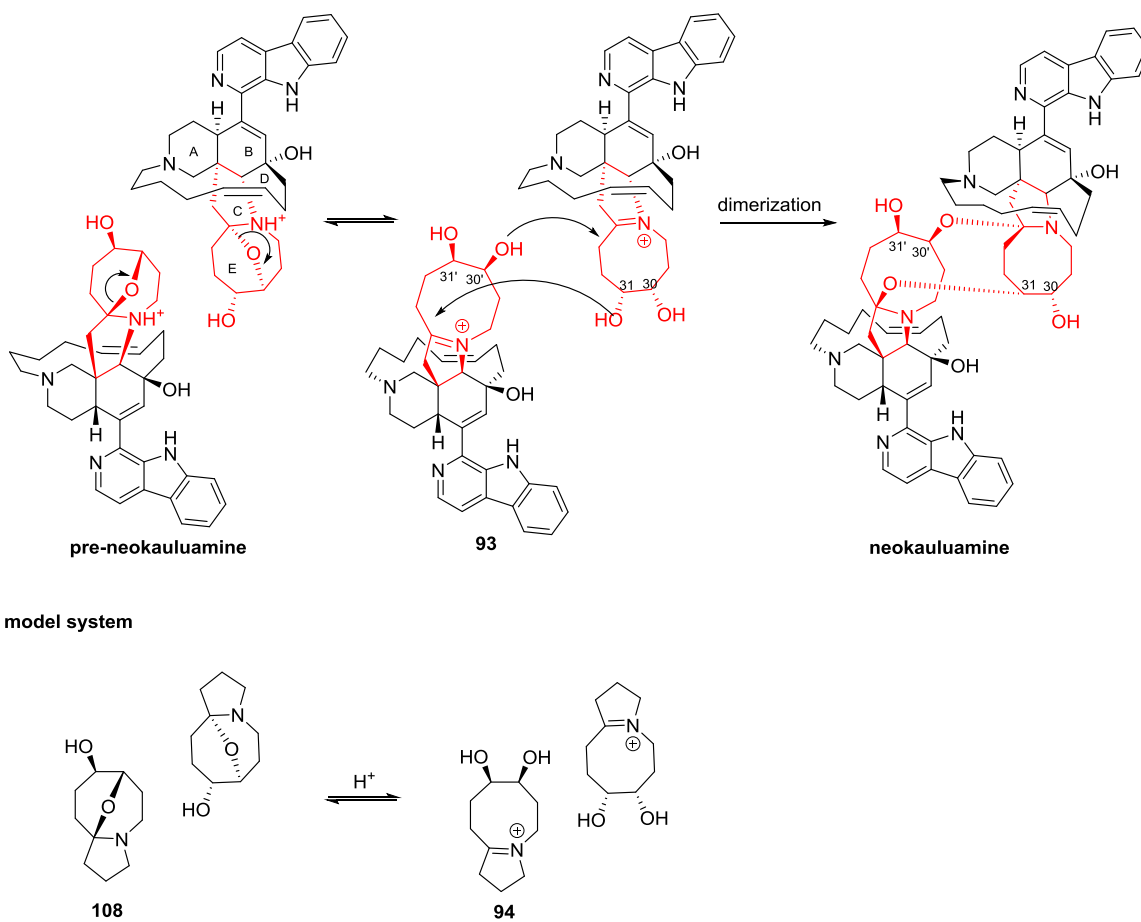
To convert manzamine A to neokauluamine, we envisioned a three step pathway (**Scheme 2.8**): 1) isomerization of the alkene functionality from the $\Delta^{32,33}$ alkene in manzamine A to the $\Delta^{30,31}$ alkene in **94** 2) dihydroxylation of the $\Delta^{30,31}$ alkene to form the diol **95** and selective C-H activation at C-34 to form the requisite iminium in **93**; followed by 3) “double” nucleophilic attack of the appropriate hydroxyl group to the iminium to form the desired dimeric structure neokauluamine.



Scheme 2. 8 Key steps for the dimerization of manzamine A toward neokauluamine.

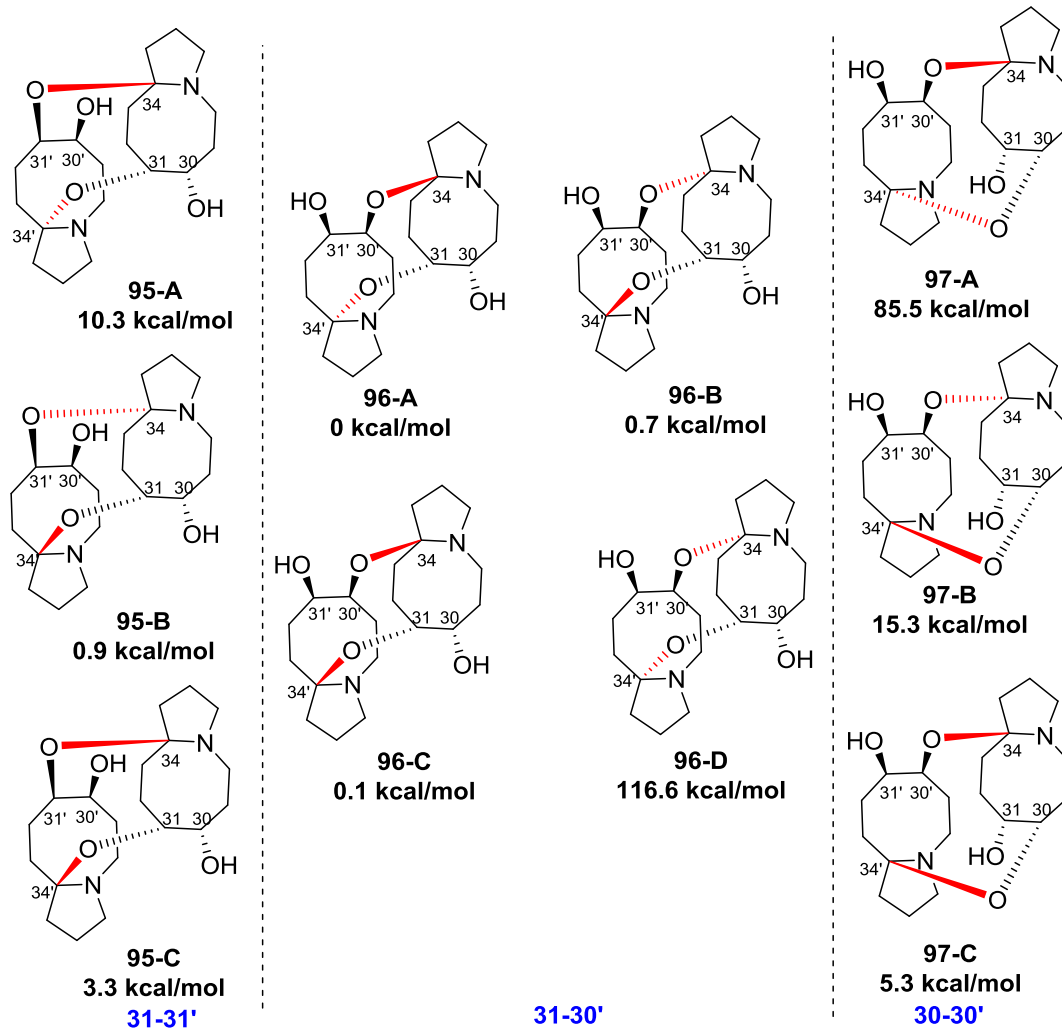
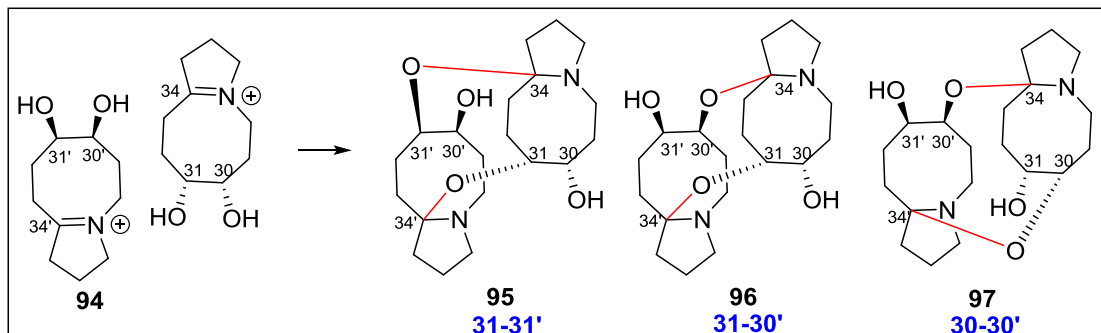
2.4. Model study for the key dimerization step

The key dimerization step proposed by Tsukamoto *et.al.* is shown in **Scheme 2.9**. Since the dimerization reaction involves only rings C and E, we planned to study the dimerization using the partial structure labeled in red in **Scheme 2.9**.



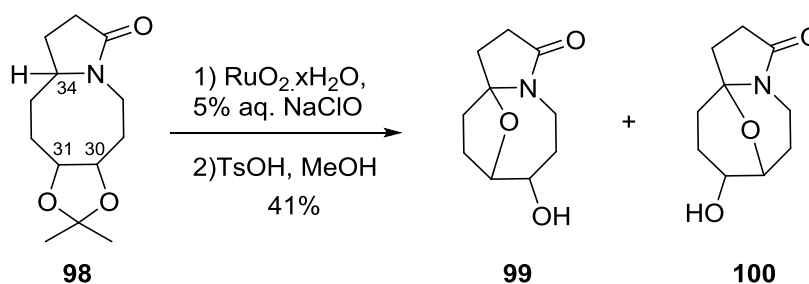
Scheme 2.9 Model system for the study of the dimerization step.

Although the structure of neokauluamine was fully assigned from the observation that it is a dimer of pre-neokauluamine by Tsukamoto *et.al.*, the dimerization of the model system **94** could theoretically yield eight different isomers, as shown in **Scheme 2.10**. Isomers **95** and **97** are homodimers from the linkages at the C-31-C-31' hydroxyls and the C-30-C-30' hydroxyls, as labeled in **Scheme 2.10**, respectively. Isomers **96** are heterodimers from the amination of the C-30'- C-31 or the C-30- C-31'hydroxyls. There are three stereoisomers for each of **95** and **97** and four stereoisomers for **96**. Among them, only isomers **95-C**, **96**, **97-C** are not symmetrical. We used Gaussian with B3LYP/6-31G(d) to perform geometry optimization calculation for each of these possible isomers. Interestingly, the lowest energy isomer is **96-A** which does not correspond to the reported structure of neokauluamine. These results add further significance to the proposed model studies, which could lead to the stereochemistry of the natural product or, alternatively, to the lowest-energy structure based on these calculations.



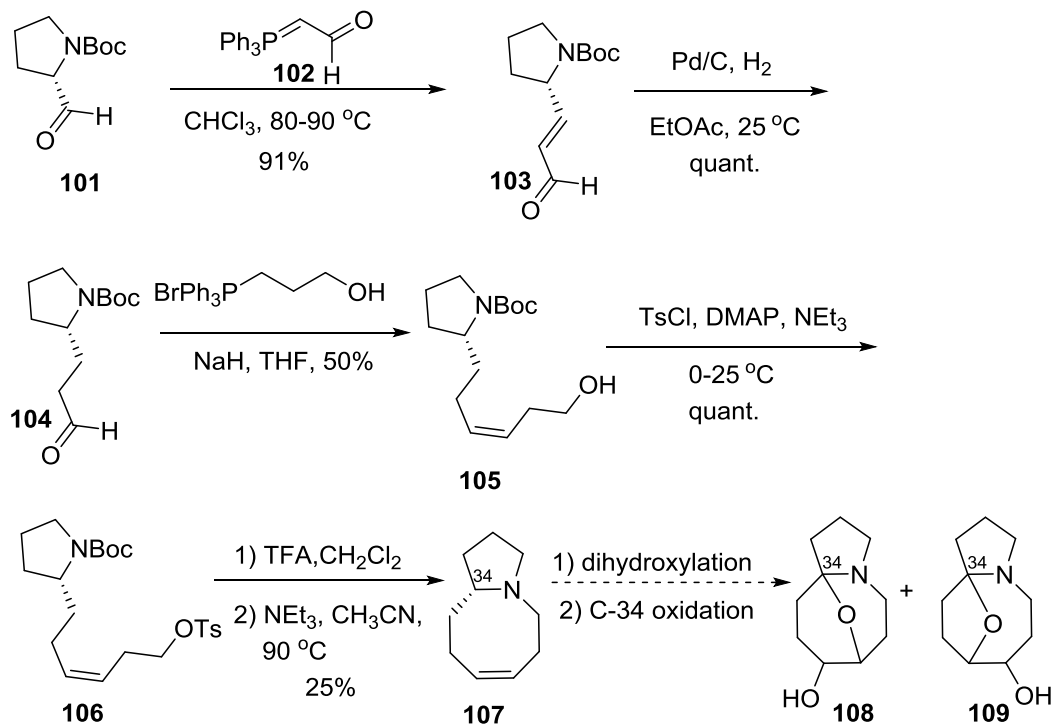
Scheme 2. 10 Possible isomers from the dimerization of the model system **94** and relative energy of the possible dimers from geometry optimization calculation using Gaussian with B3LYP/6-31G(d) .

In previous work from our laboratory, Dr. Matilda Bingham had discovered that compound **98** could be selectively oxidized at C-34 by $\text{RuO}_2 \cdot x\text{H}_2\text{O} / \text{NaOCl}$ to form a mixture of transannular cyclization products **99** and **100** after acid-catalyzed acetal deprotection (**Scheme 2.11**), of which **100** shares the ring system of pre-neokaulamine. However, no dimerization was observed from either **99** or **100**, a result that we attributed to the attenuated electron-density of the aminal nitrogen, which could impede the ring-opening that is required for the key dimerization step. We reasoned that reduction of lactam **98** to the corresponding tertiary amine would promote the requisite ring-opening of the hemiaminal.



Scheme 2.11 Previous effort to study the dimerization of the model system **94**.

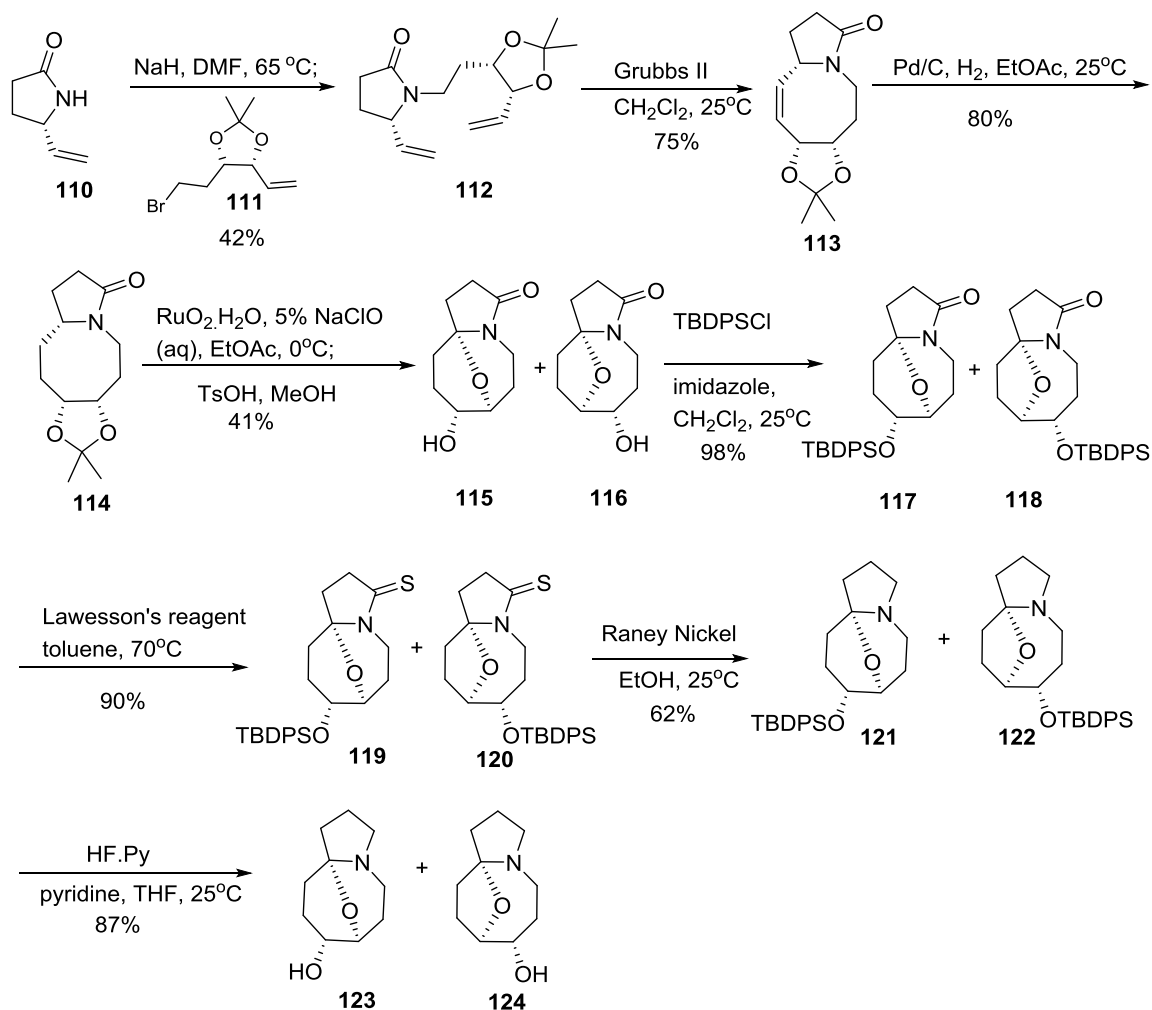
Our initial efforts to make the amine version of **98** was to prepare compound **107**, shown in **Scheme 2.12**. We reasoned that compound **107** could be dihydroxylated and oxidized to form the desired aminals **108** and **109**. Starting from the commercially available (S)-1-Boc-2-formylpyrrolidine **101**, compound **107** was prepared in 5 steps involving Wittig and $\text{S}_{\text{N}}2$ reactions. Unfortunately, compound **107** was found to be difficult to handle because of its volatility, hydrophilicity and high polarity.



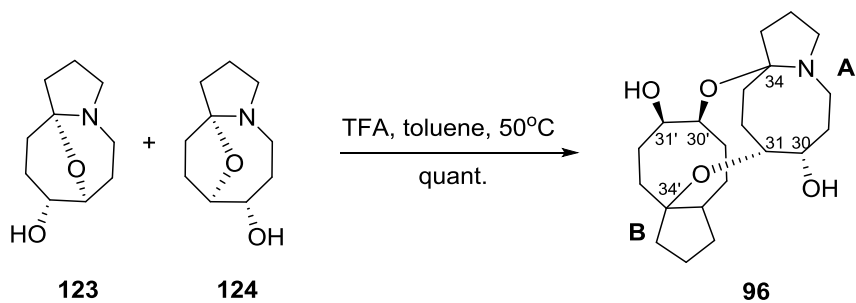
Scheme 2. 12 Initial effort to prepare model system **94**.

We envisioned that selective reduction of the lactam in compound **99** and **100** could yield the designed models **108** and **109**. The model molecule **98** prepared by Bingham was a mixture of diastereomers. To simplify the characterization in later steps, we therefore revised the synthetic route for the preparation of the enantiopure version of **98**, lactam **114**. Shown in **Scheme 2.13**, S_N2 reaction of the known lactam **110**⁴² and the alkyl bromide **111** yielded the diene **112**. Ring-closing metathesis and Pd-catalyzed hydrogenation of compound **113** gave the enantiopure compound **114** in good yield. The oxidation of **114** by the same reaction condition gave similar result to what observed by Bingham. The successfully selective reduction of the lactams **115** and **116** in the presence of hemiaminals was performed by conversion of the lactams to thioamides and subsequently reduction with Raney nickel, yielding the pre-neokaulamine-like compounds **123** and **124**.

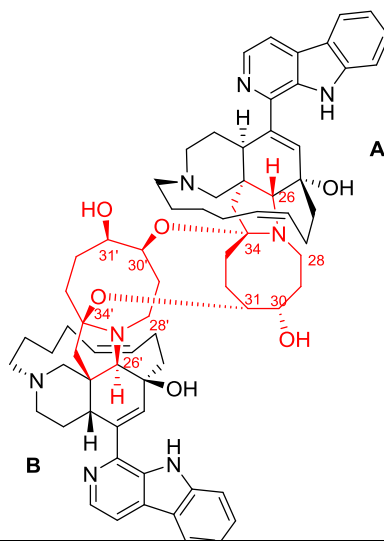
To study the dimerization of pre-neokauluamine, we treated a mixture of **123** and **124** with catalytic amount of different kinds of acids (TFA, TsOH and PPTS) in various solvents (CH₂Cl₂, CHCl₃, THF and toluene) to initiate the iminium formation. We observed no reaction when the dimerization was performed at 25°C using the acids and solvents listed above. However, when a mixture of **123** and **124** was treated with a catalytic amount of TFA in toluene and warmed up to 50°C (**Scheme 2.14**), we observed 100% conversion from the pre-neokauluamine-like compounds **123** and **124** to a compound that has 32 and 20 different protons and carbons, respectively, as determined by ¹H- and ¹³C NMR spectroscopy. This result strongly suggests the formation of the asymmetric isomers **95-C**, **96**, **97-C** (**Scheme 2.10**). The structure of the resulting dimer was further explored by COSY, HSQC and HMBC experiments that allowed us to assign its proton and carbon peaks and indicated the heterodimer **96**. Shown in **Table 2.2**, the ¹³C peak for C-34 is more downfield compared to the one for C-34'. This is opposite to what observed for neokauluamine. NOE experiments on the dimeric product gave correlations of H31-H31' and H26-26', which are consistent with the dimeric structure **96-A**, for which the indicated distances are all within 5 Å, according to the structures optimized by the geometry optimization on WebMO computational server, as shown in **Table 2.3**. These NMR data and the relatively lowest energy isomer of **96-A** (**Scheme 2.10**) are all consistent with our conclusion that the model dimer that we have prepared has the structure shown in **96-A**. However, X-ray analysis of a crystalline derivative will be needed to unambiguously confirm the proposed structure.



Scheme 2. 13 Stereoselective synthesis of the model system for the study of the dimerization of pre-neokauluamine.



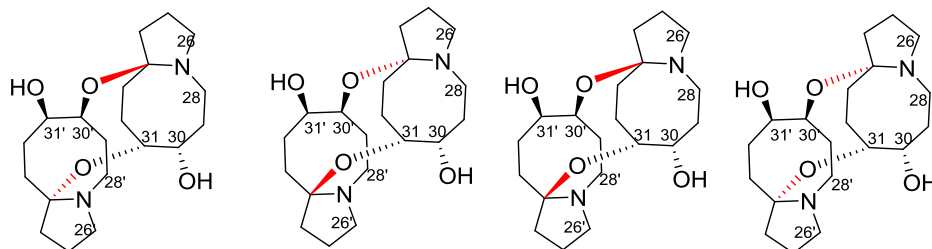
Scheme 2. 14 Model study for the dimerization of the pre-neokauluamine like compounds **123** and **124**.



neokauluamine					
Hemisphere A	¹³ C	¹ H	Hemisphere B	¹³ C	¹ H
26	75.5	3.85	26'	75.9	3.66
28	47.2	3.15	28'	44.6	3.57, 3.18
30	72.2	3.76	30'	72.7	4.14
31	84.4	4.41	31'	67.2	3.69
34	89.7	-	34'	104.5	-

Dimer 96					
Hemisphere A	¹³ C	¹ H	Hemisphere B	¹³ C	¹ H
26	56.8	3.55, 2.38	26'	54	3.42, 2.57
28	45.5	3.08, 2.88	28'	43.6	3.35, 2.51
30	70.1	3.39	30'	71.9	3.84
31	86.2	4.27	31'	65.7	3.28
34	108.3	-	34'	95.5	-

Table 2.2 ¹H- and ¹³C NMR data (ppm, CDCl₃, 500 MHz) for neokauluamine and dimer **96**.

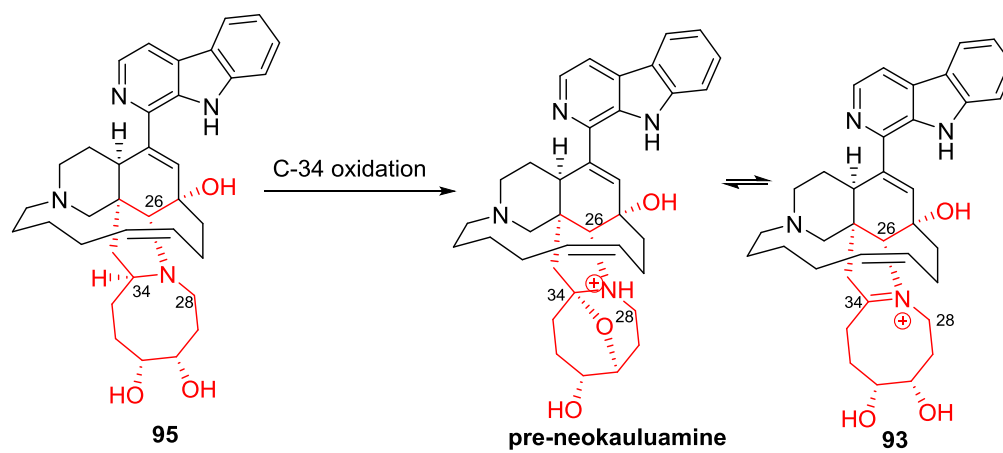


		96-A	96-B	96-C	96-D
distance (Å)	H31-H31'	4.1	6.2	4.7	5.7
	H26-H26'	5.3	8.6	8.0	8.5

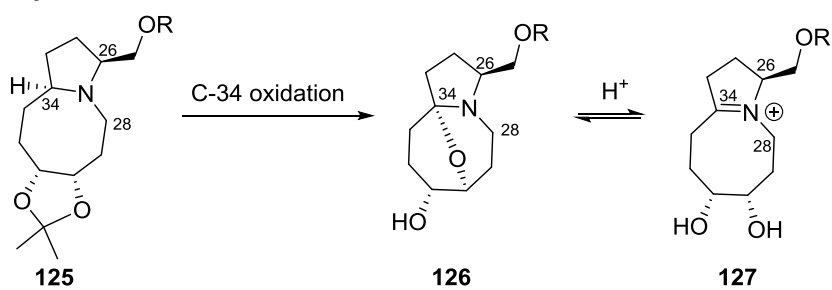
Table 2.3 Calculated distances in space between H-atoms in isomer **96**.

2.5. Model study of the oxidation key step

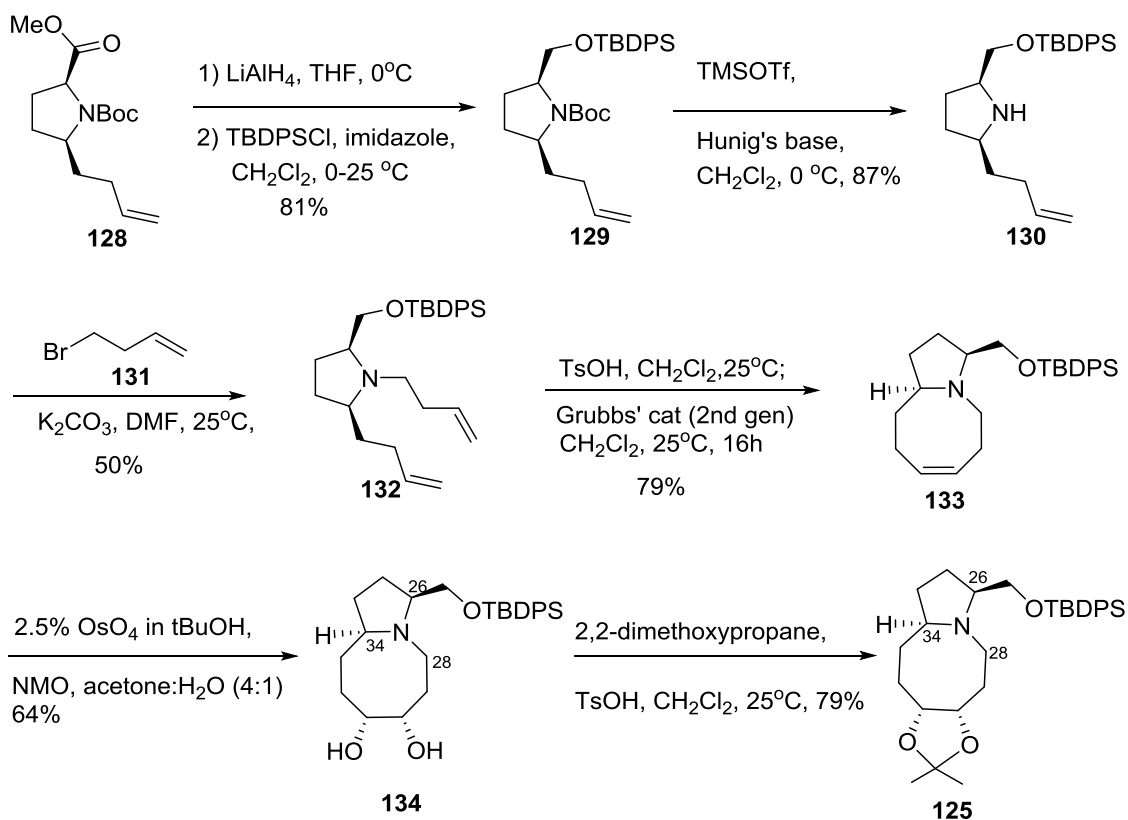
Since compound **107** (**Scheme 2.12**) was found to be difficult to handle, to study the selective C-H activation at C-34 as opposed to C-26 or C-28 (**Scheme 2.15**), we planned to use the model system **125** in **Scheme 2.15**. The free hydroxyl group could allow us to put on functionalities that make the compound non-volatile, less polar and UV active. The synthesis of the **125** (a model system for **95**) is shown in **Scheme 2.16**. The alkene **133** could be prepared from the known enantiopure alkene **128**⁴³ in 5 steps involving S_N2 and ring closing metathesis reactions. The dihydroxylation of the alkene **133** with OsO₄ gave **134** as a pure diastereomer, similar to the product obtained by the Sharpless reagent, AD-mix-β. Protection of the resulting diol with 2, 2-dimethoxypropane gave the model system **125** which was ready for the study of the selective oxidation at C-34.



model system

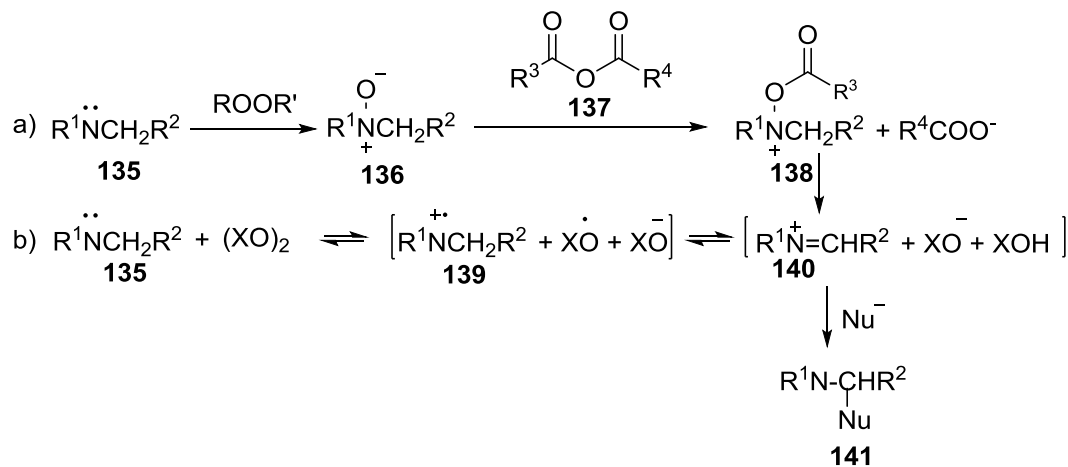


Scheme 2. 15 Model system for the study of the key oxidation step.

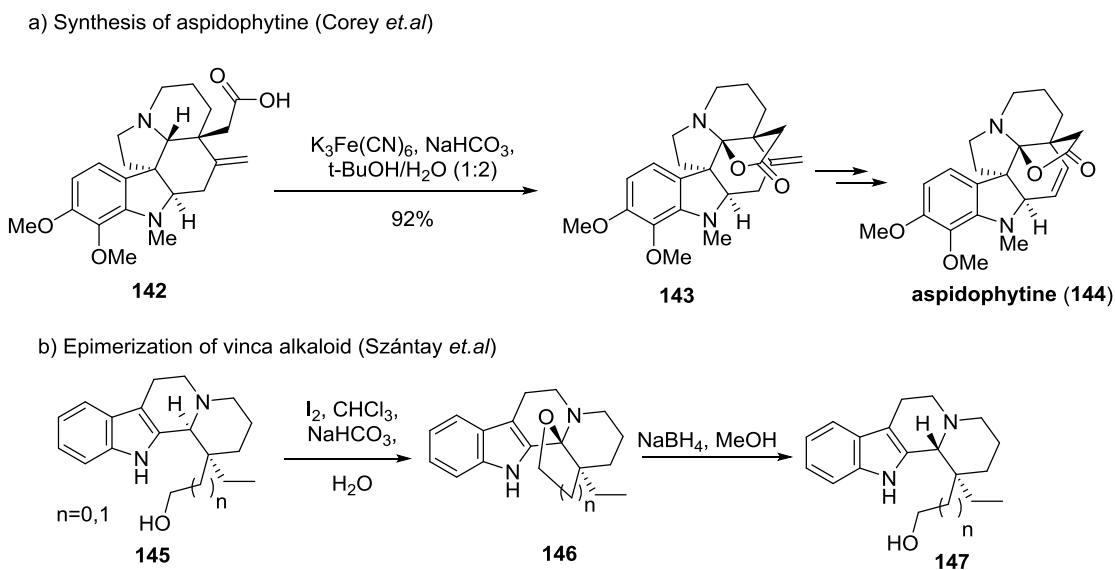


Scheme 2. 16 Synthesis of the model system **125**.

C-H activation of tertiary amines has been studied and utilized in natural product synthesis.^{18,44–47} The reaction usually proceeds through oxidation of the tertiary nitrogen to form N-oxide (**136**) or ammonium radical (**139**) and subsequent α -H abstraction to form reactive iminium species (**140**), shown in **Scheme 2.17**.⁴⁸ Selectivity for the α -H abstraction depends on thermodynamic, kinetic and stereoelectronic effects. In his synthesis of aspidophytine, Corey *et.al.* performed oxidative lactonization using potassium ferricyanide to selectively form the aminolactone **143** in excellent yield.¹⁸ Szántay *et.al.* reported iodine-aided epimerization of vinca alkaloid **145** via the hemiaminal **146** (**Scheme 2.18**).⁴⁹ However, only recovered starting material was observed when **125** was subjected to these reaction conditions.



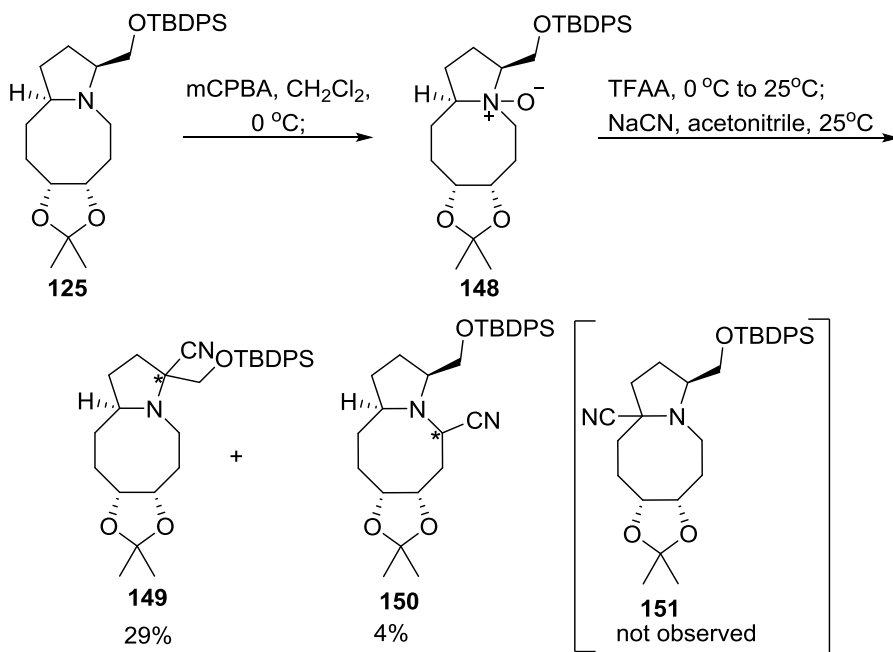
Scheme 2. 17 Proposed mechanism for C-H activation of tertiary amine **135** by a) Polonovski-Potier Reaction and by b) one-electron oxidation of tertiary amine **135**.



Scheme 2. 18 Examples of selective oxidation of tertiary amines in natural product synthesis.

We further investigated the oxidation of the model compound **125** and found that by treating with *m*CPBA in CH_2Cl_2 at 0°C , the tertiary amine was quantitatively converted to the corresponding N-oxide (**148**) in 1 hour. We therefore performed Polonovski-Potier reaction by treating the N-oxide (**148**) with trifluoroacetic anhydride to form the corresponding reactive iminium ions which were

then trapped with cyanide ions (**Scheme 2.19**).⁴⁷ Unfortunately, we observed only **149** and **150** as major and minor products, respectively with no desired isomer **151**. Working with Dr. Simon Berritt at UPenn Parallel Reaction Screening Service Center, we screened for the conditions that would yield the desired product by variations of solvents (dioxane, acetonitrile, dichloromethane, methanol, toluene and tetrahydrofuran) and anhydrides (Ac₂O, Ms₂O, Tf₂O, TFAA). Unfortunately, none of them was promising.

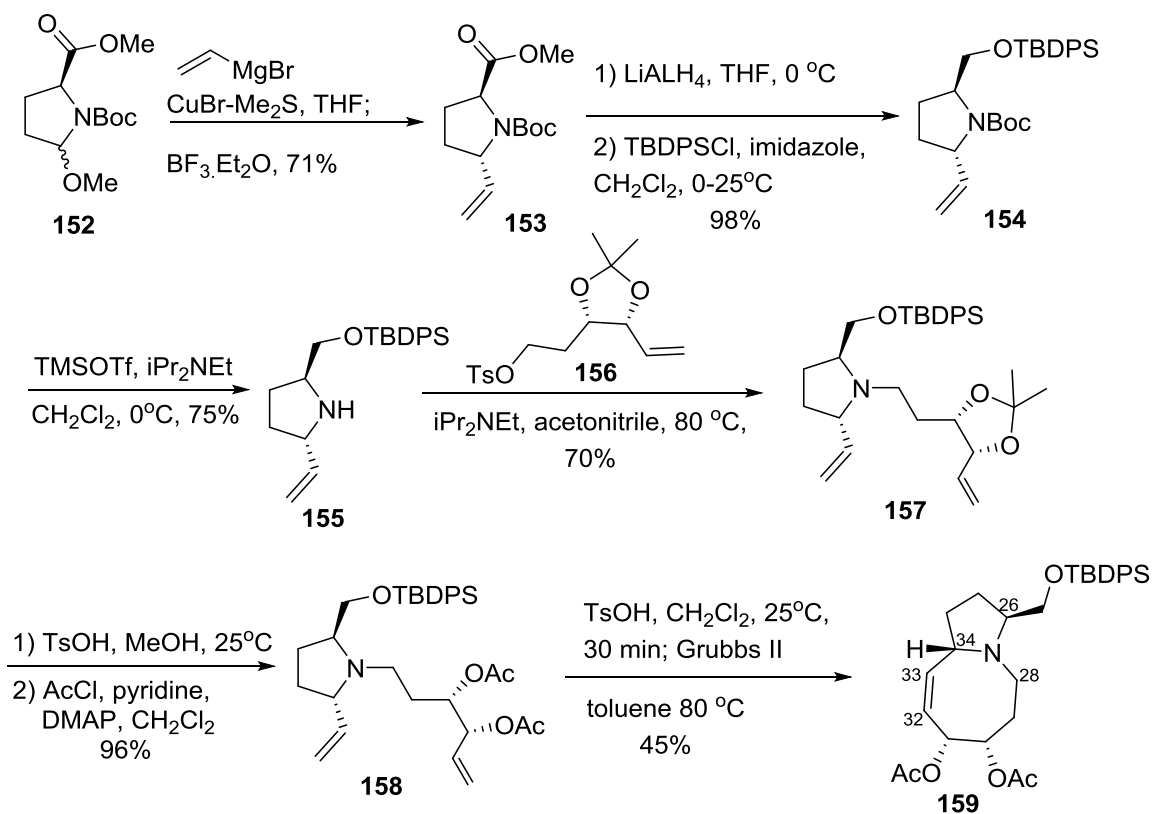


Scheme 2. 19 Polonovski-Potier reaction of model **125**.

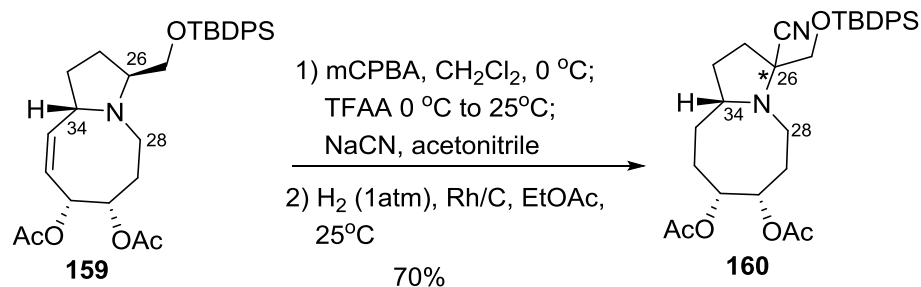
(Note: * configuration not determined)

Selective oxidation at C-34 was attempted by first introducing a double bond at $\Delta^{32,33}$ in **159**. In this case, the C-34 position is made allylic and therefore expected to be more susceptible to oxidation. The model compound **159** was prepared as outlined in **Scheme 2.20**. Following a known procedure,⁵⁰ the hemiaminal **152** was stereoselectively attacked by the vinyl cuprate, yielding the alkene **153**. Ester reduction of **153** with LiAlH₄, subsequent protection of the resulting

alcohol and Boc-deprotection led to the amine **155**. Alkylation of the amine **155** with tosylate **156** yielded the diene **157** which was then underwent ring-closing metathesis to afford the model compound **159**. Unfortunately, **159** treated with the same Polonovski-Potier reaction condition led to an inseparable mixture (**Scheme 2.21**). After hydrogenation, we observed the oxidation at C-26 (**160**) as the product, similar to the selectivity observed previously for the oxidation of model **125** (**Scheme 2.19**).



Scheme 2. 20 Synthesis of model system **159**.



Scheme 2. 21 Polonovski-Potier reaction of model **159**.

(Note: * configuration not determined)

2.6. Conclusions

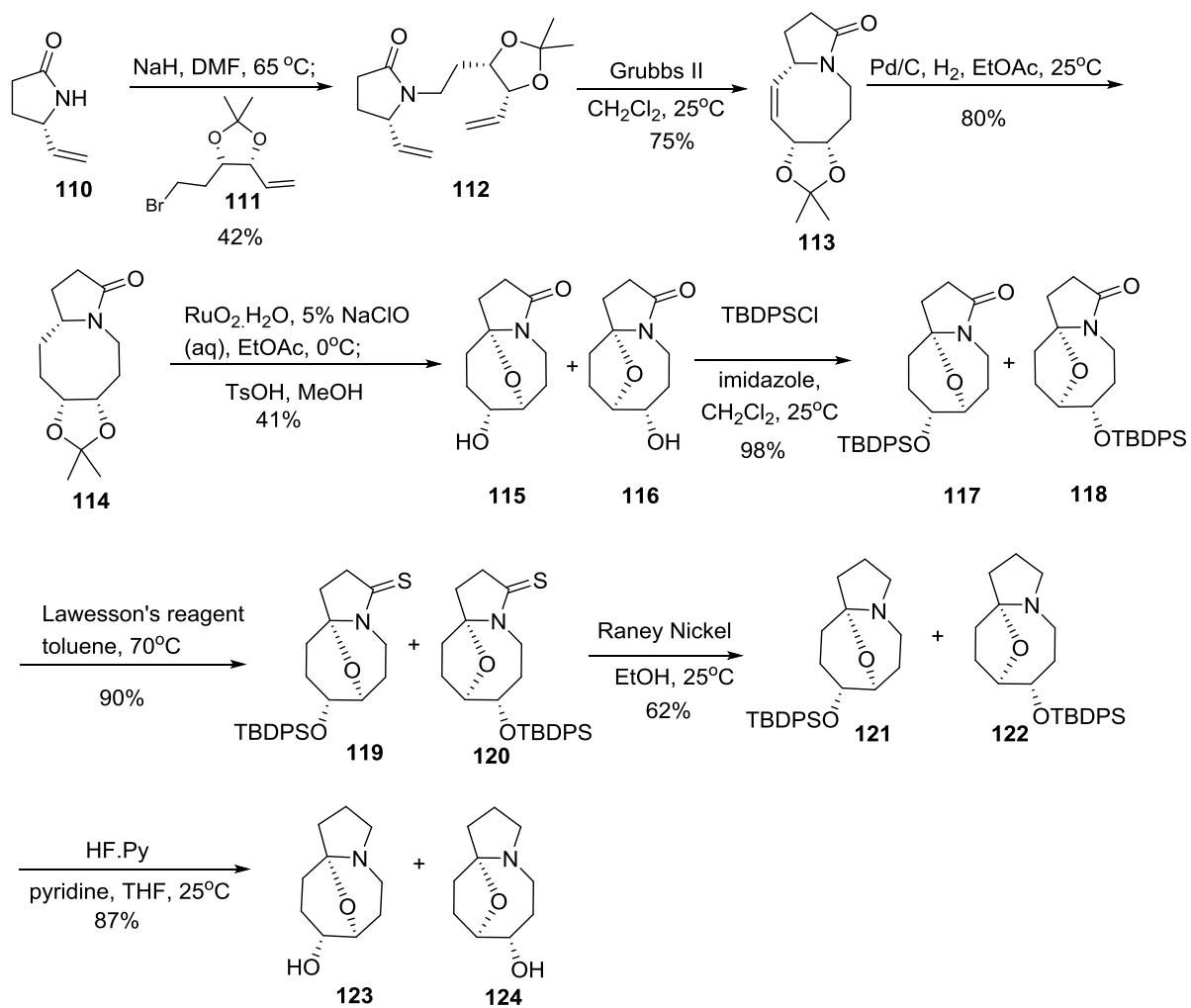
The dimerization of manzamine A toward neokauluamine involves three key steps: 1) double bond isomerization from $\Delta^{32,33}$ to $\Delta^{30,31}$, 2) C-34 selective oxidation to pre-neokauluamine, and 3) selective C-31-C-30' hydroxyl dimerization, respectively. We studied the key dimerization step from the pre-neokauluamine-like structures, **123** and **124**, and found that they were selectively dimerized to a single hetero dimer after being warmed up to 50 °C with catalytic TFA in toluene. Our extensive NMR experiments and computational data suggest that the resulting dimer is the isomer **96-A**. However, X-ray crystal analysis is needed to confirm the structure. Since **96-A** does not correspond to the structure present in the reported structure of neokauluamine, we reason that the other functionalities in the structure of pre-neokauluamine, e.g. the macrocyclic 13-membered ring, crucially affect the stereoselectivity of the dimerization step. A model study for the key oxidation step was also performed. Unfortunately, the Polonovski reaction of both the saturated (**125**) and unsaturated (**159**) model systems led to C-26 oxidation as the major product with no observation of the desired oxidation product **151**. Further investigation to alter the selectivity for the oxidation at 34-C is therefore necessary.

2.7. General method and experimental procedures

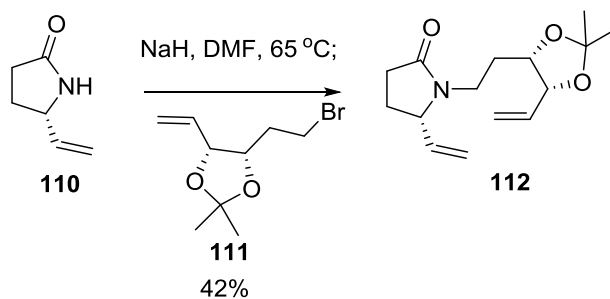
2.7.1. General information

Unless otherwise stated, all reagents were purchased from Sigma Aldrich, Alfa Aesar, Acros Organic or TCI America and used without further purification. ^1H and ^{13}C NMR spectra were recorded on Bruker AVII500B (500 MHz) and DRX-500 (500 MHz) spectrometers. Chemical shifts are reported relative to the solvent resonance peak δ 7.26 (CDCl_3) for ^1H NMR and δ 77.16 (CDCl_3) for ^{13}C NMR. Infrared spectra were recorded on a NaCl plate using a Perkin-Elmer 1600 series Fourier transform spectrometer. High-resolution mass spectra were obtained by Dr. Rakesh Kohli at the University of Pennsylvania Mass Spectrometry Service Center.

2.6.2. Procedure for the synthesis of model system **123** and **124**

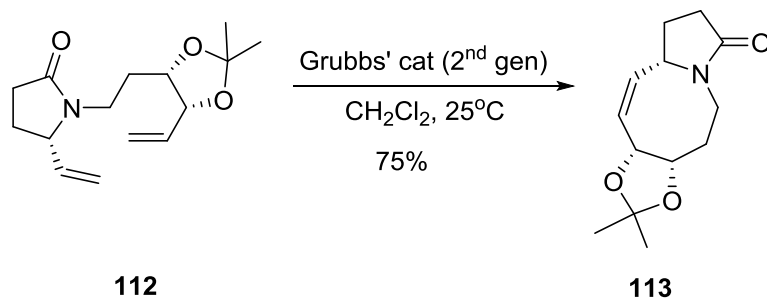


(S)-1-(2-((4S,5R)-2,2-dimethyl-5-vinyl-1,3-dioxolan-4-yl)ethyl)-5-vinylpyrrolidin-2-one (**112**)



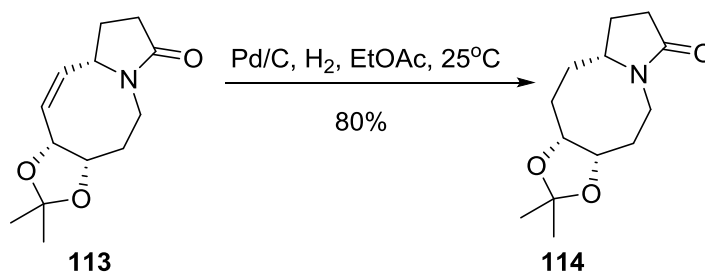
NaH (0.043 g, 1.08 mmol, 1 eq.) was added to a solution of **110** (prepared in 5 steps⁴² from L-pyrroglutamic acid) (0.12 g, 1.08 mmol, 1 eq.) in DMF (1 mL). The suspension was stirred at 25°C for 1h under argon atmosphere. A solution of **111**⁵¹ (0.3 g, 1.276 mmol, 1.2 eq.) in DMF (1 mL) was then added and the reaction mixture was stirred at 25°C for 16h. H₂O (5mL) was then added. The mixture was extracted with EtOAc (5mL) three times. The combined organic layer was washed with brine, dried over Na₂SO₄ and concentrated under reduced pressure. The residue was purified by silica gel chromatography (gradient 1-50% EtOAc/Hexane) to yield **112** as a colorless oil (0.12 g, 42% yield). ¹H NMR (500 MHz, Chloroform-*d*) δ 5.63 (dddd, *J* = 17.7, 10.1, 7.5, 1.8 Hz, 1H), 5.52 (dddd, *J* = 16.9, 10.1, 8.3, 1.8 Hz, 1H), 5.22 – 5.01 (m, 4H), 4.36 (t, *J* = 6.9 Hz, 1H), 4.03 – 3.95 (m, 1H), 3.90 (dddd, *J* = 13.7, 7.7, 6.2, 1.8 Hz, 1H), 3.45 – 3.36 (m, 1H), 2.94 – 2.85 (m, 1H), 2.31 – 2.02 (m, 3H), 1.60 (dddd, *J* = 12.5, 9.4, 6.2, 1.8 Hz, 1H), 1.49 (dddd, *J* = 11.7, 9.8, 5.6, 2.6 Hz, 1H), 1.39 (dddd, *J* = 13.3, 9.5, 5.6, 3.8, 1.8 Hz, 1H), 1.31 (d, *J* = 1.7 Hz, 3H), 1.19 (d, *J* = 1.8 Hz, 3H). ¹³C NMR (126 MHz, Chloroform-*d*) δ 174.58, 137.65, 133.76, 118.18, 117.74, 108.10, 79.22, 76.07, 61.23, 38.06, 29.79, 28.35, 28.03, 25.43. FTIR (CHCl₃ film): 2984.3, 2935.13, 1689.34, 1419.35, 1216.86 cm⁻¹. HRMS: [M+H]⁺ calc. 266.1756, found 266.1757.

(3a*S*,9a*S*,11a*R*,*Z*)-2,2-dimethyl-4,5,8,9,9a,11a-hexahydro-[1,3]dioxolo[4,5-*e*]pyrrolo[1,2-*a*]azocin-7(3a*H*)-one (**113**)



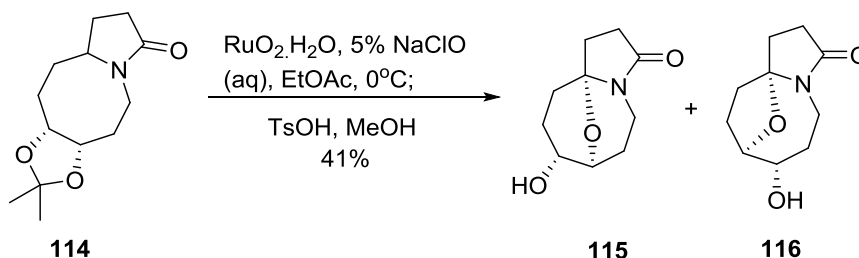
A solution of **112** (0.07 g, 0.26 mmol, 1 eq.) in CH₂Cl₂ (50 mL) was degassed before adding Grubbs' cat. (2nd gen) (0.022 g, 0.026 mmol, 0.1 eq.). The mixture was stirred for 24 h under argon atmosphere and concentrated under reduced pressure. The residue was purified by silica gel chromatography (gradient 20-80% EtOAc/Hexane) to yield **113** as a colorless oil (0.046g, 75% yield). ¹H NMR (500 MHz, Chloroform-*d*) δ 5.70 – 5.64 (m, 2H), 5.16 (dd, *J* = 6.5, 3.1 Hz, 1H), 4.43 (dd, *J* = 15.0, 8.9 Hz, 1H), 4.31 (ddd, *J* = 10.3, 6.3, 3.6 Hz, 1H), 4.06 – 3.97 (m, 1H), 2.73 (dd, *J* = 15.0, 9.9 Hz, 1H), 2.51 (dt, *J* = 16.4, 9.5 Hz, 1H), 2.33 – 2.07 (m, 3H), 1.90 – 1.76 (m, 2H), 1.47 (s, 3H), 1.37 (s, 3H). ¹³C NMR (126 MHz, Chloroform-*d*) δ 173.97, 135.87, 130.91, 108.76, 81.49, 75.51, 55.66, 39.10, 29.39, 29.18, 27.79, 26.06, 25.58. FTIR (CHCl₃ film): 2983.34, 1681.62, 1423.21, 1379.82, 1248.68, 1062.59 cm⁻¹. HRMS: [M+H]⁺ calc. 238.1443, found 238.1446.

(3a*S*,9a*R*,11a*R*)-2,2-dimethyloctahydro-[1,3]dioxolo[4,5-*e*]pyrrolo[1,2-*a*]azocin-7(3a*H*)-one (**114**)



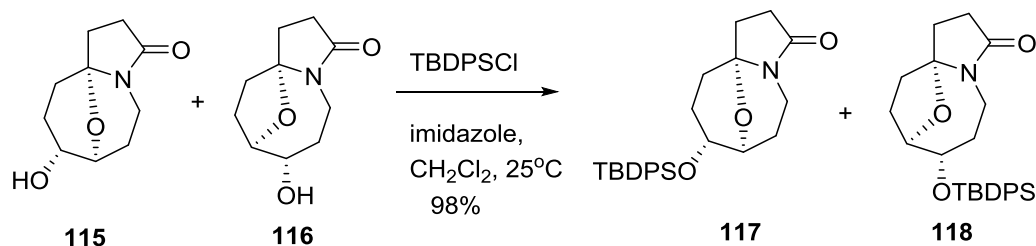
Pd/C (0.002 g, 0.0169 mmol, 0.1 eq.) was added to a solution of **113** (0.04 g, 0.169 mmol, 1 eq.) in EtOAc (5 mL). The suspension was charged with a H₂ balloon and stirred at 25°C for 16h. The reaction mixture was then filtered through a thin pad of Celite to yield **114** as a colorless film (0.032 g, 80% yield). ¹H NMR (500 MHz, Chloroform-*d*) δ 4.22 (dt, *J* = 11.1, 5.1 Hz, 1H), 4.15 – 4.07 (m, 2H), 3.62 (tdd, *J* = 7.1, 5.0, 3.4 Hz, 1H), 2.46 – 2.35 (m, 2H), 2.29 (dt, *J* = 17.1, 9.1 Hz, 1H), 2.04 (dddd, *J* = 13.5, 11.6, 5.6, 3.5 Hz, 1H), 1.97 – 1.82 (m, 2H), 1.80 – 1.69 (m, 2H), 1.61 – 1.46 (m, 3H), 1.36 (s, 3H), 1.29 (s, 3H). ¹³C NMR (126 MHz, Chloroform-*d*) δ 175.86, 107.61, 80.09, 58.35, 39.17, 32.52, 30.48, 28.35, 26.11, 25.81, 24.92, 20.17. FTIR (CHCl₃ film): 2930.31, 1680.66, 1420.32, 1046.19 cm⁻¹. HRMS: [M+H]⁺ calc. 240.1600, found 240.1593.

(7*S*,8*R*,10*aR*)-8-hydroxyoctahydro-3*H*-7,10*a*-epoxypyrrolo[1,2-*a*]azocin-3-one (**115**) and (7*S*,8*R*,10*aR*)-7-hydroxyoctahydro-3*H*-8,10*a*-epoxypyrrolo[1,2-*a*]azocin-3-one (**116**)



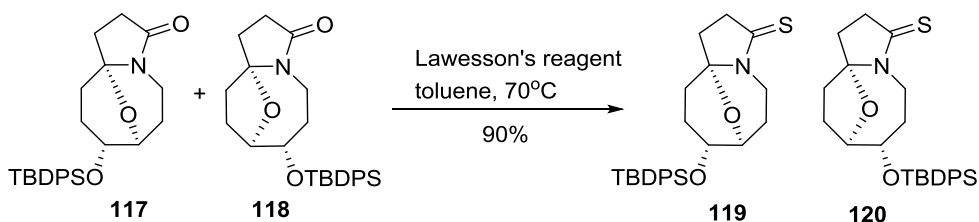
RuO₄·H₂O (0.005 g, 0.038 mmol, cat.) was added into a solution of **114** (0.2 g, 0.84 mmol, 1eq.) in EtOAc (3 mL) at 0°C under argon. 5%NaClO (aq) (1.68 ml) was added in 3 portions over 3 h. The reaction was kept at 0°C until **114** was completely consumed (monitored by LCMS). Isopropanol (1.5 mL) was then added. The mixture was extracted three time with EtOAc (10 mL). The combined organic layer was washed with brine, dried over Na₂SO₄ and concentrated under reduced pressure. The residue was then brought up into MeOH (1 mL). TsOH (0.01 g) was added and the mixture was stirred at 25°C for 16h. The mixture was concentrated under reduced pressure and purified by silica gel chromatography (2-5 % MeOH/CH₂Cl₂) to yield a mixture of the two isomers (**115:116** = 10:2) (0.067g, 41% yield). ¹H NMR (500 MHz, Chloroform-*d*) δ 4.49 (dt, *J* = 9.4, 2.2 Hz, 0.2H), 4.15 – 4.06 (m, 1.8H), 3.83 (td, *J* = 5.3, 4.7, 2.6 Hz, 0.2H), 3.78 (dt, *J* = 4.7, 2.3 Hz, 1H), 3.76 – 3.70 (m, 0.2H), 3.50 – 3.40 (m, 1H), 3.18 (ddd, *J* = 14.7, 8.6, 2.4 Hz, 0.2H), 2.55 – 2.10 (m, 7H), 2.06 (ddd, *J* = 13.6, 10.2, 6.7 Hz, 1H), 1.99 – 1.91 (m, 1.8H), 1.86 – 1.75 (m, 1.5H), 1.55 (dd, *J* = 14.3, 5.5 Hz, 1H). ¹³C NMR (126 MHz, Chloroform-*d*) δ 174.15, 173.59, 101.67, 88.00, 84.65, 74.59, 66.93, 36.61, 35.85, 35.20, 33.42, 32.07, 31.87, 30.72, 30.25, 28.85, 28.27, 28.00, 23.72. FTIR (CHCl₃ film): 3335.28, 2947.66, 1669.09, 1368.25, 1175.4, 1029.8 cm⁻¹. HRMS: [M+Na]⁺ calc. 220.0950, found 220.0955.

(7*S*,8*R*,10*aR*)-8-((*tert*-butyldiphenylsilyl)oxy)octahydro-3*H*-7,10*a*-epoxy pyrrolo[1,2-*a*]azocin-3-one (**117**) and (7*S*,8*R*,10*aR*)-7-((*tert*-butyldiphenylsilyl)oxy)octahydro-3*H*-8,10*a*-epoxy pyrrolo[1,2-*a*]azocin-3-one (**118**)



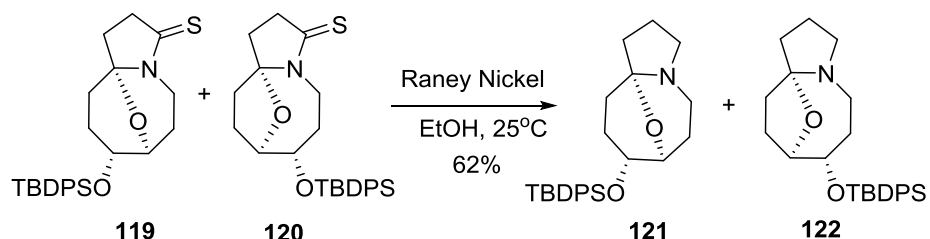
Imidazole (0.06 g, 0.9 mmol, 1.5 eq.) and TBDPSCI (0.247 g, 0.9 mmol, 1.5 eq.) were added to a mixture of **115** and **116** (0.12g, 0.6 mmol, 1 eq.) in CH₂Cl₂ (3 mL). The mixture was stirred at 25°C for 16 h. The solvent was then removed under reduced pressure. The residue was purified by silica gel chromatography (20 % EtOAc/Hexane) to yield a mixture of the two isomers (**117**:**118** = 10:2) (0.26g, 98% yield). **Compound 117**: ¹H NMR (500 MHz, Chloroform-*d*) δ 7.67 (ddq, *J* = 9.3, 7.9, 1.5 Hz, 4H), 7.46 – 7.35 (m, 6H), 4.00 (dd, *J* = 14.1, 7.9 Hz, 2H), 3.76 (dq, *J* = 3.5, 1.7 Hz, 1H), 3.36 – 3.26 (m, 1H), 2.50 – 2.28 (m, 3H), 2.15 – 1.91 (m, 4H), 1.84 (dd, *J* = 15.2, 6.1 Hz, 1H), 1.73 (dd, *J* = 13.6, 5.5 Hz, 1H), 1.28 – 1.16 (m, 1H), 1.09 (d, *J* = 1.2 Hz, 9H). ¹³C NMR (126 MHz, Chloroform-*d*) δ 174.08, 135.86, 133.98, 129.94, 127.83, 87.97, 68.28, 36.15, 33.77, 31.21, 29.00, 28.51, 27.09, 23.75, 19.42. **Compound 118**: ¹H NMR (500 MHz, Chloroform-*d*) δ 7.72 – 7.59 (m, 4H), 7.46 – 7.33 (m, 6H), 4.44 – 4.36 (m, 1H), 3.91 – 3.80 (m, 1H), 3.80 – 3.72 (m, 1H), 2.94 – 2.84 (m, 1H), 2.57 (ddd, *J* = 16.8, 9.8, 5.7 Hz, 1H), 2.40 (ddd, *J* = 16.5, 9.5, 6.3 Hz, 1H), 2.32 (ddd, *J* = 13.4, 9.8, 6.2 Hz, 1H), 2.13 (ddd, *J* = 13.4, 9.5, 5.7 Hz, 1H), 2.06 – 1.94 (m, 3H), 1.83 (td, *J* = 7.0, 3.2 Hz, 2H), 1.54 – 1.44 (m, 1H), 1.06 (s, 9H). ¹³C NMR (126 MHz, Chloroform-*d*) δ 173.48, 135.95, 134.08, 133.83, 129.94, 127.83, 101.60, 85.60, 36.30, 35.13, 33.21, 31.63, 30.33, 28.90, 27.09, 19.30. FTIR (CHCl₃ film): 2931.27, 1698.02, 1407.78, 1111.76 cm⁻¹. HRMS: [M+Na]⁺ calc. 458.2127, found 458.2131.

(7*S*,8*R*,10*aR*)-8-((*tert*-butyldiphenylsilyl)oxy)octahydro-3*H*-7,10*a*-epoxy pyrrolo[1,2-*a*]azocine-3-thione (**119**) and (7*S*,8*R*,10*aR*)-7-((*tert*-butyldiphenylsilyl)oxy)octahydro-3*H*-8,10*a*-epoxy pyrrolo[1,2-*a*]azocine-3-thione (**120**)



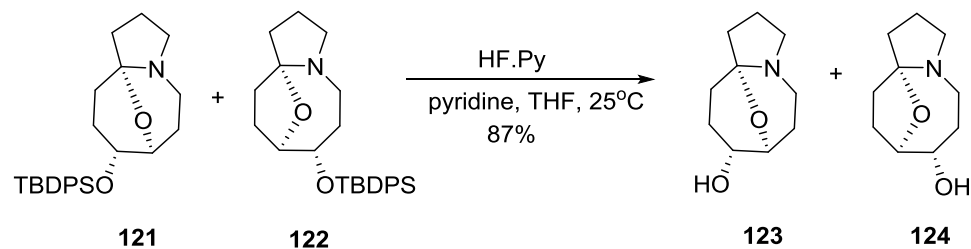
A mixture of **117** and **118** (0.18 g, 0.4 mmol, 1 eq.) and Lawesson's reagent (0.184 g, 0.45 mmol, 1.1 eq.) in toluene (2 mL) was heated up to 70°C for 1h. The mixture was then cooled down to 25°C and absorbed on silica gel for silica gel chromatography (dry load). The eluent was 3-5% EtOAc/Hexane to obtain **119** (0.126 g, 70% yield) and 10-20% EtOAc/Hexane to obtain **120** (0.036 g, 20% yield). **Compound 119**: ¹H NMR (500 MHz, Chloroform-*d*) δ 7.67 (ddt, *J* = 13.0, 6.6, 1.4 Hz, 4H), 7.46 – 7.33 (m, 6H), 4.56 (dd, *J* = 14.9, 8.4 Hz, 1H), 4.07 – 4.00 (m, 1H), 3.81 (dt, *J* = 3.8, 2.1 Hz, 1H), 3.46 (tdd, *J* = 12.5, 6.4, 2.3 Hz, 1H), 3.08 – 2.96 (m, 1H), 2.85 (dtd, *J* = 18.3, 9.3, 2.3 Hz, 1H), 2.35 (td, *J* = 13.5, 6.3 Hz, 1H), 2.17 – 2.11 (m, 2H), 2.11 – 2.04 (m, 1H), 1.95 (dddd, *J* = 14.7, 13.2, 5.5, 3.7 Hz, 1H), 1.85 (ddt, *J* = 12.9, 6.3, 2.1 Hz, 1H), 1.78 (ddd, *J* = 13.6, 5.5, 2.0 Hz, 1H), 1.45 – 1.36 (m, 1H), 1.10 (s, 9H). ¹³C NMR (126 MHz, Chloroform-*d*) δ 199.26, 135.69, 133.58, 129.91, 127.75, 94.47, 73.72, 67.82, 41.41, 40.58, 35.87, 29.60, 27.82, 26.95, 23.20, 19.27. **Compound 120**: ¹H NMR (500 MHz, Chloroform-*d*) δ 7.75 – 7.60 (m, 4H), 7.48 – 7.34 (m, 6H), 4.38 (d, *J* = 8.8 Hz, 1H), 4.19 – 4.08 (m, 1H), 3.94 – 3.86 (m, 1H), 3.85 – 3.73 (m, 1H), 3.12 (ddd, *J* = 17.7, 9.3, 2.6 Hz, 1H), 2.95 (dt, *J* = 17.6, 8.8 Hz, 1H), 2.38 (dt, *J* = 12.8, 9.3 Hz, 1H), 2.21 – 2.08 (m, 3H), 2.06 – 1.98 (m, 1H), 1.84 (dt, *J* = 6.8, 4.0 Hz, 2H), 1.56 – 1.48 (m, 1H), 1.07 (s, 9H). ¹³C NMR (126 MHz, Chloroform-*d*) δ 198.96, 135.99, 133.54, 129.97, 127.86, 107.69, 85.28, 75.61, 42.66, 40.46, 36.74, 34.98, 29.79, 27.64, 27.10, 19.38. FTIR (CHCl₃ film): 2952.48, 1463.71, 1426.1, 1110.8, 1029.8 cm⁻¹. HRMS: [M+H]⁺ calc. 452.2080, found 452.2083.

(7*S*,8*R*,10*aS*)-8-((*tert*-butyldiphenylsilyl)oxy)octahydro-1*H*-7,10*a*-epoxy pyrrolo[1,2-*a*]azocine (**121**) and (7*S*,8*R*,10*aS*)-7-((*tert*-butyldiphenylsilyl)oxy)octahydro-1*H*-8,10*a*-epoxy pyrrolo[1,2-*a*]azocine (**122**)



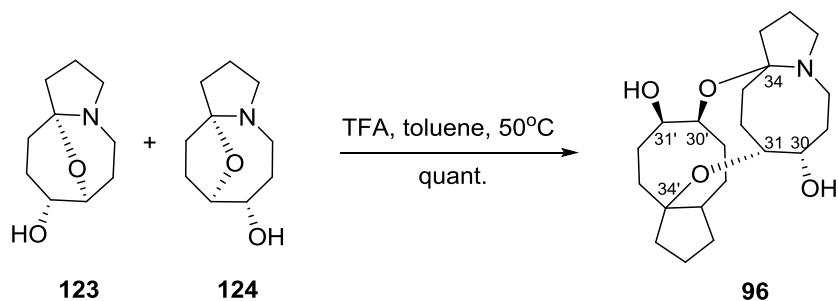
Raney Nickel (activated in H₂O) (0.9 g) was washed two times with H₂O (1 mL) and EtOH (1 mL) before suspending in EtOH (5 mL). The suspension was then added to a solution of **119** and **120** (0.12 g, 0.266 mmol, 1 eq.) in EtOH (5 mL). The mixture was stirred under argon for 30 min at 25°C before being filtered through a thin pad of Celite (washed with MeOH (20 mL)) to afford a mixture of **121** and **122** in (0.069 g, 62% yield). ¹H NMR (500 MHz, Chloroform-*d*) δ 7.69 (td, *J* = 6.7, 3.3 Hz, 4H), 7.44 – 7.34 (m, 6H), 4.01 – 3.93 (m, 1H), 3.72 (td, *J* = 3.7, 1.7 Hz, 1H), 3.44 (d, *J* = 2.1 Hz, 1H), 3.33 (ddd, *J* = 13.6, 11.4, 5.1 Hz, 1H), 3.17 (q, *J* = 8.3 Hz, 1H), 2.94 (td, *J* = 8.4, 2.6 Hz, 1H), 2.73 (ddd, *J* = 14.1, 6.6, 3.1 Hz, 1H), 2.29 (td, *J* = 12.6, 6.0 Hz, 1H), 2.21 – 2.06 (m, 2H), 1.95 (qd, *J* = 8.0, 4.8 Hz, 1H), 1.89 – 1.70 (m, 3H), 1.56 (ddd, *J* = 13.4, 5.4, 3.6 Hz, 1H), 1.09 (d, *J* = 2.6 Hz, 9H), 0.90 – 0.81 (m, 1H). ¹³C NMR (126 MHz, Chloroform-*d*) δ 136.03, 134.42, 129.69, 127.63, 89.51, 74.11, 69.50, 52.60, 41.93, 40.48, 29.49, 27.46, 27.06, 20.82, 20.57, 19.35. FTIR (CHCl₃ film): 2931.27, 2856.06, 1698.02, 1427.07, 1110.8 cm⁻¹. HRMS: [M+H]⁺ calc. 422.2515, found 422.2519.

(7*S*,8*R*,10*aS*)-octahydro-1*H*-7,10*a*-epoxy pyrrolo[1,2-*a*]azocin-8-ol (**123**) and (7*S*,8*R*,10*aS*)-octahydro-1*H*-8,10*a*-epoxy pyrrolo[1,2-*a*]azocin-7-ol (**124**)



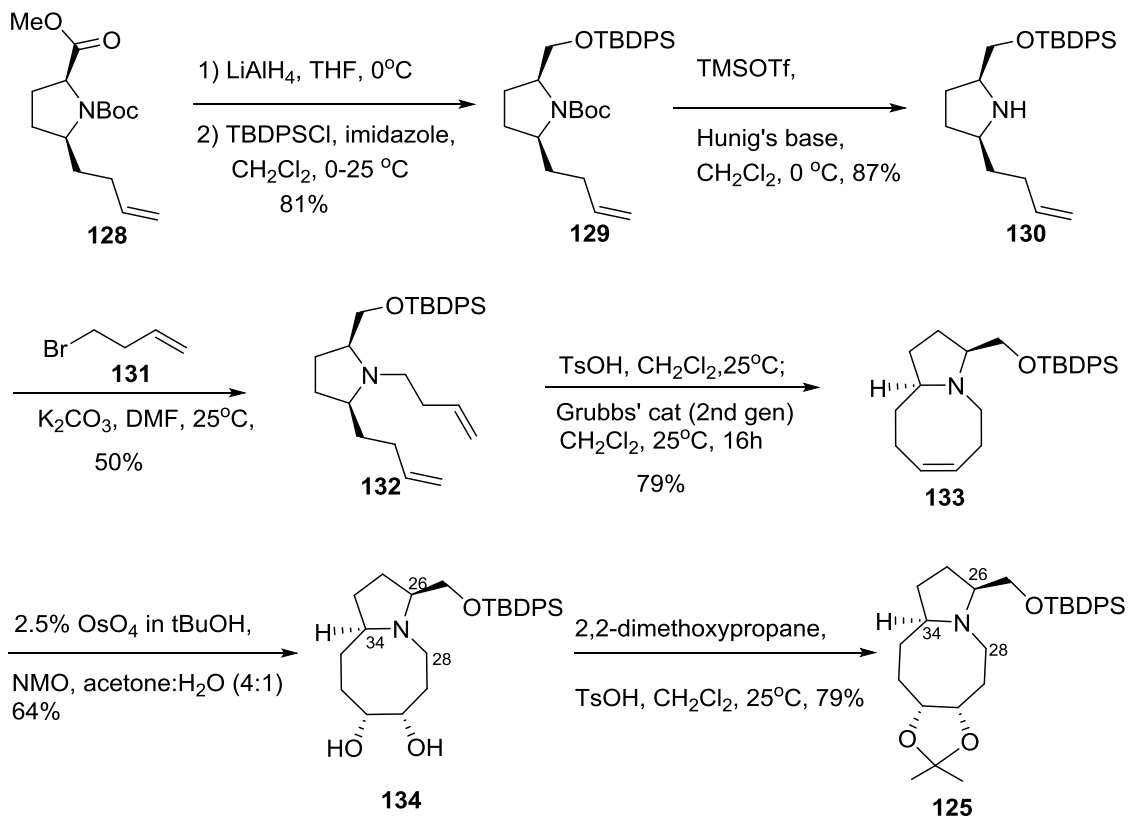
A solution of **121** and **122** (0.05 g, 0.119 mmol, 1eq.) and pyridine (150 μL) in THF (300 μL) was cooled down to 0°C. HF.Py (70%HF) (150 μL) was then added and the reaction was stirred at 25°C for 16h. Sat. NaHCO_3 (5mL) was then added. The mixture was extracted with 25%isopropanol/ CHCl_3 (5 mL) three times. The combined organic layer was washed with brine (2 mL) and concentrated under reduced pressure to afford a mixture of **123** and **124** (0.018 g, 87%yield). ^1H NMR (500 MHz, Chloroform-*d*) δ 4.02 (d, $J = 7.3$ Hz, 1H), 3.73 – 3.62 (m, 1H), 3.58 – 3.48 (m, 1H), 3.21 (h, $J = 7.4, 6.7$ Hz, 1H), 2.94 (t, $J = 8.6$ Hz, 1H), 2.87 – 2.74 (m, 1H), 2.36 (ddt, $J = 18.1, 14.2, 5.8$ Hz, 2H), 2.16 (dq, $J = 13.7, 6.8$ Hz, 1H), 2.13 – 2.00 (m, 1H), 1.93 – 1.78 (m, 2H), 1.81 – 1.68 (m, 2H), 1.72 – 1.58 (m, 1H), 1.24 – 1.12 (m, 1H). ^{13}C NMR (126 MHz, Chloroform-*d*) δ 89.59, 73.81, 67.93, 52.59, 41.81, 40.36, 29.01, 27.42, 20.70, 19.99. FTIR (CHCl_3 film): 3303.46, 2959.23, 1258.32 cm^{-1} . HRMS: $[\text{M}+\text{H}]^+$ calc. 184.1338, found 184.1346.

2.6.3. Procedure for acid-catalyzed dimerization of model **123** and **124**

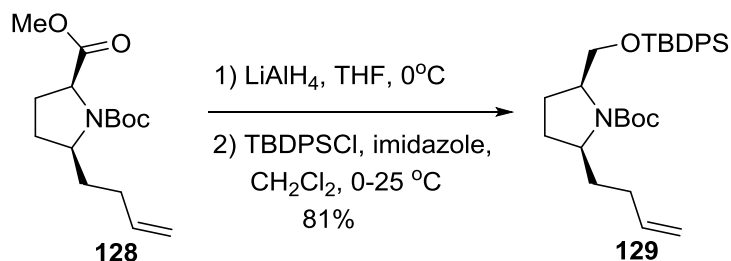


A mixture of **123** and **124** (0.01 g, 0.05 mmol, 1 eq.) with catalytic amount of TFA in toluene (100 μ L) was heated up to 50°C for 16h. The mixture was then cooled down to 25°C and concentrated under reduced pressure to afford the product **96** in quantitative yield. ^1H NMR (500 MHz, Chloroform-*d*) δ 4.28 (ddt, J = 8.8, 4.0, 1.9 Hz, 1H), 3.88 – 3.80 (m, 1H), 3.57 (dt, J = 11.4, 5.8 Hz, 1H), 3.46 – 3.33 (m, 3H), 3.29 (q, J = 2.8 Hz, 1H), 3.09 (t, J = 12.3 Hz, 1H), 2.93 – 2.82 (m, 2H), 2.58 (dt, J = 11.3, 7.1 Hz, 1H), 2.51 (ddd, J = 12.5, 9.4, 5.6 Hz, 1H), 2.39 (ddd, J = 11.2, 8.6, 6.4 Hz, 1H), 2.20 (dddd, J = 15.5, 11.3, 7.4, 3.5 Hz, 1H), 2.12 (ddt, J = 16.4, 11.9, 2.0 Hz, 1H), 2.01 – 1.62 (m, 14H), 1.63 – 1.54 (m, 1H), 1.52 – 1.45 (m, 1H), 1.40 (ddq, J = 14.8, 9.7, 4.8 Hz, 1H). ^{13}C NMR (126 MHz, Chloroform-*d*) δ 108.24, 95.40, 86.20, 71.93, 70.12, 65.73, 55.78, 53.94, 45.50, 43.59, 39.02, 37.13, 36.11, 28.20, 25.72, 24.95, 23.51, 22.86, 20.78, 20.16. FTIR (CHCl₃ film): 3388.32, 1425.14, 1200.47, 1129.12 cm^{-1} . HRMS: $[\text{M}+\text{H}]^+$ calc. 367.2597, found 367.2343.

2.6.4. Procedure for the synthesis of model system **125**



tert-butyl (2S,5S)-2-(but-3-en-1-yl)-5-(((tert-butyldiphenylsilyl)oxy)methyl)pyrrolidine-1-carboxylate
(129)



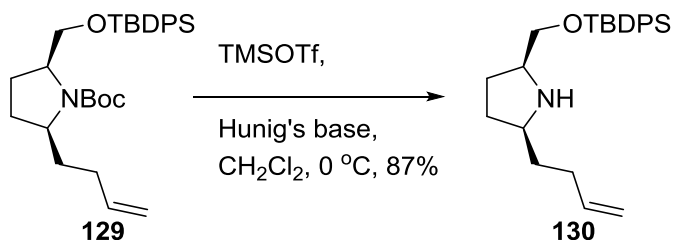
Step1: A solution of **128** (prepared in 3 steps from L-pyrroglutamic acid methyl ester⁴³) (0.21 g, 0.741 mmol, 1 eq.) in THF (15 mL) was cooled to 0°C under argon before adding LiAlH₄ (0.042 g, 1.11 mmol, 1.5 eq.). The mixture was stirred at 0°C for 45 min. An aqueous solution of saturated Potassium sodium tartrate (aq) (5 mL) was then added and the mixture was stirred vigorously for 15 min. The mixture was diluted in EtOAc (20 mL) and the layers were separated. The organic layer was wash with brine (10 mL) and concentrated under reduced pressure. The resulting colorless oil was used in the next step without further purification.

Step2: Imidazole (0.1 g, 1.48 mmol, 2 eq.) and TBDPSCI (0.3g, 1.11 mmol, 1.5 eq.) were added to a solution of the residue from step 1 in CH₂Cl₂ (5 mL) at 0°C. The mixture was allowed to warm to 25°C and stirred at 25°C for 16h. The reaction was then quenched with saturated aqueous NH₄Cl (5 mL). The layers were separated. The aqueous layer was extracted three times with CH₂Cl₂ (5 mL). The combined organic layer was washed with brine (10mL), dried over Na₂SO₄ and concentrated under reduced pressure. The residue was purified by silica gel chromatography (5% EtOAc/Hexane) to yield **129** as a colorless oil (0.296 g, 81% yield). ¹H NMR (500 MHz, Chloroform-*d*) δ 7.74 – 7.65 (m, 4H), 7.41 (dt, *J* = 13.5, 7.0 Hz, 7H), 5.89 – 5.72 (m, 1H), 5.13 – 4.87 (m, 2H), 4.07 – 3.40 (m, 3H), 2.22 – 1.80 (m, 7H), 1.73 – 1.56 (m, *J* = 6.2, 5.4 Hz, 1H), 1.55 – 1.25 (m, 9H), 1.16 – 1.04 (m, 10H). ¹³C NMR (126 MHz, Chloroform-*d*) δ 154.97, 138.49, 135.65, 133.70, 129.69, 127.74, 114.48, 79.12, 59.72, 58.53, 34.57, 30.88, 28.57, 26.97, 19.37. FTIR (CHCl₃ film): 3071.57,

2961.64, 2857.99, 2278.97, 1958.84, 1887.97, 1823.37, 1694.16, 1392.35, 1173.95, 1112.24 cm⁻¹

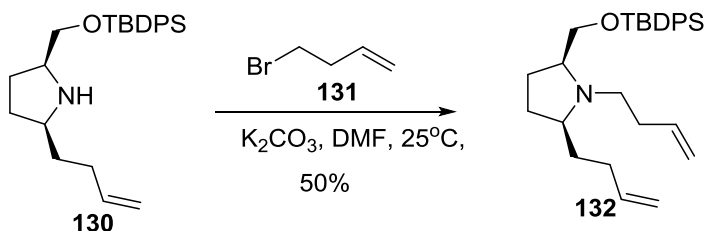
¹. HRMS: [M+H]⁺ calc. 494.3090, found 494.3093.

(2*S*,5*S*)-2-(but-3-en-1-yl)-5-(((*tert*-butyldiphenylsilyl)oxy)methyl)pyrrolidine (**130**)



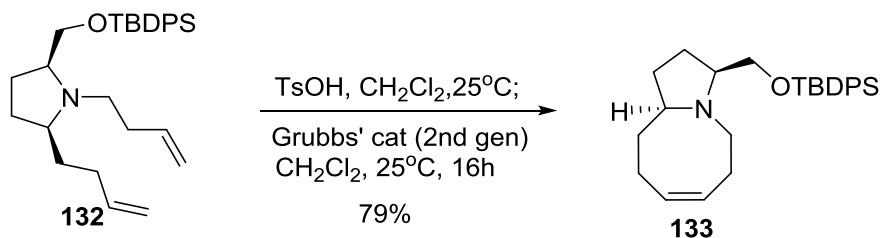
A solution of **129** (0.42 g, 0.85 mmol, 1 eq.), Hunig's base (0.22 g, 1.7 mmol, 2eq.) in CH₂Cl₂ (6 mL) was cooled to 0°C. TMSOTf (0.27 g, 1.02 mmol, 1.2 eq.) was then added and the mixture was stirred at 0°C for 1h. The reaction was then quenched with sat. NaHCO₃ (aq) (10 mL). The layers were then separated. The aqueous layer was extracted with CH₂Cl₂ (5 mL) three times. The combined organic layers were washed with sat. NH₄Cl (aq.) (10 mL) and brine (10 mL), dried over Na₂SO₄ and concentrated under reduced pressure. The residue was purified by silica gel chromatography (10% EtOAc/Hexane) to yield **130** as a colorless oil (0.29 g, 87% yield). ¹H NMR (500 MHz, Chloroform-*d*) δ 7.75 – 7.63 (m, 4H), 7.48 – 7.33 (m, 6H), 5.84 (ddt, *J* = 16.8, 10.1, 6.6 Hz, 1H), 5.04 (dq, *J* = 17.1, 1.7 Hz, 1H), 4.97 (ddt, *J* = 10.2, 2.1, 1.3 Hz, 1H), 3.73 (dd, *J* = 10.1, 4.8 Hz, 1H), 3.64 (dd, *J* = 10.2, 5.4 Hz, 1H), 3.28 (tt, *J* = 7.4, 5.1 Hz, 1H), 3.08 (dq, *J* = 8.7, 6.7 Hz, 1H), 2.71 (s, 1H), 2.13 (tddd, *J* = 8.0, 6.2, 2.9, 1.2 Hz, 1H), 1.89 (dddd, *J* = 11.9, 8.6, 6.6, 4.8 Hz, 1H), 1.77 (ddt, *J* = 12.6, 8.6, 7.4 Hz, 1H), 1.63 (dddd, *J* = 16.0, 9.9, 7.9, 4.5 Hz, 2H), 1.54 (ddd, *J* = 13.1, 6.6, 2.2 Hz, 1H), 1.39 – 1.27 (m, 1H), 1.08 (s, 9H). ¹³C NMR (126 MHz, Chloroform-*d*) δ 138.71, 135.80, 133.77, 133.75, 129.85, 127.88, 127.85, 114.75, 66.89, 60.35, 59.37, 35.72, 31.81, 31.63, 27.55, 27.11, 27.05, 19.49. FTIR (CHCl₃ film): 3366.14, 2929.34, 2856.06, 1642.09, 1427.07, 1111.76 cm⁻¹. HRMS: [M+H]⁺ calc. 394.2566, found 394.2565.

(2*S*,5*S*)-1,2-di(*but-3-en-1-yl*)-5-(((*tert-butyl*diphenylsilyl)oxy)methyl)pyrrolidine (**132**)



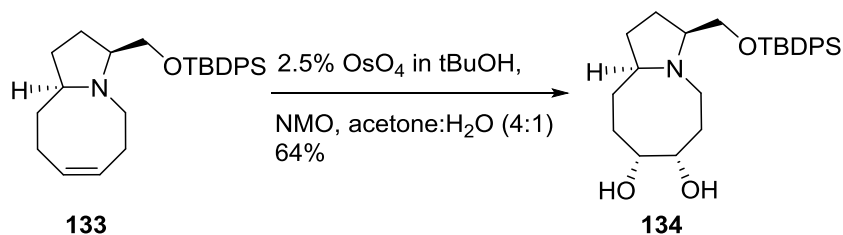
A mixture of **130** (0.25 g, 0.635 mmol, 1 eq.), 4-bromo-1-butene (**131**) (0.129 g, 0.953 mmol, 1.5 eq.) and K_2CO_3 (0.263 g, 1.905 mmol, 3 eq.) in DMF (10 mL) was stirred at 25°C for 16h. H_2O (20 mL) was then added and the mixture was extracted three times with EtOAc (3 x 10mL). The combined organic layers were washed two times with H_2O (15 mL) and brine (15 mL). The crude product was dried over Na_2SO_4 and concentrated under reduced pressure. The residue was purified by silica gel chromatography (3% EtOAc/Hexane) to yield **132** as a colorless oil (0.14 g, 50% yield). 1H NMR (500 MHz, Chloroform-*d*) δ 7.78 – 7.70 (m, 4H), 7.49 – 7.38 (m, 6H), 5.86 (ddt, $J = 16.9, 10.2, 6.5$ Hz, 1H), 5.74 (ddt, $J = 17.0, 10.2, 6.7$ Hz, 1H), 5.10 – 4.91 (m, 2H), 3.64 (dd, $J = 10.0, 4.8$ Hz, 1H), 3.44 (dd, $J = 10.0, 8.1$ Hz, 1H), 2.90 (tt, $J = 8.0, 4.7$ Hz, 1H), 2.75 – 2.64 (m, 2H), 2.64 – 2.56 (m, 1H), 2.18 – 1.97 (m, 4H), 1.91 – 1.75 (m, 3H), 1.75 – 1.64 (m, 1H), 1.46 – 1.36 (m, 1H), 1.32 (dtd, $J = 13.2, 9.5, 5.2$ Hz, 1H), 1.12 (s, 9H). ^{13}C NMR (126 MHz, Chloroform-*d*) δ 139.16, 137.12, 137.10, 135.78, 135.75, 134.14, 134.05, 129.65, 127.70, 115.38, 114.22, 114.19, 68.12, 65.57, 64.85, 53.62, 34.82, 32.73, 30.93, 29.79, 27.33, 27.06, 27.03, 19.36. FTIR (CHCl₃ film): 3072.05, 2930.79, 2857.51, 1640.64, 1428.03, 1112.73 cm^{-1} . HRMS: $[M+H]^+$ calc. 448.3036, found 448.3034.

(3*S*,10*aS*,*Z*)-3-(((*tert*-butyldiphenylsilyl)oxy)methyl)-1,2,3,5,6,9,10,10*a*-octahydropyrrolo [1,2-*a*]azocine (**133**)



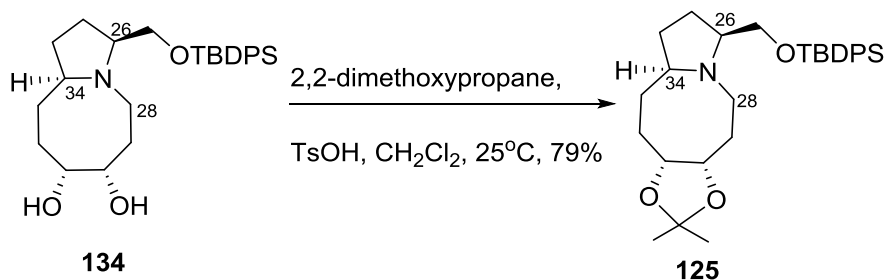
A solution of **132** (0.03 g, 0.0628 mmol, 1 eq.) in CH₂Cl₂ (13 mL) was degassed by bubbling through argon gas for 30 min before adding TsOH (0.01 g, 0.0628 mmol, 1 eq.). The mixture was stirred at 25°C for 30 min before adding Grubbs' cat (2nd Gen) (0.006 g, 0.0063 mmol, 0.1 eq.). The mixture was stirred at 25°C under argon atmosphere for 24h. Sat. NaHCO₃ (aq) (5 mL) was then added. The mixture was then extracted with CH₂Cl₂ (5 mL) three times. The combined organic layers were then washed with brine (5 mL), dried over Na₂SO₄ and concentrated under reduced pressure. The residue was purified by silica gel chromatography (gradient: 20-100% EtOAc/Hexane) to yield **133** as a colorless oil (0.02 g, 79% yield). ¹H NMR (500 MHz, Chloroform-*d*) δ 7.77 – 7.70 (m, 4H), 7.46 – 7.35 (m, 6H), 5.74 – 5.57 (m, 2H), 3.69 (dd, *J* = 9.9, 5.1 Hz, 1H), 3.55 (dd, *J* = 9.9, 6.1 Hz, 1H), 2.88 (tq, *J* = 15.3, 5.4, 4.4 Hz, 2H), 2.81 (td, *J* = 9.1, 5.0 Hz, 1H), 2.59 (tdd, *J* = 11.9, 7.8, 5.8 Hz, 1H), 2.41 – 2.25 (m, 2H), 2.09 – 1.97 (m, 1H), 1.94 – 1.80 (m, 3H), 1.56 – 1.45 (m, 1H), 1.45 – 1.36 (m, 1H), 1.36 – 1.25 (m, 2H), 1.08 (s, 9H). ¹³C NMR (126 MHz, Chloroform-*d*) δ 135.81, 135.79, 134.15, 130.97, 129.62, 129.53, 127.70, 69.61, 68.73, 63.17, 55.46, 36.70, 30.61, 29.83, 28.31, 26.97, 23.98, 19.36. FTIR (CHCl₃ film): 3012.75, 2929.82, 2857.02, 1471.9, 1428.03, 1112.73 cm⁻¹. HRMS: [M+H]⁺ calc. 420.2723, found 420.2728.

(3*S*,10*aR*)-3-(((*tert*-butyldiphenylsilyl)oxy)methyl)decahydropyrrolo[1,2-*a*]azocine-7,8-diol (**134**)



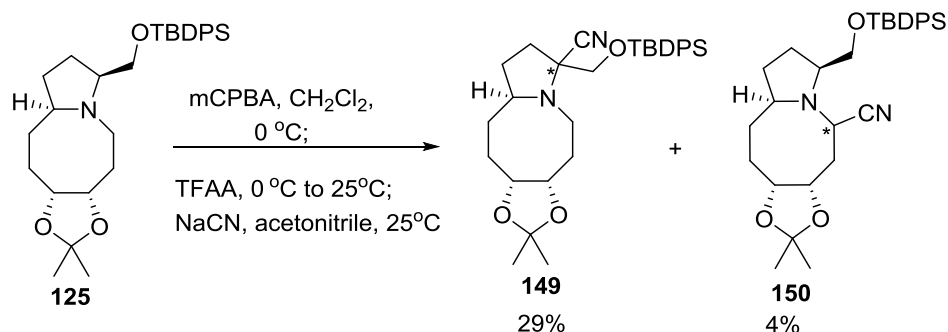
A solution of **133** (0.03 g, 0.0715 mmol, 1 eq.) in acetone:H₂O (4:1)(1mL) was cooled to 0°C. 2.5% OsO₄ in tBuOH (0.002 g, 0.007 mmol, 0.1 eq.) and NMO (0.01 g, 0.079 mmol, 1.1 eq.) were added and the mixture was stirred at 0°C under argon atmosphere for 30 min. Solid Na₂SO₃ (0.1 g) was then added and the mixture was stirred at 25°C for 10 min. The solvent was removed under reduced pressure. The residue was extracted with CH₂Cl₂ (5 mL) three times. The combined organic layers were then washed with brine (5 mL), dried over Na₂SO₄ and concentrated under reduced pressure. The residue was purified by silica gel (gradient 10-80% EtOAc/Hexane) to yield **134** as a colorless oil (0.02 g, 64% yield). ¹H NMR (500 MHz, Chloroform-*d*) δ 7.68 (ddq, *J* = 8.1, 5.9, 2.1 Hz, 4H), 7.46 – 7.34 (m, 6H), 3.93 (d, *J* = 7.4 Hz, 1H), 3.73 (dd, *J* = 10.4, 5.5 Hz, 1H), 3.67 (s, 1H), 3.63 (dd, *J* = 10.4, 5.8 Hz, 1H), 3.34 (s, 1H), 3.14 (ddd, *J* = 13.2, 12.0, 3.7 Hz, 1H), 2.91 (ddt, *J* = 11.7, 8.8, 2.9 Hz, 1H), 2.79 (dq, *J* = 9.3, 5.6 Hz, 1H), 2.19 (ddd, *J* = 12.0, 4.6, 2.7 Hz, 1H), 2.05 – 1.87 (m, 2H), 1.86 – 1.73 (m, 3H), 1.66 (dddd, *J* = 12.4, 11.0, 9.4, 6.9 Hz, 1H), 1.55 (dq, *J* = 14.2, 3.6 Hz, 1H), 1.47 – 1.34 (m, 2H), 1.07 (s, 9H). ¹³C NMR (126 MHz, Chloroform-*d*) δ 135.70, 133.53, 133.51, 129.80, 127.81, 70.70, 69.88, 68.60, 66.34, 61.00, 47.85, 32.97, 31.23, 30.68, 28.08, 27.74, 26.95, 26.92, 19.3. FTIR (CHCl₃ film): 3397.96, 3070.12, 3048.91, 2930.31, 2857.02, 1668.12, 1589.06, 1471.42, 1428.03 cm⁻¹. HRMS: [M+H]⁺ calc. 454.2777, found 454.2780.

(7*S*,9*aR*)-7-(((*tert*-butyldiphenylsilyl)oxy)methyl)-2,2-dimethyldecahydro-[1,3]dioxolo[4,5-*e*]pyrrolo[1,2-*a*]azocine (**125**)



A mixture of **134** (0.015 g, 0.033 mmol, 1 eq.), 2,2-dimethoxypropane (0.034 g, 0.33 mmol, 10 eq.) and TsOH (0.006 g, 0.033 mmol, 1 eq.) in CH₂Cl₂ (1 mL) was stirred at 25°C for 30 min. Sat. NaHCO₃ (aq) (5 mL) was added. The mixture was extracted with CH₂Cl₂ (5 mL) three times. The combined organic layers were then washed with brine (5 mL), dried over Na₂SO₄ and concentrated under reduced pressure. The residue was purified by silica gel (5% EtOAc/Hexane) to yield **125** as a colorless oil (0.19 g, 79% yield). ¹H NMR (500 MHz, Chloroform-*d*) δ 7.85 – 7.62 (m, 4H), 7.55 – 7.32 (m, 6H), 4.17 (dd, *J* = 11.1, 6.0 Hz, 1H), 4.10 (ddd, *J* = 11.4, 6.0, 2.6 Hz, 1H), 3.64 (dd, *J* = 10.1, 5.2 Hz, 1H), 3.54 (dd, *J* = 10.0, 5.5 Hz, 1H), 2.99 (ddd, *J* = 12.9, 4.8, 3.0 Hz, 1H), 2.80 (dq, *J* = 10.6, 5.2 Hz, 1H), 2.41 – 2.29 (m, 2H), 2.22 (qd, *J* = 12.9, 3.9 Hz, 1H), 2.04 (dtd, *J* = 14.5, 11.6, 2.9 Hz, 1H), 1.96 – 1.87 (m, 1H), 1.84 (dq, *J* = 12.1, 6.6, 6.2 Hz, 1H), 1.77 (dq, *J* = 13.3, 3.4 Hz, 1H), 1.54 – 1.45 (m, 2H), 1.42 (s, 3H), 1.41 – 1.36 (m, 2H), 1.34 (s, 3H), 1.27 (ddd, *J* = 16.9, 8.4, 3.8 Hz, 1H), 1.07 (s, 9H). ¹³C NMR (126 MHz, Chloroform-*d*) δ 135.75, 135.70, 134.02, 133.98, 129.66, 127.78, 127.72, 105.73, 80.76, 69.43, 68.29, 63.58, 54.97, 34.66, 34.05, 30.96, 28.21, 28.03, 26.97, 26.95, 25.27, 24.84, 19.32. FTIR (CHCl₃ film): 2931.27, 2857.99, 1651.73, 1428.03, 1365.35, 1112.73 cm⁻¹. HRMS: [M+H]⁺ calc. 494.3090, found 494.3107.

2.6.5. Procedure for Polonovski-Potier reaction of the model system **125**



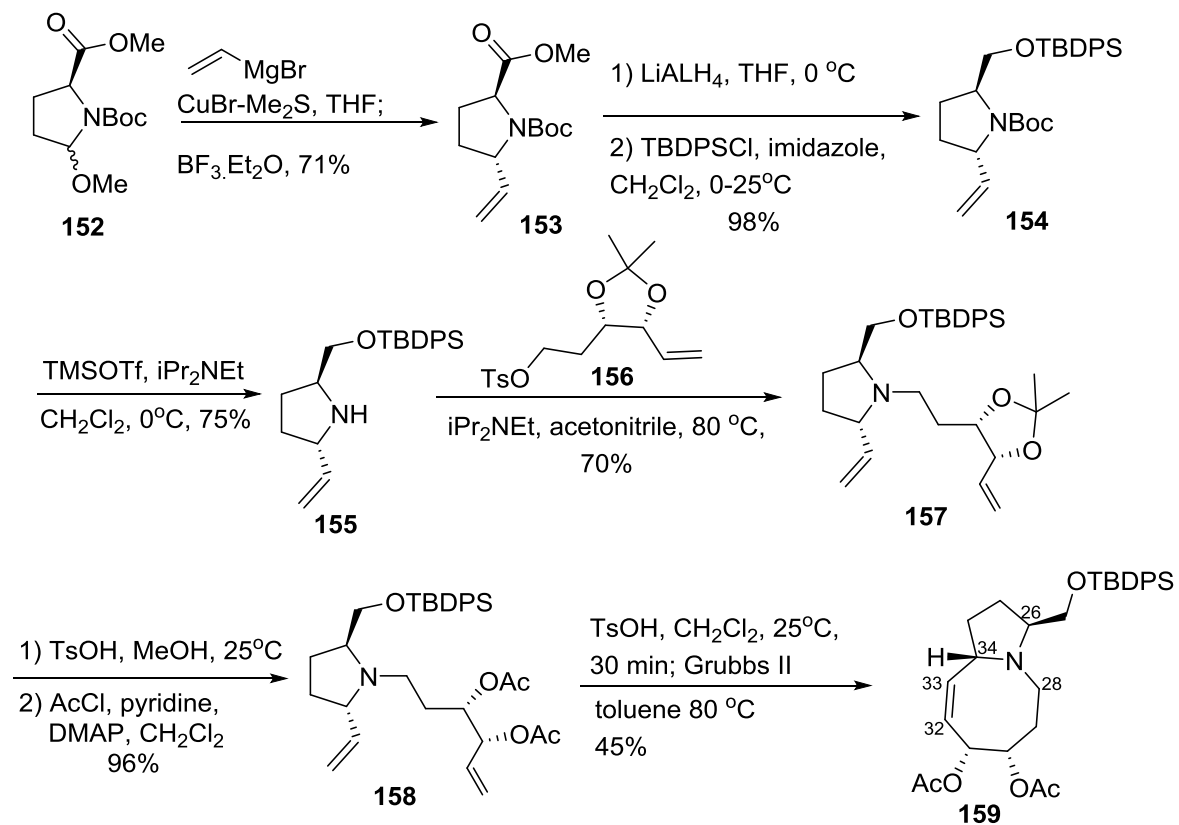
A solution of **125** (0.05 g, 0.1 mmol, 1eq.) in CH₂Cl₂ (1 mL) was cooled to 0°C and treated with *m*CPBA (0.021 g, 0.12 mmol, 1.2 eq.) The reaction was stirred at 0°C until the starting material was all consumed (monitored by TLC, mobile phase: 20% EtOAc/Hexane, R_f = 0.4). TFAA (0.042 g, 0.2 mmol, 2eq.) was then added and the reaction was allowed to warm to 25°C and stirred at 25°C until the preformed N-oxide was all consumed (monitored by LCMS). The solvent and excess TFAA were removed under reduced pressure. The residue was dissolved in acetonitrile (1 mL). NaCN (0.01 g, 0.15 mmol, 1.5 eq.) was added and the mixture was stirred at 25°C for 16h. To the reaction was then added sat. NaHCO₃ (aq.) (5 mL) and the aqueous layer was extracted three times with EtOAc (5 mL). The combined organic layers were then washed with brine, dried over Na₂SO₄ and concentrated under reduced pressure. The residue was purified by preparative TLC (5% Et₂O/Hexane) to yield **149** (0.015 g, 29% yield) and **150** (0.002 g 4% yield).

Compound 149: ¹H NMR (500 MHz, Chloroform-*d*) δ 7.69 (td, *J* = 7.6, 1.5 Hz, 4H), 7.49 – 7.32 (m, 6H), 4.13 (dd, *J* = 10.9, 6.0 Hz, 1H), 4.08 (ddd, *J* = 11.4, 6.0, 2.7 Hz, 1H), 3.73 (d, *J* = 10.0 Hz, 1H), 3.56 (d, *J* = 9.9 Hz, 1H), 3.07 (ddd, *J* = 13.2, 5.1, 2.9 Hz, 1H), 2.65 (t, *J* = 12.5 Hz, 1H), 2.55 (ddd, *J* = 12.4, 8.2, 4.2 Hz, 1H), 2.33 – 2.18 (m, 2H), 2.00 (dddd, *J* = 26.3, 14.9, 12.5, 3.3 Hz, 2H), 1.89 – 1.73 (m, 2H), 1.64 – 1.55 (m, 3H), 1.51 (dd, *J* = 12.2, 6.2 Hz, 1H), 1.39 (s, 3H), 1.32 (s, 3H), 1.08 (s, 9H). ¹³C NMR (126 MHz, Chloroform-*d*) δ 135.79, 135.77, 134.94, 132.86, 132.74, 130.09, 128.00, 127.98, 127.86, 119.67, 106.17, 80.14, 77.81, 70.46, 68.93, 63.02, 52.31, 33.73, 33.69,

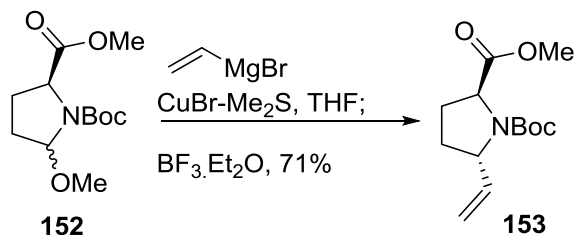
30.60, 28.16, 26.83, 25.27, 24.44, 19.38. FTIR (CHCl₃ film): 2932.23, 1428.03, 1112.73, 1046.19 cm⁻¹. HRMS: [M+H]⁺ calc. 519.3043, found 519.3040.

Compound 150: ¹H NMR (500 MHz, Chloroform-*d*) δ 7.67 (ddt, *J* = 15.6, 6.5, 1.6 Hz, 4H), 7.49 – 7.36 (m, 6H), 4.48 (dd, *J* = 11.1, 5.9 Hz, 1H), 4.40 (t, *J* = 4.0 Hz, 1H), 4.13 (ddd, *J* = 11.5, 5.9, 2.8 Hz, 1H), 3.68 (dd, *J* = 10.3, 3.7 Hz, 1H), 3.59 – 3.49 (m, 1H), 3.19 – 3.08 (m, 1H), 2.84 – 2.73 (m, 1H), 2.25 (ddd, *J* = 15.1, 11.3, 3.8 Hz, 1H), 2.03 (dd, *J* = 17.9, 10.4 Hz, 2H), 1.88 – 1.69 (m, 3H), 1.47 – 1.41 (m, 3H), 1.41 (s, 3H), 1.33 (s, 3H), 1.26 (s, 1H), 1.04 (s, 9H). ¹³C NMR (126 MHz, Chloroform-*d*) δ 135.73, 135.70, 133.24, 130.00, 127.96, 118.67, 106.34, 77.75, 76.26, 68.91, 67.08, 59.92, 54.02, 36.00, 30.99, 30.69, 28.08, 27.00, 26.94, 25.06, 24.71, 19.26. HRMS: [M+H]⁺ calc. 519.3043, found 519.3042.

2.6.6. Procedure for the synthesis of model system **159**

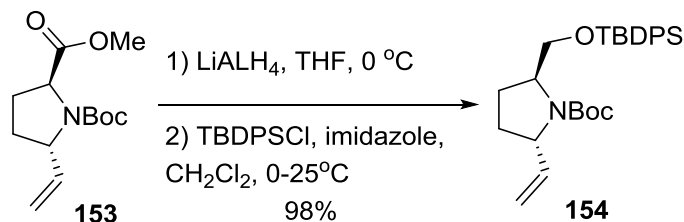


1-(*tert*-butyl) 2-methyl (2*S*,5*S*)-5-vinylpyrrolidine-1,2-dicarboxylate (**153**)



Under argon atmosphere, 1 M vinyl bromide in THF (36.1 mL, 36.1 mmol, 4 eq.) was added to Mg° (turnings) (1.05 g, 43.3 mmol, 4.8 eq.) and small amount of iodine. The mixture was heated to reflux for 1h. The resulting vinyl magnesium bromide solution was then cooled to 25°C before being transferred to a suspension of $\text{CuBr-Me}_2\text{S}$ (7.1 g, 34.56 mmol, 3.83 eq.) in THF (20 mL) at -40°C. The resulting mixture was stirred for 45 min at -40°C. The reaction mixture was cooled to -78°C and $\text{BF}_3\cdot\text{Et}_2\text{O}$ (4.45 ml, 36.096 mmol, 4 eq.) was added. After 30 min, compound **152** (prepared in 3 steps from L-pyrroglutamic acid methyl ester⁵⁰) (2.34 g, 9.024 mmol, 1eq.) in THF (15 mL) was added and the solution was stirred at -78°C for 2 h and at 25°C for 2 h. The mixture of sat. aq. NH_4Cl (22 mL) and conc. NH_4OH (3 mL) was added and the solution was stirred at 25°C for 45 min. The reaction mixture was diluted with EtOAc (100 mL), washed with water (3x30 mL), brine (30 mL) and was dried over Na_2SO_4 . After the solvent was evaporated under reduced pressure, the residue (3 g) was purified by silica gel chromatography (10% EtOAc/Hexane) to yield **153** as a colorless oil (1.63 g, 71% yield). ^1H NMR (500 MHz, Chloroform-*d*) δ 5.84 – 5.66 (m, 1H), 5.15 – 4.98 (m, 2H), 4.50 (dt, $J = 59.3, 7.0$ Hz, 1H), 4.41 – 4.26 (m, 1H), 3.72 (dd, $J = 4.0, 1.8$ Hz, 4H), 2.29 – 2.11 (m, 2H), 1.97 – 1.87 (m, 1H), 1.76 – 1.62 (m, 1H), 1.41 (dd, $J = 10.4, 1.7$ Hz, 12H). ^{13}C NMR (126 MHz, Chloroform-*d*) δ 173.71, 173.38, 154.49, 153.57, 138.48, 137.96, 114.25, 114.02, 80.14, 80.09, 59.76, 59.59, 59.21, 52.25, 52.09, 30.11, 29.33, 28.44, 28.41, 28.39, 27.43. FTIR (CHCl_3 film): 2977.55, 1749.12, 1698.02, 1390.42, 1166.72 cm^{-1} . HRMS: $[\text{M}+\text{Na}]^+$ calc. 278.1368, found 278.1367.

tert-butyl (2S,5S)-2-(((tert-butyl)diphenylsilyl)oxy)methyl)-5-vinylpyrrolidine-1-carboxylate (154)

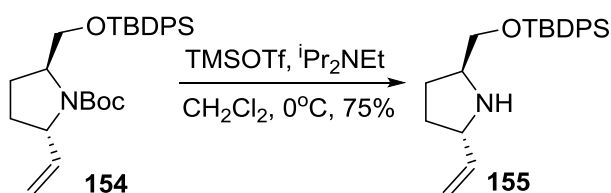


Step1: A solution of **153** (0.9 g, 3.525 mmol, 1 eq.) in THF (40 mL) was cooled to 0°C and treated with LiAlH₄ (0.2 g, 5.29 mmol, 1.5 eq.). The mixture was stirred at 0°C for 1h before adding sat. Rochelle salt solution (20 mL). The mixture was allowed to warm to 25°C and stirred vigorously at 25°C for 30 min. The mixture was then diluted with EtOAc (50mL). The layers were then separated. The aqueous layer was extracted with EtOAc (10mL) for three times. The combined organic layer was washed with brine (15 mL), dried over Na₂SO₄ and concentrated under reduced pressure. The resulting residue was used in the next step without further purification. ¹H NMR (500 MHz, Chloroform-*d*) δ 5.71 (ddd, *J* = 16.8, 10.8, 6.4 Hz, 1H), 5.11 – 4.93 (m, 2H), 4.45 – 4.19 (m, 2H), 4.15 – 4.03 (m, 1H), 3.78 – 3.65 (m, 1H), 3.65 – 3.54 (m, 1H), 2.12 – 1.99 (m, 2H), 1.69 – 1.54 (m, 1H), 1.49 (t, *J* = 5.2 Hz, 1H), 1.43 (d, *J* = 9.2 Hz, 9H). ¹³C NMR (126 MHz, Chloroform-*d*) δ 156.91, 138.36, 113.93, 67.99, 60.97, 60.11, 30.2, 28.48, 26.41.

Step2: The residue from the first step was dissolved in CH₂Cl₂ (15 mL) and cooled to 0°C. Imidazole (0.58 g, 8.6 mmol, 2.5 eq.) and TBDPSCl (1.9 g, 6.86 mmol, 2 eq.) were then added. The reaction was allowed to warm to 25°C and stirred at 25°C for 12h. Sat. NH₄Cl (aq) solution (10 mL) was then added. The mixture was extracted with CH₂Cl₂ (5 mL) three times. The combined organic layer was then washed with brine, dried over Na₂SO₄ and concentrated under reduced pressure. The residue was purified by silica gel chromatography (3% EtOAc/Hexane) to yield **154** as a colorless oil (1.6 g, 98% yield). ¹H NMR (500 MHz, Chloroform-*d*) δ 7.72 – 7.59 (m, 4H), 7.48 – 7.33 (m, 6H), 5.78 (dddd, *J* = 21.1, 16.7, 10.3, 5.8 Hz, 1H), 5.12 – 4.95 (m, 2H), 4.33 (dt, *J* = 44.5, 7.0 Hz, 1H), 4.10 – 3.89 (m, 1H), 3.86 – 3.45 (m, 2H), 2.30 – 1.93 (m, 3H), 1.61 (ddd, *J* = 17.0, 12.1, 6.1 Hz,

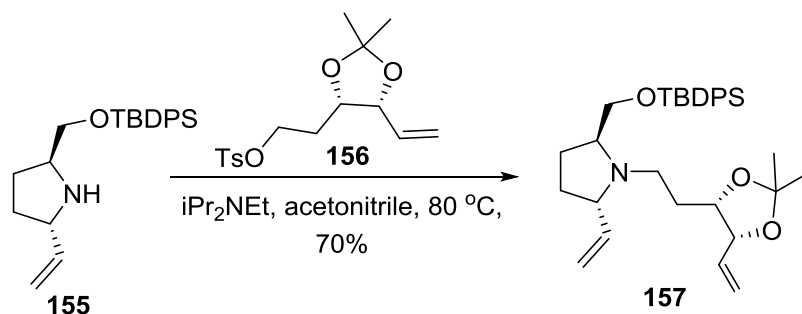
1H), 1.38 (d, $J = 52.9$ Hz, 9H), 1.08 (d, $J = 1.7$ Hz, 9H). ^{13}C NMR (126 MHz, Chloroform- d) δ 154.28, 153.76, 139.30, 138.37, 135.69, 135.67, 135.65, 135.62, 134.93, 133.88, 133.80, 133.70, 133.55, 129.78, 129.64, 127.84, 127.80, 127.74, 127.72, 113.53, 113.35, 64.09, 63.86, 60.27, 59.65, 58.78, 58.68, 31.71, 30.21, 28.82, 28.54, 28.49, 26.98, 26.69, 25.81, 25.56, 19.41, 19.37. FTIR (CHCl₃ film): 3071.08, 2961.16, 2931.27, 2857.99, 1693.19, 1387.53, 1111.76 cm⁻¹. HRMS: [M+H]⁺ calc. 466.2777, found 466.2793.

(2*S*,5*S*)-2-(((*tert*-butyldiphenylsilyl)oxy)methyl)-5-vinylpyrrolidine (**155**)



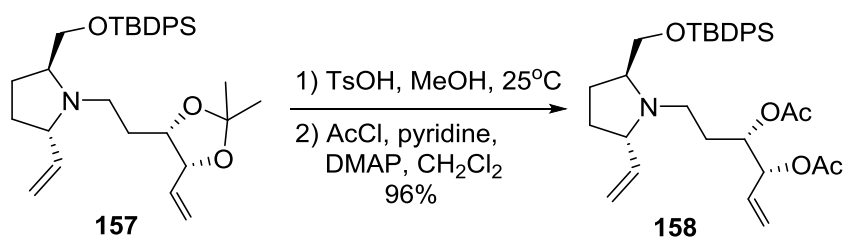
A solution of **154** (1.597 g, 3.43 mmol, 1 eq.) and Hunig's base (0.89 g, 6.86 mmol, 2eq.) in CH₂Cl₂ (6 mL) was cooled to 0°C. TMSOTf (0.915 g, 4.12 mmol, 1.2 eq.) was then added and the mixture was stirred at 0°C for 1h. The reaction was then quenched with sat. NaHCO₃ (aq) (10 mL). The layers were then separated. The aqueous layer was extracted with CH₂Cl₂ (5 mL) three times. The combined organic layer was washed with brine (10 mL), dried over Na₂SO₄ and concentrated under reduced pressure. The residue was purified by silica gel chromatography (10-50% EtOAc/Hexane) to yield **155** as a colorless oil (0.94 g, 75% yield). ^1H NMR (500 MHz, Chloroform- d) δ 7.71 – 7.62 (m, 4H), 7.47 – 7.34 (m, 6H), 5.81 (dddd, $J = 17.2, 10.1, 7.1, 1.4$ Hz, 1H), 5.10 (dt, $J = 17.1, 1.4$ Hz, 1H), 4.99 (dq, $J = 10.1, 1.3$ Hz, 1H), 3.63 – 3.49 (m, 3H), 3.44 (p, $J = 6.3$ Hz, 1H), 2.00 – 1.83 (m, 3H), 1.58 – 1.37 (m, 2H), 1.07 (d, $J = 1.3$ Hz, 9H). ^{13}C NMR (126 MHz, Chloroform- d) δ 141.83, 135.73, 133.79, 129.78, 127.82, 113.99, 67.12, 60.08, 59.15, 32.19, 27.49, 27.04, 19.42. FTIR (CHCl₃ film): 3071.08, 2959.23, 2930.31, 2857.51, 1589.06, 1471.9, 1427.55, 1112.73 cm⁻¹. HRMS: [M+H]⁺ calc. 366.2253, found 366.2264.

(2*S*,5*S*)-2-(((*tert*-butyldiphenylsilyl)oxy)methyl)-1-(2-(((4*S*,5*R*)-2,2-dimethyl-5-vinyl-1,3-dioxolan-4-yl)ethyl)-5-vinylpyrrolidine (**157**)



A mixture of **155** (0.34 g, 0.93 mmol, 1 eq.), **156**⁵¹ (0.33 g, 1 mmol, 1.1 eq.), Hunig's base (0.24 g, 1.86 mmol, 2 eq.) in acetonitrile (10 mL) was heated to 80°C for 16h. The reaction was cooled down to 25°C and concentrated under reduced pressure. The residue was purified by silica gel chromatography (2-5% EtOAc/CH₂Cl₂) to yield **157** as a colorless oil (0.34 g, 70% yield). ¹H NMR (500 MHz, Chloroform-*d*) δ 7.68 (dddd, *J* = 8.0, 6.5, 3.1, 1.4 Hz, 4H), 7.45 – 7.33 (m, 6H), 5.73 (dddd, *J* = 16.9, 12.7, 10.2, 8.5 Hz, 2H), 5.23 – 5.05 (m, 4H), 4.40 (dd, *J* = 7.8, 6.3 Hz, 1H), 4.12 – 4.08 (m, 1H), 3.65 (dd, *J* = 10.1, 4.1 Hz, 1H), 3.50 (ddd, *J* = 12.2, 9.7, 6.6 Hz, 2H), 3.07 (dp, *J* = 10.6, 3.6 Hz, 1H), 2.71 (ddd, *J* = 13.2, 9.0, 4.5 Hz, 1H), 2.60 (ddd, *J* = 12.4, 9.3, 7.0 Hz, 1H), 2.03 – 1.93 (m, 1H), 1.83 – 1.74 (m, 1H), 1.56 (dddd, *J* = 15.6, 12.4, 9.1, 4.0 Hz, 2H), 1.48 – 1.41 (m, 1H), 1.40 (s, 3H), 1.31 – 1.26 (m, 4H), 1.06 (d, *J* = 4.1 Hz, 9H). ¹³C NMR (126 MHz, Chloroform-*d*) δ 139.62, 135.74, 135.70, 135.68, 134.66, 133.91, 133.84, 129.68, 129.63, 127.79, 127.72, 118.19, 116.13, 108.08, 79.82, 65.92, 65.25, 61.97, 45.15, 30.41, 29.63, 28.32, 26.99, 26.66, 25.69, 19.33, 19.33. FTIR (CHCl₃ film): 2931.75, 2857.51, 1472.38, 1428.03, 1112.24 cm⁻¹. HRMS: [M+H]⁺ calc. 520.3247, found 520.3241.

(3*R*,4*S*)-6-((2*S*,5*S*)-2-(((*tert*-butyldiphenylsilyl)oxy)methyl)-5-vinylpyrrolidin-1-yl)hex-1-ene-3,4-diyl diacetate (**158**)

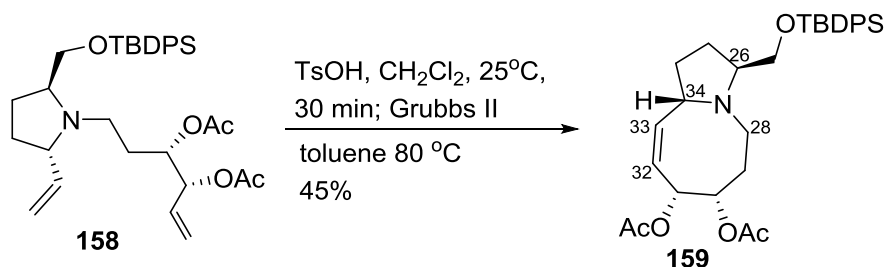


Step 1: A solution of **157** (0.6 g, 1.15 mmol, 1 eq.), TsOH.H₂O (0.5 g, 2.3 mmol, 2eq.) in MeOH (10 mL) was stirred at 25°C under argon atmosphere for 16h. The solvent was removed under reduced pressure. The residue was dissolved in CH₂Cl₂ (10 mL) and neutralized with sat. aq. NaHCO₃ (15 mL). The layers were separated. The aqueous layer was extracted with CH₂Cl₂ (10 mL) three times. The combined organic layer was washed with brine (10 mL), dried over Na₂SO₄ and concentrated under reduced pressure. The resulting colorless oil was used in the next step without further purification.

Step 2: The residue from step 1 was dissolved in CH₂Cl₂ (15 ml). Pyridine (1.9 ml), DMAP (0.014 g, 0.115 mmol, 0.1 eq.) and AcCl (0.361 g, 4.6 mmol, 4eq.) were added to the solution. The resulting mixture was then stirred at 25°C for 6h. H₂O (2 mL) was then added and the mixture was stirred further at 25°C for 15 min. The reaction was neutralized with sat. aq. NaHCO₃ (10 mL). The mixture was extracted with EtOAc (10 mL) three times. The combined organic layer was washed with brine (10 mL), dried over Na₂SO₄ and concentrated under reduced pressure. The residue was purified by silica gel chromatography (10% EtOAc/Hexane) to yield **158** as a colorless oil (0.62 g, 96% yield). ¹H NMR (500 MHz, Chloroform-*d*) δ 7.67 (ddt, *J* = 7.7, 6.0, 1.6 Hz, 4H), 7.49 – 7.35 (m, 6H), 5.83 – 5.57 (m, 2H), 5.43 – 4.99 (m, 4H), 3.65 – 3.37 (m, 2H), 3.05 (qd, *J* = 7.1, 4.1, 3.6 Hz, 1H), 2.68 – 2.45 (m, 1H), 2.11 – 2.03 (m, 3H), 2.03 – 1.92 (m, 1H), 1.92 – 1.84 (m, 3H), 1.76 (ddd, *J* = 9.3, 7.4, 3.1 Hz, 1H), 1.69 – 1.49 (m, 1H), 1.35 – 1.23 (m, 1H), 1.13 – 1.02 (m, 9H). ¹³C NMR (126 MHz, Chloroform-*d*) δ 170.43, 170.03, 139.89, 135.70, 135.68, 133.86, 133.76, 132.23, 129.73

, 127.77 , 127.75 , 119.00 , 115.94 , 71.80 , 65.66 , 65.10 , 61.44 , 43.43 , 31.69 , 30.29 , 27.77 , 26.96 , 26.74 , 20.95 , 19.30. FTIR (CHCl₃ film): 3071.08, 2932.23, 2857.99, 1745.26, 1428.03, 1371.14, 1243.86, 1225.54, 1111.76 cm⁻¹. HRMS: [M+H]⁺ calc. 564.3145, found 564.3139.

(3*S*,7*S*,8*R*,10*aS*,*Z*)-3-(((*tert*-butyldiphenylsilyl)oxy)methyl)-1,2,3,5,6,7,8,10*a*-octahydropyrrolo[1,2-*a*]azocine-7,8-diyl diacetate (**159**)



TsOH (0.015g, 0.088 mmol, 1 eq.) was added to a solution of **158** (0.05 g, 0.088 mmol, 1 eq.) in CH₂Cl₂ (5 mL). The mixture was stirred at 25°C for 30 min before concentrated under reduced pressure. The residue was dissolved in toluene (15 mL) and degassed by bubbling with argon gas for 30 min. Grubbs' catalyst (2nd Gen) (0.008g, 0.0088 mmol, 0.1 eq.) was then added. The mixture was stirred at 25°C under argon atmosphere for 24h. The mixture was concentrated under reduced pressure. Sat. NaHCO₃ (aq) (5 mL) was then added. The mixture was then extracted with CH₂Cl₂ (5mL) three times. The combined organic layer was then washed with brine (5 mL), dried over Na₂SO₄ and concentrated under reduced pressure. The residue was purified by silica gel chromatography (gradient 15-100% EtOAc/Hexane) to yield **159** as a colorless oil (0.021g, 45% yield). ¹H NMR (500 MHz, Chloroform-*d*) δ 7.77 – 7.65 (m, 4H), 7.44 – 7.32 (m, 6H), 5.72 (p, *J* = 6.2 Hz, 2H), 5.37 (dq, *J* = 13.4, 4.0 Hz, 2H), 3.94 (dd, *J* = 9.9, 5.9 Hz, 1H), 3.65 (dd, *J* = 10.1, 4.8 Hz, 1H), 3.50 (dd, *J* = 10.1, 6.1 Hz, 1H), 2.73 (dt, *J* = 14.0, 8.2 Hz, 3H), 2.23 – 2.12 (m, 1H), 2.11 (s, 2H), 2.04 (s, 3H), 1.90 – 1.73 (m, 2H), 1.70 – 1.55 (m, 1H), 1.35 – 1.17 (m, 2H), 1.07 (s, 9H), 0.89 (q, *J* = 6.6 Hz, 1H). ¹³C NMR (126 MHz, Chloroform-*d*) δ 170.15, 170.03, 135.57, 135.52,

133.75, 133.63, 129.53, 129.51, 129.06, 128.97, 127.56, 73.40, 72.25, 67.15, 63.58, 57.77, 41.72, 29.83, 29.04, 26.81, 26.79, 21.03, 20.99, 19.17. FTIR (CHCl₃ film): 3071.08, 2932.23, 2857.99, 1744.3 1428.03, 1371.14, 1225.54, 1111.76 cm⁻¹. HRMS: [M+H]⁺ calc. 536.2832, found 536.2806.

CHAPTER 3. ANTAGONISTS OF THE F PROSTANOID (FP) RECEPTER AS A NOVEL DRUG TARGET FOR HYPERTENSION TREATMENT

3.1. Causes and treatments of hypertension

High blood pressure is one of major causes of death in the US and around the world because it can lead to other deadly conditions, such as heart failure, stroke and kidney failure. Recent updates from the American Heart Association state that the proportion of U.S. adults who have high blood pressure may reach 41% by 2030.⁵² The development of new chemotherapeutic strategies for the treatment and prevention of hypertension is therefore critical.

Blood pressure regulation is complex and involves many factors and systems in our bodies.⁵³ The renin-angiotensin system (RAS) is one of the well-known systems. Shown in **Figure 3.1**, angiotensin II (Ang II) is a vasoconstrictor that causes blood pressure elevation. The production of Ang II is controlled by two enzymes called renin and angiotensin converting enzyme (ACE). There are currently three classes of marketed drugs for the treatment of hypertension via the inhibition of the RAS: ACE inhibitors (ACEIs), angiotensin receptor blockers (ARBs) and direct renin inhibitors.⁵⁴ However, most of these are taken in combination with other drugs and have potential adverse effects. It is therefore important to develop novel targets for hypertension treatment.

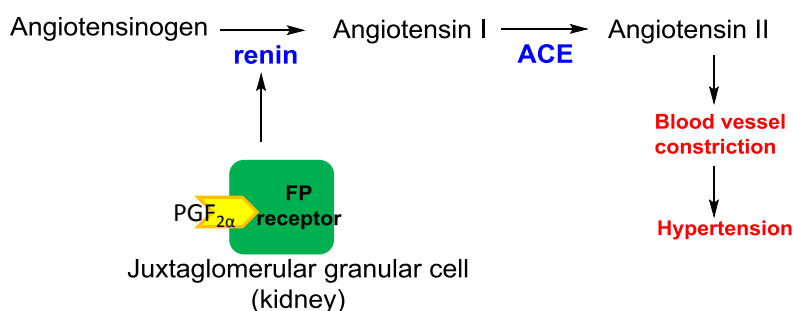


Figure 3.1 Blood pressure regulation through the renin-angiotensin system (RAS).⁵⁴

3.2. FP receptor inhibition as a novel target for treatment of hypertension

Prostaglandin F_{2α} (PGF_{2α}) is a naturally occurring prostaglandin that specifically binds to the FP receptor, a G protein-coupled receptor. It exists in many organs and affects a wide range of body functions,^{55,56,57} such as uterine contraction, water and electrolyte reabsorption, vasoconstriction, renin secretion and blood pressure regulation.

In 2009, the FitzGerald group in the Department of Pharmacology at the University of Pennsylvania discovered that the activation of PGF_{2α} increased plasma renin concentration and consequently led to the production of Ang II and blood pressure elevation (**Figure 3.1**).⁵⁸ Thus, antagonists of FP receptor can function as novel agents for reduction of blood pressure and the treatment of hypertension.

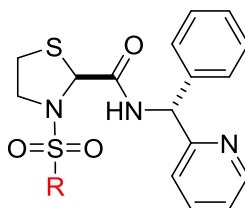
Collaborating with the FitzGerald group to prove this hypothesis, we have designed and synthesized small molecules to serve as antagonists of the FP receptor and have screened them as potential agents to reduce blood pressure.

3.3 Lead compound and previous efforts for FP antagonists

Only a few FP antagonists have been previously described in the scientific literature (e.g. AL-8810 and THG113), which underscores the challenge in the development of new FP antagonists.^{59,60,61} More recently, a non-prostaglandin small molecule, AS604872, was reported and patented as an orally active, potent and selective antagonist of the FP receptor for the arrest of preterm labor. AS604872 had K_i of 35±4 nM and no agonist activity for the human FP receptor.⁵⁵ However, this compound was not sufficiently soluble in aqueous solution for IV administration in rats. Using AS604872 as the lead compound, we have designed and synthesized derivatives of AS604872 in order to improve the solubility and FP antagonist activity, with the long-term goal of the development of for pressure-lowering agents.

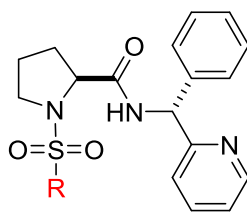
For the first set of AS604872 derivatives, Timothy S. Bush, a former student in our research group, made variations at the sulfonamide part (compound **162-171**, **Table 3.1**) and found that they were not active or not as potent as the lead compound. Moreover, replacing the thiazolidine core

with proline (compound **172-175**, **Table 3.2**) to remove the easily oxidized sulfur atom and facilitate synthetic accessibility also led to analogs with reduced potency. This suggests that the biaryl and sulfur atom in the thiazolidine ring are important to the antagonist activity.



compound	R	IC ₅₀ (nM)	compound	R	IC ₅₀ (nM)	compound	R	IC ₅₀ (nM)
AS604872		29	165		241	169		947
162		ND	166		472	170		1565
163		7629	167		ND	171		ND
164		ND	168		169			

Table 3.1 Structures and PGF_{2α} antagonist activities of the lead compound, AS604872, and previous thiazolidine analogs (ND= not determined)



compound	R	IC ₅₀ (nM)	compound	R	IC ₅₀ (nM)
172		208	174		ND
173		ND	175		ND

Table 3.2 Structures and PGF_{2α} antagonist activities of the previous proline analogs. (ND=not determined)

3.4 Structural design and synthetic plans for PGF_{2α} antagonist analogs

For a Structure-Activity Relationship (SAR) study of AS604872, we envisioned that AS604872 could be divided into 3 parts; sulfonamide (A), thiazolidine core (B) and amide branch (C). The derivatives of each part could be combined by peptide coupling and N-sulfonylation reactions, shown in **Figure 3.2**.

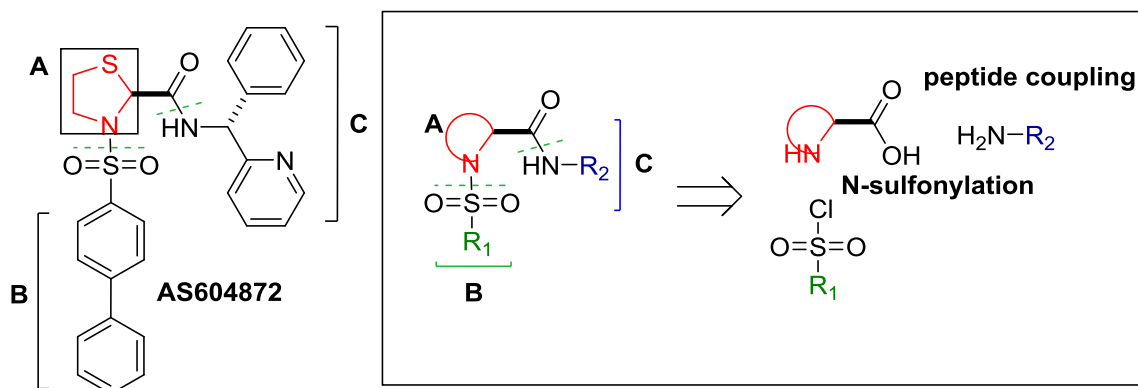


Figure 3.2 Structure analysis of AS604872.

To screen for the more potent and more water soluble compounds, we envisioned variations of each of the three portions of the parent structure as outlined below:

Variation at the sulfonamide part (A)

The previous work by Bush suggests that the biaryl sulfonamide is crucial for activity. We envisioned that the biaryl portion could be diversified by Suzuki-Miyaura cross-coupling Reaction of the bromophenyl (**177**) and various heteroaromatic- and substituted phenyl- boronic acids (**178**), shown in **Figure 3.3**.

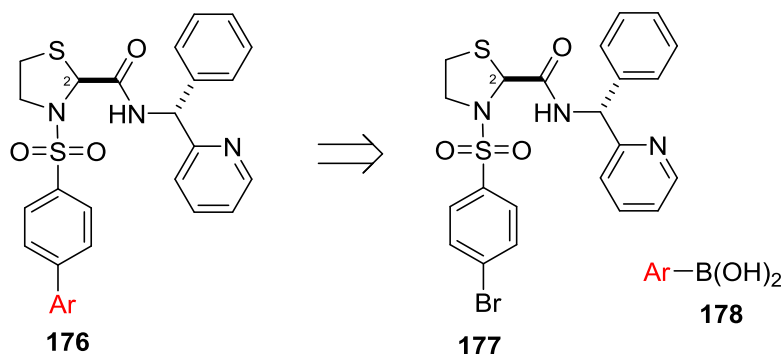
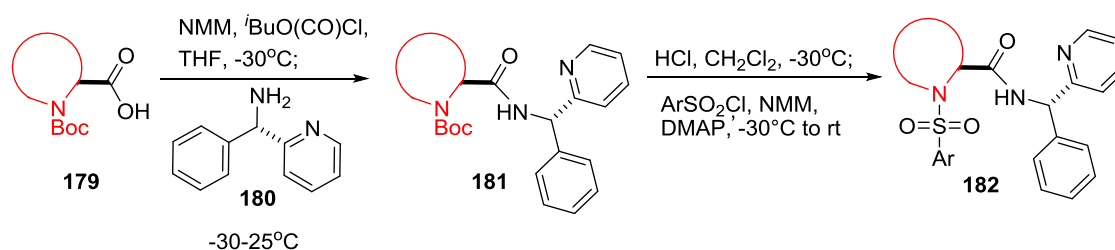


Figure 3.3 Synthetic strategy for the variation at the sulfonamide moiety (A).

Variation at the thiazolidine core (B)

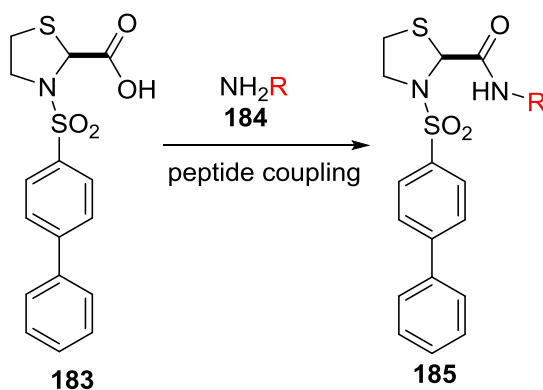
The sulfur atom in the lead compound AS604872 could be subject to oxidation under physiological conditions. Moreover, loss of the chiral center at C2 could happen via ring opening of the thiazolidine ring. We therefore planned to replace the thiazolidine core with amino acid derivatives which could improve stability as well as water solubility. The synthesis of these analogs could be achieved in the same fashion (peptide coupling and N-sulfonylation) as the synthesis of the lead compound, AS604872, shown in **Scheme 3.1**.



Scheme 3.1 Synthetic plan for the variation at the thiazolidine core (B).

Variation at the amide portion (C)

To study the effect of phenyl and pyridine ring on the amide portion, the thiazolidine compound could be diversified by peptide coupling with different amines.

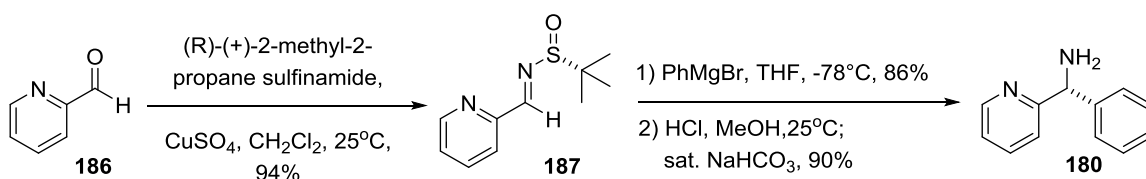


Scheme 3.2 Synthetic plan for the variation at the amide portion (C).

3.5. Synthesis of the designed PGF_{2α} antagonist analogs

Synthesis of the chiral amine (180)

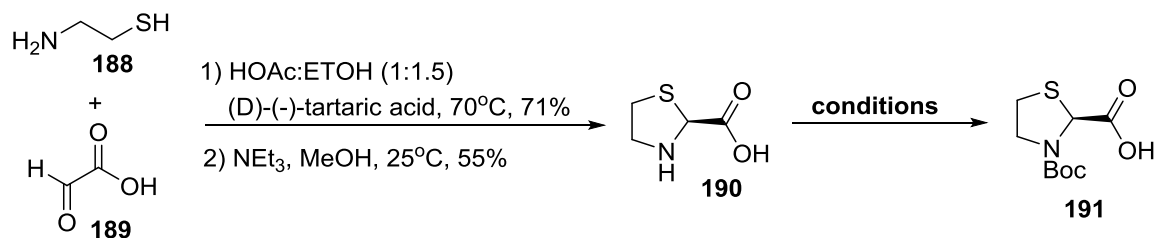
Following precedent literature,⁶² the synthesis of chiral amines **180** using Ellman's chiral sulfinamide methodology was straightforward and the requisite amines were successfully obtained in good yield (**Scheme 3.3**). The commercially available aldehyde **186** was condensed with the chiral auxiliary 1-(+)-2-methyl-2-propane sulfinamide to form the chiral sulfinamide **187**. The stereoselective attack of PhMgBr on **187** yielded the corresponding enantiomeric pure amine **180** after the acid-catalyzed removal of the chiral auxiliary.



Scheme 3.3 Synthesis of the chiral amine (**180**) by using Ellman's chiral sulfinamide.

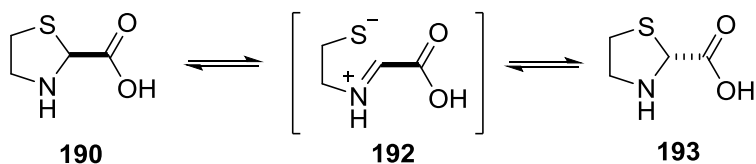
Synthesis of the enantiopure N-protected thiazolidine carboxylic core (191)

Following literature precedent,⁵⁹ the enantiopure carboxylic acid **190** was prepared from the cyclization of cystamine **188** and glyoxylic acid **189** in the presence of (D)-(-)-tartaric acid in moderate yield. Unfortunately, Boc protection of the free amine before the peptide coupling step was not straightforward. We found that treating the chiral carboxylic acid **190** with different sources of the Boc group and a variety of different reaction conditions led to the racemic mixture of **191** (**Scheme 3.4**). This was similar to the observation reported by Bush. A mechanism for the epimerization is shown in **Scheme 3.5**.⁶³ However, this problem was solved by the preparation of the thiazolidine ethyl ester **196**⁶⁴ which could be Boc protected and hydrolyzed to the key compound **191** without loss of stereochemistry integrity (**Scheme 3.5**).

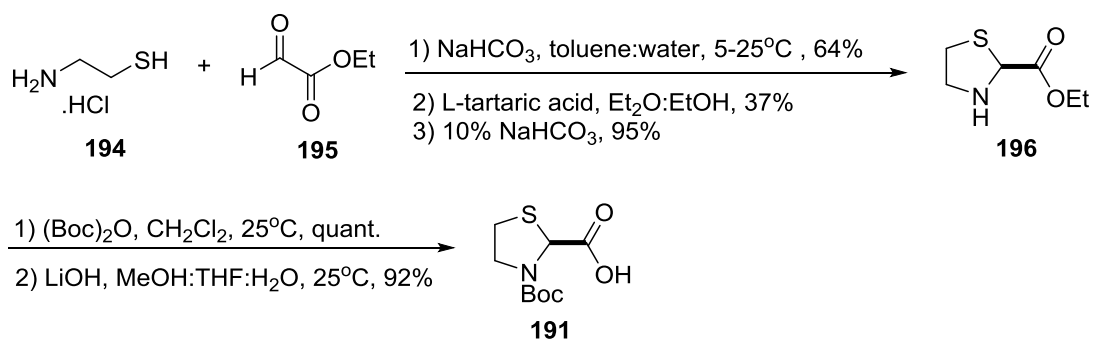


conditions	%yield
A. (Boc) ₂ O, NEt ₃ , CH ₃ CN, reflux	57 (racemic)
B. (Boc) ₂ O, DMAP, CH ₃ CN, 0-25°C	NR
C. tert-Butyl phenyl carbonate, NEt ₃ , CH ₃ CN, 25°C	NR
D. BOC-ON, NEt ₃ , Dioxane:water (1:1), 25°C	75 (racemic)
E. (Boc) ₂ O, NaHCO ₃ , THF, 0-25°C	47 (racemic)

Scheme 3.4 Initial efforts for the synthesis of the enantiopure N-protected thiazolidine carboxylic core (**191**).



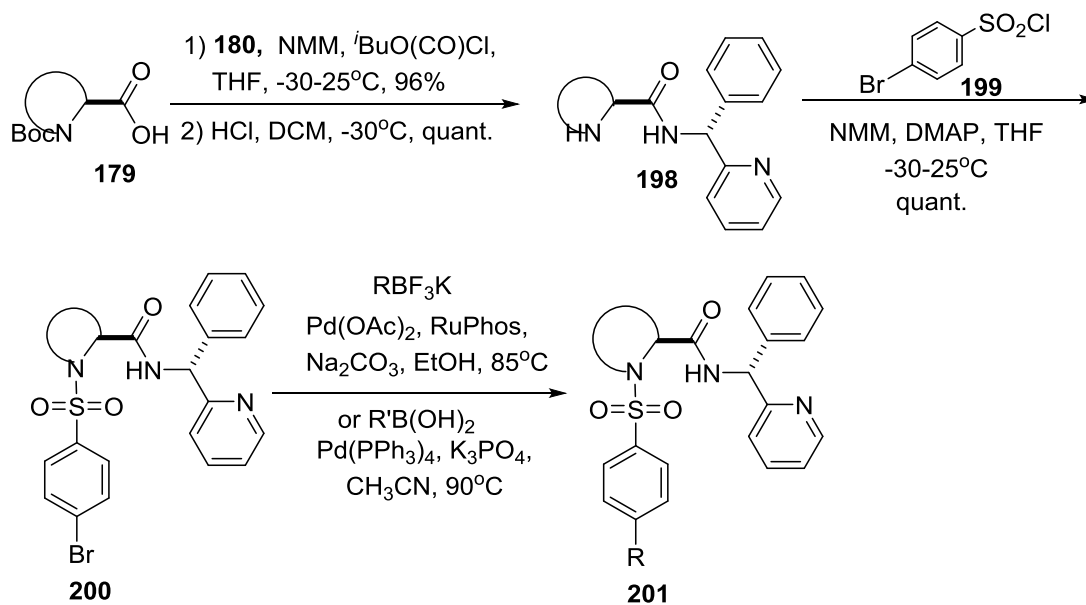
Scheme 3.5 Propose mechanism for epimerization of the thiazolidine carboxylic acid (**190**).



Scheme 3.6 Synthesis of the the enantiopure thiazolidine carboxylic core (**191**).

Synthesis of the $PGF_{2\alpha}$ antagonist analogs

The general synthetic route for the lead compound, AS604872, and its derivatives is shown in **Scheme 3.7**. The N-protected thiazolidine or N-protected amino acids **179** was coupled with the prepared chiral amine **180**. After Boc-deprotection, the free amine in **198** was subsequently sulfonated with *p*-bromosulfonylchloride **199** to give the corresponding arylbromide **200**. The preparation of a variety of biphenyl derivatives **201** in rapid fashion was performed by Suzuki-Miyaura coupling of the arylbromide **200** with various aryl trifluoroborates or aryl boronicacids.

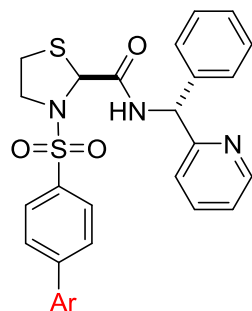


Scheme 3.7 Synthesis of the lead compound, AS604872, and its derivatives.

3.6 Biological evaluations of PGF_{2α} antagonist analogs

Collaborating with the FitzGerald group, we evaluated the FP antagonist activities of our analogs by an assay that measures the change in inositol triphosphate (IP3) signaling when PGF_{2α} interacts with FP receptor. Therefore, FP agonists would lead to an increase in IP3 signaling. An FP antagonist would lead to a decrease in IP3 signaling. The IC₅₀ shown here was measured at a PGF_{2α} concentration of 100 nM.

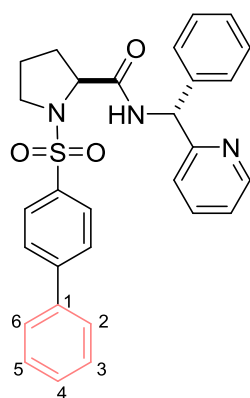
Although most biaryl derivatives with different heteroaromatic and substituted phenyl groups (**Table 3.3**) showed lower FP antagonist activity than AS604872, compound **205** was about 3 times more potent than the lead compound. Similarly, the corresponding proline derivative **213** was about 4 times more potent than **172**. This intriguing result led us to further study the effect of N-atom position. As shown in **Table 3.4**, the synthetically accessible biaryl proline analogs were prepared. Having a nitrogen atom at the 4-position in compound **215** destroyed the activity of the compound. Interestingly, having one extra nitrogen atom, as shown at the 5-position in compound **214**, also led to the loss of antagonist activity. This result is somewhat correlated to the difference in IC₅₀ of compound **210** and **212**. These data suggest that there might be an important interaction of the C-H bond at the 4-position of these ligands to the target or that steric hindrance at the 4-position might significantly affects the interactions of compound to the target.



compound	Ar	IC ₅₀ (nM)	compound	Ar	IC ₅₀ (nM)	compound	Ar	IC ₅₀ (nM)
202		ND	206		113	210		262
203		56	207		334	211		ND
204		1612	208		22260	212		45
205		9	209		375			

Table 3.3 FP antagonist activity (IC₅₀) of biaryl thiazolidine derivatives.

Note: 1) ND = not determined 2) None of them showed agonist activity.



compound	Ar	IC ₅₀ (nM)
213		51
214		1514
215		47350

Table 3.4 FP antagonist activity (IC₅₀) of biaryl proline derivatives.

Note: 1) ND = not determined 2) None of them showed agonist activity.

For the variation of the amide branch, compound **229** and **230** showed a significant loss in PGF_{2α} antagonist activity, compared to the lead compound AS604872. The phenyl ring proved to be more important than the pyridine ring, from the IC₅₀ values shown in **Figure 3.5**. We therefore kept the phenyl ring for the variation at the thiazolidine core to simplify the synthesis (compound **220** to **228**). Amino acids were thought to be a good choice because they are readily available and could potentially improve the solubility in aqueous media. Unfortunately, all of them (compound **216** to **228**) led to complete loss of antagonist potency (**Figure 3.4**). This suggests that the thiazolidine ring is critical for the potency of these compounds.

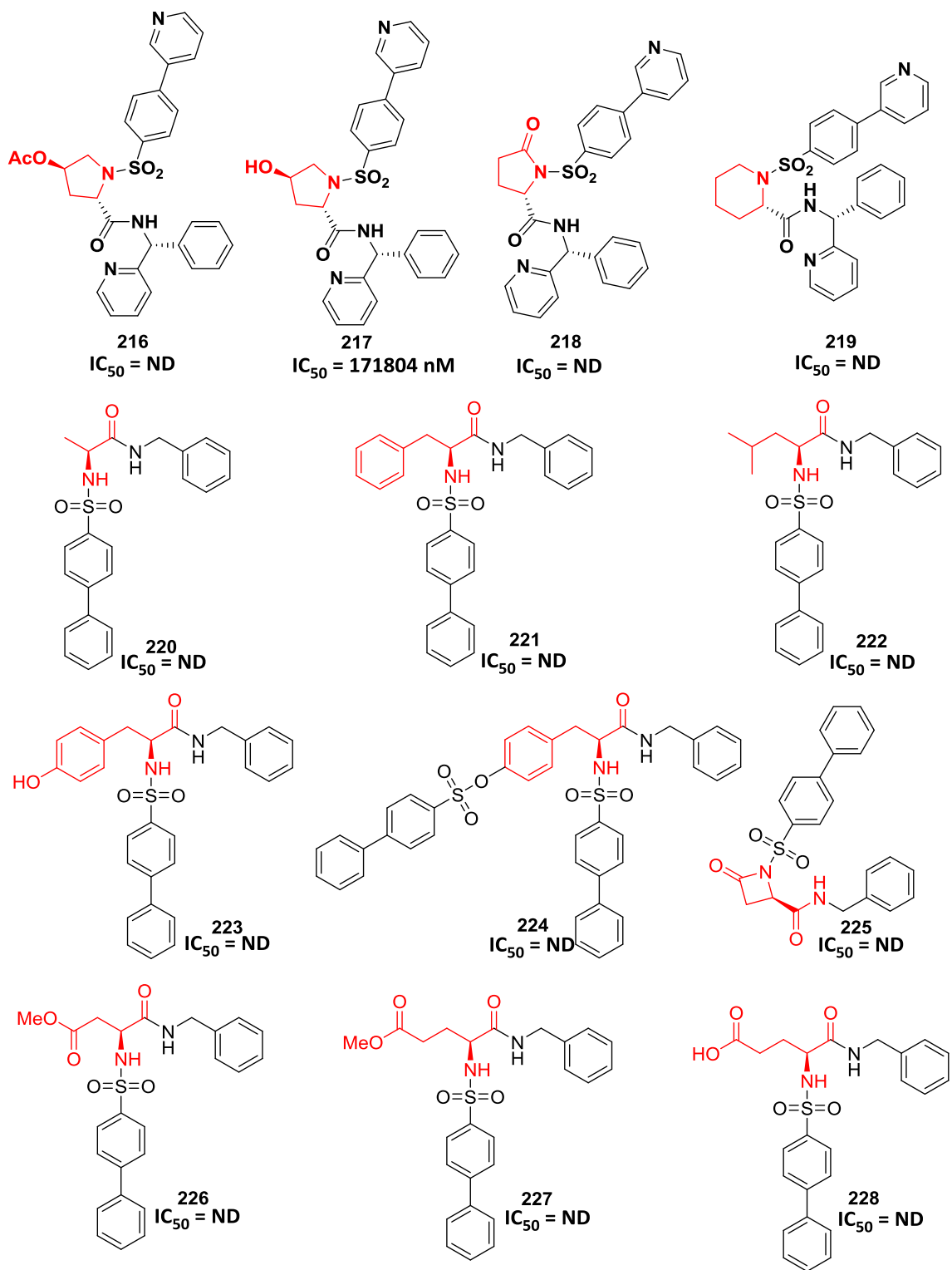


Figure 3.4 FP antagonist activity (IC_{50}) of the amino acid derivatives

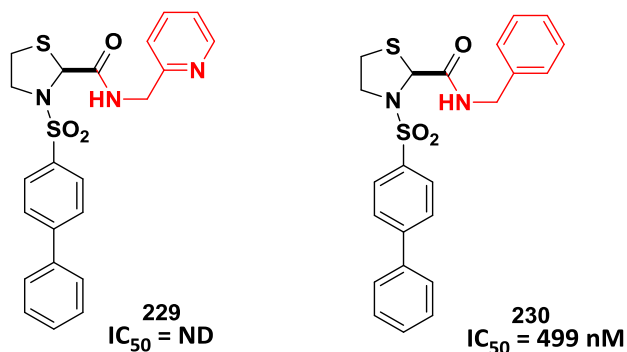


Figure 3.5 FP antagonist activity (IC_{50}) for derivatives with variation of the amide branch.

3.7. Conclusions

In conclusion, we have designed, synthesized and evaluated analogs of AS604872 as $PGF_{2\alpha}$ antagonists. Our preliminary SAR studies indicate that the lead structure is very sensitive to substitution. Among the prepared analogs, only **205** exhibited improvement in $PGF_{2\alpha}$ antagonist activity *in vitro* by ca. 3x lower IC_{50} than the one of AS604872. However, diversification of the structure in an effort to improve water solubility led to the loss of potency. The SAR study showed that the substituents at the 4-position of the biphenyl portions (**207-211** and **215**) caused the loss in potency more than the one at the 3-position (**205** and **212**). This result suggests that the C-H bond or the steric hindrance at the 4-position may be an important factor for the interaction between the compound and target. Replacement of the thiazolidine ring with other ring systems (**216-228**) also led to the loss of antagonist activity. This result suggests that the orientation of the biphenyl and the chiral amine moieties is crucial for the activity.

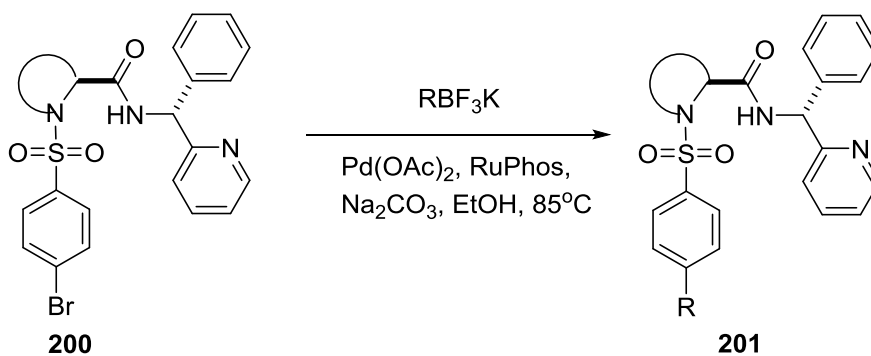
3.8 General method and experimental procedures

3.8.1. General information

Unless otherwise stated, all reagents were purchased from Sigma Aldrich, Alfa Aesar, Acros Organic or TCI America and used without further purification. ^1H and ^{13}C NMR spectra were recorded on Bruker AVII500B (500 MHz) and DRX-500 (500 MHz) spectrometers. Chemical shifts are reported relative to the solvent resonance peak δ 7.26 (CDCl_3) for ^1H NMR and δ 77.16 (CDCl_3) for ^{13}C . Infrared spectra were recorded on a NaCl plate using a Perkin-Elmer 1600 series Fourier transform spectrometer. High-resolution mass spectra were obtained by Dr. Rakesh Kohli at the University of Pennsylvania Mass Spectrometry Service Center.

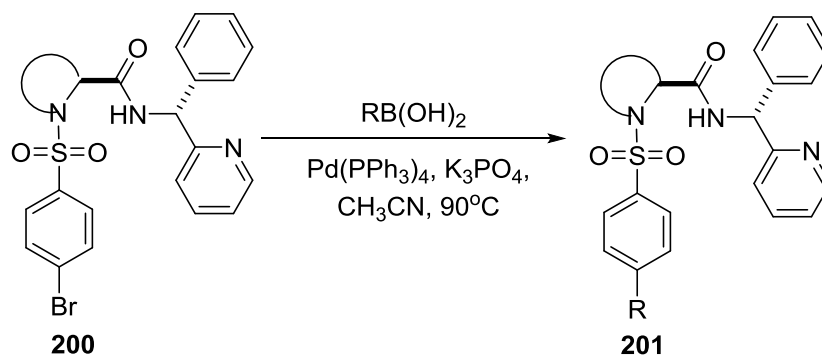
3.8.2. General procedure for the synthesis of PGF $_{2\alpha}$ antagonist analogs

Suzuki Coupling of the bromoaryl **200** and a variety of RBF $_3$ K (for compounds **202-208**)



Compound **200** (1 eq.), $\text{Pd}(\text{OAc})_2$ (3mol%), RuPhos (6mol%), RBF_3K (1.05 eq.) and Na_2CO_3 (2eq.) were placed in a sealable glass tube and purged with argon gas. Degassed EtOH (0.2M) was then added. The mixture was then heated up to 85°C for 12-16h (monitored by TLC). The reaction was cooled to 25°C and then filtered through a thin pad of Celite, which was washed with 25% MeOH/EtOAc . The filtrate was concentrated under reduced pressure and purified by silica gel chromatography (50% $\text{EtOAc}/\text{Hexane}$) to yield the corresponding biphenyl compounds.

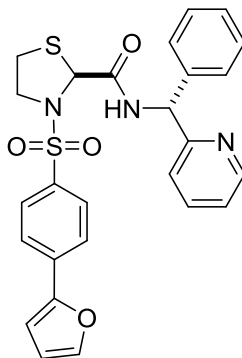
Suzuki Coupling of the bromoaryl **200** and a variety of RB(OH)₂ (for compounds **209-215**)



Compound **200** (1 eq.), Pd(OAc)₂ (6mol%), BINAP (12mol%), RB(OH)₂ (1.1 eq.) and K₃PO₄ (2eq.) were placed in a sealable glass tube and purged with argon gas. Degassed CH₃CN (0.2M) was then added. The mixture was then heated to 80°C for 12-16h (monitored by TLC, mobile phase 50% EtOAc/Hexane). The reaction was cooled to 25°C and then filtered through a thin pad of Celite, which was washed with 25%MeOH/EtOAc. The filtrate was concentrated under reduced pressure and purified by silica gel chromatography (50%EtOAc/Hexane) to yield the corresponding biphenyl compounds.

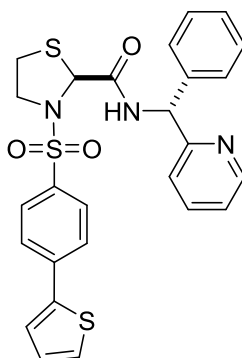
3.8.3. Characterization data for PGF_{2α} antagonist analogs

(S)-3-((4-(furan-2-yl) phenyl) sulfonyl)-N-((R)-phenyl(pyridin-2-yl)methyl)thiazolidine-2-carboxamide (**202**)



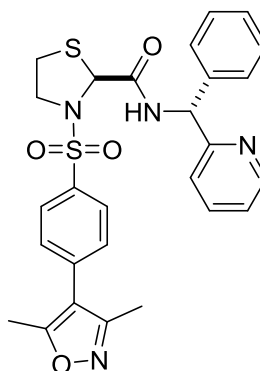
¹H NMR (500 MHz, Chloroform-*d*) δ 8.61 – 8.55 (m, 2H), 7.90 (d, *J* = 8.6 Hz, 2H), 7.84 (s, 1H), 7.65 – 7.58 (m, 3H), 7.53 (t, *J* = 1.8 Hz, 1H), 7.33 (d, *J* = 6.8 Hz, 2H), 7.28 (t, *J* = 7.1 Hz, 2H), 7.25 – 7.17 (m, 3H), 6.73 (s, 1H), 6.08 (d, *J* = 7.4 Hz, 1H), 5.48 (s, 1H), 4.06 (dt, *J* = 11.5, 5.5 Hz, 1H), 3.74 (ddd, *J* = 11.7, 7.6, 6.0 Hz, 1H), 2.96 (dt, *J* = 10.9, 5.4 Hz, 1H), 2.59 (ddd, *J* = 10.6, 7.6, 6.0 Hz, 1H). ¹³C NMR (126 MHz, Chloroform-*d*) δ 168.07, 158.48, 149.14, 144.55, 141.17, 140.19, 137.04, 135.05, 128.80, 128.65, 127.73, 127.35, 126.52, 124.99, 122.81, 122.68, 108.62, 77.36, 65.33, 57.75, 52.80, 31.66. FTIR (CHCl₃ film): 2925.48 (sp³ C-H str), 1678.73 (amide I C=O), 1508.06 (amide II C=O), 1349.93 (sym SO₂), 1159.97 (asym SO₂) cm⁻¹. [α]_D^{23.9 °C} = -120.8° (c 2.07, CHCl₃). HRMS: [M+H]⁺ calc. 506.1208, found 506.1204.

(S)-N-((R)-phenyl(pyridin-2-yl)methyl)-3-((4-(thiophen-2-yl)phenyl)sulfonyl)thiazolidine-2-carboxamide (**203**)



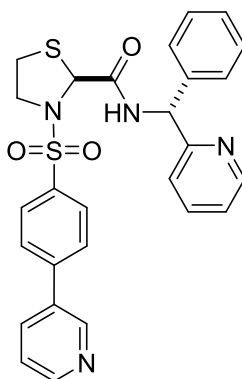
^1H NMR (500 MHz, Chloroform-*d*) δ 8.60 – 8.53 (m, 2H), 7.89 (d, J = 8.6 Hz, 2H), 7.73 (d, J = 8.6 Hz, 2H), 7.63 (tt, J = 7.7, 1.7 Hz, 1H), 7.45 (dd, J = 3.7, 1.1 Hz, 1H), 7.41 (dd, J = 5.1, 1.2 Hz, 1H), 7.35 – 7.27 (m, 4H), 7.24 – 7.17 (m, 4H), 7.14 (dd, J = 5.0, 3.7 Hz, 1H), 6.08 (d, J = 7.4 Hz, 1H), 5.49 (s, 1H), 4.06 (ddd, J = 11.9, 6.1, 4.9 Hz, 1H), 3.74 (ddd, J = 11.9, 7.6, 6.0 Hz, 1H), 2.98 (ddd, J = 10.9, 6.0, 4.9 Hz, 1H), 2.62 (ddd, J = 10.8, 7.6, 6.1 Hz, 1H). ^{13}C NMR (126 MHz, Chloroform-*d*) δ 168.05, 158.45, 149.12, 141.87, 141.15, 139.73, 137.08, 135.32, 128.81, 128.72, 128.68, 127.76, 127.37, 126.37, 125.48, 122.83, 122.69, 77.36, 65.31, 57.75, 52.77, 31.70. FTIR (CHCl₃ film): 2925.48 (sp³ C-H str), 1678.73 (amide I C=O), 1496.49 (amide II C=O), 1348.96 (sym SO₂), 1163.83 (asym SO₂) cm⁻¹. $[\alpha]_{\text{D}}^{23.9\text{ }^\circ\text{C}} = -111.5^\circ$ (c 1.7, CHCl₃). HRMS: $[\text{M}+\text{H}]^+$ calc. 522.0980, found 522.0974.

(S)-3-((4-(3,5-dimethylisoxazol-4-yl)phenyl)sulfonyl)-N-((R)-phenyl(pyridin-2-yl)methyl)thiazolidine-2-carboxamide (**204**)



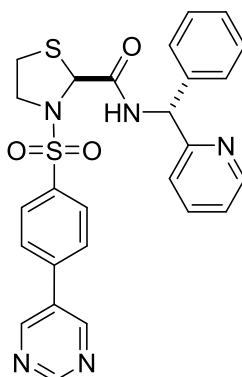
^1H NMR (500 MHz, Chloroform-*d*) δ 8.64 – 8.53 (m, 2H), 7.98 (d, J = 8.6 Hz, 2H), 7.65 – 7.61 (m, 1H), 7.42 (d, J = 8.6 Hz, 2H), 7.33 (ddt, J = 4.4, 3.3, 1.5 Hz, 2H), 7.30 – 7.26 (m, 2H), 7.24 – 7.18 (m, 4H), 6.08 (d, J = 7.4 Hz, 1H), 5.49 (s, 1H), 4.08 – 4.02 (m, 1H), 3.77 (ddd, J = 11.8, 7.2, 6.1 Hz, 1H), 3.03 (dt, J = 11.1, 5.7 Hz, 1H), 2.68 (ddd, J = 10.9, 7.3, 6.1 Hz, 1H), 2.43 (s, 3H), 2.28 (d, J = 1.7 Hz, 3H). ^{13}C NMR (126 MHz, Chloroform-*d*) δ 167.97, 158.40, 158.25, 149.11, 141.17, 137.09, 136.53, 136.24, 129.83, 128.81, 128.55, 127.77, 127.33, 122.85, 122.72, 115.32, 77.36, 65.18, 57.78, 52.76, 31.68, 11.94, 11.04. FTIR (CHCl₃ film): 2925.48 (sp³ C-H str), 1678.73 (amide I C=O), 1499.38 (amide II C=O), 1351.86 (sym SO₂), 1165.76 (asym SO₂) cm⁻¹. $[\alpha]_{\text{D}}^{23.9\text{ }^\circ\text{C}}$ = -124.9 $^\circ$ (c 0.1, CHCl₃). HRMS: $[\text{M}+\text{H}]^+$ calc. 535.1474, found 535.1465.

(S)-N-((R)-phenyl(pyridin-2-yl)methyl)-3-((4-(pyridin-3-yl)phenyl)sulfonyl)thiazolidine-2-carboxamide (205)



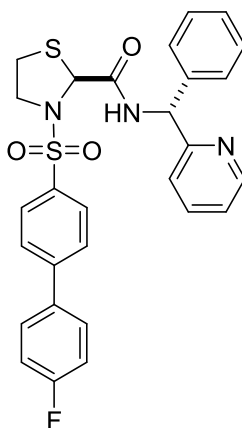
^1H NMR (500 MHz, Chloroform-*d*) δ 8.86 (d, J = 2.4 Hz, 1H), 8.68 (dd, J = 4.9, 1.6 Hz, 1H), 8.60 – 8.53 (m, 2H), 8.02 (d, J = 8.7 Hz, 2H), 7.90 (ddd, J = 8.0, 2.4, 1.7 Hz, 1H), 7.75 – 7.71 (m, 2H), 7.63 (td, J = 7.6, 1.8 Hz, 1H), 7.43 (ddd, J = 8.0, 4.8, 0.9 Hz, 1H), 7.33 (d, J = 7.1 Hz, 2H), 7.28 (d, J = 7.1 Hz, 1H), 7.25 – 7.18 (m, 3H), 6.08 (d, J = 7.4 Hz, 1H), 5.50 (s, 1H), 4.06 (ddd, J = 11.5, 6.1, 5.1 Hz, 1H), 3.77 (ddd, J = 11.8, 7.3, 6.1 Hz, 1H), 3.01 (ddd, J = 11.0, 6.0, 5.1 Hz, 1H), 2.67 (ddd, J = 10.9, 7.3, 6.1 Hz, 1H). ^{13}C NMR (126 MHz, Chloroform-*d*) δ 167.98, 158.42, 149.90, 149.11, 148.42, 141.15, 137.10, 136.79, 134.80, 128.81, 128.15, 127.76, 127.35, 123.94, 122.85, 122.73, 77.36, 65.20, 57.76, 52.75, 31.70. FTIR (CHCl₃ film): 2925.48 (sp³ C-H str), 1678.73 (amide I C=O), 1498.42 (amide II C=O), 1351.86 (sym SO₂), 1165.76 (asym SO₂) cm⁻¹. $[\alpha]_D^{23.9} = -133.4^\circ$ (c 0.07, CHCl₃). HRMS: [M+H]⁺ calc. 517.1368, found 517.1371.

(S)-N-((R)-phenyl(pyridin-2-yl)methyl)-3-((4-(pyrimidin-5-yl)phenyl)sulfonyl)thiazolidine-2-carboxamide (**206**)



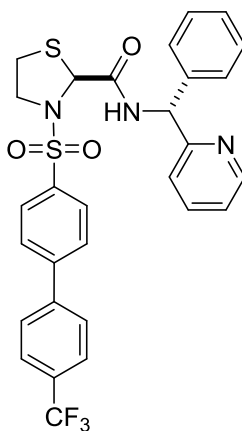
^1H NMR (500 MHz, Chloroform-*d*) δ 2.70 (dt, $J=10.99, 6.56$ Hz, 1 H) 3.04 (dt, $J=10.91, 5.68$ Hz, 1 H) 3.78 (dt, $J=18.01, 6.10$ Hz, 1 H) 4.03 - 4.08 (m, 1 H) 5.50 - 5.55 (m, 1 H) 6.08 (d, $J=7.32$ Hz, 1 H) 7.19 - 7.25 (m, 3 H) 7.29 (d, $J=7.02$ Hz, 2 H) 7.32 - 7.34 (m, 2 H) 7.73 (d, $J=8.54$ Hz, 2 H) 8.06 (d, $J=8.24$ Hz, 2 H) 8.59 (d, $J=3.97$ Hz, 1 H) 8.60 (br. s., 1 H) 8.98 (s, 2 H) 9.29 (s, 1 H). ^{13}C NMR (126 MHz, Chloroform-*d*) δ 31.73, 52.66, 57.78, 65.14, 107.57, 122.78, 122.90, 127.37, 127.81, 128.05, 128.85, 129.12, 137.13, 137.96, 139.71, 141.18, 149.14, 155.26, 156.97, 158.39, 167.87. FTIR (CHCl_3 film): 2926.45 (sp^3 C-H str), 1676.8 (amide I C=O), 1497.45 (amide II C=O), 1348.96 (sym SO_2), 1166.72 (asym SO_2) cm^{-1} . $[\alpha]_{\text{D}}^{23.9}$ $^{\circ}\text{C} = -149.9^{\circ}$ (c 0.07, CHCl_3). HRMS: $[\text{M}+\text{H}]^+$ calc. 518.1321, found 518.1329.

(S)-3-((4'-fluoro-[1,1'-biphenyl]-4-yl)sulfonyl)-N-((R)-phenyl(pyridin-2-yl)methyl)thiazolidine-2-carboxamide (**207**)



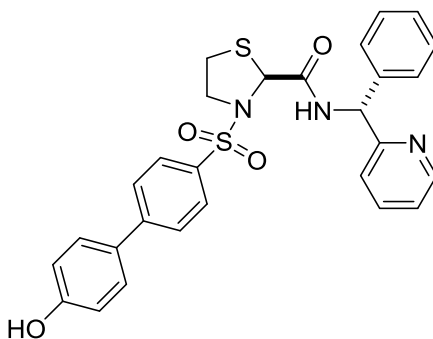
^1H NMR (500 MHz, Chloroform-*d*) δ 8.65 – 8.55 (m, 2H), 7.96 (d, $J = 9.1$ Hz, 2H), 7.68 (d, $J = 9.1$ Hz, 2H), 7.65 – 7.60 (m, 1H), 7.57 (ddd, $J = 10.0, 5.1, 2.6$ Hz, 2H), 7.34 (d, $J = 8.2$ Hz, 2H), 7.28 (d, $J = 7.2$ Hz, 2H), 7.24 – 7.15 (m, 5H), 6.10 (d, $J = 7.4$ Hz, 1H), 5.50 (s, 1H), 4.06 (ddd, $J = 11.5, 6.1, 5.1$ Hz, 1H), 3.77 (ddd, $J = 11.9, 7.4, 6.0$ Hz, 1H), 2.98 (ddd, $J = 11.0, 5.9, 5.1$ Hz, 1H), 2.63 (ddd, $J = 10.9, 7.4, 6.1$ Hz, 1H). ^{13}C NMR (126 MHz, Chloroform-*d*) δ 168.16, 158.46, 149.14, 145.68, 141.09, 137.10, 135.64, 129.25, 129.18, 128.80, 128.60, 127.92, 127.74, 127.33, 122.87, 122.72, 116.33, 116.16, 65.27, 57.78, 52.85, 31.65. FTIR (CHCl₃ film): 2925.48 (sp³ C-H str), 1674.87 (amide I C=O), 1517.7 (amide II C=O), 1351.86 (sym SO₂), 1161.9 (asym SO₂) cm⁻¹. $[\alpha]_{\text{D}}^{23.9\text{ }^\circ\text{C}} = -148.9^\circ$ (c 0.07, CHCl₃). HRMS: $[\text{M}+\text{H}]^+$ calc. 534.1321, found 534.1317.

(S)-N-((R)-phenyl(pyridin-2-yl)methyl)-3-((4'-(trifluoromethyl)-[1,1'-biphenyl]-4-yl)sulfonyl)thiazolidine-2-carboxamide (**208**)



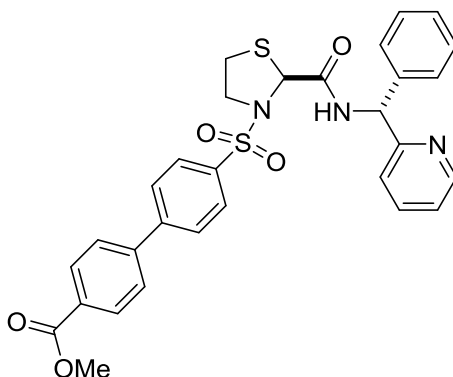
^1H NMR (500 MHz, Chloroform-*d*) δ 8.63 – 8.57 (m, 2H), 8.01 (d, J = 8.8 Hz, 2H), 7.77 – 7.67 (m, 7H), 7.64 (td, J = 7.7, 1.8 Hz, 1H), 7.33 (tt, J = 5.3, 1.4 Hz, 2H), 7.30 – 7.27 (m, 2H), 7.26 – 7.17 (m, 4H), 6.10 (d, J = 7.5 Hz, 1H), 5.51 (s, 1H), 4.06 (dt, J = 11.6, 5.7 Hz, 1H), 3.79 (ddd, J = 11.8, 7.2, 6.1 Hz, 1H), 3.01 (dt, J = 11.1, 5.6 Hz, 1H), 2.66 (ddd, J = 10.9, 7.2, 6.1 Hz, 1H). ^{13}C NMR (126 MHz, Chloroform-*d*) δ 168.12, 158.40, 149.09, 145.14, 141.06, 137.17, 136.71, 128.83, 128.71, 128.34, 127.88, 127.78, 127.33, 126.19, 126.16, 122.90, 122.77, 65.21, 57.79, 52.81, 31.66. FTIR (CHCl₃ film): 2925.48 (sp³ C-H str), 1679.69 (amide I C=O), 1504.2 (amide II C=O), 1352.82 (sym SO₂), 1165.76 (asym SO₂) cm⁻¹. $[\alpha]_{\text{D}}^{23.9\text{ }^\circ\text{C}}$ = -116.7^o (c 0.05, CHCl₃). HRMS: $[\text{M}+\text{H}]^+$ calc. 584.1289, found 584.1293.

(S)-3-((4'-hydroxy-[1,1'-biphenyl]-4-yl)sulfonyl)-N-((R)-phenyl(pyridin-2-yl)methyl)thiazolidine-2-carboxamide (**209**)



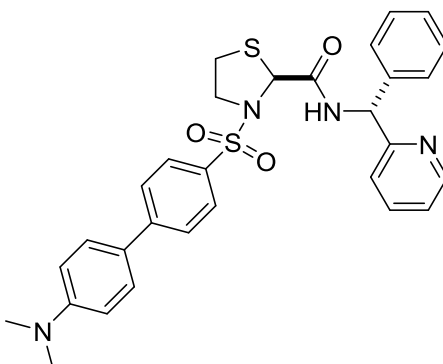
^1H NMR (500 MHz, Chloroform-*d*) δ 8.64 – 8.59 (m, 2H), 7.91 – 7.89 (m, 2H), 7.69 – 7.60 (m, 4H), 7.47 – 7.43 (m, 2H), 7.36 – 7.27 (m, 3H), 7.25 – 7.18 (m, 2H), 6.95 – 6.86 (m, 3H), 6.11 (d, $J = 7.5$ Hz, 2H), 5.49 (s, 1H), 4.05 (dt, $J = 11.5, 5.6$ Hz, 1H), 3.80 – 3.72 (m, 1H), 3.01 (dt, $J = 11.1, 5.6$ Hz, 1H), 2.67 (ddd, $J = 10.9, 7.3, 6.0$ Hz, 1H). FTIR (CHCl₃ film): 3334.32, 2923.56, 1652.7, 1520.6, 1349.93, 1268.93, 1162.87 cm⁻¹. HRMS: [M+Na]⁺ calc. 554.1184, found 554.1202.

methyl 4'-(((S)-2-(((R)-phenyl(pyridin-2-yl)methyl)carbamoyl)thiazolidin-3-yl)sulfonyl)-[1,1'-biphenyl]-4-carboxylate (**210**)



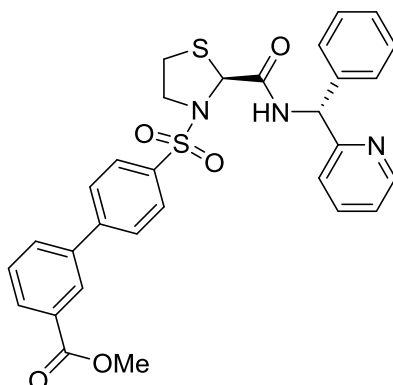
^1H NMR (500 MHz, Chloroform-*d*) δ 8.61 – 8.54 (m, 2H), 8.17 – 8.12 (m, 2H), 8.02 – 7.98 (m, 2H), 7.78 – 7.73 (m, 2H), 7.69 – 7.65 (m, 2H), 7.63 (td, $J = 7.6, 1.7$ Hz, 1H), 7.33 (tt, $J = 6.0, 1.5$ Hz, 2H), 7.30 – 7.27 (m, 1H), 7.25 – 7.18 (m, 3H), 6.08 (d, $J = 7.4$ Hz, 1H), 5.50 (s, 1H), 4.09 – 4.03 (m, 1H), 3.96 (s, 3H), 3.77 (ddd, $J = 12.0, 7.5, 6.1$ Hz, 1H), 3.00 (ddd, $J = 11.0, 6.0, 5.0$ Hz, 1H), 2.65 (ddd, $J = 10.9, 7.4, 6.1$ Hz, 1H). ^{13}C NMR (126 MHz, Chloroform-*d*) δ 168.03, 166.74, 158.43, 149.06, 145.45, 143.30, 136.63, 130.47, 130.40, 128.83, 128.65, 128.63, 128.32, 127.78, 127.51, 127.40, 127.37, 122.88, 122.74, 76.91, 65.25, 57.77, 52.79, 52.44, 31.72. FTIR (CHCl₃ film): 3353.12, 1720.19, 1682.59, 1504.69, 1283.39, 1166.24 cm⁻¹. HRMS: [M+H]⁺ calc. 574.1470, found 574.1459.

(S)-3-((4'-(dimethylamino)-[1,1'-biphenyl]-4-yl)sulfonyl)-N-((R)-phenyl(pyridin-2-yl)methyl)thiazolidine-2-carboxamide (**211**)



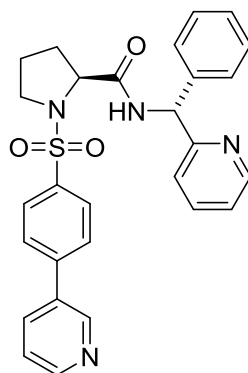
^1H NMR (500 MHz, Chloroform-*d*) δ 8.64 – 8.57 (m, 2H), 7.90 (dd, J = 8.6, 1.8 Hz, 2H), 7.69 (dq, J = 8.9, 2.4 Hz, 2H), 7.58 – 7.50 (m, 2H), 7.39 – 7.32 (m, 1H), 7.32 – 7.27 (m, 3H), 7.25 – 7.16 (m, 3H), 6.82 (d, J = 8.4 Hz, 2H), 6.09 (d, J = 7.5 Hz, 1H), 5.50 (d, J = 3.3 Hz, 1H), 4.10 – 4.05 (m, 1H), 3.74 (ddd, J = 11.7, 7.7, 5.9 Hz, 1H), 3.04 (s, 6H), 2.96 (dt, J = 10.8, 5.4 Hz, 1H), 2.60 (ddd, J = 10.7, 7.7, 5.9 Hz, 1H). ^{13}C NMR (126 MHz, Chloroform-*d*) δ 168.30, 158.54, 149.05, 146.72, 141.10, 137.20, 133.75, 130.42, 128.85, 128.55, 128.19, 127.78, 127.41, 126.65, 122.89, 122.72, 112.84, 65.40, 57.80, 52.93, 40.66, 31.73. FTIR (CHCl₃ film): 2922.59, 1682.59, 1506.13, 1352.82, 1160.94 cm⁻¹. HRMS: [M+H]⁺ calc. 559.1838, found 559.1838.

methyl 4'-(((S)-2-(((R)-phenyl(pyridin-2-yl)methyl)carbamoyl)thiazolidin-3-yl)sulfonyl)-[1,1'-biphenyl]-3-carboxylate (**212**)



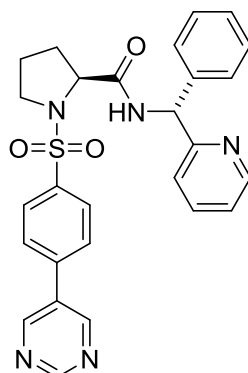
^1H NMR (500 MHz, Chloroform- d) δ 8.60 (ddd, $J = 5.0, 1.8, 0.9$ Hz, 1H), 8.57 (d, $J = 7.6$ Hz, 1H), 8.29 (t, $J = 1.8$ Hz, 1H), 8.10 (dt, $J = 7.8, 1.4$ Hz, 1H), 8.03 – 7.97 (m, 2H), 7.79 (ddd, $J = 7.8, 2.0, 1.1$ Hz, 1H), 7.77 (s, 1H), 7.67 (td, $J = 7.7, 1.8$ Hz, 1H), 7.57 (t, $J = 7.8$ Hz, 1H), 7.37 – 7.32 (m, 2H), 7.31 – 7.27 (m, 3H), 7.25 – 7.18 (m, 2H), 6.11 (d, $J = 7.5$ Hz, 1H), 5.51 (s, 1H), 4.09 – 4.01 (m, 1H), 3.97 (s, 3H), 3.79 (ddd, $J = 11.8, 7.4, 6.1$ Hz, 1H), 3.03 (dt, $J = 11.0, 5.6$ Hz, 1H), 2.66 (ddd, $J = 10.9, 7.3, 6.1$ Hz, 1H). ^{13}C NMR (126 MHz, Chloroform- d) δ 168.18, 166.76, 158.38, 148.72, 145.59, 139.37, 136.35, 131.78, 131.24, 129.87, 129.40, 128.89, 128.67, 128.64, 128.18, 127.87, 127.43, 123.08, 122.86, 65.22, 60.53, 57.76, 52.83, 52.50, 31.71. FTIR (CHCl_3 film): 2951.04, 1721.16, 1684.03, 1506.61, 1248.2, 1165.76 cm^{-1} . HRMS: $[\text{M}+\text{H}]^+$ calc. 574.1470, found 574.1477.

(S)-N-((R)-phenyl(pyridin-2-yl)methyl)-1-((4-(pyridin-3-yl)phenyl)sulfonyl)pyrrolidine-2-carboxamide (**213**)



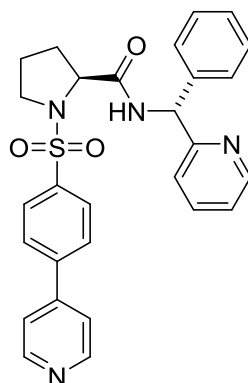
^1H NMR (500 MHz, Chloroform-*d*) δ 8.85 (s, 1H), 8.68 (d, $J = 7.5$ Hz, 1H), 8.65 (dd, $J = 4.9, 1.6$ Hz, 1H), 8.59 (d, $J = 4.7$ Hz, 1H), 8.01 – 7.95 (m, 2H), 7.88 (dt, $J = 8.0, 2.1$ Hz, 1H), 7.71 (d, $J = 8.3$ Hz, 2H), 7.60 (td, $J = 7.6, 1.8$ Hz, 1H), 7.43 – 7.36 (m, 3H), 7.26 (dt, $J = 16.3, 7.7$ Hz, 2H), 7.21 – 7.13 (m, 2H), 6.11 (d, $J = 7.5$ Hz, 1H), 4.25 (dd, $J = 8.7, 3.0$ Hz, 1H), 3.63 (ddd, $J = 10.1, 7.1, 3.1$ Hz, 1H), 3.32 (td, $J = 9.7, 6.3$ Hz, 1H), 2.16 (ddt, $J = 12.0, 6.0, 2.8$ Hz, 1H), 1.85 – 1.74 (m, 1H), 1.68 (dtd, $J = 10.7, 8.0, 7.0, 4.2$ Hz, 2H). ^{13}C NMR (126 MHz, Chloroform-*d*) δ 170.29, 158.95, 149.79, 149.29, 148.38, 142.78, 141.29, 136.85, 136.08, 134.71, 134.66, 128.76, 128.69, 127.94, 127.54, 127.29, 123.84, 122.48, 62.68, 57.90, 49.88, 30.47, 24.52. FTIR (CHCl₃ film): 3386.39, 3055.66, 1953.45, 1671.98, 1508.061347.03, 1162.87 cm⁻¹. HRMS: [M+H]⁺ calc. 499.1804, found 499.1794.

(S)-N-((R)-phenyl(pyridin-2-yl)methyl)-1-((4-(pyrimidin-5-yl)phenyl)sulfonyl)pyrrolidine-2-carboxamide (**214**)



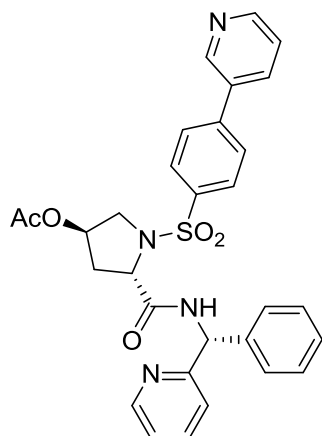
^1H NMR (500 MHz, Chloroform- d) δ 9.26 (s, 1H), 8.96 (s, 2H), 8.65 (d, J = 7.5 Hz, 1H), 8.58 (dd, J = 4.9, 1.6 Hz, 1H), 8.02 (d, J = 8.1 Hz, 2H), 7.71 (d, J = 8.1 Hz, 2H), 7.60 (td, J = 7.8, 1.8 Hz, 1H), 7.37 (d, J = 7.6 Hz, 2H), 7.30 – 7.21 (m, 3H), 7.21 – 7.12 (m, 2H), 6.10 (d, J = 7.5 Hz, 1H), 4.25 (dd, J = 8.5, 3.0 Hz, 1H), 3.63 (ddd, J = 10.1, 7.2, 3.1 Hz, 1H), 3.31 (td, J = 9.7, 6.2 Hz, 1H), 2.16 (ddt, J = 10.8, 8.1, 3.9 Hz, 1H), 1.86 – 1.76 (m, 1H), 1.69 (td, J = 10.9, 9.0, 5.3 Hz, 2H). ^{13}C NMR (126 MHz, Chloroform- d) δ 170.17, 158.86, 158.52, 155.14, 149.26, 141.28, 137.20, 136.87, 129.03, 128.69, 127.85, 127.55, 127.29, 122.53, 122.51, 62.67, 57.85, 49.84, 30.53, 24.53. FTIR (CHCl₃ film): 3383.5, 3052.76, 1671.98, 1590.99, 1508.06, 1345.11, 1162.87 cm⁻¹. HRMS: [M+H]⁺ calc. 500.1756, found 500.1755.

(S)-N-((R)-phenyl(pyridin-2-yl)methyl)-1-((4-(pyridin-4-yl)phenyl)sulfonyl)pyrrolidine-2-carboxamide (**215**)



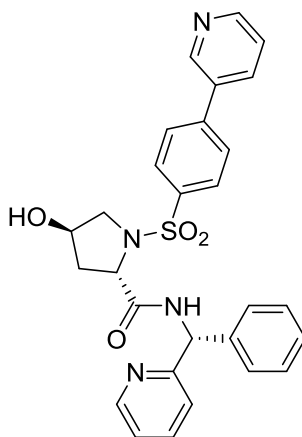
^1H NMR (500 MHz, Chloroform-*d*) δ 8.74 – 8.62 (m, 3H), 8.56 (d, J = 4.8 Hz, 1H), 7.97 (d, J = 7.9 Hz, 2H), 7.74 (d, J = 8.0 Hz, 2H), 7.57 (t, J = 7.7 Hz, 1H), 7.48 (d, J = 5.1 Hz, 2H), 7.37 (d, J = 7.6 Hz, 2H), 7.23 (q, J = 8.0 Hz, 3H), 7.14 (dt, J = 12.0, 6.8 Hz, 2H), 6.10 (d, J = 7.5 Hz, 1H), 4.24 (dd, J = 8.3, 2.9 Hz, 1H), 3.70 – 3.48 (m, 1H), 3.29 (td, J = 9.6, 9.2, 6.0 Hz, 1H), 2.13 (dd, J = 9.5, 5.7 Hz, 1H), 1.77 (dt, J = 17.0, 8.3 Hz, 1H), 1.70 – 1.59 (m, 2H). ^{13}C NMR (126 MHz, Chloroform-*d*) δ 170.16, 158.80, 150.54, 149.18, 146.14, 142.90, 141.22, 136.79, 128.65, 128.59, 127.86, 127.44, 127.17, 122.41, 122.38, 121.67, 62.59, 57.79, 49.78, 30.39, 24.42. FTIR (CHCl₃ film): 1672.95, 1590.99, 1506.13, 1348, 1161.9 cm⁻¹. HRMS: [M+H]⁺ calc. 499.1804, found 499.1790.

(3*R*,5*S*)-5-(((*R*)-phenyl(pyridin-2-yl)methyl)carbamoyl)-1-((4-(pyridin-3-yl)phenyl) sulfonyl)pyrrolidin-3-yl acetate (**216**)



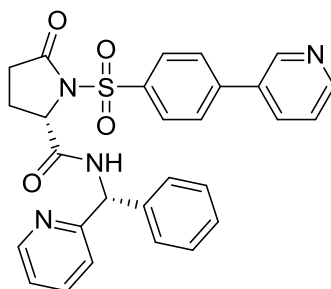
^1H NMR (500 MHz, Chloroform-*d*) δ 8.83 (dd, $J = 2.4, 0.9$ Hz, 1H), 8.67 (dd, $J = 4.8, 1.6$ Hz, 1H), 8.60 (ddd, $J = 4.9, 1.8, 0.9$ Hz, 1H), 8.56 (d, $J = 7.3$ Hz, 1H), 7.99 (d, $J = 8.7$ Hz, 2H), 7.87 (ddd, $J = 7.9, 2.4, 1.6$ Hz, 1H), 7.70 (d, $J = 8.7$ Hz, 2H), 7.62 (td, $J = 7.7, 1.8$ Hz, 1H), 7.42 (ddd, $J = 8.0, 4.8, 0.9$ Hz, 1H), 7.40 – 7.37 (m, 2H), 7.32 – 7.26 (m, 2H), 7.25 – 7.17 (m, 3H), 6.10 (d, $J = 7.3$ Hz, 1H), 5.09 (dh, $J = 4.4, 2.0$ Hz, 1H), 4.41 (t, $J = 8.1$ Hz, 1H), 3.79 (dd, $J = 13.0, 4.1$ Hz, 1H), 3.71 (dt, $J = 13.0, 1.7$ Hz, 1H), 2.37 – 2.23 (m, 2H), 1.61 (s, 3H). ^{13}C NMR (126 MHz, Chloroform-*d*) δ 169.98, 169.77, 149.93, 149.27, 148.28, 142.80, 137.00, 136.64, 134.59, 129.12, 128.75, 127.81, 127.67, 127.40, 123.98, 122.67, 122.63, 72.63, 61.73, 57.88, 54.90, 37.10, 20.67. FTIR (CHCl₃ film): 3370, 3059.03, 2926.93, 2247.15, 1738.51, 1673.91, 1515.29, 1349.93, 1162.87 cm⁻¹. HRMS: [M+H]⁺ calc. 557.1859, found 557.1857.

(2*S*,4*R*)-4-hydroxy-*N*-((*R*)-phenyl(pyridin-2-yl)methyl)-1-((4-(pyridin-3-yl)phenyl)sulfonyl)pyrrolidine-2-carboxamide (**217**)



^1H NMR (500 MHz, Chloroform-*d*) δ 8.79 – 8.74 (m, 1H), 8.64 – 8.55 (m, 3H), 7.97 (d, *J* = 8.7 Hz, 2H), 7.86 (dddd, *J* = 7.6, 5.2, 2.4, 1.6 Hz, 1H), 7.64 (d, *J* = 8.0 Hz, 2H), 7.42 – 7.36 (m, 3H), 7.33 (tt, *J* = 6.4, 1.3 Hz, 1H), 7.31 – 7.27 (m, 2H), 7.25 – 7.14 (m, 3H), 6.09 (d, *J* = 7.2 Hz, 1H), 4.44 – 4.34 (m, 1H), 4.32 (p, *J* = 3.9 Hz, 1H), 3.66 (ddd, *J* = 11.3, 8.7, 4.3 Hz, 1H), 3.45 (d, *J* = 2.1 Hz, 1H), 2.15 (tdd, *J* = 19.4, 6.9, 4.7 Hz, 1H), 2.09 – 1.99 (m, 1H). ^{13}C NMR (126 MHz, Chloroform-*d*) δ 170.52, 158.82, 149.51, 149.26, 148.20, 137.08, 136.22, 134.96, 134.89, 129.16, 128.87, 128.78, 127.73, 127.69, 127.38, 123.98, 122.69, 122.66, 69.72, 61.58, 57.98, 39.63, 29.82. FTIR (CHCl₃ film): 3353.05, 2924.52, 2853.65, 1668.12, 1515.78, 1338.84, 1159.97 cm⁻¹. HRMS: [M+Na]⁺ calc. 537.1572, found 537.1568.

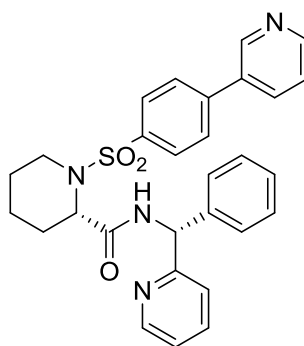
(S)-5-oxo-N-((R)-phenyl(pyridin-2-yl)methyl)-1-((4-(pyridin-3-yl)phenyl)sulfonyl)pyrrolidine-2-carboxamide (**218**)



^1H NMR (500 MHz, Chloroform- d) δ 8.84 (s, 1H), 8.67 (s, 1H), 8.62 (d, J = 4.8 Hz, 1H), 8.22 (d, J = 6.5 Hz, 1H), 8.11 (d, J = 8.3 Hz, 2H), 7.88 (dt, J = 7.9, 1.9 Hz, 1H), 7.68 (td, J = 7.7, 1.8 Hz, 1H), 7.62 (d, J = 8.3 Hz, 2H), 7.42 (dd, J = 7.9, 4.7 Hz, 1H), 7.36 – 7.27 (m, 5H), 7.25 – 7.20 (m, 1H), 6.11 (d, J = 6.5 Hz, 1H), 4.93 (dd, J = 6.7, 2.1 Hz, 1H), 2.74 – 2.60 (m, 1H), 2.46 – 2.31 (m, 2H), 2.09 (td, J = 10.1, 2.5 Hz, 1H). ^{13}C NMR (126 MHz, Chloroform- d) δ 173.52, 169.04, 157.95, 149.74, 149.02, 148.48, 143.57, 141.41, 137.33, 137.29, 134.90, 129.97, 128.98, 127.97, 127.41, 127.39, 123.93, 122.95, 122.84, 60.85, 57.81, 30.87, 24.08. FTIR (CHCl_3 film): 2925.48, 1741.89, 1682.59, 1360.53, 1169.62 cm^{-1} . HRMS: $[\text{M}+\text{H}]^+$ calc. 513.1597, found 513.1595.

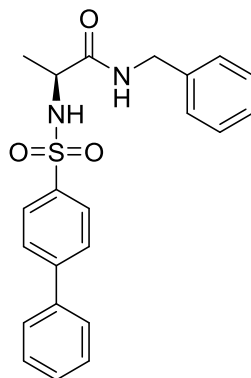
(S)-N-((R)-phenyl(pyridin-2-yl)methyl)-1-((4-(pyridin-3-yl)phenyl)sulfonyl)piperidine-2-carboxamide

(219)



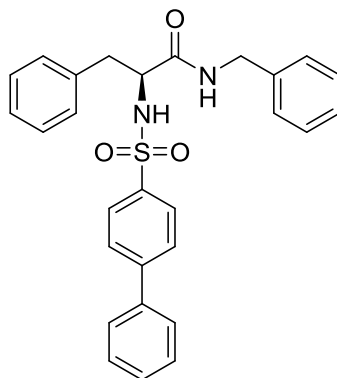
^1H NMR (500 MHz, Chloroform-*d*) δ 8.83 (d, $J = 2.3$ Hz, 1H), 8.66 (dd, $J = 4.8, 1.6$ Hz, 1H), 8.57 (ddd, $J = 4.9, 1.8, 0.9$ Hz, 1H), 8.46 (d, $J = 7.2$ Hz, 1H), 8.00 (d, $J = 8.6$ Hz, 2H), 7.87 (ddd, $J = 7.9, 2.4, 1.6$ Hz, 1H), 7.66 (d, $J = 8.6$ Hz, 3H), 7.60 (td, $J = 7.7, 1.8$ Hz, 1H), 7.41 (ddd, $J = 7.9, 4.9, 0.8$ Hz, 1H), 7.22 (d, $J = 4.3$ Hz, 3H), 7.18 (dddd, $J = 11.1, 6.4, 2.4, 1.4$ Hz, 3H), 6.03 (d, $J = 7.3$ Hz, 1H), 4.62 (d, $J = 4.2$ Hz, 1H), 4.04 (ddd, $J = 14.0, 4.0, 2.1$ Hz, 1H), 3.24 (ddd, $J = 14.1, 12.4, 3.0$ Hz, 1H), 2.34 – 2.26 (m, 1H), 1.81 (s, 1H), 1.56 (q, $J = 3.4$ Hz, 1H), 1.52 – 1.45 (m, 1H), 1.43 – 1.31 (m, 2H), 1.28 – 1.22 (m, 1H). ^{13}C NMR (126 MHz, Chloroform-*d*) δ 168.63, 158.68, 149.76, 149.00, 148.43, 142.27, 141.59, 140.03, 136.97, 134.67, 132.25, 128.78, 128.20, 127.93, 127.70, 127.37, 123.87, 122.73, 122.61, 57.63, 56.42, 43.66, 25.07, 24.17, 20.09. FTIR (CHCl₃ film): 3374.34, 2924.52, 2853.17, 1674.39, 1495.53, 1337.39, 1159.49 cm⁻¹. HRMS: [M+H]⁺ calc. 513.1960, found 513.1960.

(S)-2-([1,1'-biphenyl]-4-sulfonamido)-N-benzylpropanamide (**220**)



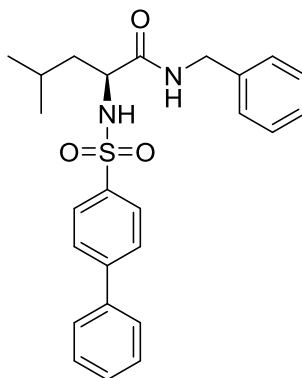
^1H NMR (500 MHz, $\text{DMSO-}d_6$) δ 8.39 (t, $J = 5.9$ Hz, 1H), 8.11 (s, 1H), 7.87 (d, $J = 1.8$ Hz, 4H), 7.74 (dd, $J = 8.2, 1.4$ Hz, 2H), 7.57 – 7.49 (m, 2H), 7.47 – 7.40 (m, 1H), 7.26 (t, $J = 7.5$ Hz, 2H), 7.22 – 7.17 (m, 1H), 7.17 – 7.12 (m, 2H), 4.22 – 4.09 (m, 2H), 3.85 (d, $J = 7.2$ Hz, 1H), 1.12 (d, $J = 7.1$ Hz, 3H). ^{13}C NMR (126 MHz, $\text{DMSO-}d_6$) δ 171.77, 144.35, 140.47, 139.63, 139.10, 129.72, 129.08, 128.81, 127.81, 127.74, 127.64, 127.63, 127.32, 52.50, 42.59, 19.77. FTIR (CHCl_3 film): 3231.63, 1647.39, 1327.27, 1159.49, 1095.85 cm^{-1} . HRMS: $[\text{M}+\text{H}]^+$ calc. 395.1429, found 395.1431.

(S)-2-([1,1'-biphenyl]-4-sulfonamido)-N-benzyl-3-phenylpropanamide (**221**)



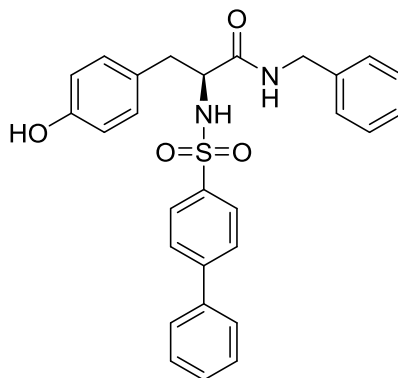
^1H NMR (500 MHz, Chloroform-*d*) δ 7.69 (dd, J = 8.3, 1.2 Hz, 2H), 7.62 – 7.56 (m, 4H), 7.51 (dd, J = 8.3, 7.0 Hz, 2H), 7.47 – 7.41 (m, 1H), 7.29 – 7.21 (m, 3H), 7.19 – 7.14 (m, 1H), 7.14 – 7.08 (m, 4H), 6.98 – 6.92 (m, 2H), 6.72 (t, J = 5.8 Hz, 1H), 5.36 (d, J = 7.0 Hz, 1H), 4.33 (d, J = 5.9 Hz, 2H), 4.00 (q, J = 6.9 Hz, 1H), 3.06 – 2.91 (m, 2H). ^{13}C NMR (126 MHz, Chloroform-*d*) δ 170.26, 145.86, 139.17, 137.51, 137.33, 135.40, 129.27, 129.24, 129.00, 128.75, 128.74, 127.82, 127.72, 127.60, 127.37, 127.31, 58.31, 43.74, 38.71. FTIR (CHCl₃ film): 3398.92, 1652.21, 1330.16, 1162.38 cm⁻¹. HRMS: [M+H]⁺ calc. 471.1742, found 471.1735.

(S)-2-([1,1'-biphenyl]-4-sulfonamido)-N-benzyl-4-methylpentanamide (**222**)



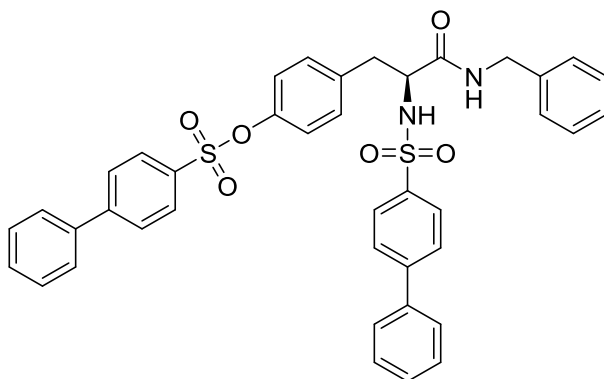
^1H NMR (500 MHz, Chloroform-*d*) δ 7.91 (d, $J = 8.7$ Hz, 2H), 7.68 (d, $J = 8.7$ Hz, 2H), 7.61 – 7.56 (m, 2H), 7.51 – 7.46 (m, 2H), 7.46 – 7.41 (m, 1H), 7.26 – 7.20 (m, 3H), 7.17 – 7.05 (m, 2H), 6.48 (t, $J = 5.8$ Hz, 1H), 5.48 (d, $J = 7.6$ Hz, 1H), 4.32 – 4.16 (m, 2H), 3.77 (ddd, $J = 9.4, 7.5, 4.4$ Hz, 1H), 1.65 – 1.41 (m, 3H), 0.84 (d, $J = 6.4$ Hz, 3H), 0.68 (d, $J = 6.2$ Hz, 3H). ^{13}C NMR (126 MHz, Chloroform-*d*) δ 171.47, 137.55, 129.23, 128.82, 128.76, 127.97, 127.82, 127.74, 127.69, 127.42, 55.76, 43.77, 42.60, 24.49, 23.12, 21.34. FTIR (CHCl₃ film): 3281.29, 2956.82, 1652.21, 1325.82, 1162.87 cm⁻¹. HRMS: [M+H]⁺ calc. 437.1899, found 437.1899.

(S)-2-([1,1'-biphenyl]-4-sulfonamido)-N-benzyl-3-(4-hydroxyphenyl)propanamide (**223**)



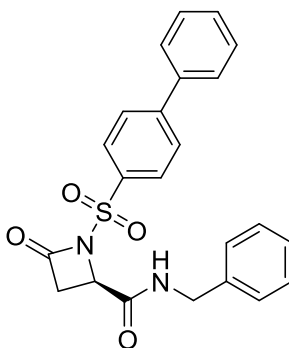
^1H NMR (500 MHz, Chloroform-*d*) δ 7.75 – 7.67 (m, 3H), 7.66 (s, 5H), 7.50 (t, J = 7.5 Hz, 2H), 7.44 (td, J = 7.2, 6.3, 2.8 Hz, 1H), 7.27 (s, 2H), 7.16 – 7.13 (m, 2H), 6.77 (d, J = 8.3 Hz, 2H), 6.58 (d, J = 8.3 Hz, 2H), 4.99 (d, J = 6.7 Hz, 1H), 4.45 – 4.29 (m, 2H), 3.88 (q, J = 6.7 Hz, 1H), 3.05 – 2.81 (m, 2H). ^{13}C NMR (126 MHz, Chloroform-*d*) δ 170.23, 155.20, 137.11, 130.44, 129.32, 128.86, 128.83, 127.85, 127.81, 127.73, 127.45, 127.04, 115.96, 58.32, 43.85, 37.80. FTIR (CHCl₃ film): 3297.68, 2924.04, 1652.21, 1515.78, 1330.16, 1161.42 cm⁻¹. HRMS: [M-H]⁻ calc. 485.1535, found 485.1548.

(S)-4-(2-([1,1'-biphenyl]-4-sulfonamido)-3-(benzylamino)-3-oxopropyl)phenyl [1,1'-biphenyl]-4-sulfonate (**224**)



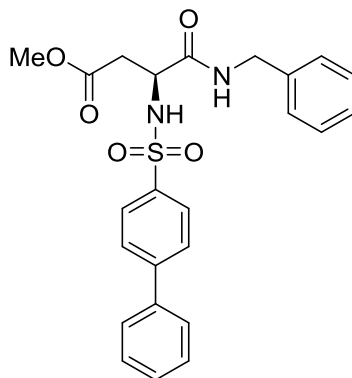
^1H NMR (500 MHz, Chloroform-*d*) δ 7.90 – 7.76 (m, 2H), 7.72 – 7.64 (m, 4H), 7.63 – 7.57 (m, 6H), 7.52 – 7.38 (m, 7H), 7.26 – 7.17 (m, 3H), 7.14 – 7.05 (m, 2H), 6.92 – 6.85 (m, 2H), 6.82 – 6.76 (m, 2H), 6.67 (t, J = 5.8 Hz, 1H), 5.34 (d, J = 7.4 Hz, 1H), 4.29 (d, J = 5.8 Hz, 2H), 3.95 (td, J = 7.6, 5.9 Hz, 1H), 3.01 (dd, J = 14.1, 5.9 Hz, 1H), 2.88 (dd, J = 14.1, 7.9 Hz, 1H). ^{13}C NMR (126 MHz, Chloroform-*d*) δ 169.93, 148.74, 147.30, 146.04, 138.93, 138.81, 137.35, 137.29, 134.72, 133.84, 130.61, 129.27, 129.02, 128.84, 128.81, 127.83, 127.80, 127.72, 127.71, 127.69, 127.48, 127.44, 122.78, 58.11, 43.80, 38.15. FTIR (CHCl₃ film): 3292.86, 1651.73, 1504.69, 1373.07, 1153.22 cm⁻¹. HRMS: [M-H]⁻ calc. 701.1780, found 701.1777.

(R)-1-([1,1'-biphenyl]-4-ylsulfonyl)-N-benzyl-4-oxoazetidine-2-carboxamide (**225**)



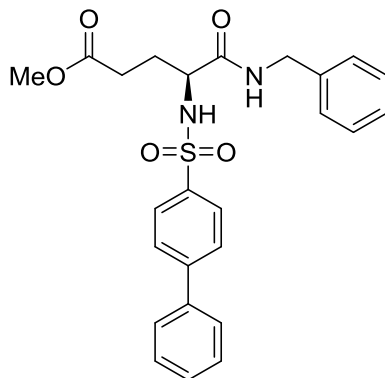
^1H NMR (500 MHz, Chloroform-*d*) δ 7.88 (d, J = 8.0 Hz, 2H), 7.67 (d, J = 8.3 Hz, 2H), 7.54 (d, J = 7.3 Hz, 2H), 7.42 (dd, J = 8.3, 6.8 Hz, 2H), 7.38 – 7.33 (m, 1H), 7.27 – 7.17 (m, 4H), 4.56 (d, J = 2.1 Hz, 2H), 4.18 (dd, J = 8.8, 5.7 Hz, 1H), 3.01 (dd, J = 18.4, 8.9 Hz, 1H), 2.68 (ddd, J = 18.3, 5.7, 0.9 Hz, 1H). ^{13}C NMR (126 MHz, Chloroform-*d*) δ 174.42, 173.84, 138.12, 135.07, 129.08, 128.79, 128.71, 128.59, 128.20, 127.85, 127.67, 127.33, 51.49, 42.75, 37.01. FTIR (CHCl₃ film): 3227.29, 1704.76, 1351.37, 1146.47 cm^{-1} . HRMS: $[\text{M}-\text{H}]^-$ calc. 419.1066, found 419.1078.

methyl (S)-3-([1,1'-biphenyl]-4-sulfonamido)-4-(benzylamino)-4-oxobutanoate (**226**)



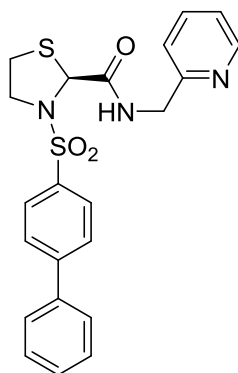
^1H NMR (500 MHz, Chloroform-*d*) δ 7.91 (dd, $J = 8.3, 1.6$ Hz, 2H), 7.78 – 7.67 (m, 2H), 7.67 – 7.54 (m, 2H), 7.50 (ddd, $J = 7.8, 6.3, 1.4$ Hz, 2H), 7.47 – 7.39 (m, 1H), 7.31 – 7.21 (m, 4H), 7.20 – 7.12 (m, 2H), 7.00 (s, 1H), 6.12 (d, $J = 9.0$ Hz, 1H), 4.48 – 4.30 (m, 2H), 4.15 (ddd, $J = 9.5, 5.8, 3.8$ Hz, 1H), 3.62 (d, $J = 1.2$ Hz, 3H), 3.07 (ddd, $J = 17.3, 3.9, 1.3$ Hz, 1H), 2.40 (ddd, $J = 17.2, 6.1, 1.5$ Hz, 1H). ^{13}C NMR (126 MHz, Chloroform-*d*) δ 169.21, 137.55, 129.27, 128.89, 128.84, 128.12, 127.71, 127.61, 127.46, 76.91, 53.58, 52.38, 43.94, 35.61. FTIR (CHCl₃ film): 3377.23, 1739.48, 1668.12, 1339.8, 1162.87 cm⁻¹. HRMS: [M-H]⁻ calc. 451.1328, found 451.1338.

methyl (S)-4-([1,1'-biphenyl]-4-sulfonamido)-5-(benzylamino)-5-oxopentanoate (**227**)



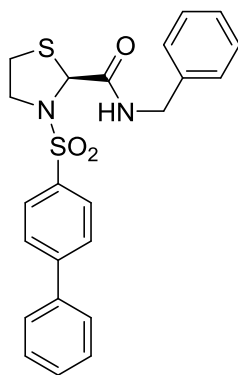
^1H NMR (500 MHz, Chloroform-*d*) δ 7.93 – 7.83 (m, 2H), 7.70 – 7.63 (m, 2H), 7.62 – 7.55 (m, 2H), 7.51 – 7.45 (m, 2H), 7.46 – 7.39 (m, 1H), 7.25 – 7.14 (m, 3H), 7.10 (dd, $J = 7.7, 1.9$ Hz, 2H), 6.78 (t, $J = 5.8$ Hz, 1H), 6.26 (d, $J = 7.5$ Hz, 1H), 4.38 – 4.22 (m, 2H), 3.86 (ddd, $J = 8.8, 7.5, 4.1$ Hz, 1H), 3.64 (s, 3H), 2.51 (ddd, $J = 17.6, 8.8, 5.1$ Hz, 1H), 2.28 (ddd, $J = 17.7, 6.9, 5.0$ Hz, 1H), 2.03 – 1.95 (m, 1H), 1.90 (dddd, $J = 14.3, 8.8, 6.9, 5.1$ Hz, 1H). ^{13}C NMR (126 MHz, Chloroform-*d*) δ 129.21, 128.78, 128.75, 127.86, 127.79, 127.65, 127.62, 127.41, 77.41, 56.40, 52.19, 43.73, 29.73, 28.25. FTIR (CHCl₃ film): 3282.25, 1733.21, 1652.7, 1161.42, 1094.89 cm⁻¹. HRMS: [M-H]⁻ calc. 465.1484, found 465.1495.

(S)-3-([1,1'-biphenyl]-4-ylsulfonyl)-N-(pyridin-2-ylmethyl)thiazolidine-2-carboxamide (**229**)



^1H NMR (500 MHz, Chloroform-*d*) δ 8.52 (dt, $J = 4.9, 1.2$ Hz, 1H), 7.95 (dd, $J = 8.6, 2.2$ Hz, 2H), 7.82 (q, $J = 5.4, 4.0$ Hz, 1H), 7.74 (d, $J = 8.4$ Hz, 2H), 7.64 (td, $J = 7.7, 1.8$ Hz, 1H), 7.61 – 7.58 (m, 2H), 7.49 – 7.45 (m, 2H), 7.44 – 7.38 (m, 1H), 7.27 (d, $J = 8.0$ Hz, 1H), 7.19 – 7.14 (m, 1H), 5.50 (s, 1H), 4.59 (d, $J = 5.3$ Hz, 2H), 4.01 – 3.94 (m, 1H), 3.77 (ddd, $J = 11.8, 7.2, 6.0$ Hz, 1H), 3.00 (dt, $J = 11.1, 5.7$ Hz, 1H), 2.59 (ddd, $J = 11.0, 7.2, 6.0$ Hz, 1H). ^{13}C NMR (126 MHz, Chloroform-*d*) δ 169.31, 156.20, 149.26, 138.92, 137.00, 135.24, 129.27, 128.95, 128.56, 128.15, 127.49, 122.57, 121.88, 65.23, 53.06, 44.83, 31.53. FTIR (CHCl₃ film): 3371.92, 3062.41, 2938.98, 2245.7, 1682.59, 1520.11, 1352.82, 1165.28 cm⁻¹. HRMS: [M+Na]⁺ calc. 462.0922, found 462.0923.

(S)-3-([1,1'-biphenyl]-4-ylsulfonyl)-N-benzylthiazolidine-2-carboxamide (**230**)



^1H NMR (500 MHz, Chloroform-*d*) δ 7.92 (d, J = 9.1 Hz, 2H), 7.75 (d, J = 8.3 Hz, 2H), 7.61 (dd, J = 8.1, 1.4 Hz, 2H), 7.49 (dd, J = 8.3, 6.6 Hz, 2H), 7.46 – 7.41 (m, 1H), 7.35 – 7.24 (m, 5H), 7.10 (t, J = 6.0 Hz, 1H), 5.45 (d, J = 5.0 Hz, 1H), 4.50 (t, J = 5.5 Hz, 2H), 3.92 (dt, J = 11.5, 5.7 Hz, 1H), 3.70 (ddd, J = 11.8, 7.1, 6.0 Hz, 1H), 2.95 (dt, J = 11.1, 5.6 Hz, 1H), 2.53 (ddd, J = 11.1, 7.1, 6.0 Hz, 1H). ^{13}C NMR (126 MHz, Chloroform-*d*) δ 169.24, 146.99, 138.89, 137.83, 134.93, 129.30, 129.01, 128.91, 128.54, 128.22, 127.71, 127.69, 127.52, 65.34, 53.22, 43.89, 31.43. FTIR (CHCl₃ film): 3381.57, 3063.85, 3031.07, 2933.68, 2246.66, 1667.64, 1520.11, 1352.82, 1165.76 cm⁻¹. HRMS: [M+Na]⁺ calc. 461.0970, found 461.0966.

References

1. Cao, R., Peng, W., Wang, Z. & Xu, A. β -Carboline alkaloids : Biochemical and pharmacological functions -Carboline Alkaloids : Biochemical and Pharmacological Functions. *Curr. Med. Chem.* **14**, 479–500 (2007).
2. Radwan, M., Hanora, A., Khalifa, S. & Abou-El-Ela, S. H. Manzamines: A potential for novel cures. *Cell Cycle* **11**, 1765–1772 (2012).
3. Ashok, P., Ganguly, S. & Murugesan, S. Manzamine alkaloids: Isolation, cytotoxicity, antimalarial activity and SAR studies. *Drug Discov. Today* **19**, 1781–1791 (2014).
4. Baldwin, J. E. & Whitehead, R. C. On the biosynthesis of Manzamines. *Tetrahedron Lett.* **33**, 2059–2062 (1992).
5. Baldwin, J. E. *et al.* Investigations into the manzamine alkaloid biosynthetic hypothesis. *Angew. Chemie - Int. Ed.* **37**, 2661–2663 (1998).
6. Sakai, R., Higa, T., Jefford, C. W. & Bernardinelli, G. Manzamine A, a Novel Antitumor Alkaloid from a Sponge. *J. Am. Chem. Soc.* **108**, 6404–6405 (1986).
7. Toma, T., Kita, Y. & Fukuyama, T. Total Synthesis of (+)-Manzamine A. *J. Am. Chem. Soc.* **132**, 10233–10235 (2010).
8. Uchida, H., Kimura, Y., Yamabe, M., Nishida, A. & Nakagawa, M. Total synthesis of manzamine A and related compounds. *J. Am. Chem. Soc.* **134**, 17482–17485 (2012).
9. Winkler, J. D. & Axten, J. M. The first total syntheses of ircinol A, ircinal A, and manzamines A and D. *J. Am. Chem. Soc.* **120**, 6425–6426 (1998).
10. El Sayed, K. A. *et al.* New Manzamine Alkaloids with Potent Activity against Infectious Diseases. *J. Am. Chem. Soc.* **123**, 1804–1808 (2001).
11. Ang, K. K. H., Holmes, M. J., Higa, T., Hamann, M. T. & Kara, U. a K. In vivo antimalarial

- activity of the β -carboline alkaloid manzamine A. *Antimicrob. Agents Chemother.* **44**, 1645–1649 (2000).
12. Fattorusso, E. & Tagliatela-Scafati, O. Marine antimalarials. *Mar. Drugs* **7**, 130–152 (2009).
 13. El-Desoky, A. H. *et al.* Acantholactam and pre-neo-kauluamine, manzamine-related alkaloids from the Indonesian marine sponge *Acanthostrongylophora ingens*. *J. Nat. Prod.* **77**, 1536–1540 (2014).
 14. Vance, D., Shah, M., Joshi, A. & Kane, R. S. Polyvalency: a promising strategy for drug design. *Biotechnol. Bioeng.* **101**, 429–34 (2008).
 15. Rao, J., Lahiri, J., Isaacs, L., Weis, R. M. & Whitesides, G. M. A Trivalent System from Vancomycin-d-Ala-d-Ala with Higher Affinity Than Avidin-Biotin. *Sci.* **280**, 708–711 (1998).
 16. McAfee, Q. *et al.* Autophagy inhibitor Lys05 has single-agent antitumor activity and reproduces the phenotype of a genetic autophagy deficiency. *Proc. Natl. Acad. Sci. U. S. A.* **109**, 8253–8258 (2012).
 17. Skouta, R., Hayano, M., Shimada, K. & Stockwell, B. R. Design and synthesis of Pictet-Spengler condensation products that exhibit oncogenic-RAS synthetic lethality and induce non-apoptotic cell death. *Bioorganic Med. Chem. Lett.* **22**, 5707–5713 (2012).
 18. He, F., Bo, Y., Altom, J. D. & Corey, E. J. Enantioselective Total Synthesis of Aspidophytine. *J. Am. Chem. Soc.* **121**, 6771–6772 (1999).
 19. Vitoria, M. *et al.* The global fight against HIV/AIDS, tuberculosis, and malaria: Current status and future perspectives. *Am. J. Clin. Pathol.* **131**, 844–848 (2009).
 20. Boursereau, Y. & Coldham, I. Synthesis and biological studies of 1-amino β -carbolines.

Bioorg. Med. Chem. Lett. **14**, 5841–5844 (2004).

21. Nascimento, A. V., Bousbaa, H., Ferreira, D. & Sarmiento, B. Non-Small Cell Lung Carcinoma: An Overview on Targeted Therapy. *Curr. Drug Targets* **16**, 1448–63 (2015).
22. Rebecca, V. W. & Amaravadi, R. K. Emerging strategies to effectively target autophagy in cancer. *Oncogene* **35**, 1–11 (2015).
23. Glick, D., Barth, S. & Macleod, K. F. Autophagy: cellular and molecular mechanisms. *J. Pathol.* **221**, 3–12 (2010).
24. Boya, P. & Kroemer, G. Lysosomal membrane permeabilization in cell death. *Oncogene* **27**, 6434–6451 (2008).
25. Kallifatidis, G., Hoepfner, D., Jaeg, T., Guzmán, E. A. & Wright, A. E. The marine natural product manzamine a targets vacuolar atpases and inhibits autophagy in pancreatic cancer cells. *Mar. Drugs* **11**, 3500–3516 (2013).
26. Turk, B. & Stoka, V. Protease signalling in cell death: caspases versus cysteine cathepsins. *FEBS Lett.* **581**, 2761–2767 (2007).
27. Giraldo, A. M. V., Appelqvist, H., Ederth, T. & Ollinger, K. Lysosomotropic agents : impact on lysosomal membrane permeabilization and cell death. *Biochem. Soc. Trans.* **42**, 1460–1464 (2014).
28. Lakhter, A. J. *et al.* Chloroquine Promotes Apoptosis in Melanoma Cells by Inhibiting BH3 Domain – Mediated PUMA Degradation. *J. Invest. Dermatol.* **133**, 2247–2254 (2013).
29. Marino, G., Niso-Santano, M., Baehrecke, E. H. & Kroemer, G. Self-consumption: the interplay of autophagy and apoptosis. *Nat Rev Mol Cell Biol* **15**, 81–94 (2014).
30. Yee, K. S., Wilkinson, S., James, J., Ryan, K. M. & Vousden, K. H. PUMA- and Bax-induced autophagy contributes to apoptosis. *Cell Death Differ.* **16**, 1135–45 (2009).

31. Nishida, K., Yamaguchi, O. & Otsu, K. Crosstalk between autophagy and apoptosis in heart disease. *Circ. Res.* **103**, 343–351 (2008).
32. Thorburn, J. *et al.* Autophagy controls the kinetics and extent of mitochondrial apoptosis by regulating PUMA levels. *Cell Rep.* **7**, 45–52 (2014).
33. Boya, P. *et al.* Inhibition of Macroautophagy Triggers Apoptosis Inhibition of Macroautophagy Triggers Apoptosis. *Mol. Cell. Biol.* **25**, 1025–1040 (2005).
34. Amaravadi, R. K. *et al.* Autophagy inhibition enhances therapy-induced apoptosis in a Myc-induced model of lymphoma. *J. Clin. Invest.* **117**, 326–336 (2007).
35. Yu, J. & Zhang, L. PUMA, a potent killer with or without p53. *Oncogene* **27**, S71–S83 (2008).
36. Ruan, Y., Hu, K. & Chen, H. Autophagy inhibition enhances isorhamnetin-induced mitochondria-dependent apoptosis in non-small cell lung cancer cells. *Mol. Med. Rep.* **12**, 5796–5806 (2015).
37. Humphrey, J. M. *et al.* Enantioselective total syntheses of manzamine A and related alkaloids. *J. Am. Chem. Soc.* **124**, 8584–8592 (2002).
38. Jakubec, P., Hawkins, A., Felzmann, W. & Dixon, D. J. Total synthesis of manzamine A and related compounds. *J. Am. Chem. Soc.* **134**, 17482–17485 (2012).
39. Winkler, J. D., Londregan, A. T. & Hamann, M. T. Synthetic modification of manzamine A via Grubbs metathesis. Novel structures with enhanced antibacterial and antiprotozoal properties. *Org. Lett.* **9**, 4467–4469 (2007).
40. Corey, E. J. & Winter, R. a. E. A New, Stereospecific Olefin Synthesis from 1,2Diols. *J. Am. Chem. Soc.* **85**, 2677–2678 (1963).
41. El Sayed, K. A. *et al.* New manzamine alkaloids with potent activity against infectious

- diseases. *J. Am. Chem. Soc.* **123**, 1804–1808 (2001).
42. Hoye, A. T. & Wipf, P. Total synthesis of (-)-sessilifoliamide C and (-)-8-epi-stemoamide. *Org. Lett.* **13**, 2634–2637 (2011).
43. Brenneman, J. B., Machauer, R. & Martin, S. F. Enantioselective synthesis of (+)-anatoxin-a via enyne metathesis. *Tetrahedron* **60**, 7301–7314 (2004).
44. Chen, C.-K., Hortmann, A. G. & Marzabadi, M. R. C102 Oxidation of Amines: Synthetic Utility and a Biomimetic Synthesis of Elaeocarpidine. *J. Am. Chem. Soc.* **110**, 4829–4831 (1988).
45. Volz, H. & Gartner, H. N-acetoxyammonium ions - Reactive intermediates in the polonovski reaction. *European J. Org. Chem.* 2791–2801 (2007).
46. Murahashi, S., Nakae, T., Terai, H. & Komiya, N. Ruthenium-Catalyzed Oxidative Cyanation of Tertiary Amines with Molecular Oxygen or Hydrogen Peroxide and Sodium Cyanide : sp^3 C - H Bond Activation and Carbon - Carbon Bond. 11005–11012 (2008).
47. Suau, R., Nájera, F. & Rico, R. The Polonovski–Potier Reaction of Berbine N-Oxides. Synthesis of 8-Hydroxymethyl and 8-Methylberbines. *Tetrahedron* **56**, 9713–9723 (2000).
48. Volla, C. M. R. & Vogel, P. Chemoselective C-H bond activation: Ligand and solvent free iron-catalyzed oxidative C-C cross-coupling of tertiary amines with terminal alkynes. Reaction scope and mechanism. *Org. Lett.* **11**, 1701–1704 (2009).
49. Kalas, G. *et al.* Synthesis of Vinca Alkaloids and Related Compounds. 90.¹ New Results in the Synthesis of Alkaloids with the Aspidospermane Skeleton. First Total Synthesis of (\pm)-3-Oxominovincine. *J. Org. Chem.* **62**, 9188–9191 (1997).
50. Stockman, R. A., McDermott, P. J., Newton, A. F. & Magnus, P. A versatile chiral pyrrolidine aldehyde building-block for synthesis and formal synthesis of ent-nakadomarin

- A. *Synlett* 559–562 (2010).
51. Moretti, J. D., Wang, X. & Curran, D. P. Minimal fluororous tagging strategy that enables the synthesis of the complete stereoisomer library of SCH725674 macrolactones. *J. Am. Chem. Soc.* **134**, 7963–7970 (2012).
 52. Mozaffarian, D. *et al.* *Heart Disease and Stroke Statistics--2015 Update: A Report From the American Heart Association.* *Circulation* **131**, (2015).
 53. Foex, P. & Sear, J. Hypertension: pathophysiology and treatment. *Contin. Educ. Anaesthesia, Crit. Care Pain* **4**, 71–75 (2004).
 54. Lou, K.-J. New axis in hypertension. *Sci. Exch.* **2**, 1–3 (2009).
 55. Cirillo, R. *et al.* Arrest of preterm labor in rat and mouse by an oral and selective nonprostanoid antagonist of the prostaglandin F₂α receptor (FP). *Am. J. Obstet. Gynecol.* **197**, 54.e1–9 (2007).
 56. Okawa, T. *et al.* Effect of lipopolysaccharide on uterine contractions and prostaglandin production in pregnant rats. *Am. J. Obstet. Gynecol.* **184**, 84–89 (2001).
 57. Olsson, K., Bergström, A., Kindahl, H. & Lagerstedt, A. S. Increased plasma concentrations of vasopressin, oxytocin, cortisol and the prostaglandin F₂α metabolite during labour in the dog. *Acta Physiol. Scand.* **179**, 281–287 (2003).
 58. Yu, Y. *et al.* Prostaglandin F₂α elevates blood pressure and promotes atherosclerosis. *Proc. Natl. Acad. Sci. U. S. A.* **106**, 7985–7990 (2009).
 59. Griffin, B. W., Klimko, P., Crider, J. Y. & Sharif, N. a. AL-8810: a novel prostaglandin F₂α analog with selective antagonist effects at the prostaglandin F₂α (FP) receptor. *J. Pharmacol. Exp. Ther.* **290**, 1278–1284 (1999).
 60. Doheny, H. C., O'Reilly, M. J., Sexton, D. J. & Morrison, J. J. THG113.31, a specific

PGF2alpha receptor antagonist, induces human myometrial relaxation and BKCa channel activation. *Reprod. Biol. Endocrinol.* **5**, 10 (2007).

61. Hirst, J. J. *et al.* Delay of preterm birth in sheep by THG113.31, a prostaglandin F_{2α} receptor antagonist. *Am. J. Obstet. Gynecol.* **193**, 256–266 (2005).
62. Kuduk, S. D., DiPardo, R. M., Chang, R. K., Ng, C. & Bock, M. G. Reversal of diastereoselection in the addition of Grignard reagents to chiral 2-pyridyl tert-butyl (Ellman) sulfinimines. *Tetrahedron Lett.* **45**, 6641–6643 (2004).
63. Tadashi Shiraiwa, Takashi Katayama, Yakehiro Kaito, Hisashi Tanigawa, H. K. syn of thiazo acid1053012.pdf. *Bull. Chem. Soc. Jpn* **71**, 1911–1914 (1998).
64. Kang, S.-K., Park, W.-S., Thopate, T. S. & Ahn, J.-H. Crystallization Induced Dynamic Resolution of Ethyl Thiazolidine-2-Carboxylate. *Bull. Korean Chem. Soc.* **31**, 2709–2711 (2010).

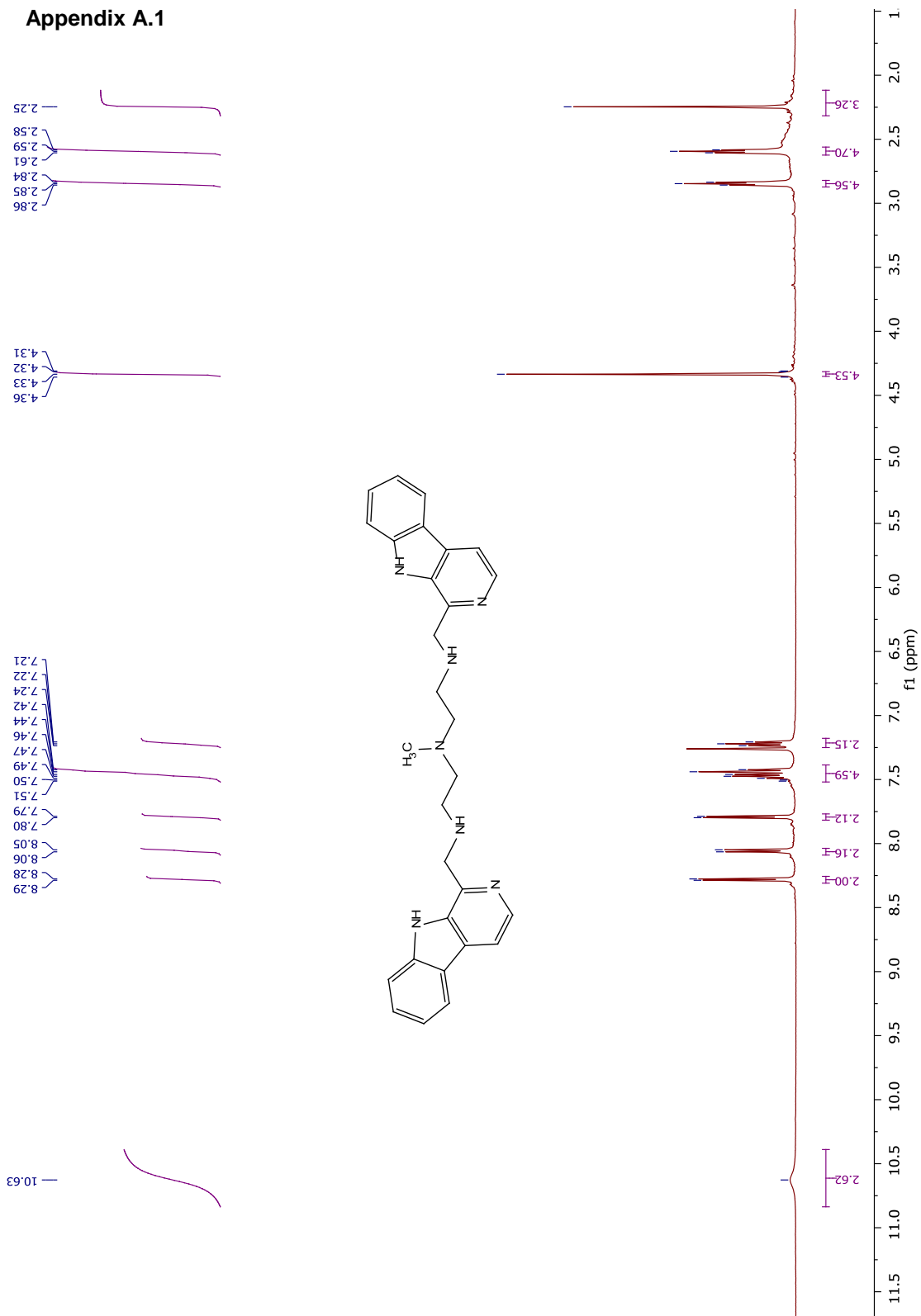
APPENDIX

A.1 Spectral Images for Chapter 1

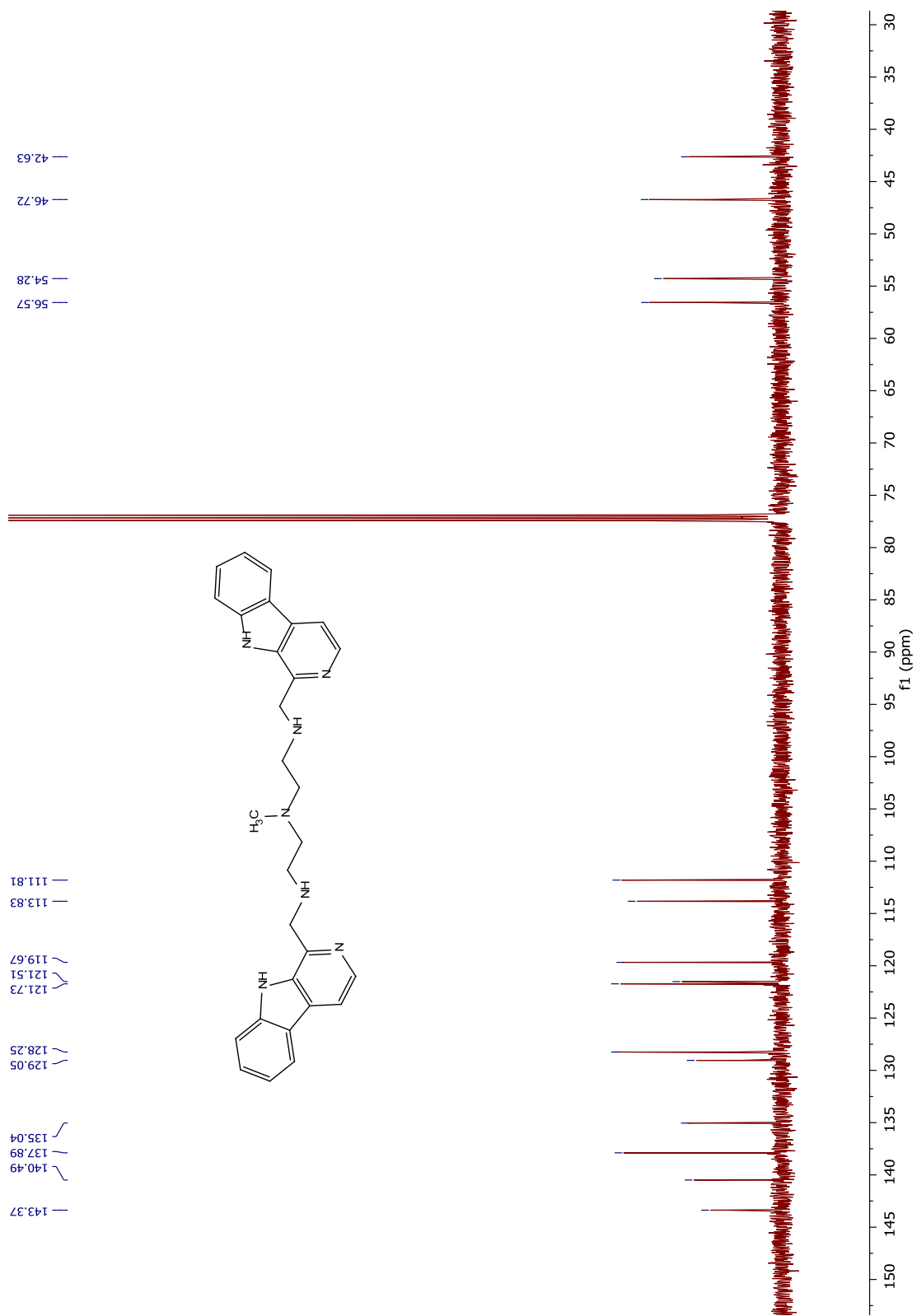
A.2 Spectral Images for Chapter 2

A.3 Spectral Images for Chapter 3

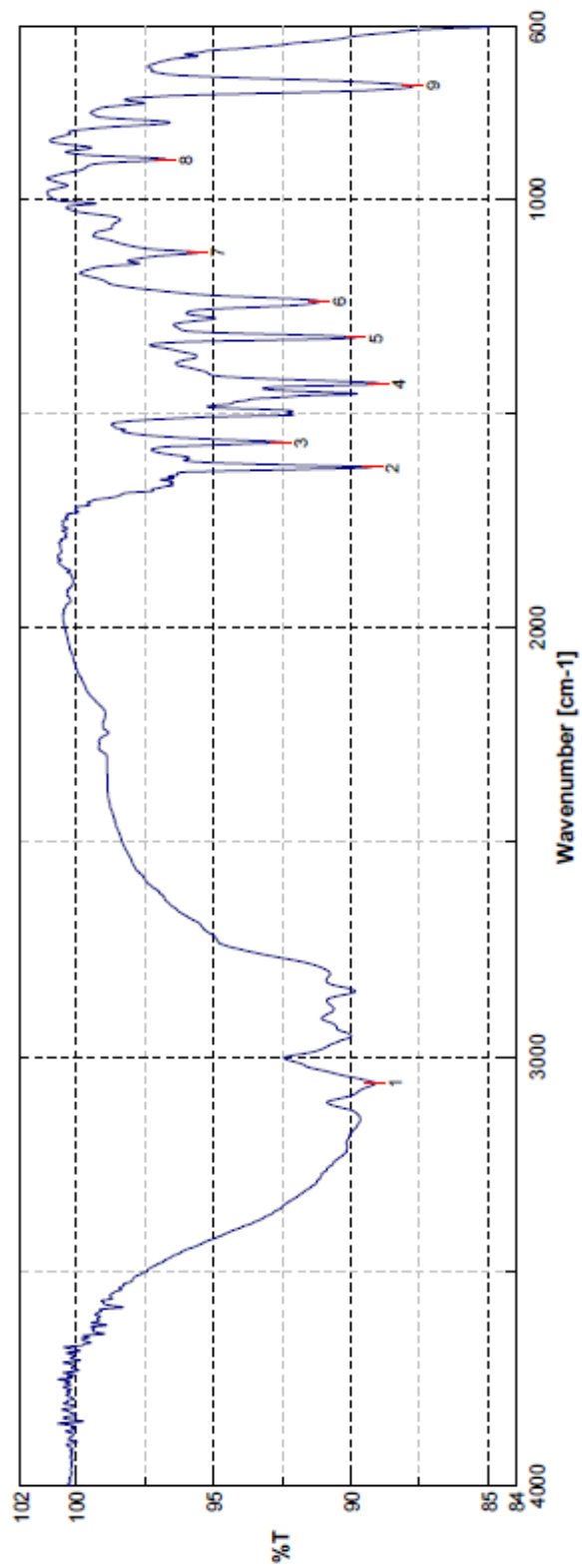
Appendix A.1



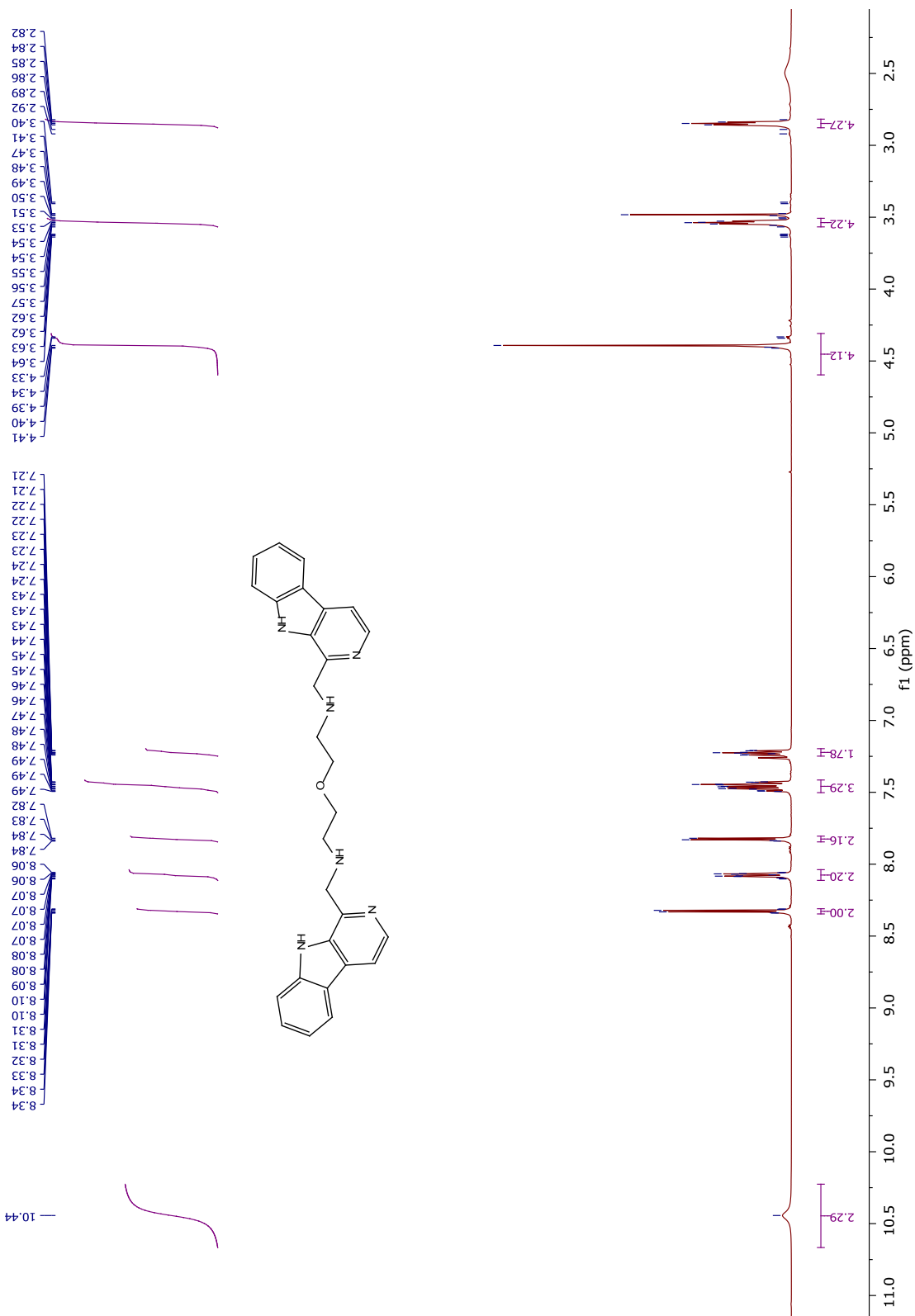
¹H NMR spectrum of compound 25



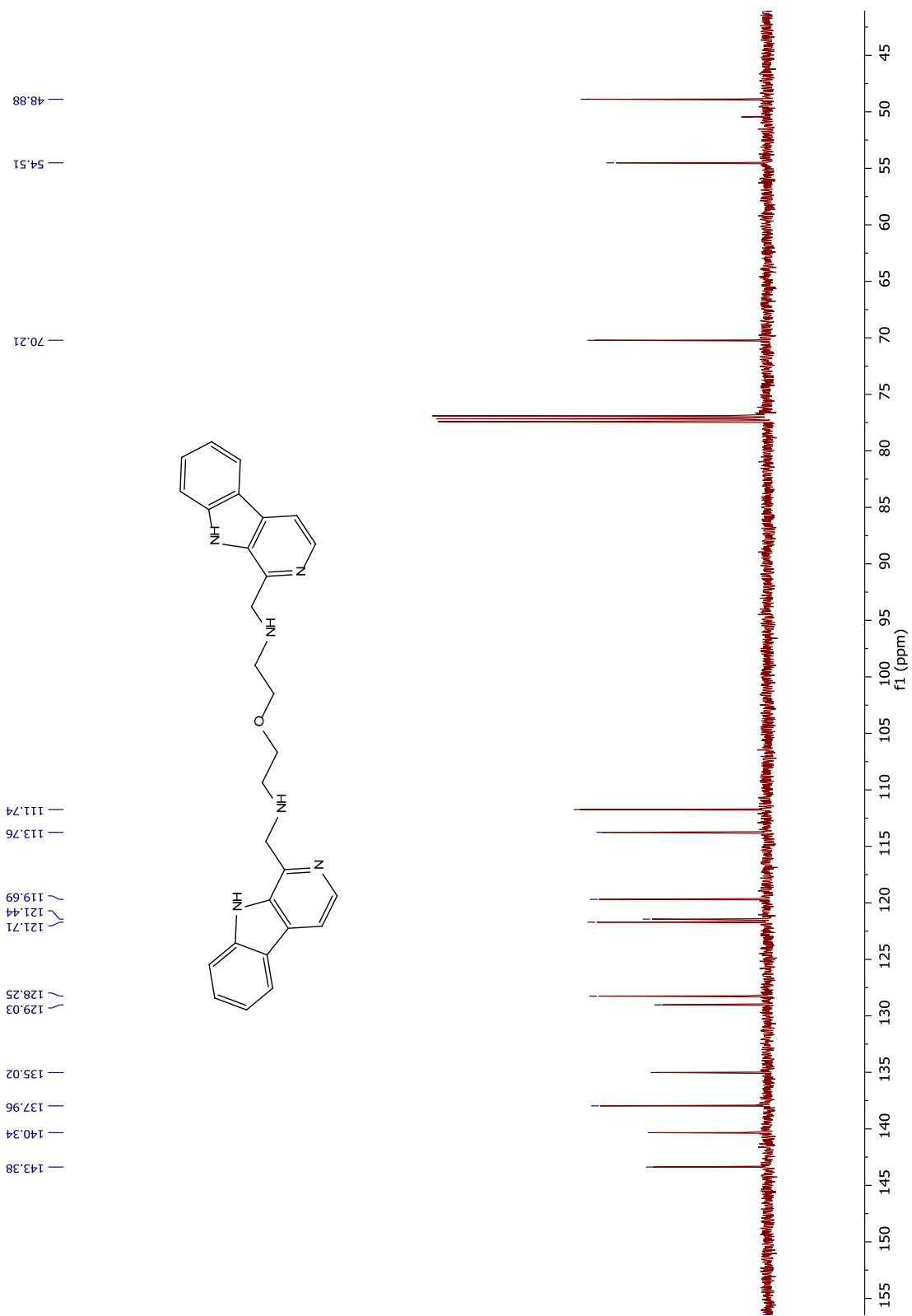
^{13}C NMR spectrum of compound **25**



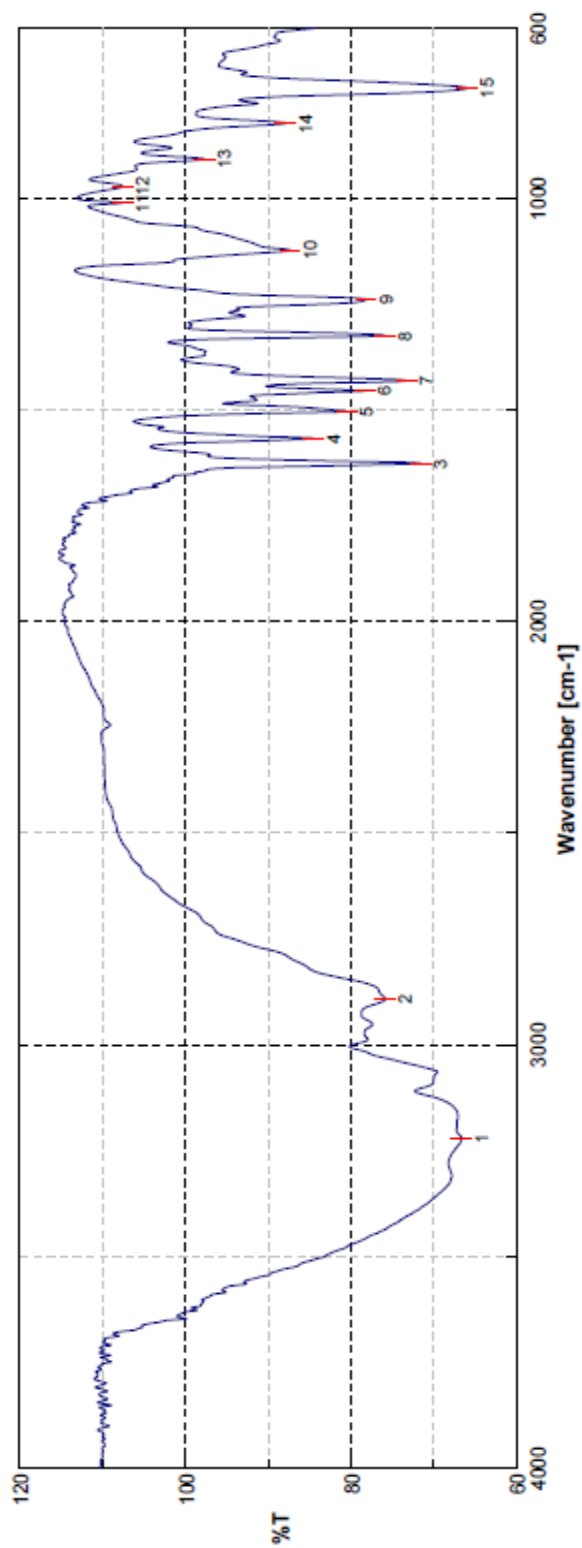
FTIR of compound 25



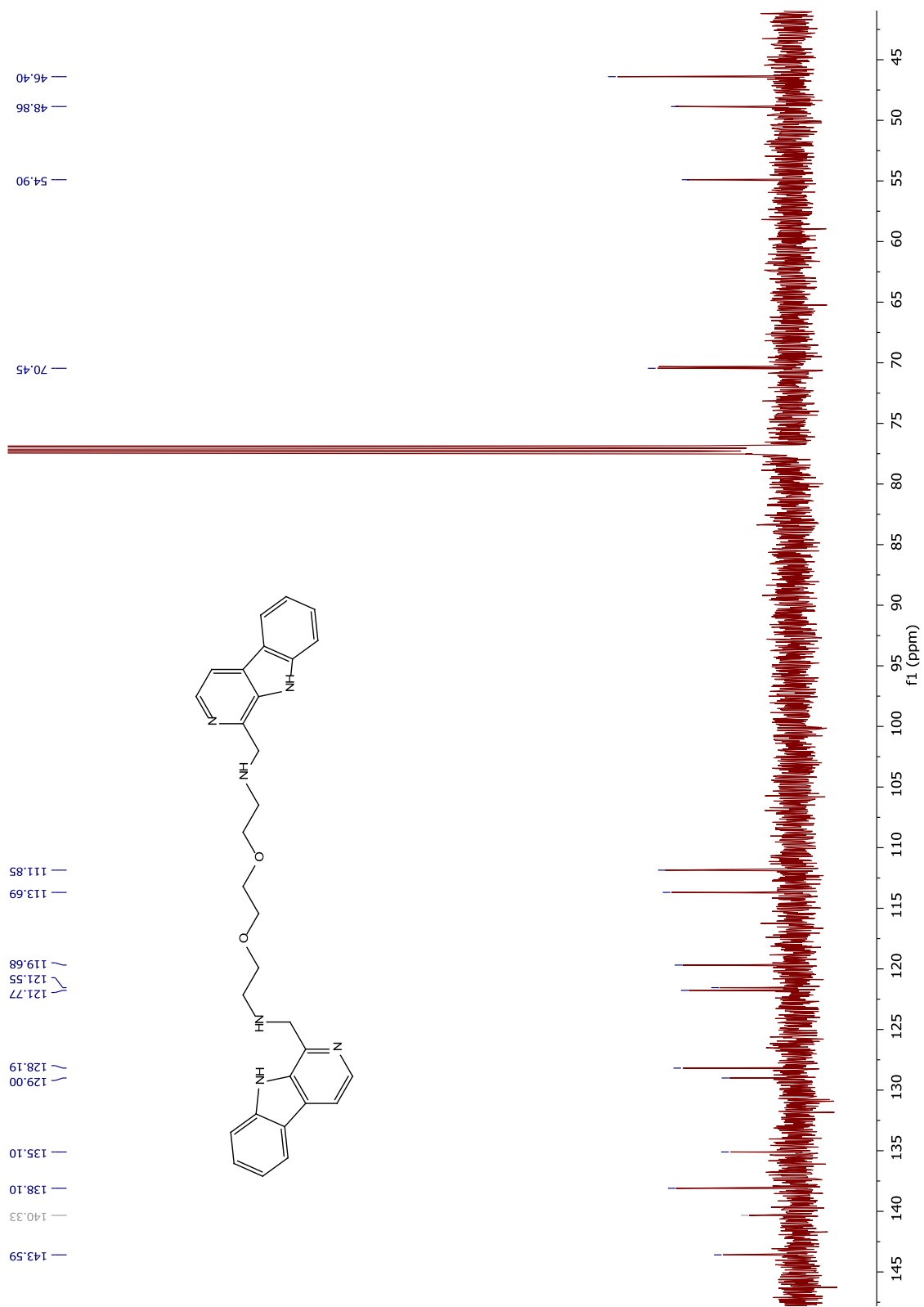
¹H NMR spectrum of compound 26



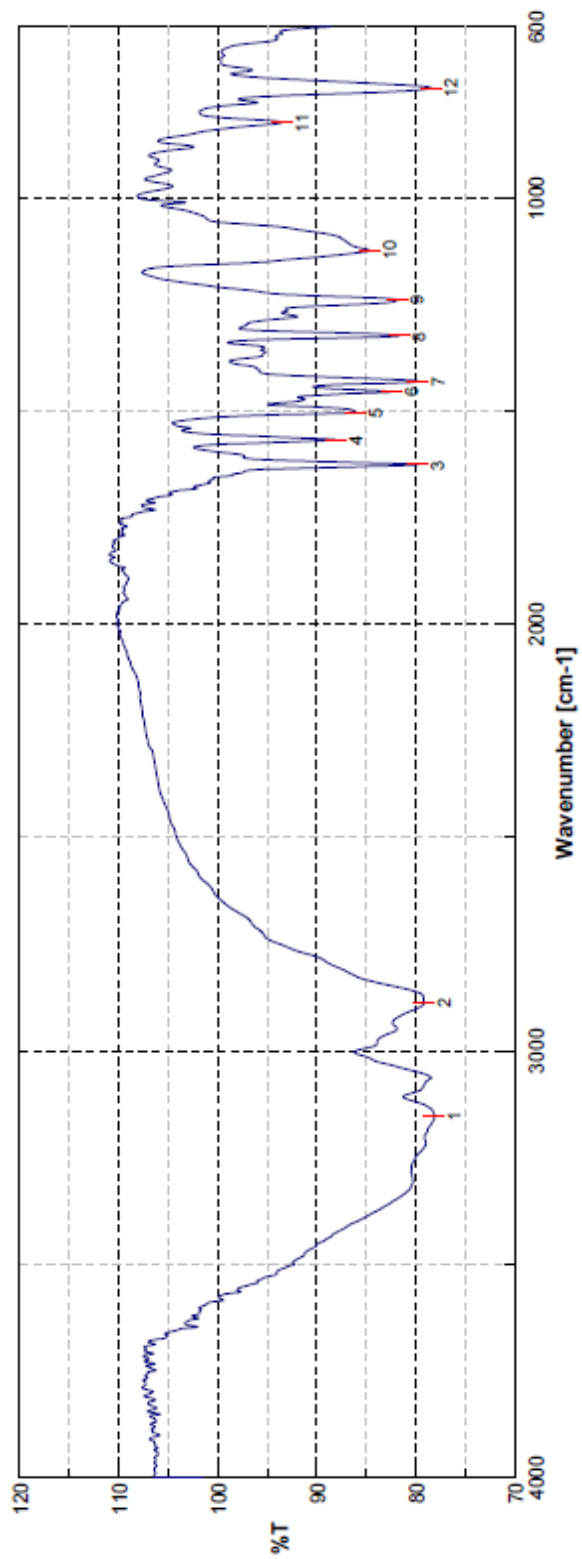
^{13}C NMR spectrum of compound 26



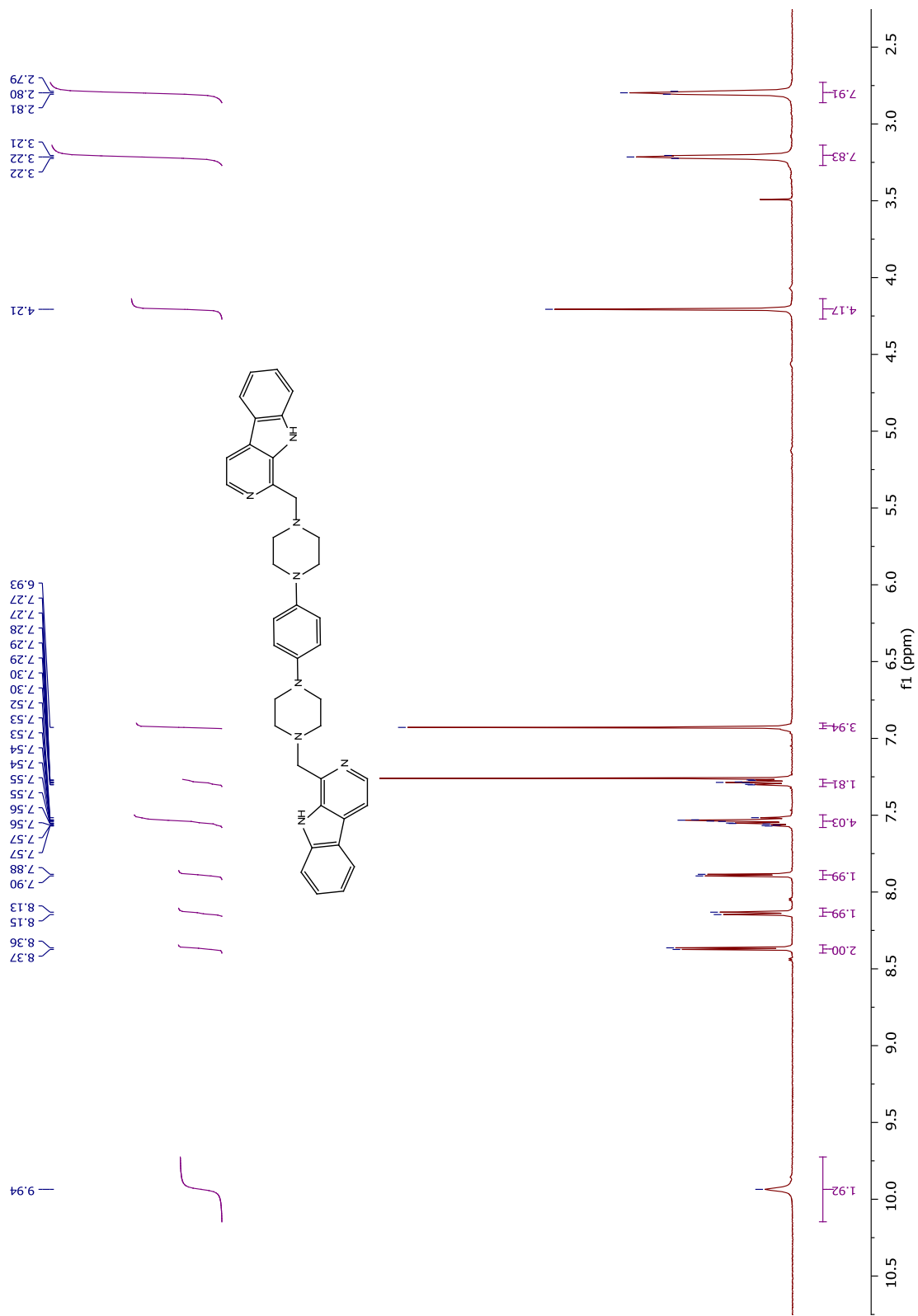
FTIR of compound **26**



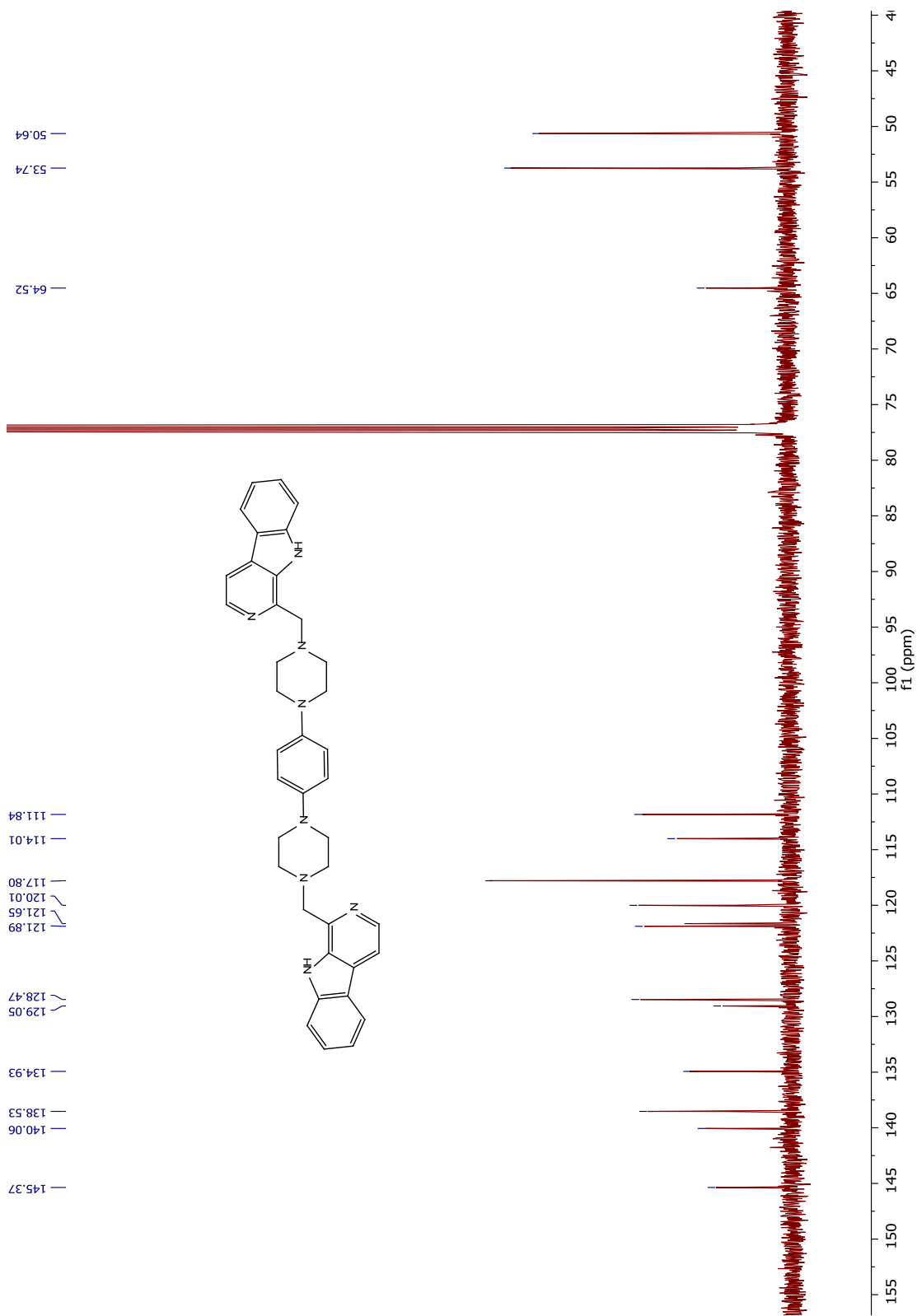
^{13}C NMR spectrum of compound 27



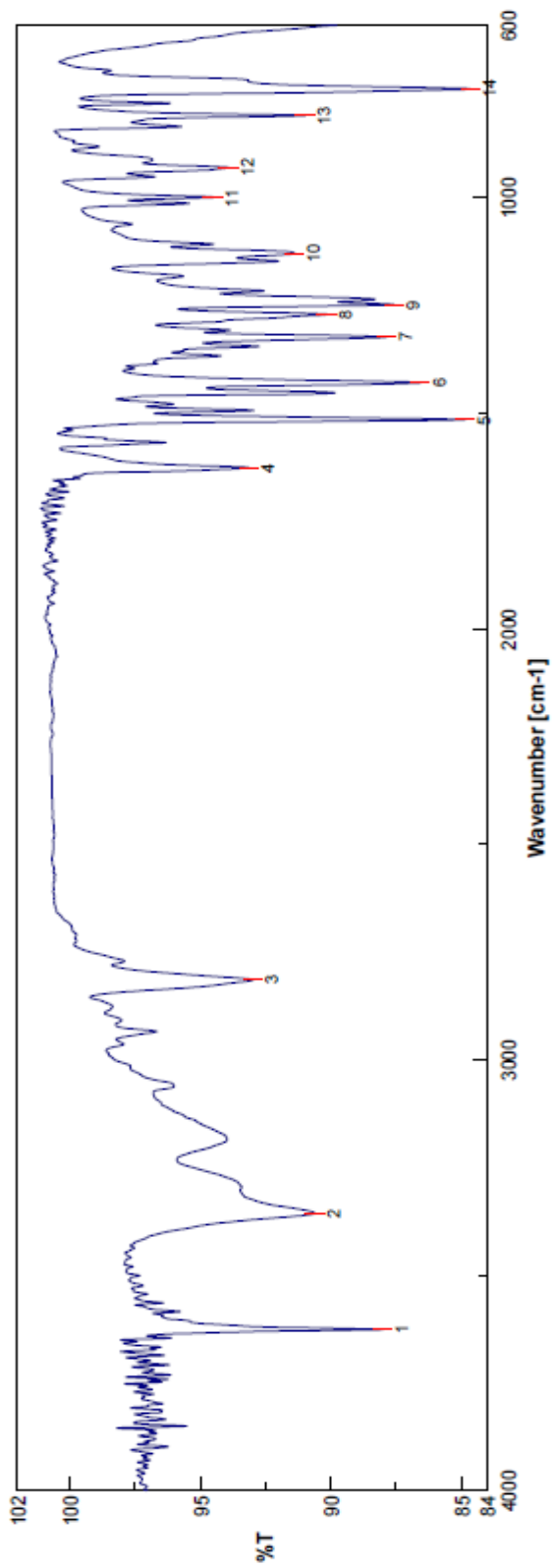
FTIR of compound 27



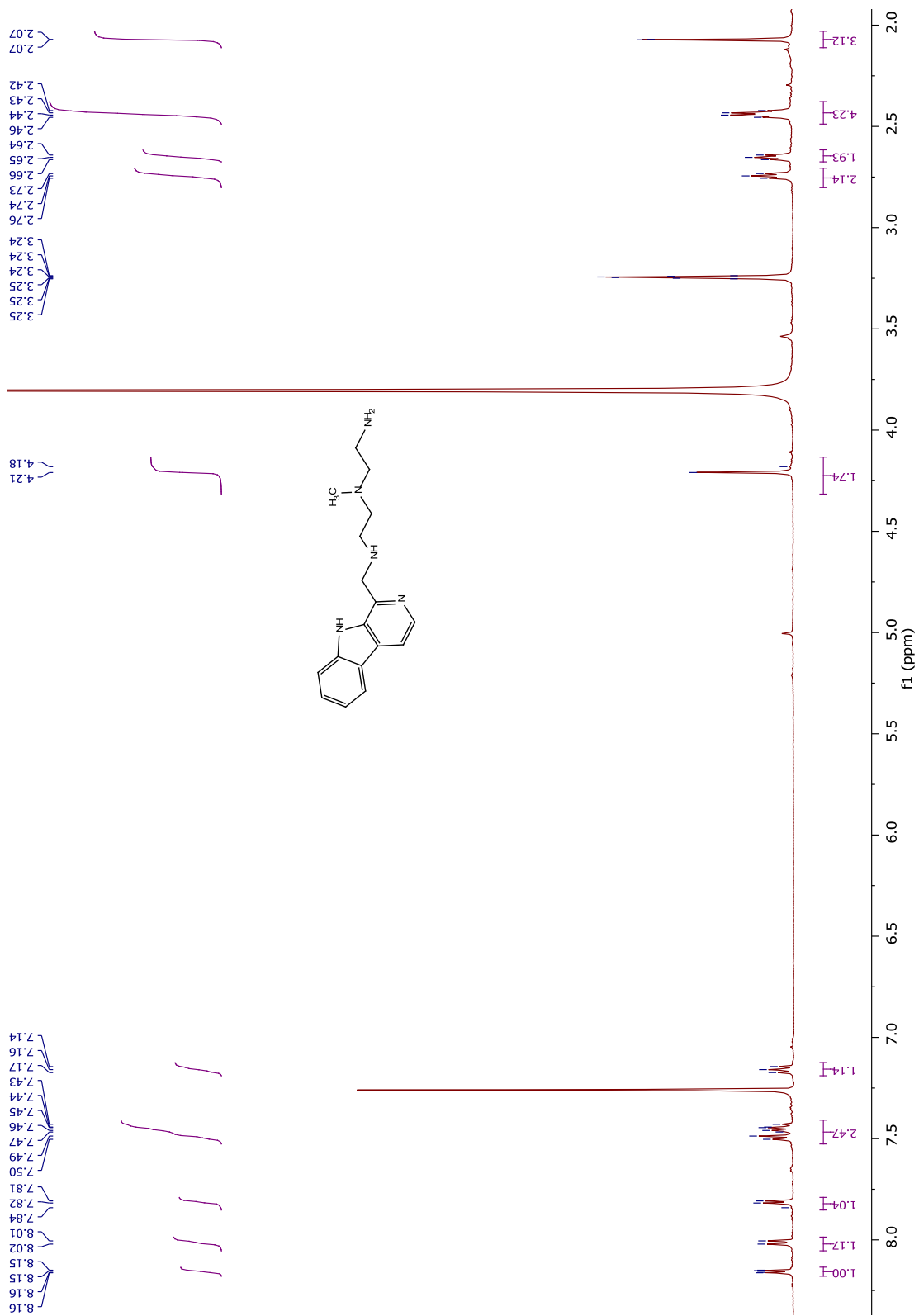
¹H NMR spectrum of compound 28



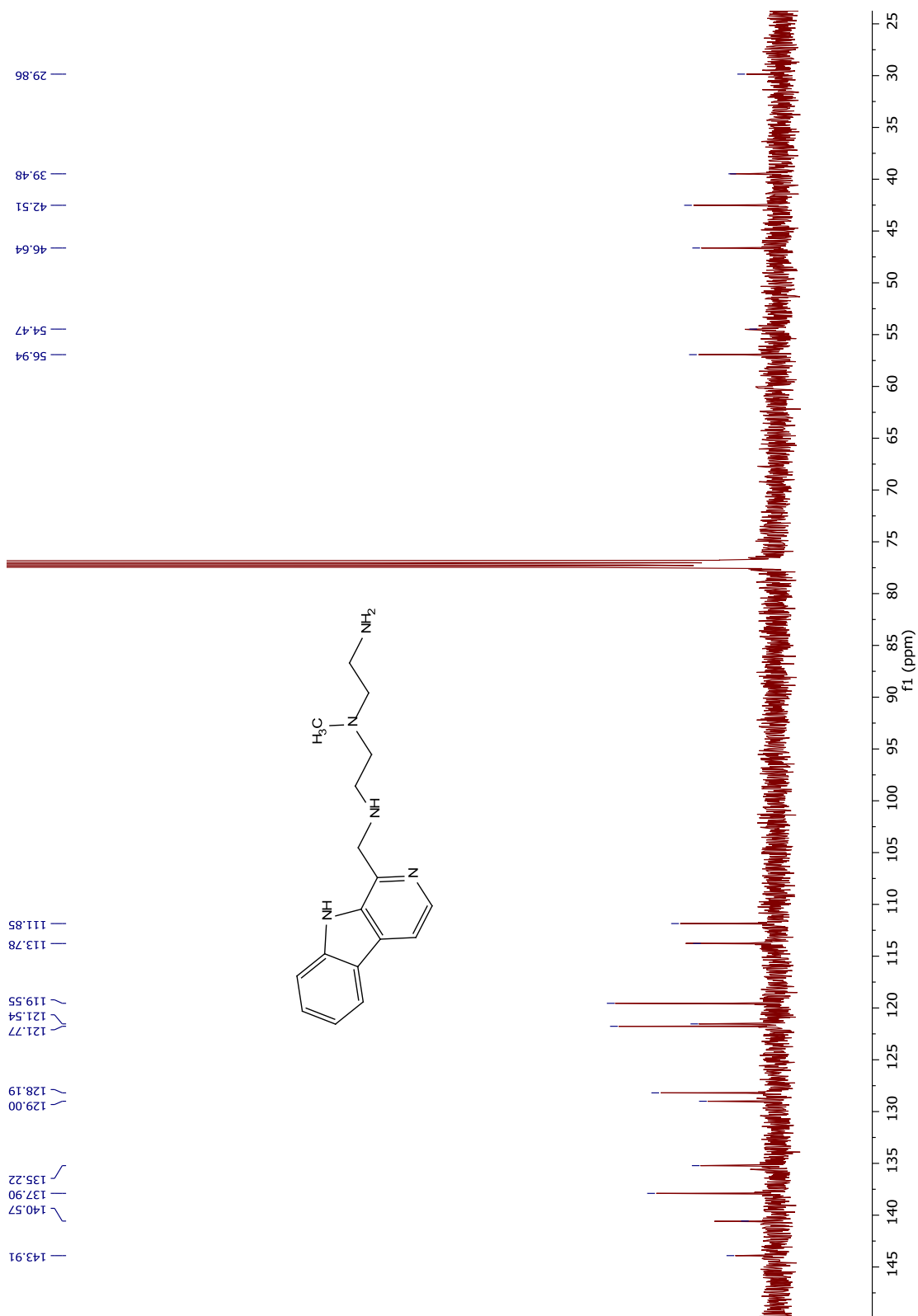
^{13}C NMR spectrum of compound **28**



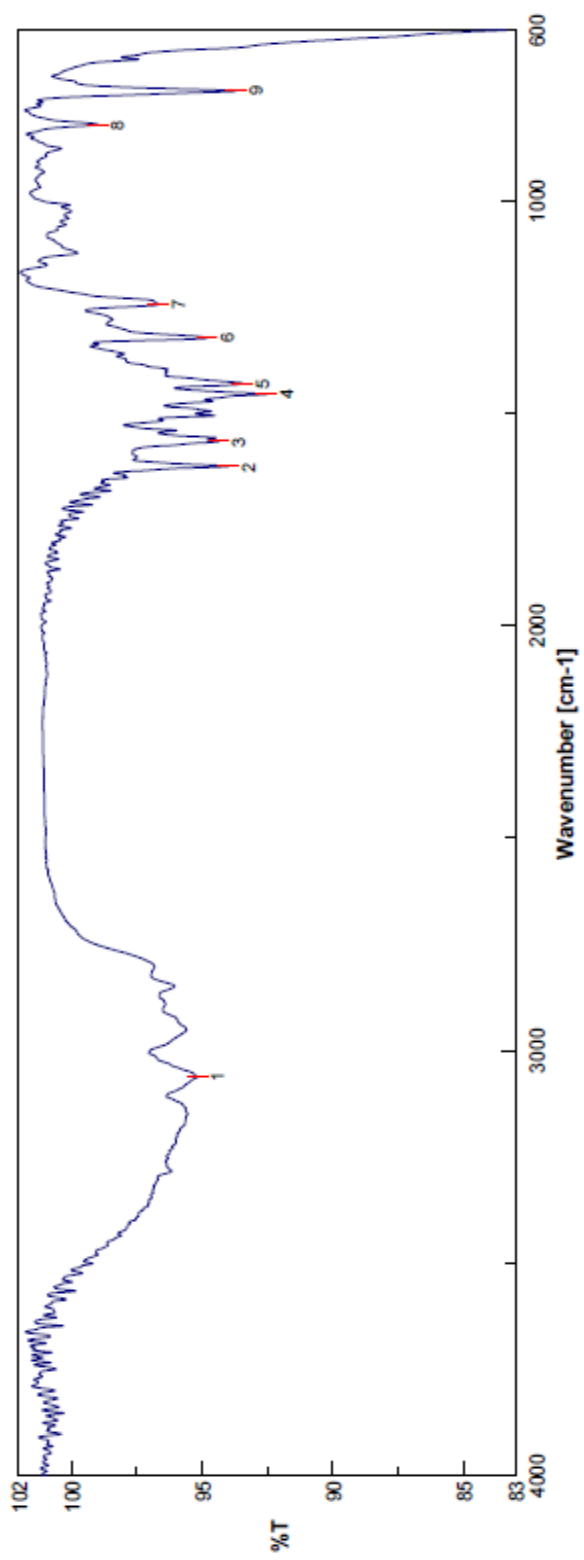
FTIR spectrum of compound **28**



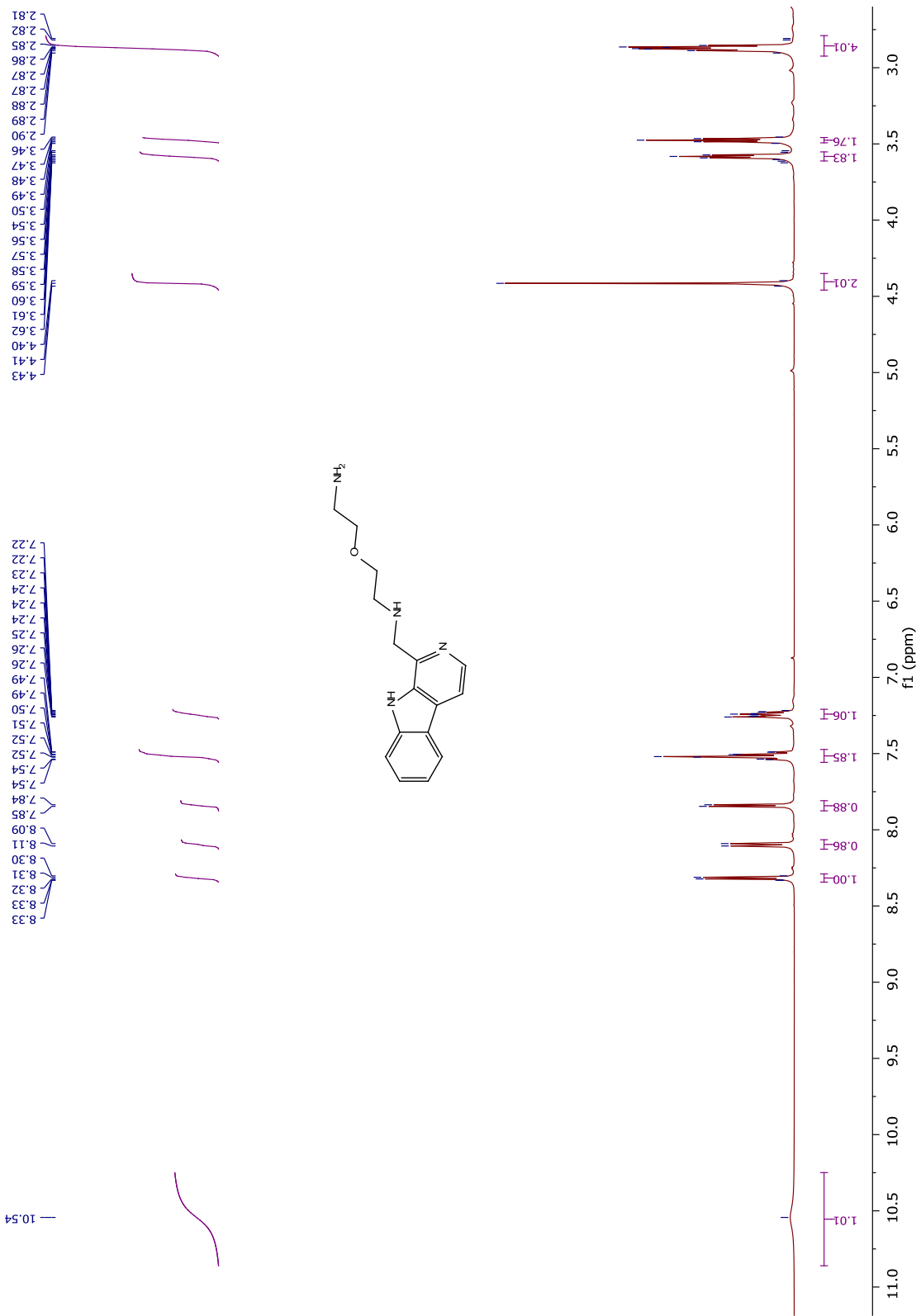
^1H NMR spectrum of compound **34**



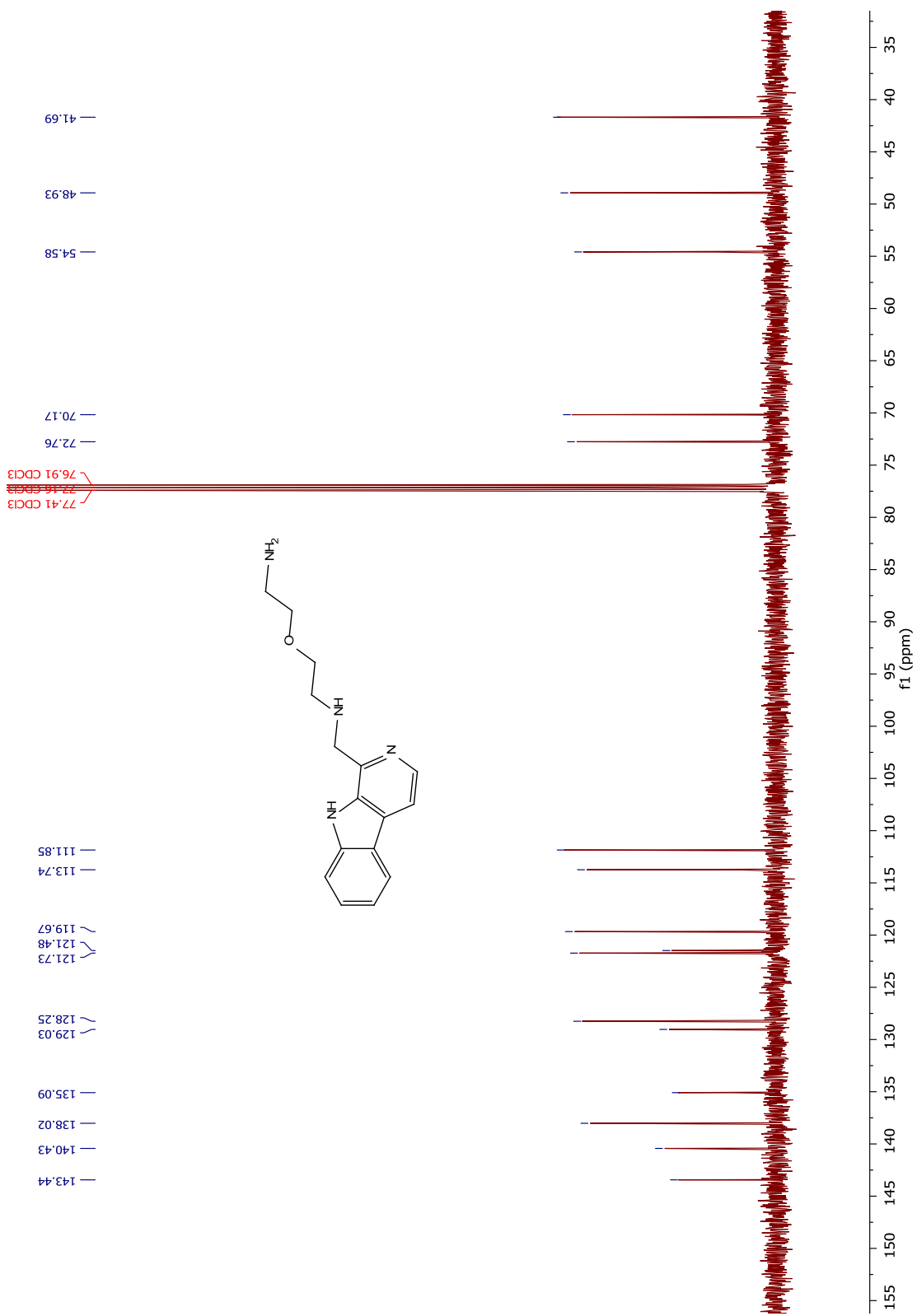
¹³C NMR spectrum of compound 34



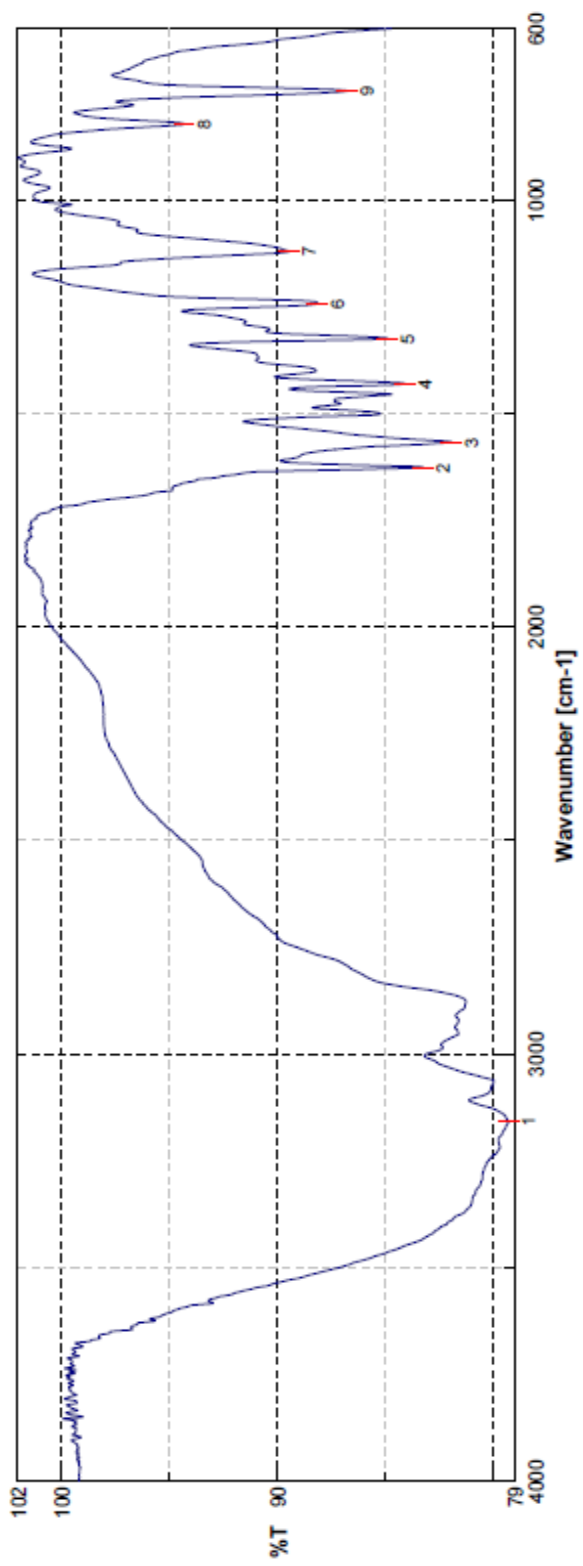
FTIR spectrum of compound 34



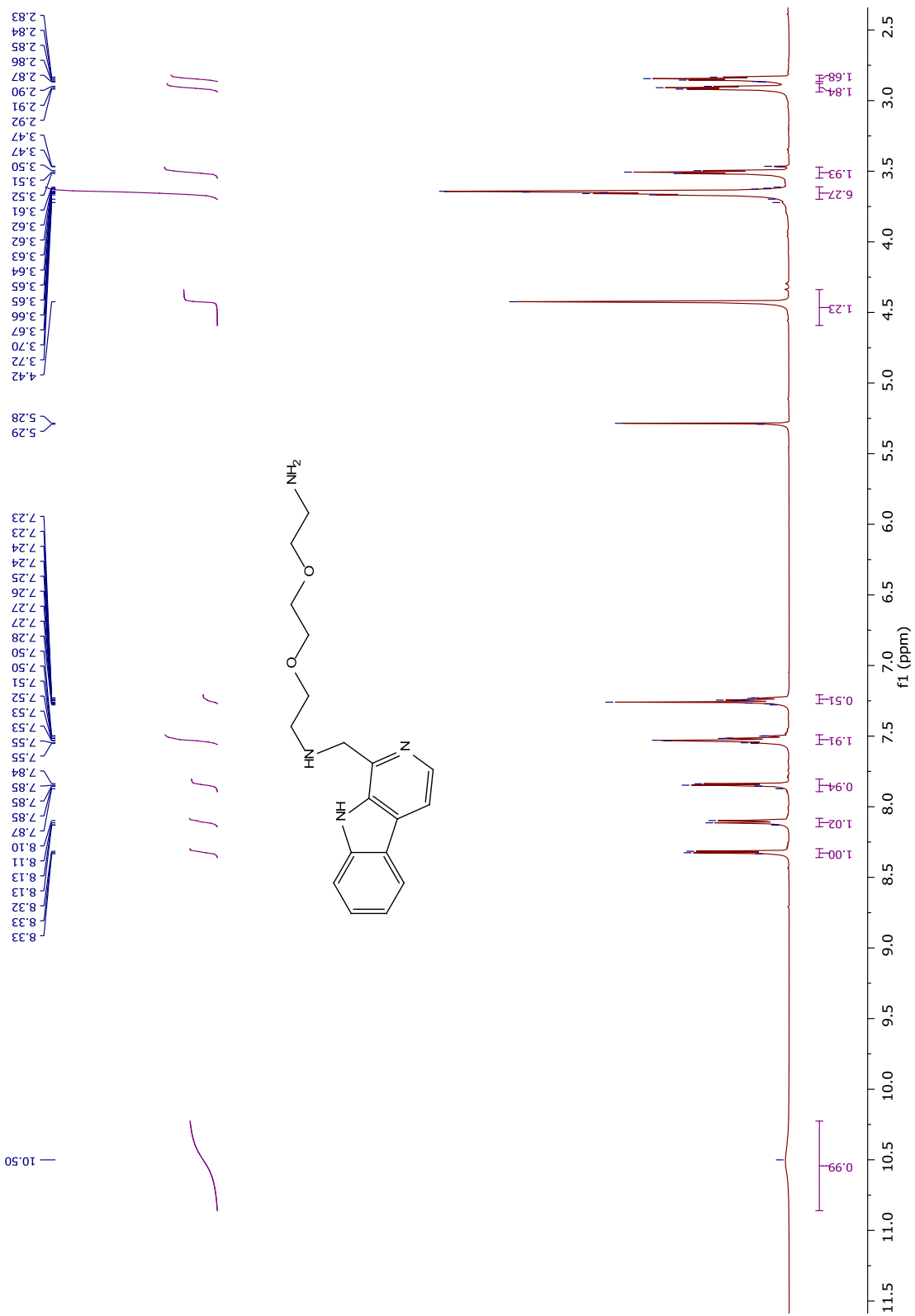
¹H NMR spectrum of compound 35



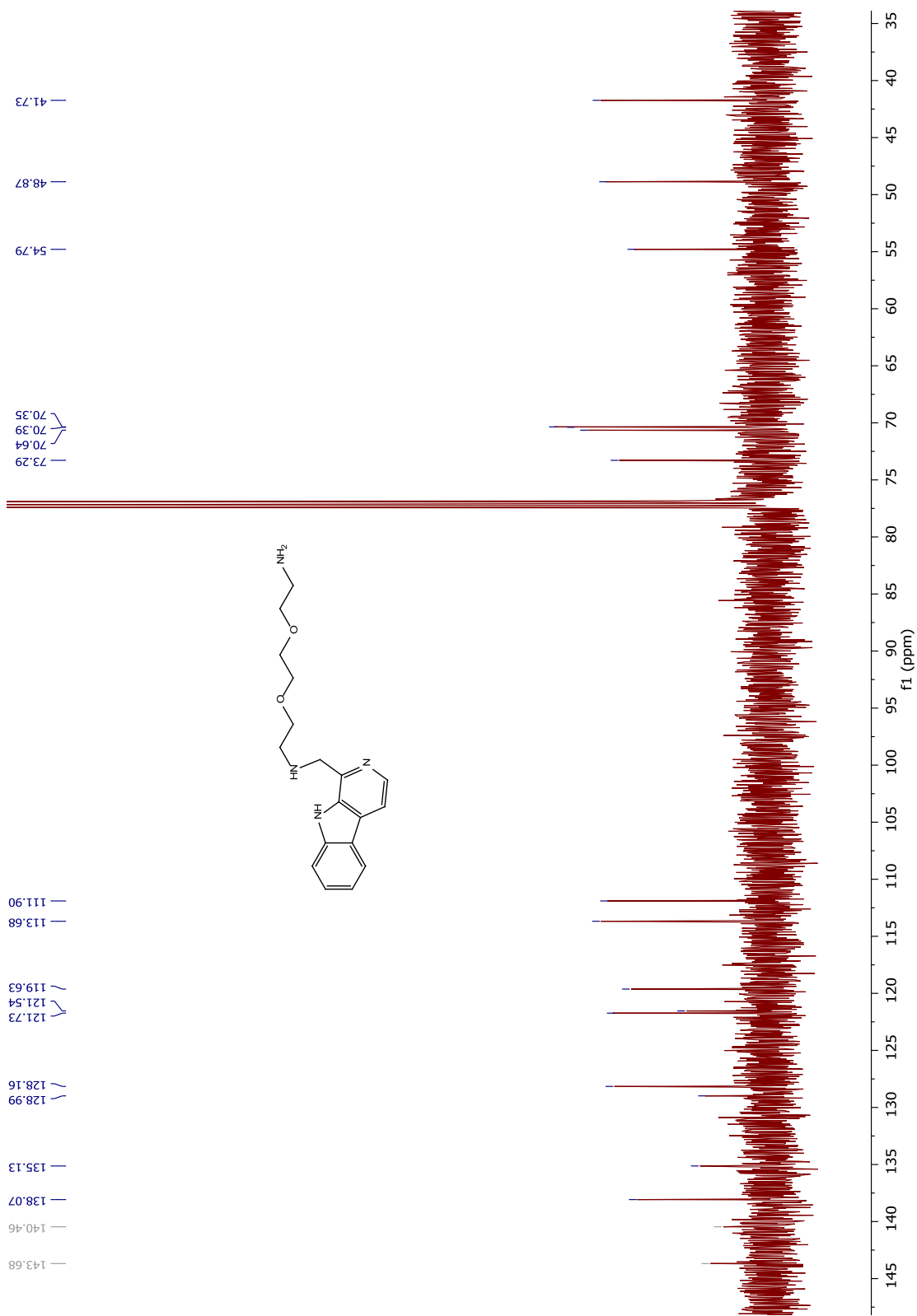
^{13}C NMR spectrum of compound **35**



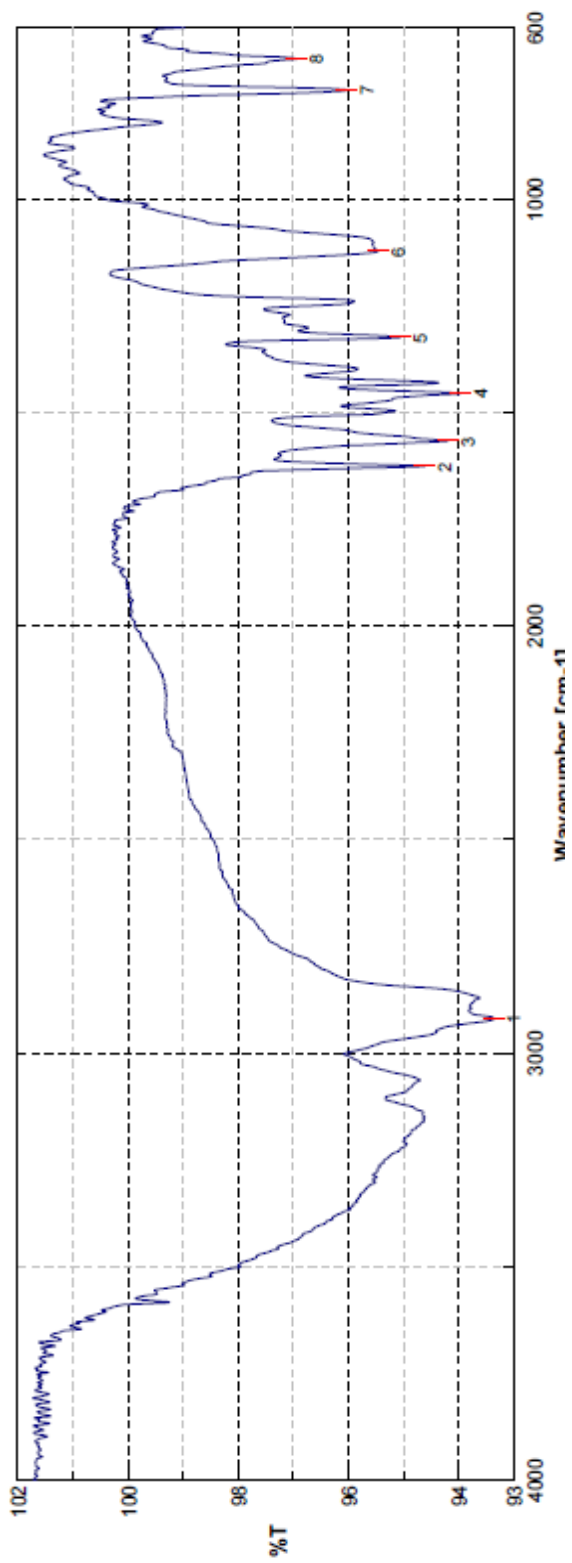
FTIR spectrum of compound 35



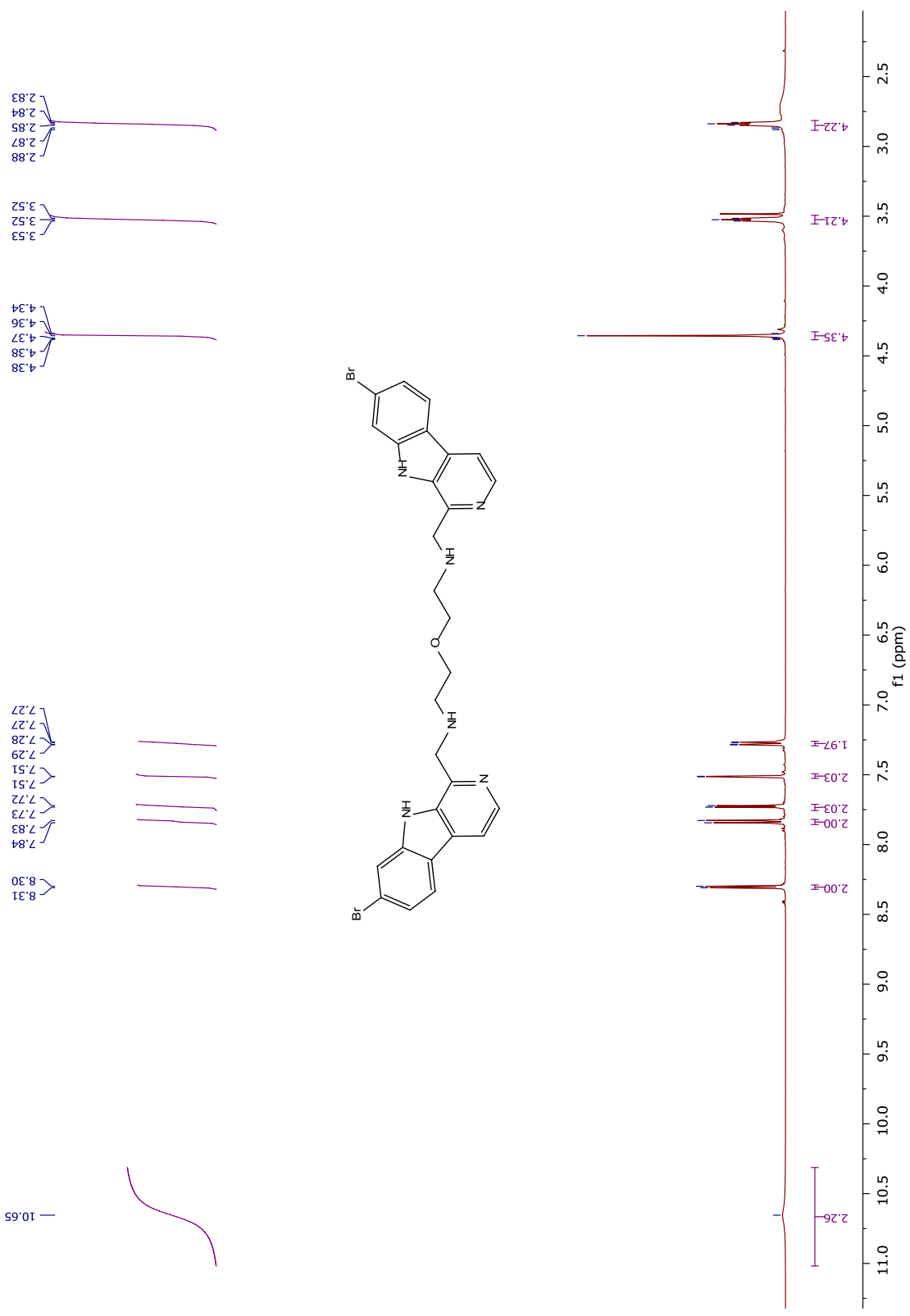
¹H NMR spectrum of compound 36



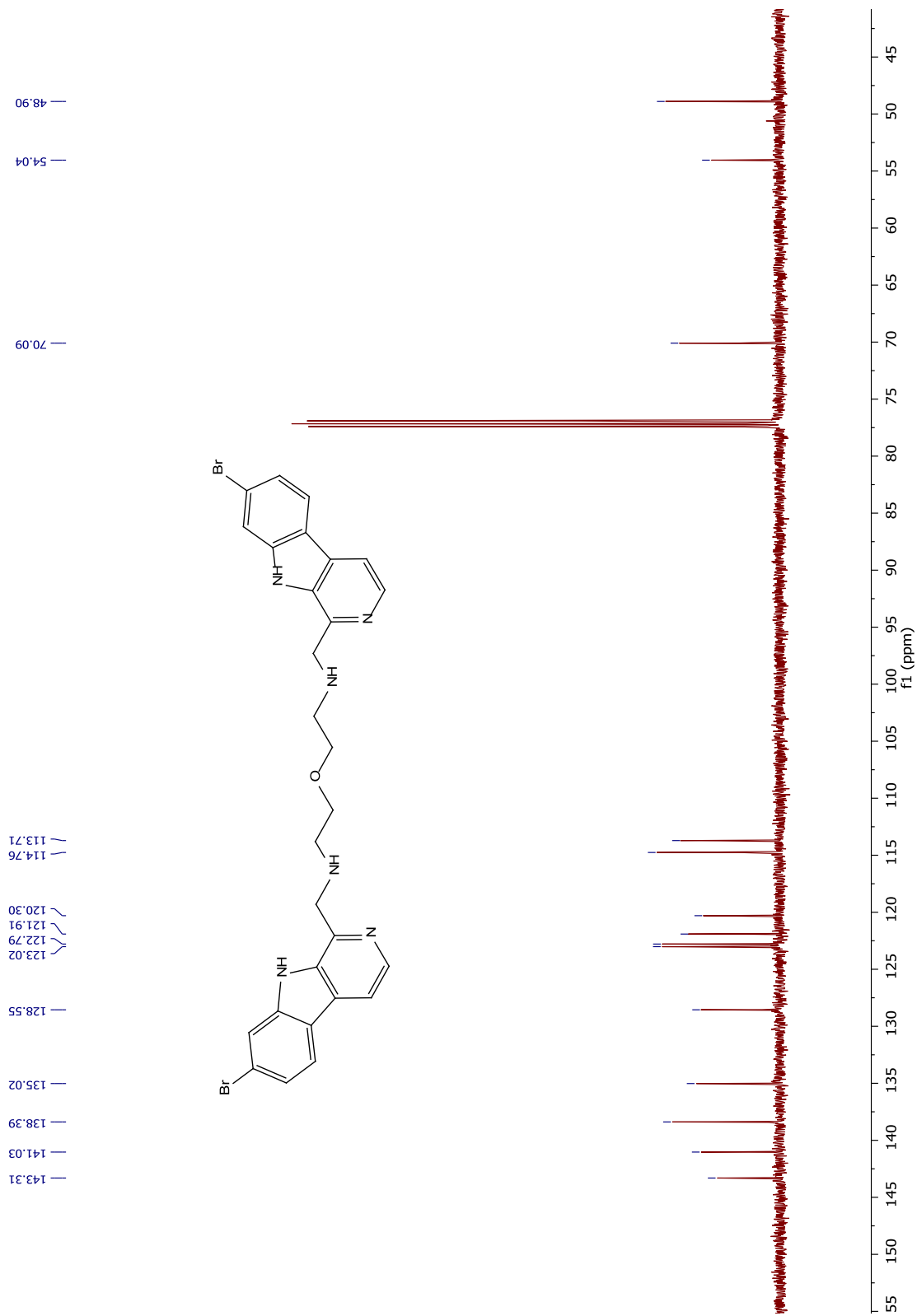
^{13}C NMR spectrum of compound **36**



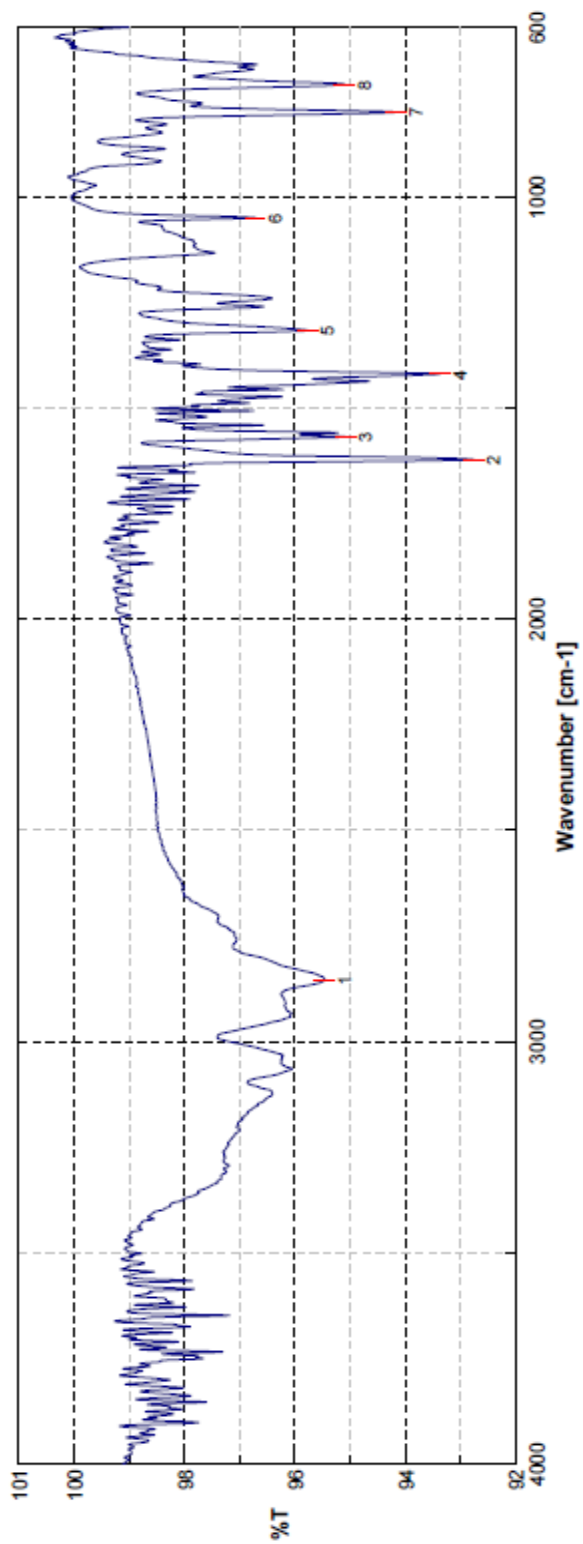
FTIR spectrum of compound 36



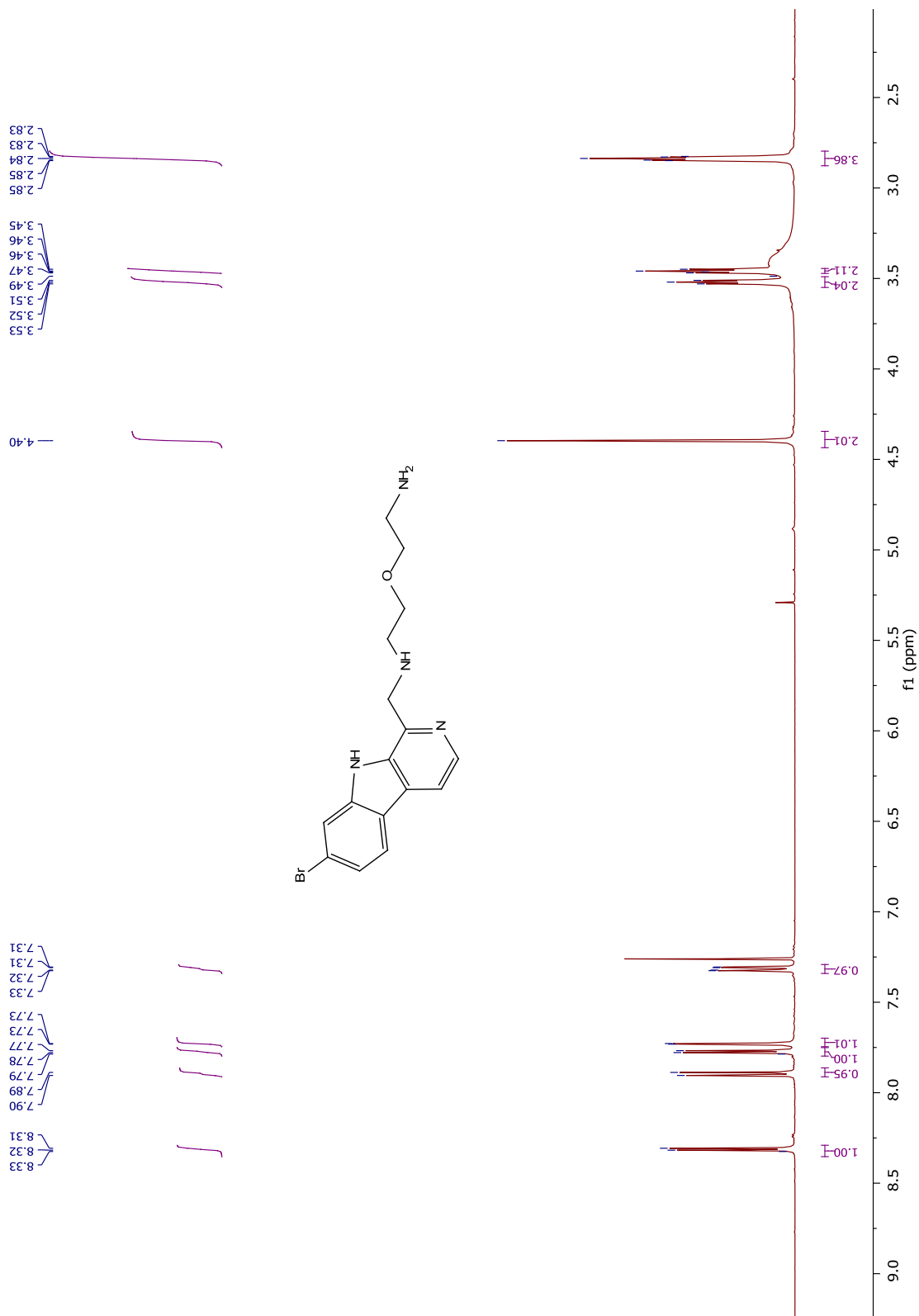
¹H NMR spectrum of compound 44



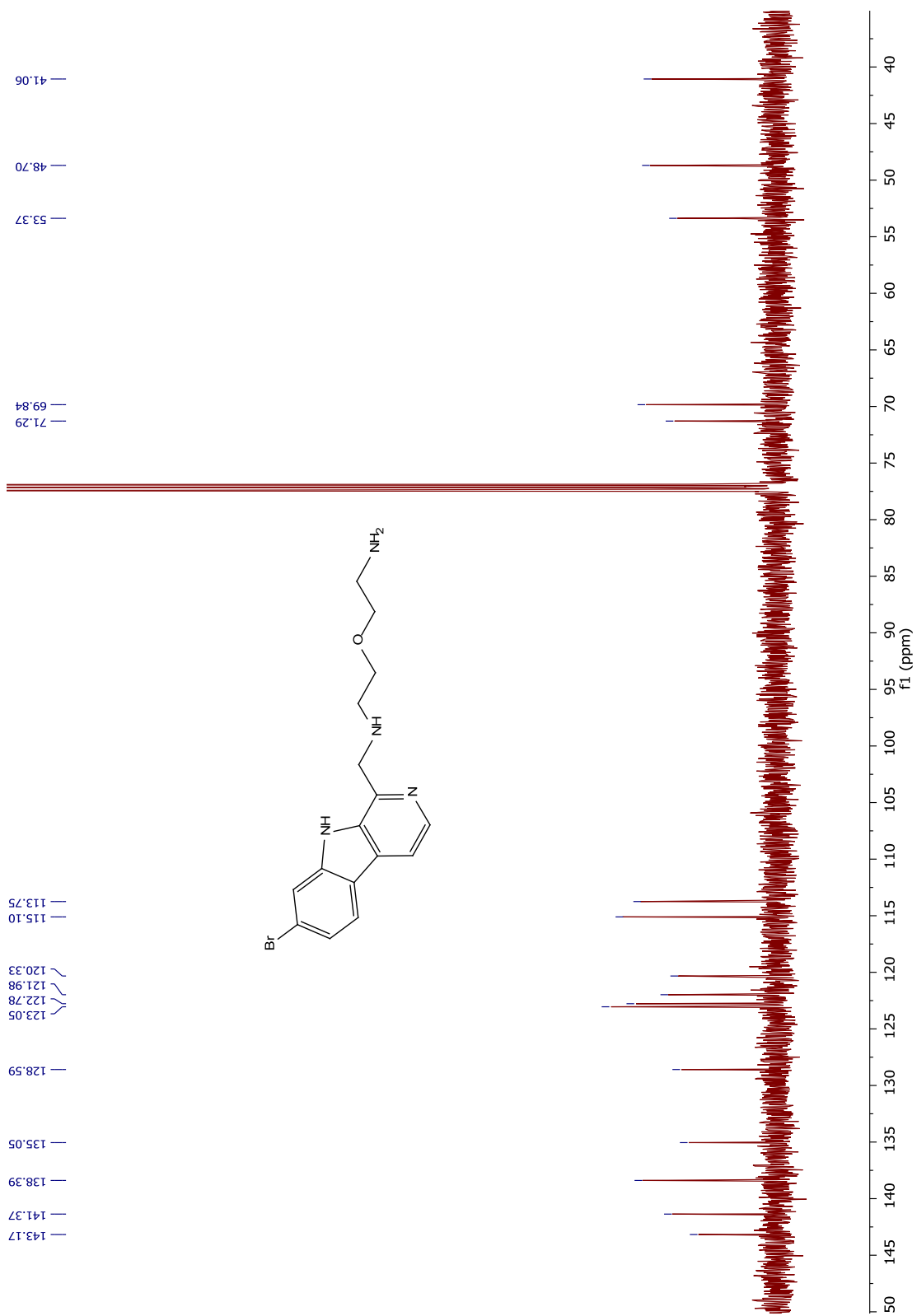
¹³C NMR spectrum of compound 44



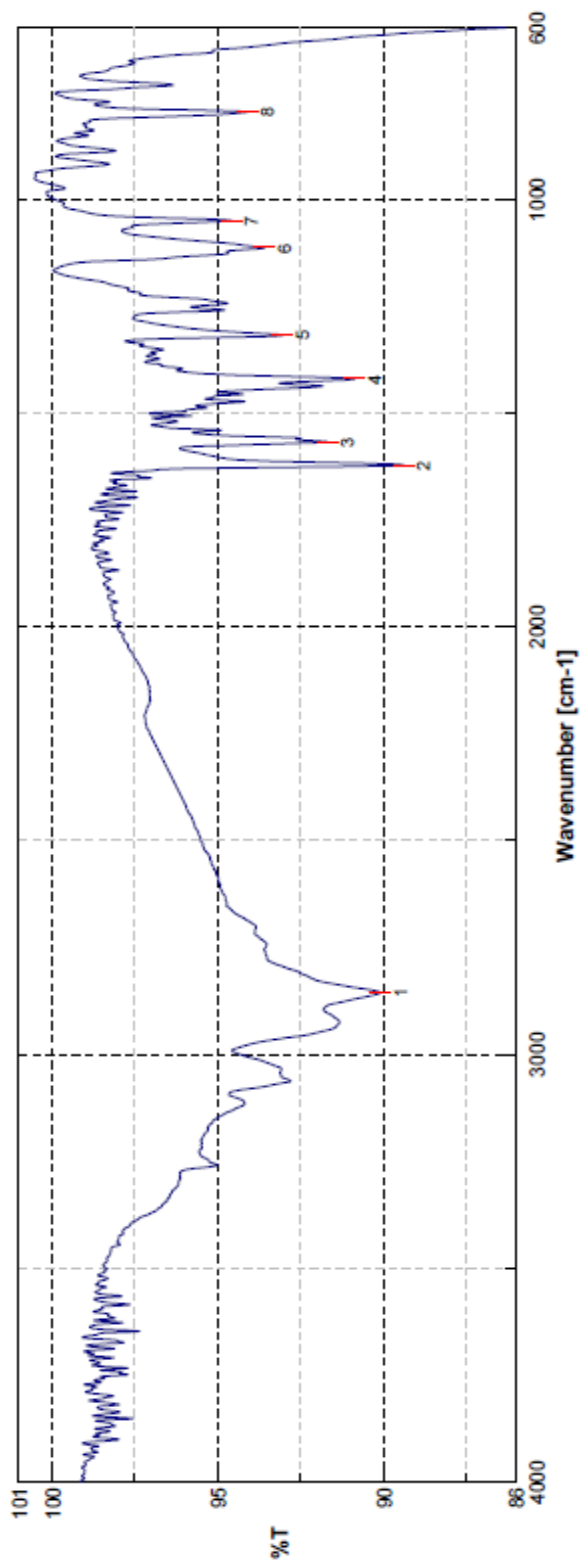
FTIR spectrum of compound 44



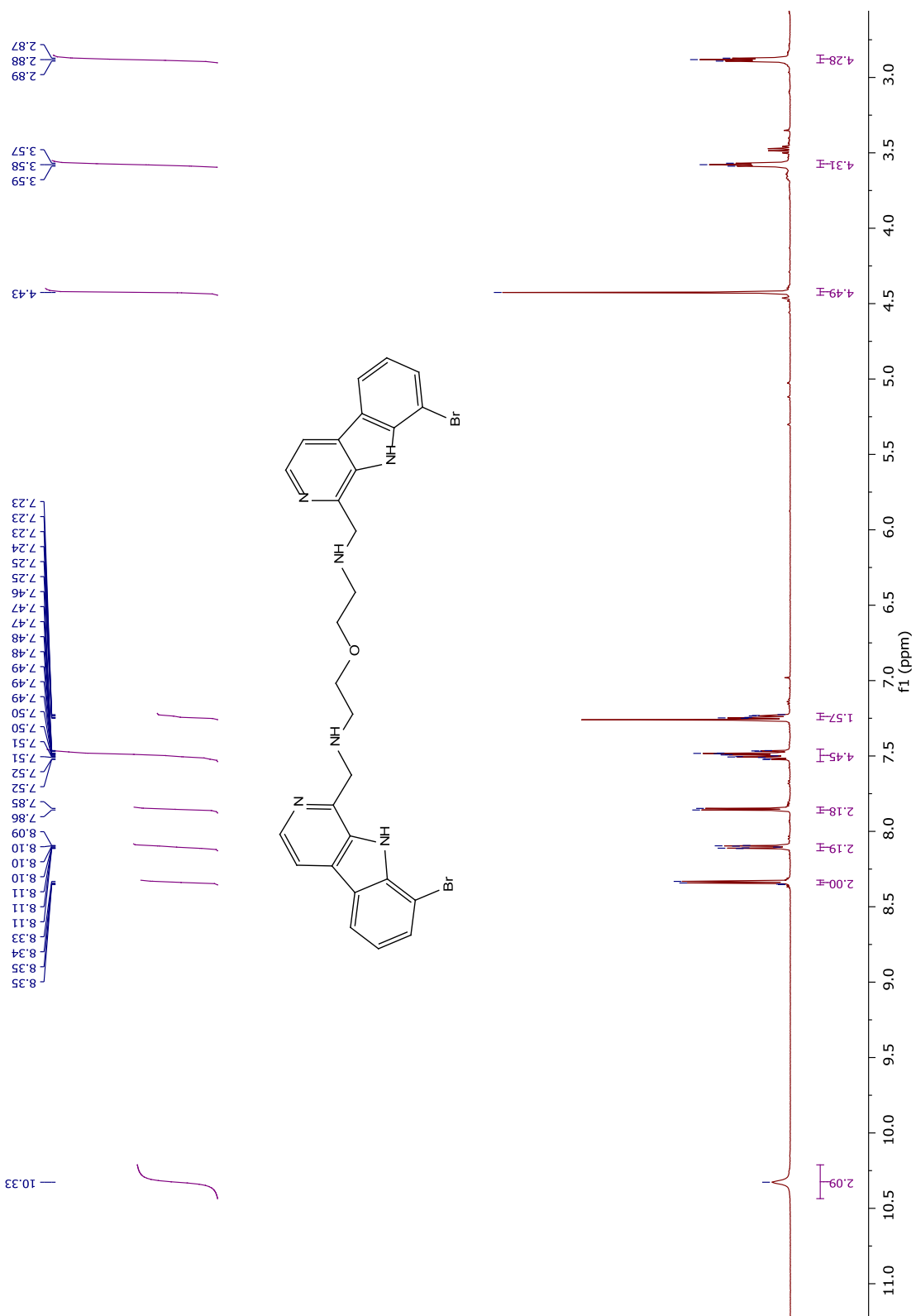
¹H NMR spectrum of compound 45



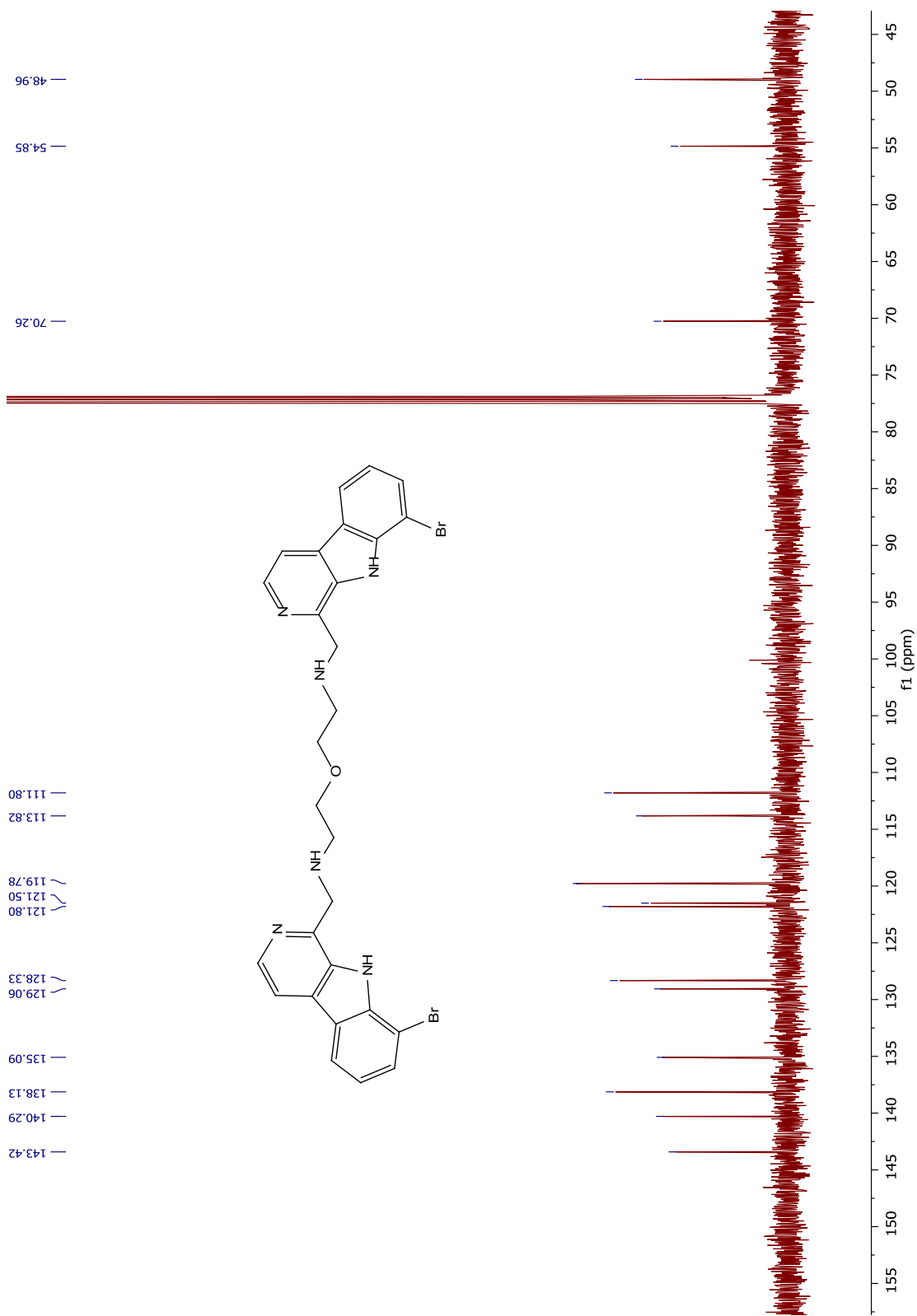
¹³C NMR spectrum of compound **45**



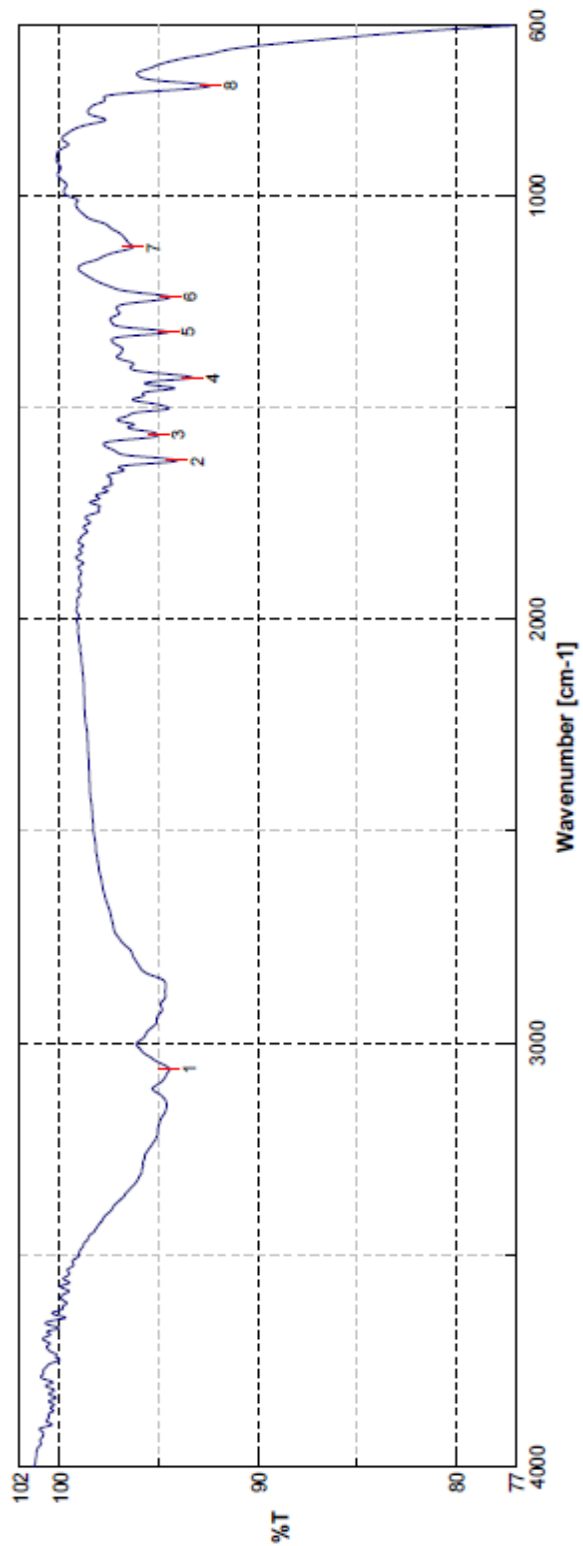
FTIR spectrum of compound 45



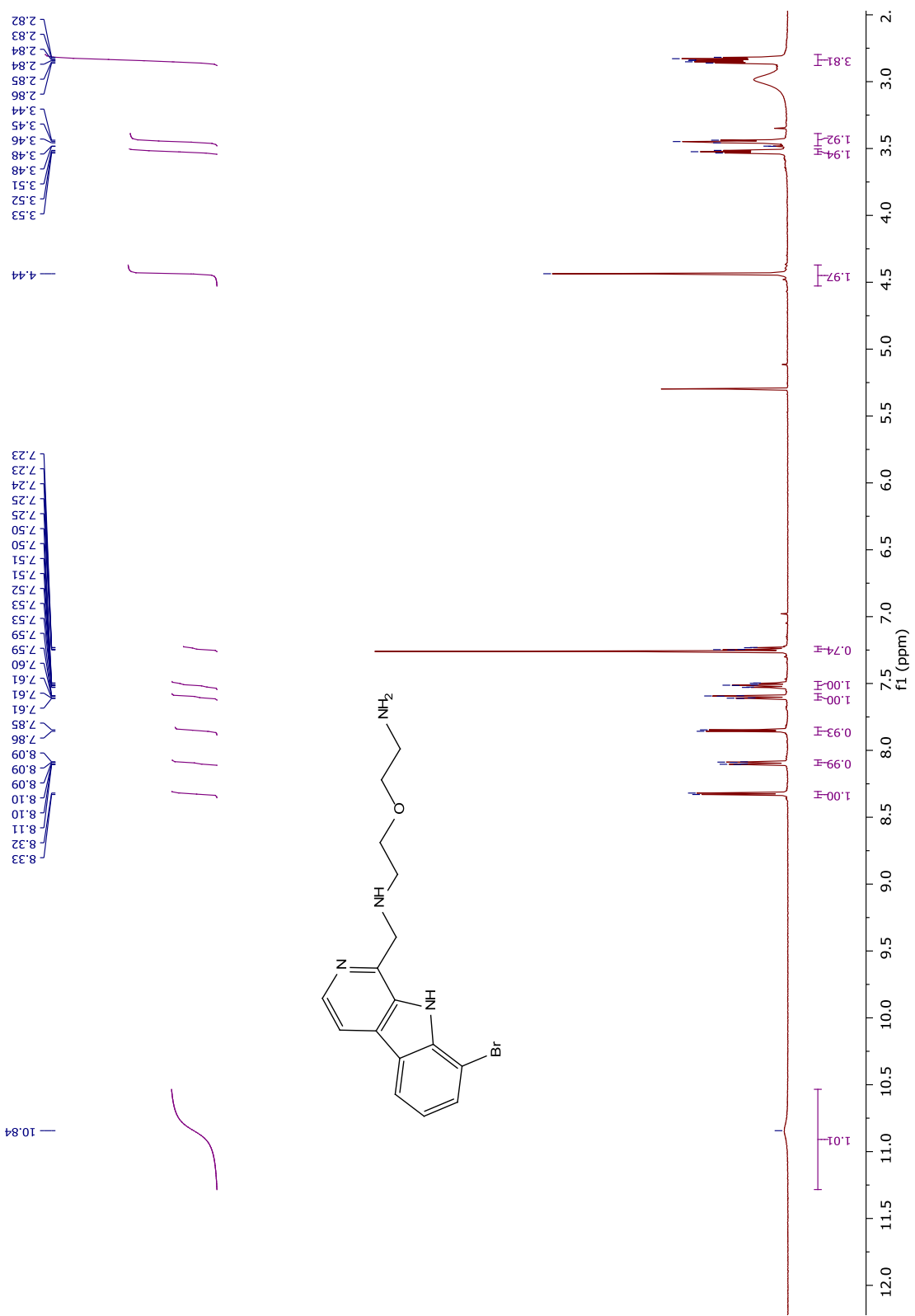
¹H NMR spectrum of compound 46



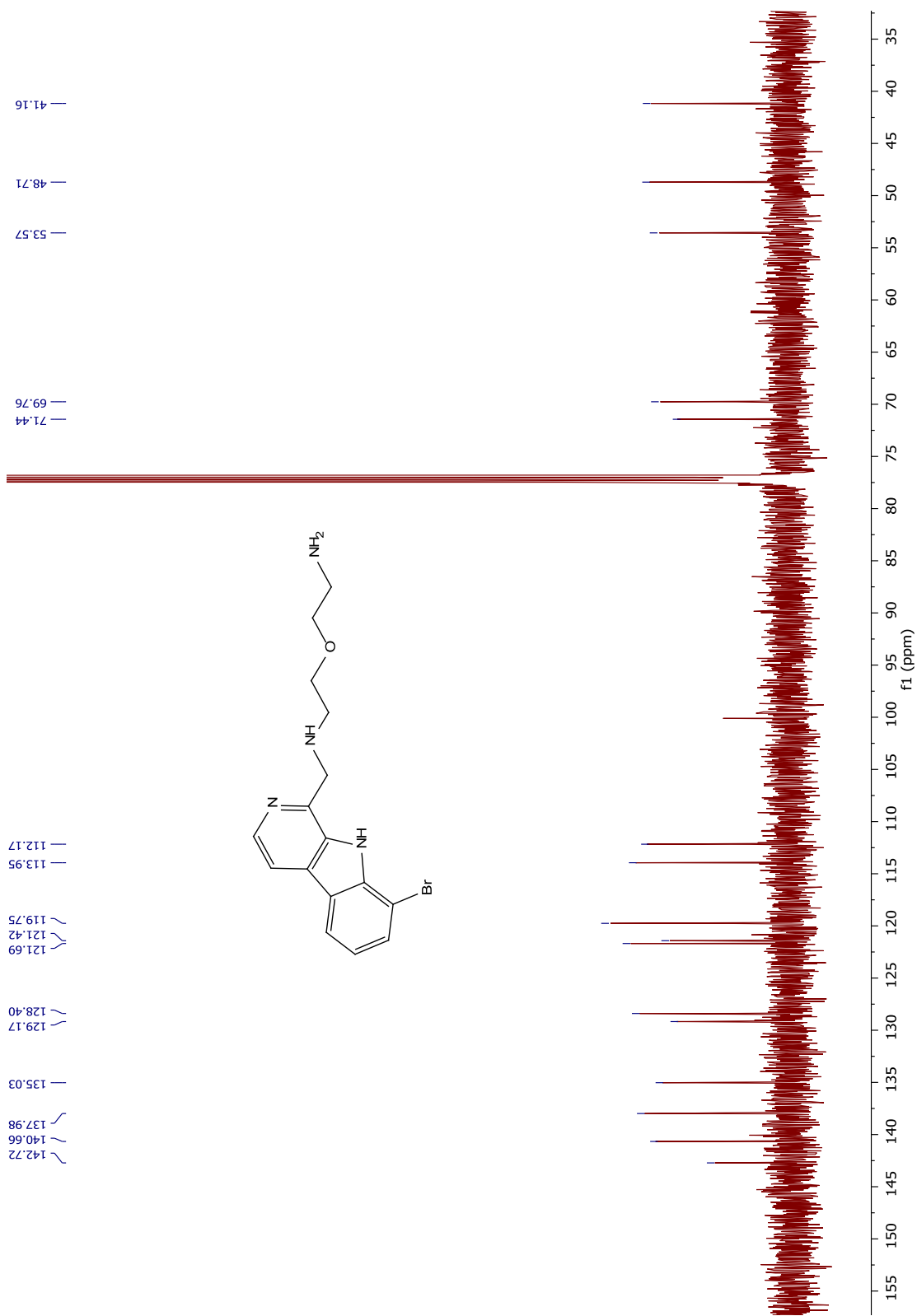
¹³C NMR spectrum of compound 46



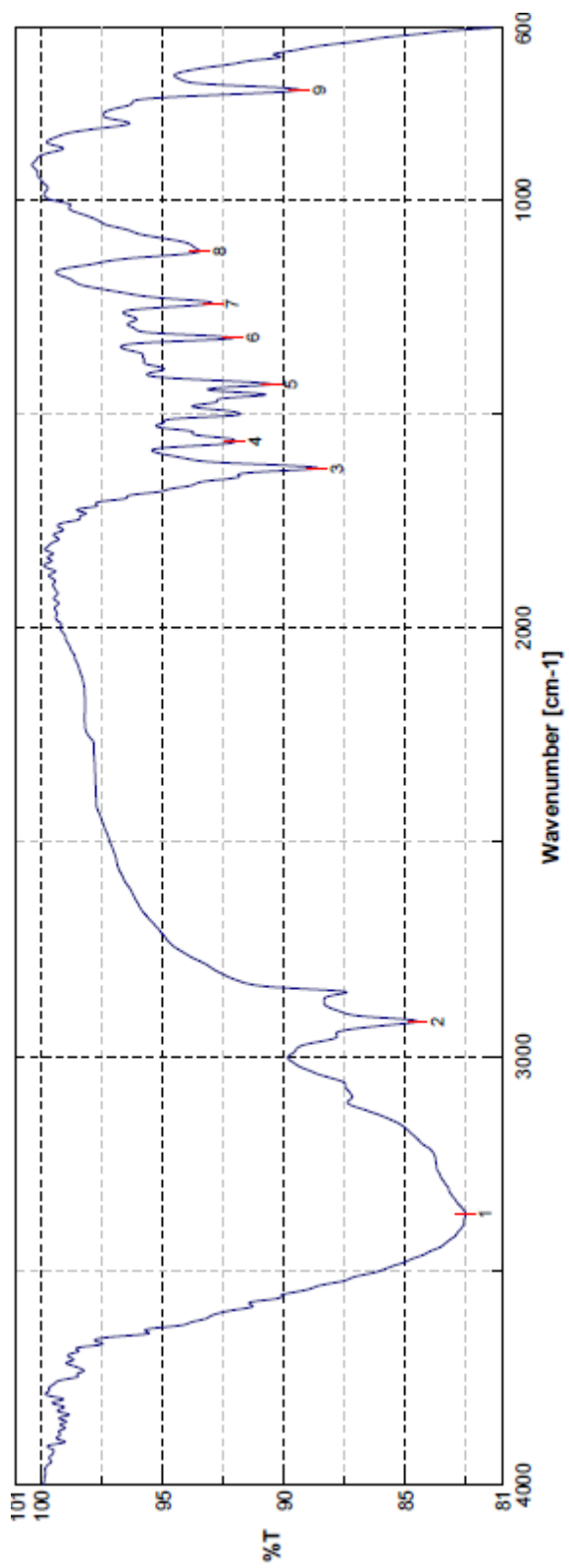
FTIR spectrum of compound 46



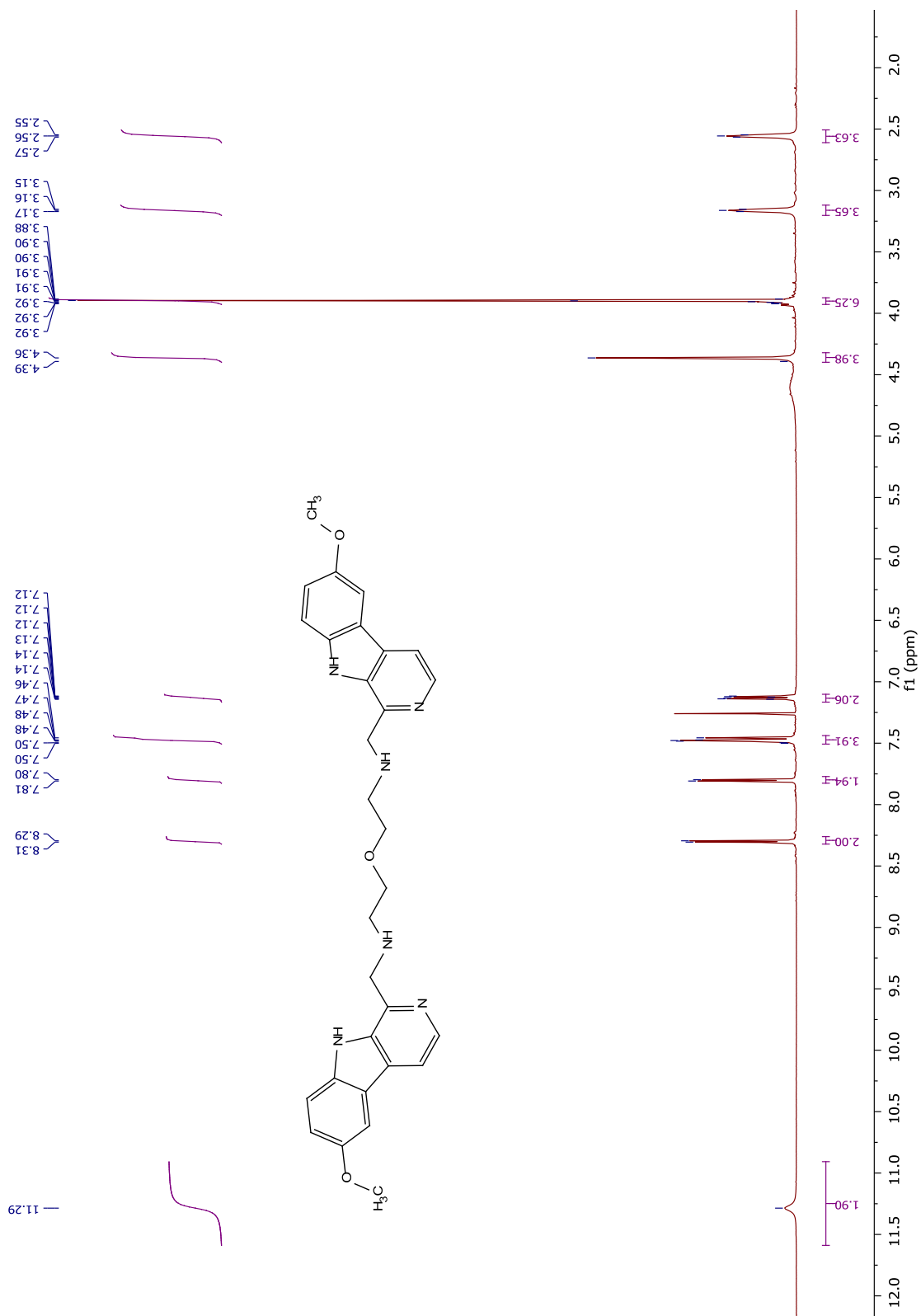
¹H NMR spectrum of compound 47



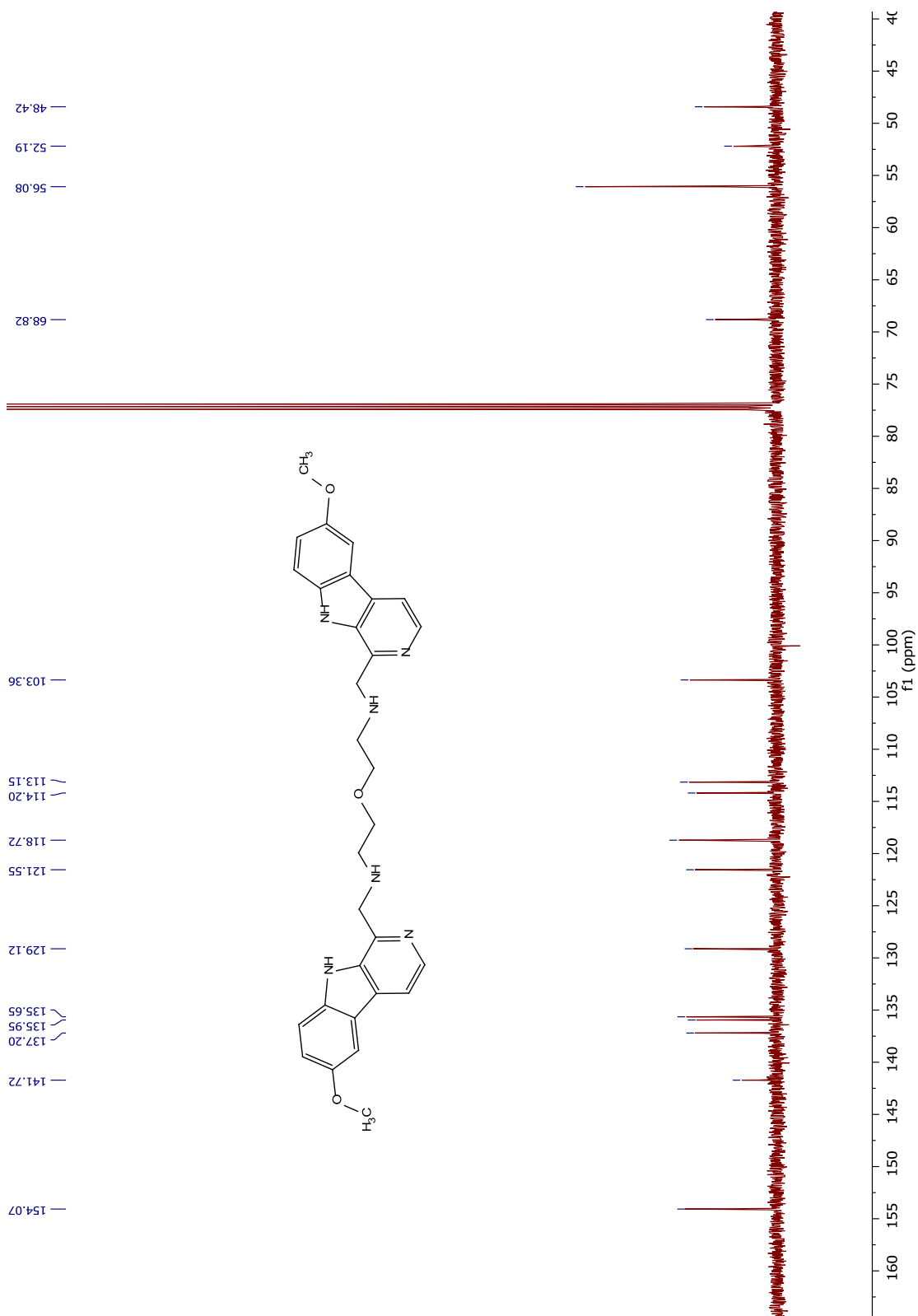
¹³C NMR spectrum of compound 47



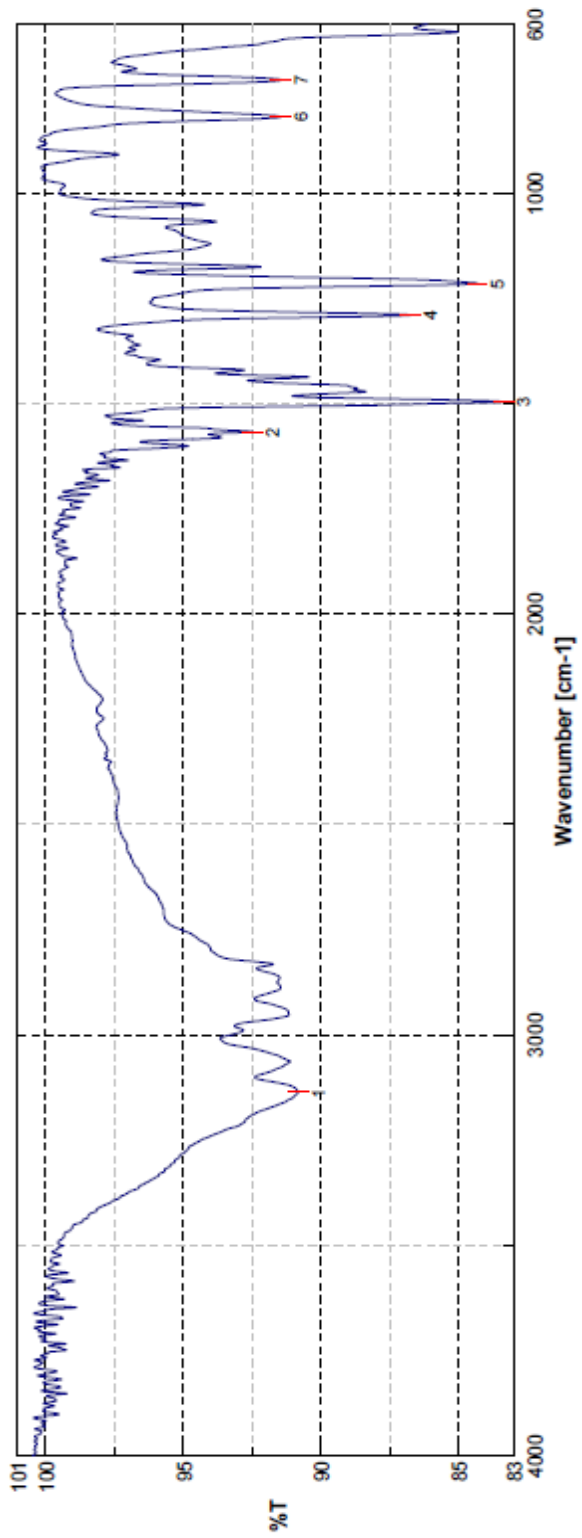
FTIR spectrum of compound 47



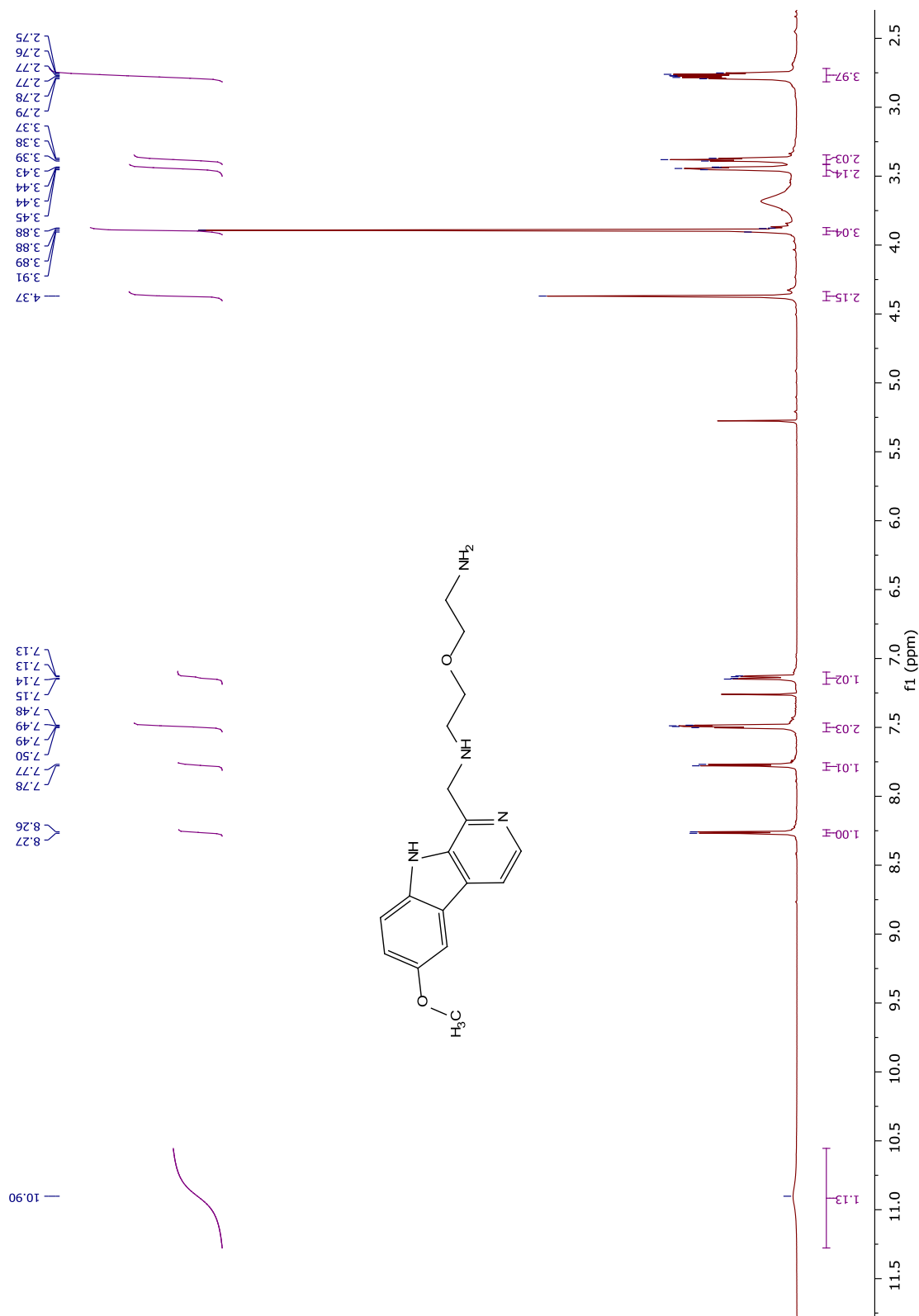
¹H NMR spectrum of compound 48



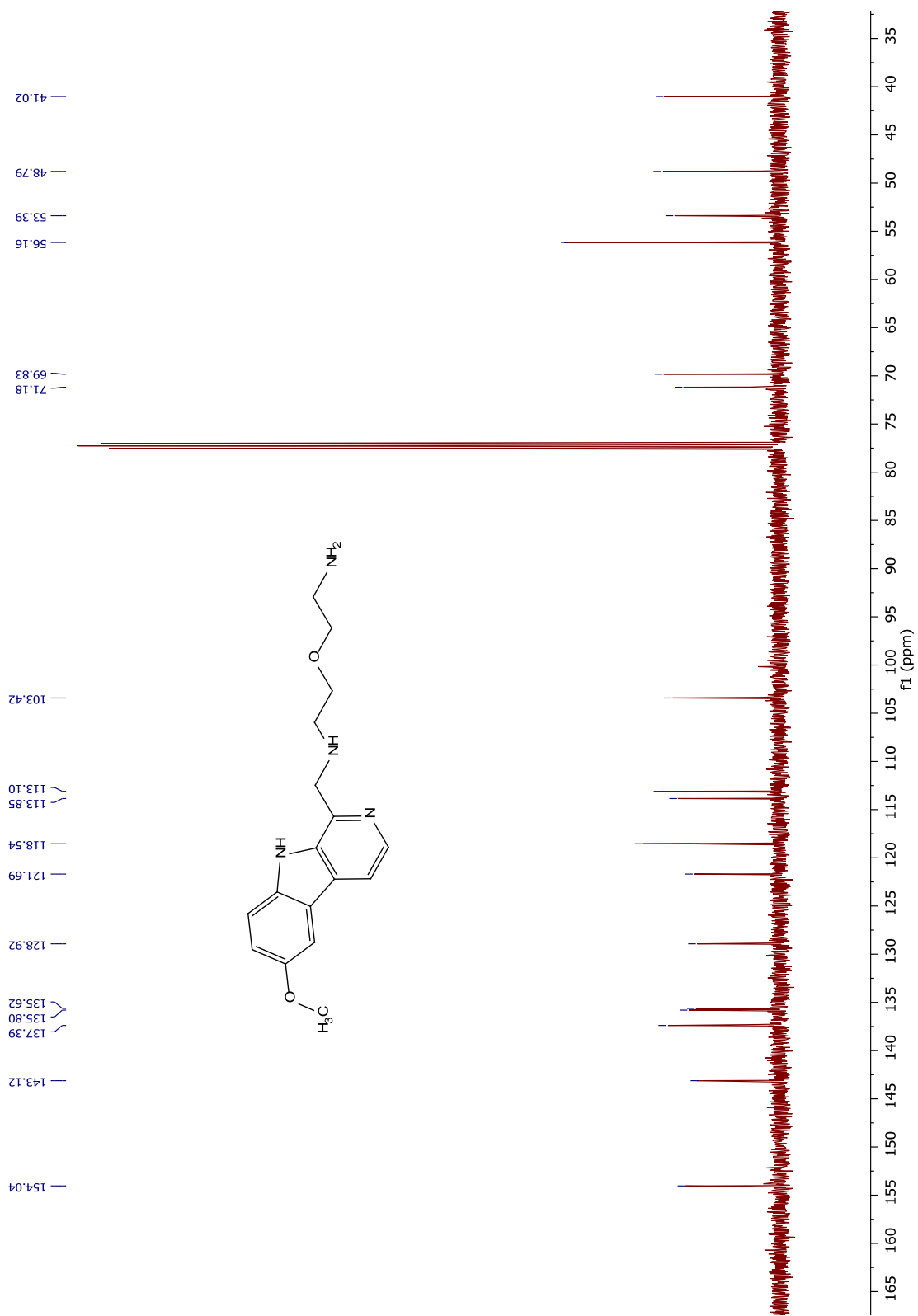
¹³C NMR spectrum of compound 48



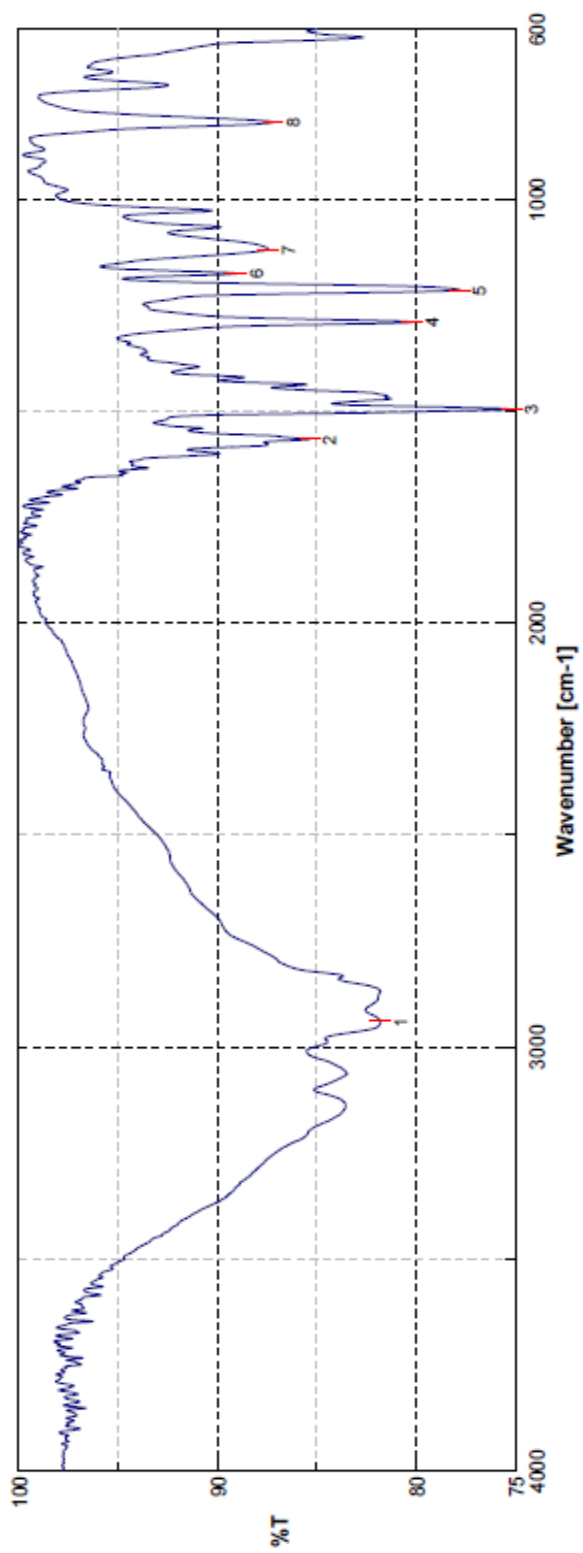
FTIR spectrum of compound 48



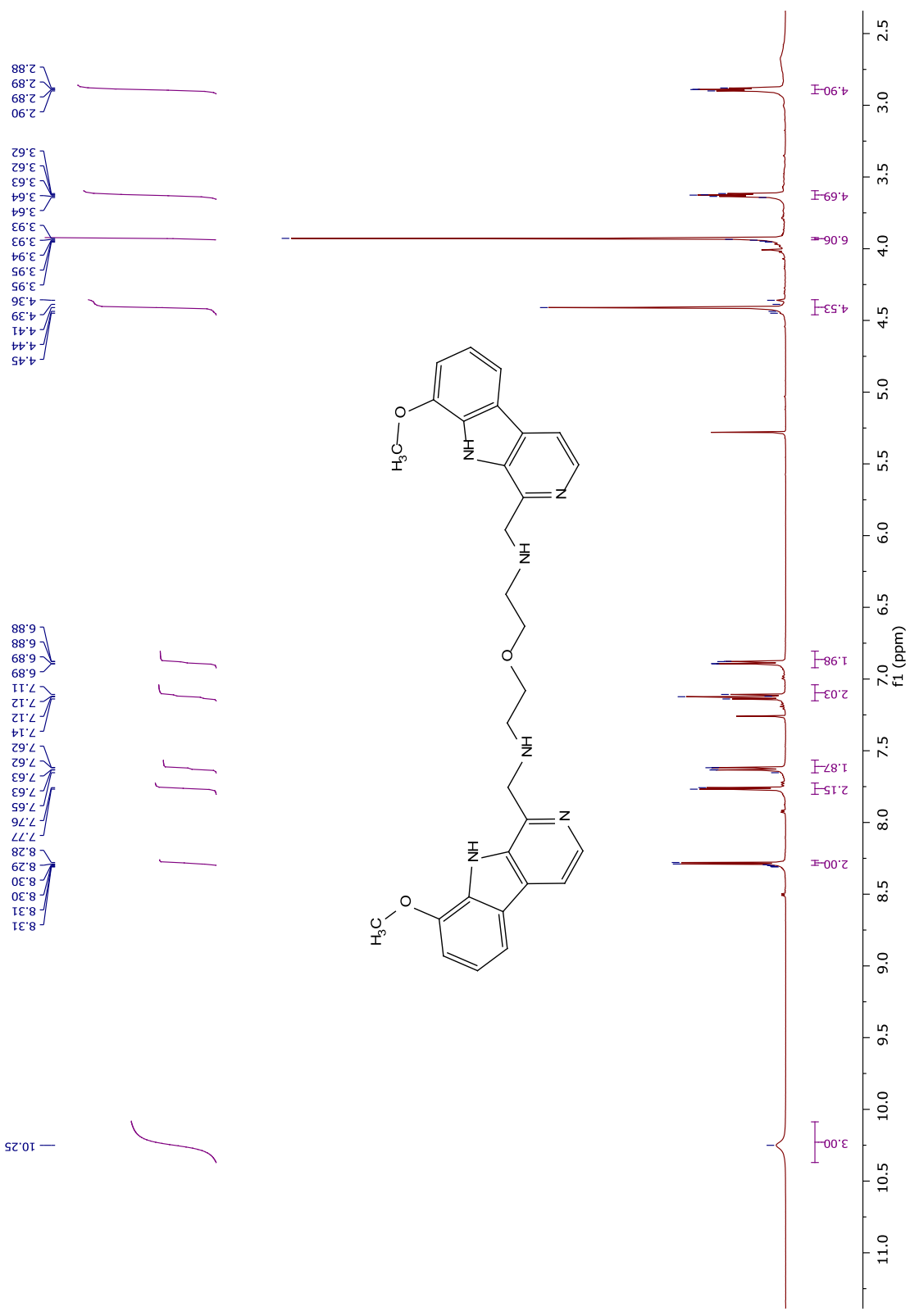
¹H NMR spectrum of compound 49



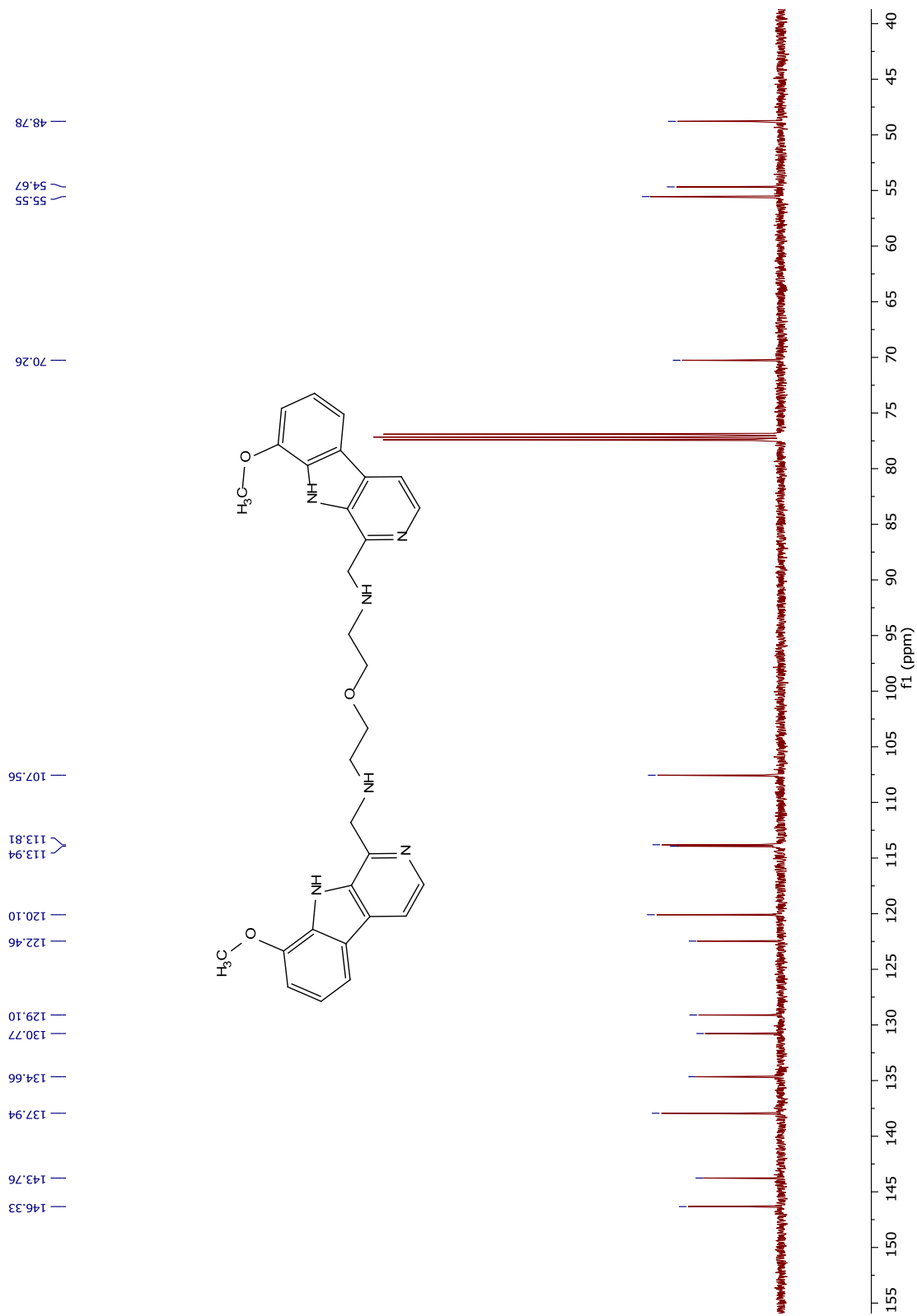
¹³C NMR spectrum of compound 49



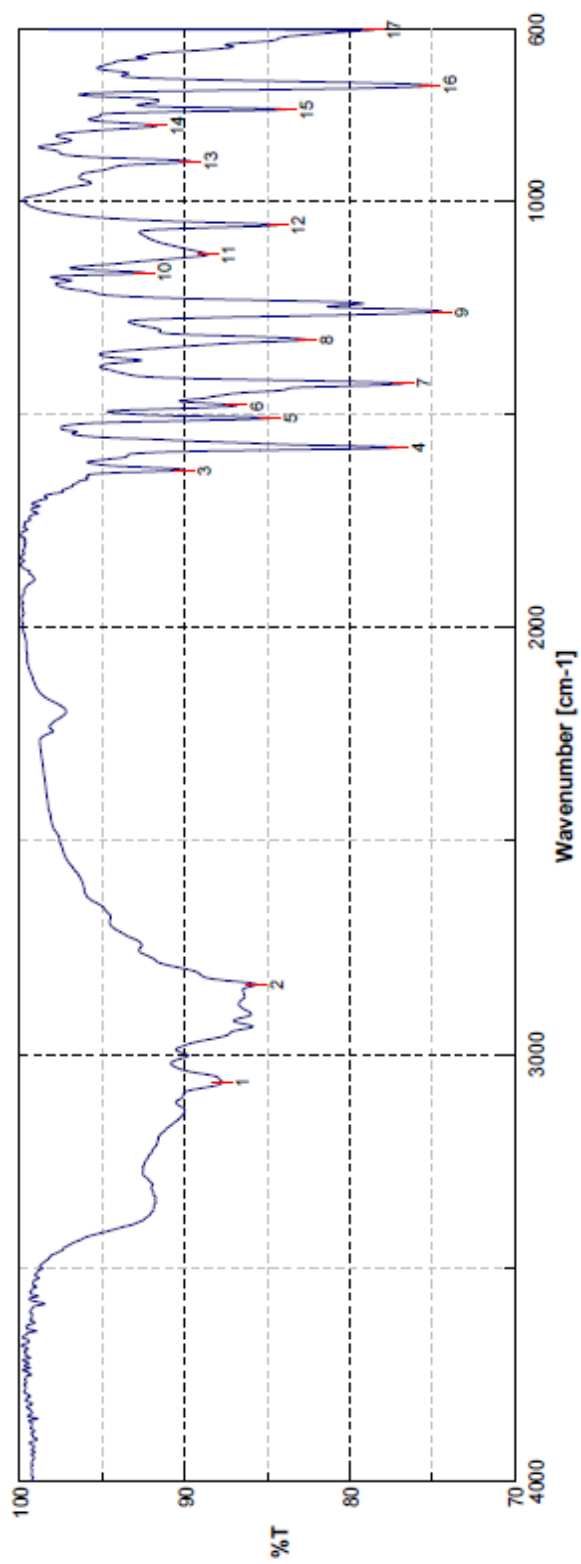
FTIR spectrum of compound 49



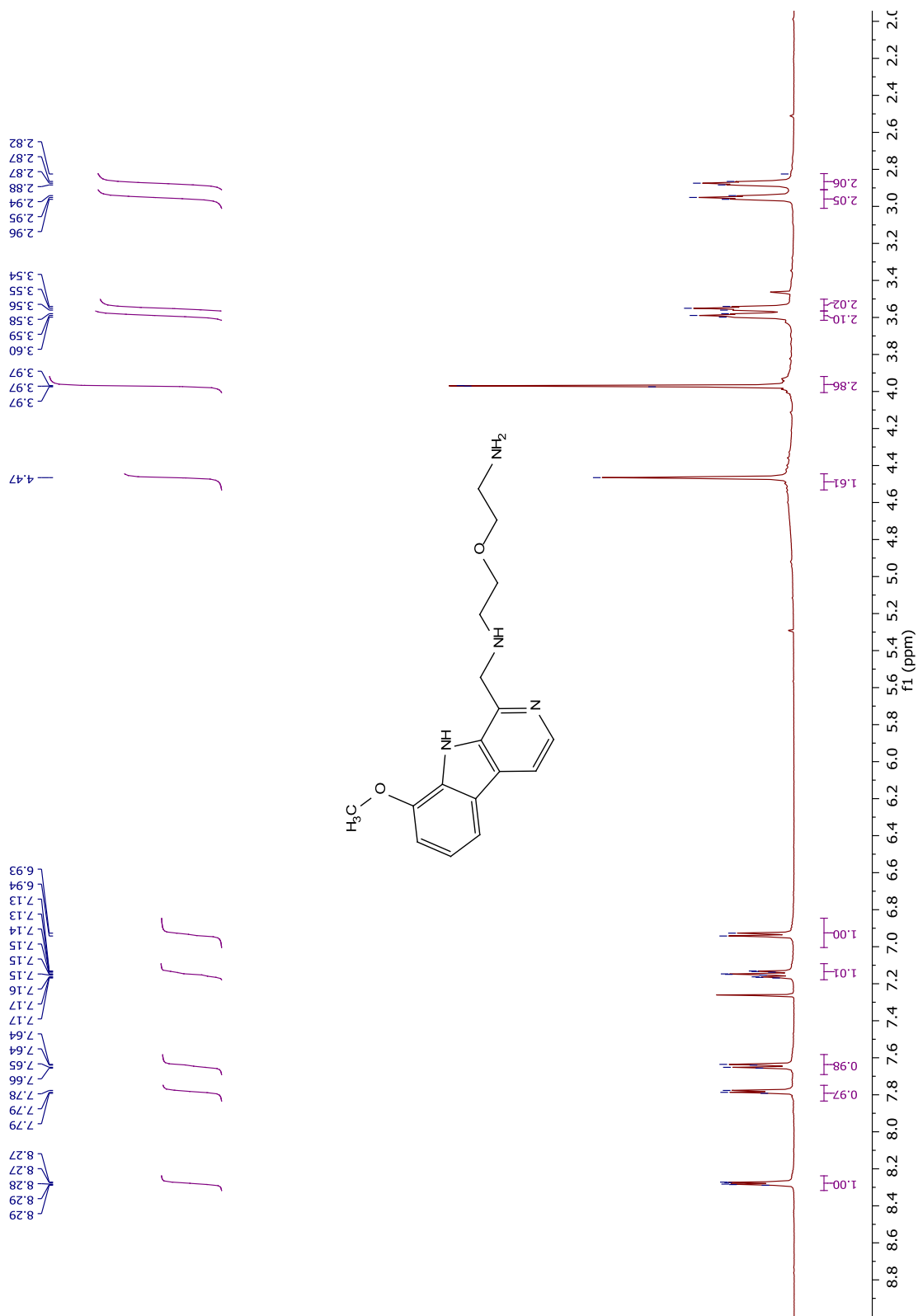
¹H NMR spectrum of compound 50



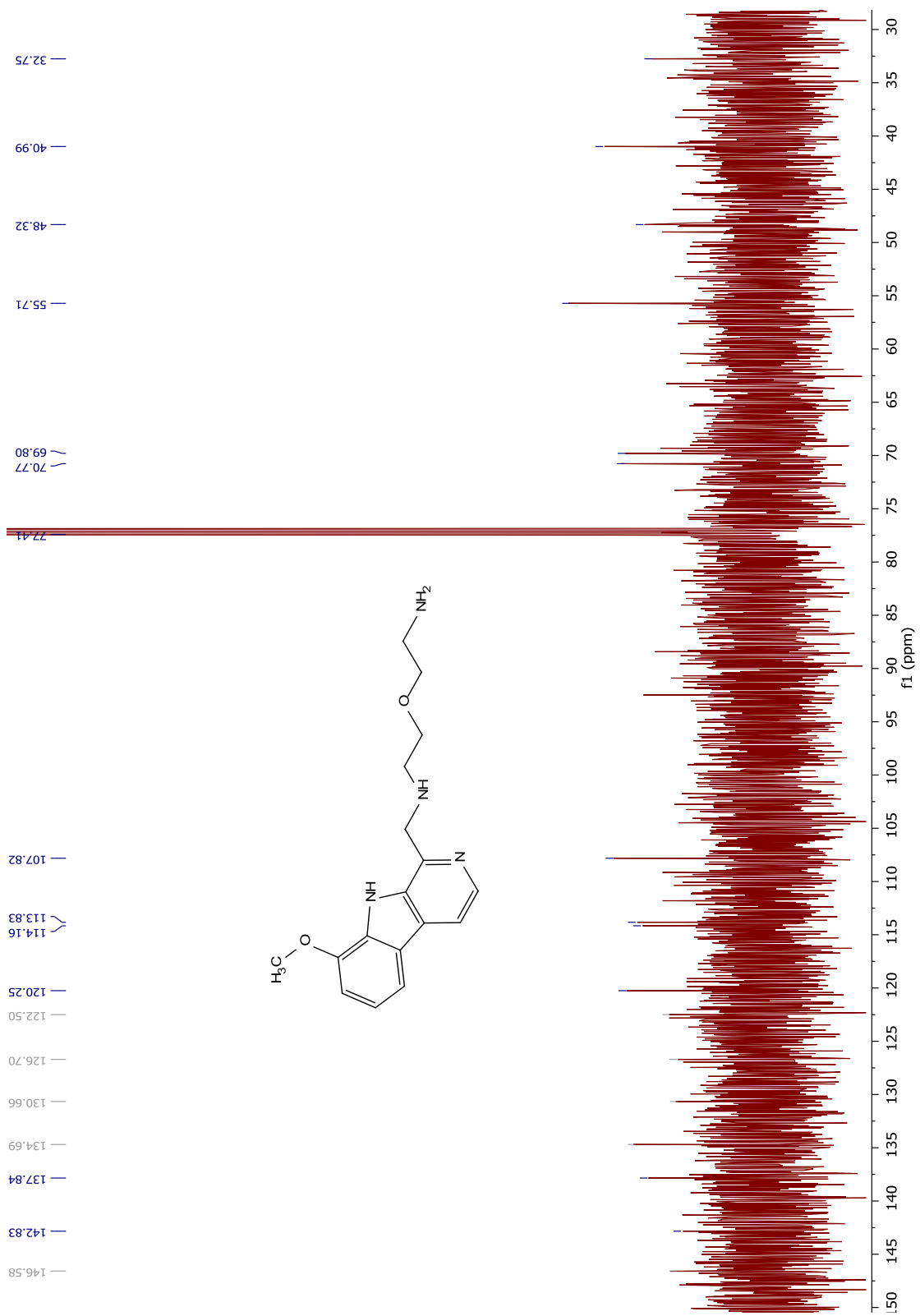
¹³C NMR spectrum of compound **50**



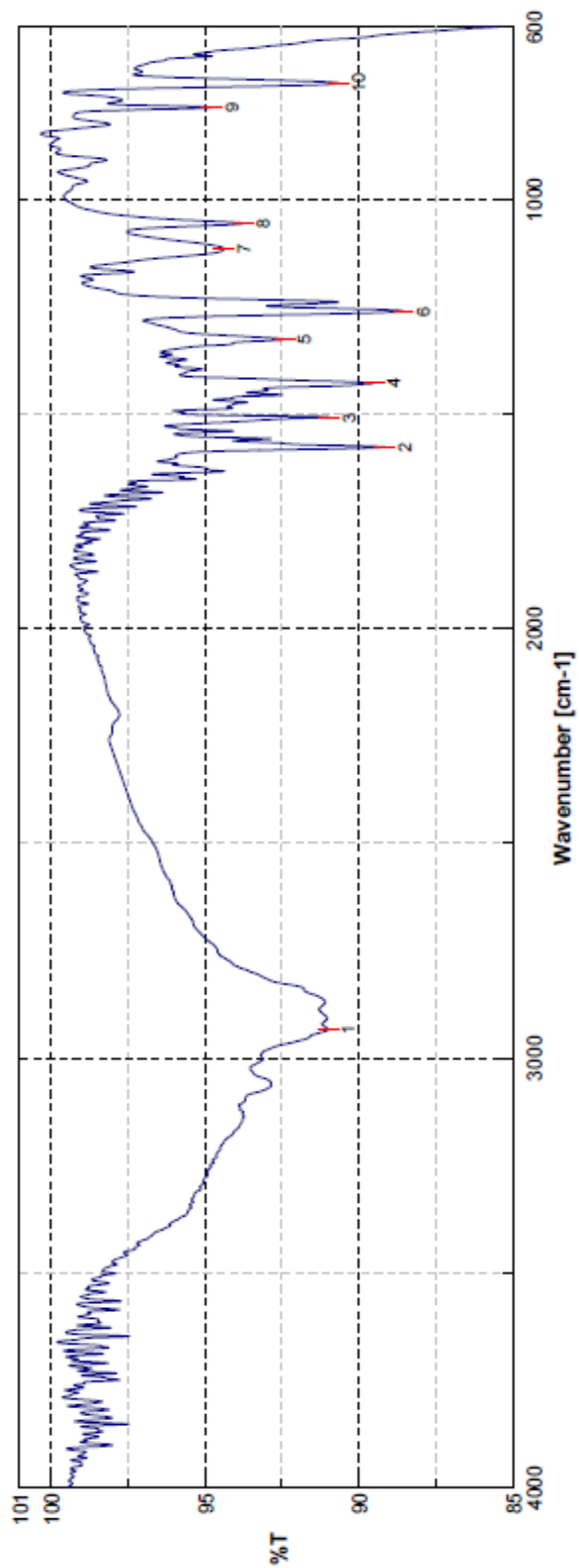
FTIR spectrum of compound 50



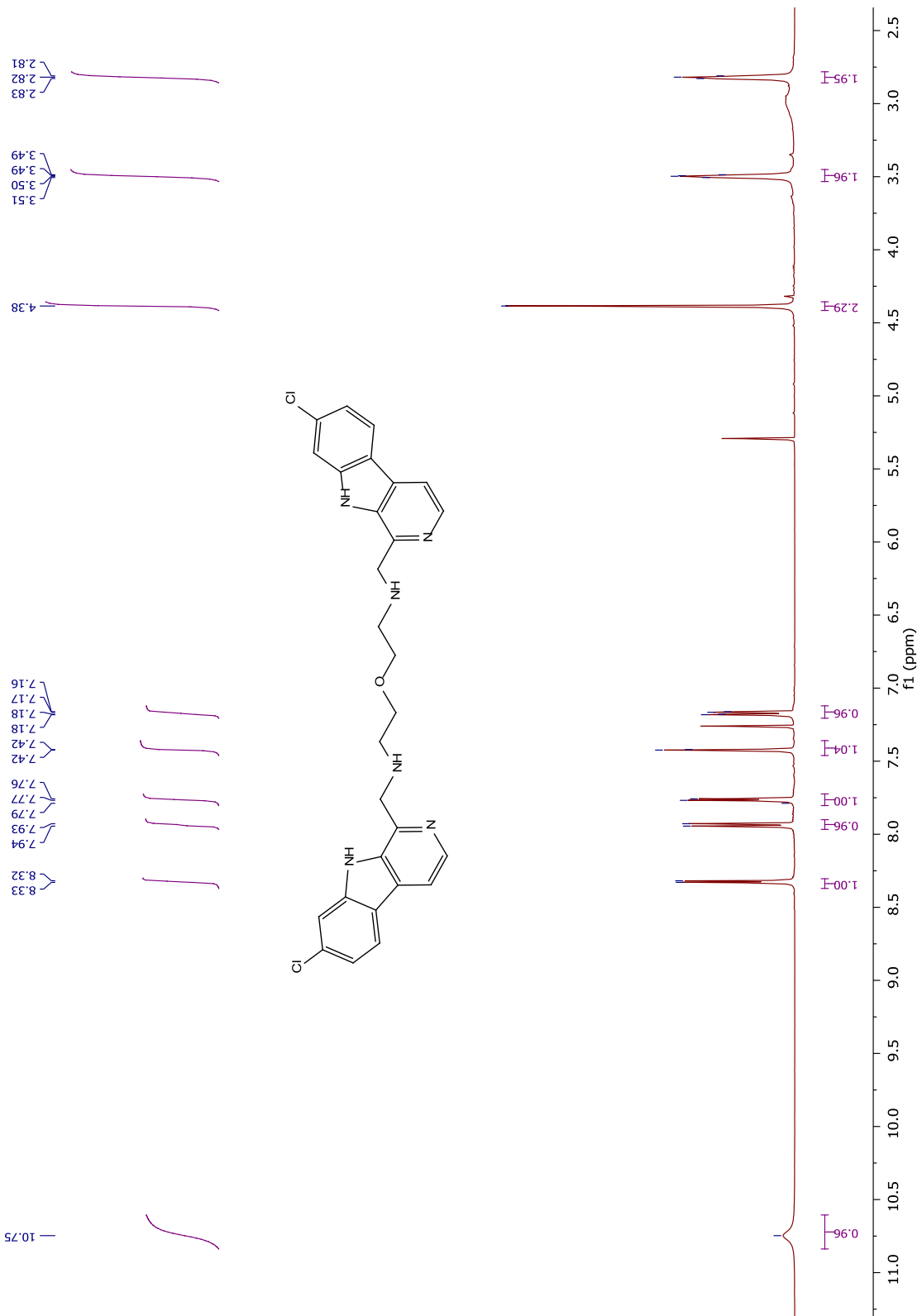
¹H NMR spectrum of compound 51



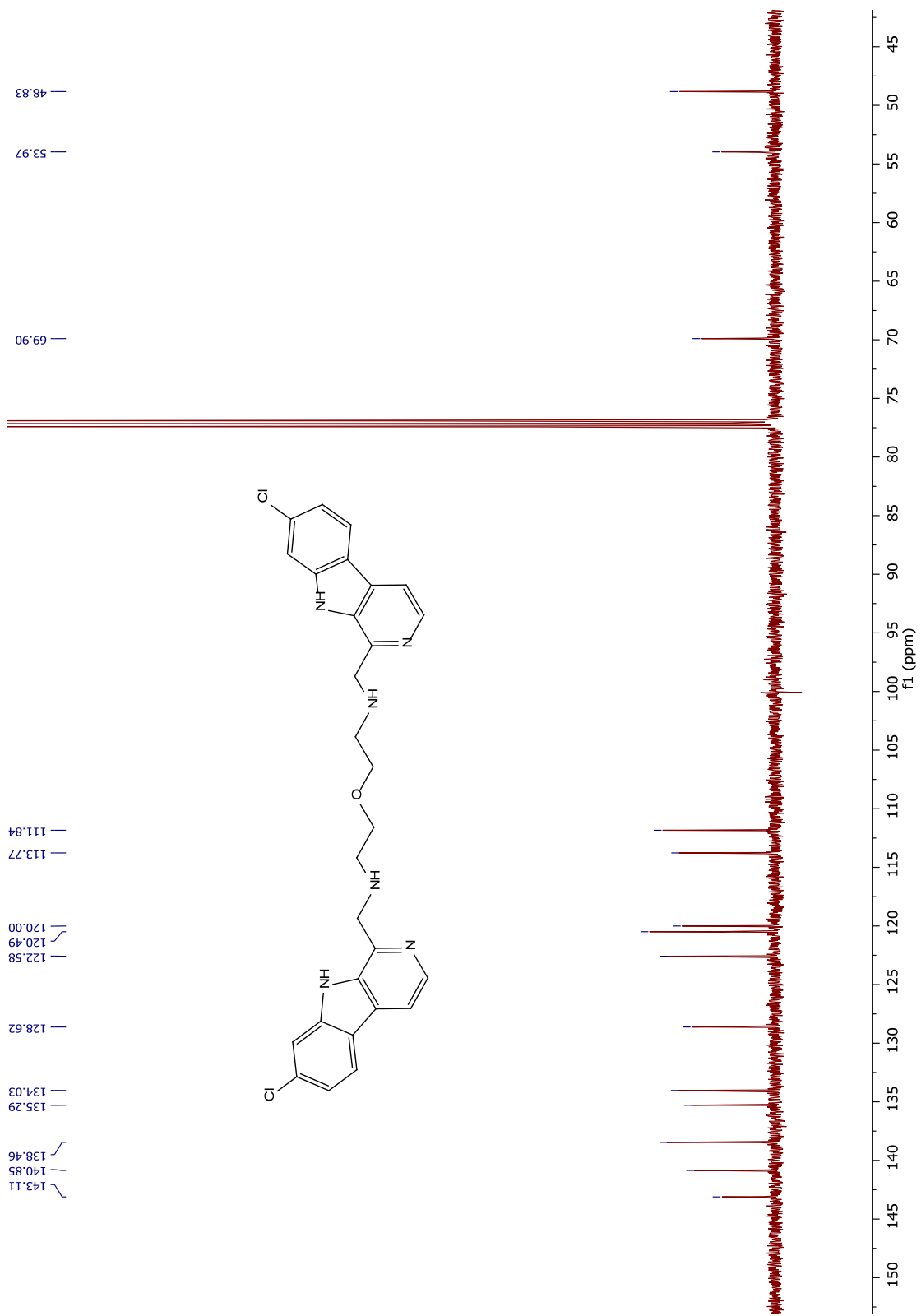
^{13}C NMR spectrum of compound 51



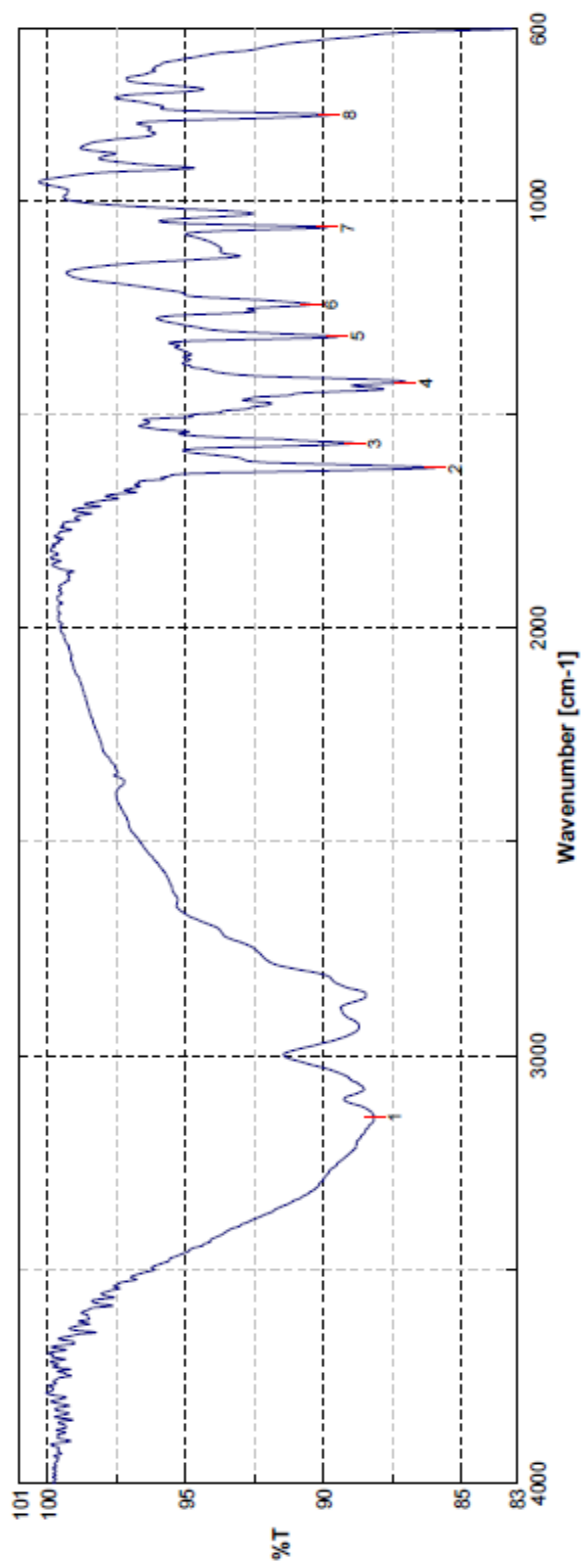
FTIR spectrum of compound 51



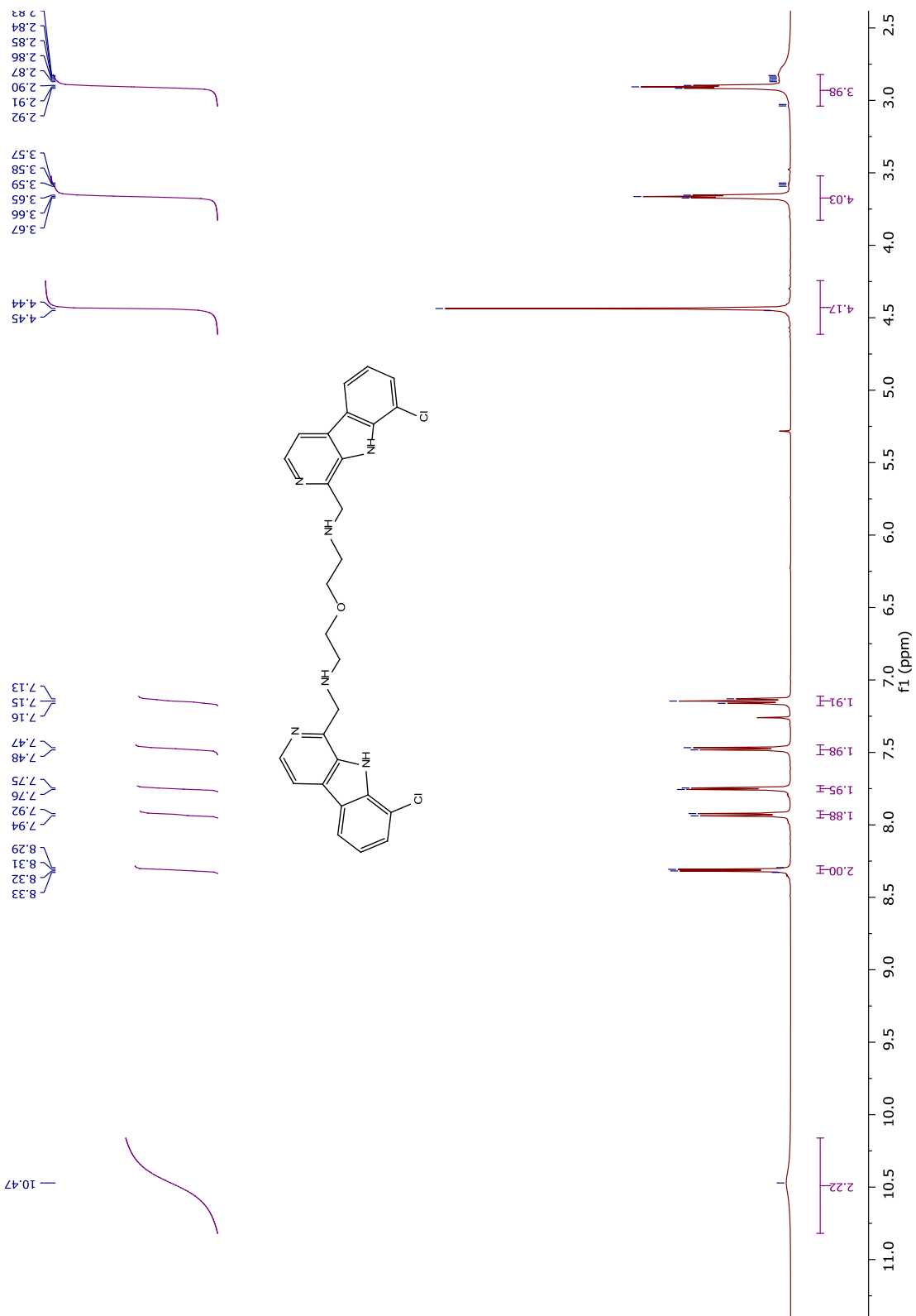
¹H NMR spectrum of compound 52



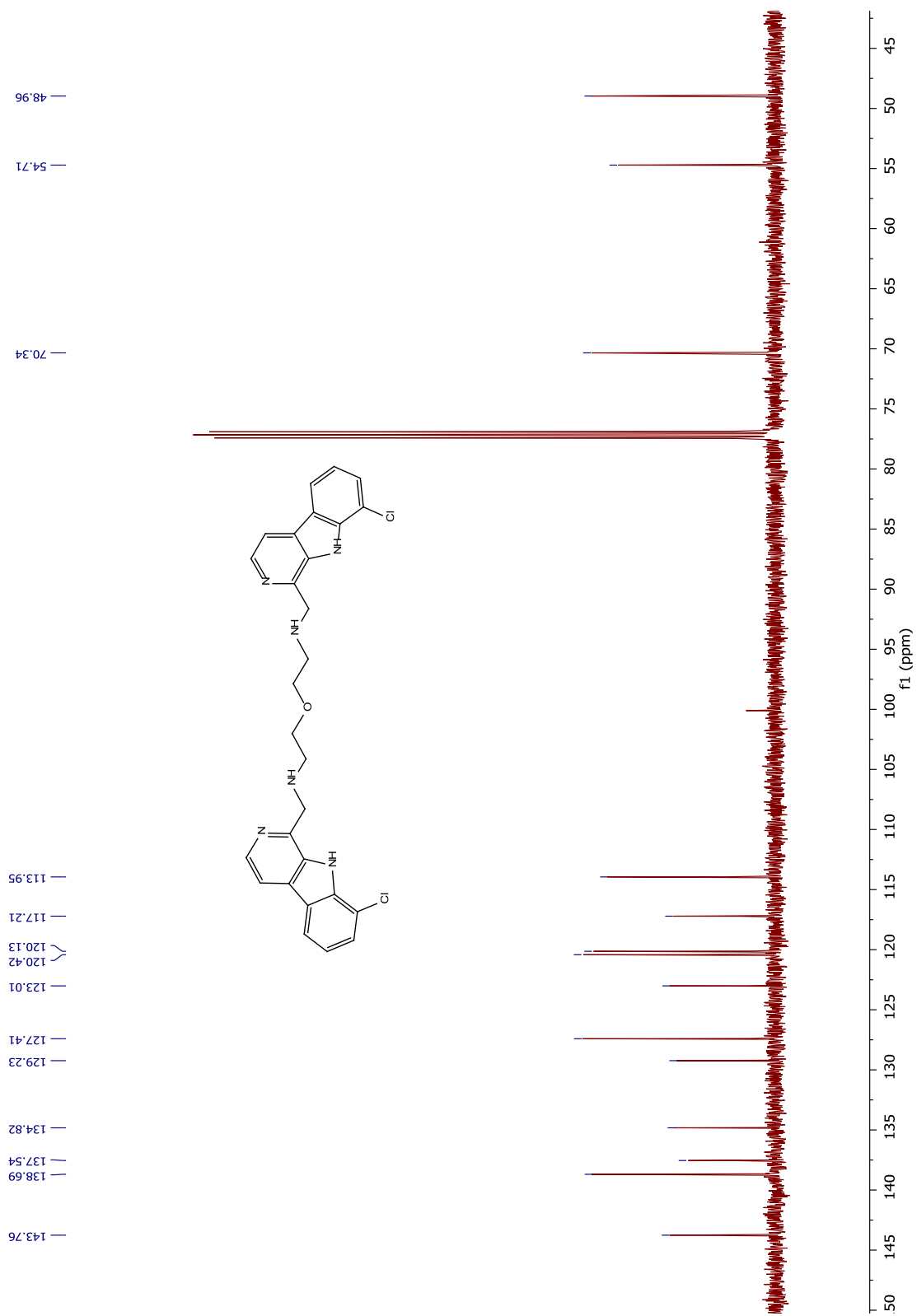
¹³C NMR spectrum of compound 52



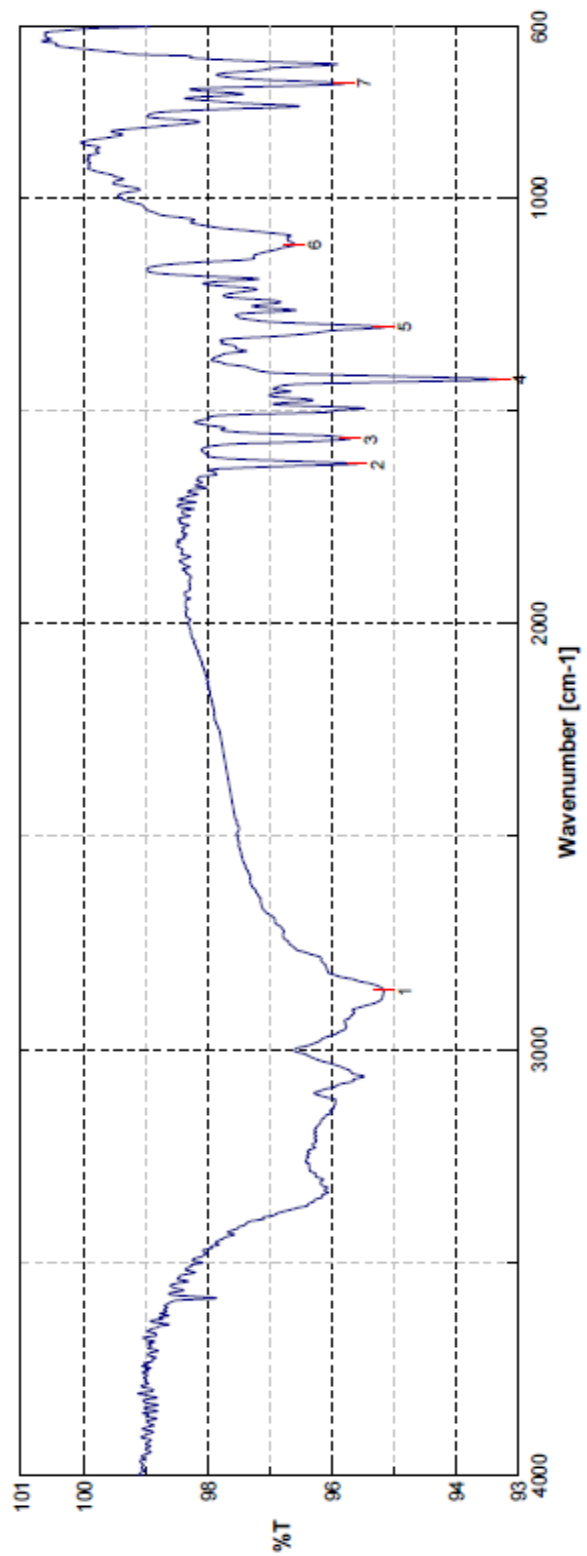
FTIR spectrum of compound **52**



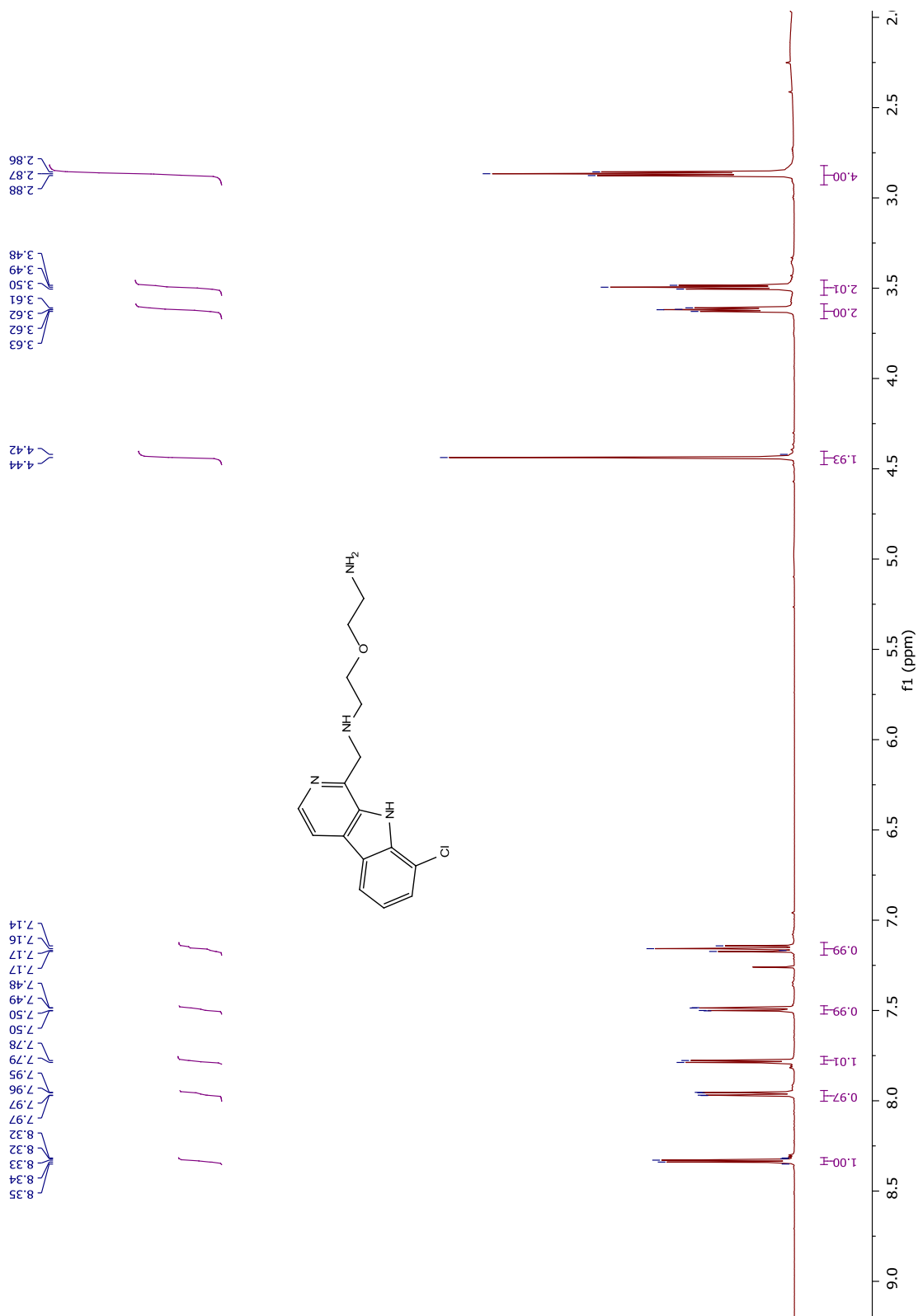
^1H NMR spectrum of compound **53**



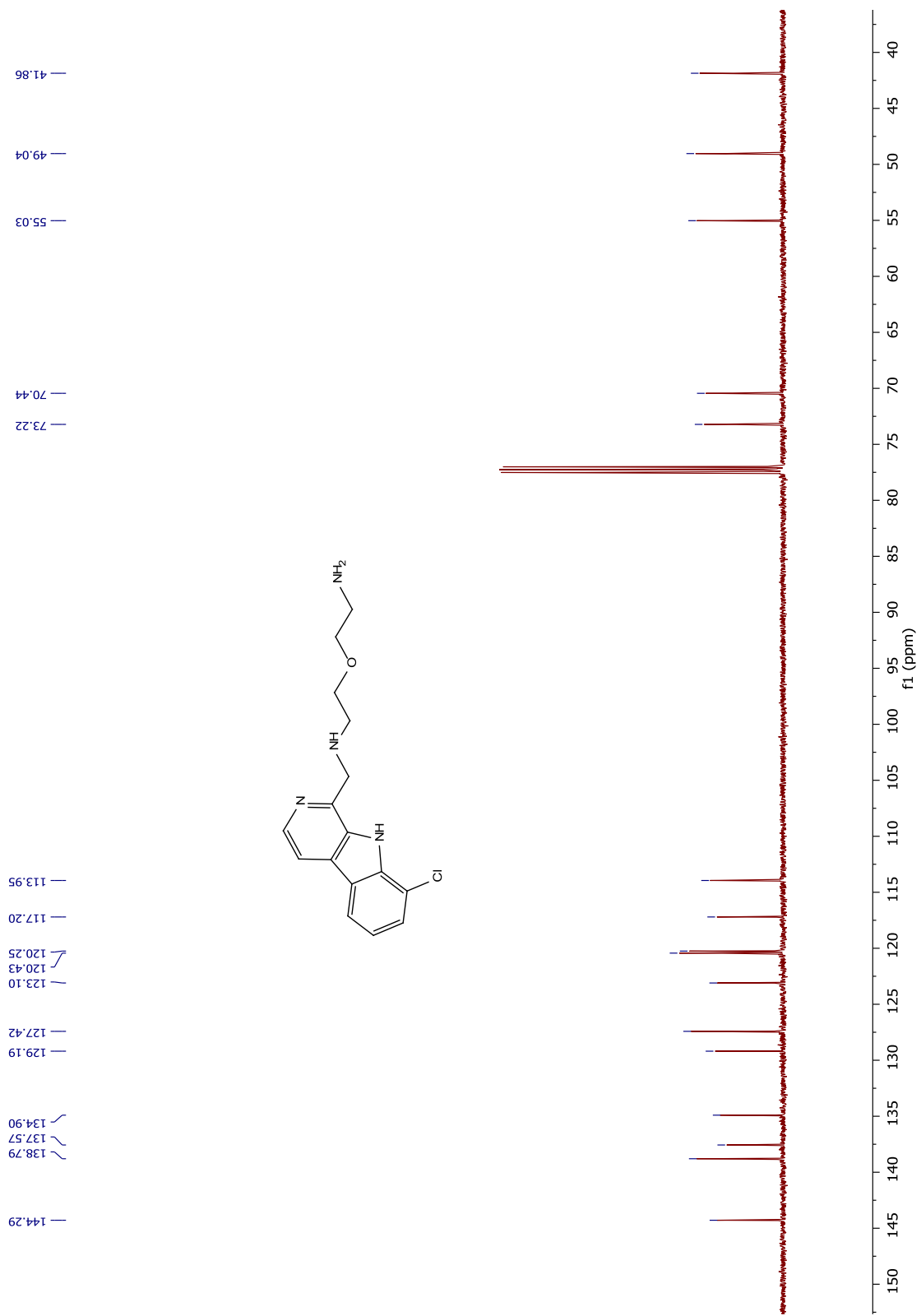
¹³C NMR spectrum of compound **53**



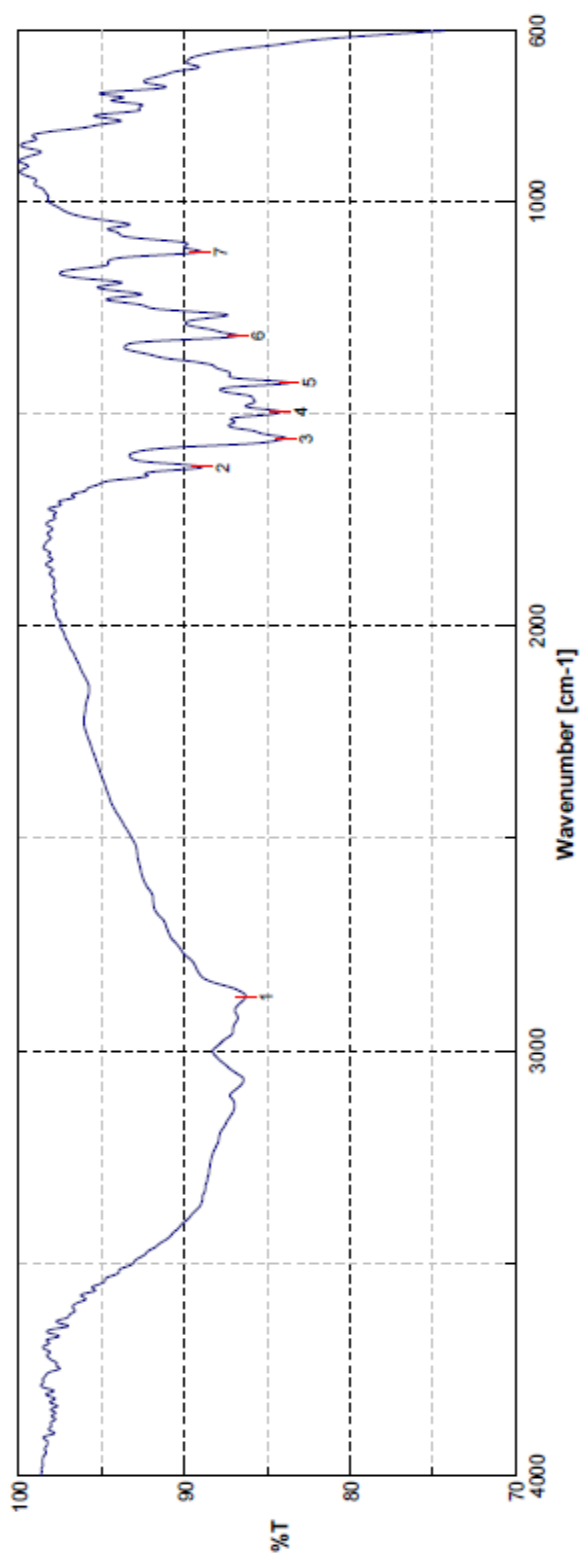
FTIR spectrum of compound 53



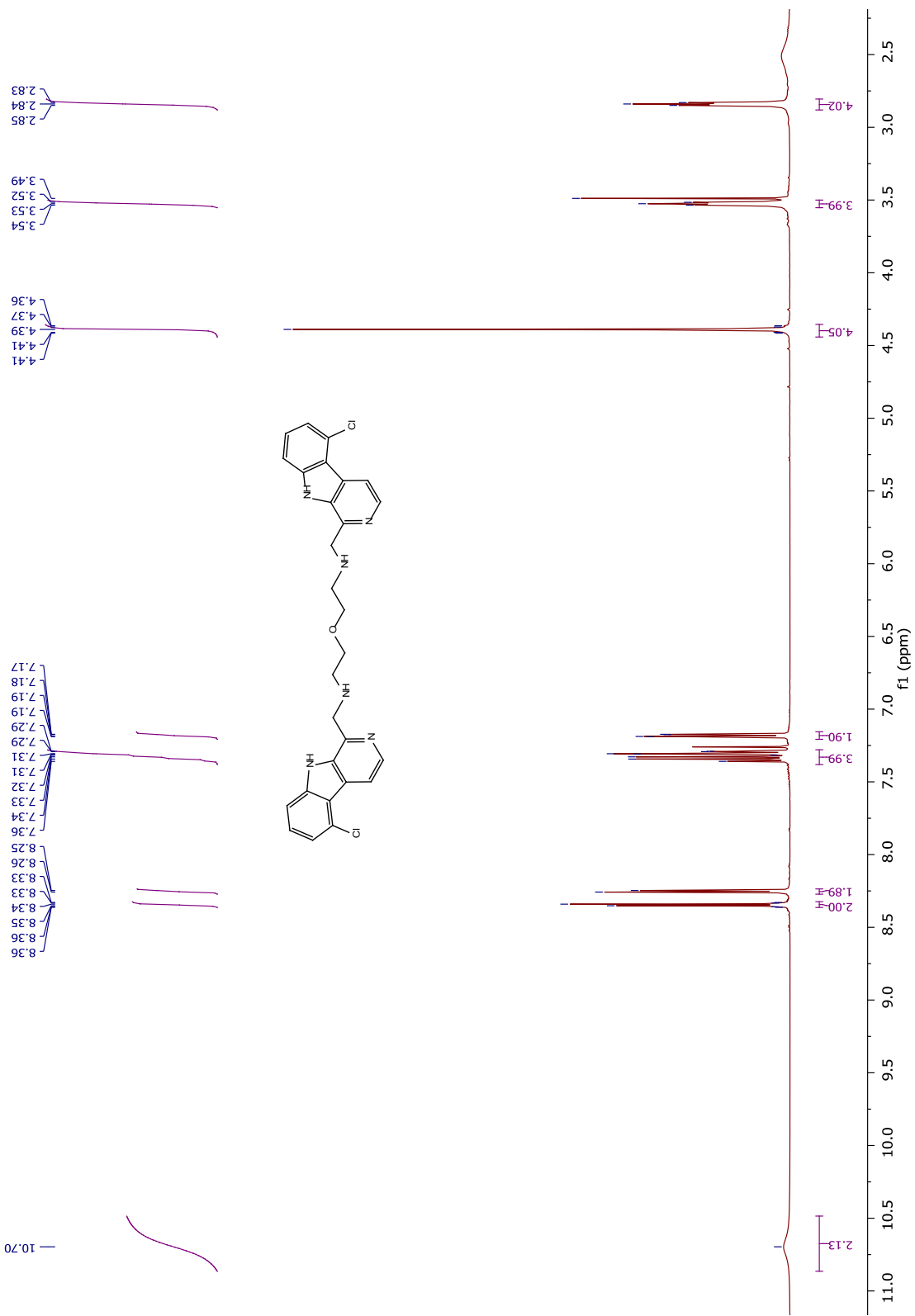
¹H NMR spectrum of compound 54



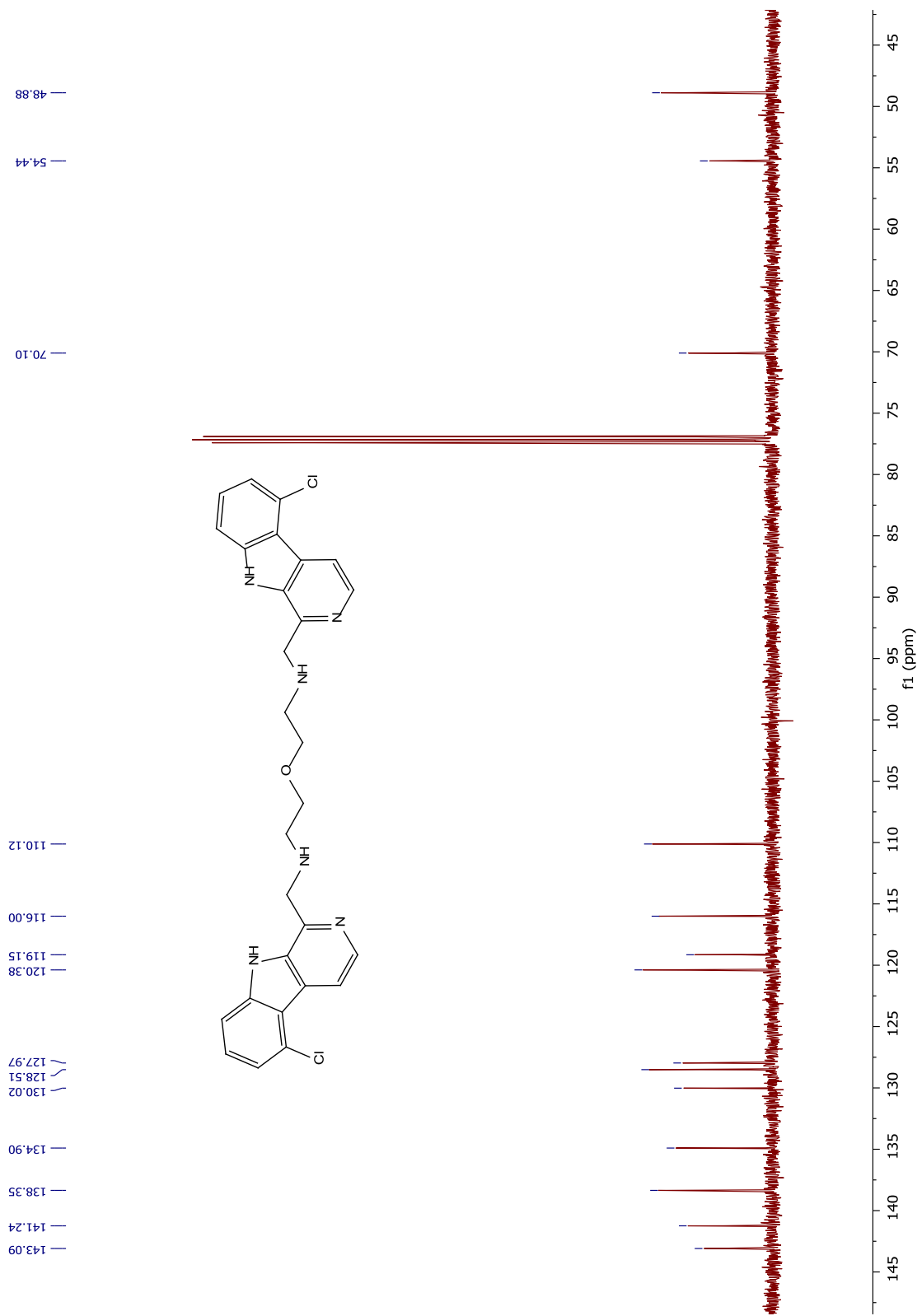
^{13}C NMR spectrum of compound 54



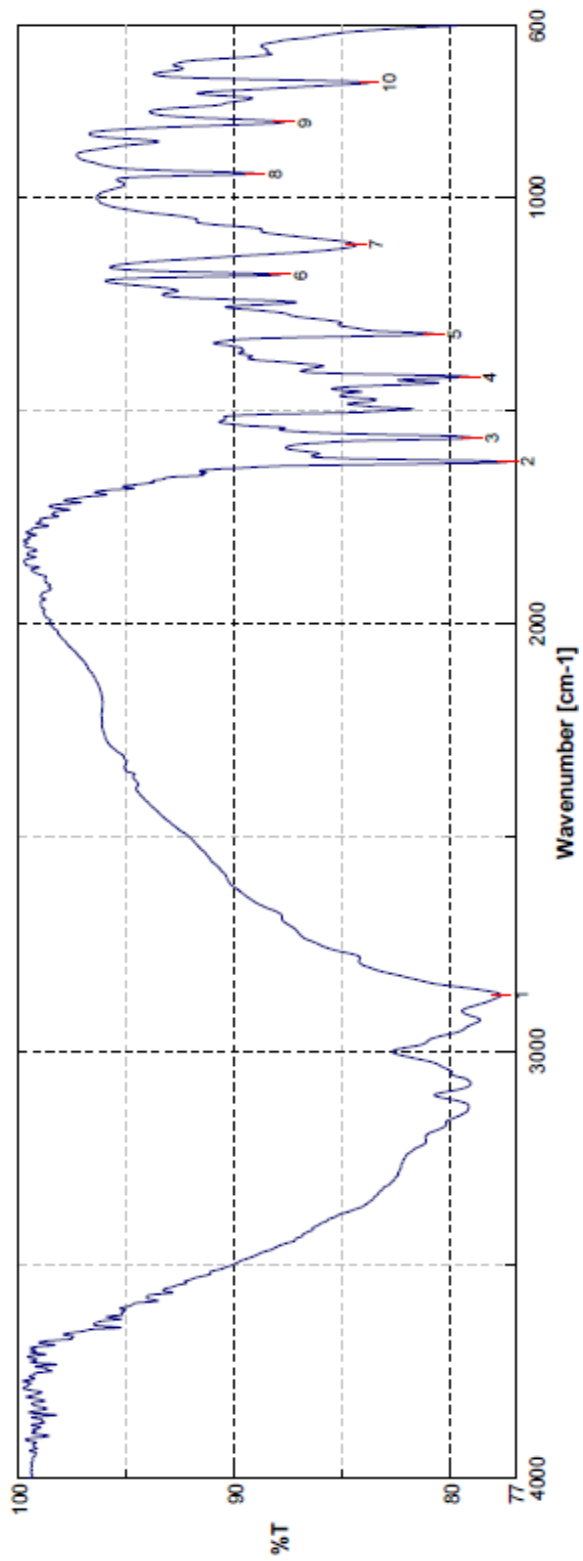
FTIR spectrum of compound **54**



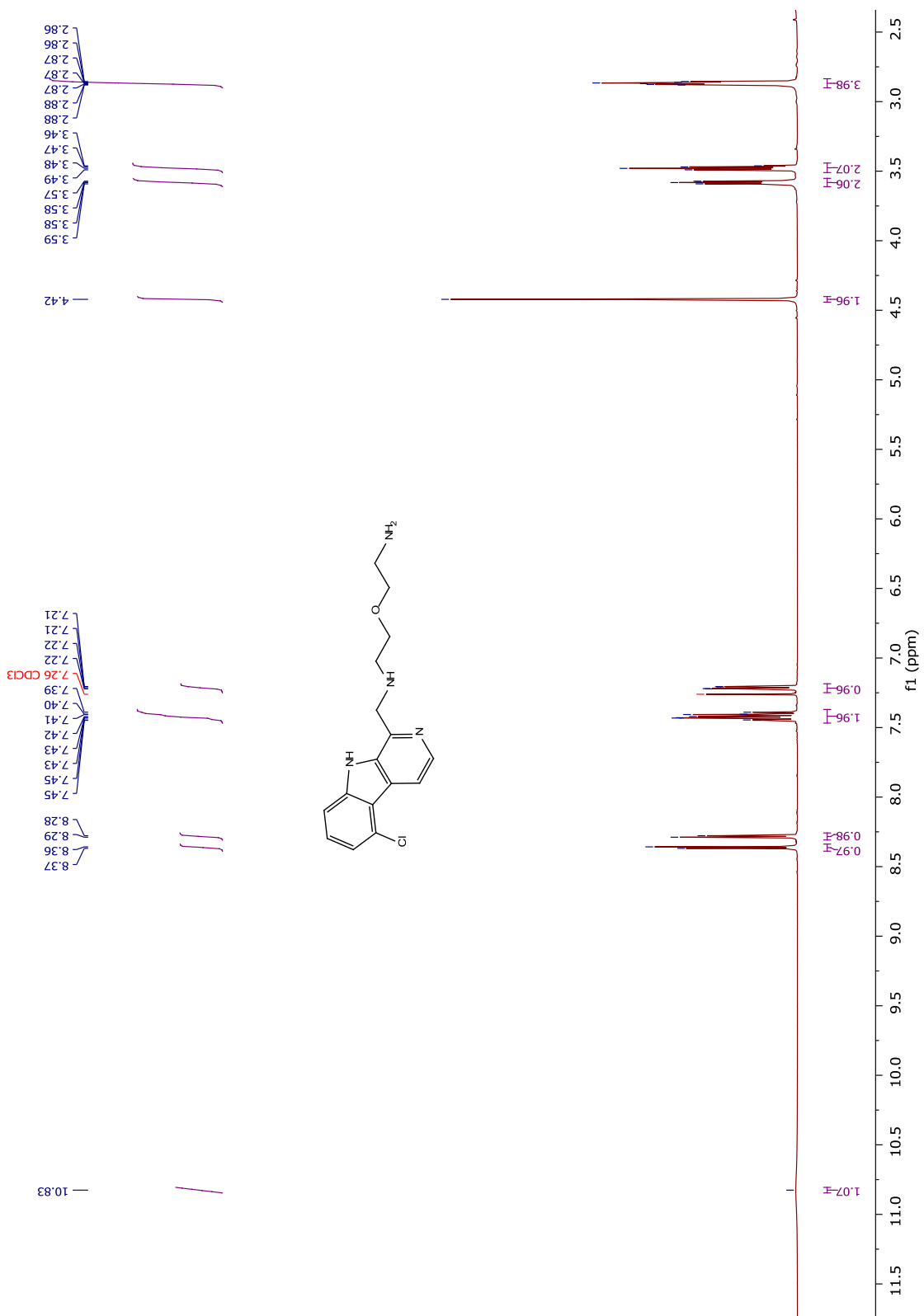
¹H NMR spectrum of compound 55



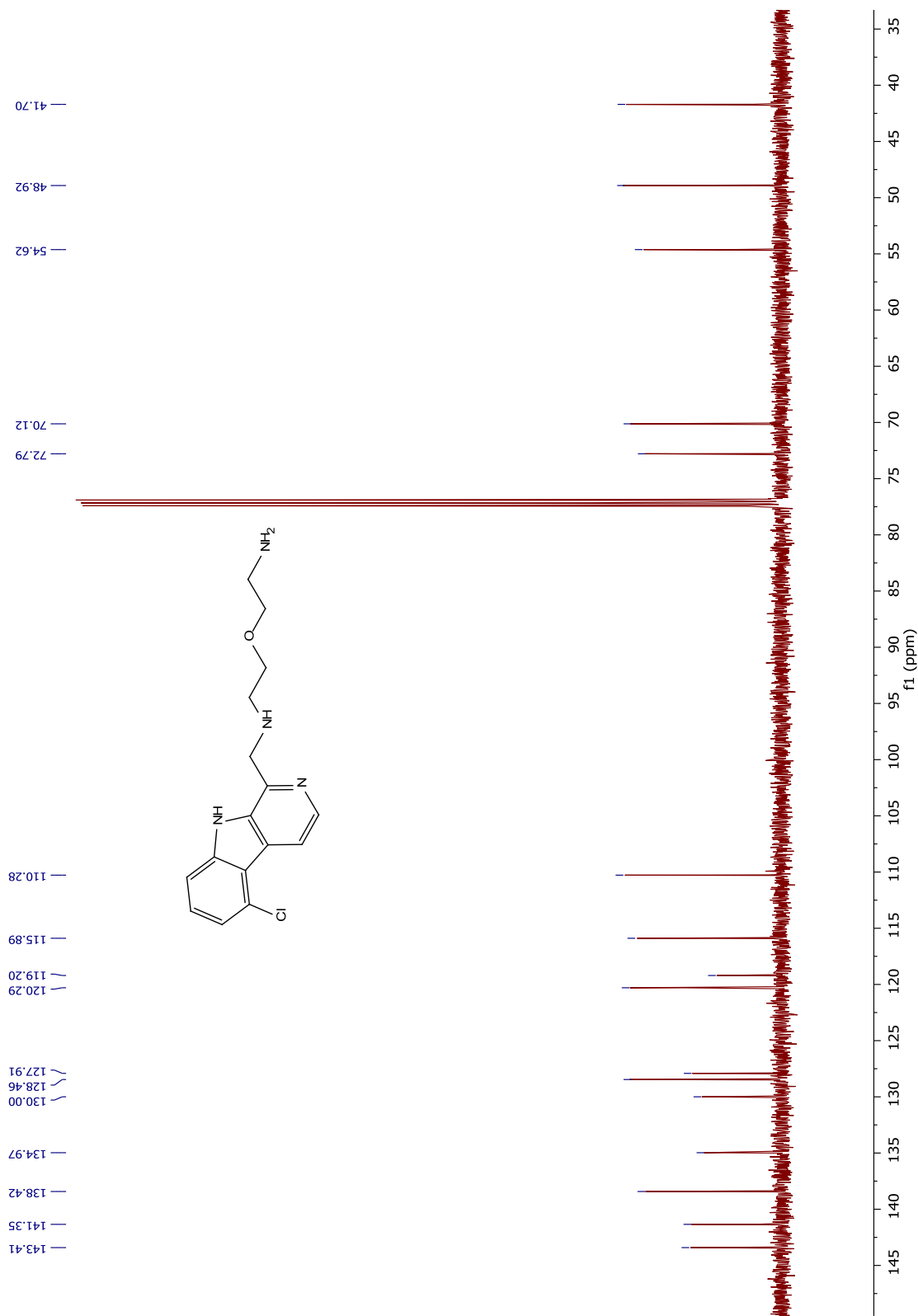
¹³C NMR spectrum of compound 55



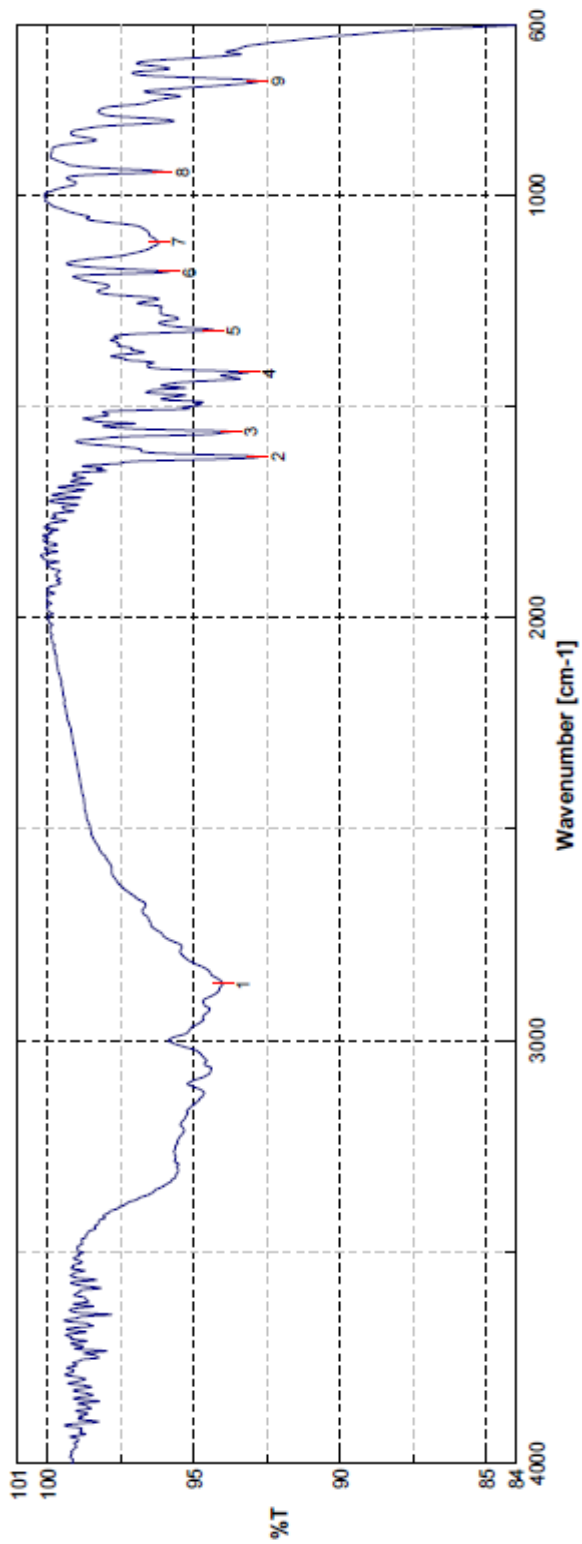
FTIR spectrum of compound 55



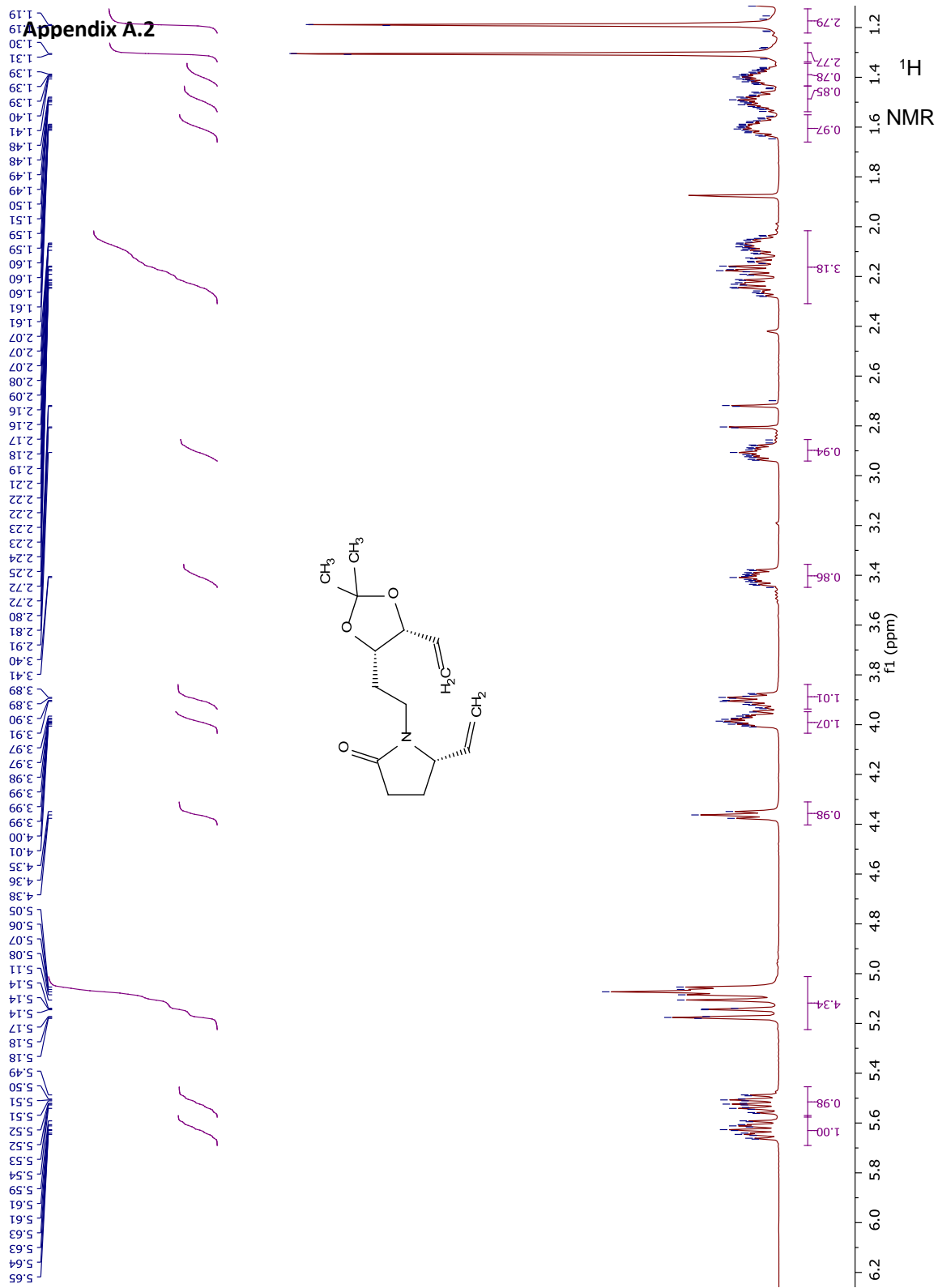
¹H NMR spectrum of compound 56



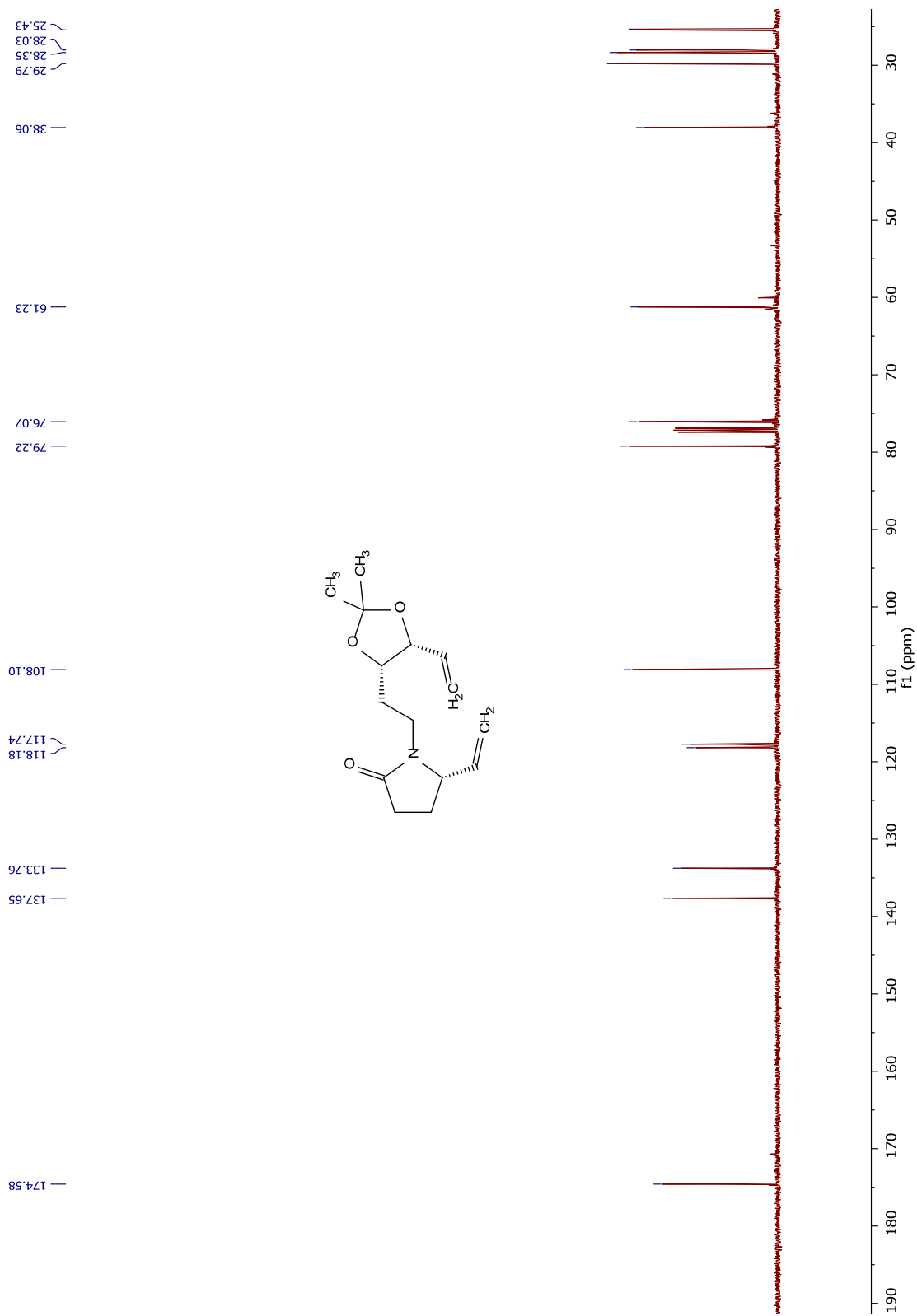
^{13}C NMR spectrum of compound **56**



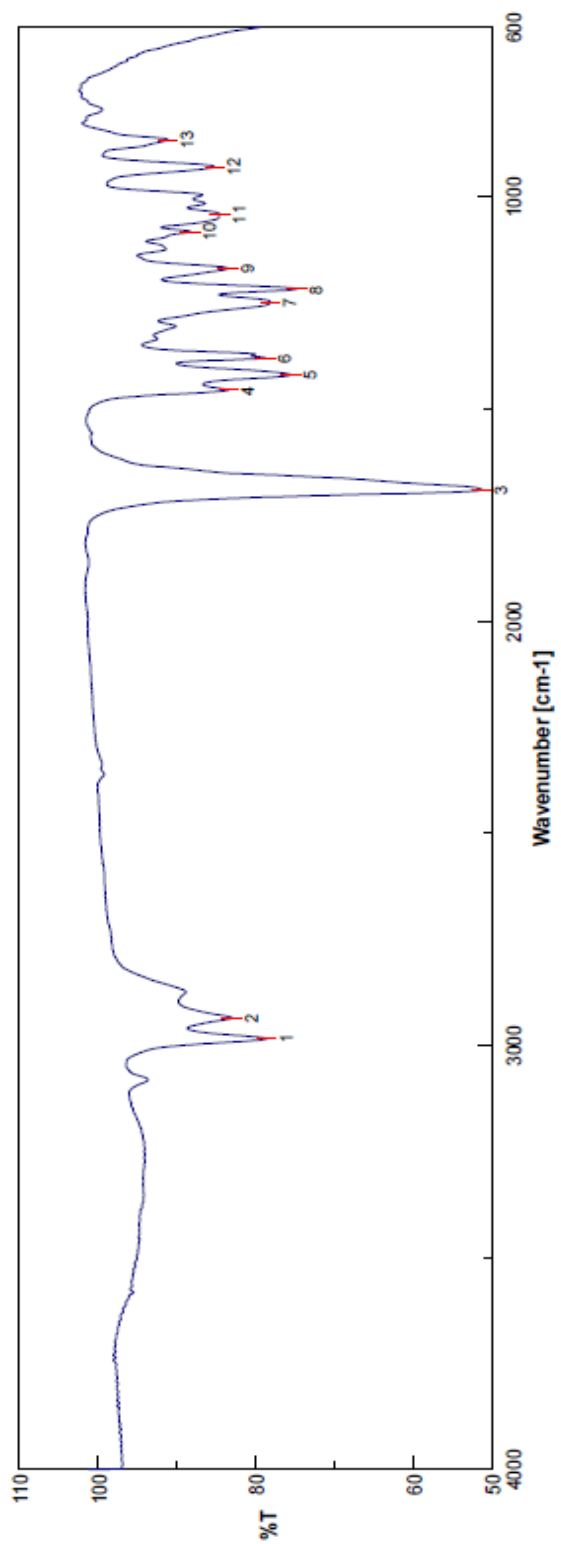
FTIR spectrum of compound 56



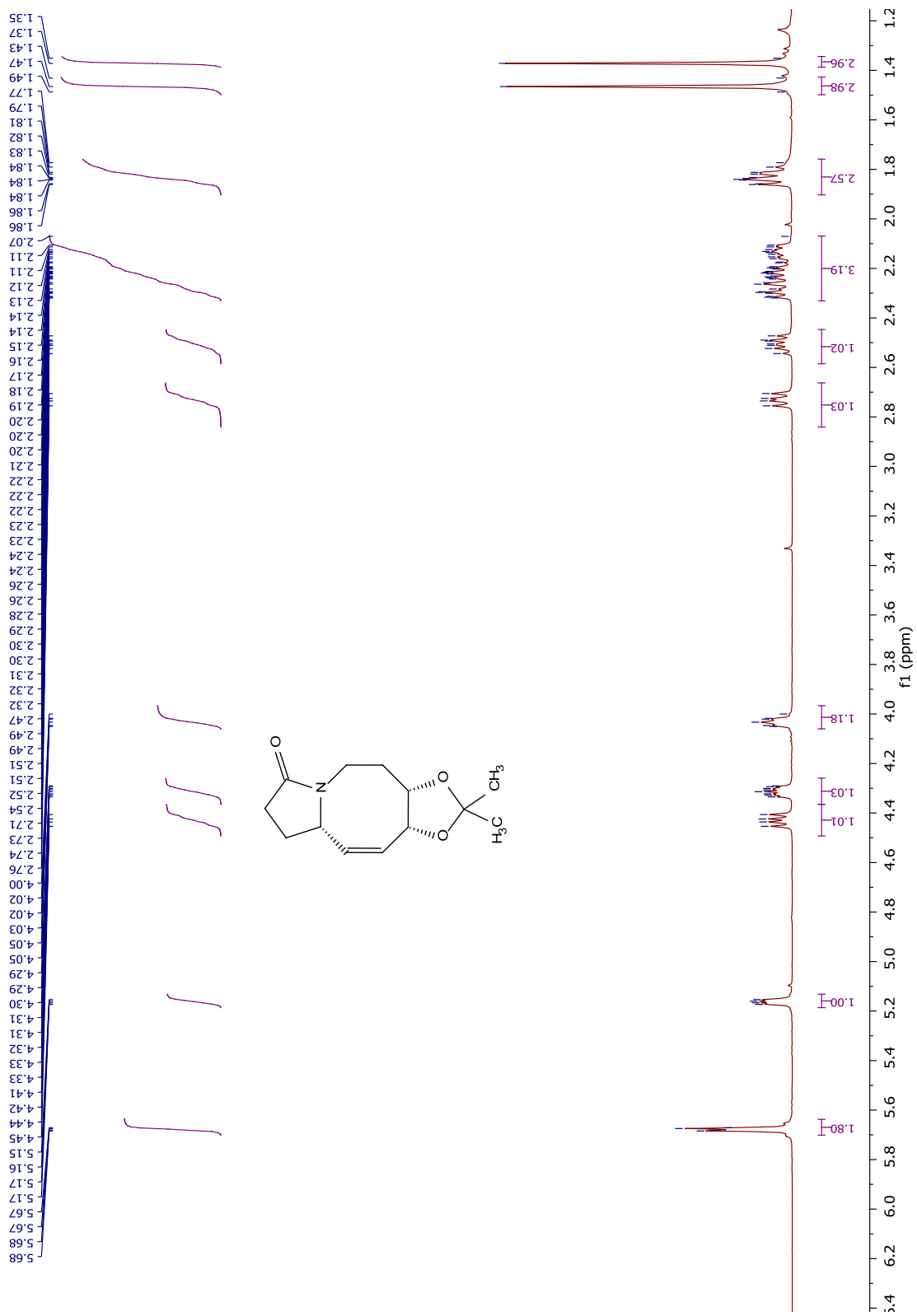
¹H NMR spectrum of compound 112



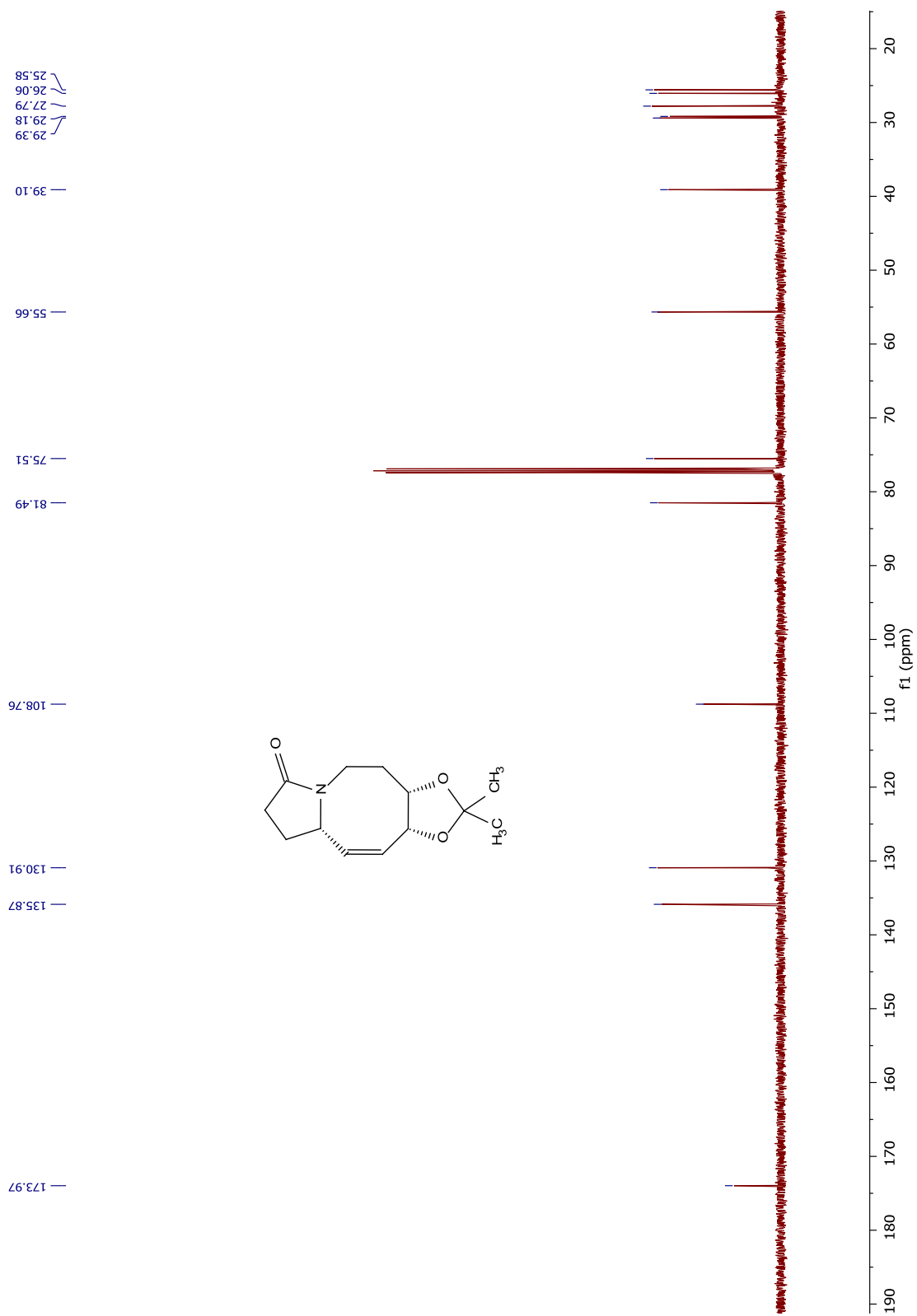
¹³C NMR spectrum of compound 112



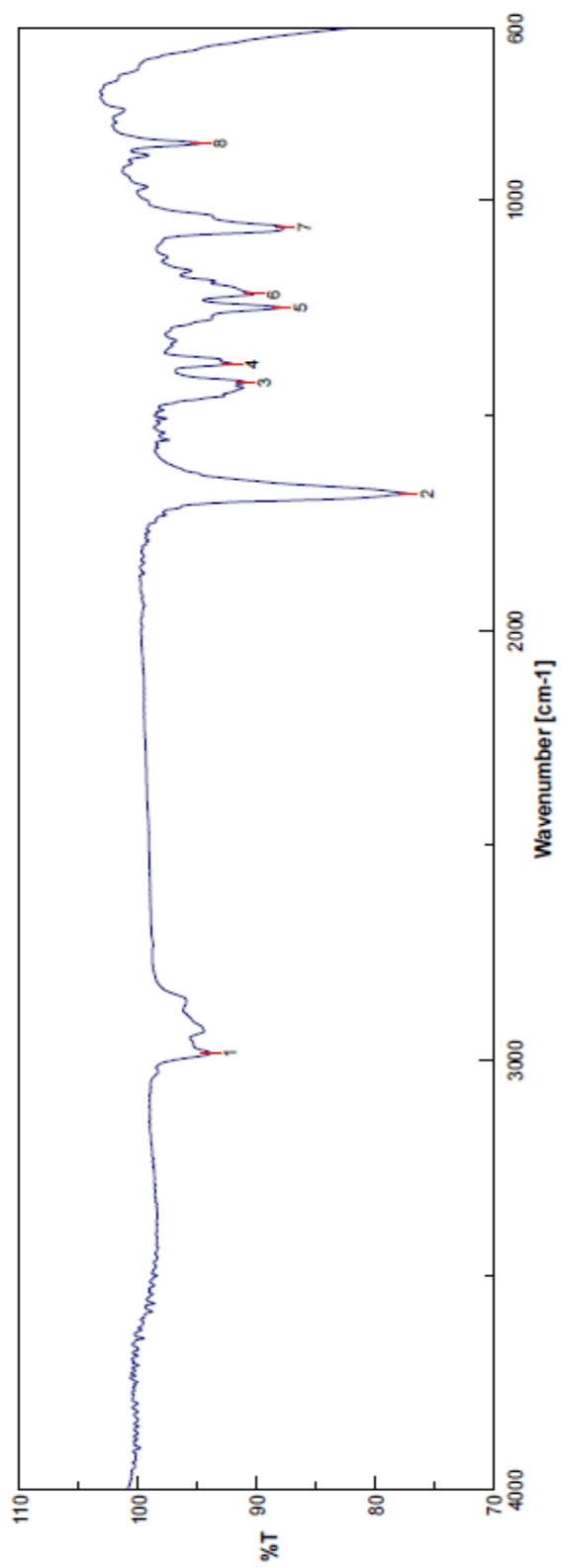
FTIR spectrum of compound **112**



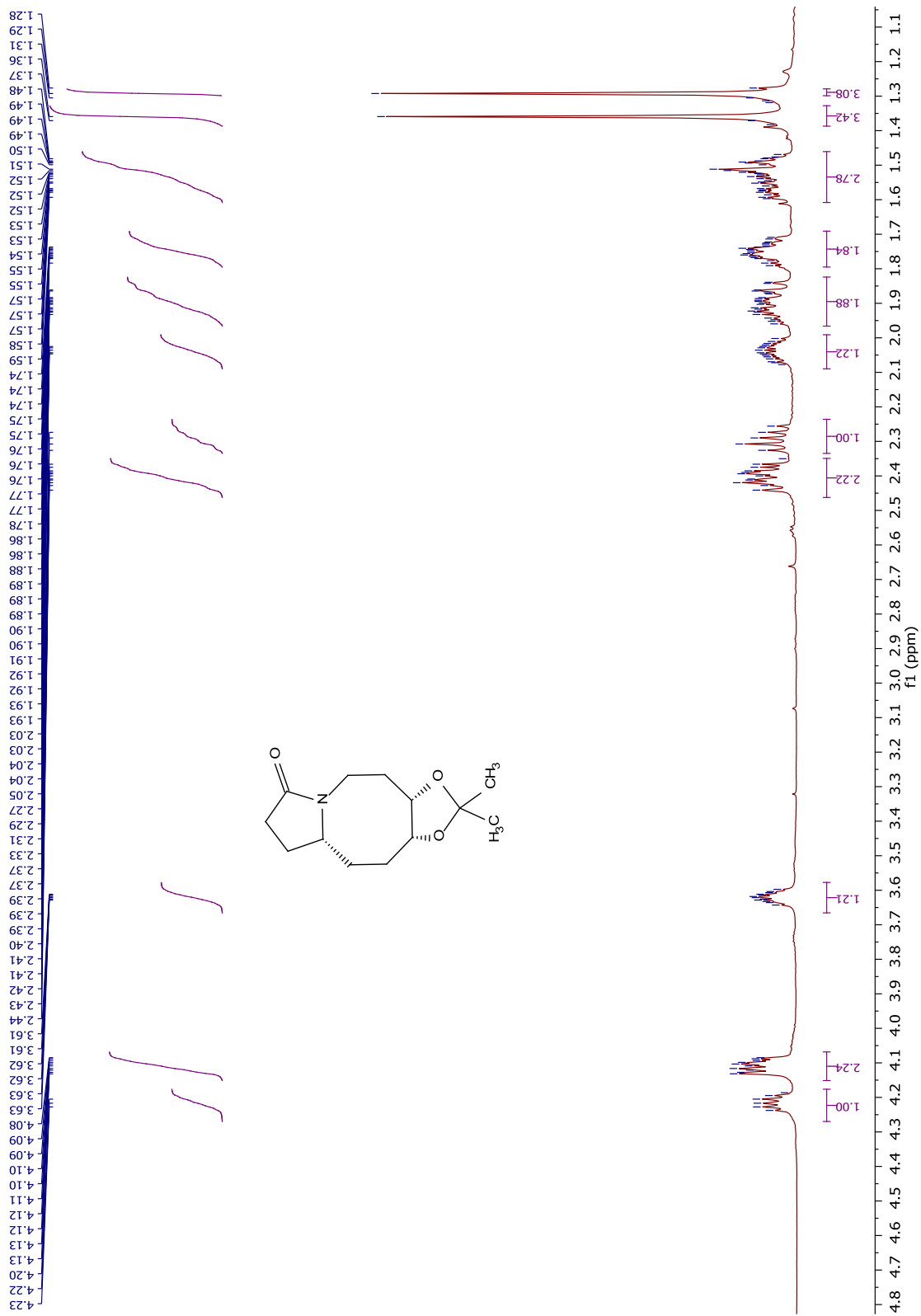
¹H NMR spectrum of compound 113



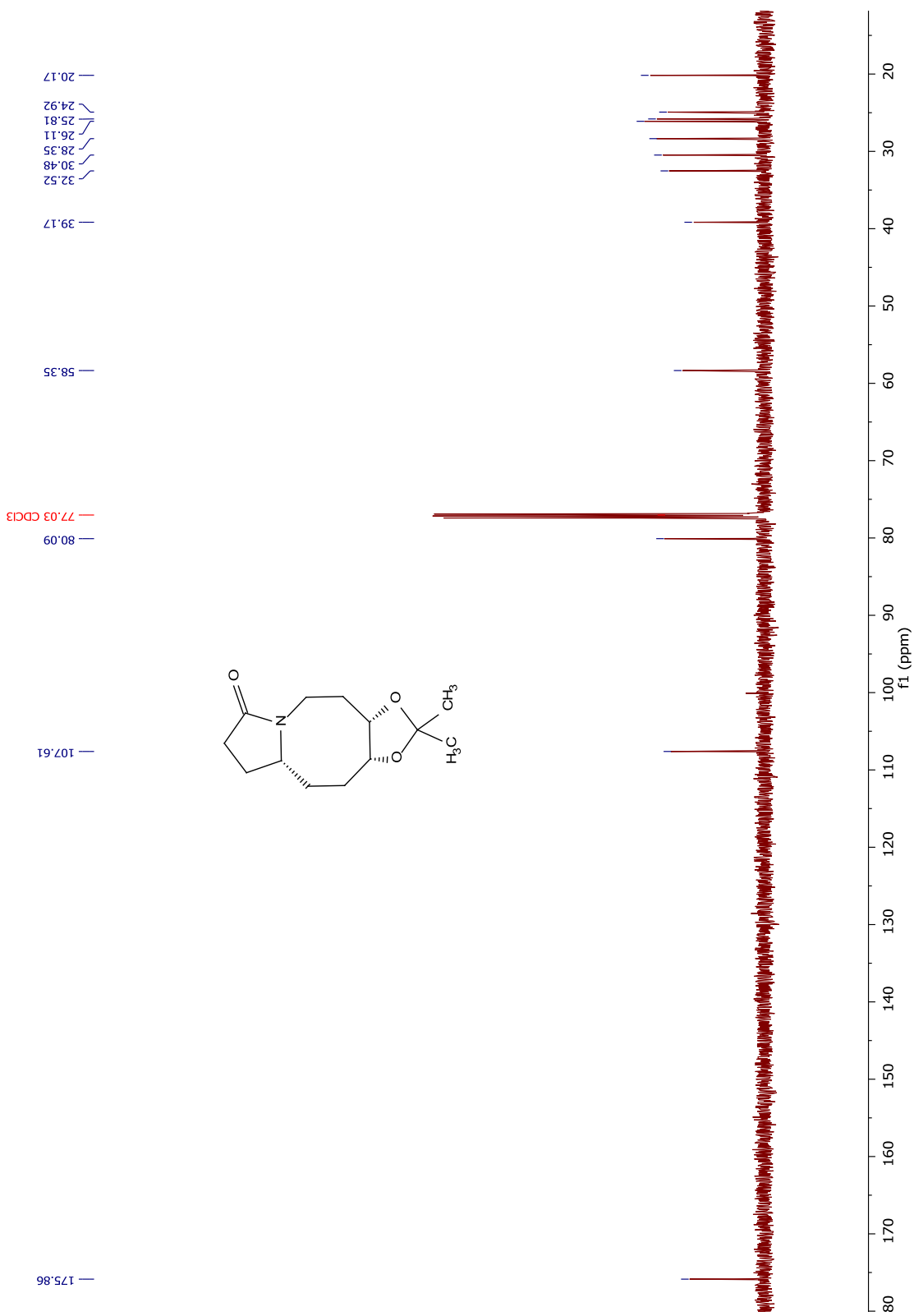
¹³C NMR spectrum of compound 113



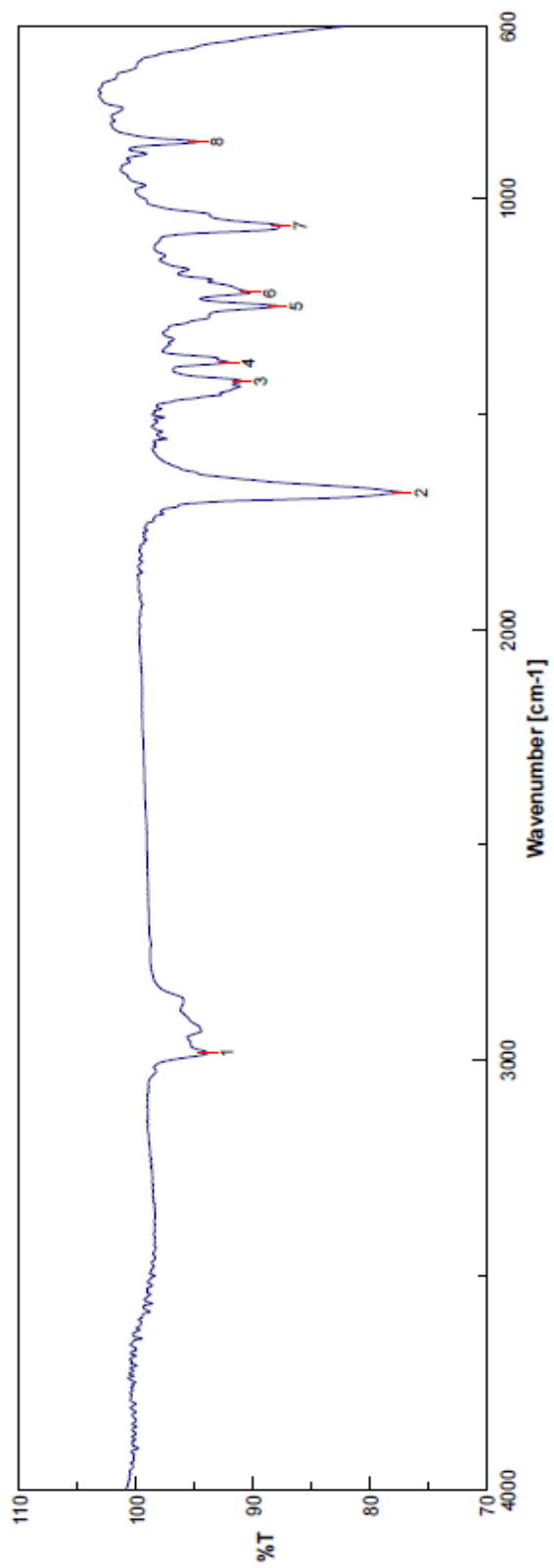
FTIR spectrum of compound 113



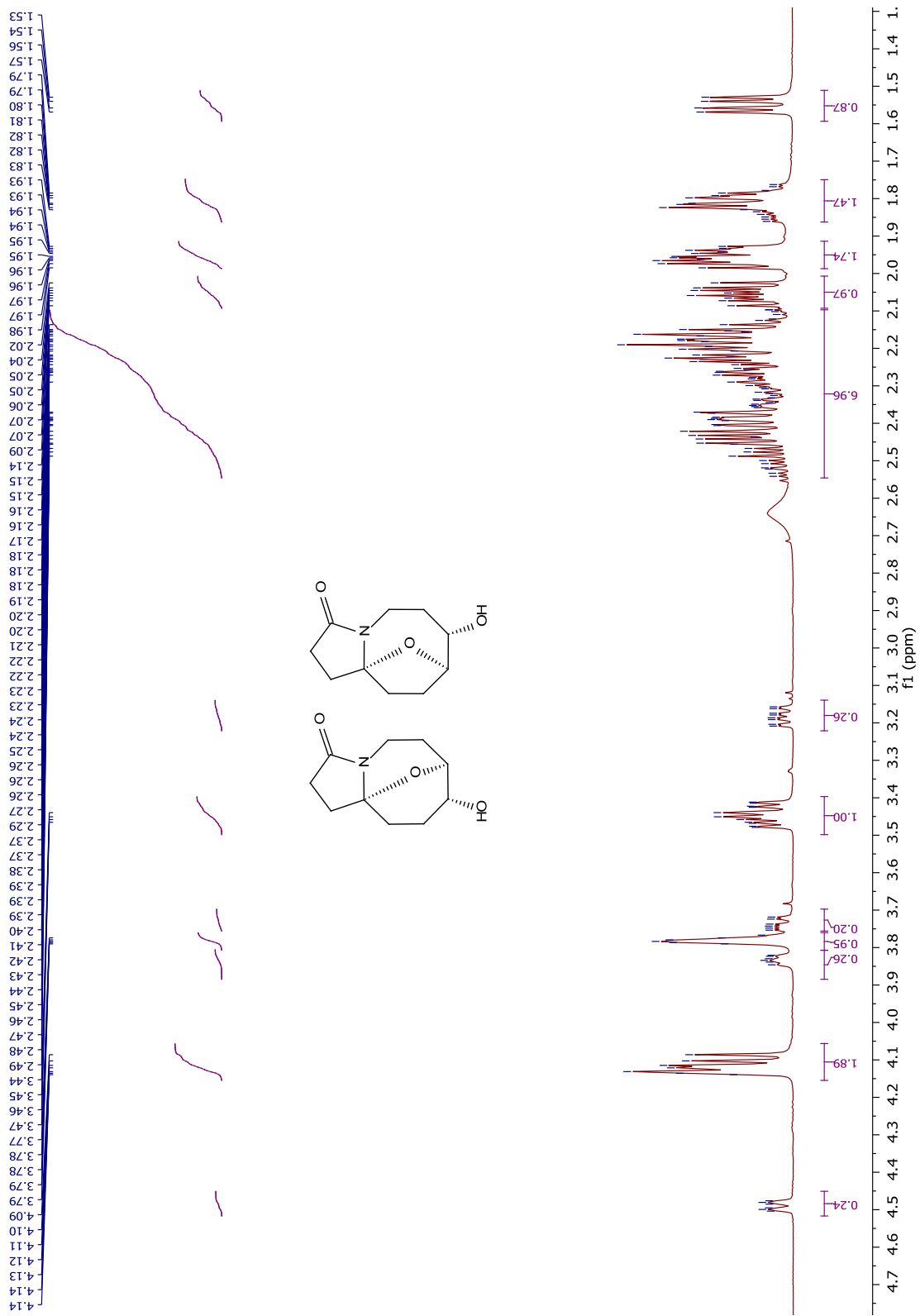
¹H NMR spectrum of compound 114



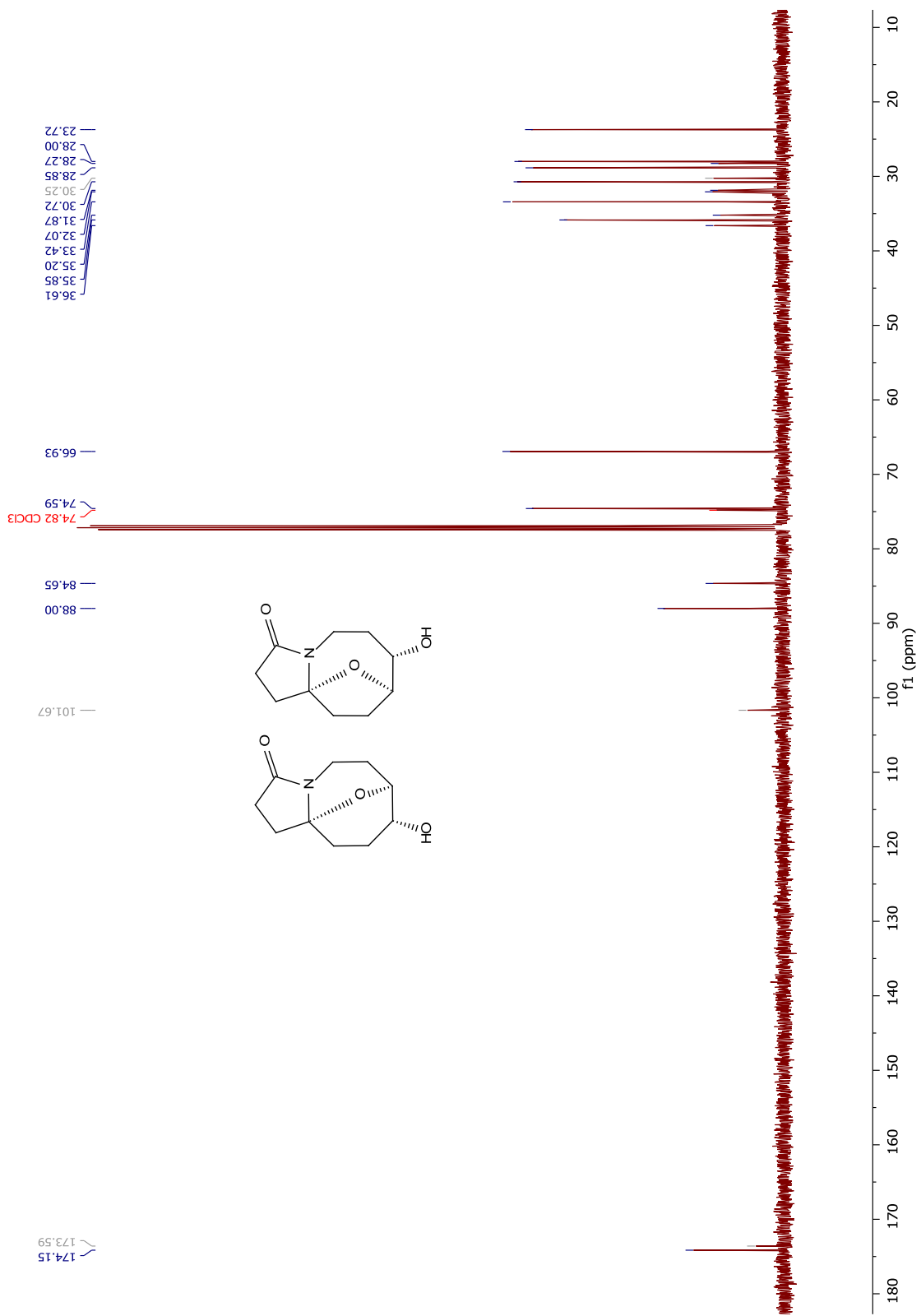
¹³C NMR spectrum of compound 114



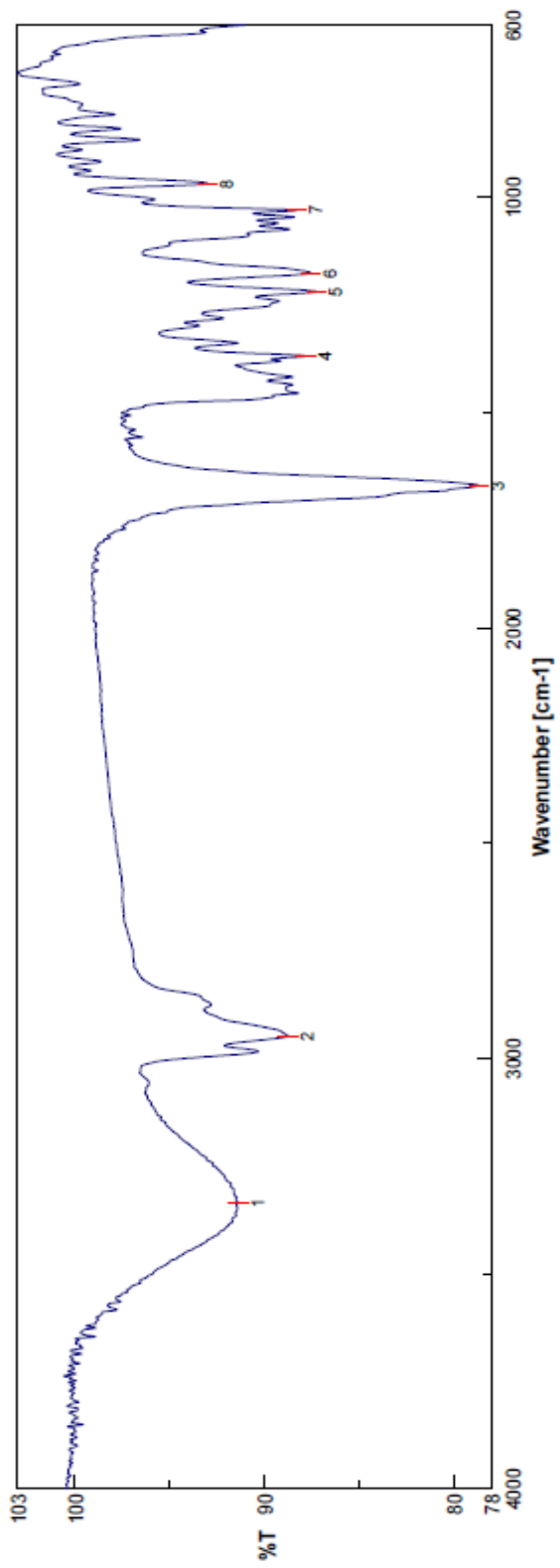
FTIR spectrum of compound 114



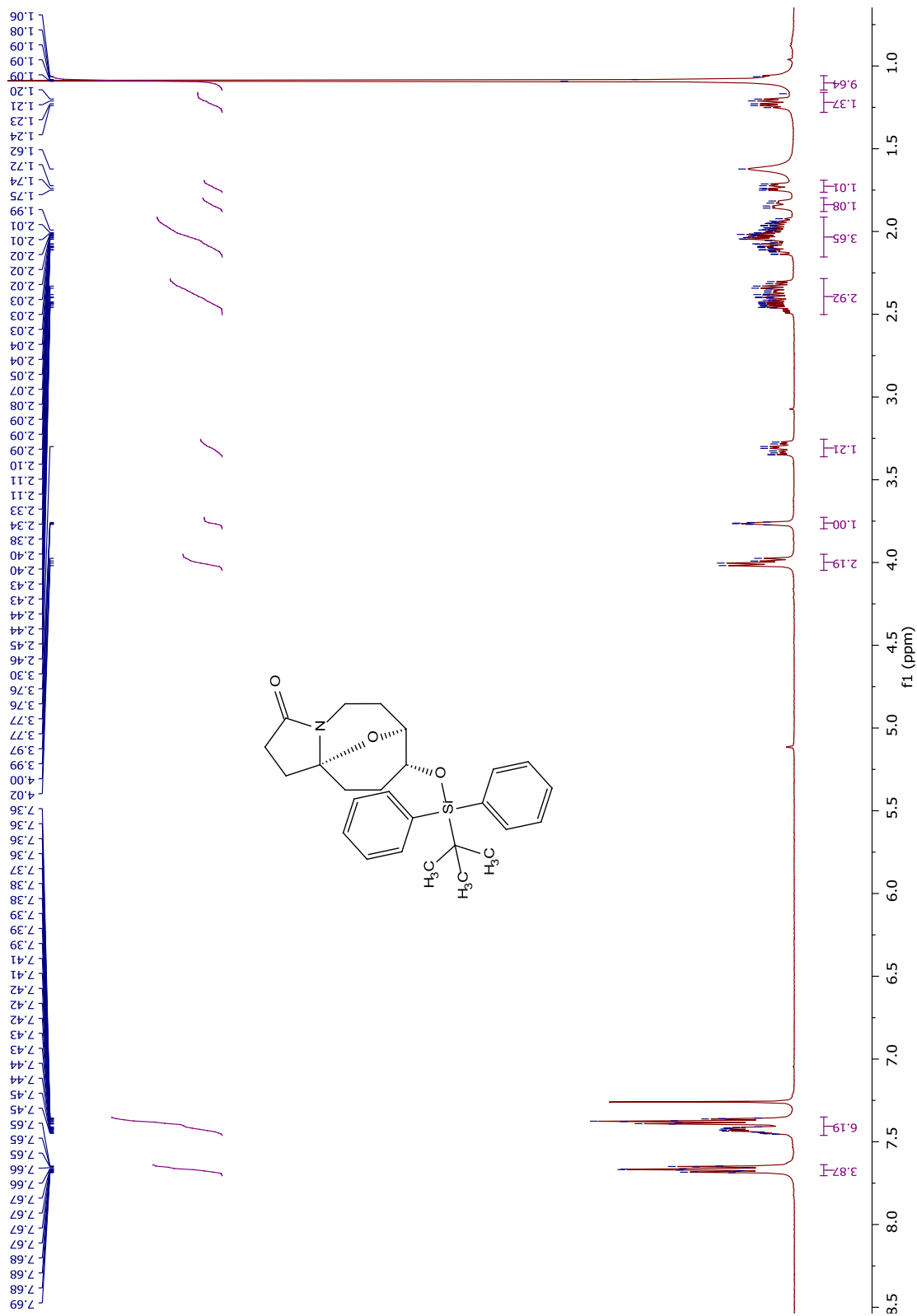
¹H NMR spectrum of compound **115** and **116**



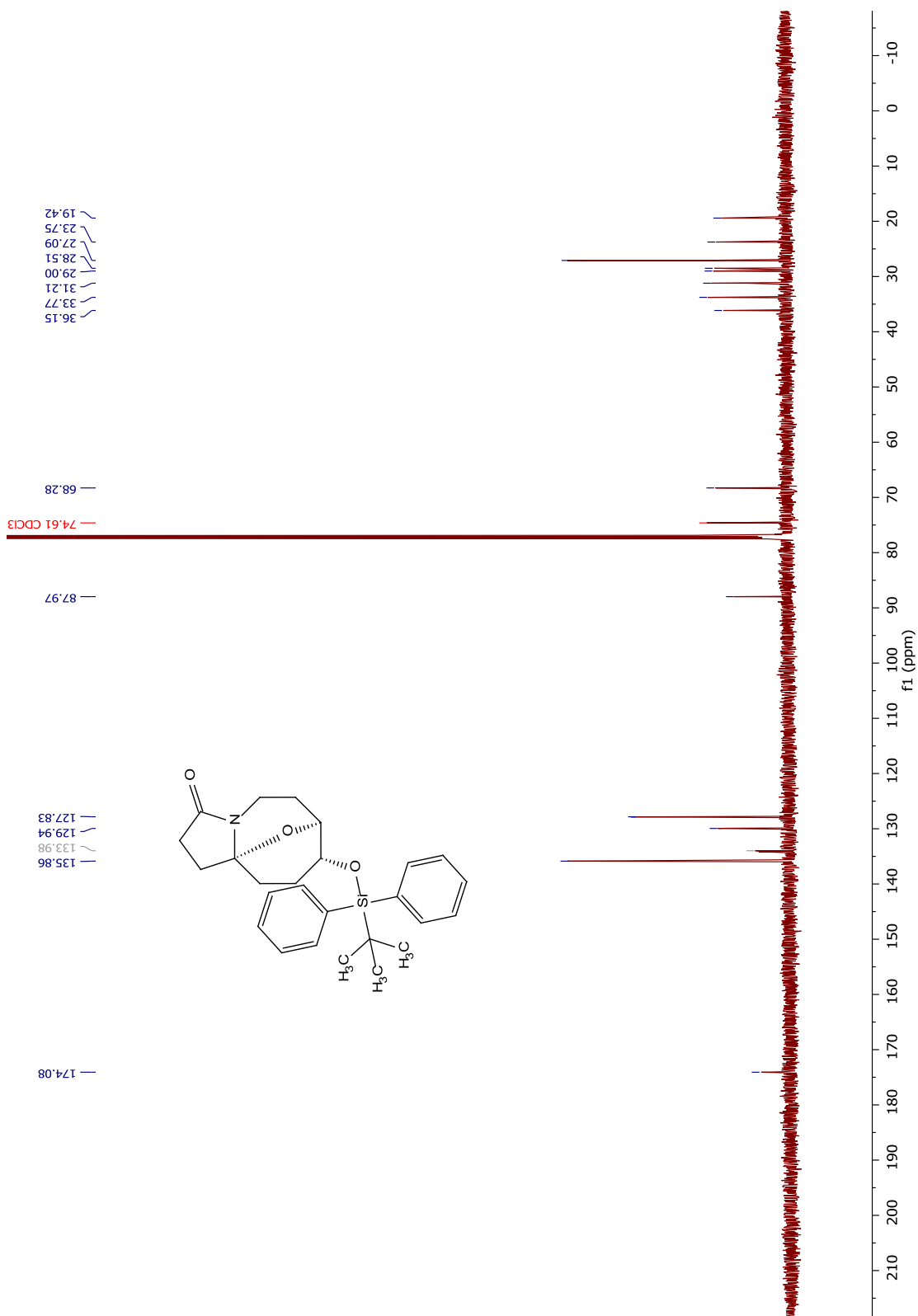
¹³C NMR spectrum of compound 115 and 116



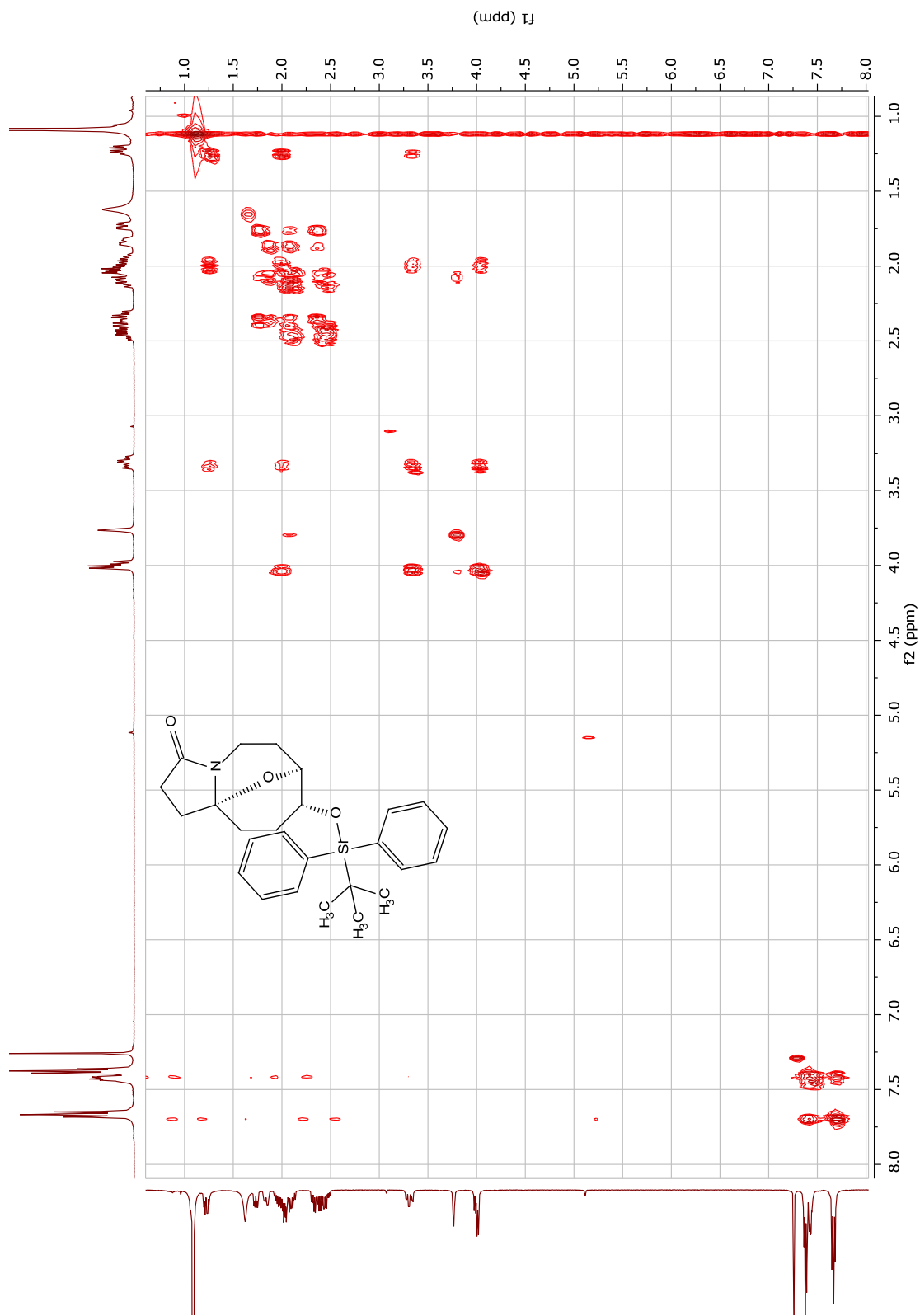
FTIR spectrum of compound **115** and **116**



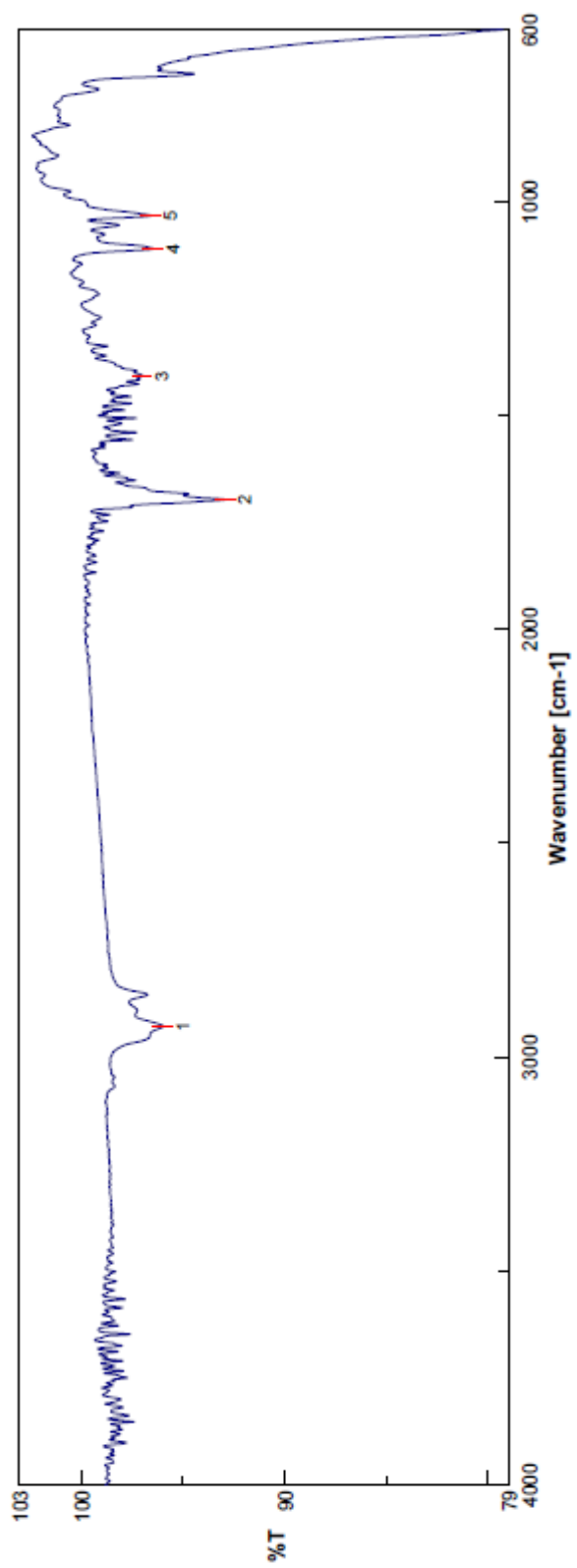
¹H NMR spectrum of compound 117



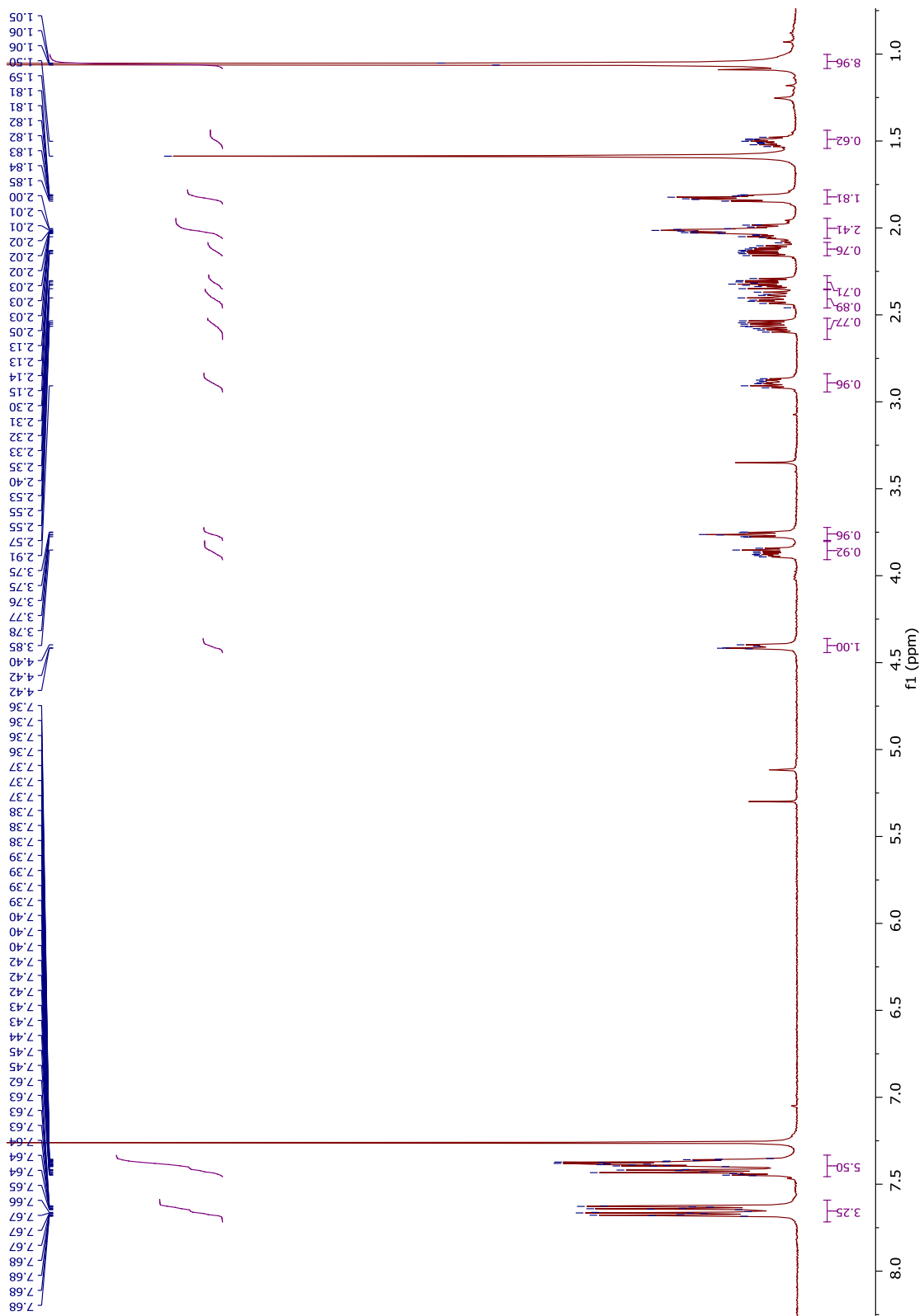
¹³C NMR spectrum of compound 117



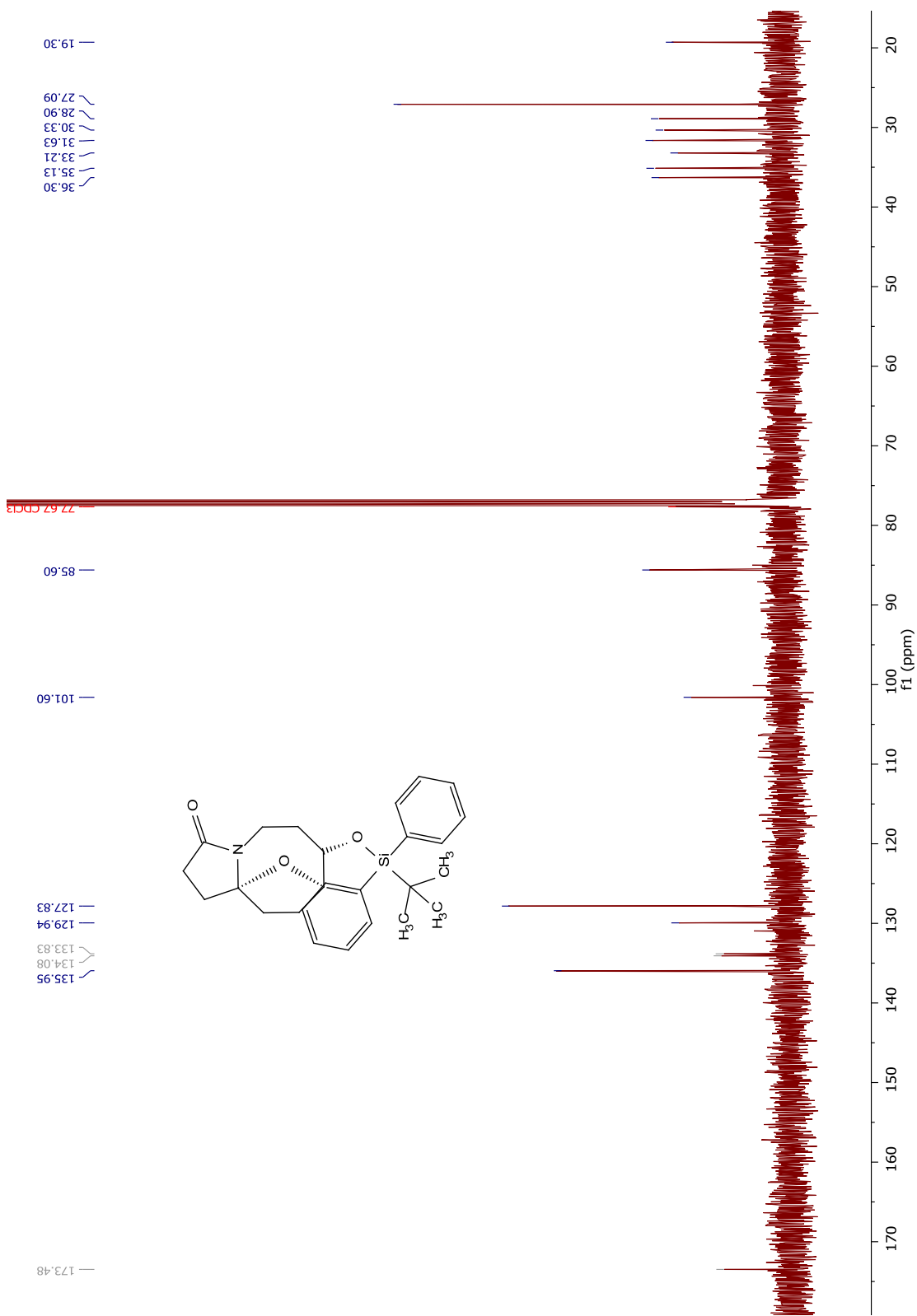
COSY NMR spectrum of compound 117



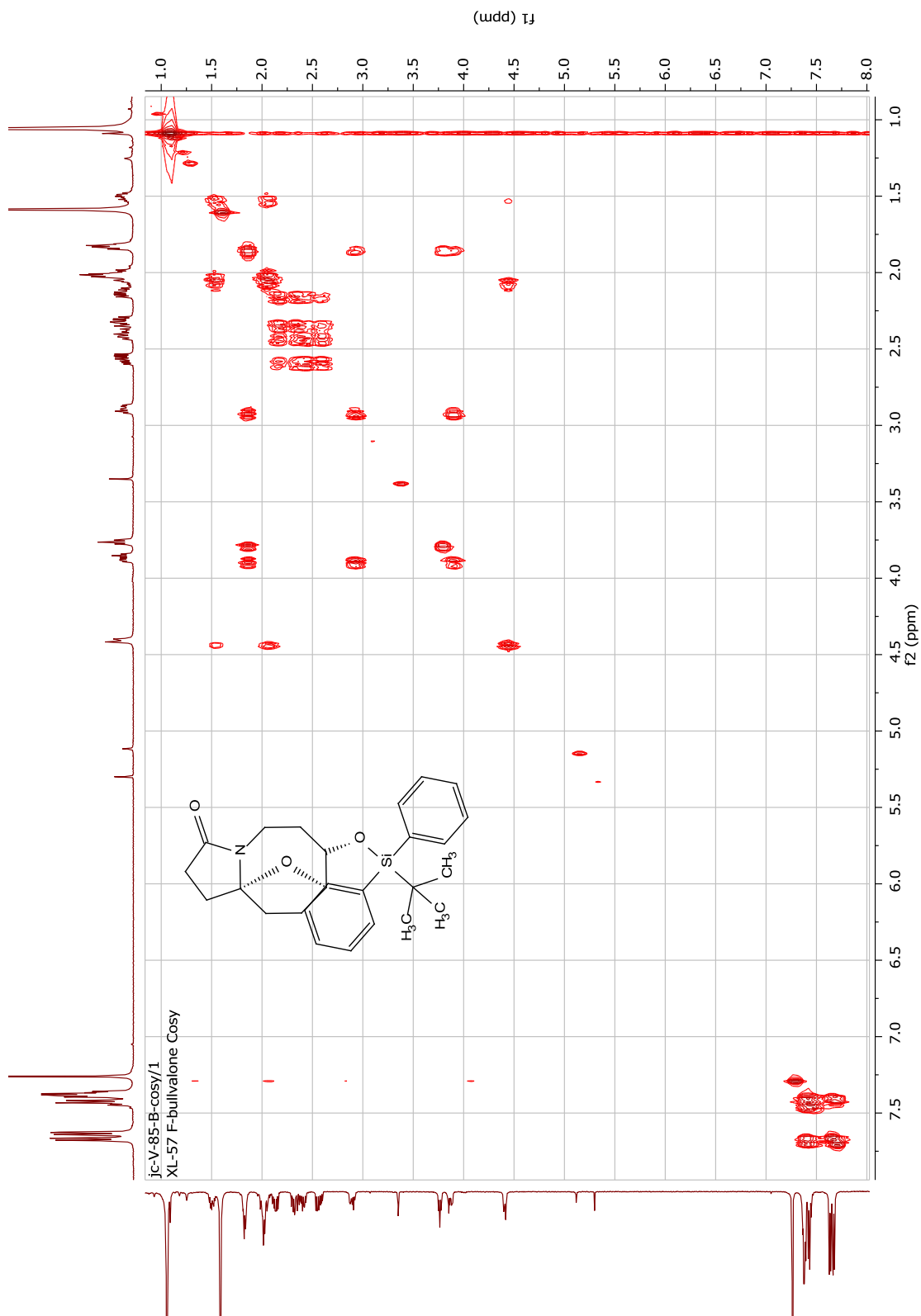
FTIR spectrum of compound 117



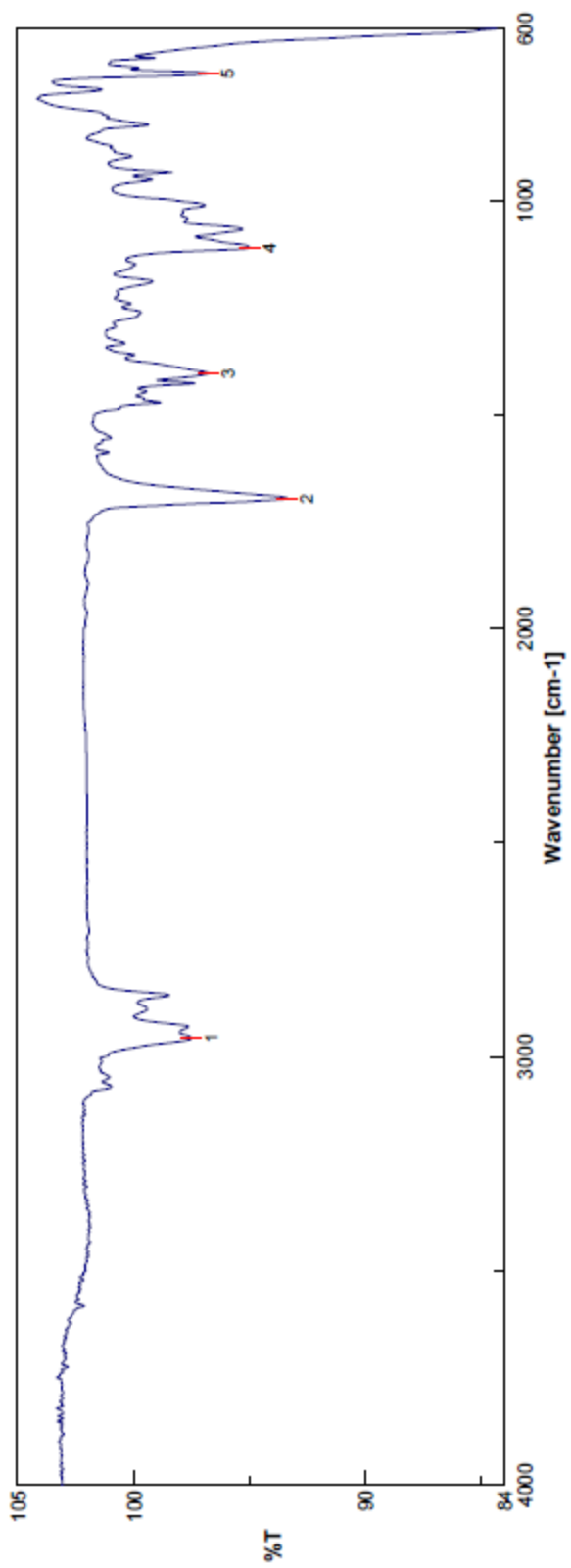
¹H NMR spectrum of compound 118



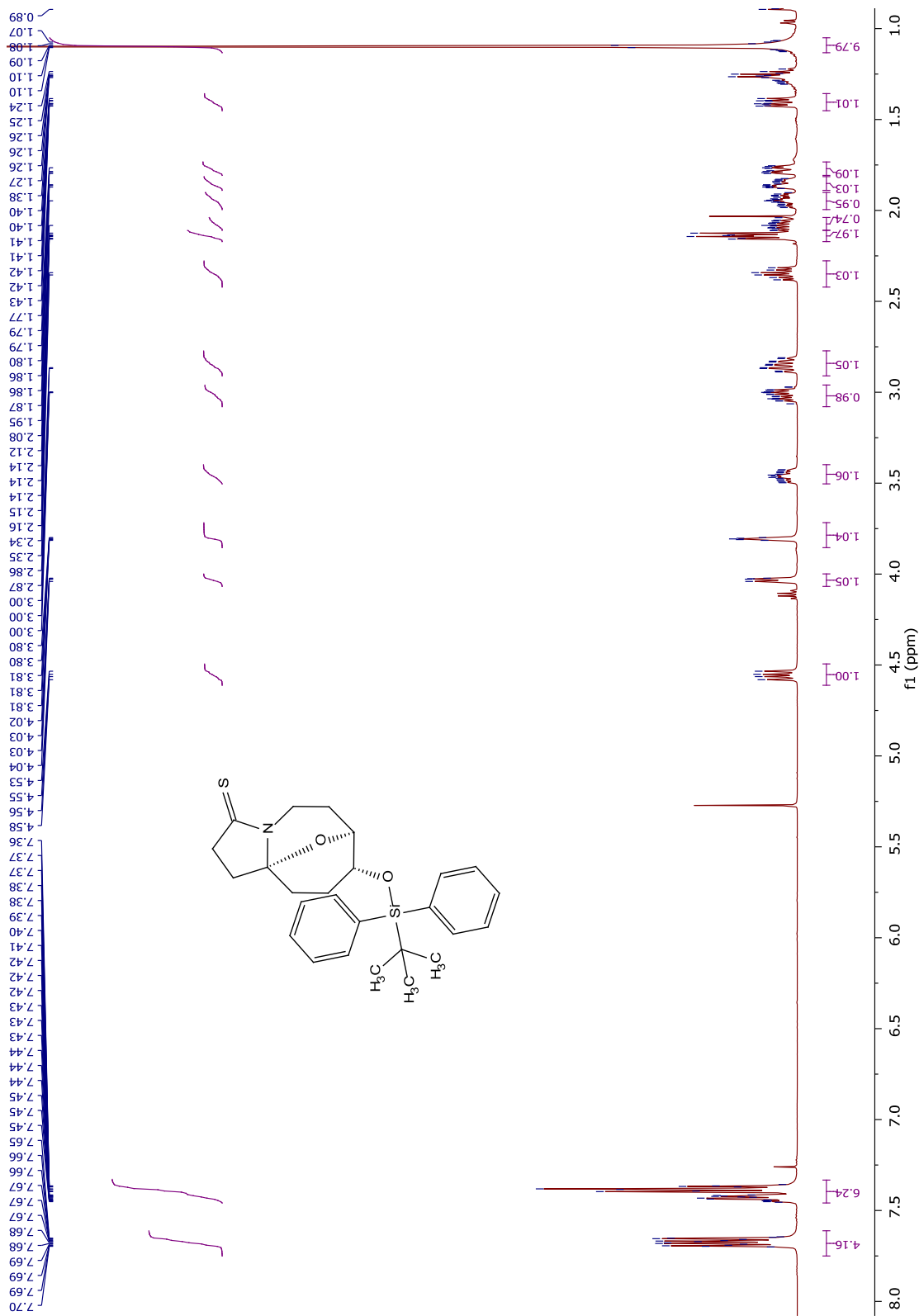
¹³C NMR spectrum of compound 118



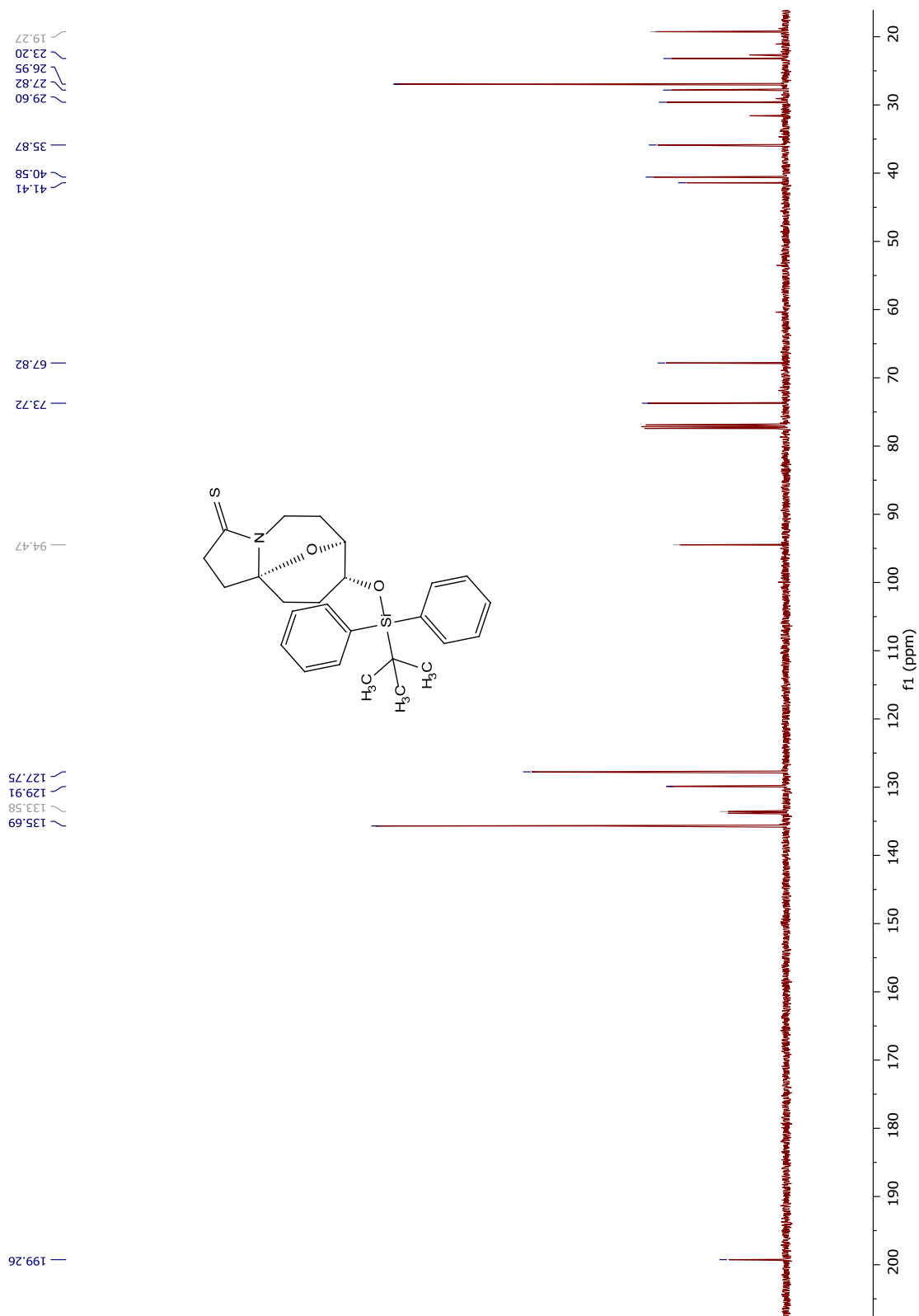
COSY NMR spectrum of compound 118



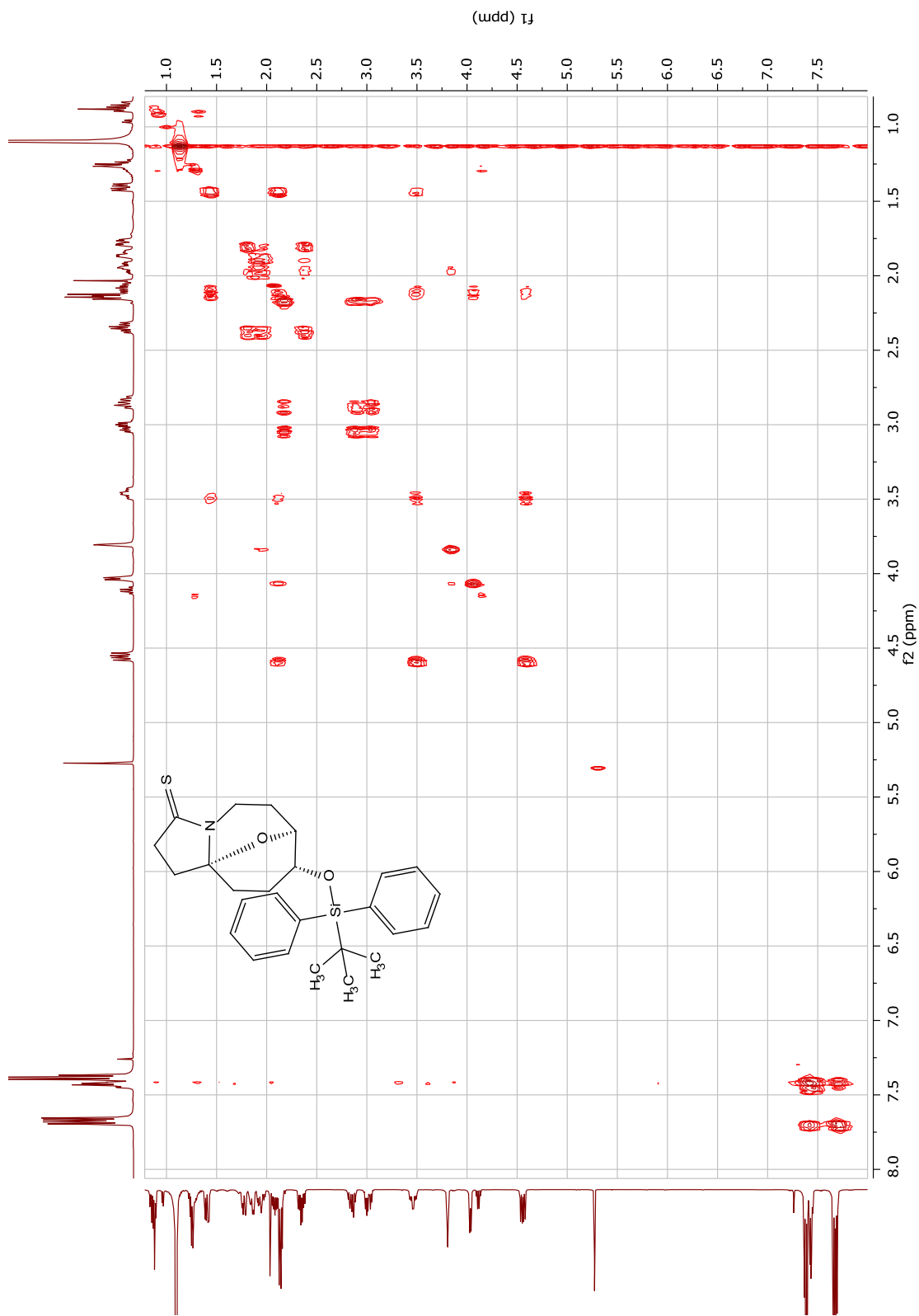
FTIR spectrum of compound **118**



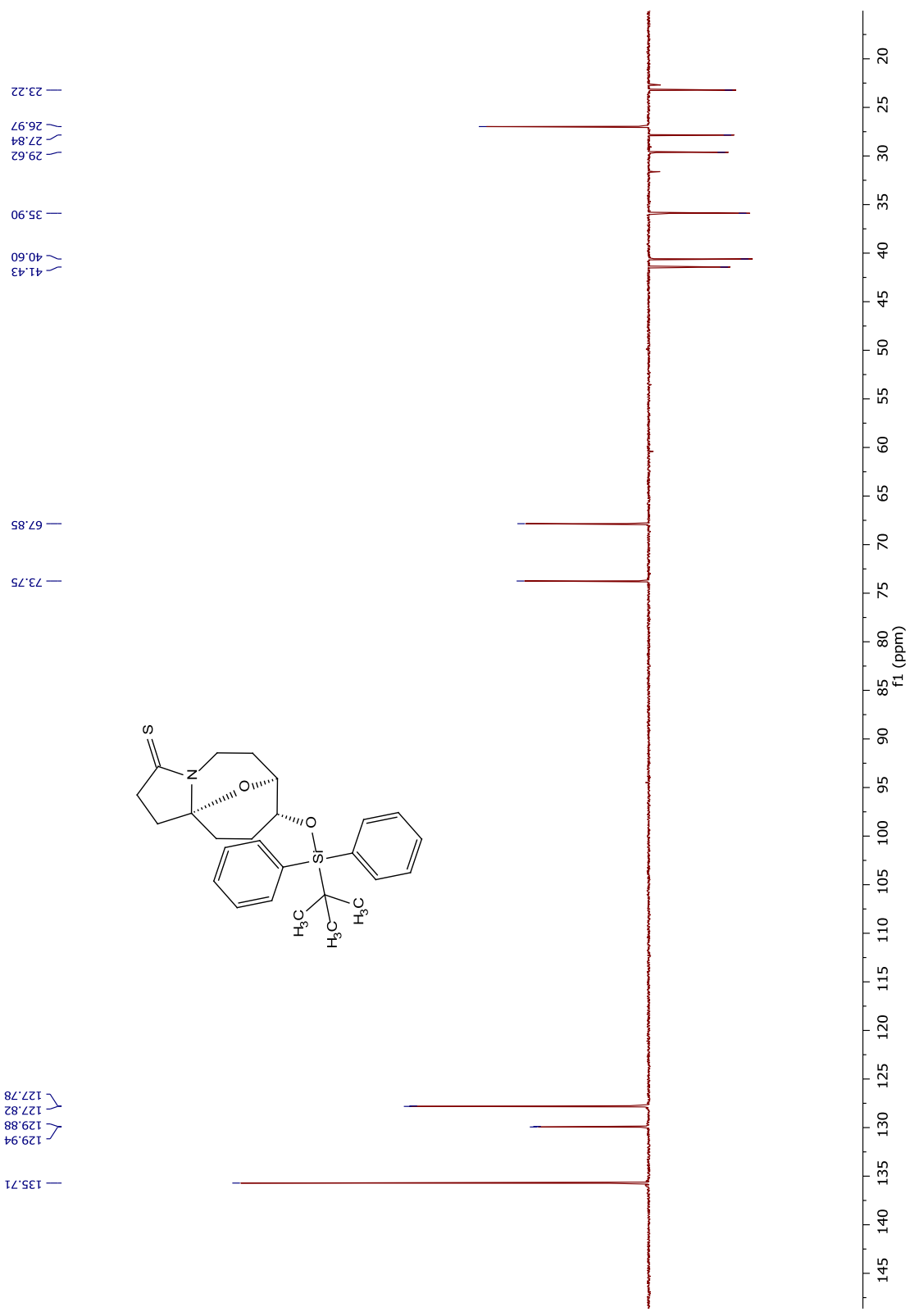
¹H NMR spectrum of compound 119



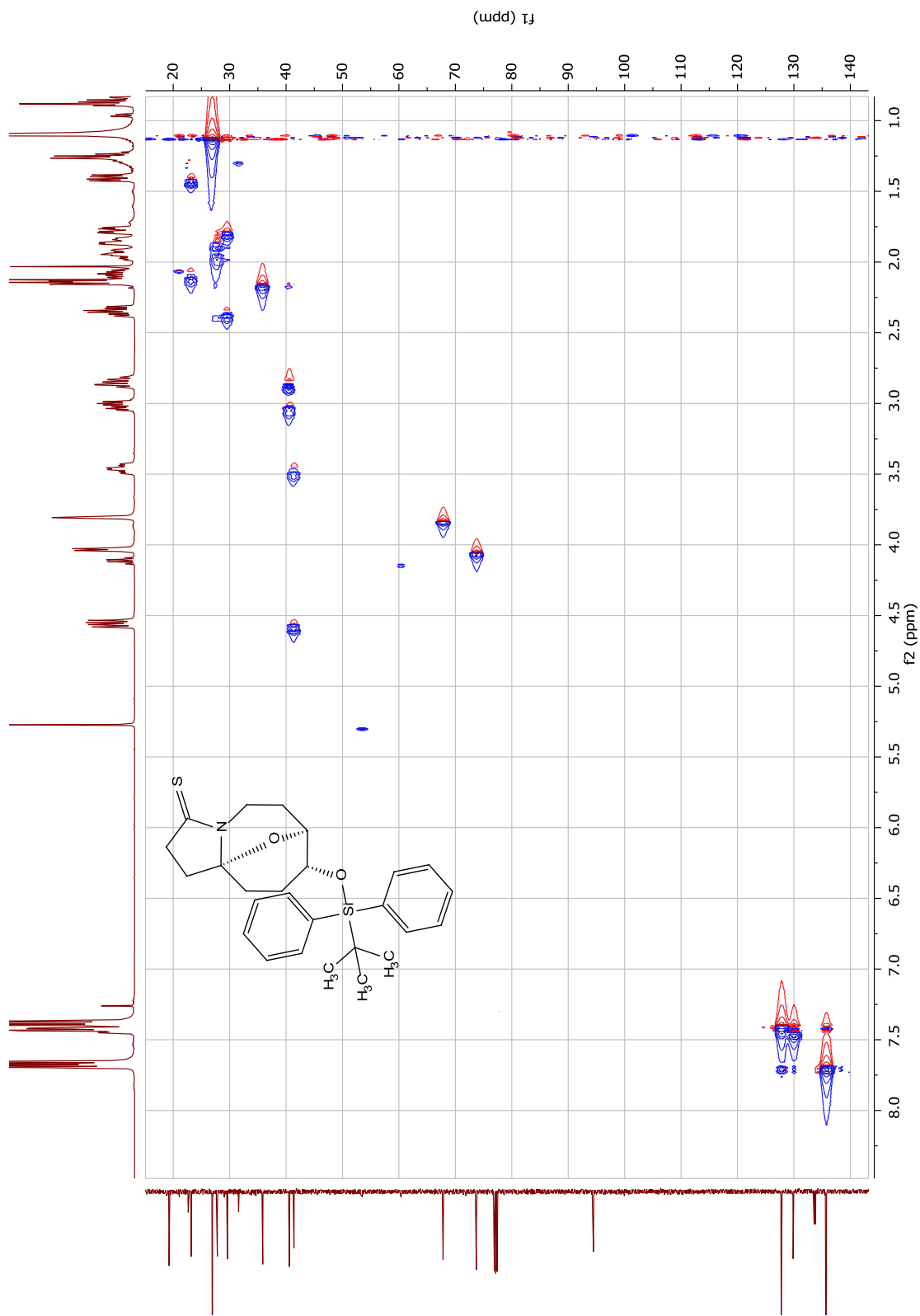
¹³C NMR spectrum of compound 119



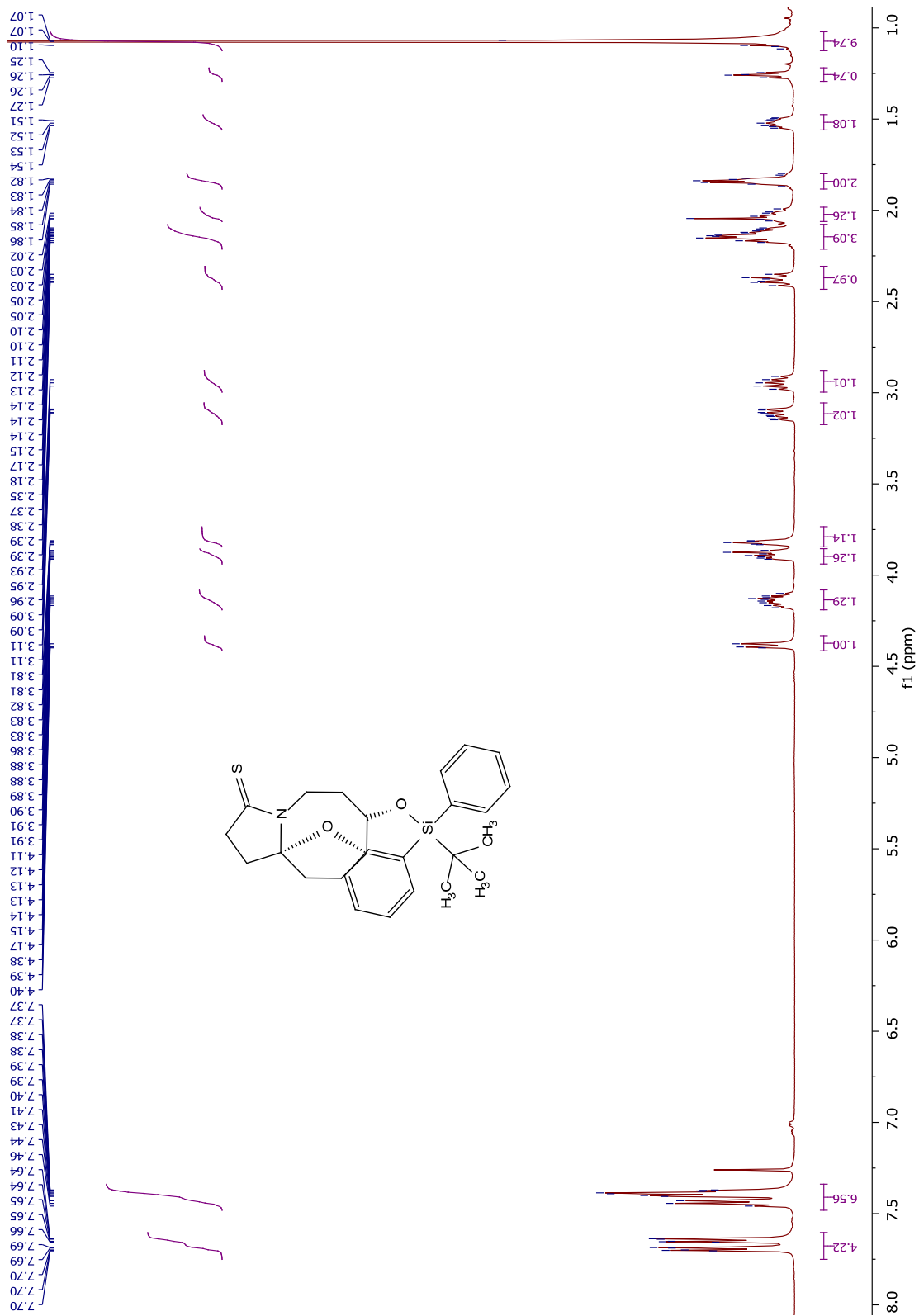
COSY NMR spectrum of compound 119



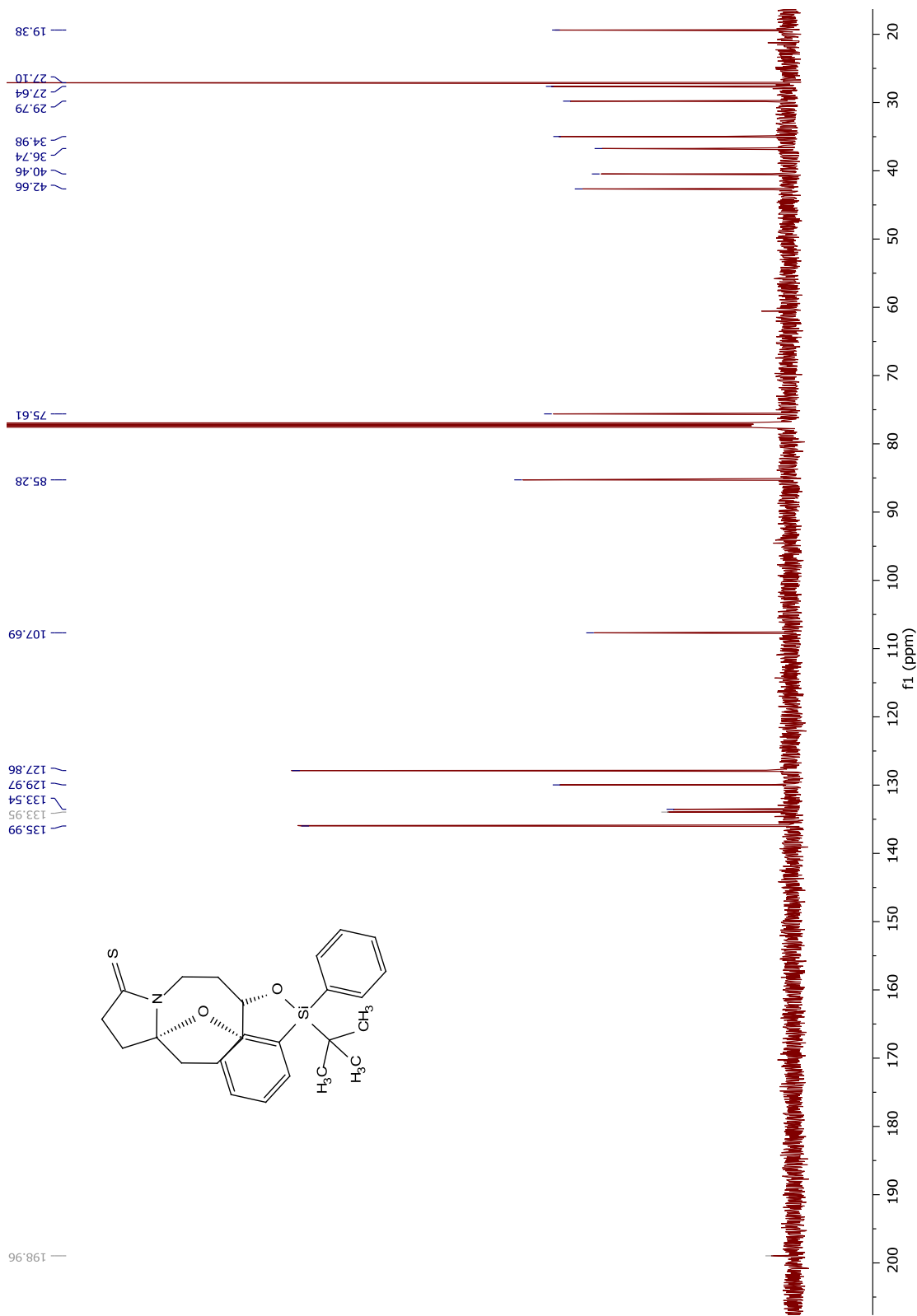
DEPT135 NMR spectrum of compound **119**



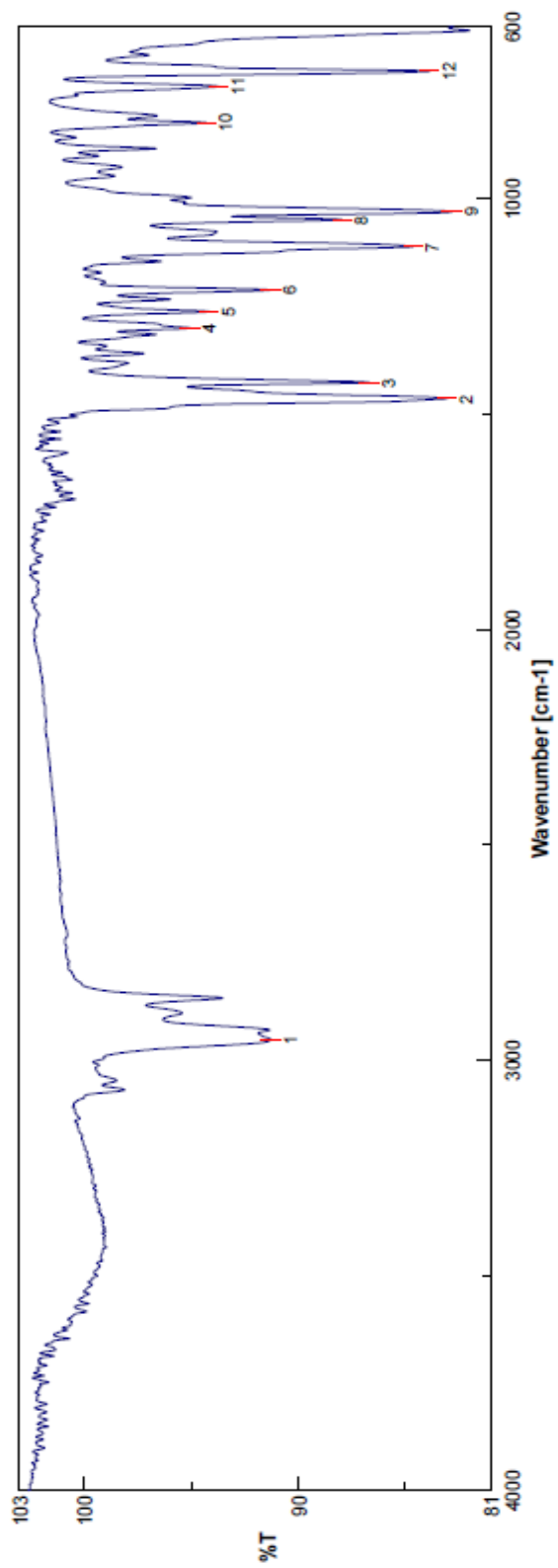
HSQC NMR spectrum of compound 119



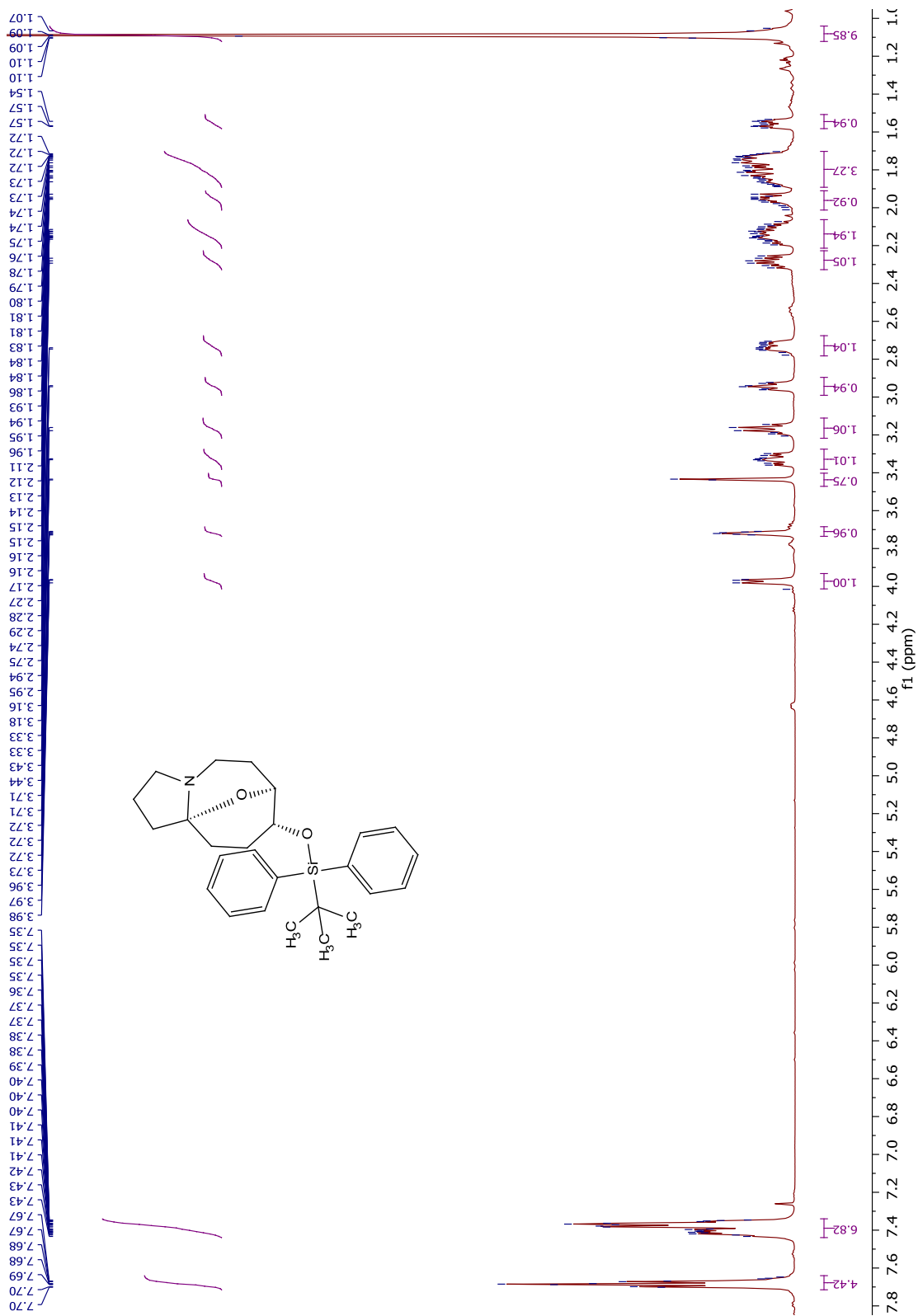
¹H NMR spectrum of compound 120



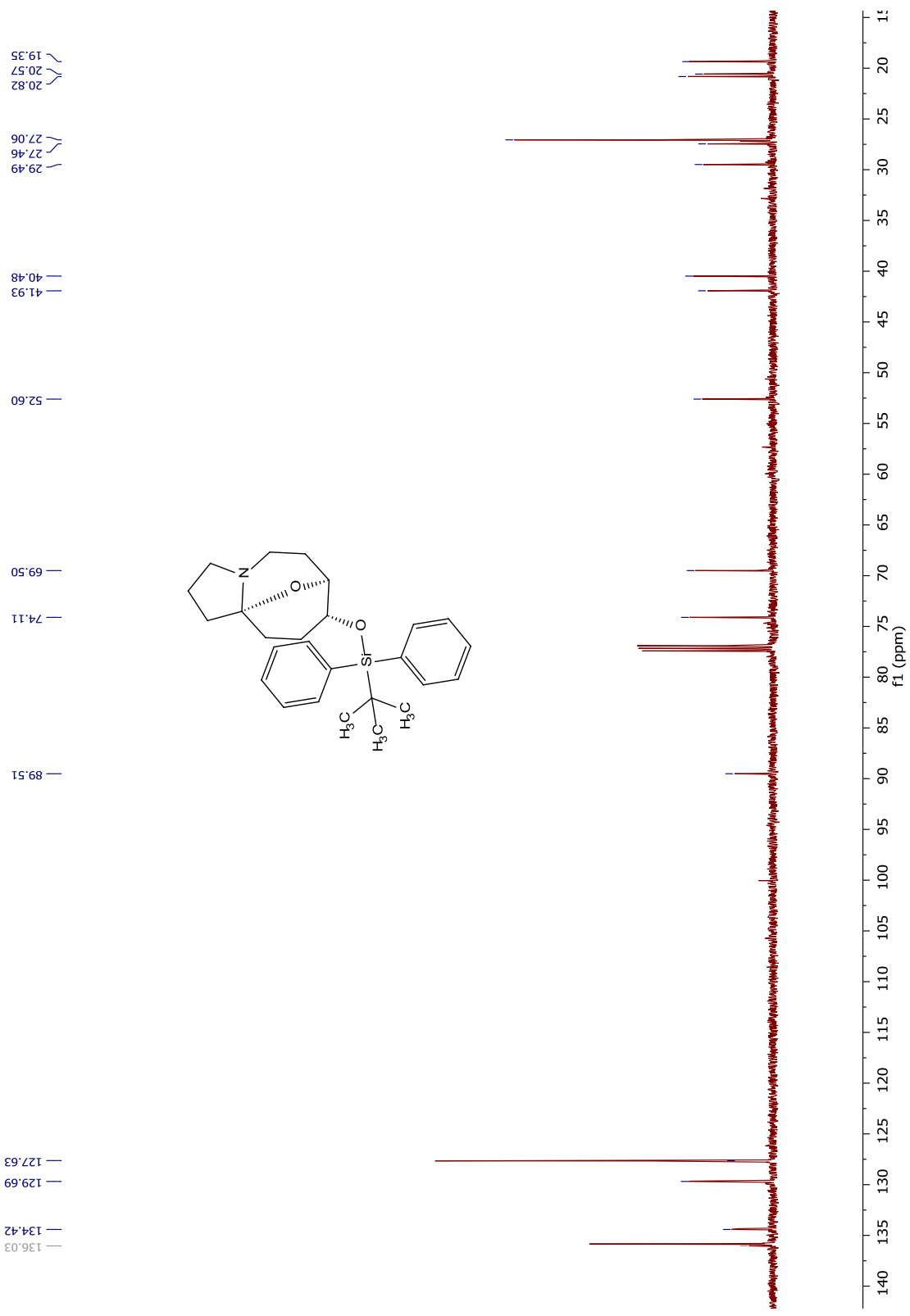
¹³C NMR spectrum of compound 120



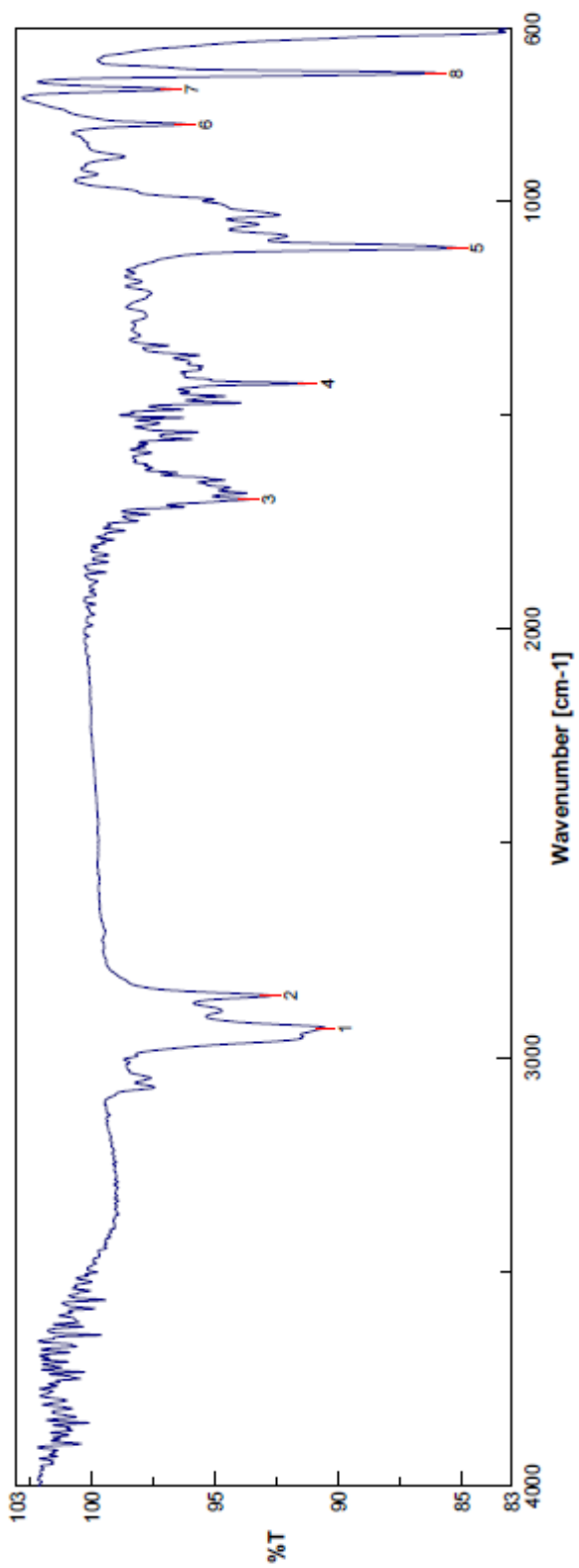
FTIR spectrum of compound **120**



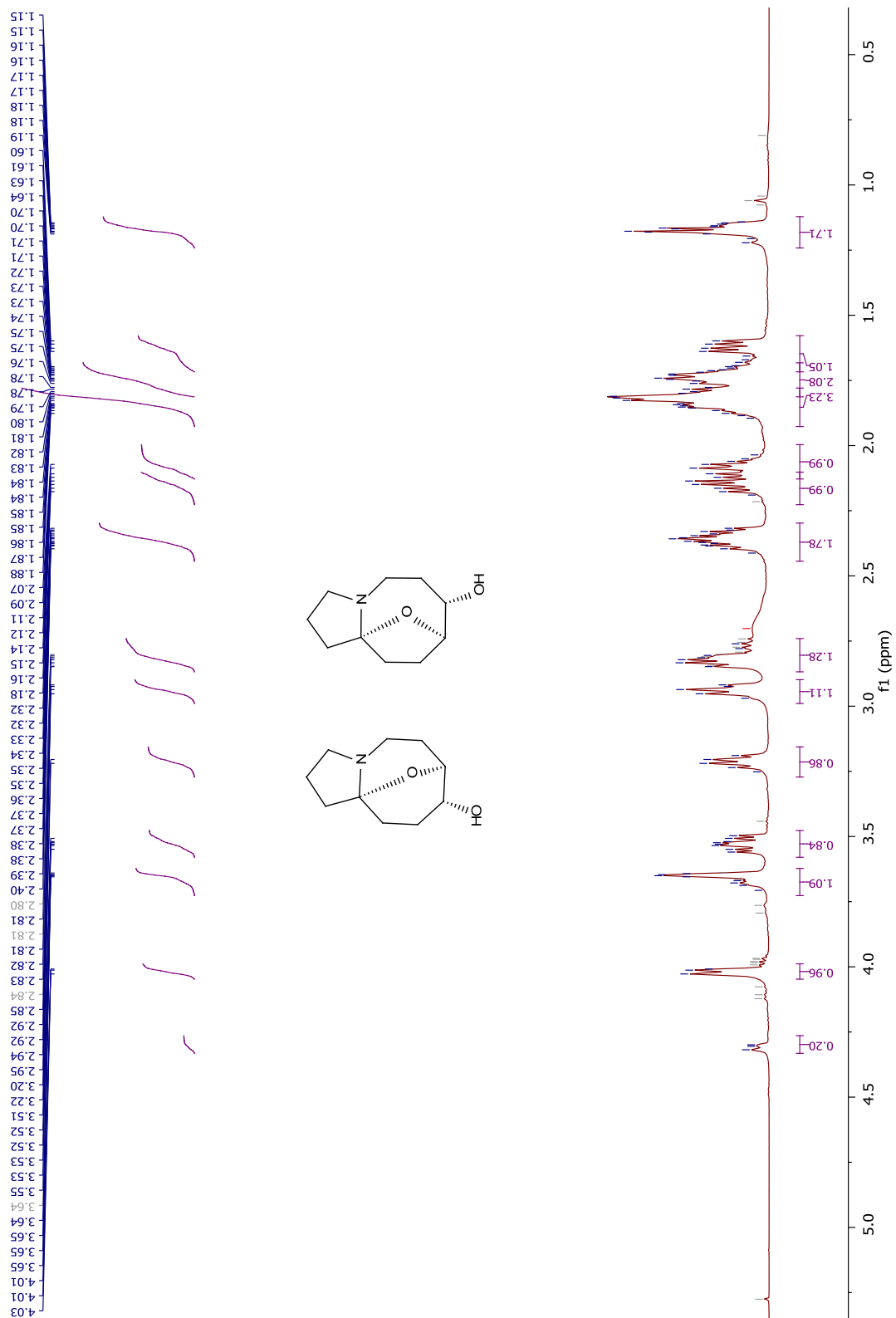
¹H NMR spectrum of compound 121



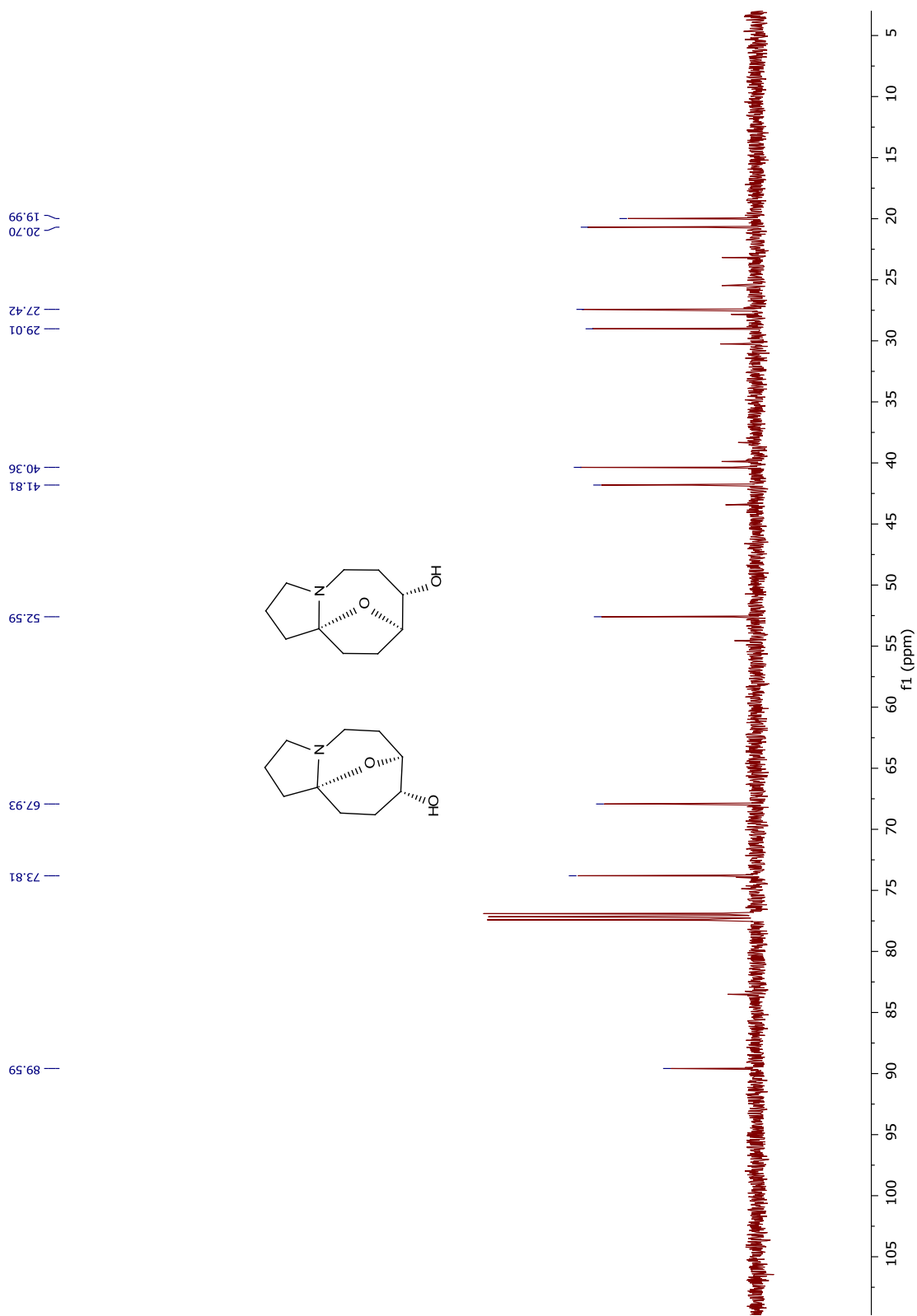
^{13}C NMR spectrum of compound **121**



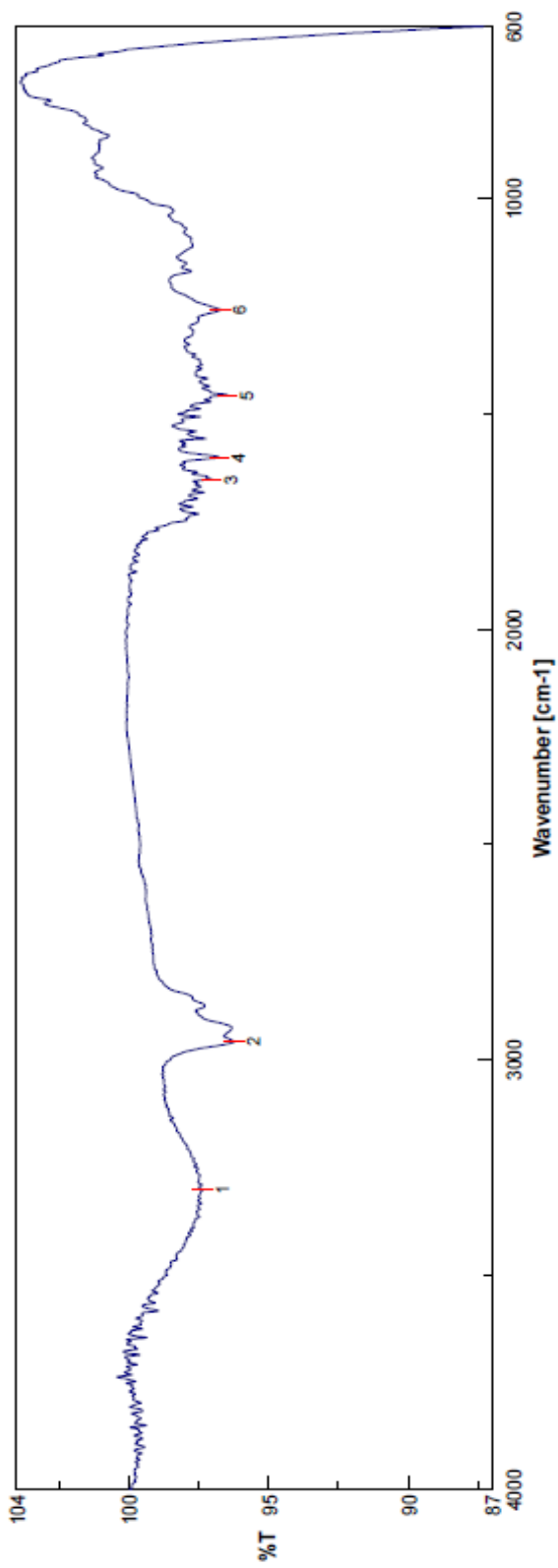
FTIR NMR spectrum of compound 121



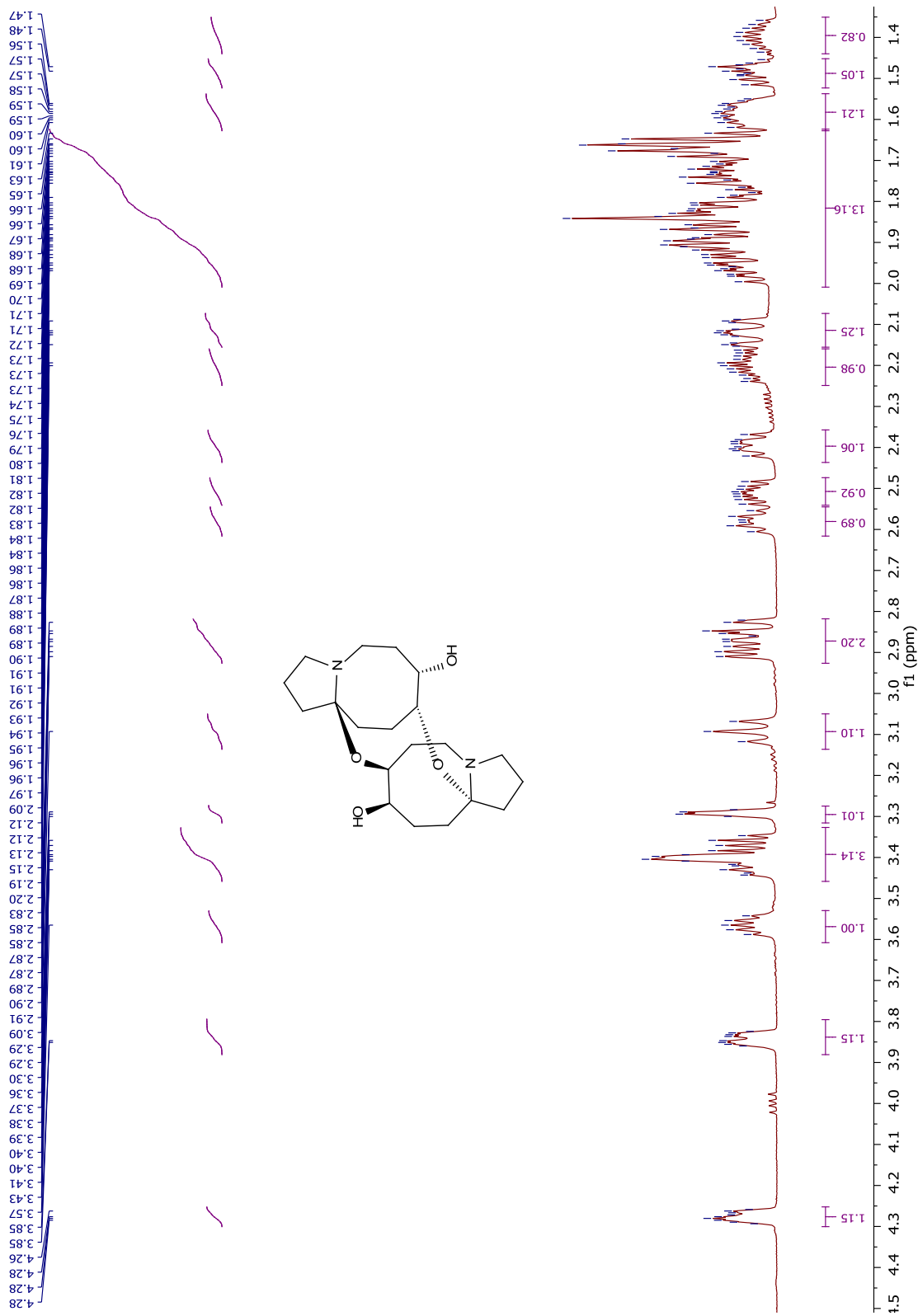
¹H NMR spectrum of compound **123** and **124**



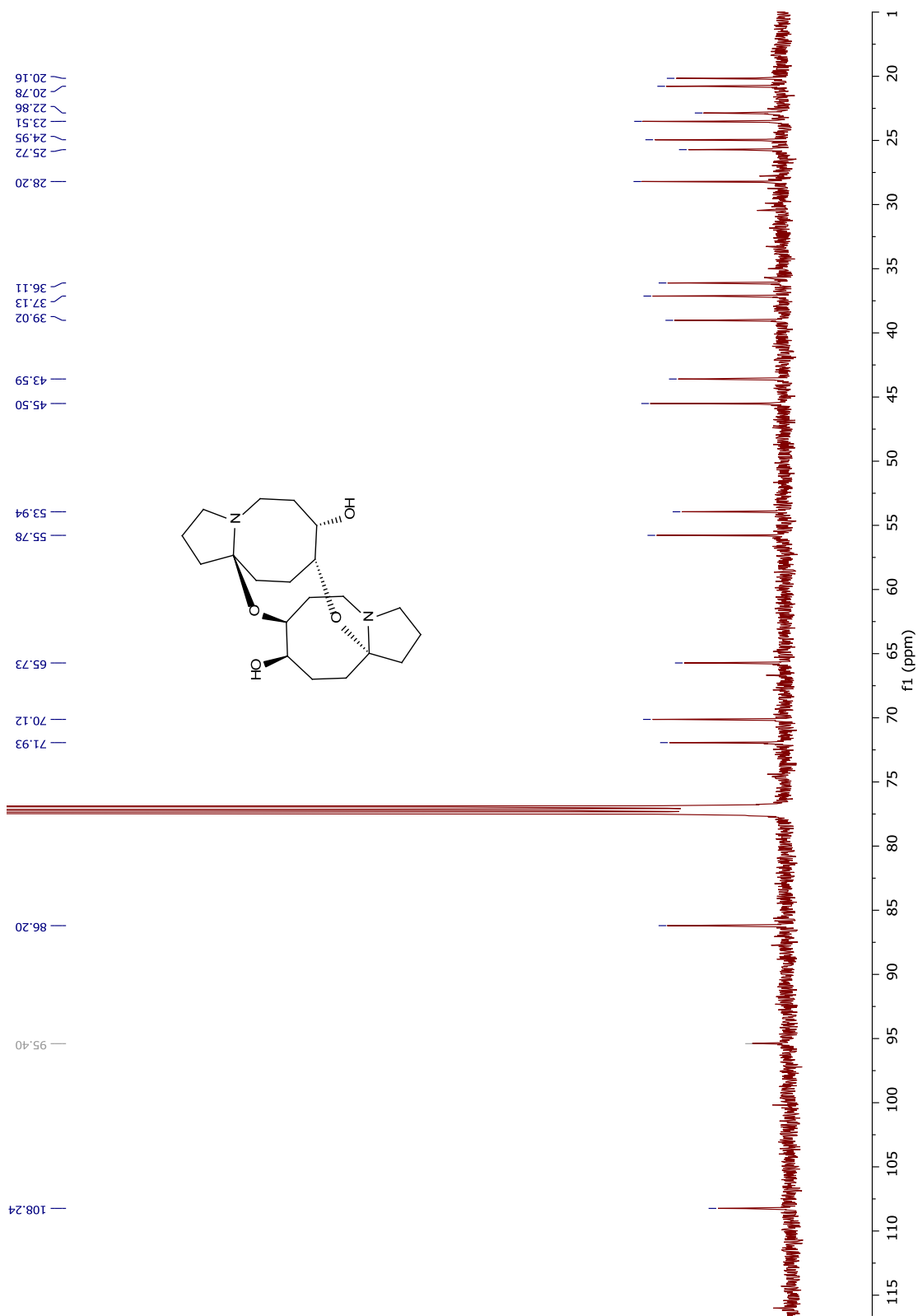
¹³C NMR spectrum of compound **123** and **124**



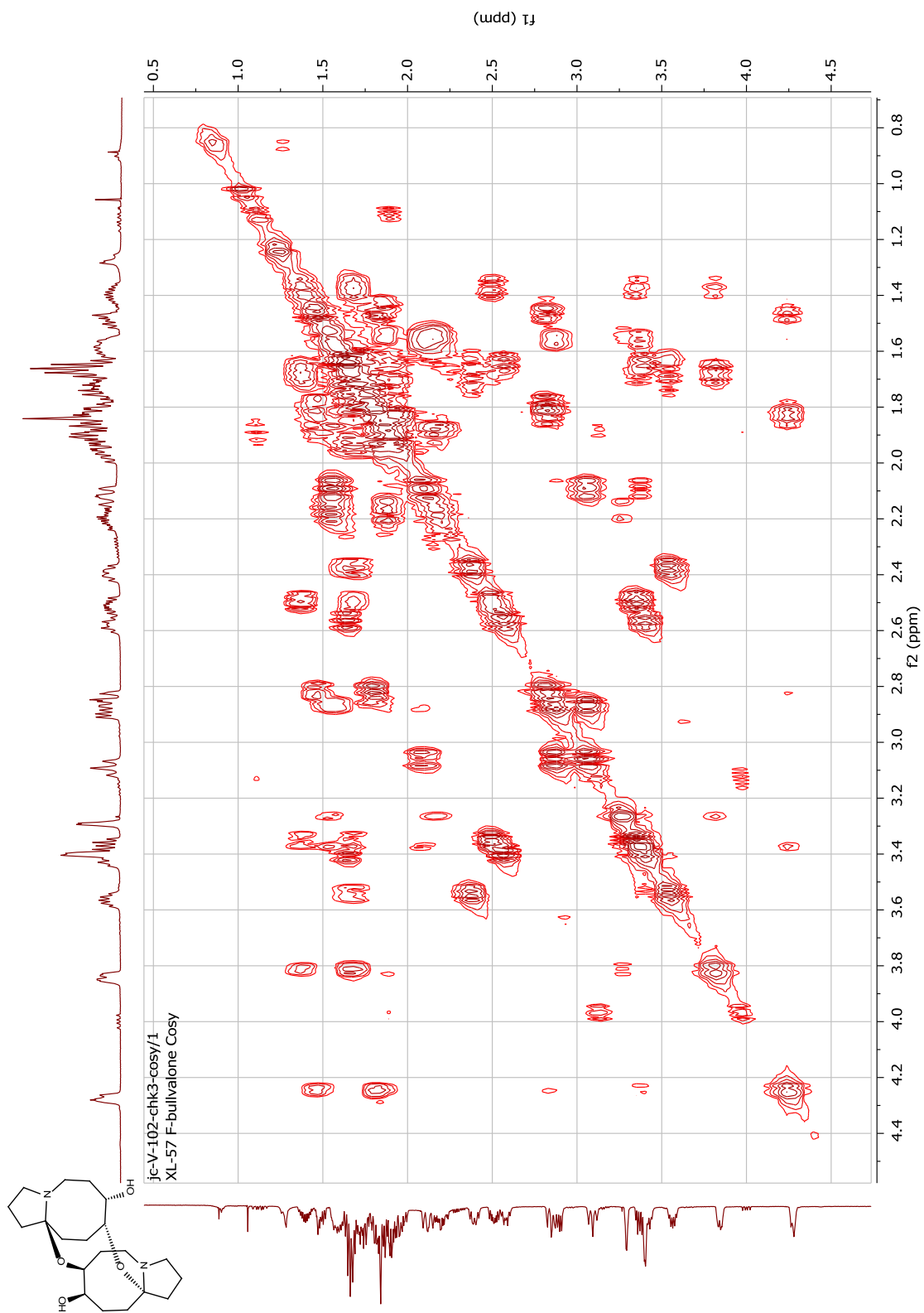
FTIR NMR spectrum of compound **123** and **124**



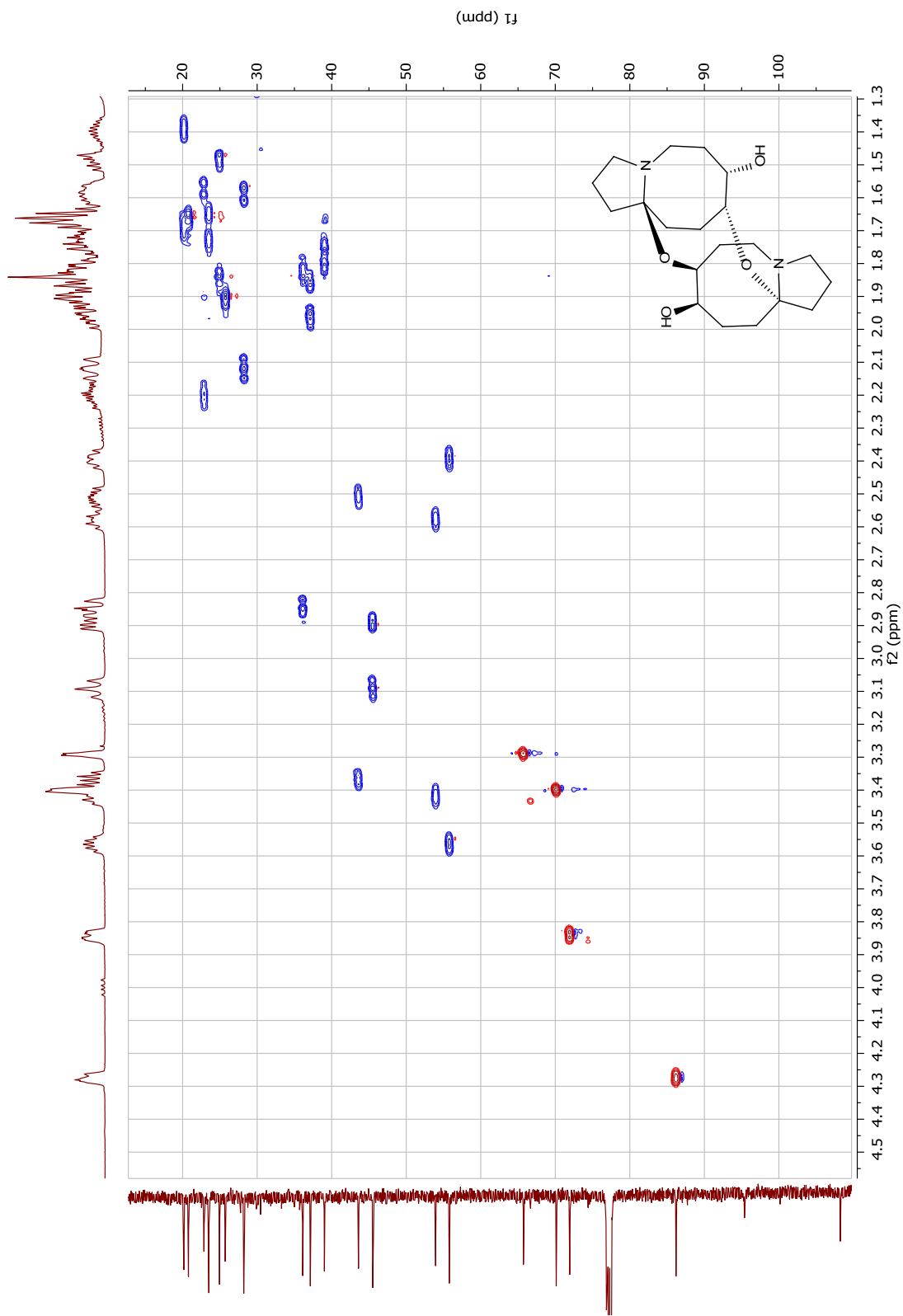
¹H NMR spectrum of compound 96



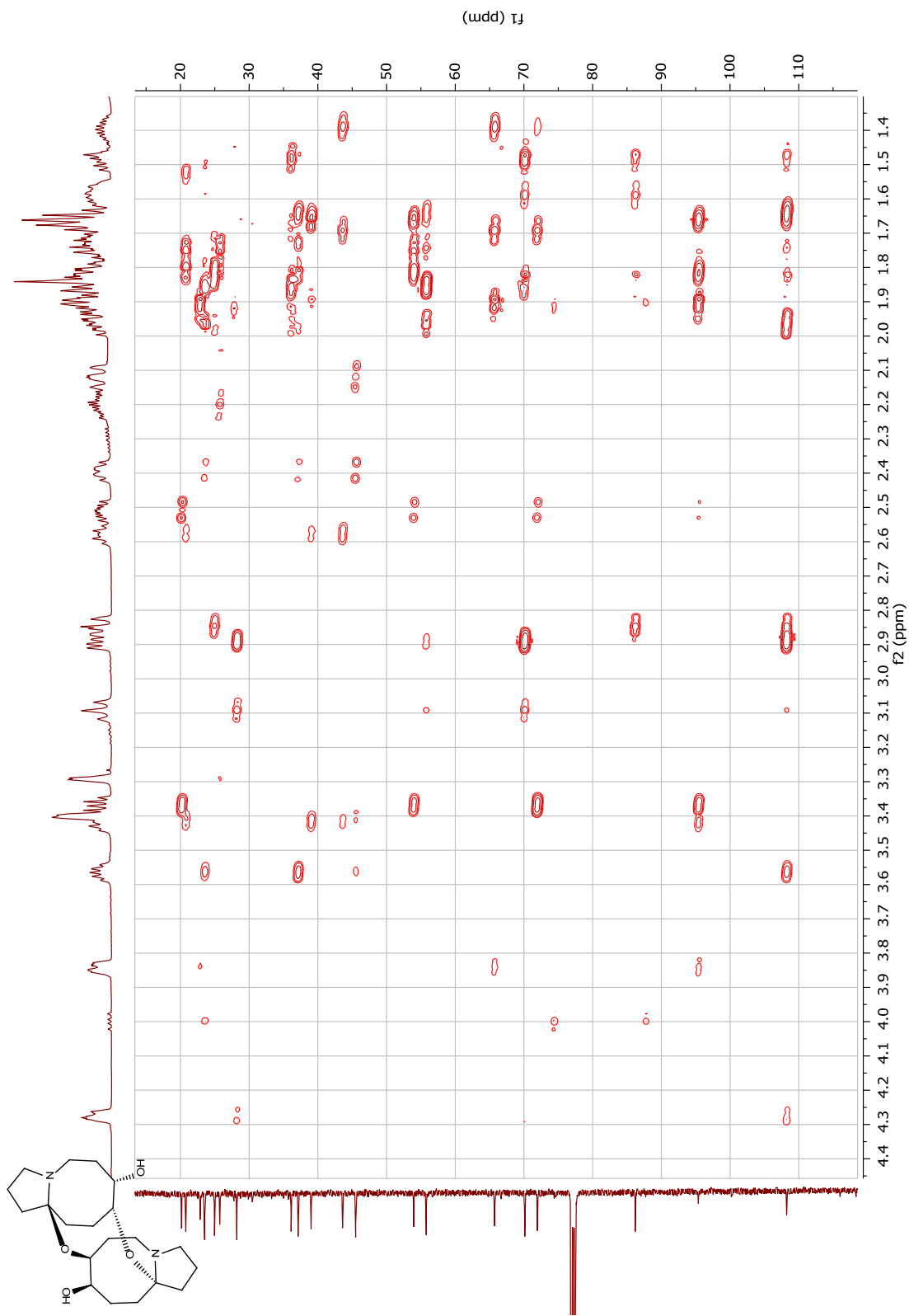
¹³C NMR spectrum of compound **96**



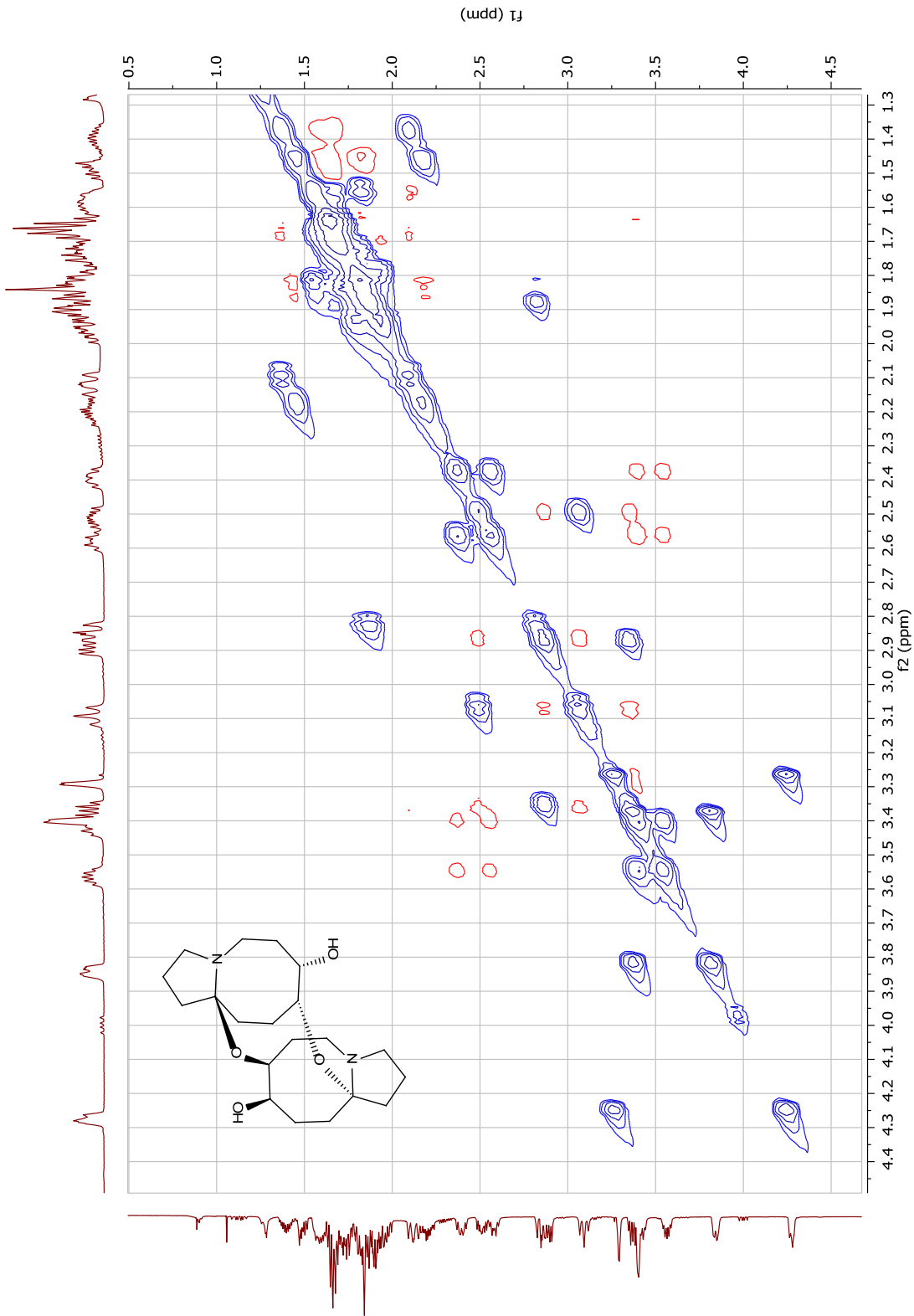
COSY NMR spectrum of compound 96



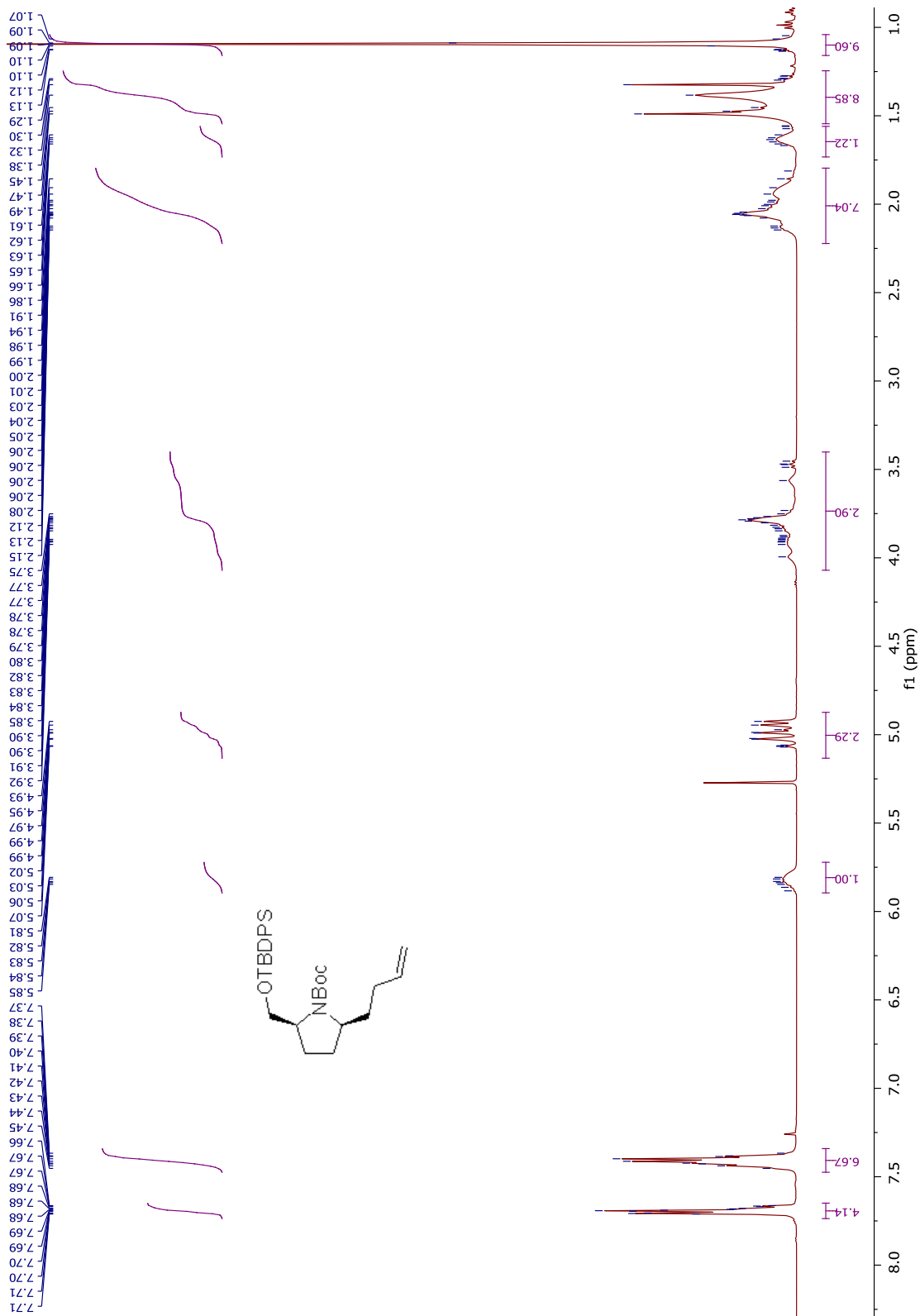
HSQC spectrum of compound **96**



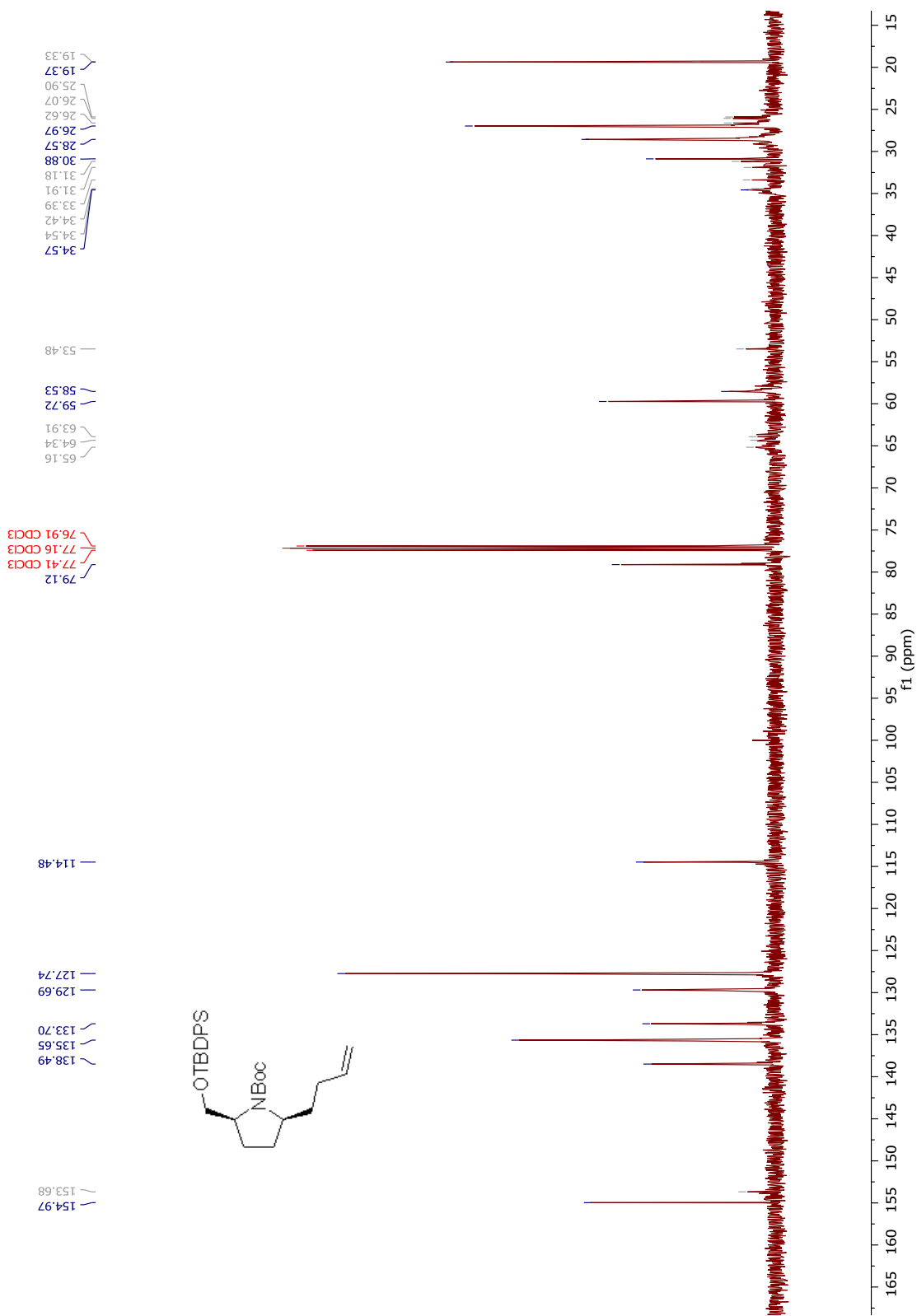
HMBC NMR spectrum of compound 96



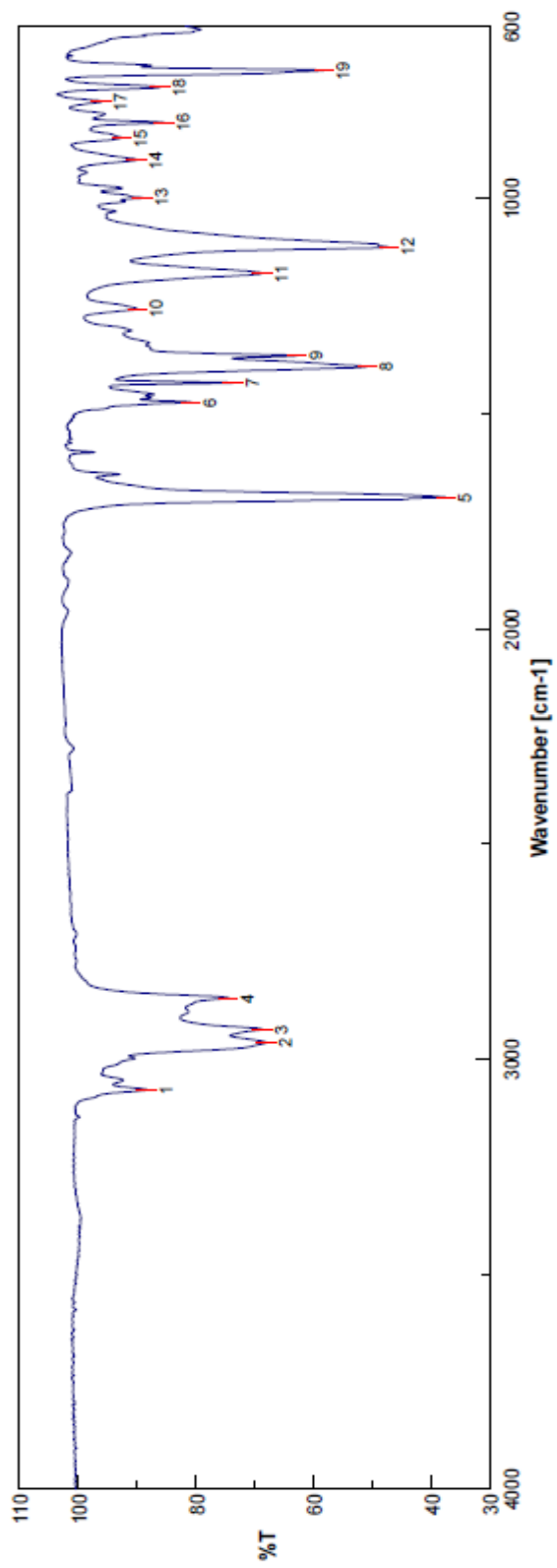
NOESY NMR spectrum of compound **96**



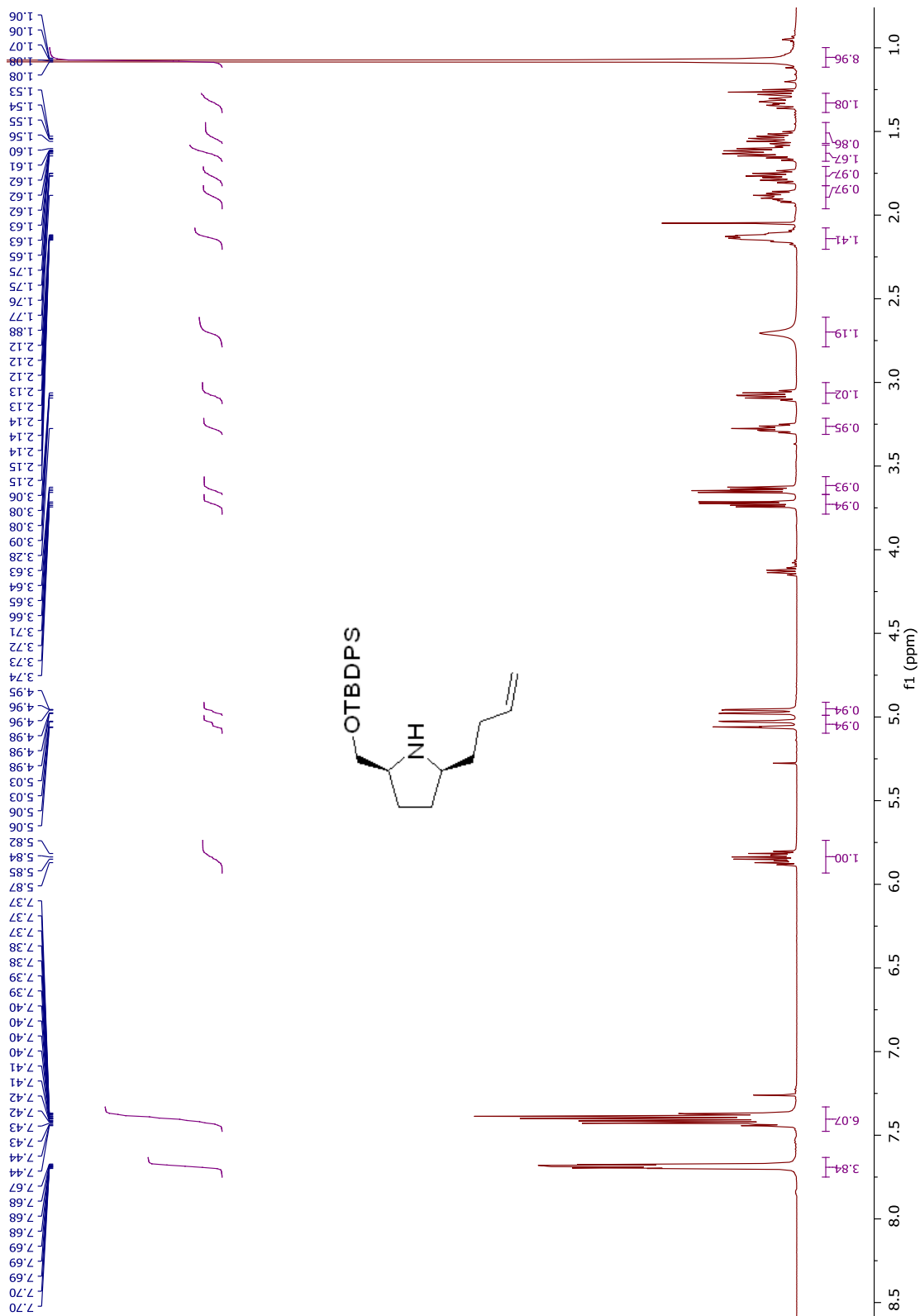
¹H NMR spectrum of compound 129



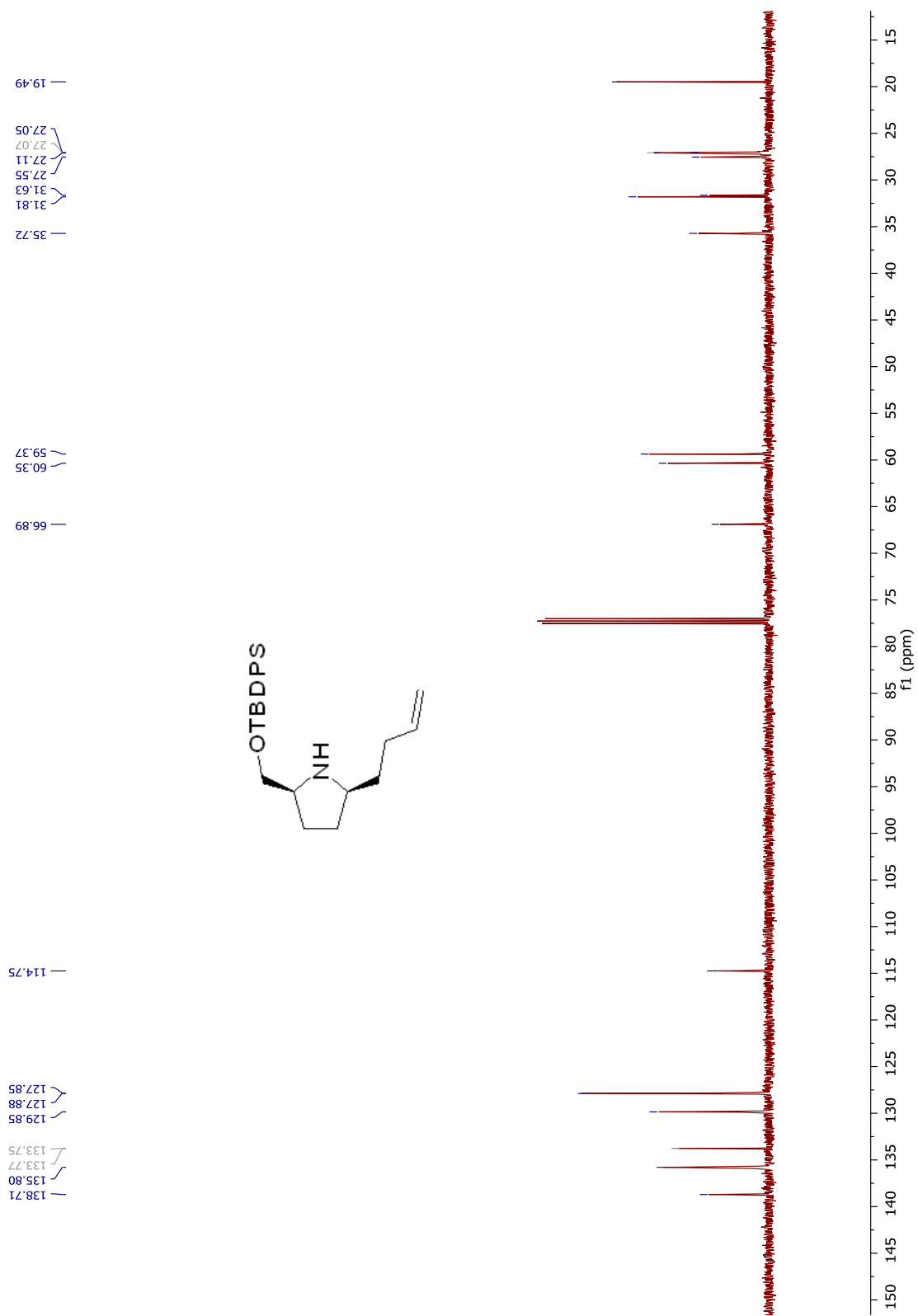
¹³C NMR spectrum of compound 129



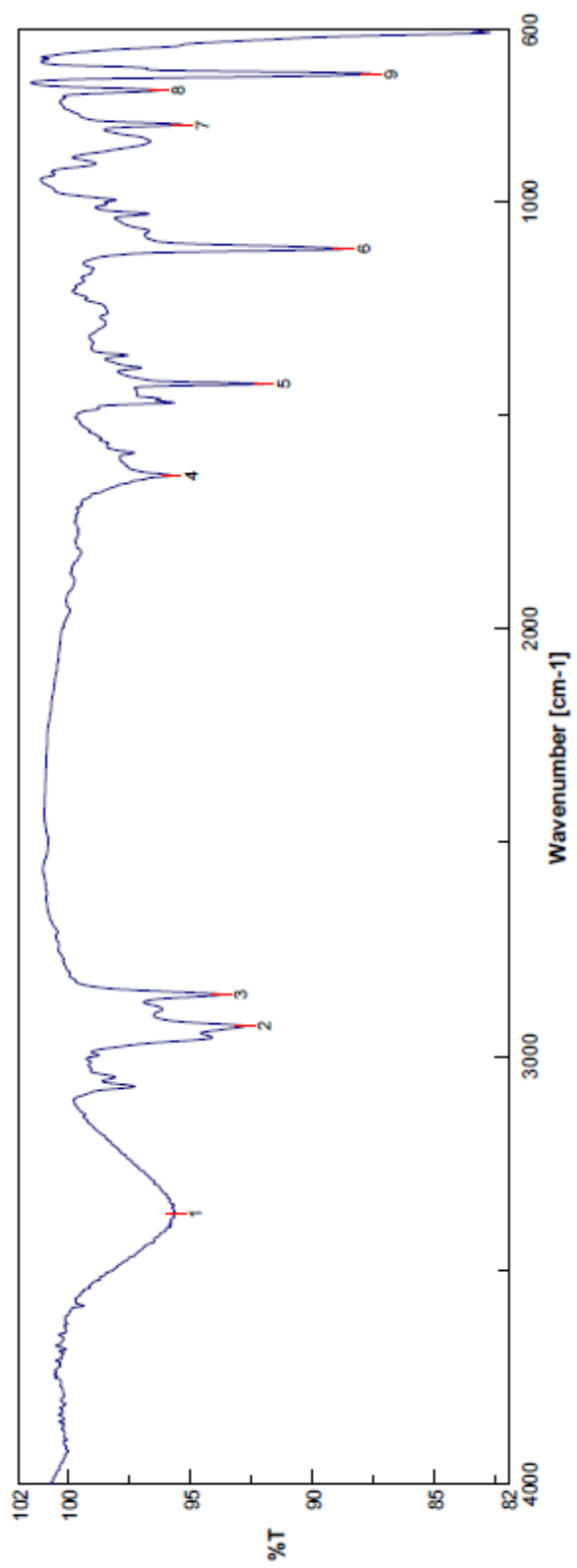
FTIR spectrum of compound **129**



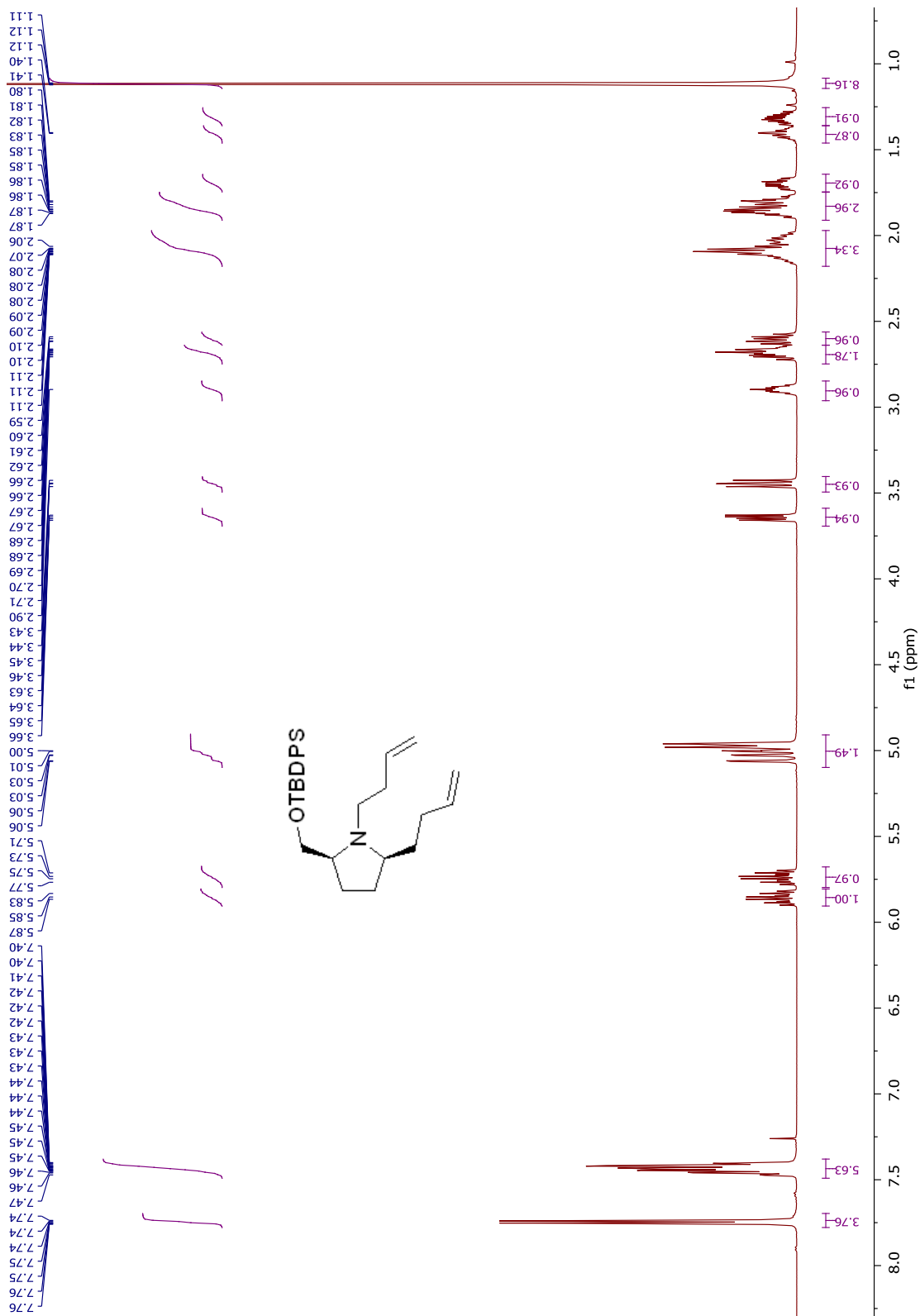
¹H NMR spectrum of compound **130**



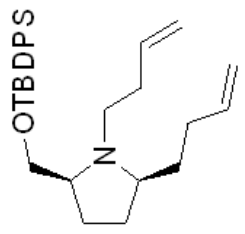
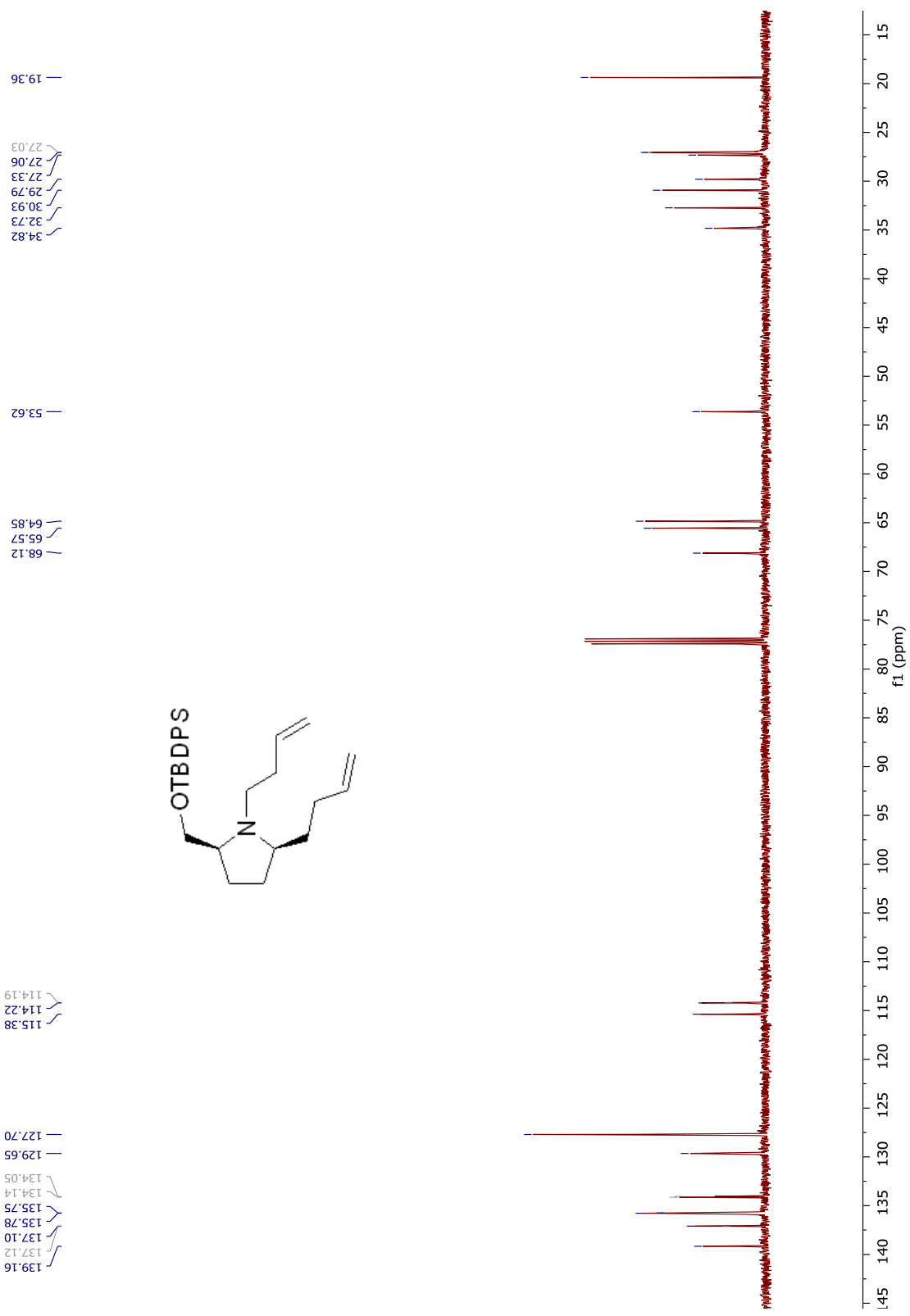
¹³C NMR spectrum of compound 130



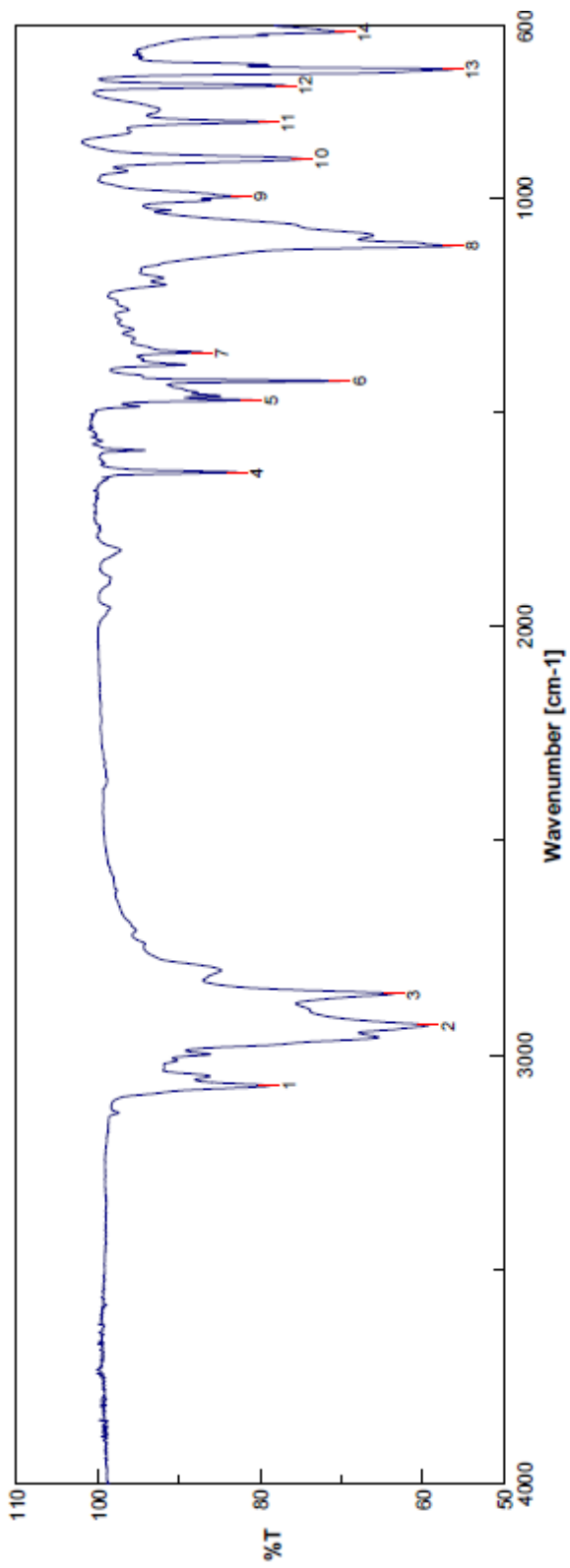
FTIR spectrum of compound **130**



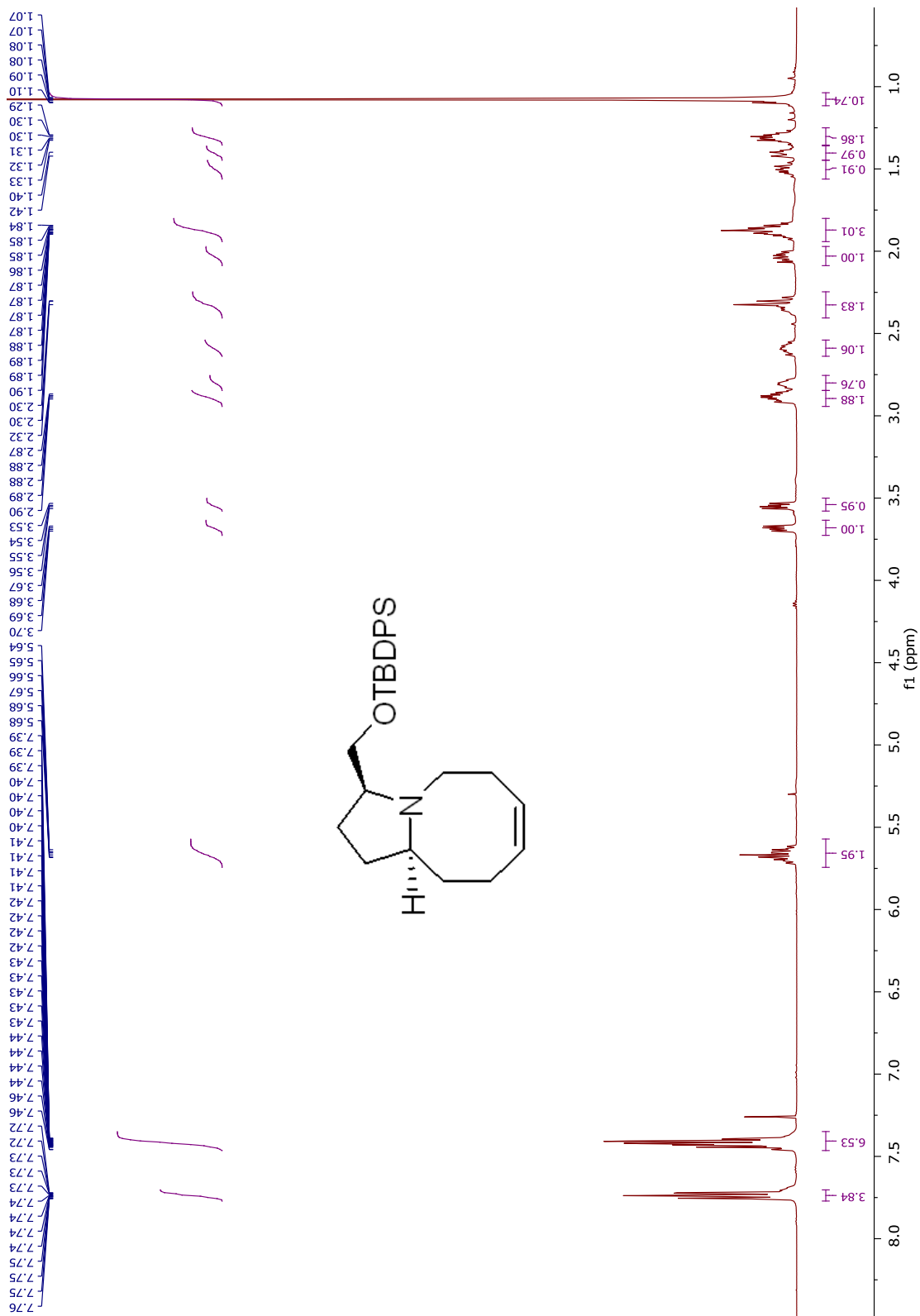
¹H NMR spectrum of compound 131



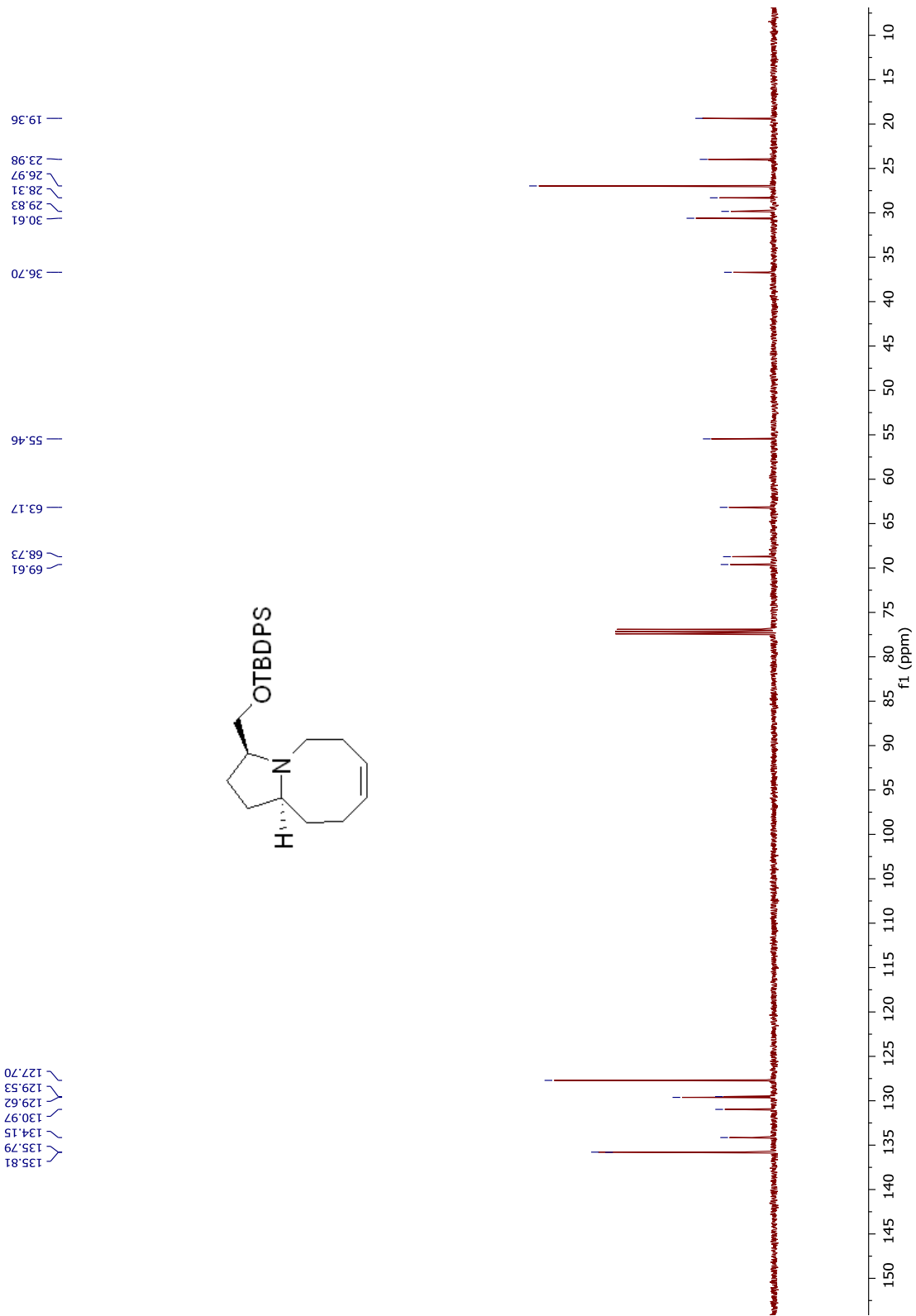
¹³C NMR spectrum of compound **131**



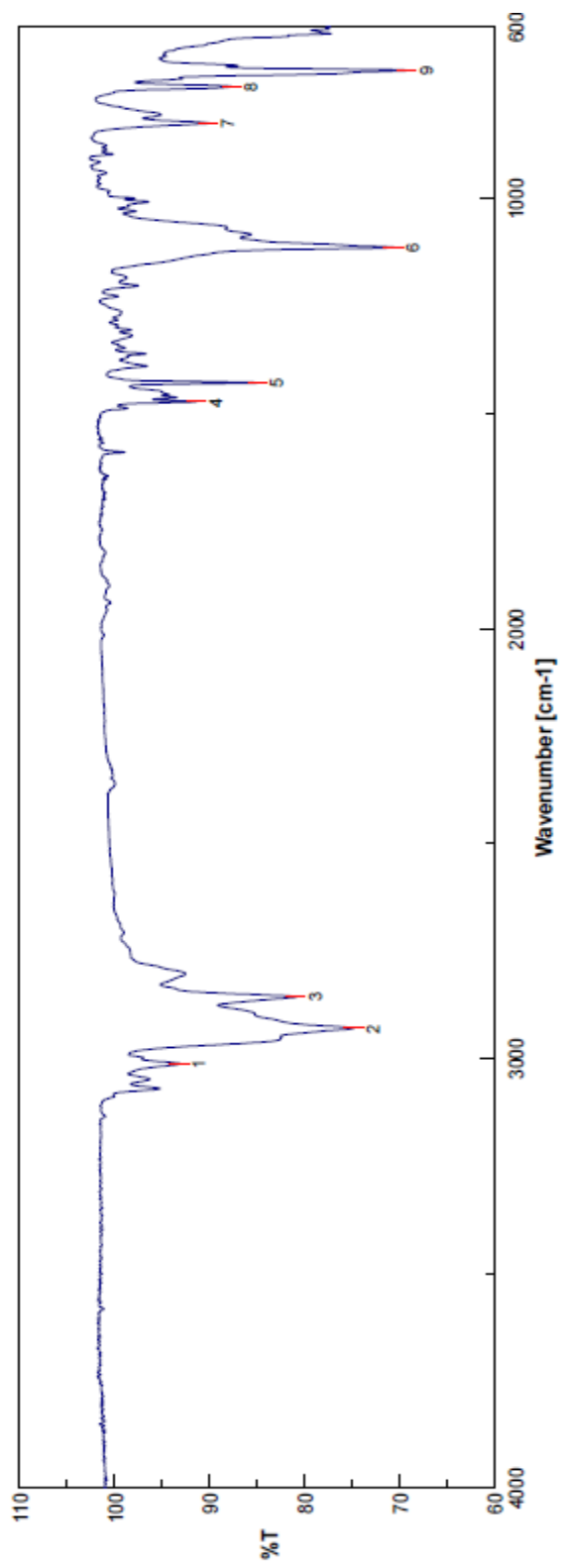
FTIR spectrum of compound 131



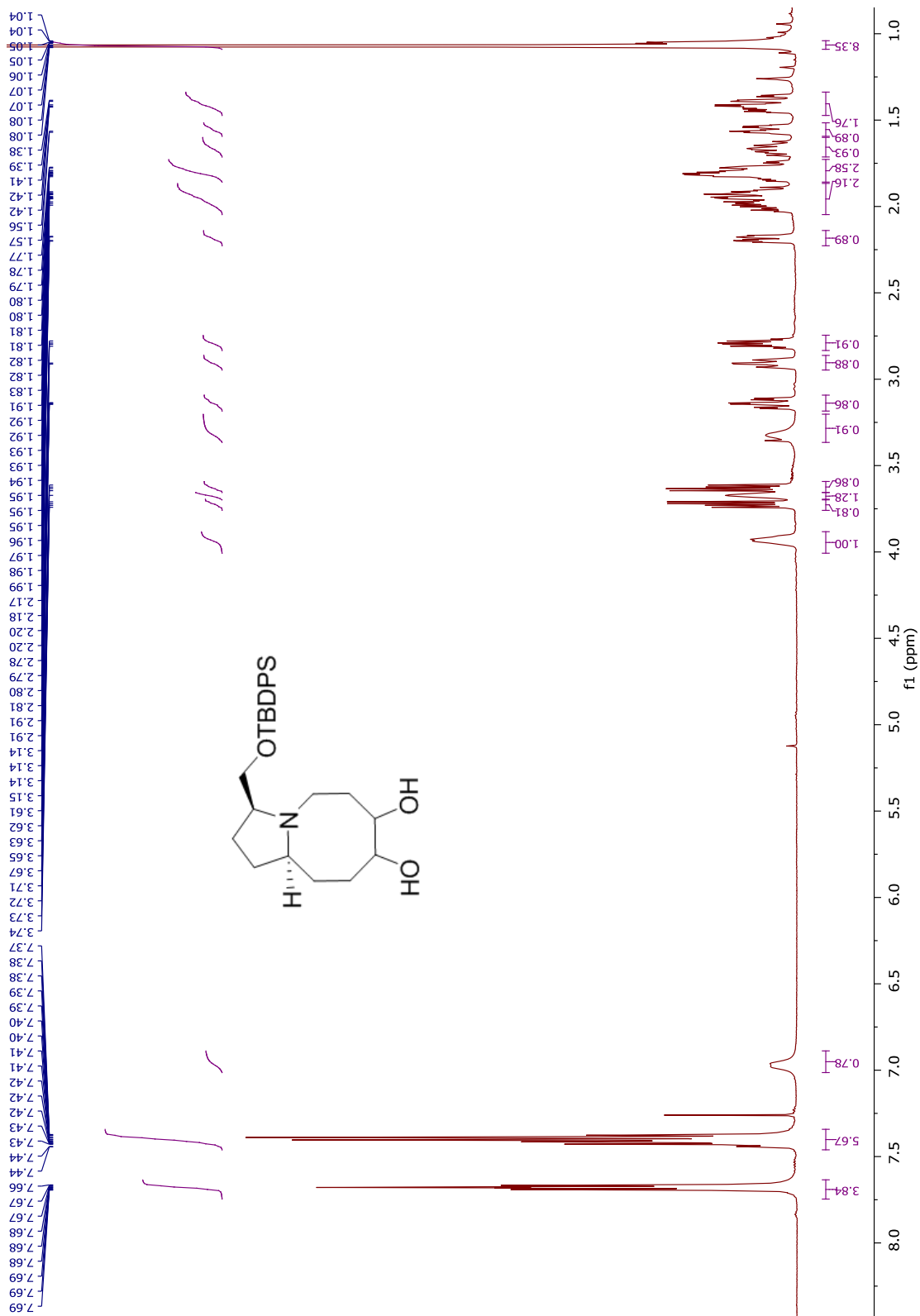
¹H NMR spectrum of compound 133



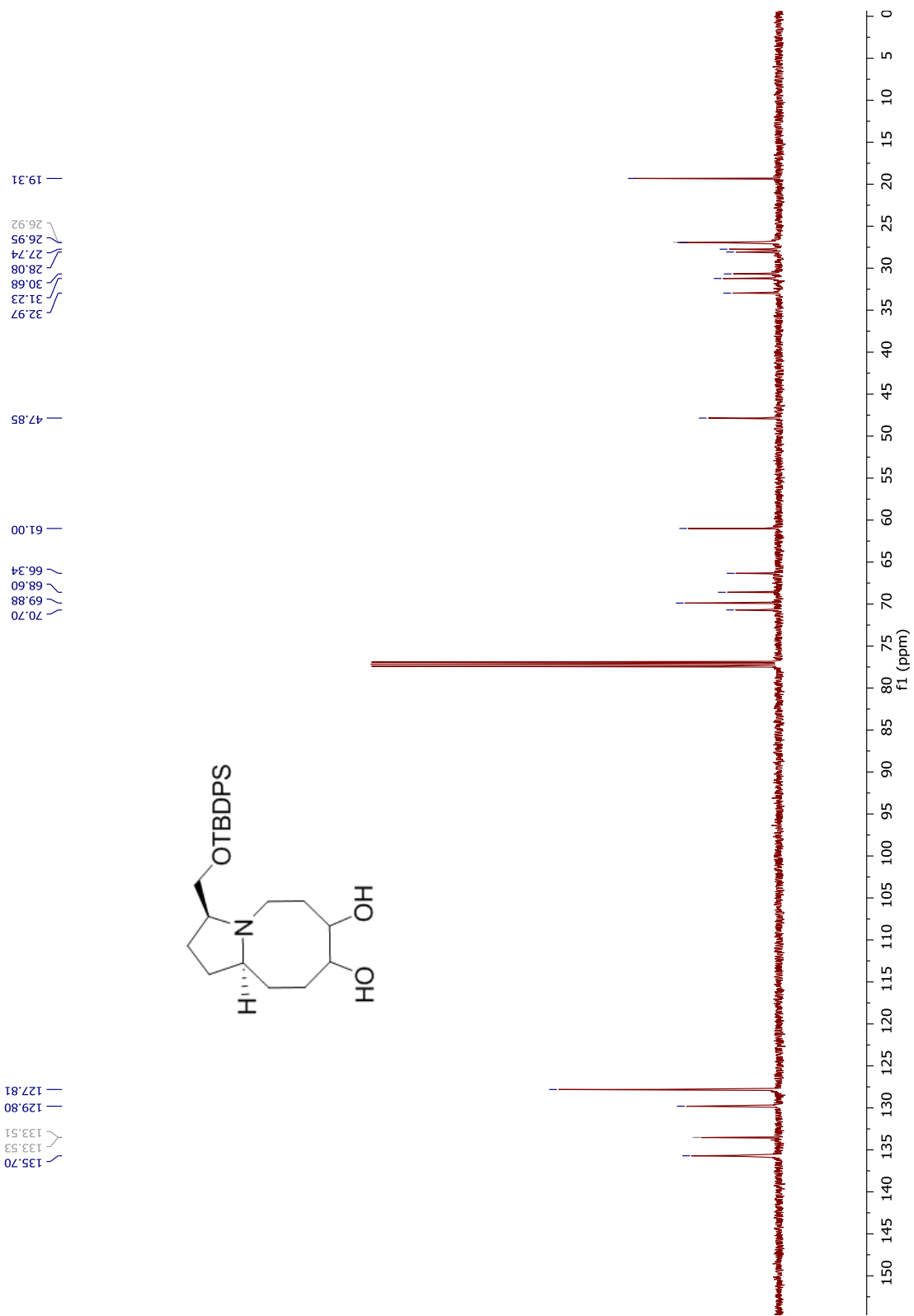
¹³C NMR spectrum of compound 133



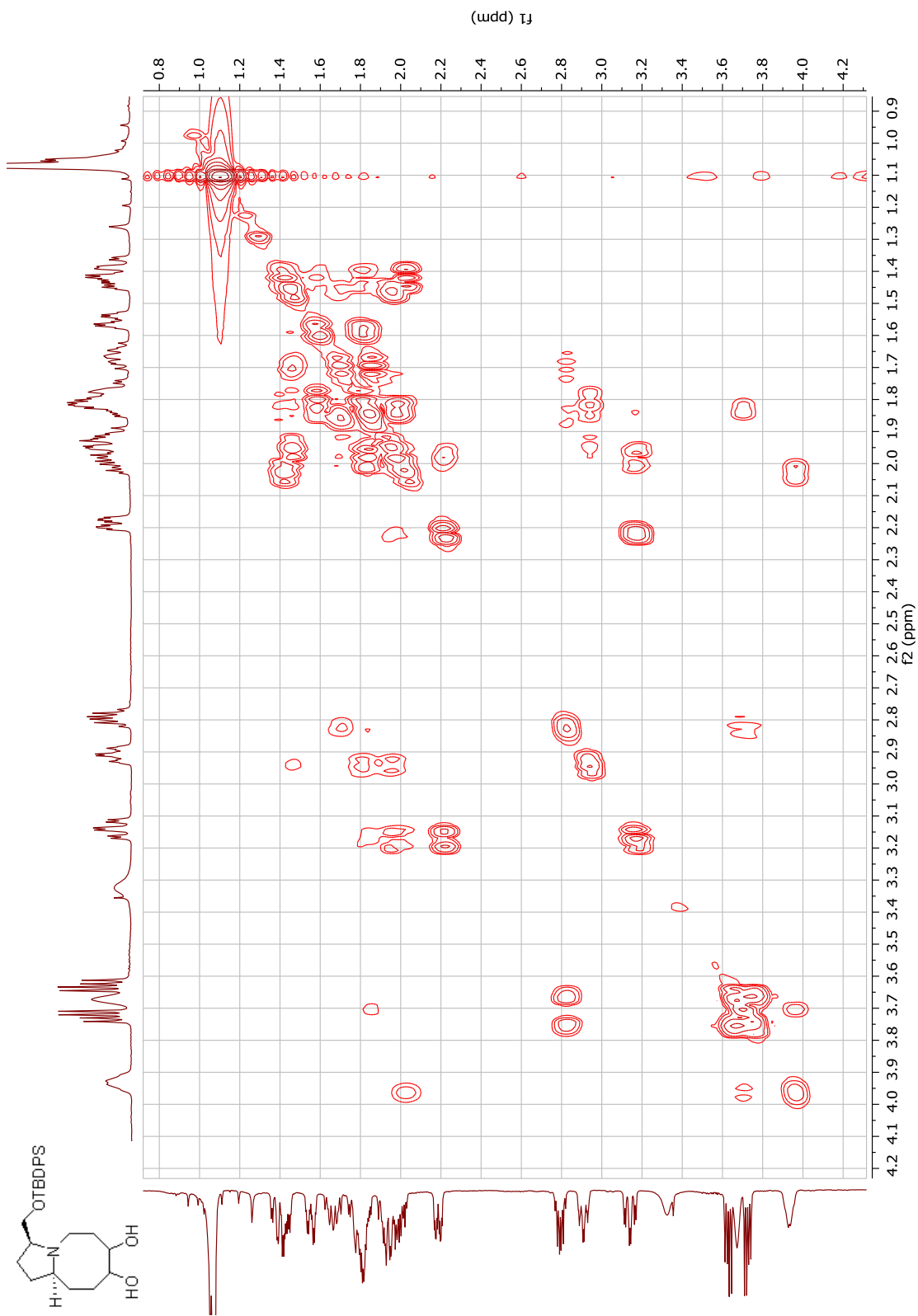
FTIR spectrum of compound 133



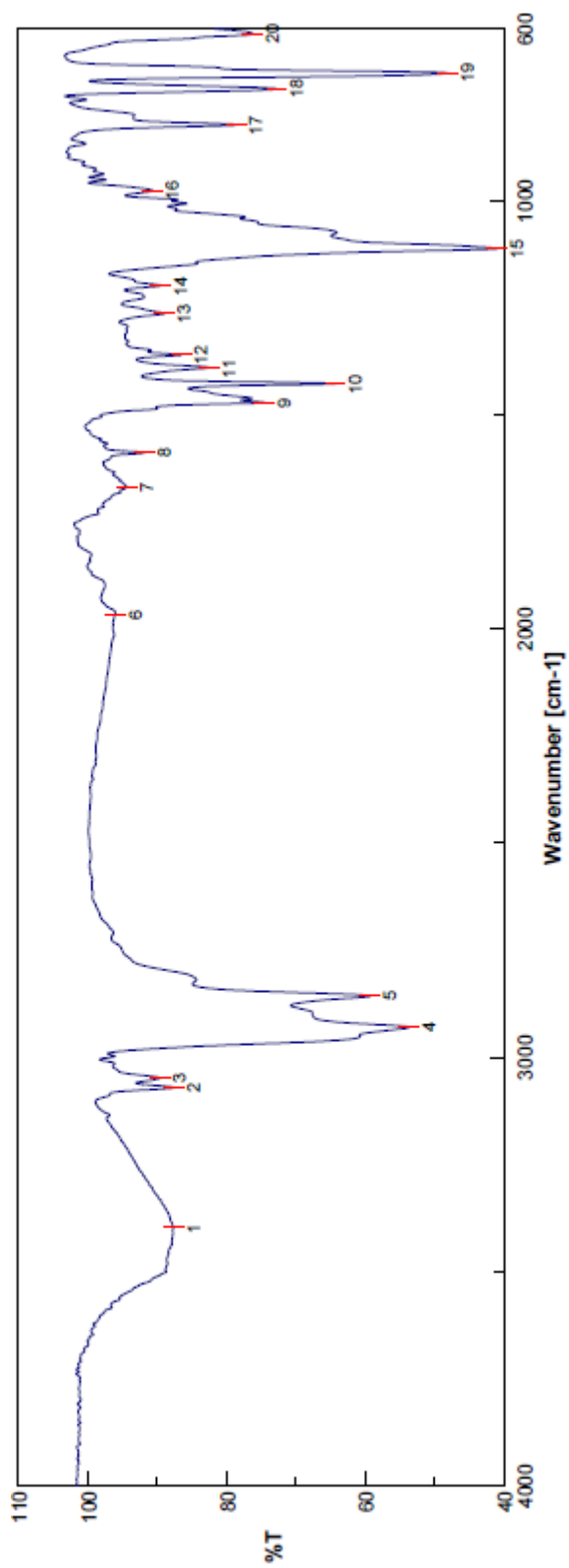
¹H NMR spectrum of compound 134



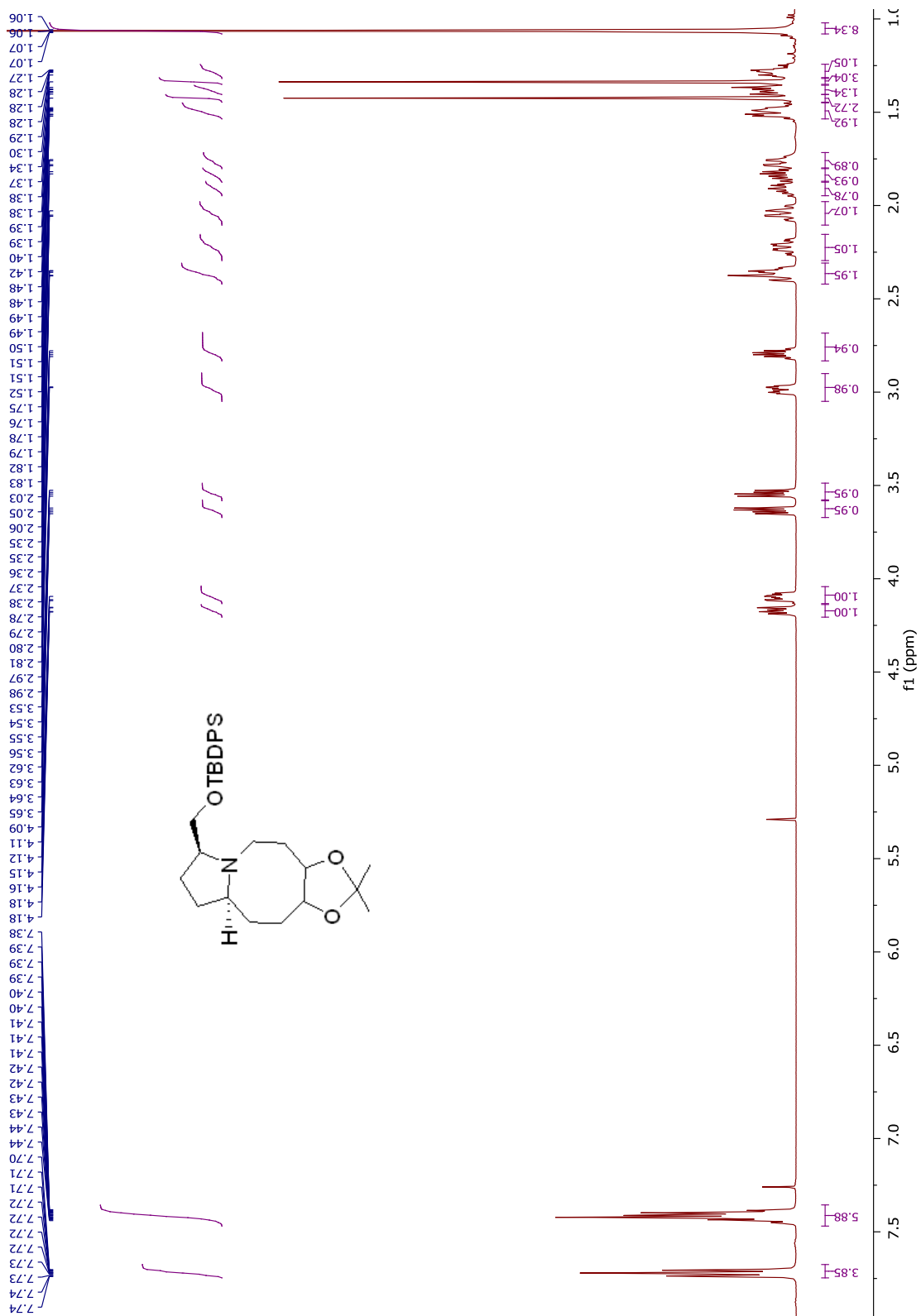
¹³C NMR spectrum of compound 134



COSY NMR spectrum of compound 134



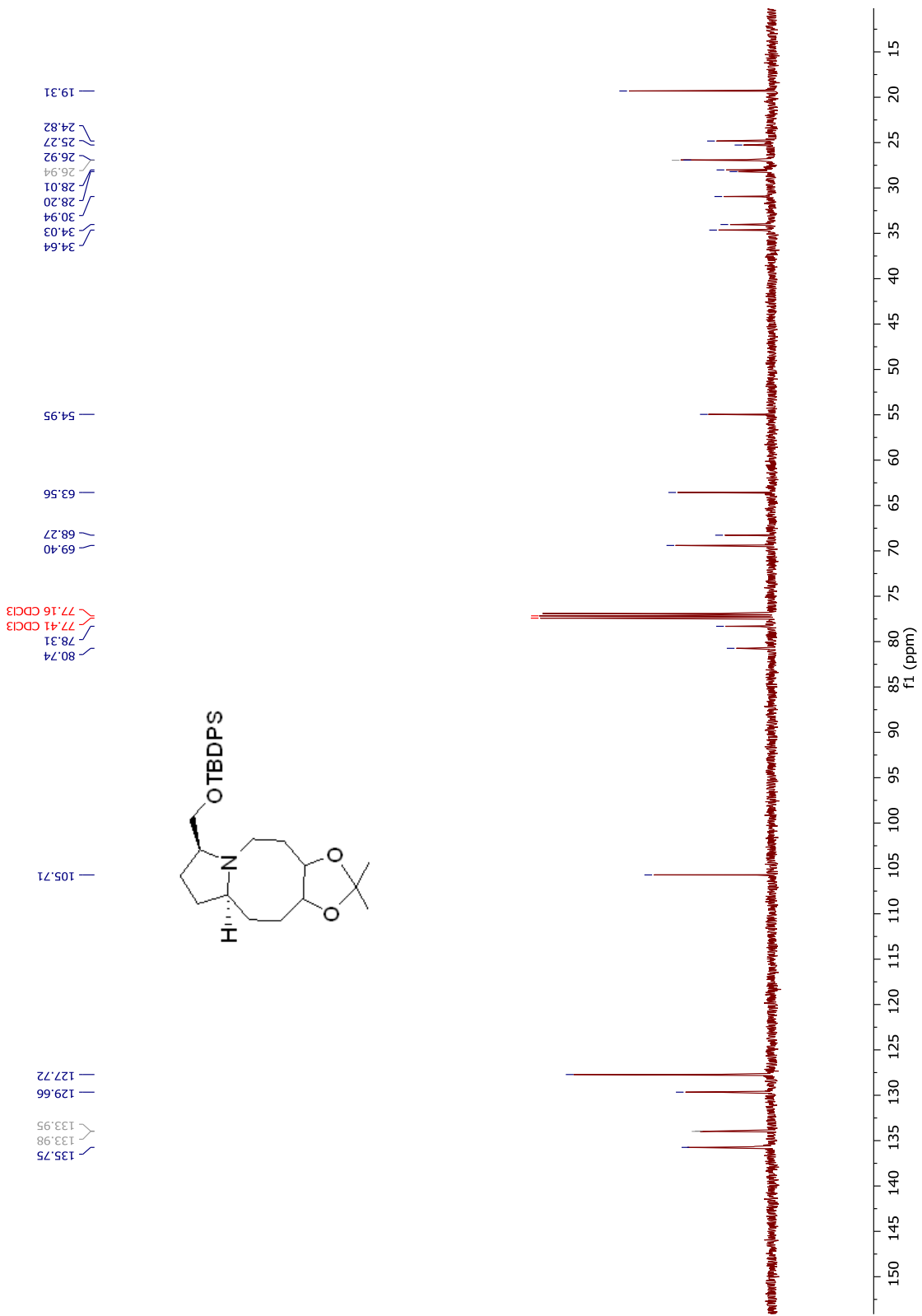
FTIR spectrum of compound **134**
261

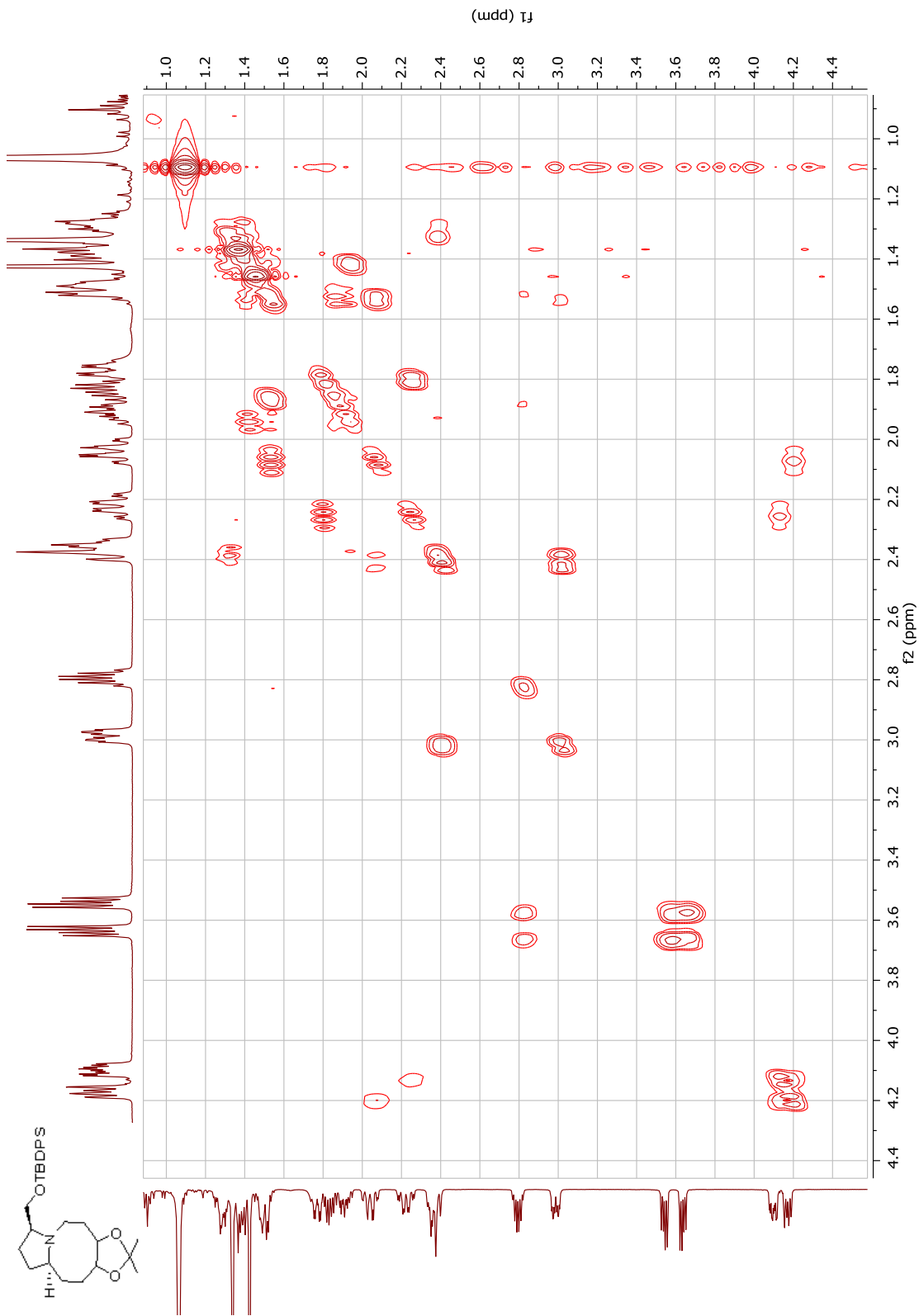


¹H NMR spectrum of compound **125**

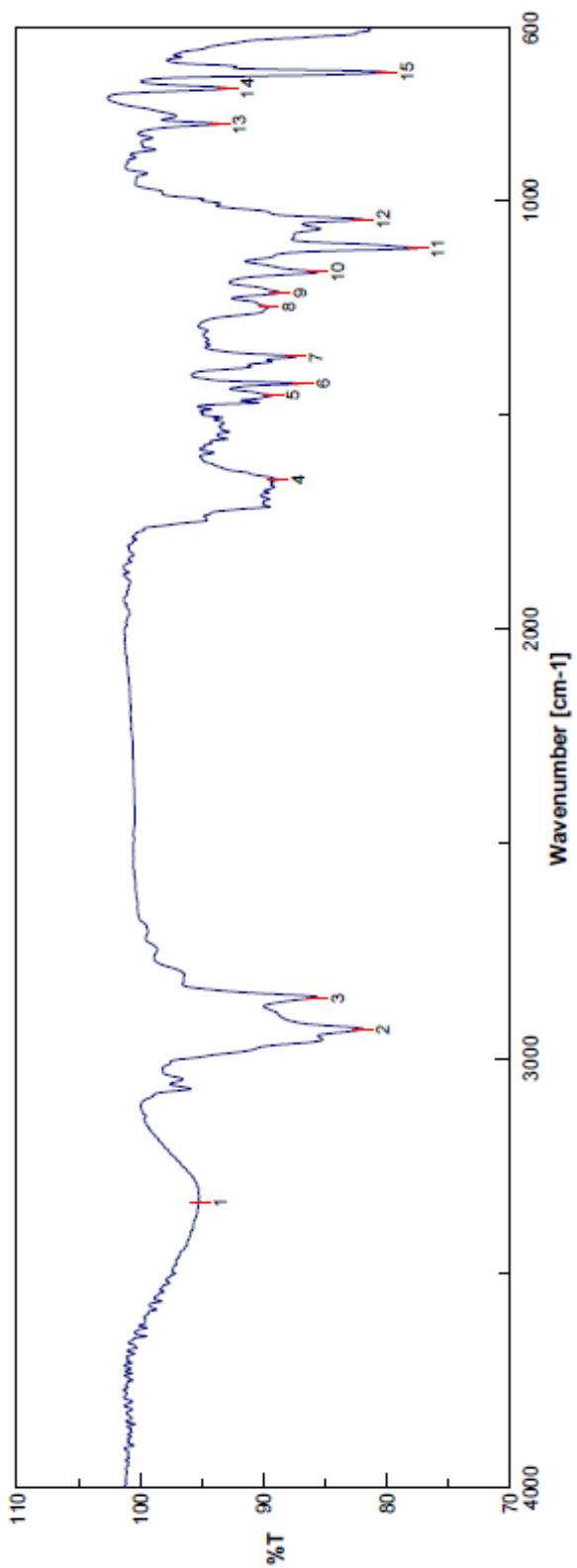
¹³C NMR spectrum of compound **125**

263

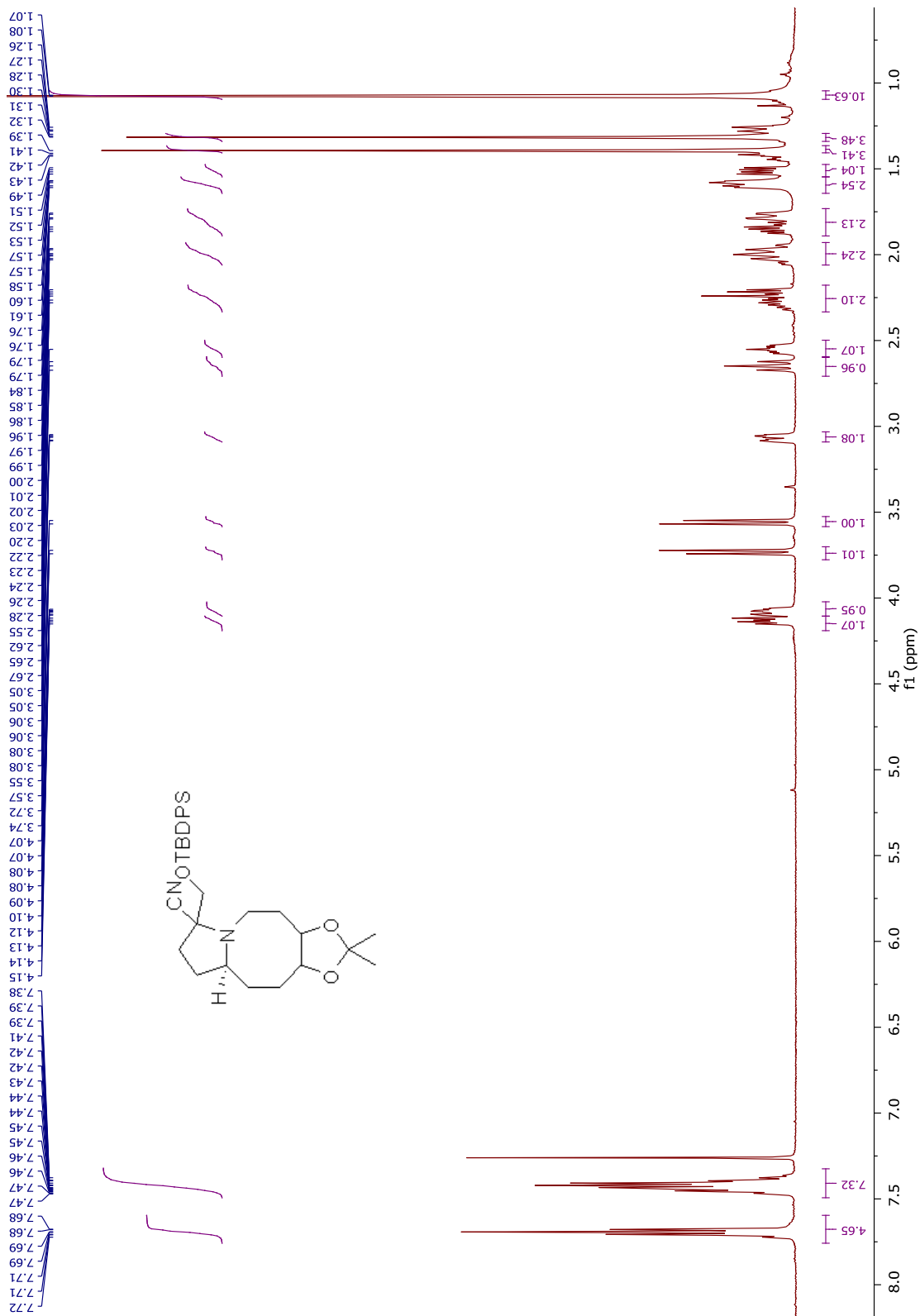




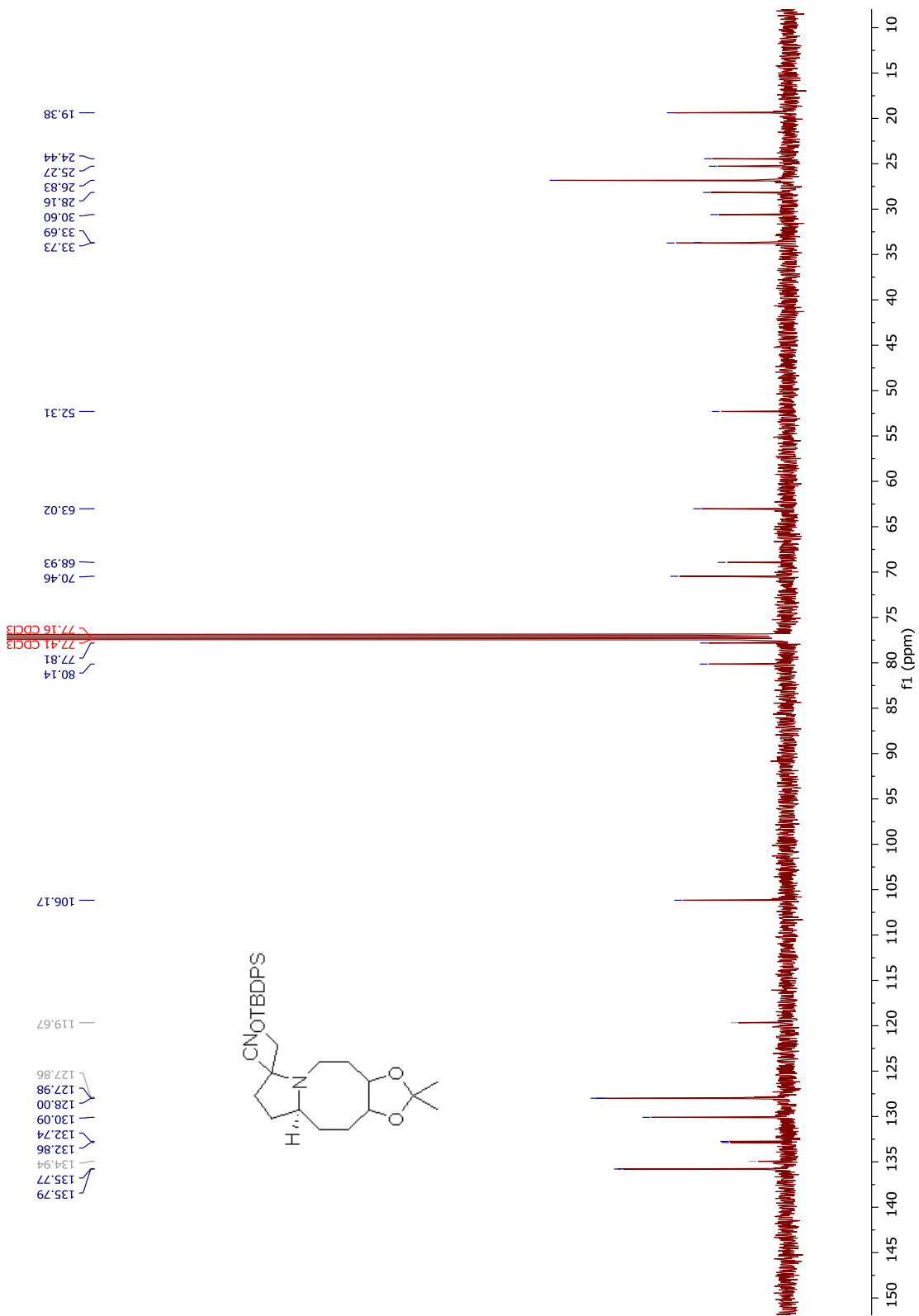
COSY NMR spectrum of compound 125



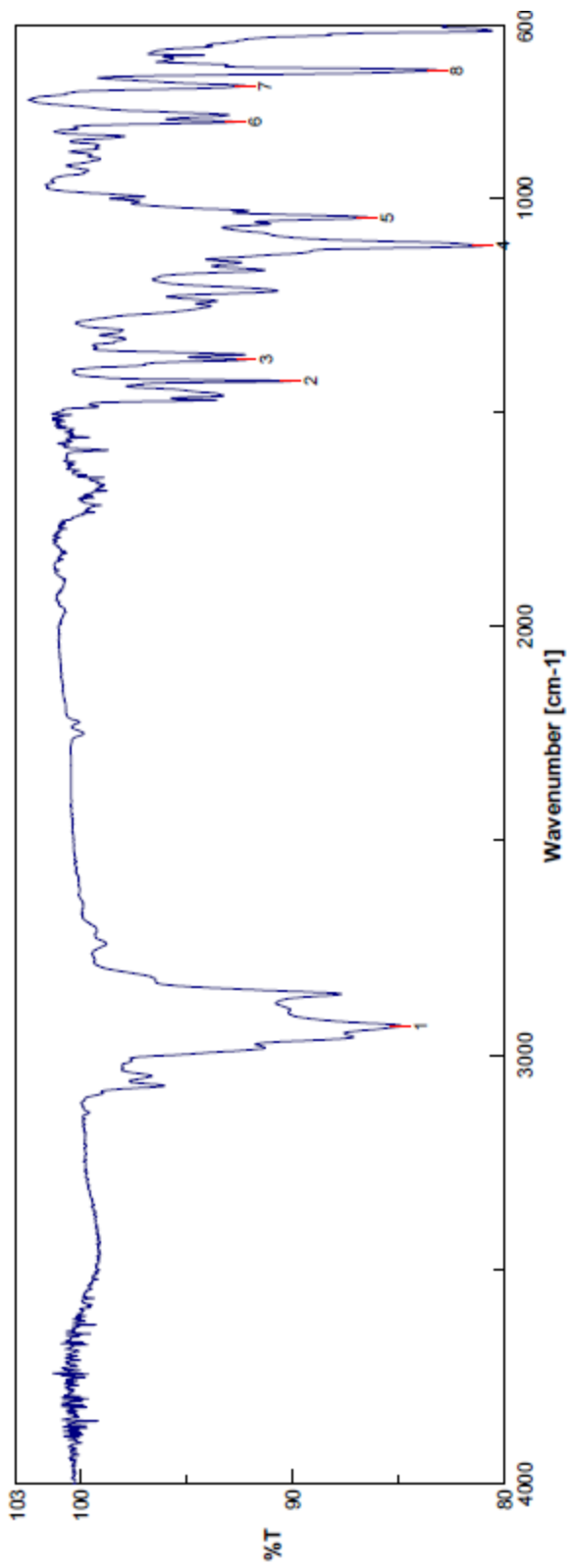
FTIR spectrum of compound **125**



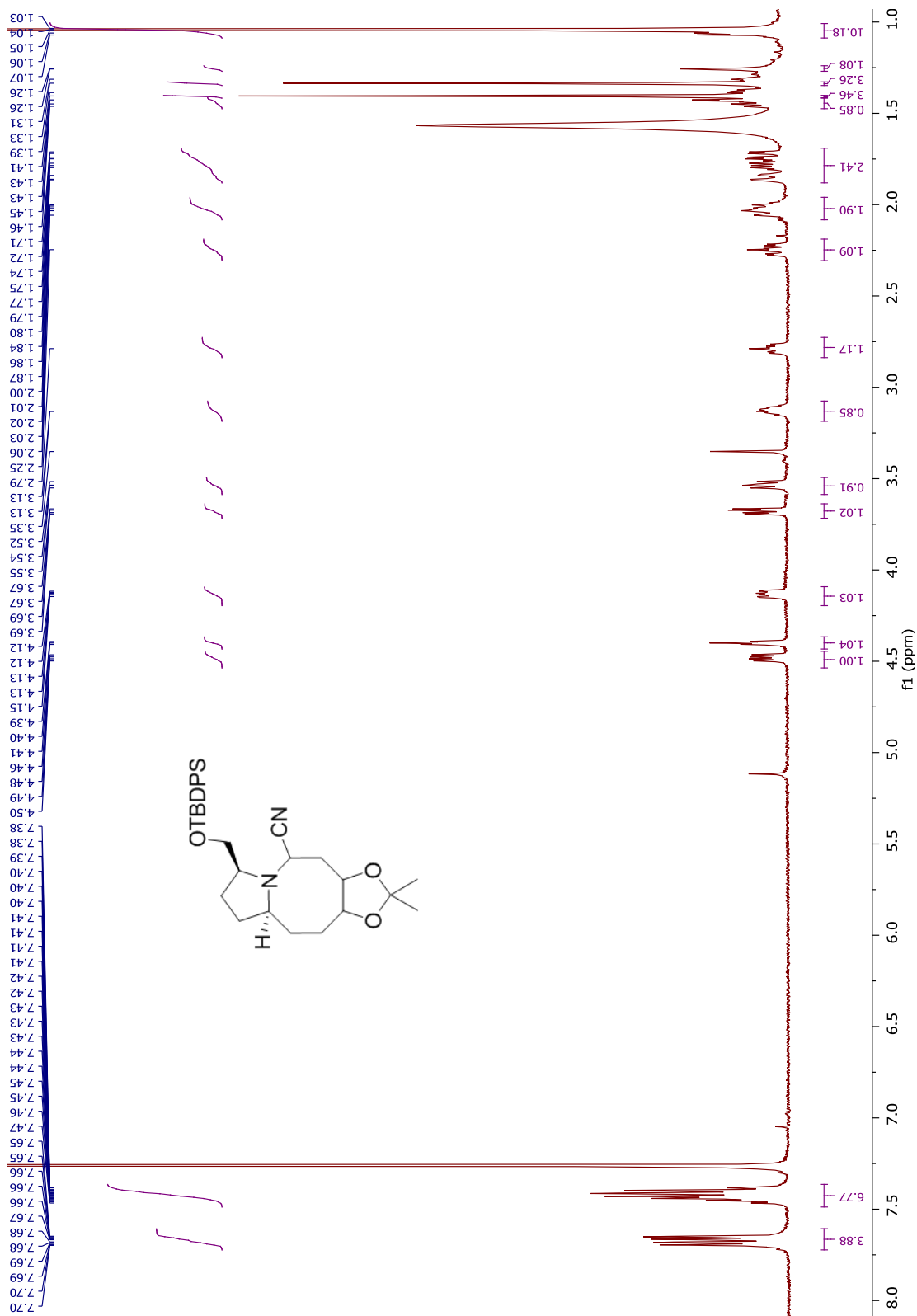
¹H NMR spectrum of compound 149



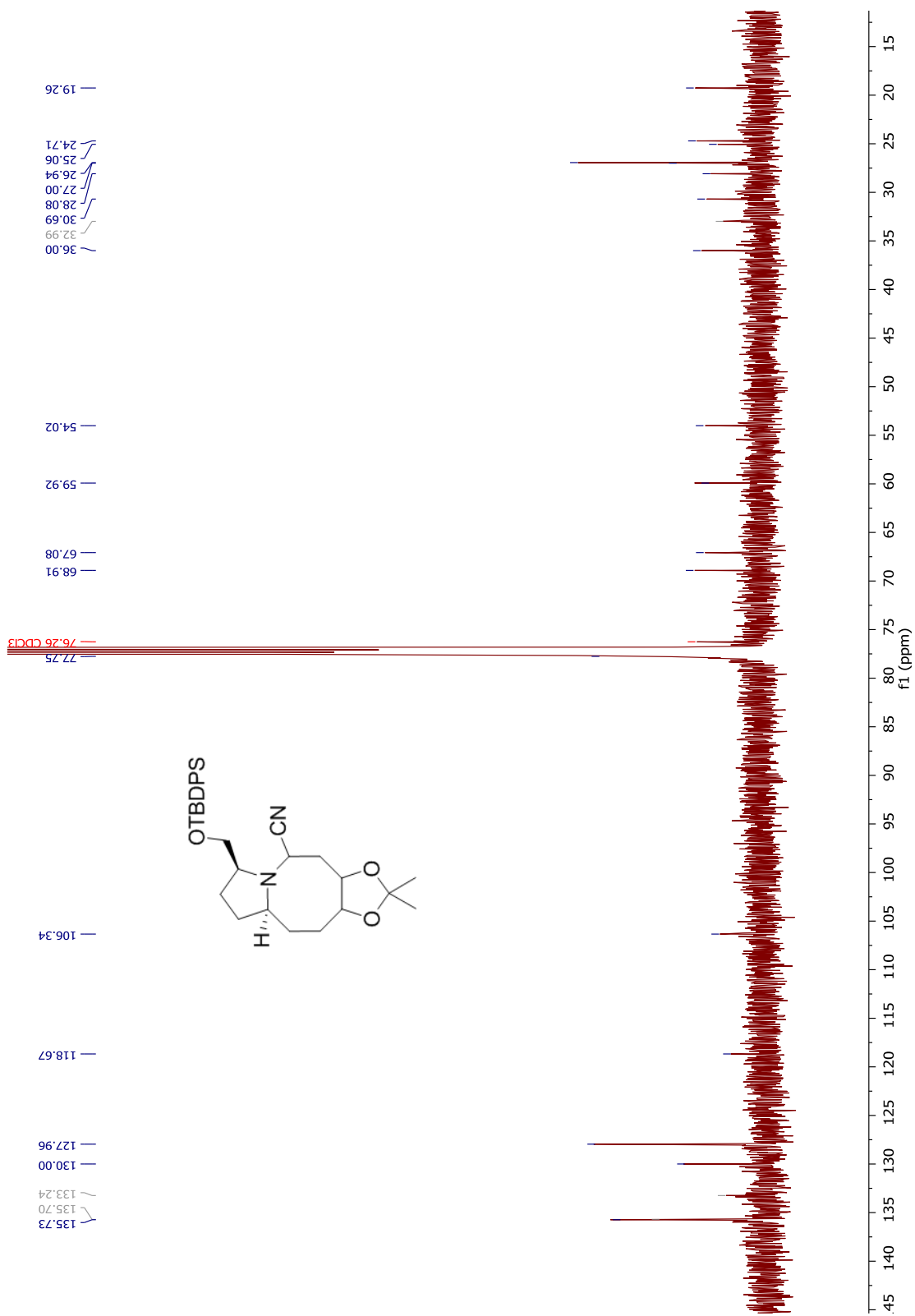
¹³C NMR spectrum of compound 149



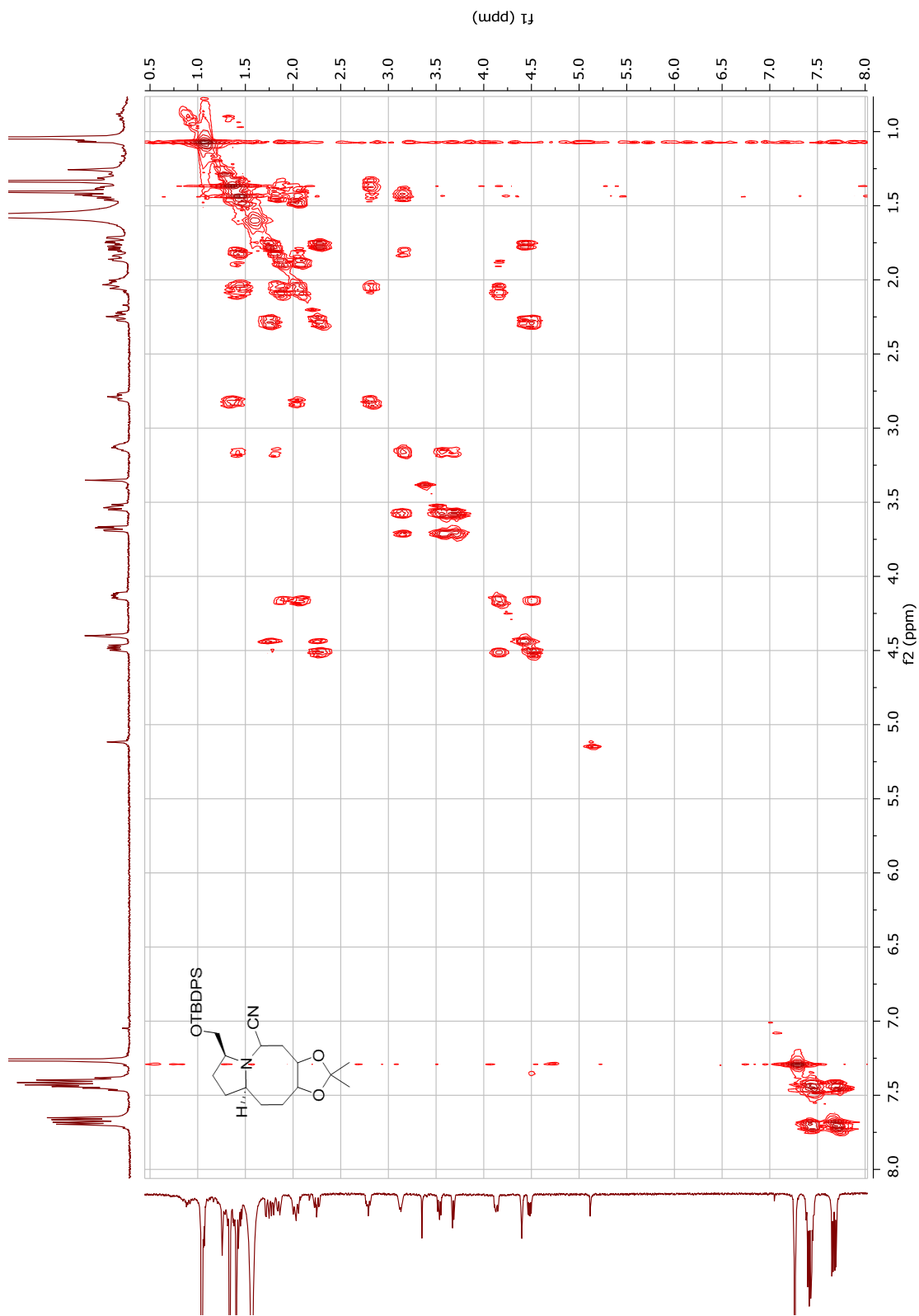
FTIR spectrum of compound **149**



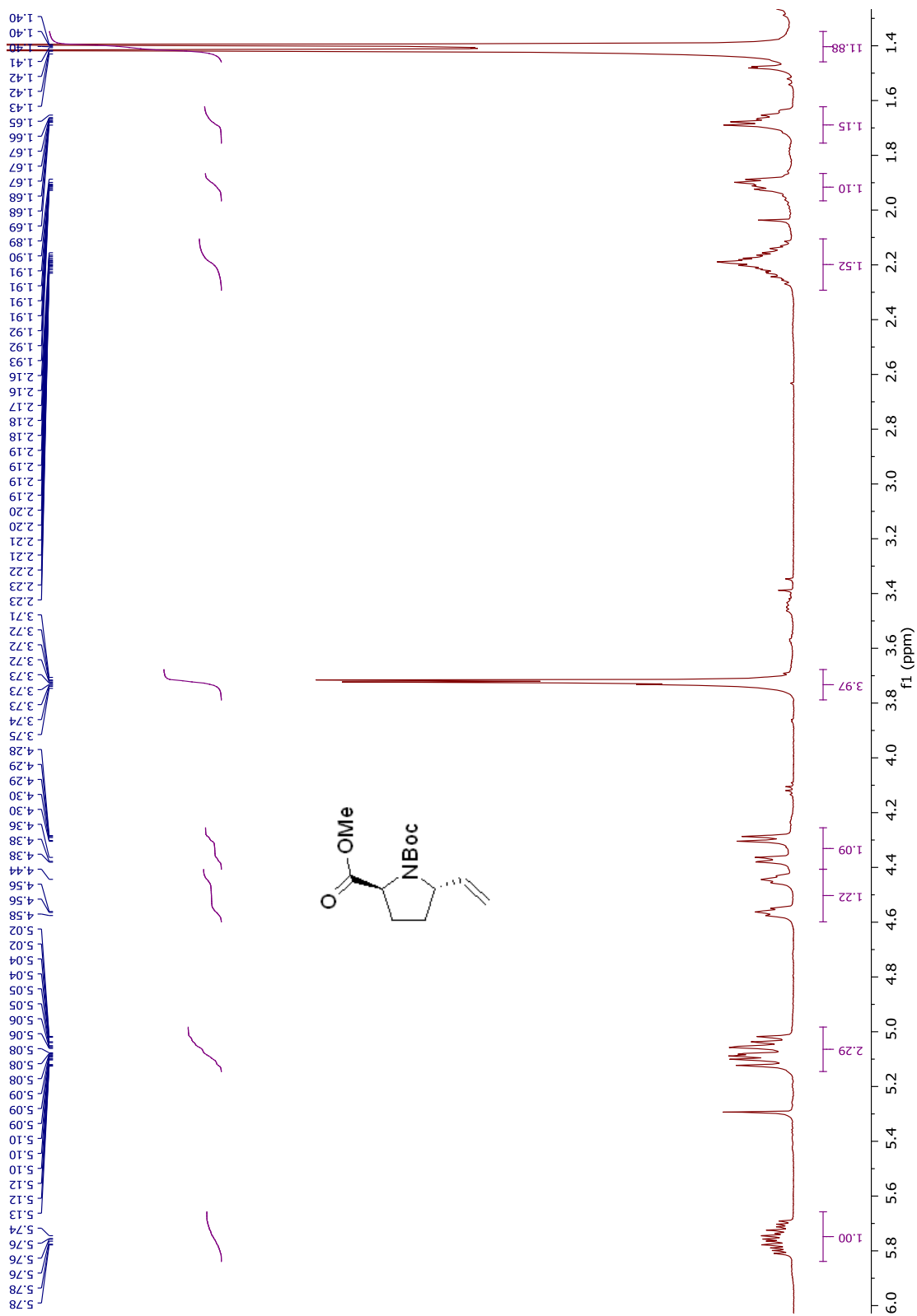
¹H NMR spectrum of compound 150



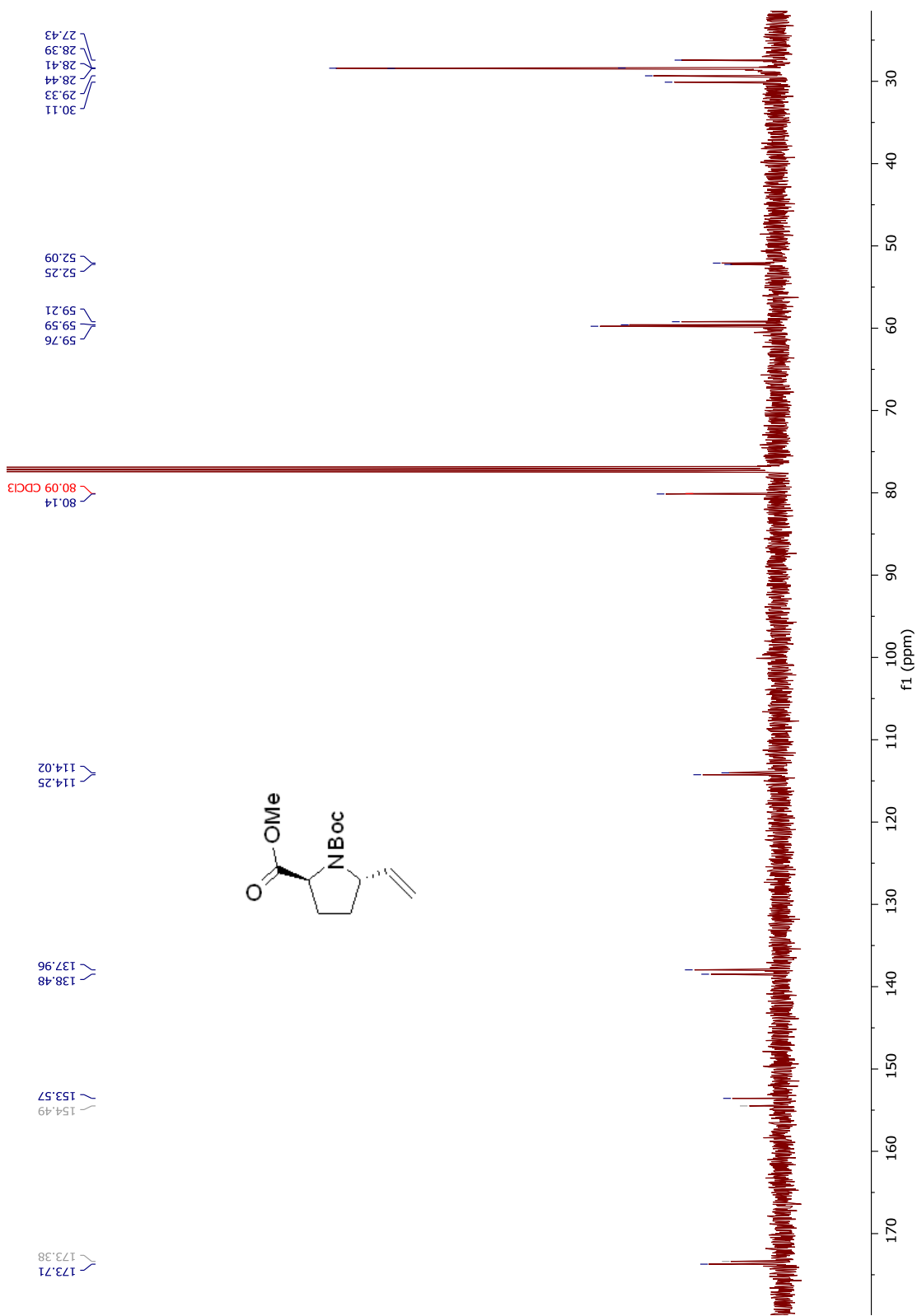
¹³C NMR spectrum of compound 150



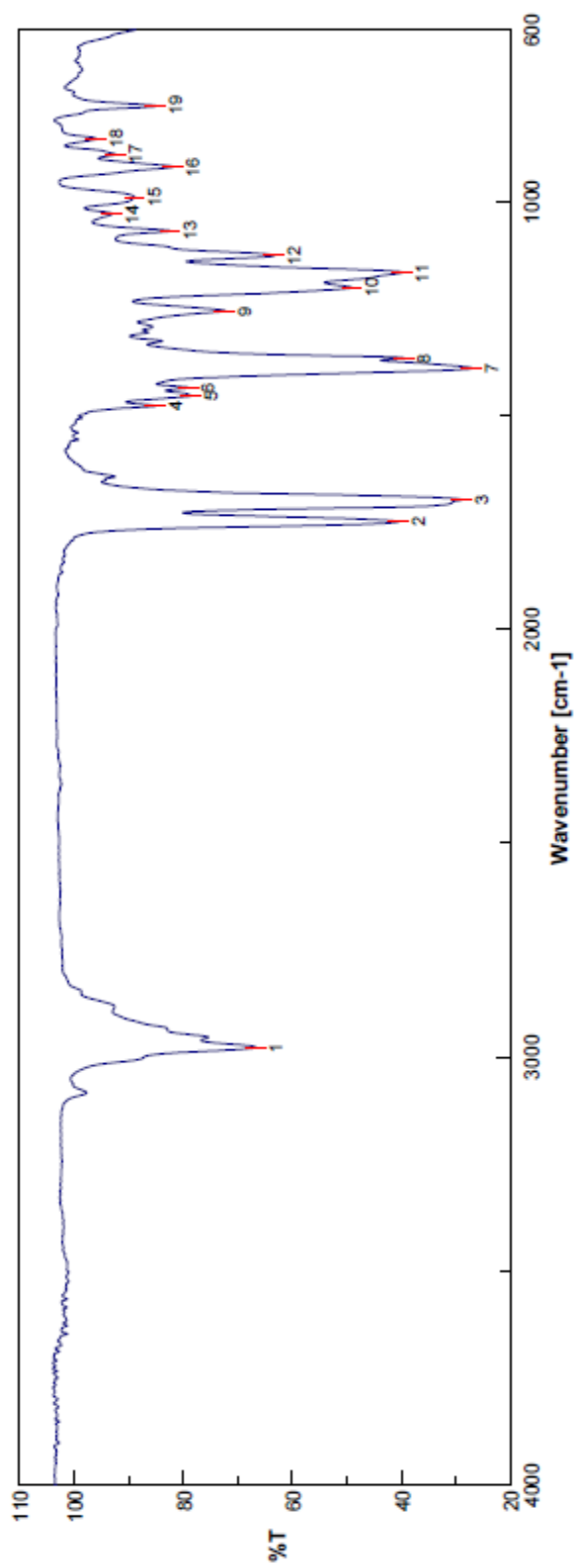
COSY NMR spectrum of compound **150**



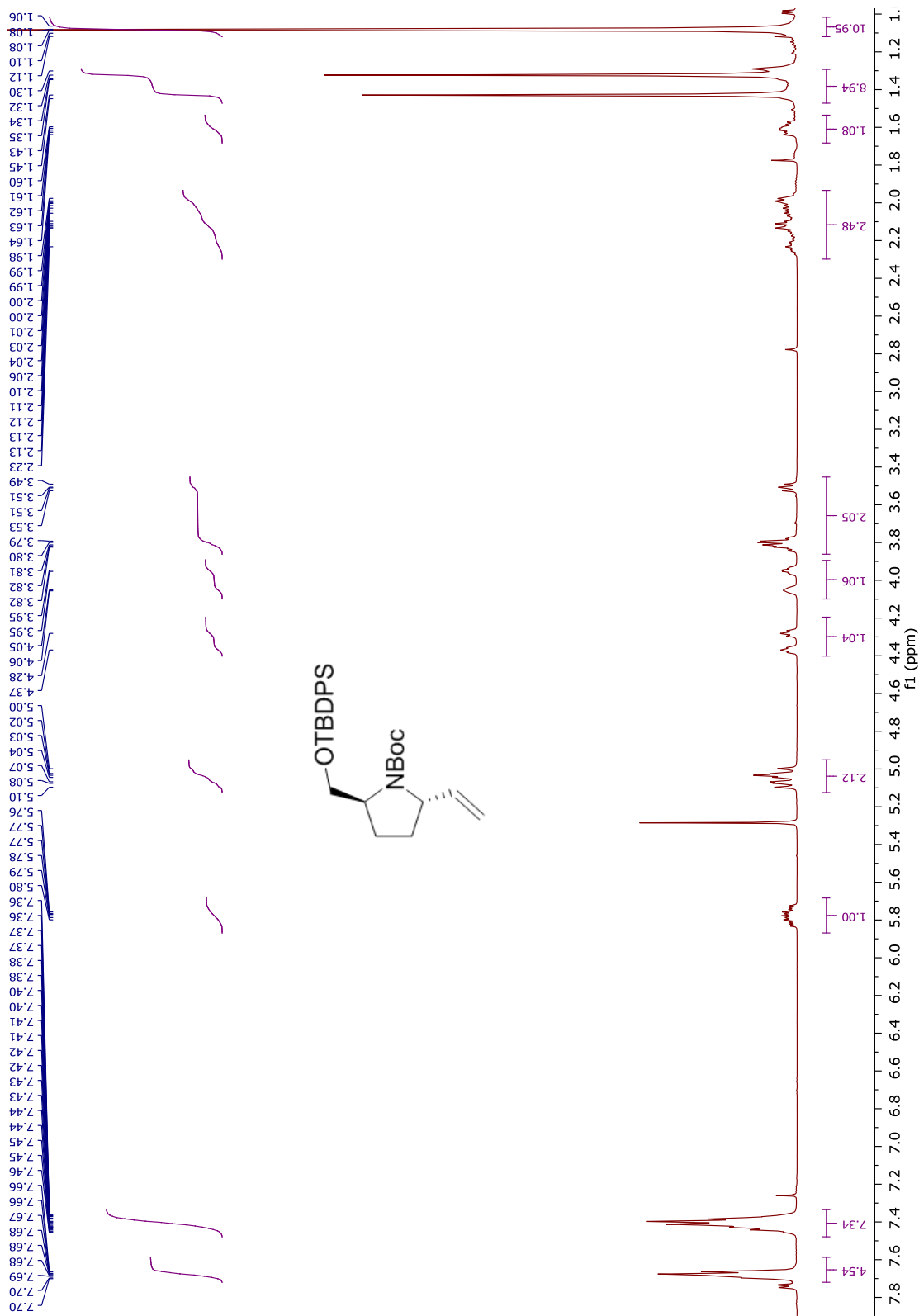
¹H NMR spectrum of compound 153



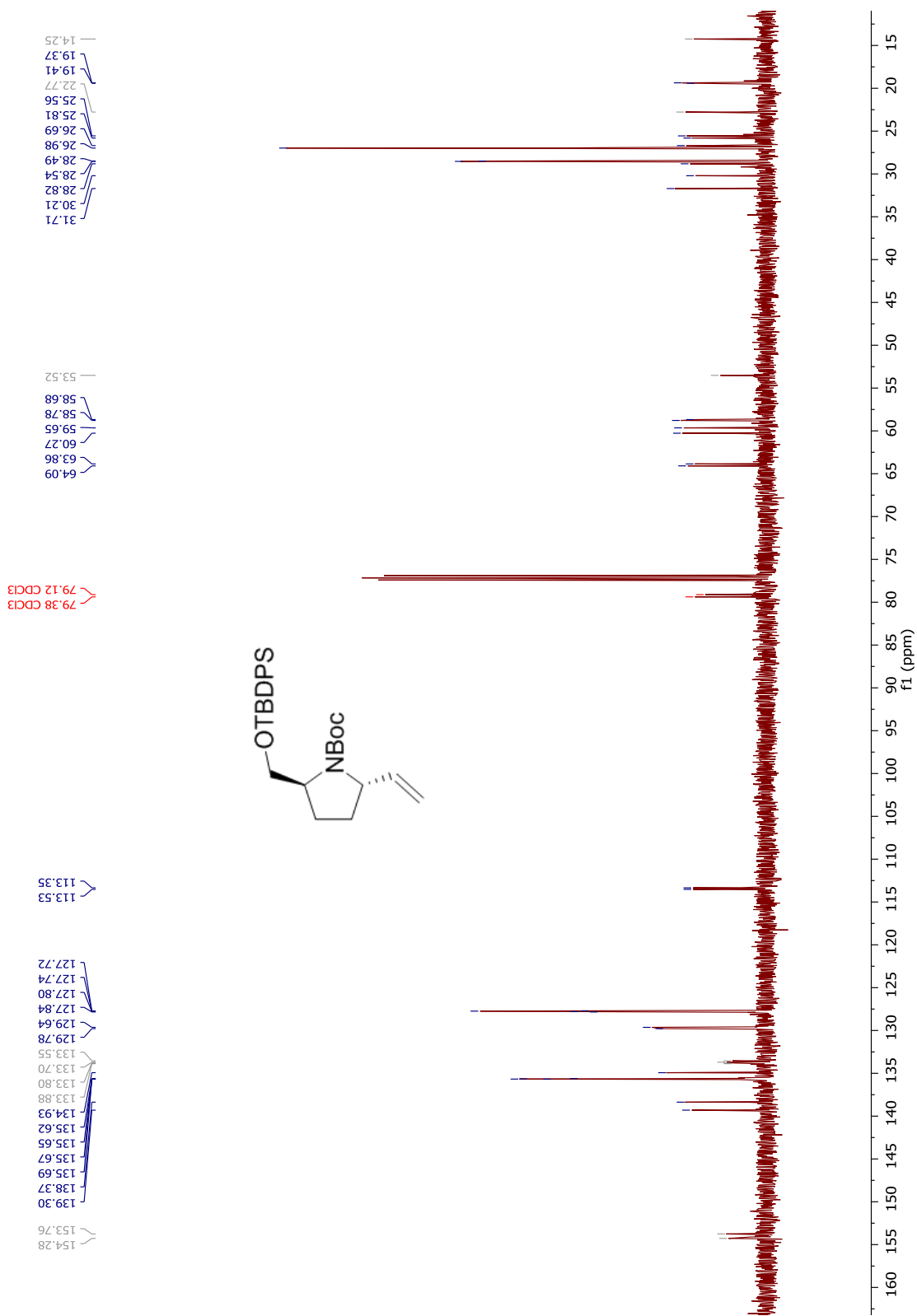
¹³C NMR spectrum of compound 153



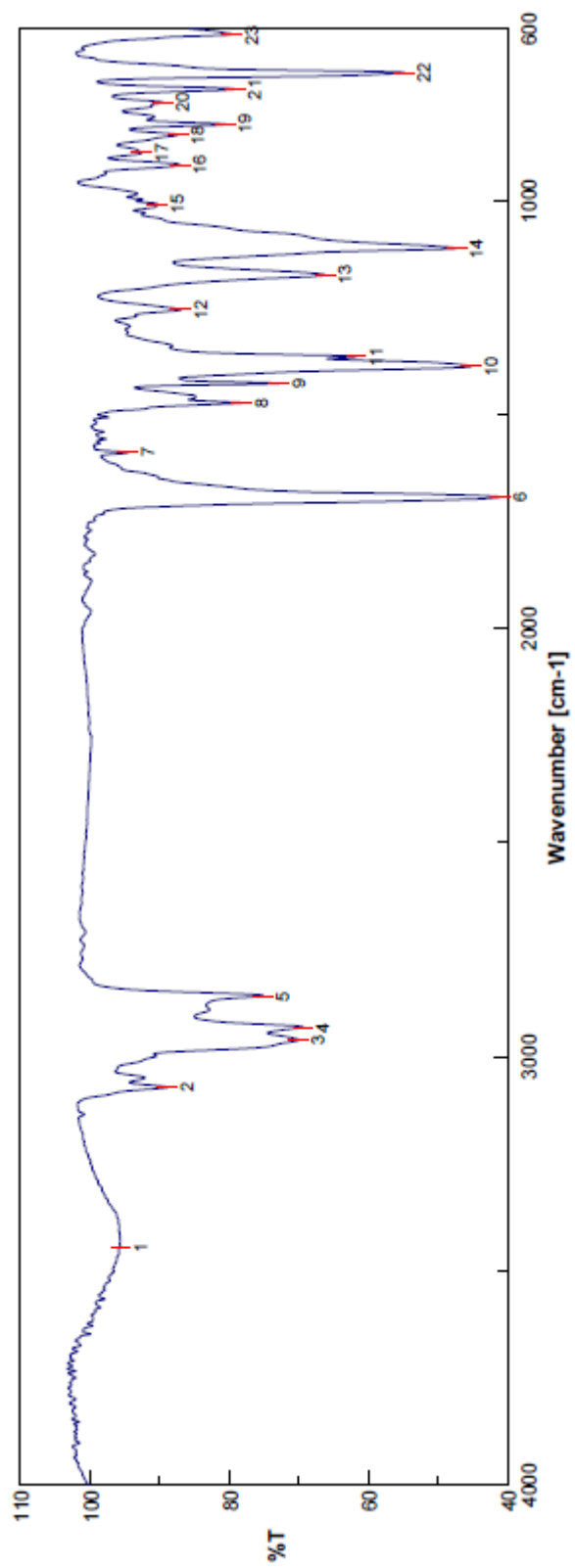
FTIR spectrum of compound **153**



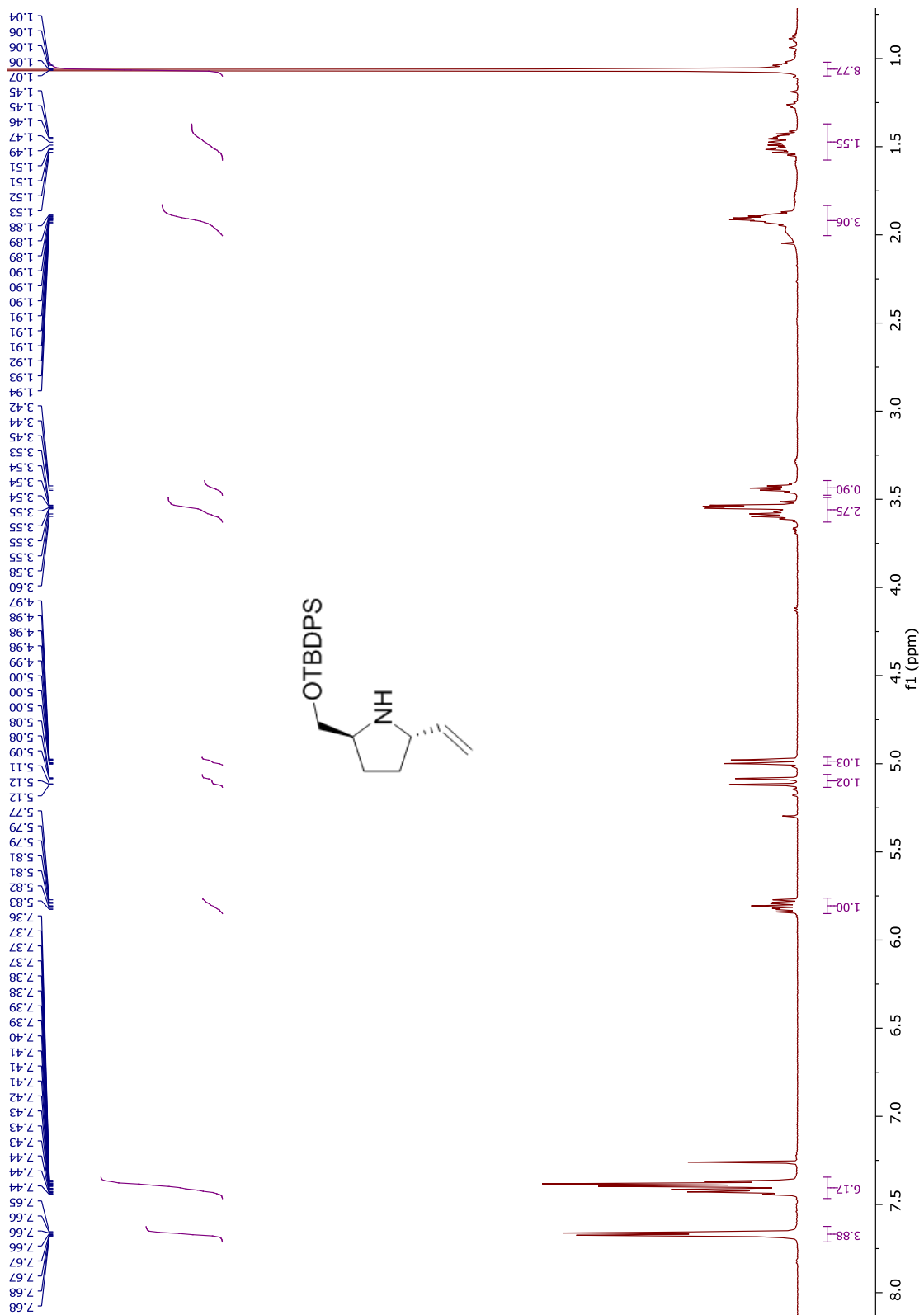
¹H NMR spectrum of compound 154



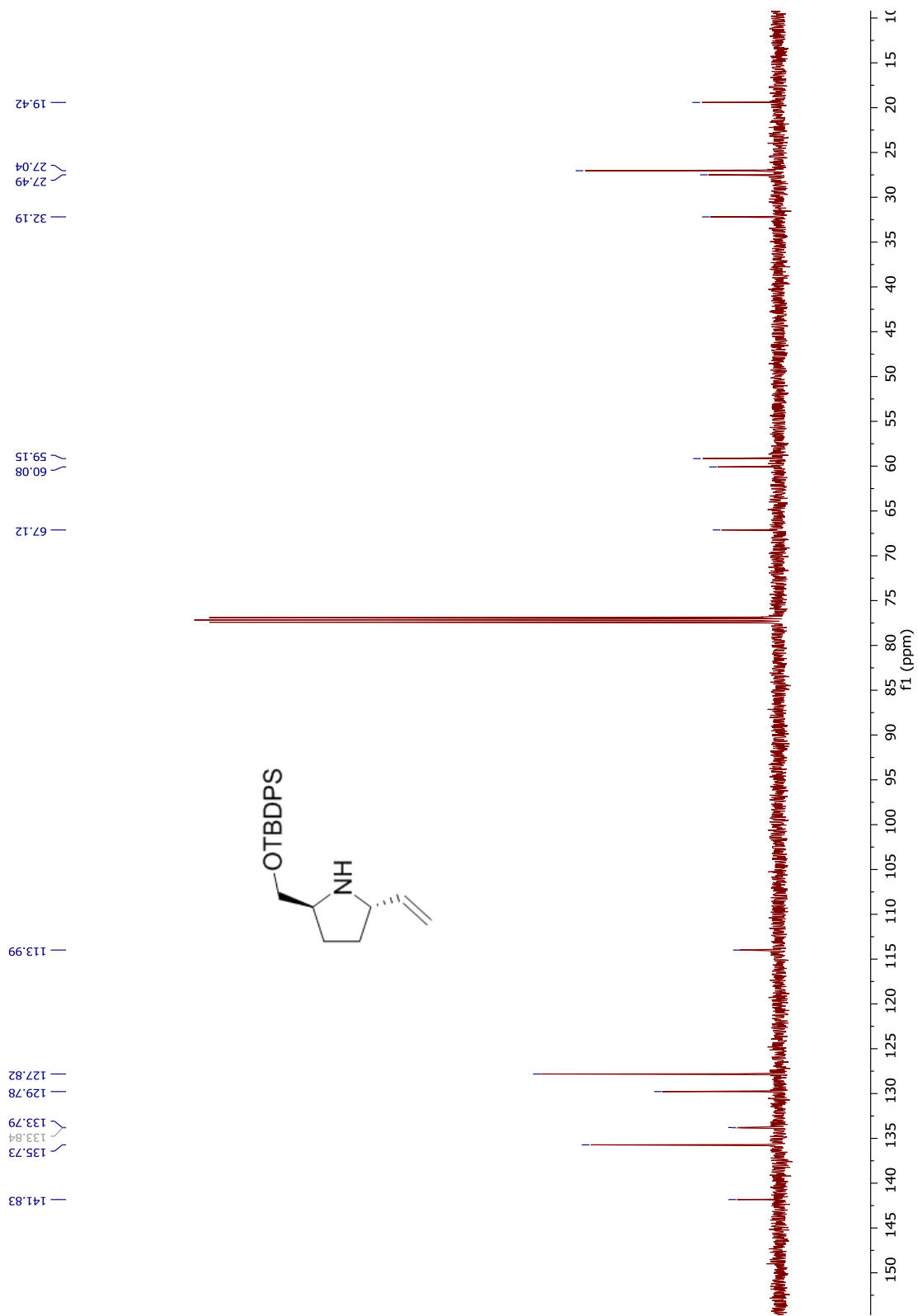
¹³C NMR spectrum of compound **154**



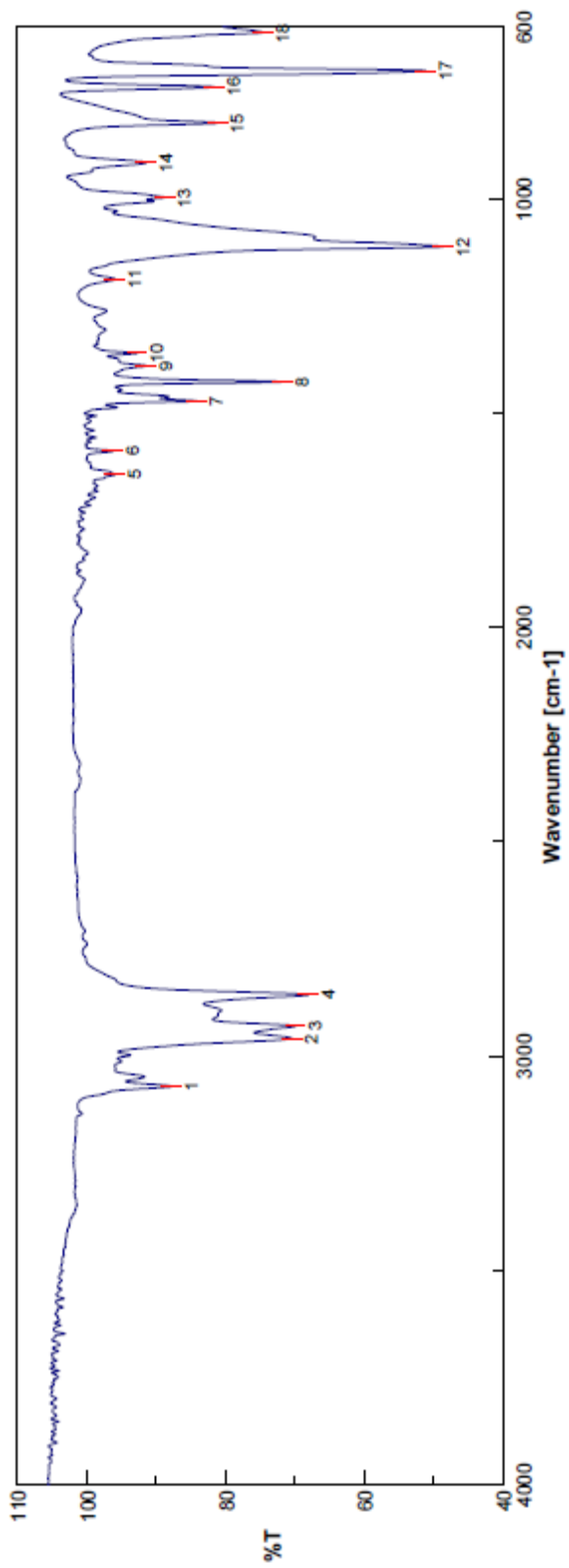
FTIR spectrum of compound 154



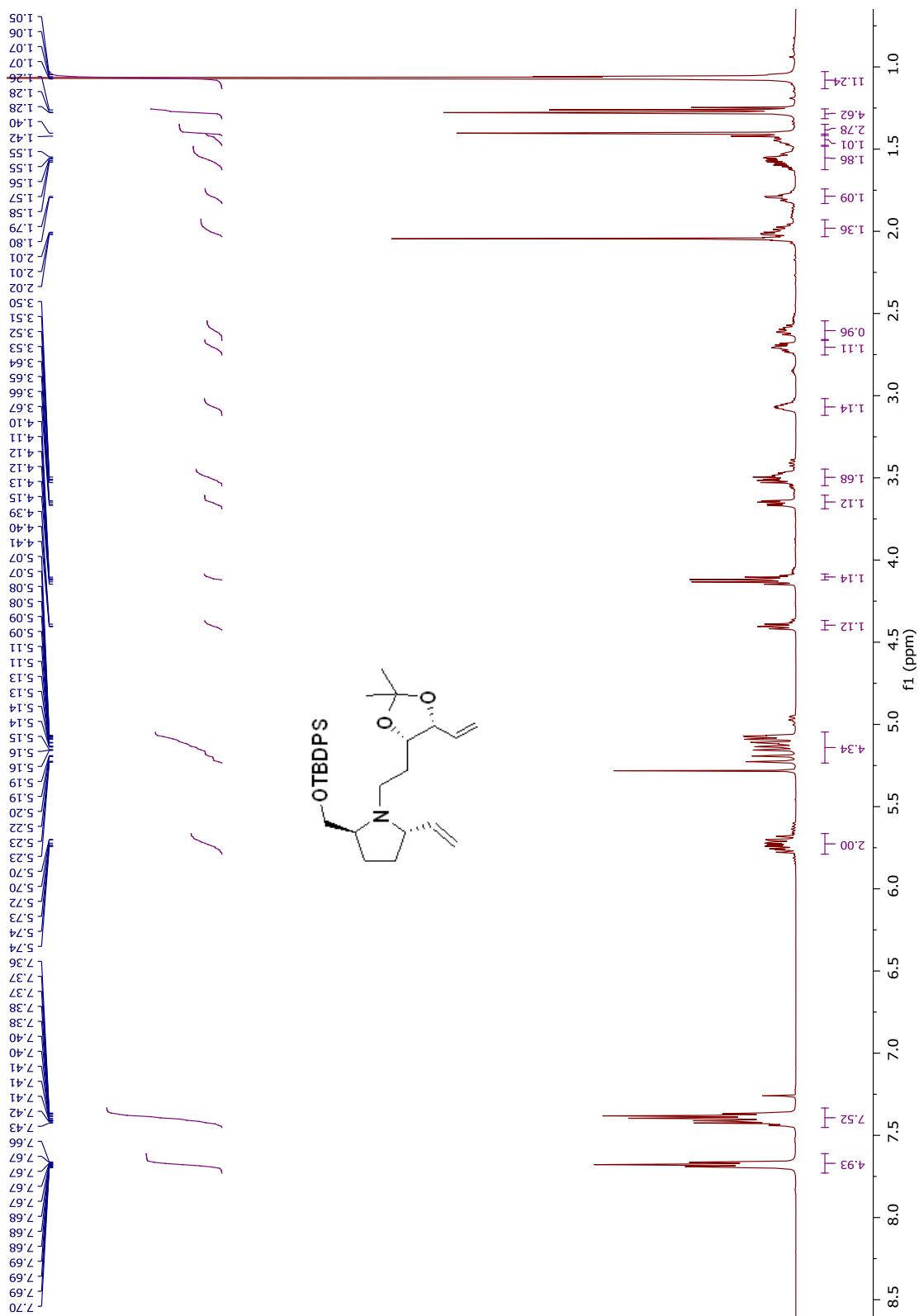
^1H NMR spectrum of compound **155**



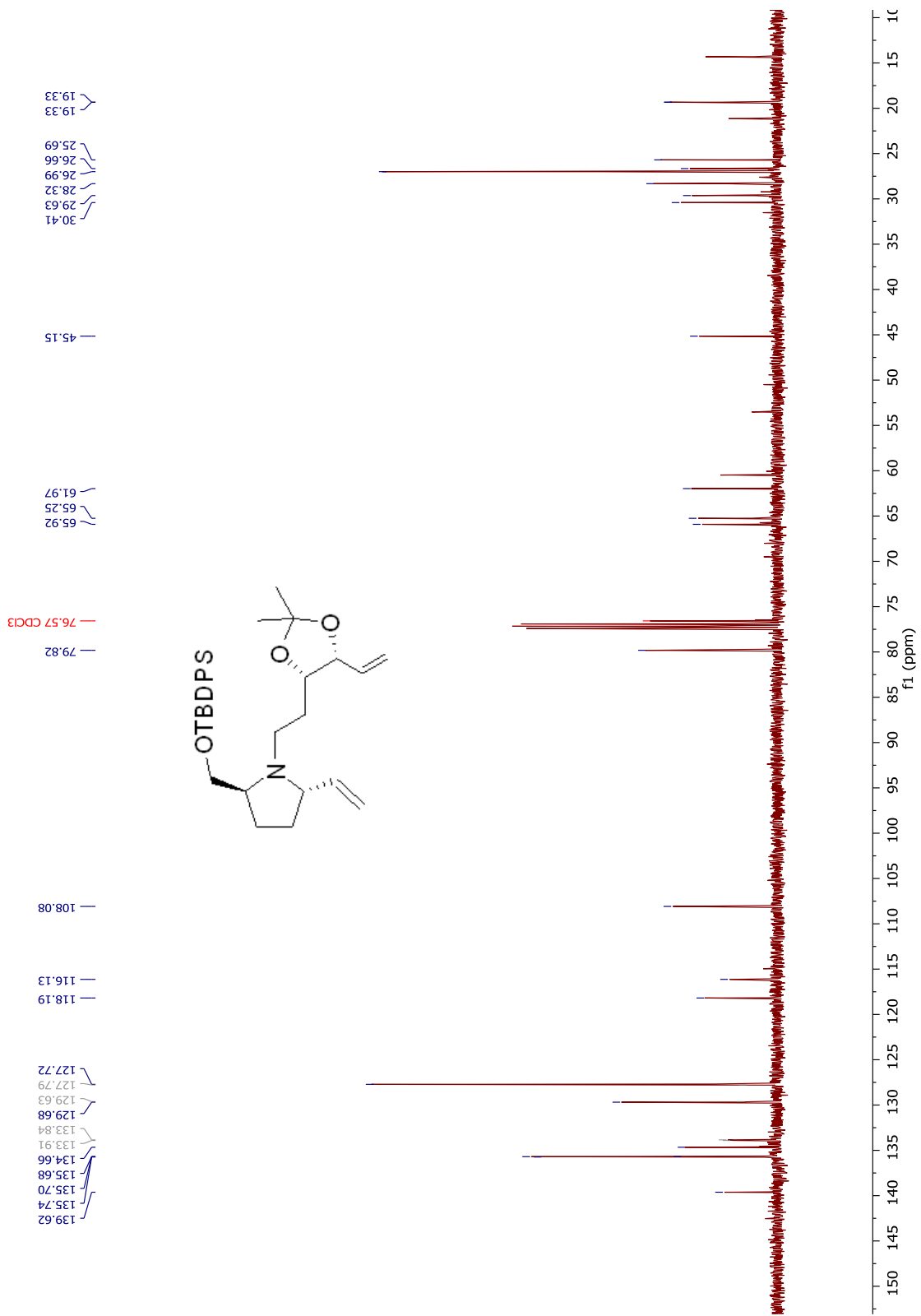
^{13}C NMR spectrum of compound **155**



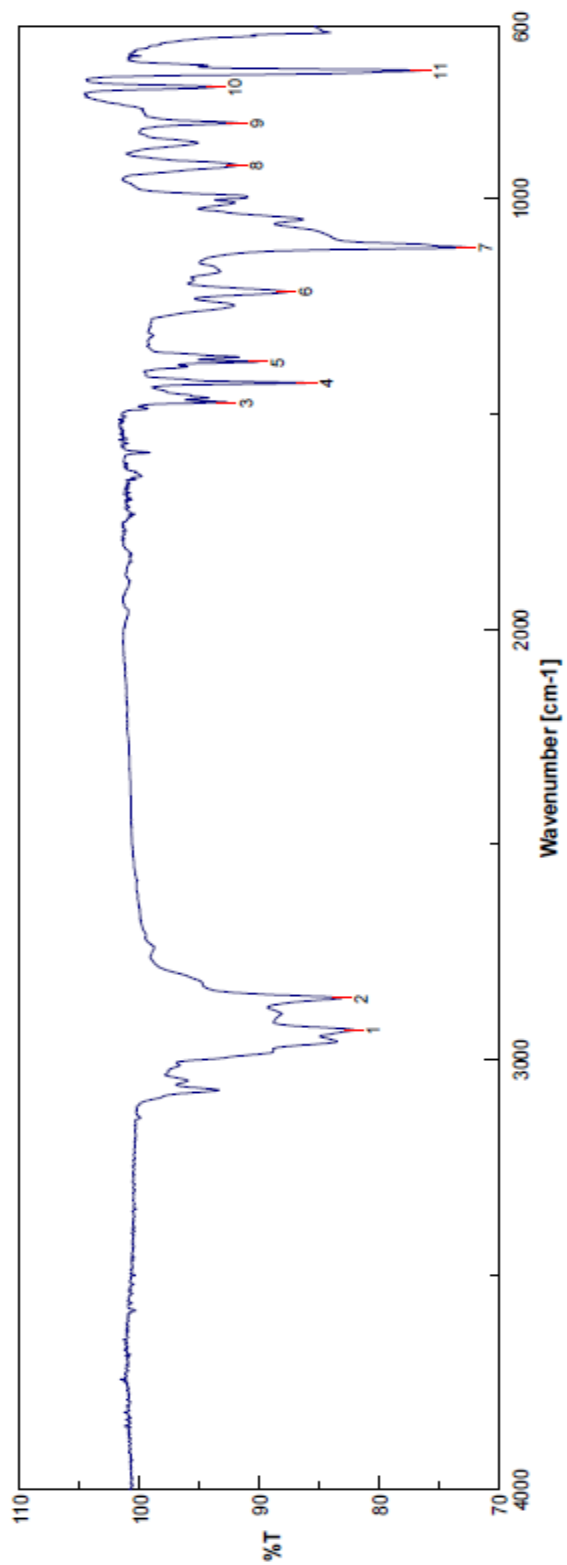
FTIR spectrum of compound **155**



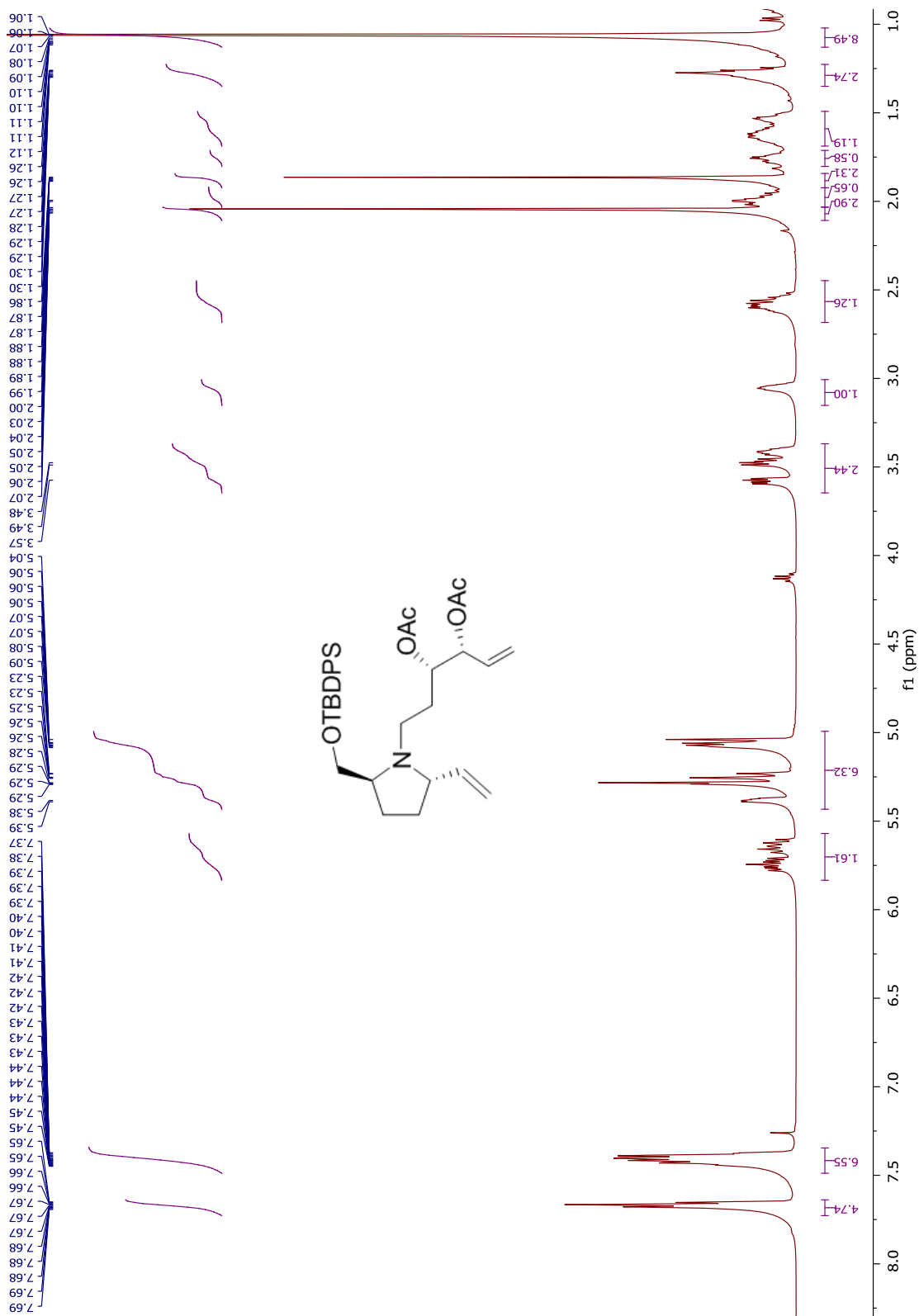
¹H NMR spectrum of compound 157



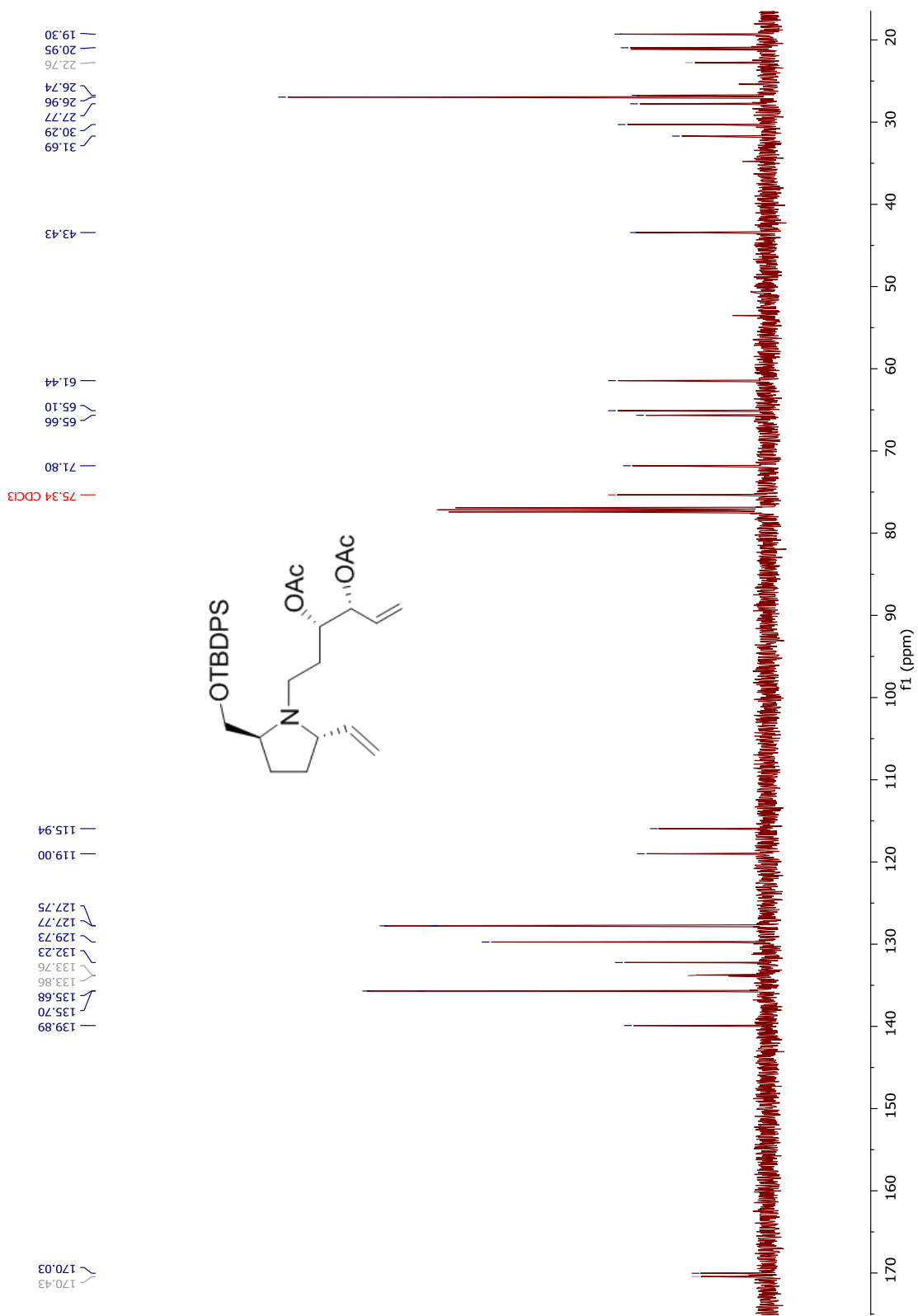
¹³C NMR spectrum of compound 157



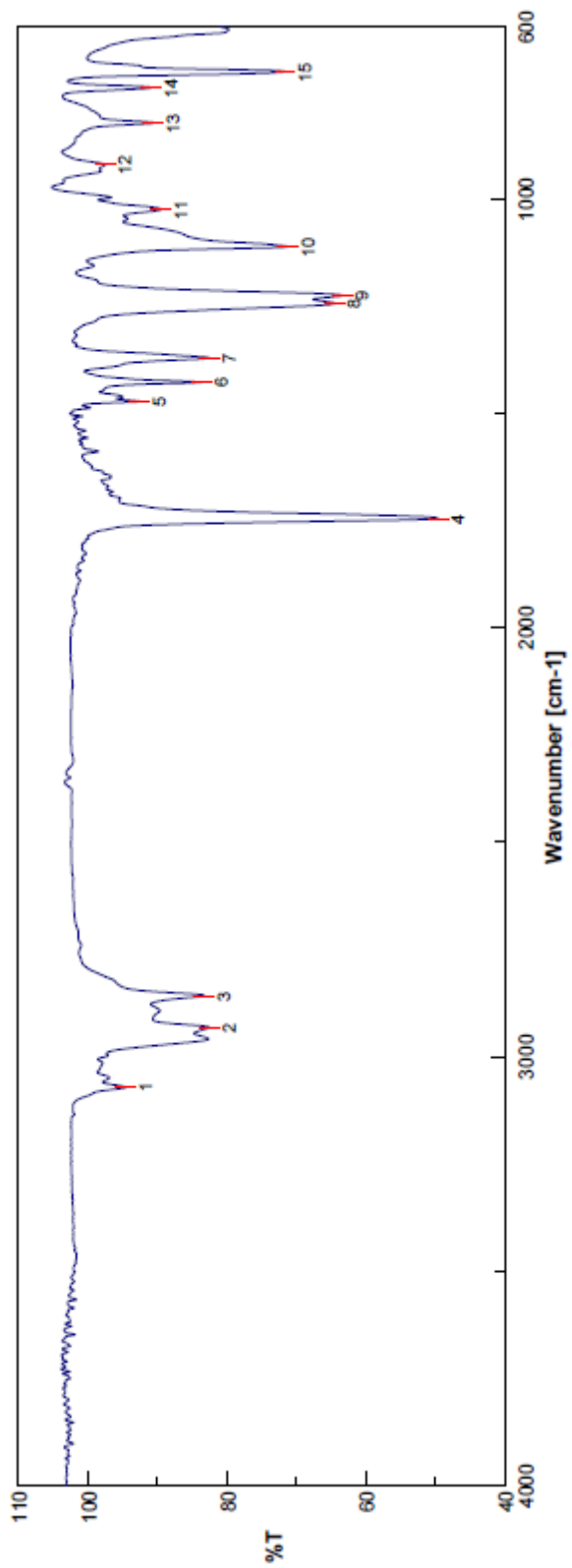
FTIR spectrum of compound **157**



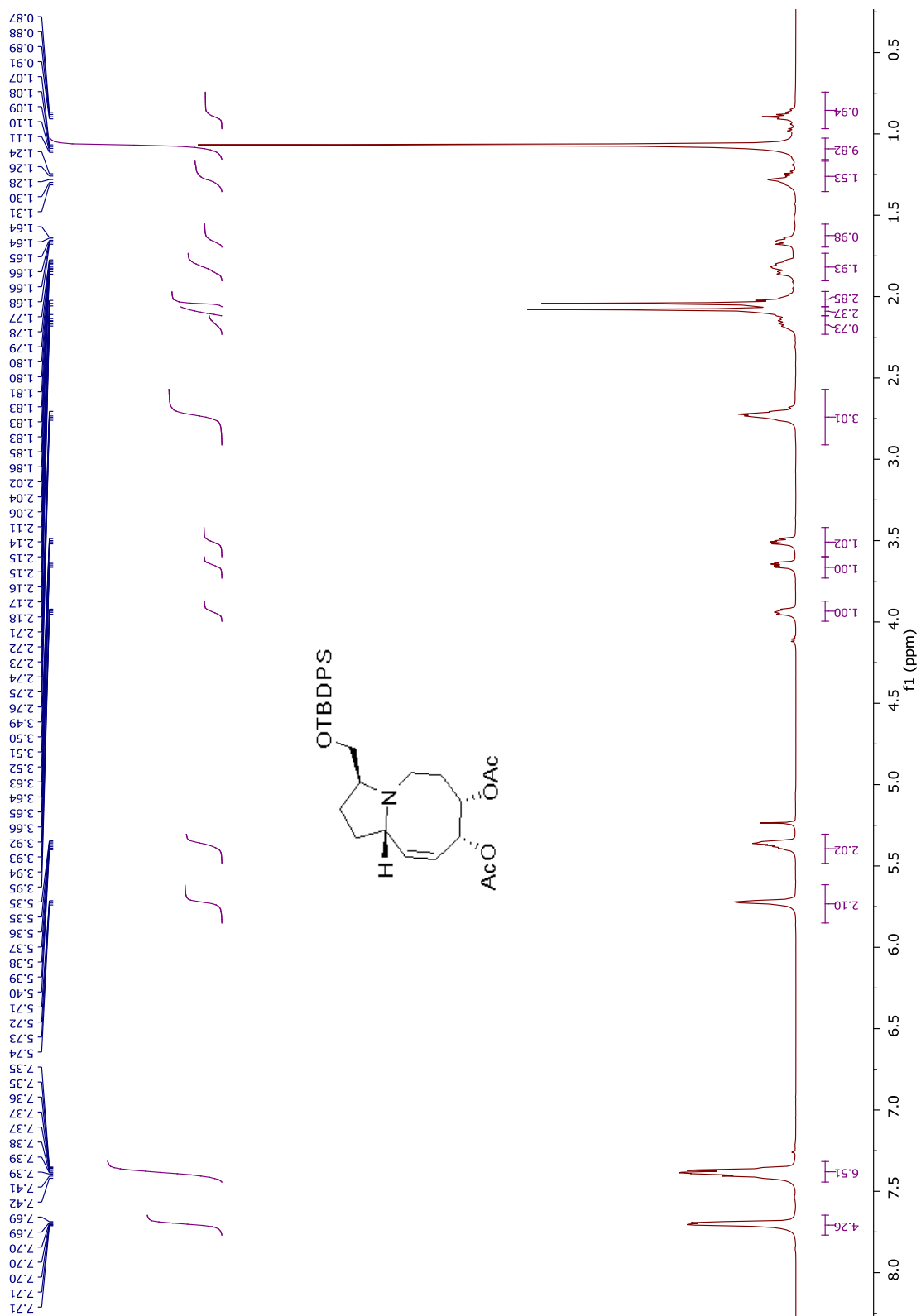
¹H NMR spectrum of compound 158



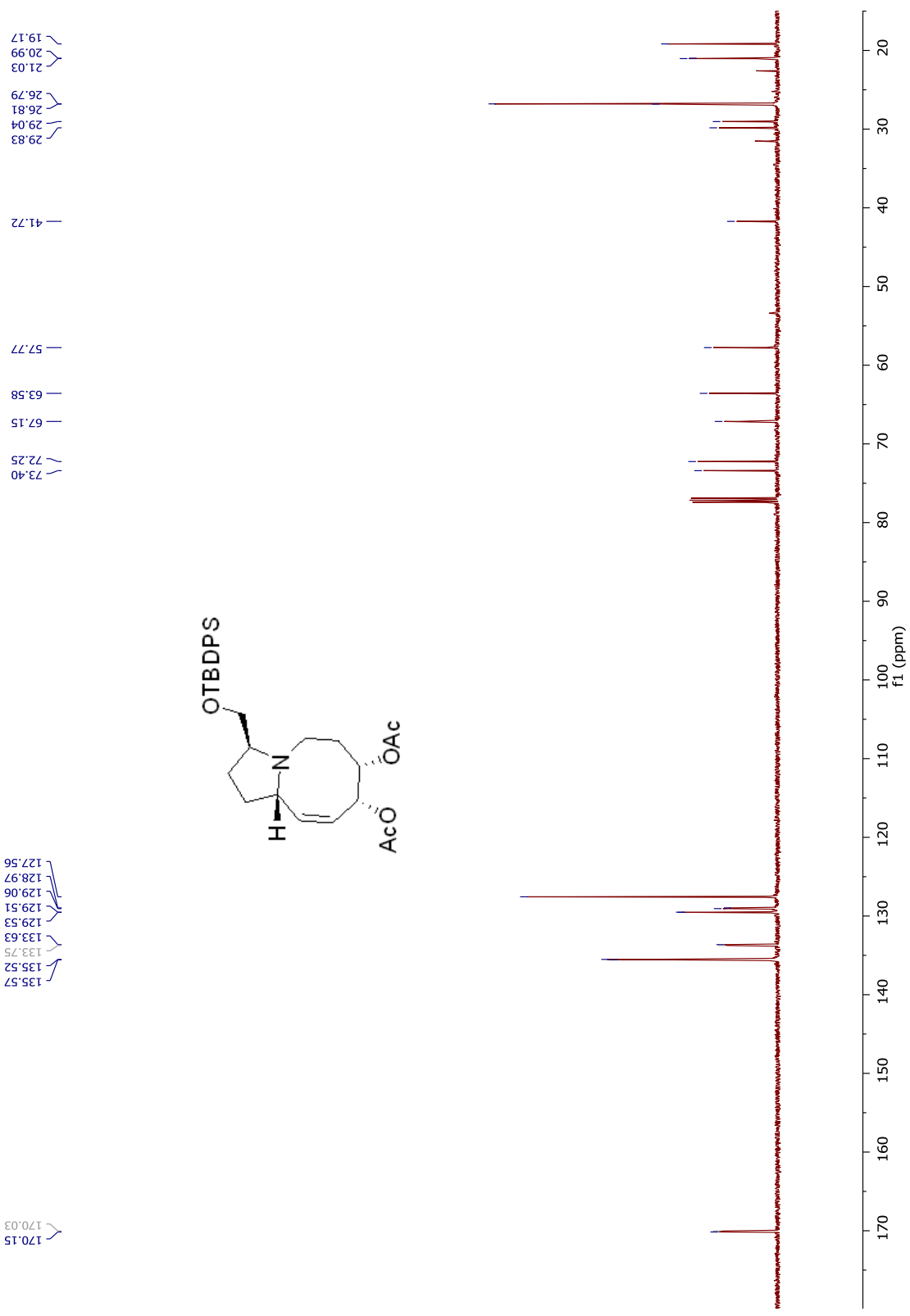
¹³C NMR spectrum of compound 158



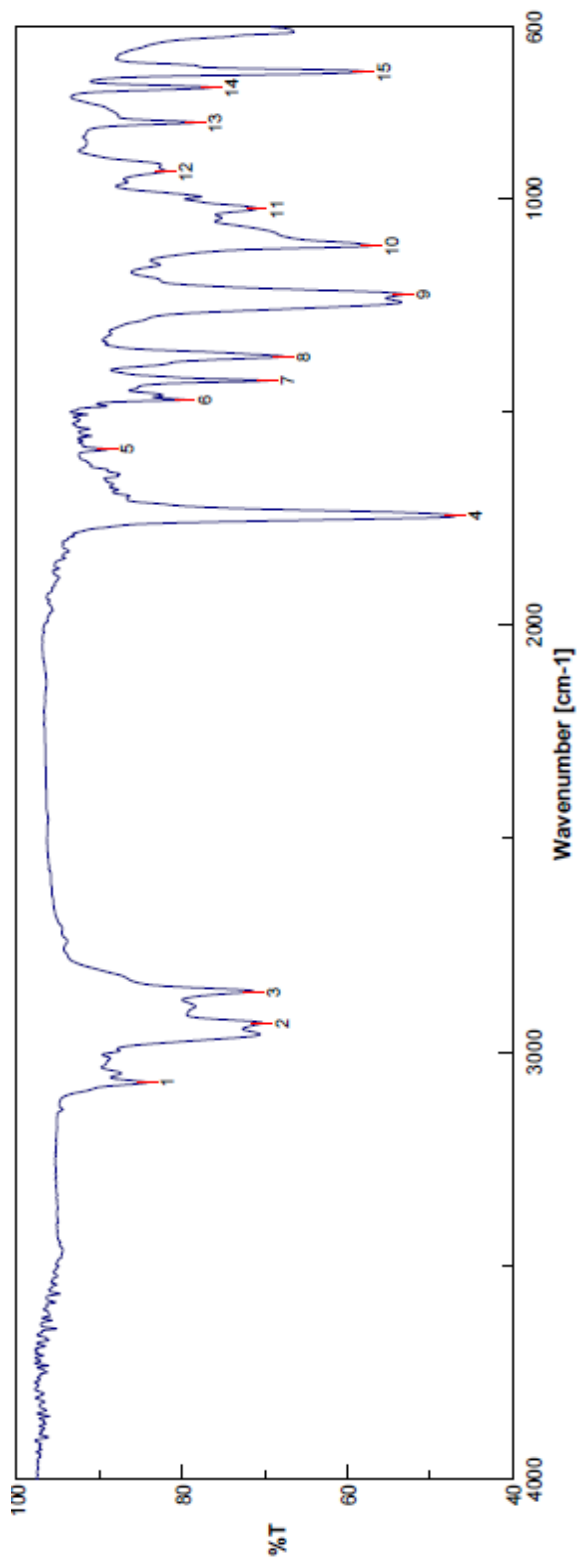
FTIR spectrum of compound **158**



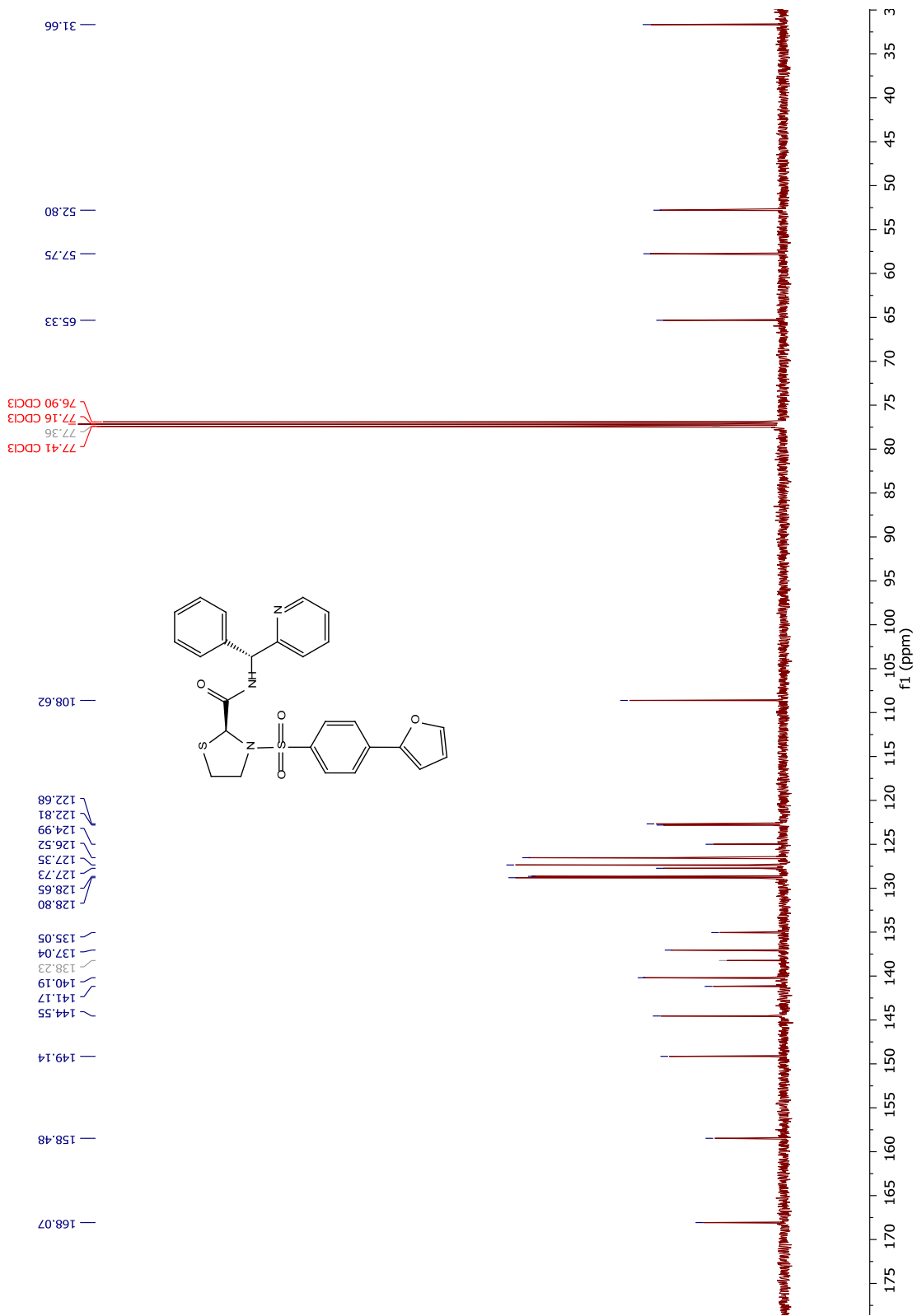
¹H NMR spectrum of compound 159



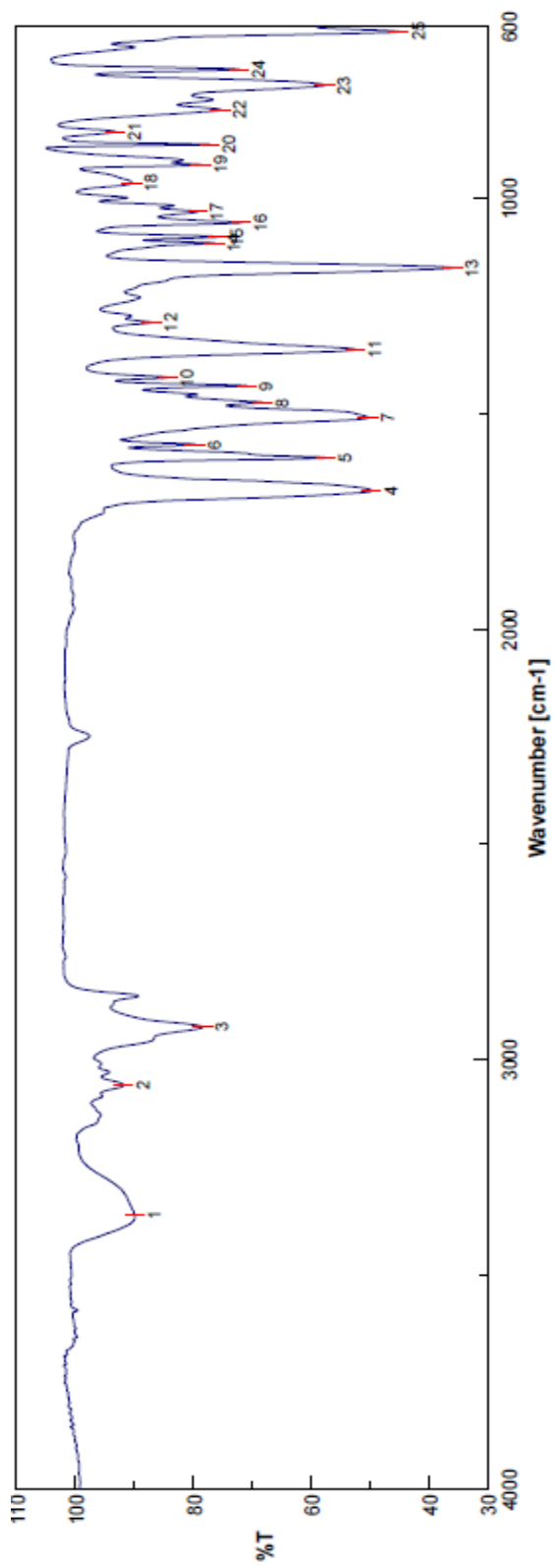
¹³C NMR spectrum of compound 159



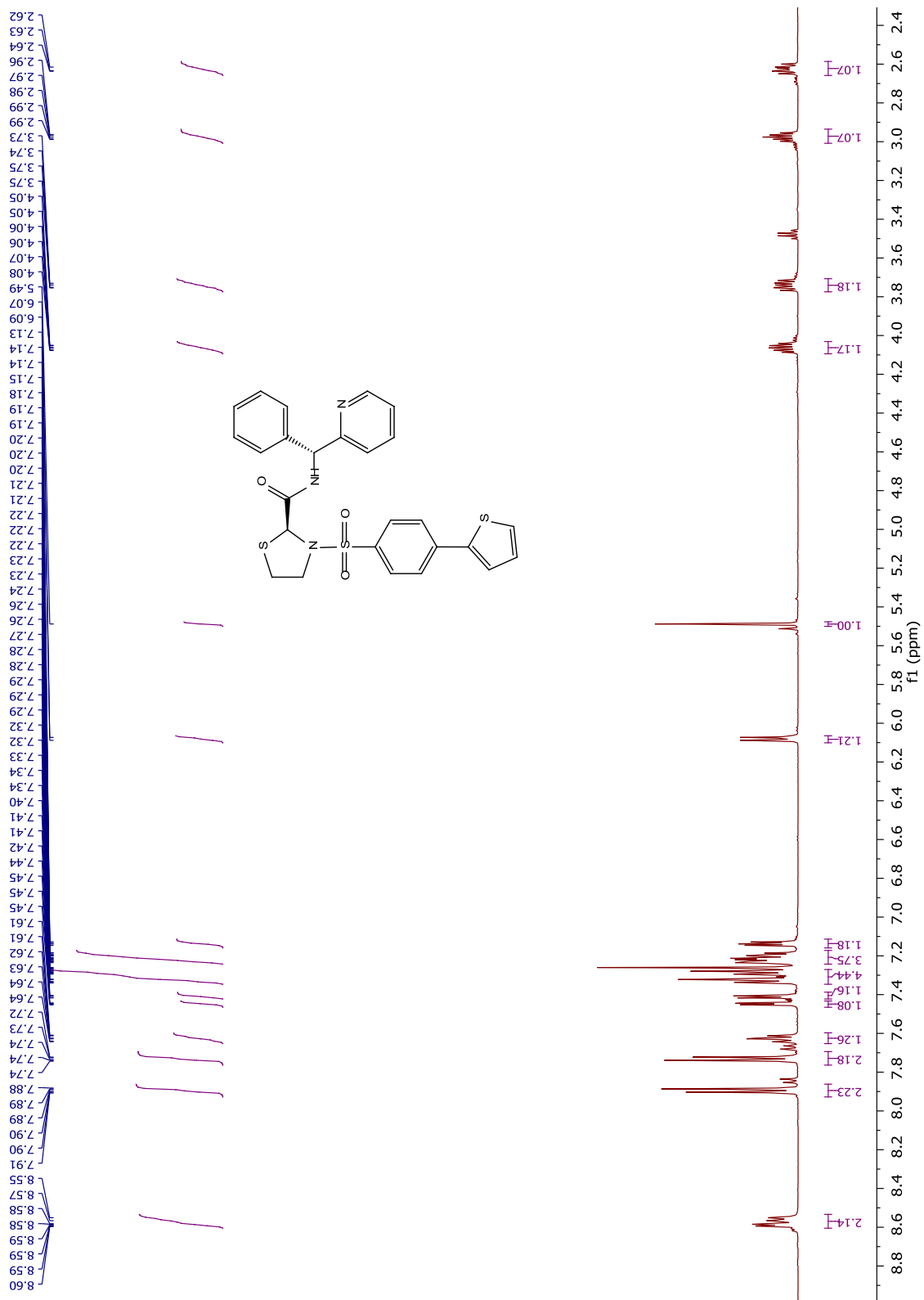
FTIR spectrum of compound **159**



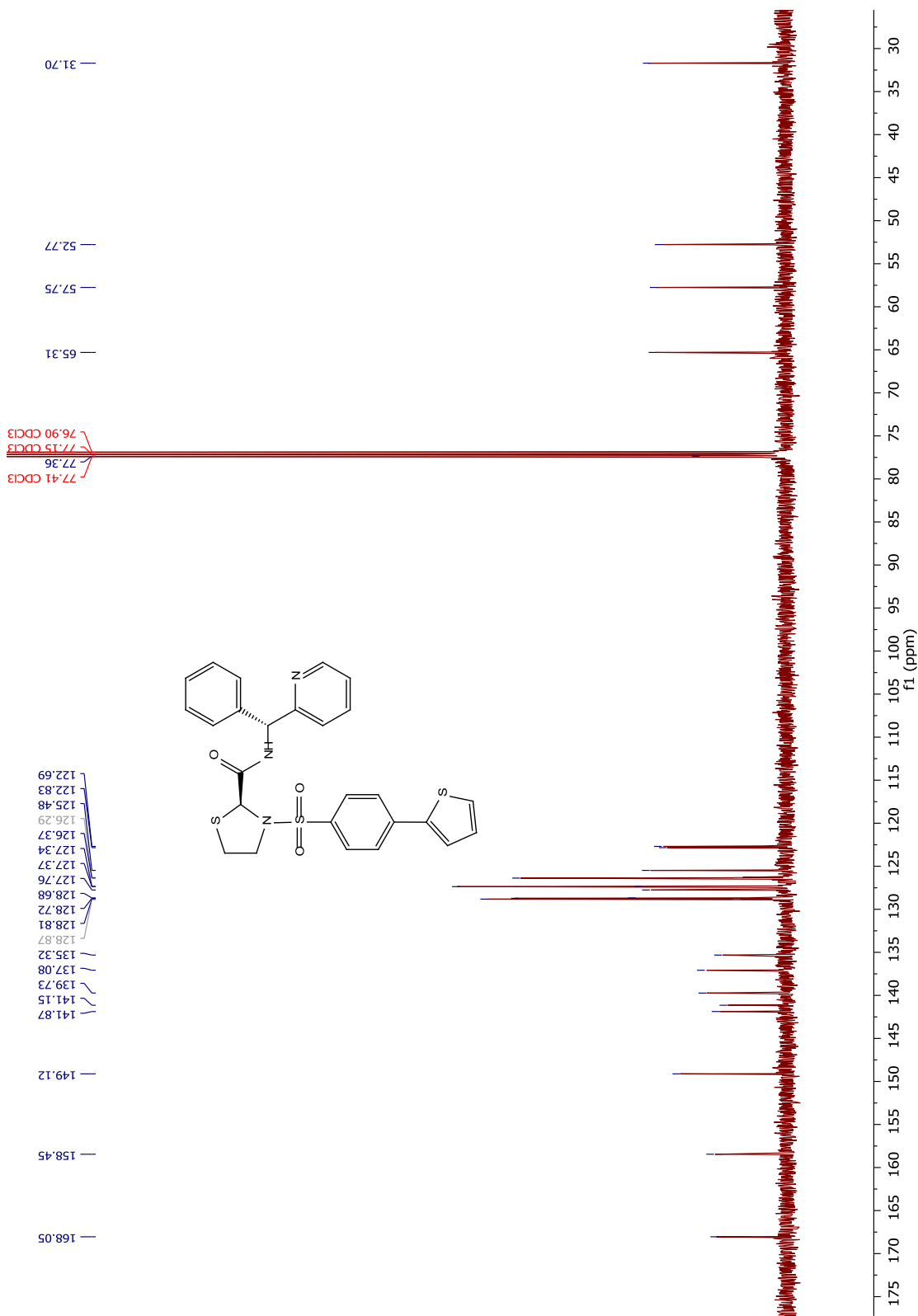
¹³C NMR spectrum of compound **202**



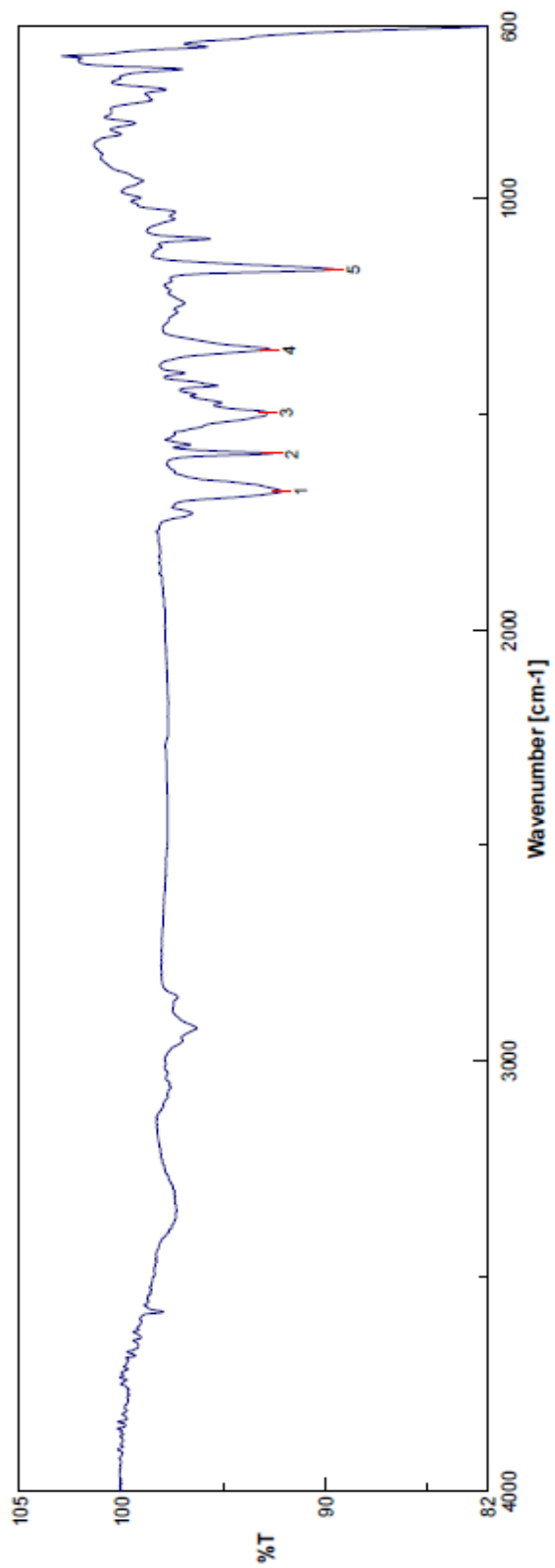
FTIR spectrum of compound **202**



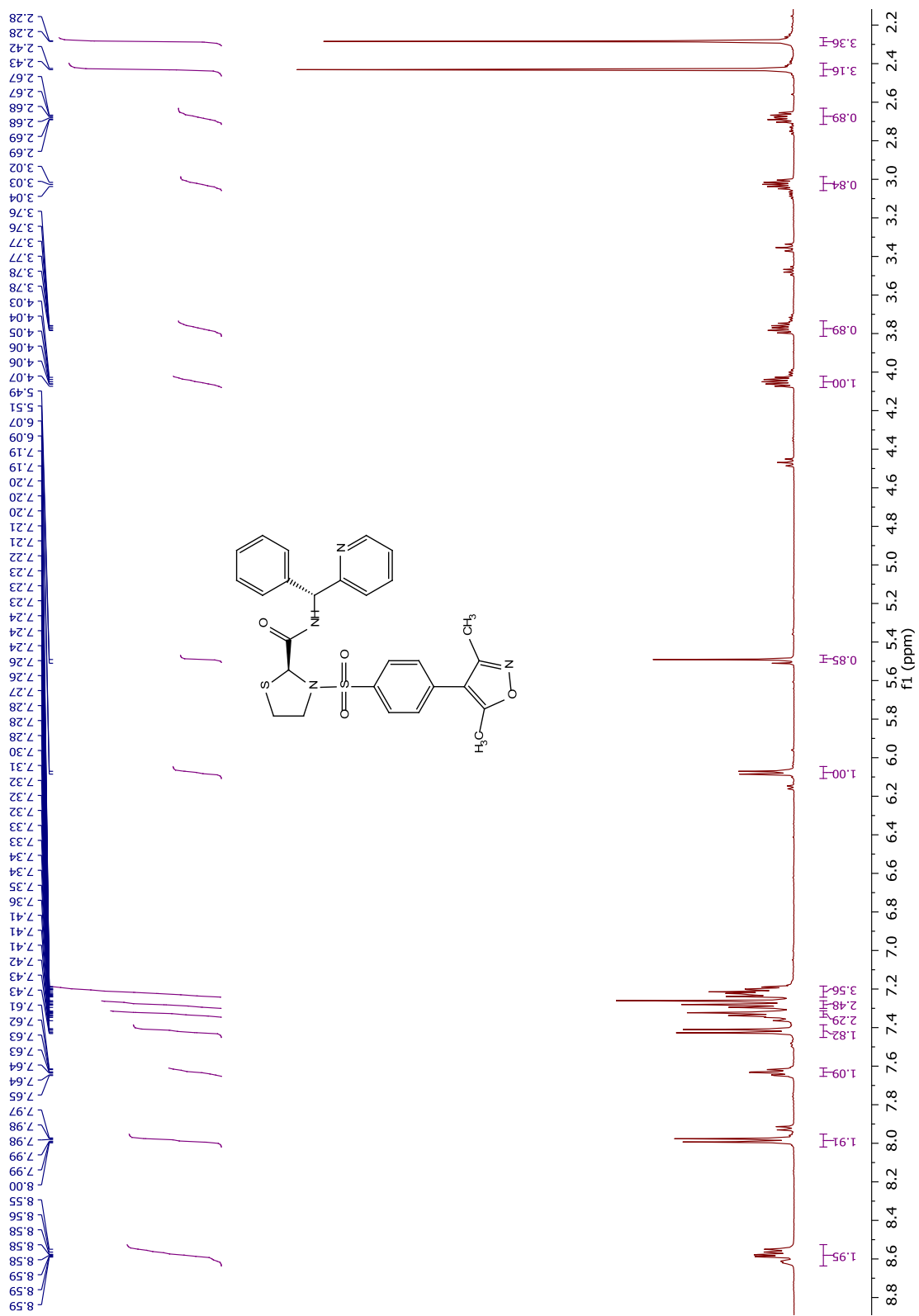
¹H NMR spectrum of compound 203



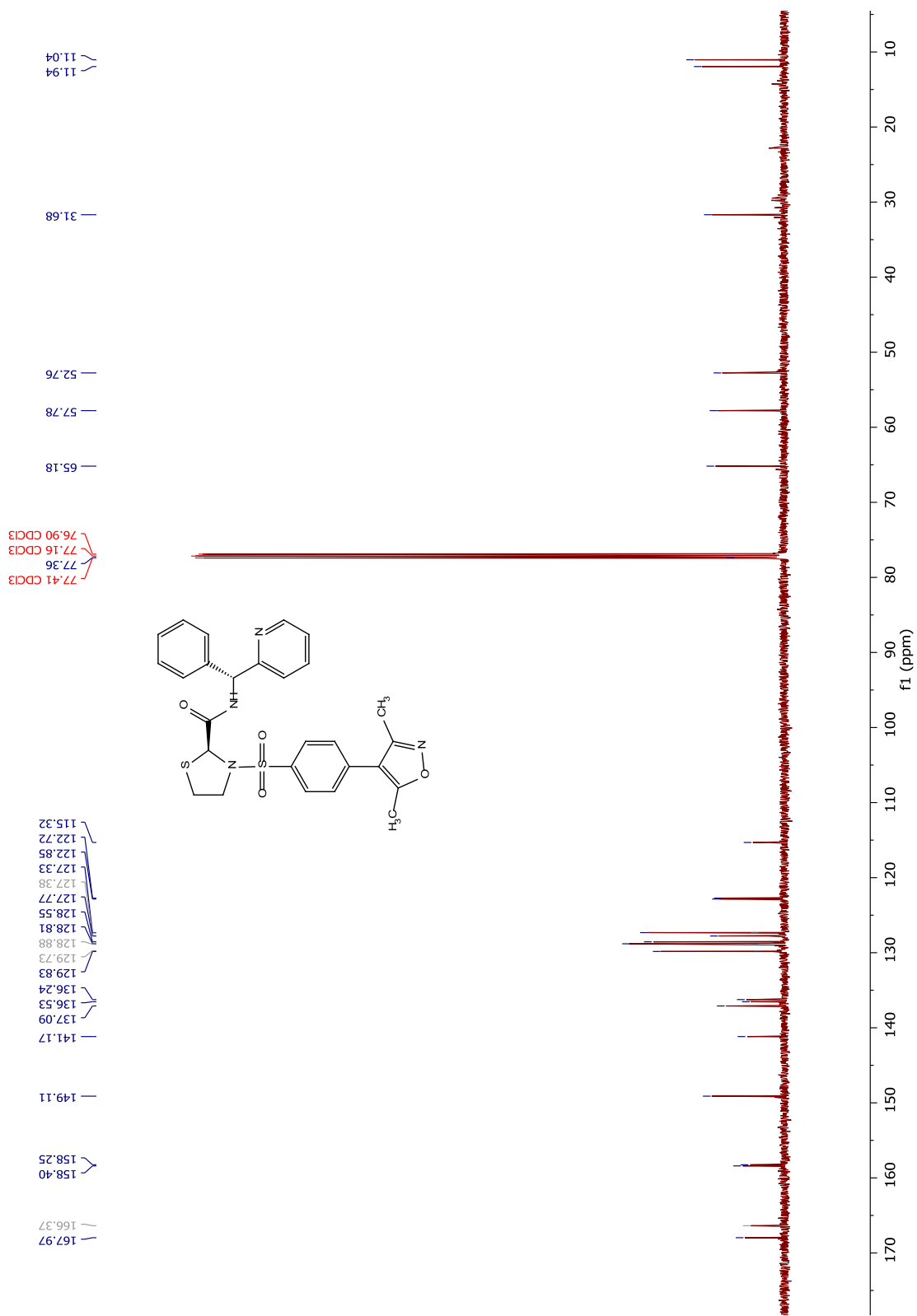
¹³C NMR spectrum of compound 203



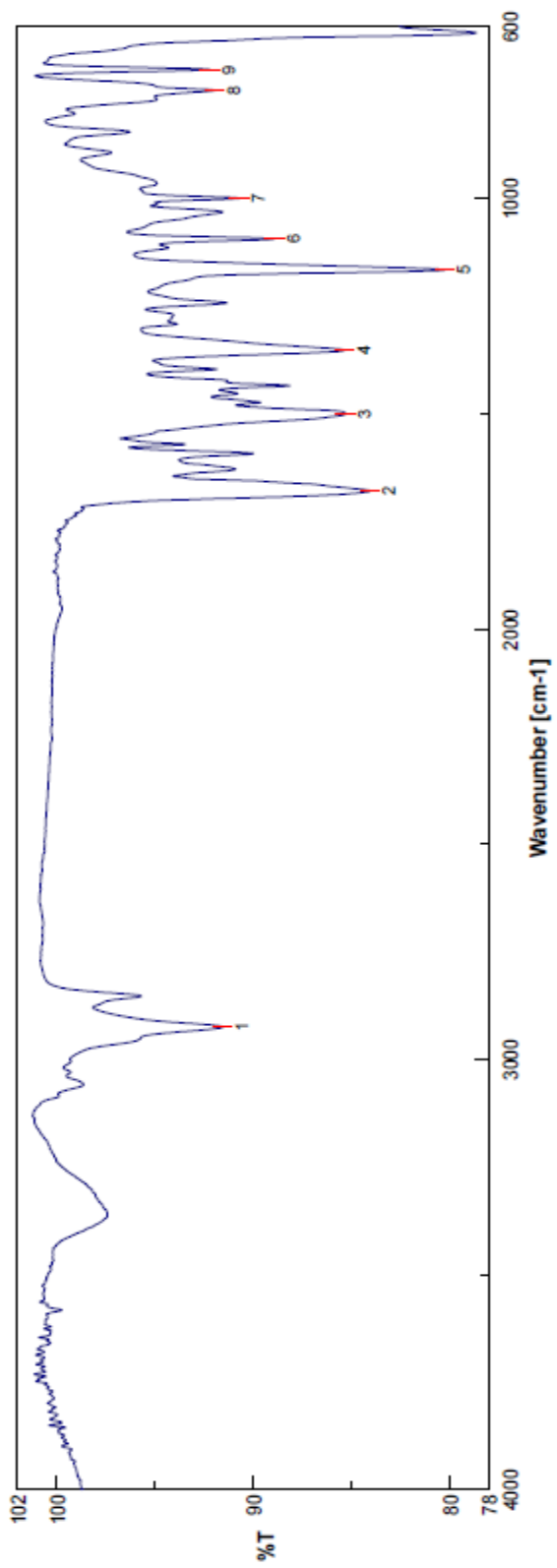
FTIR spectrum of compound **203**



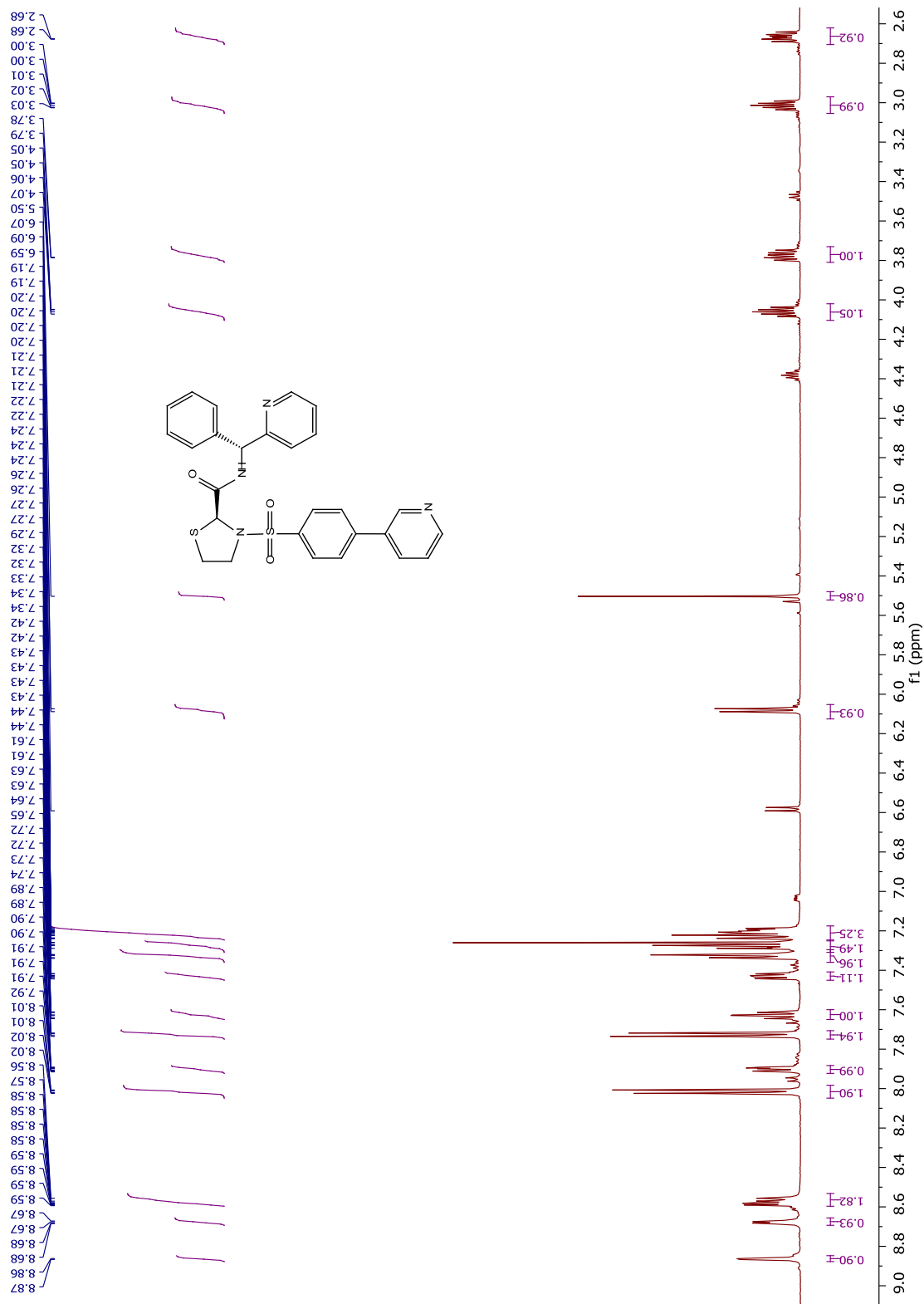
¹H NMR spectrum of compound 204



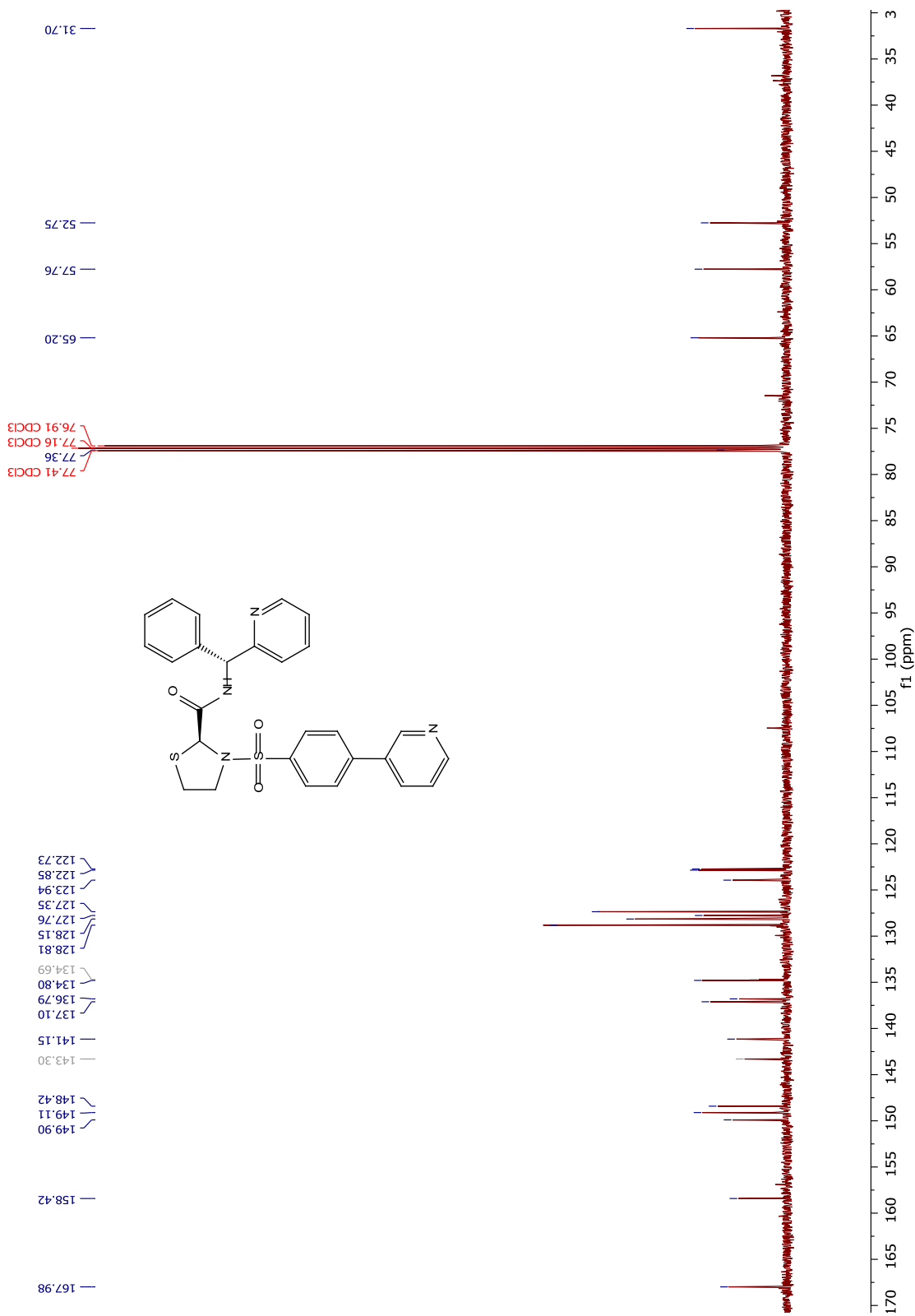
¹³C NMR spectrum of compound **204**



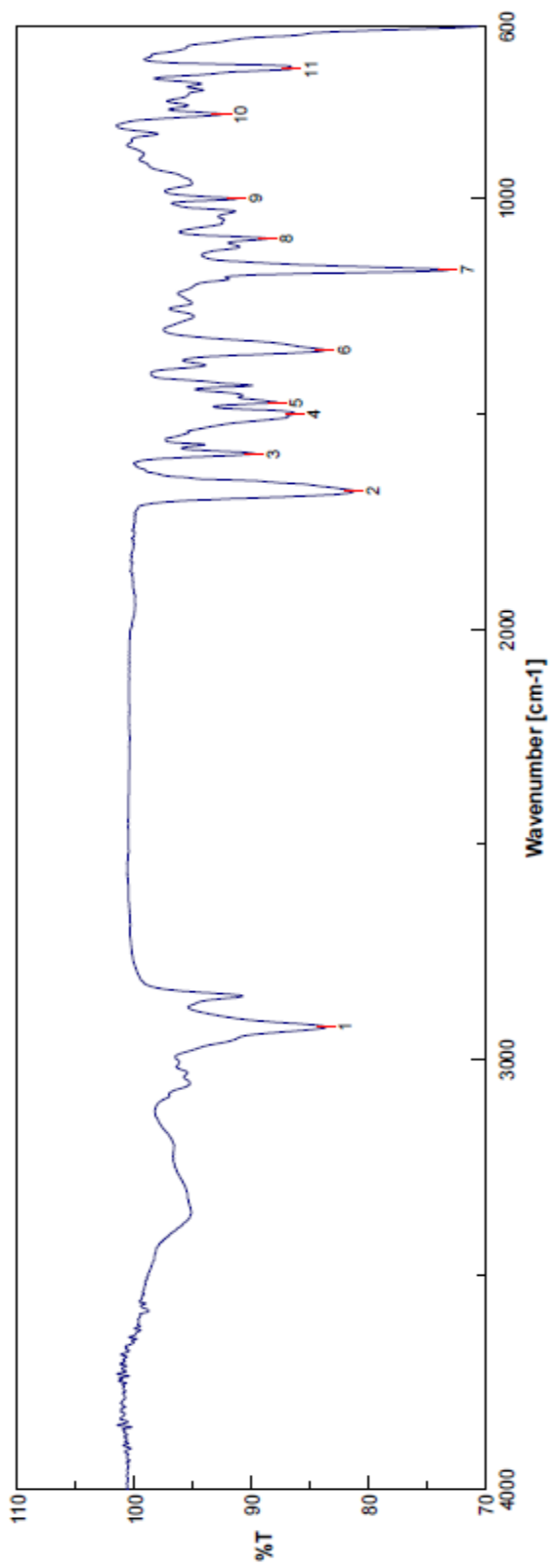
FTIR spectrum of compound **204**



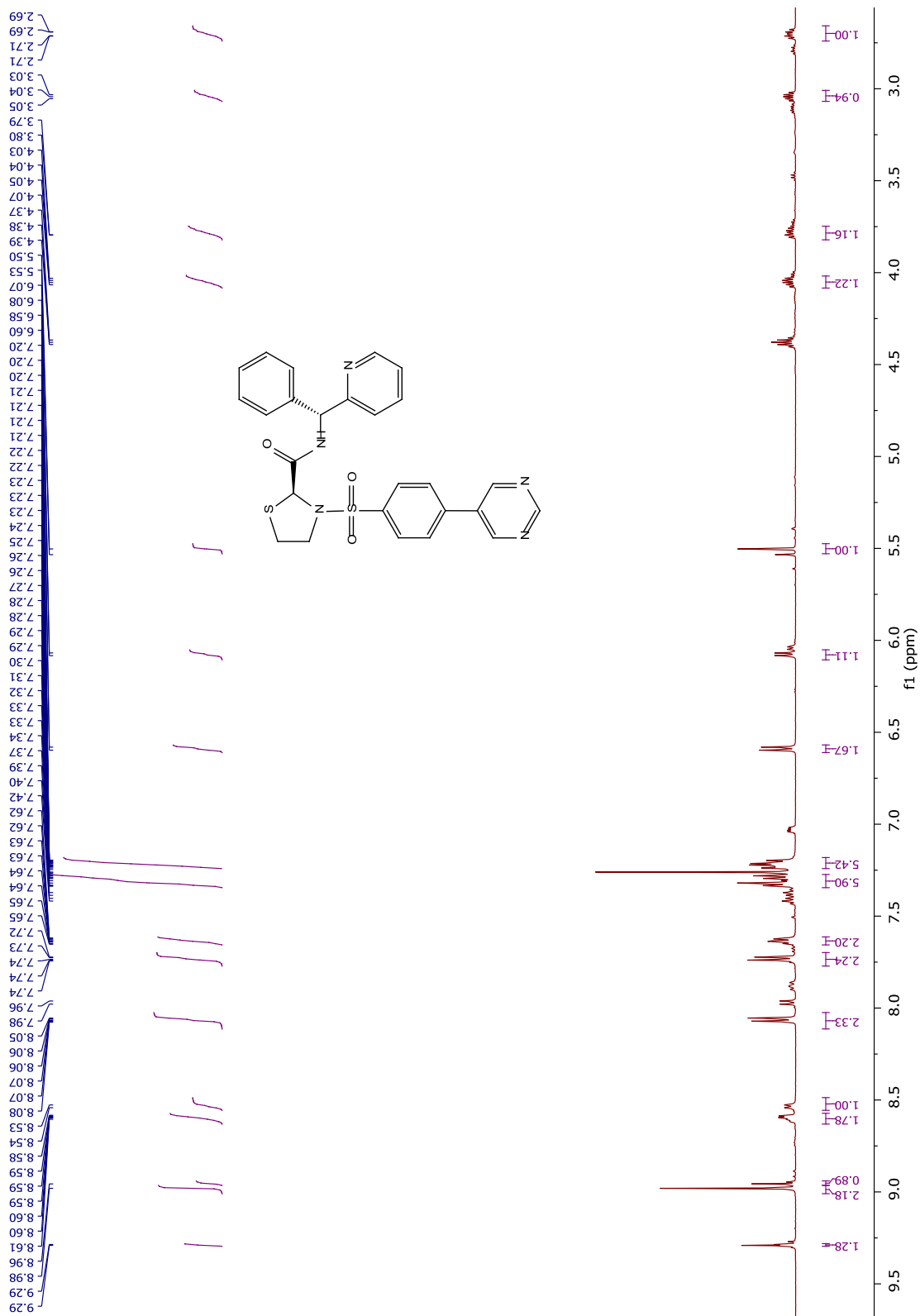
¹H NMR spectrum of compound 205



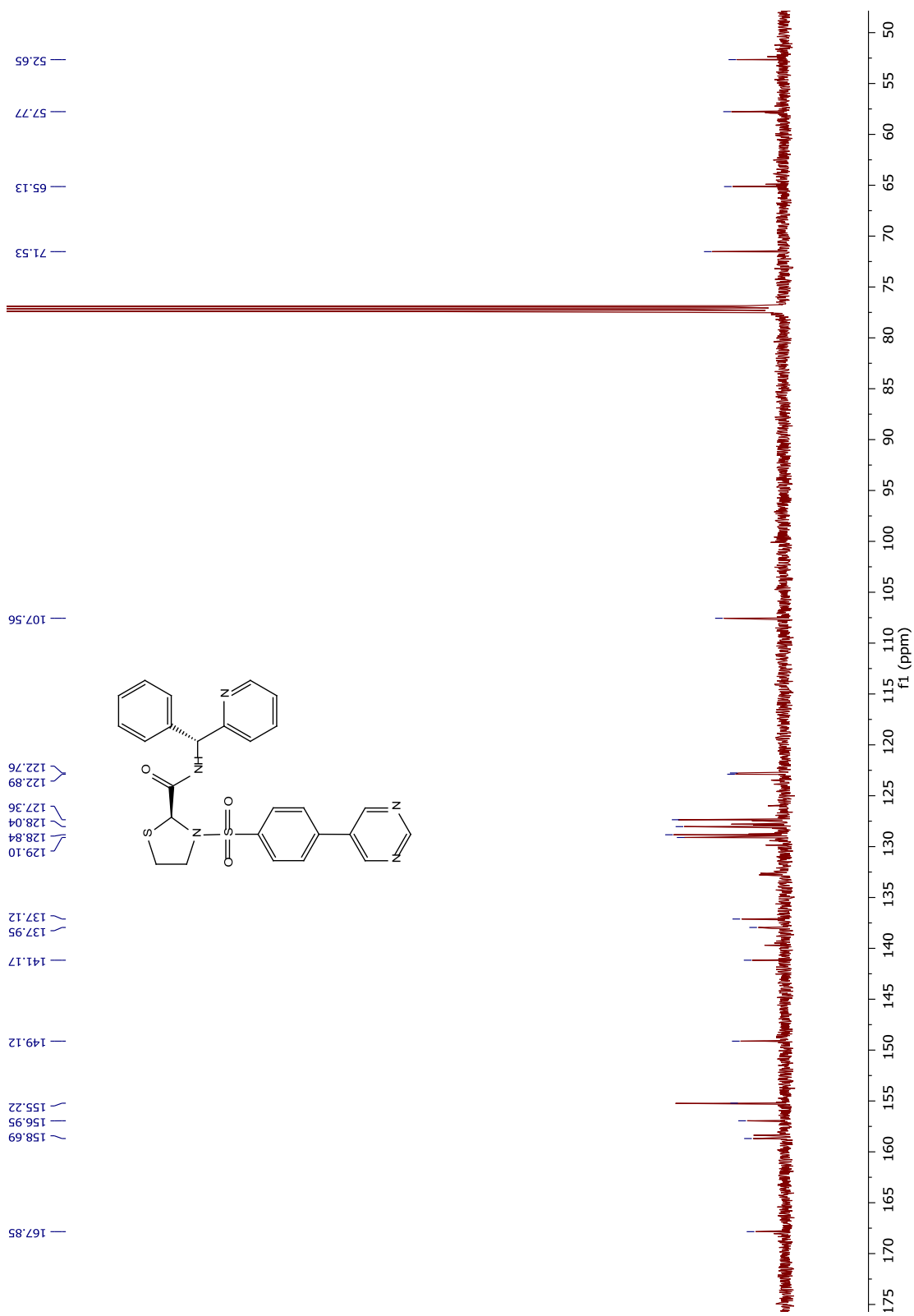
¹³C NMR spectrum of compound 205



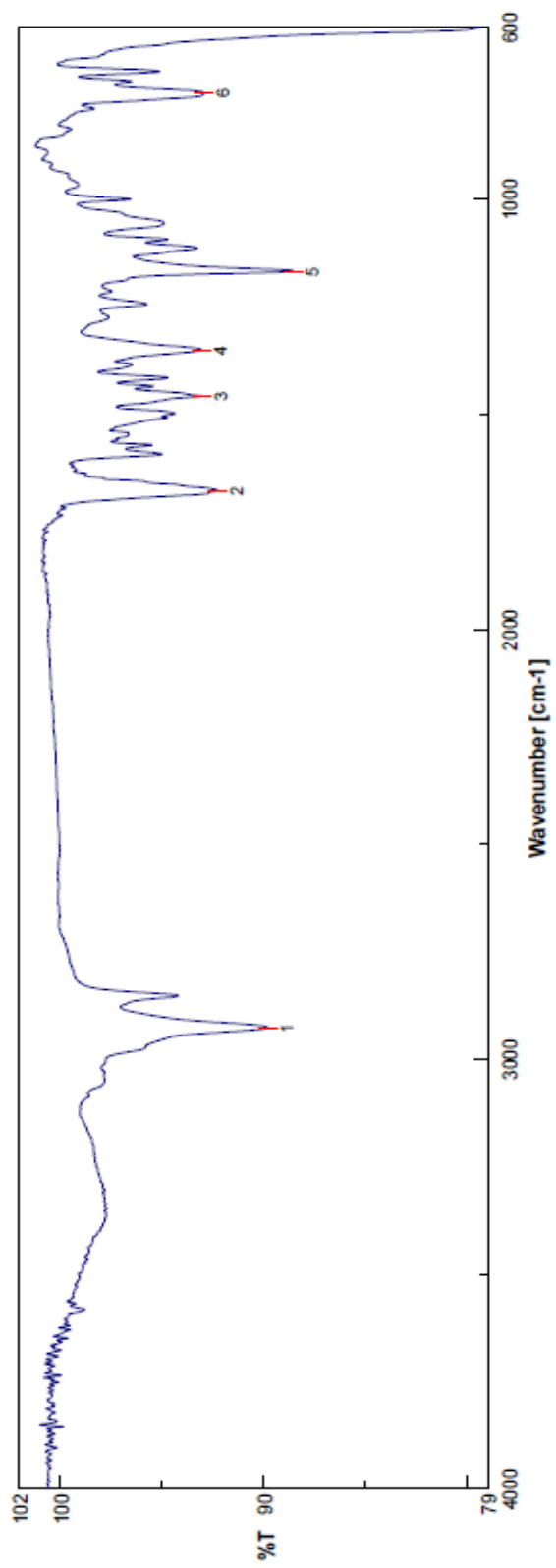
FTIR spectrum of compound **205**



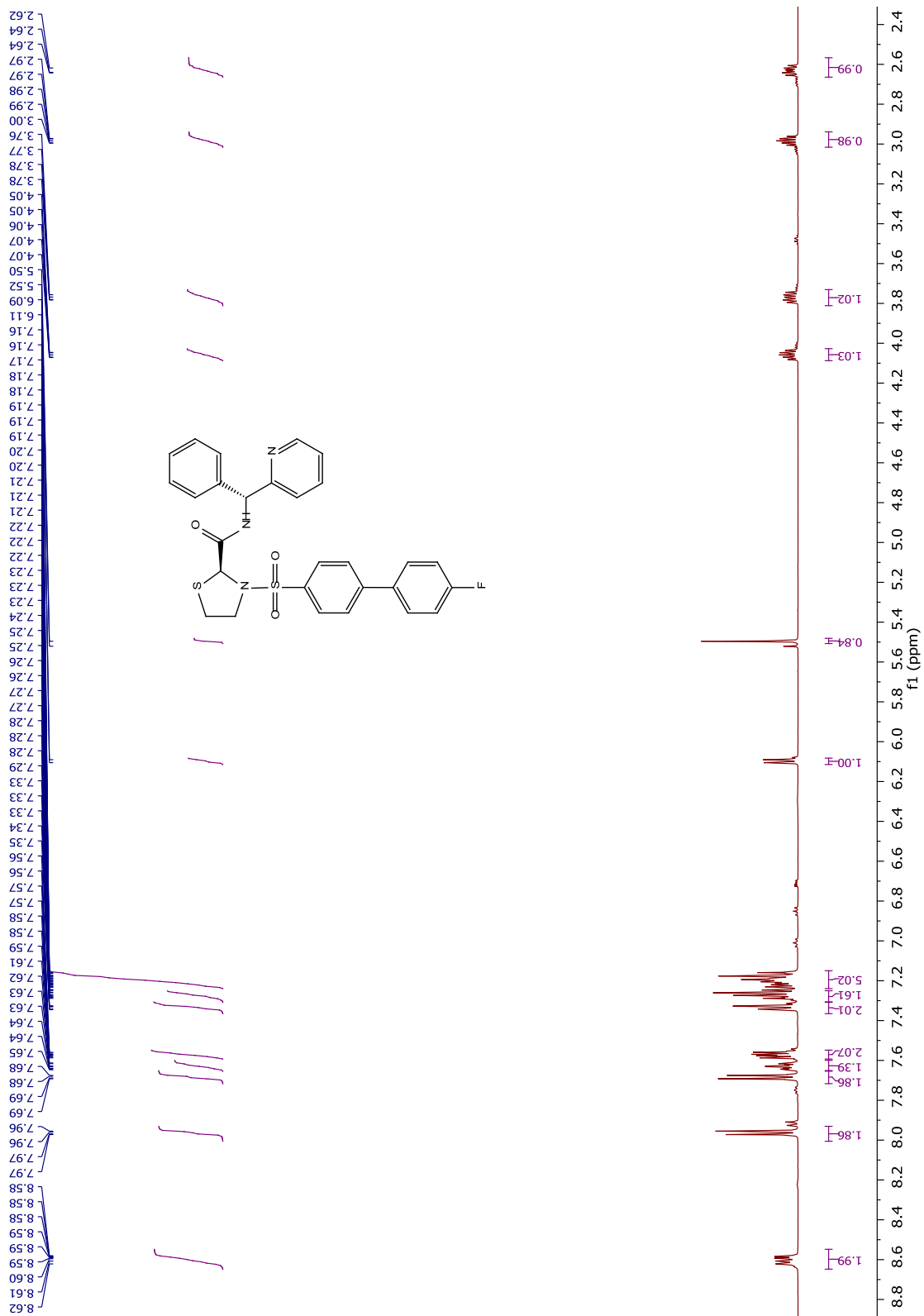
¹H NMR spectrum of compound 206



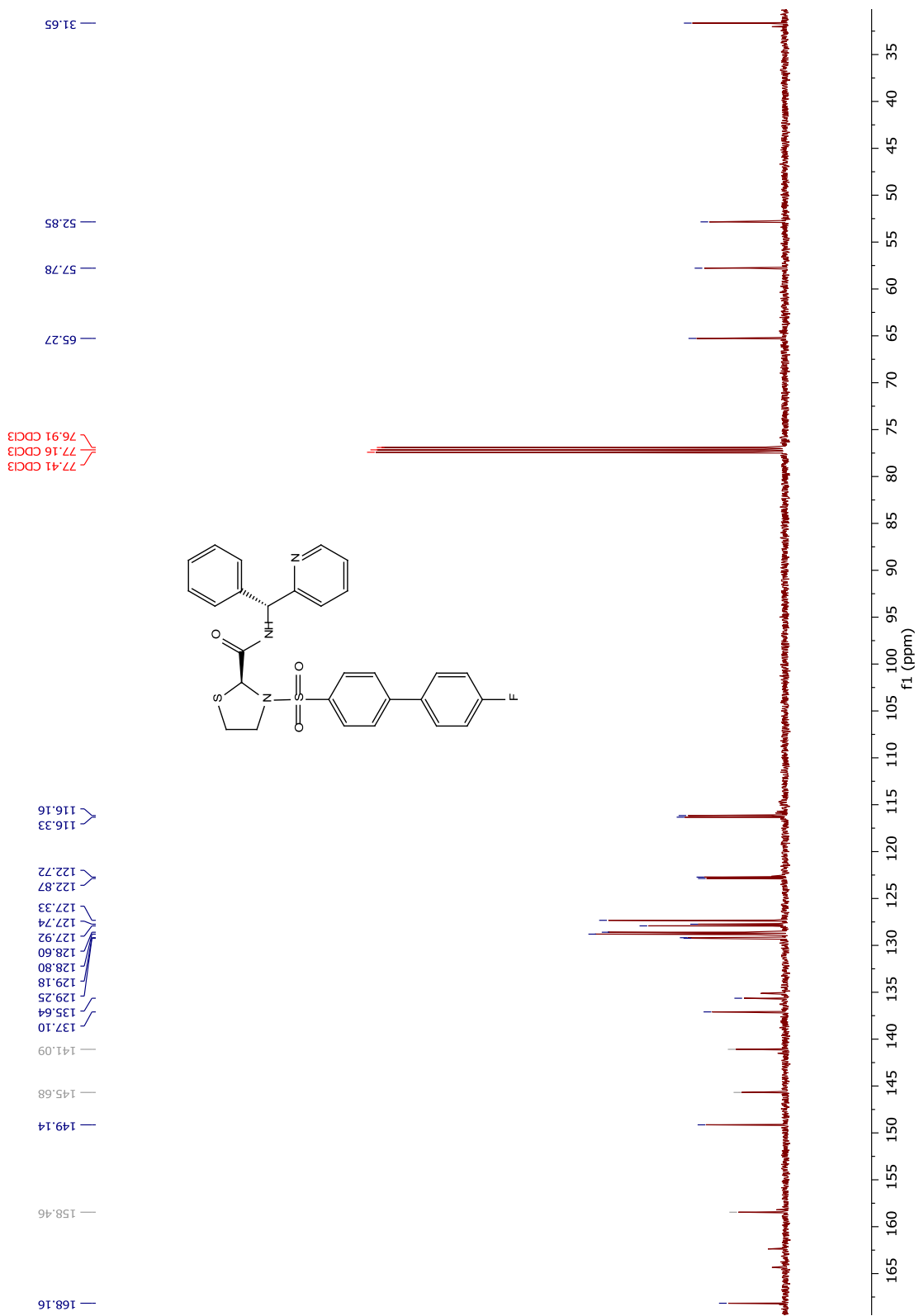
¹³C NMR spectrum of compound 206



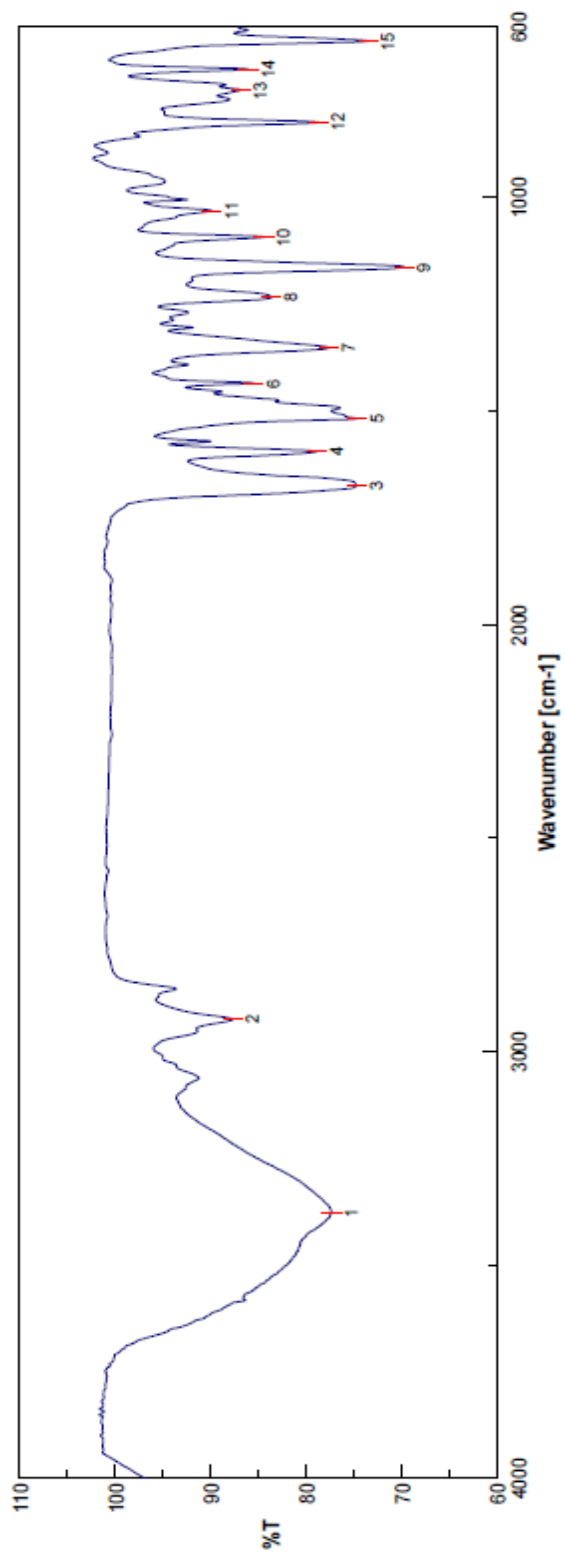
FTIR spectrum of compound **206**



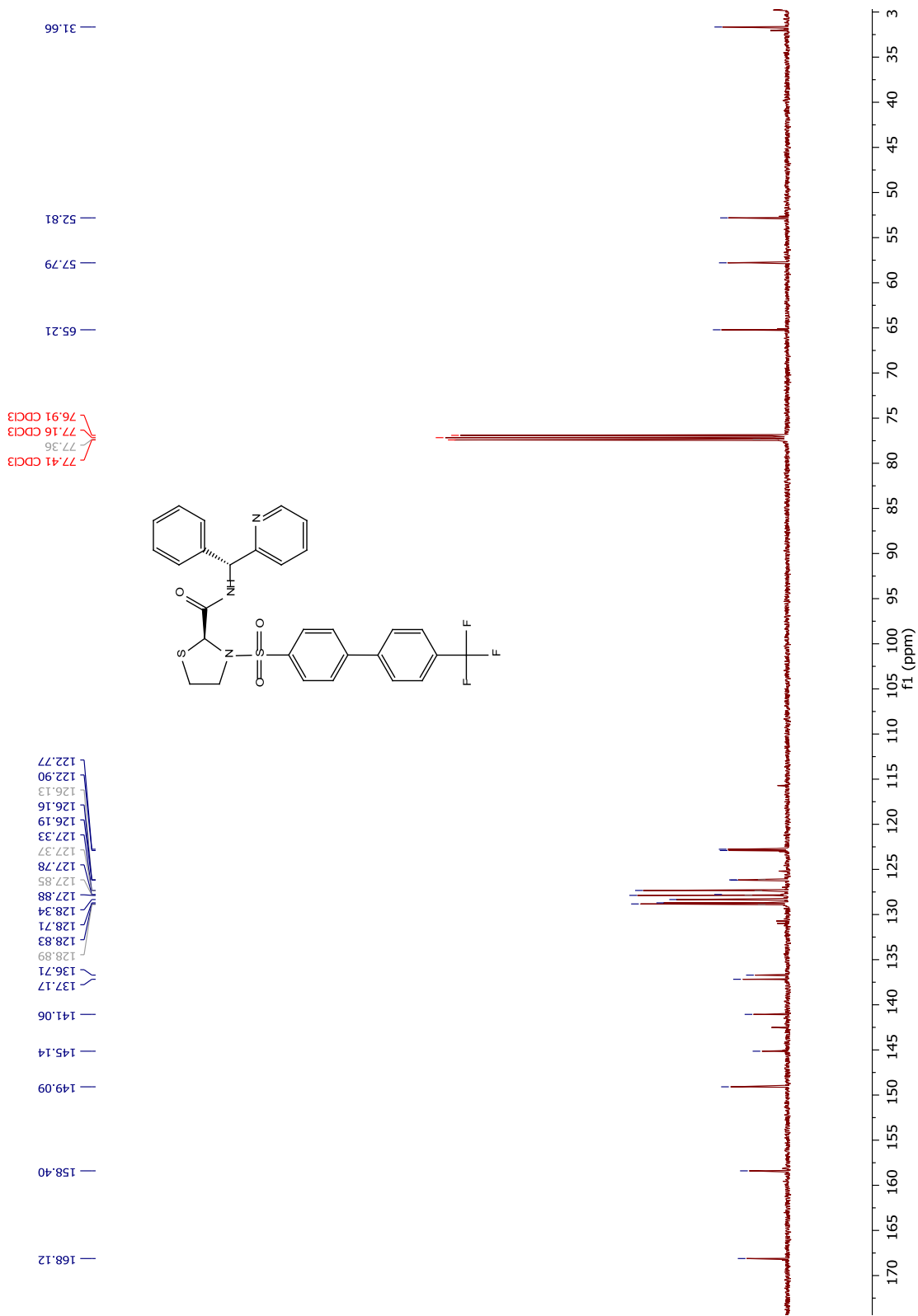
¹H NMR spectrum of compound 207



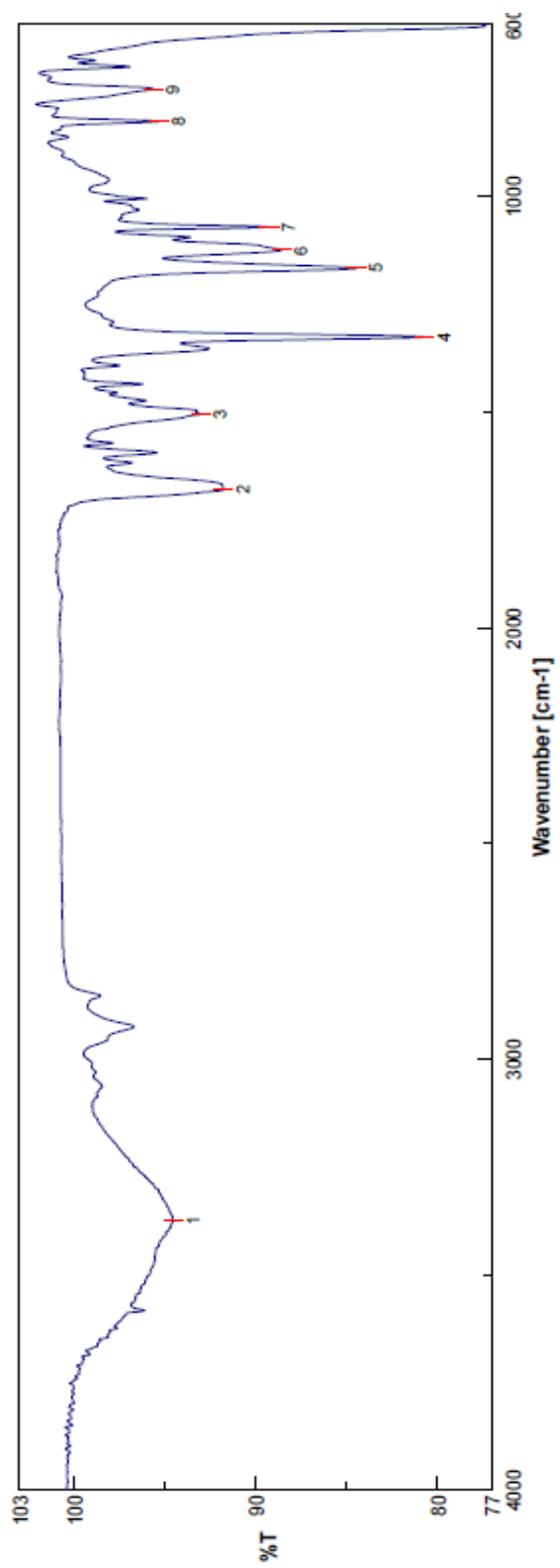
¹³C NMR spectrum of compound 207



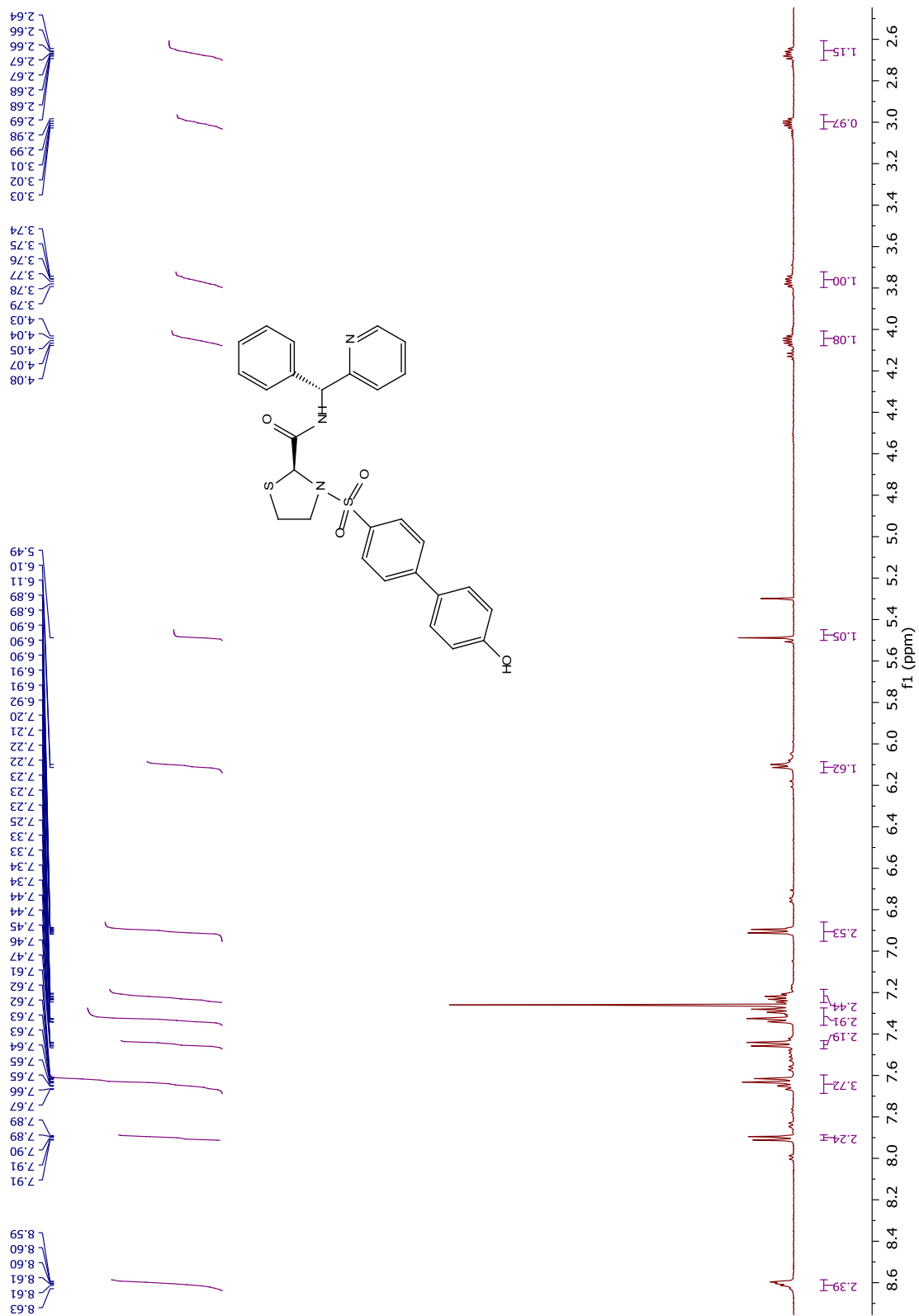
FTIR spectrum of compound **207**



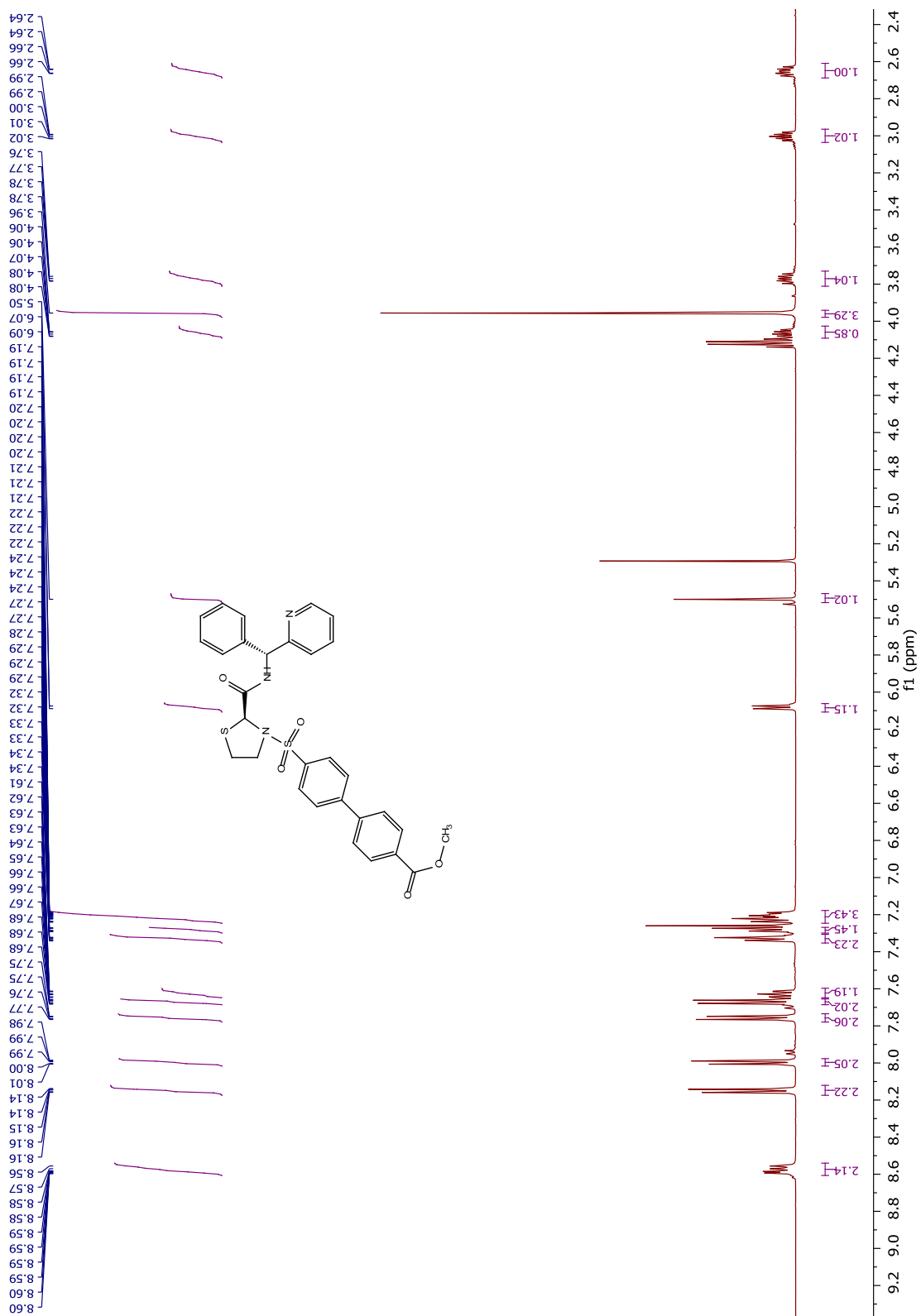
¹³C NMR spectrum of compound 208



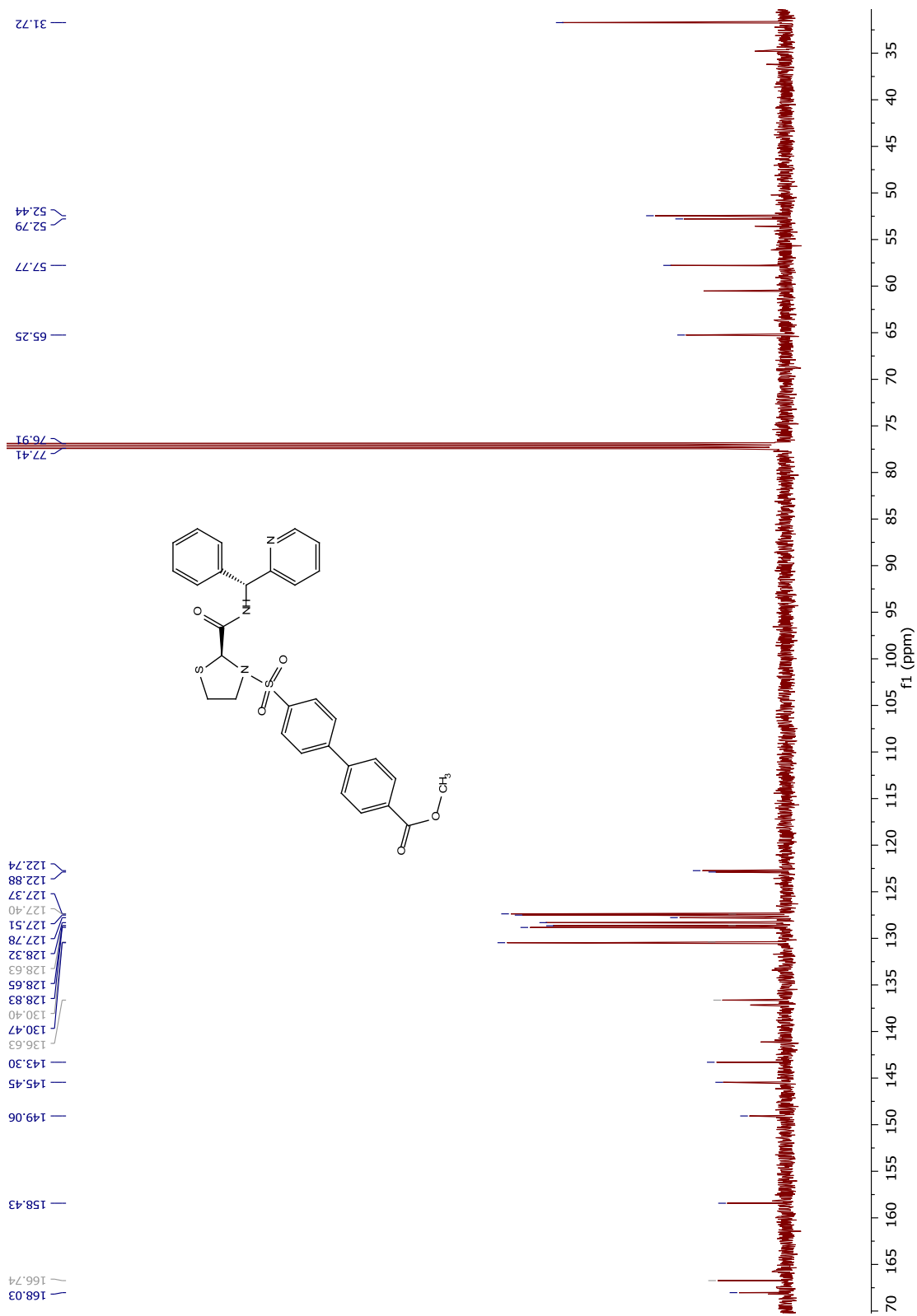
^{13}C NMR spectrum of compound **208**



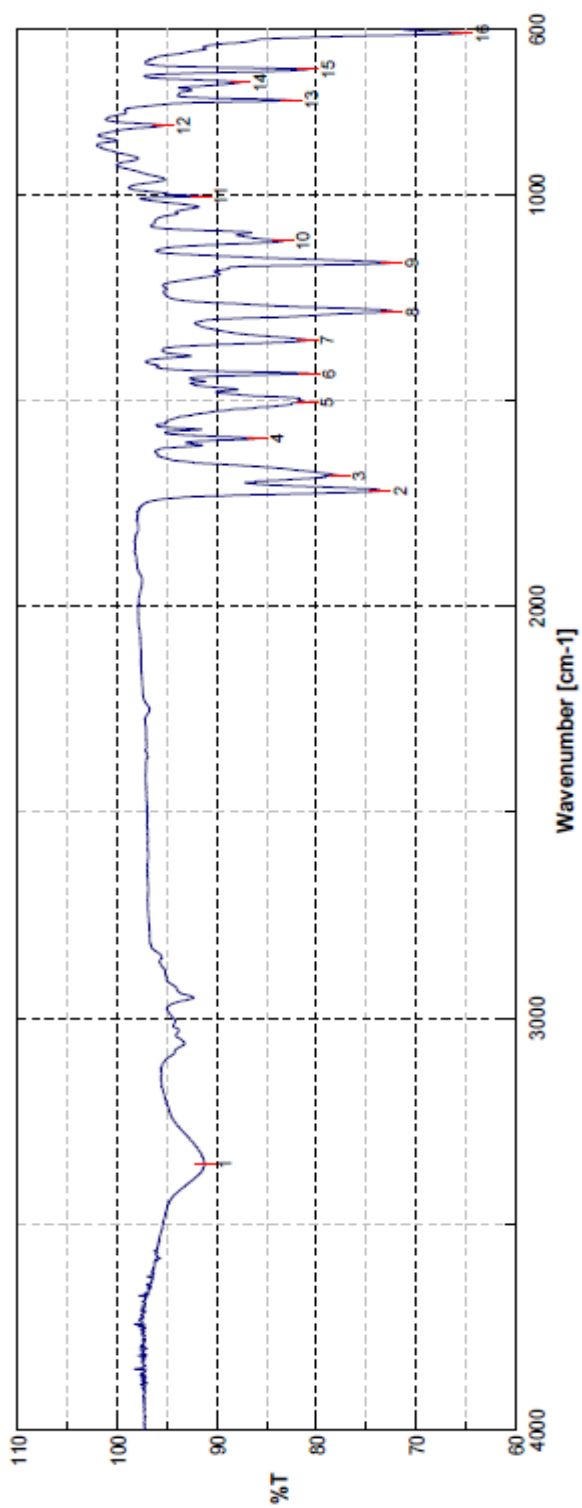
¹H NMR spectrum of compound 209



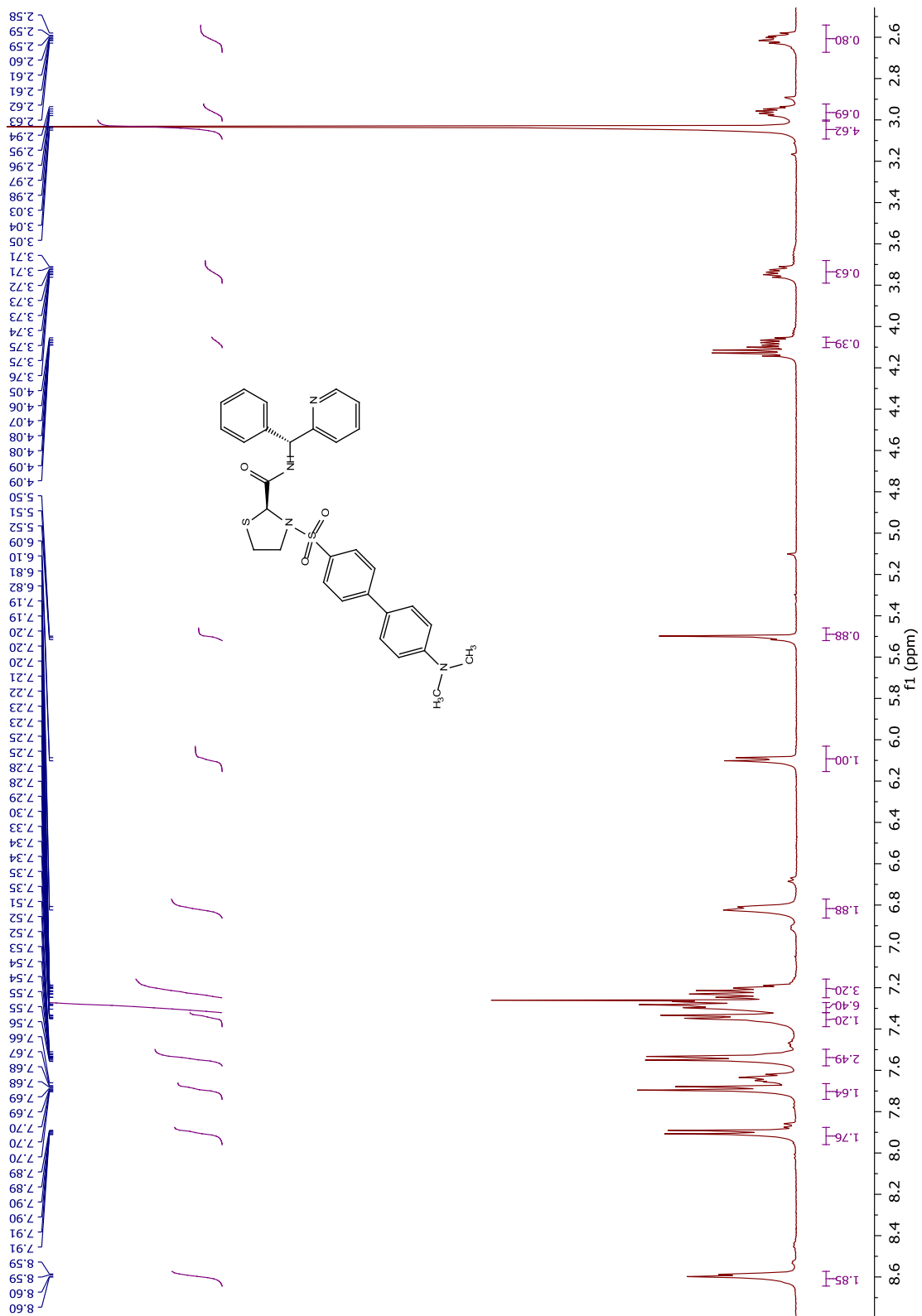
¹H NMR spectrum of compound 210



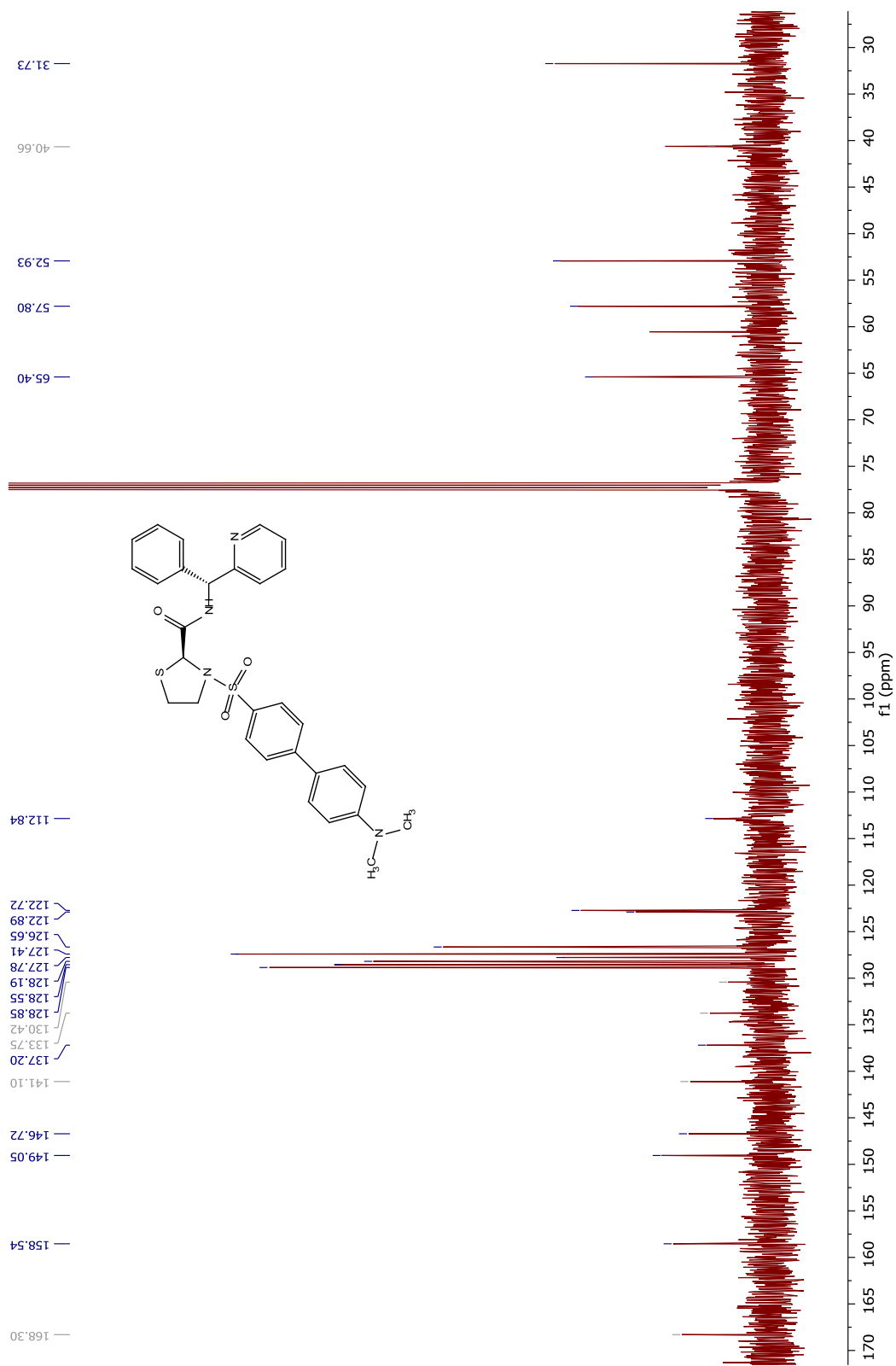
¹³C NMR spectrum of compound 210



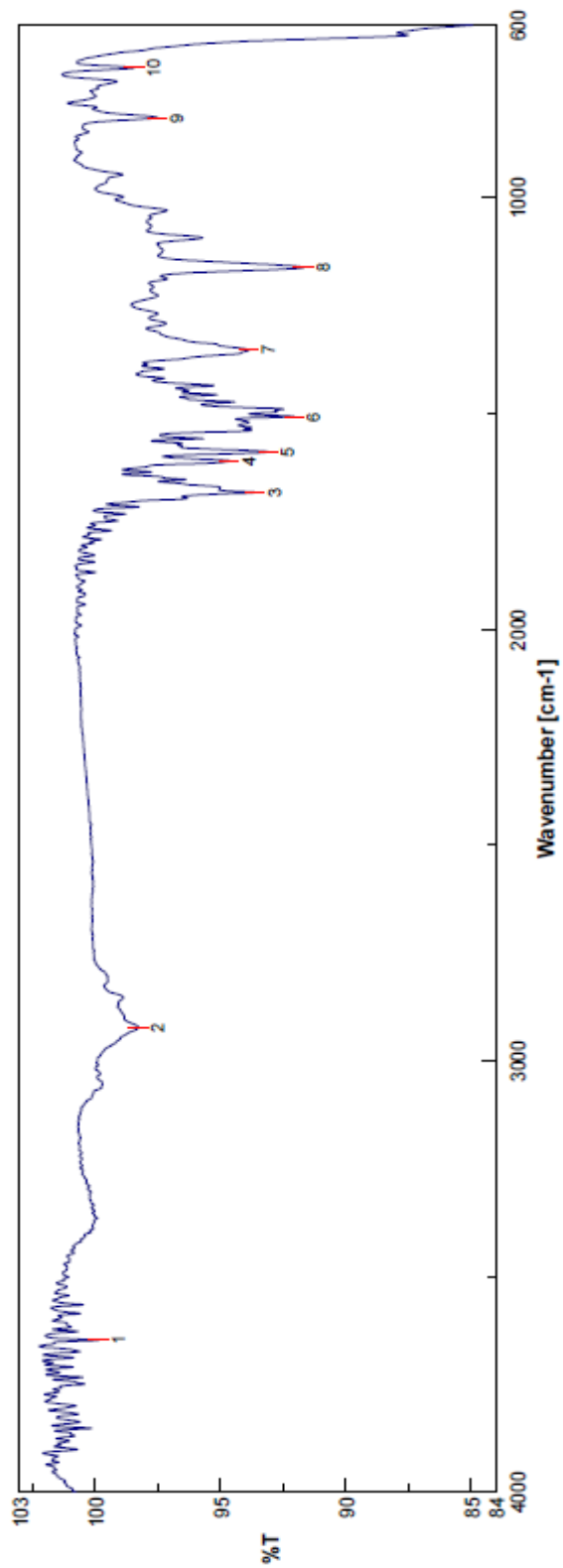
FTIR spectrum of compound **210**



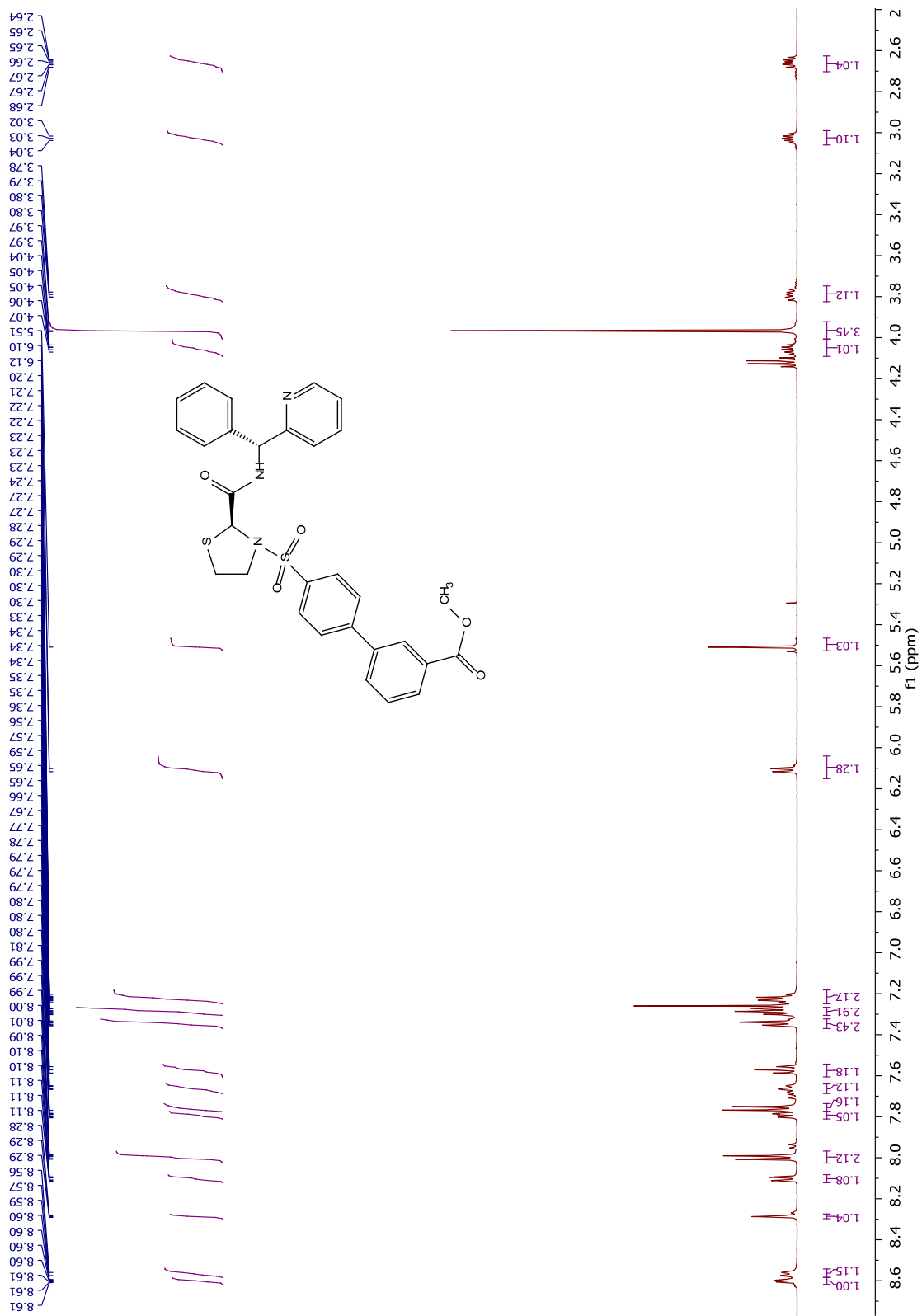
¹H NMR spectrum of compound 211



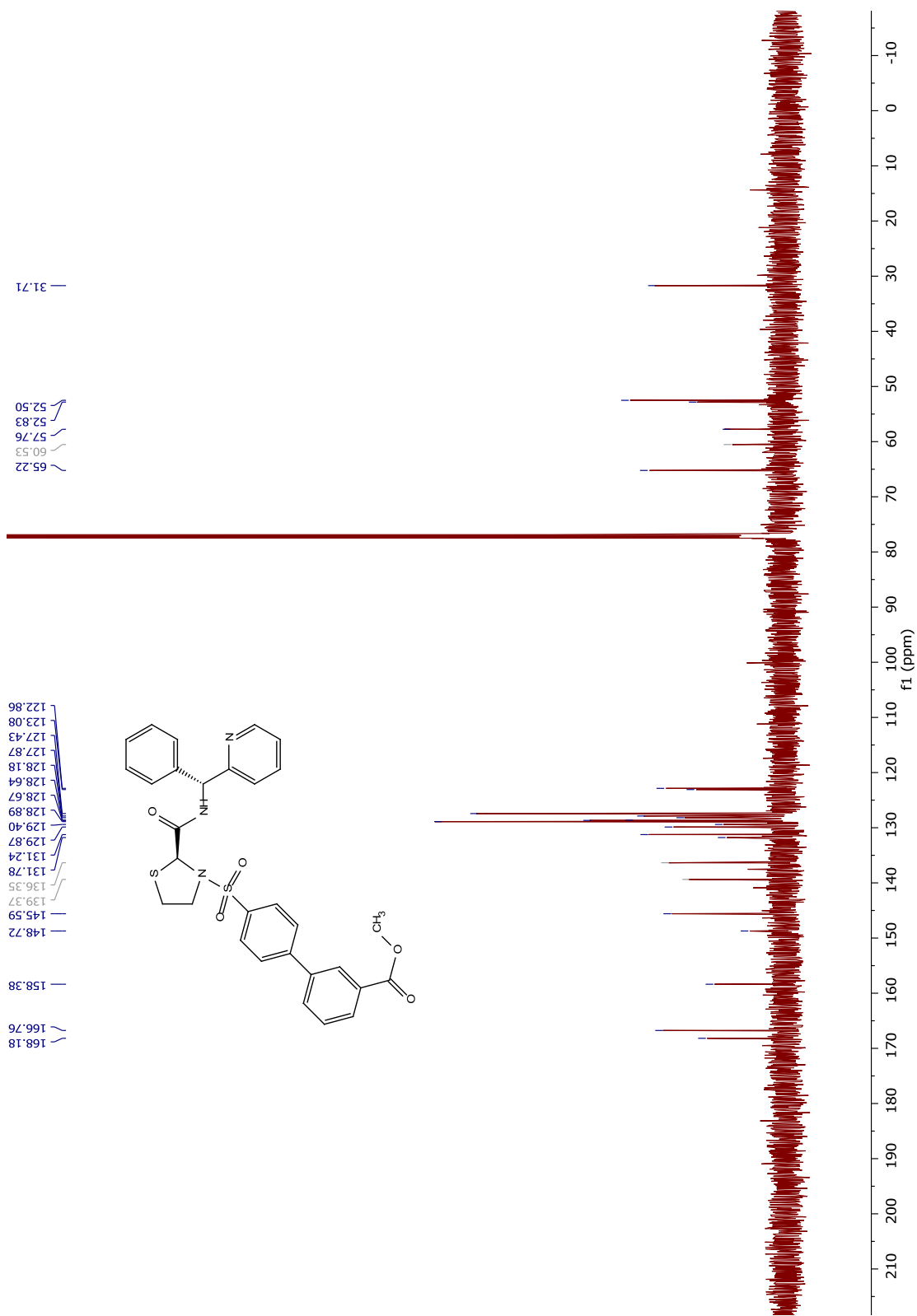
¹³C NMR spectrum of compound 211



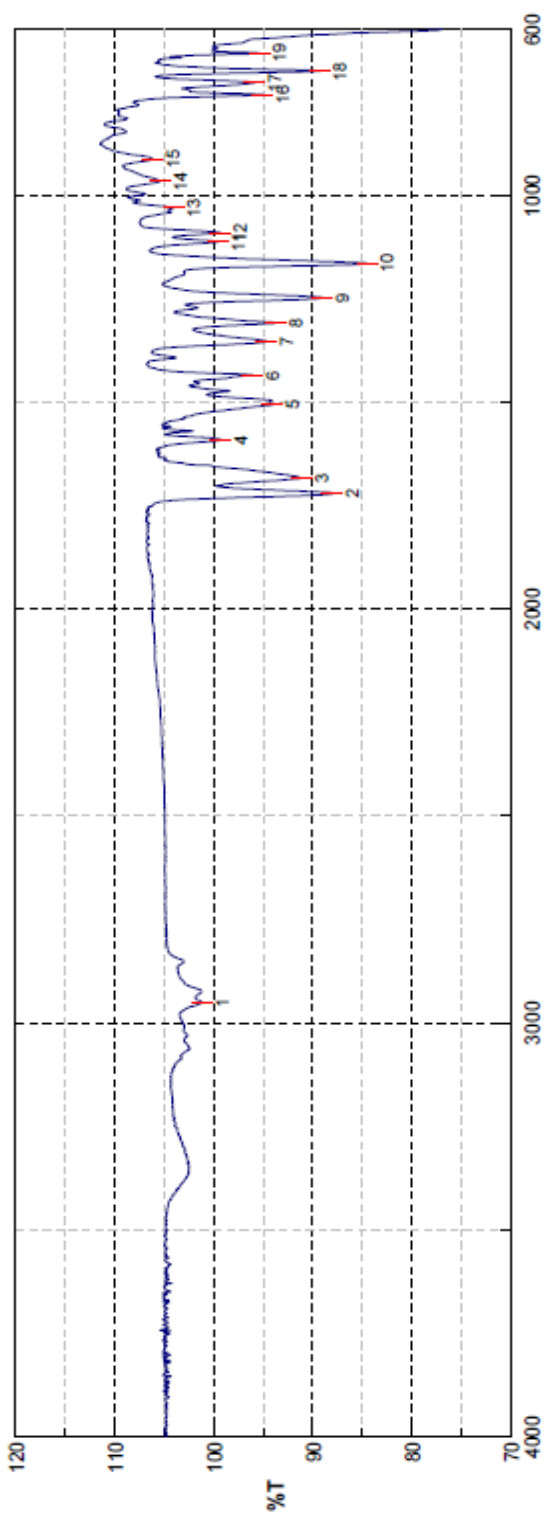
FTIR spectrum of compound 211



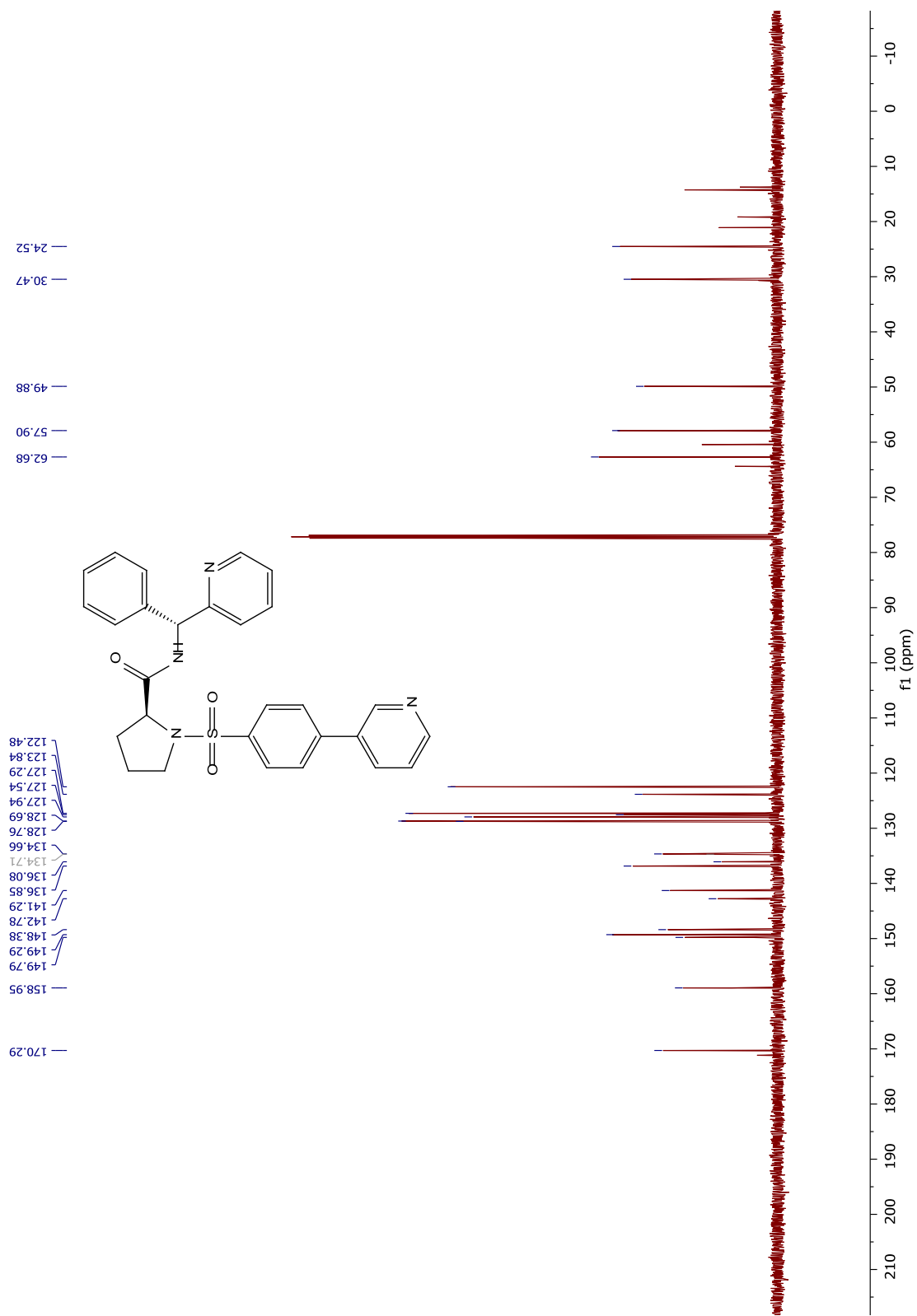
¹H NMR spectrum of compound 212



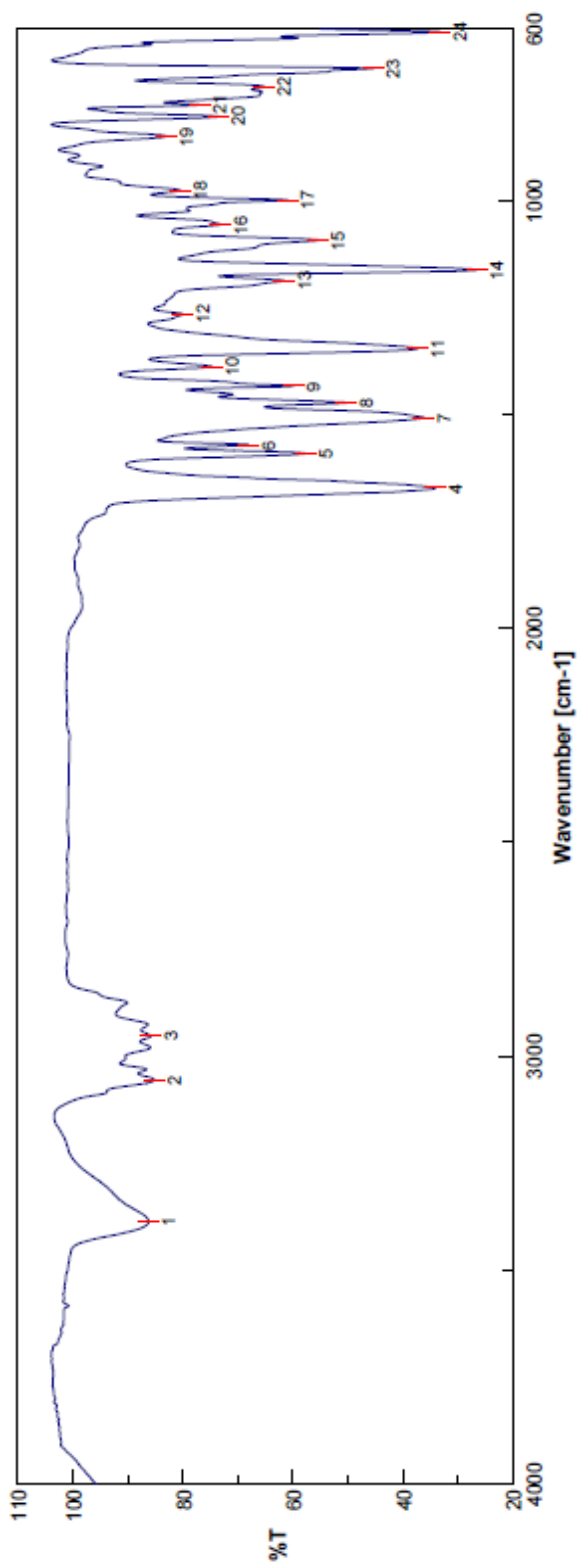
¹³C NMR spectrum of compound **212**



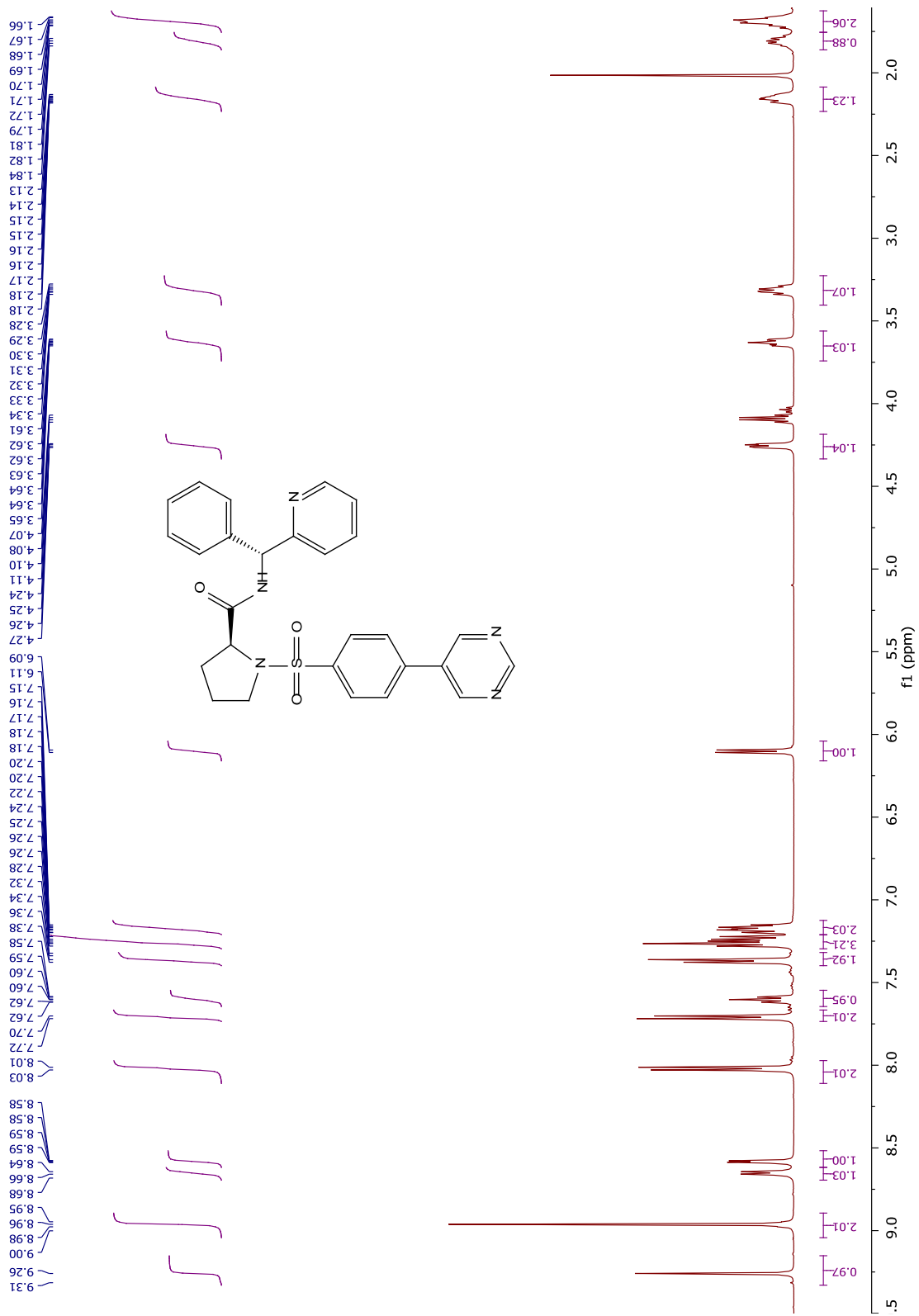
FTIR spectrum of compound 212



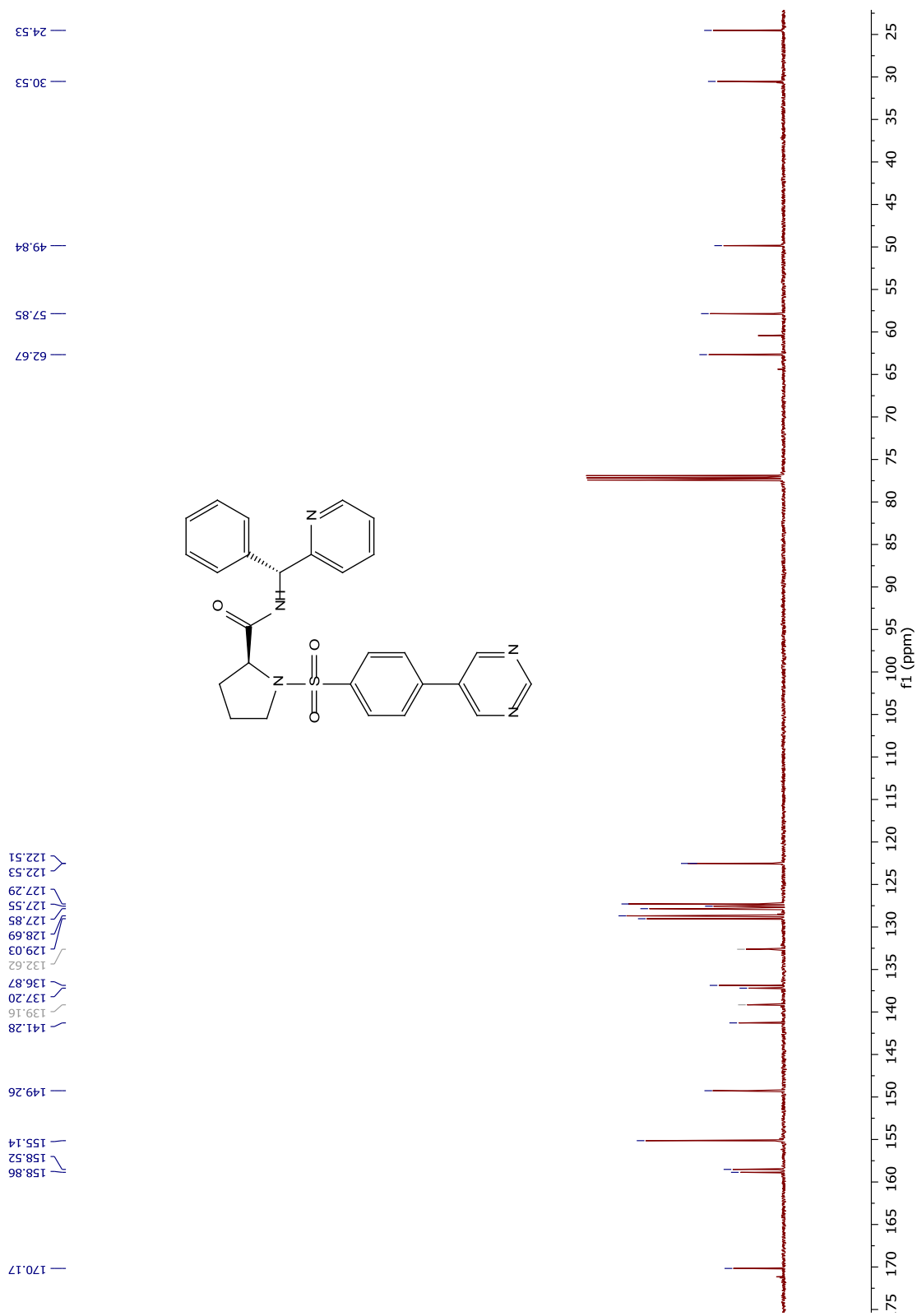
¹³C NMR spectrum of compound 213



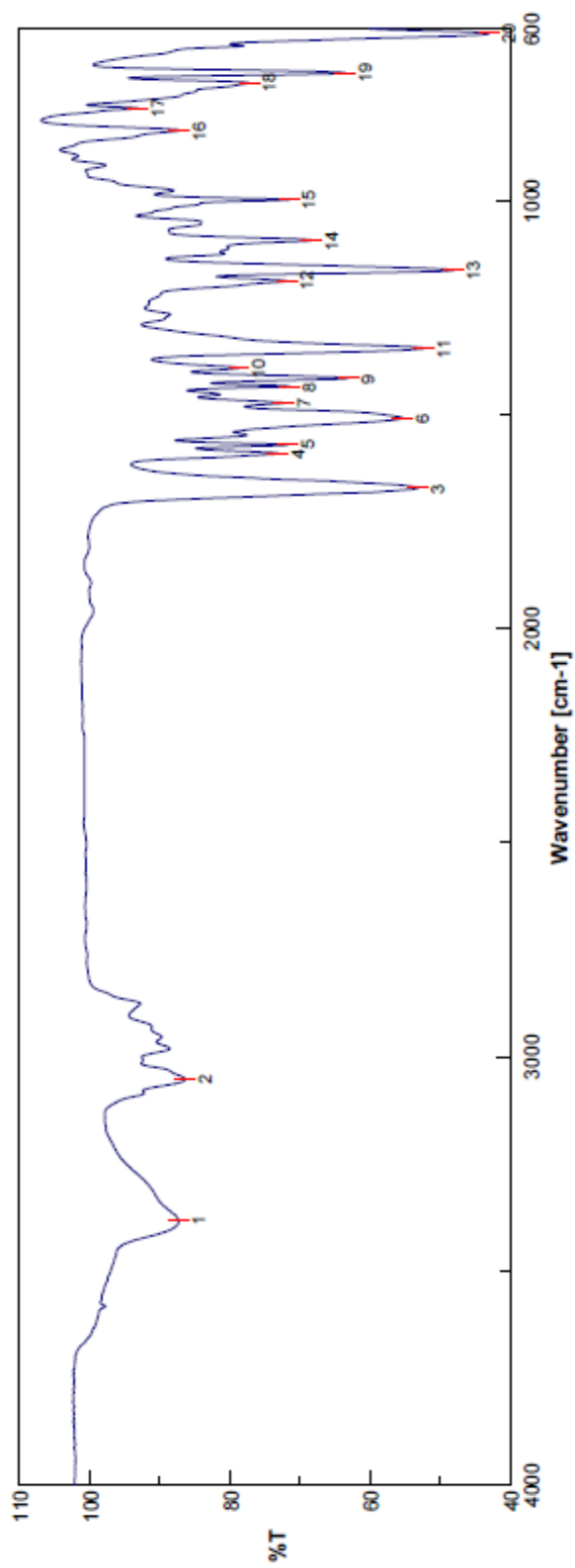
FTIR spectrum of compound **213**



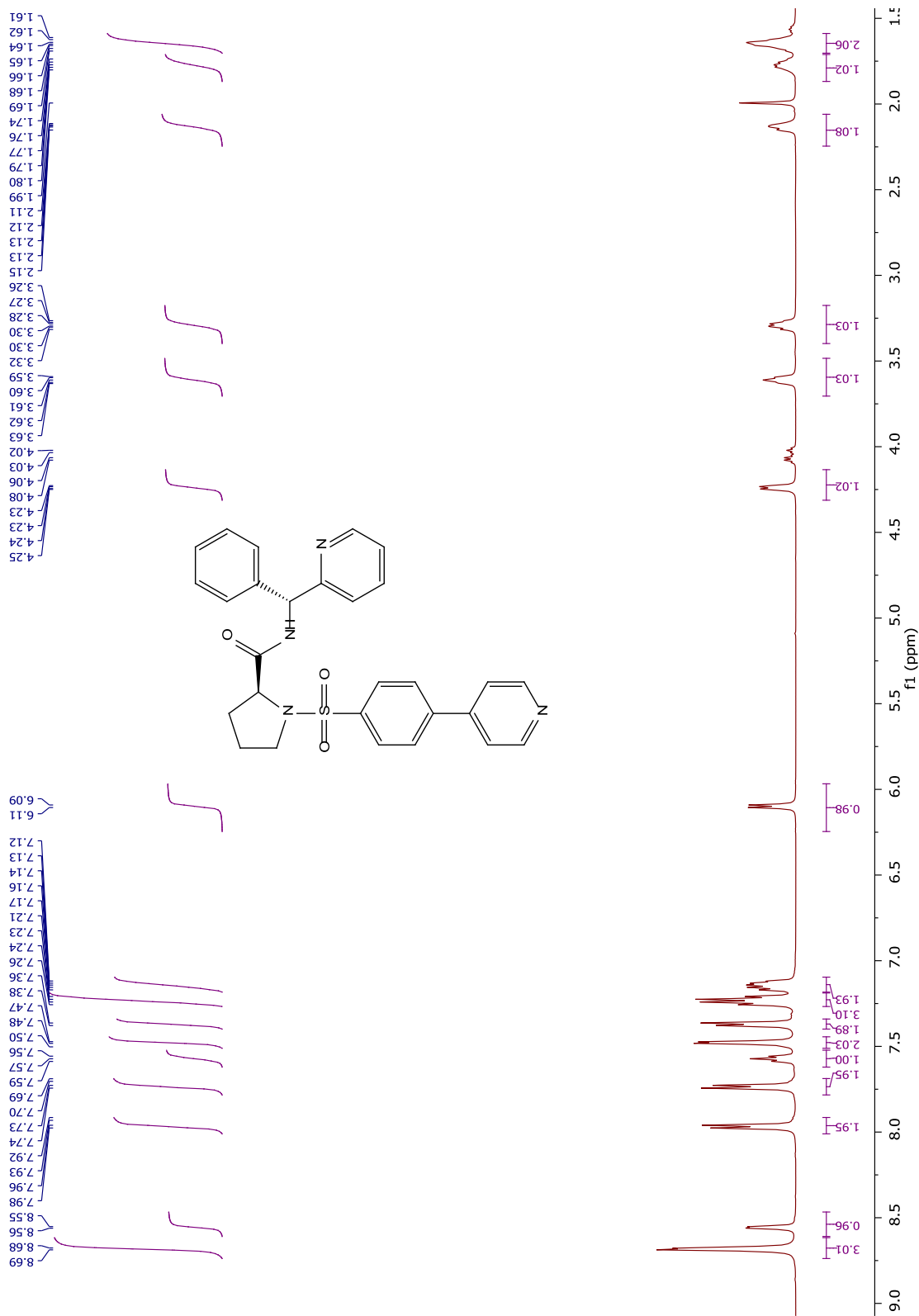
¹H NMR spectrum of compound 214



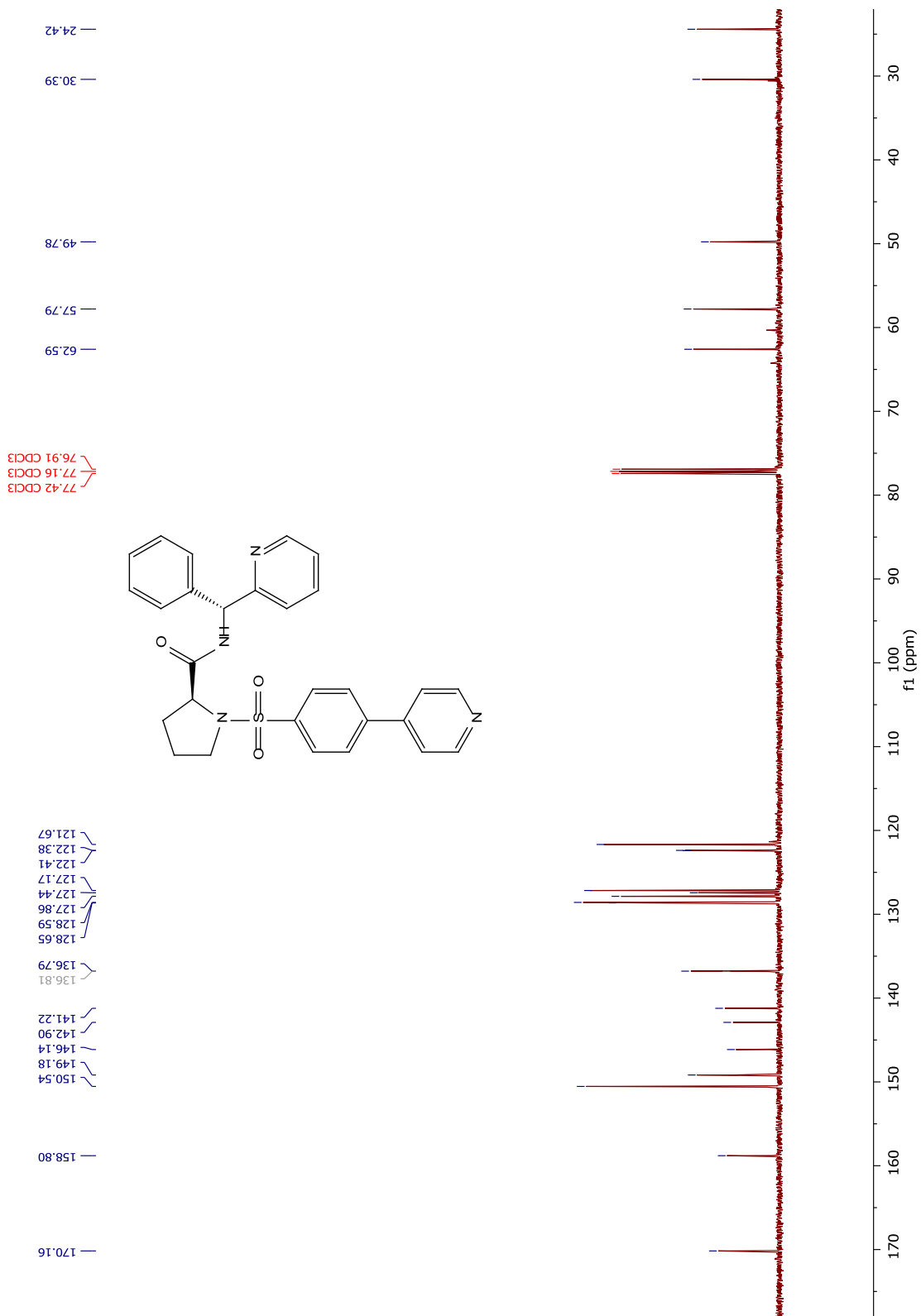
¹³C NMR spectrum of compound 214



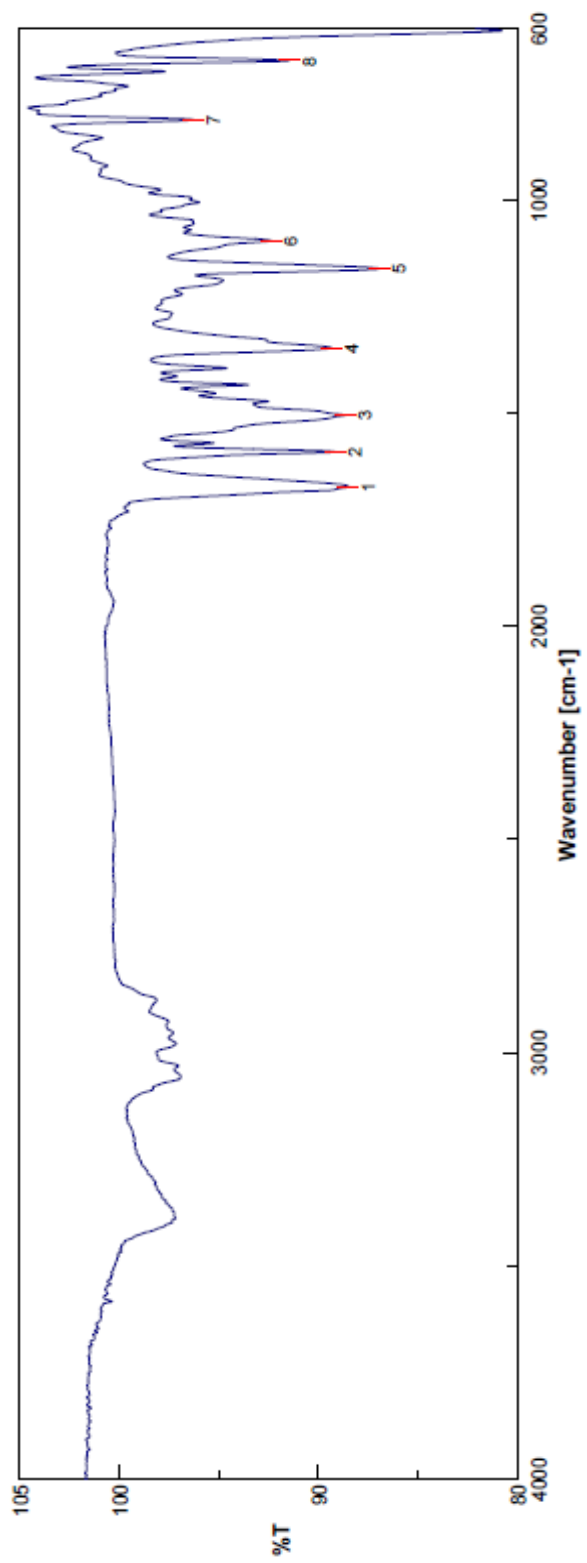
FTIR spectrum of compound **214**



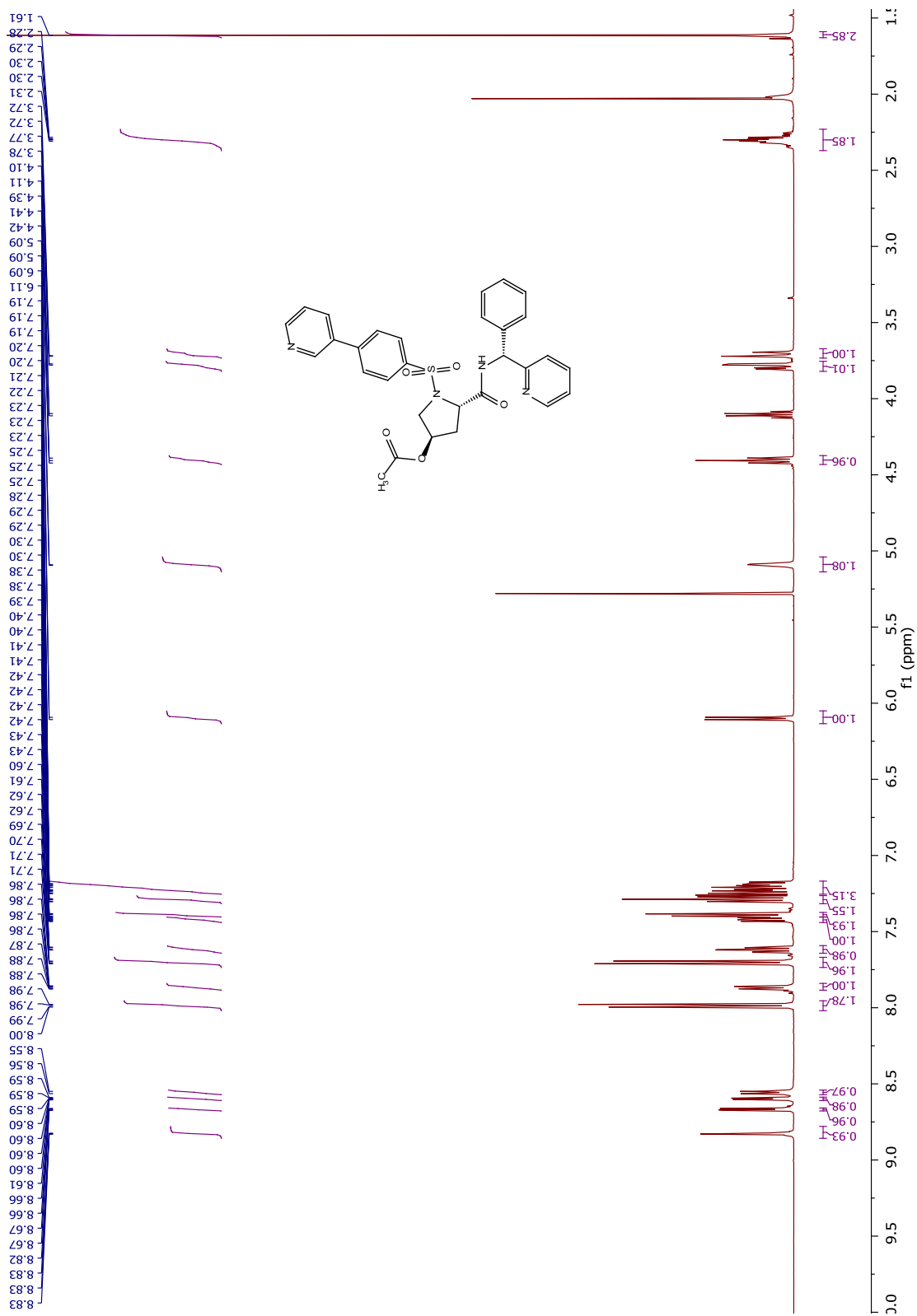
¹H NMR spectrum of compound 215



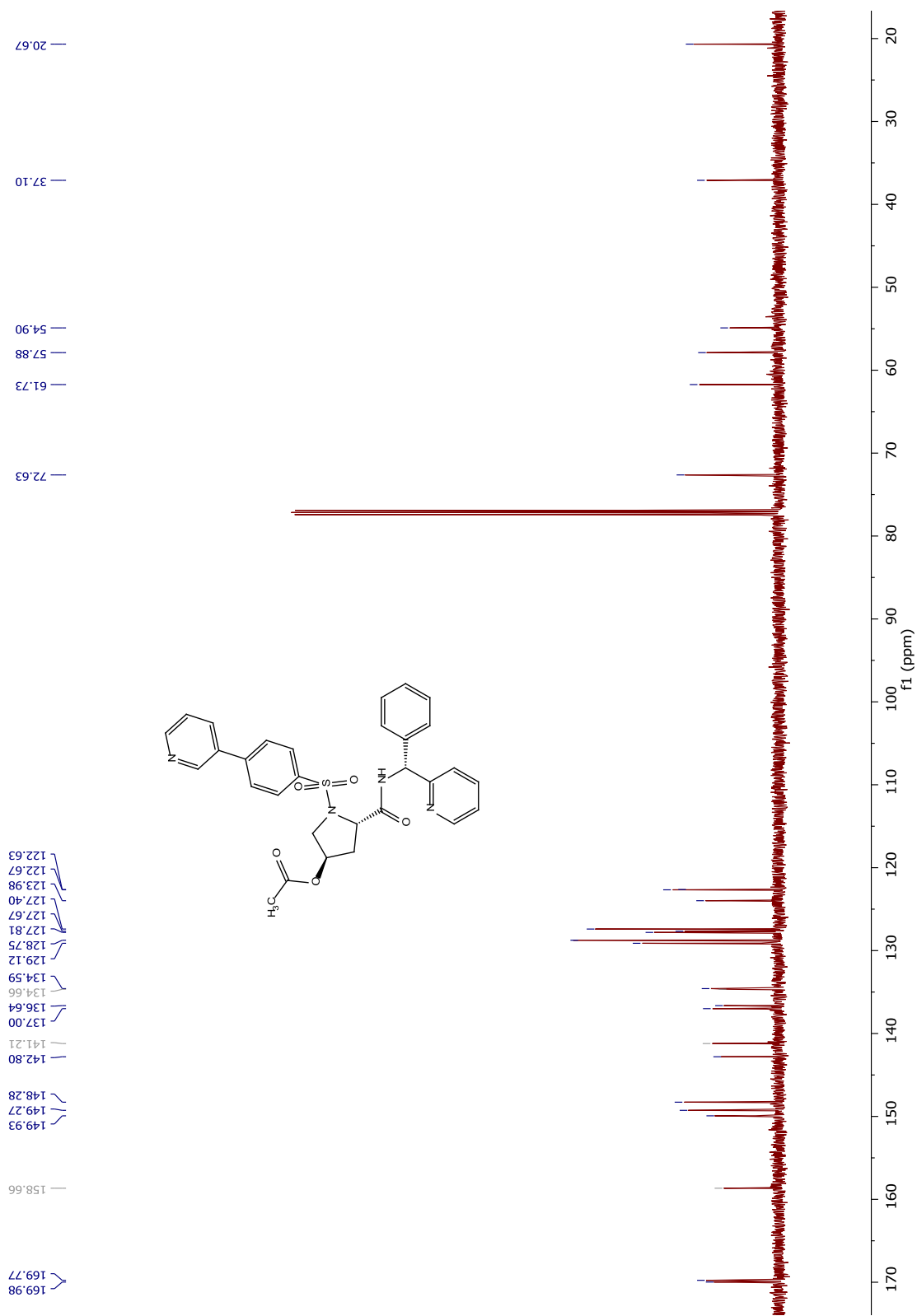
¹³C NMR spectrum of compound 215



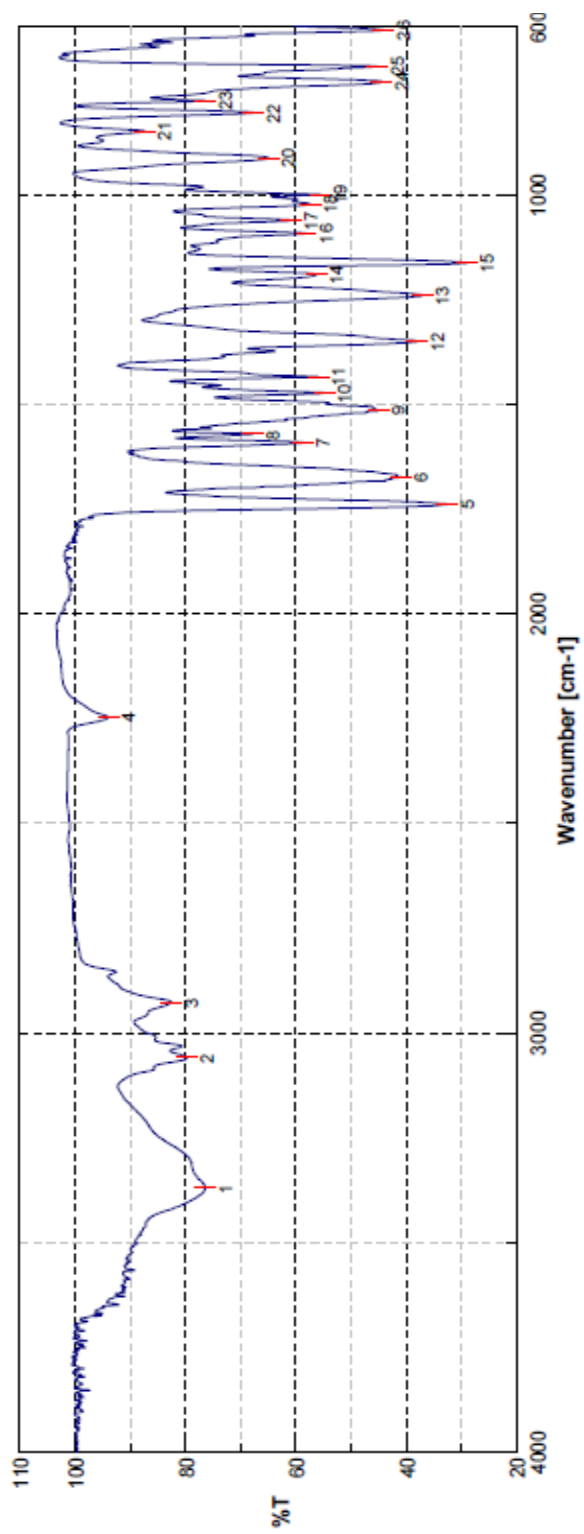
FTIR spectrum of compound 215



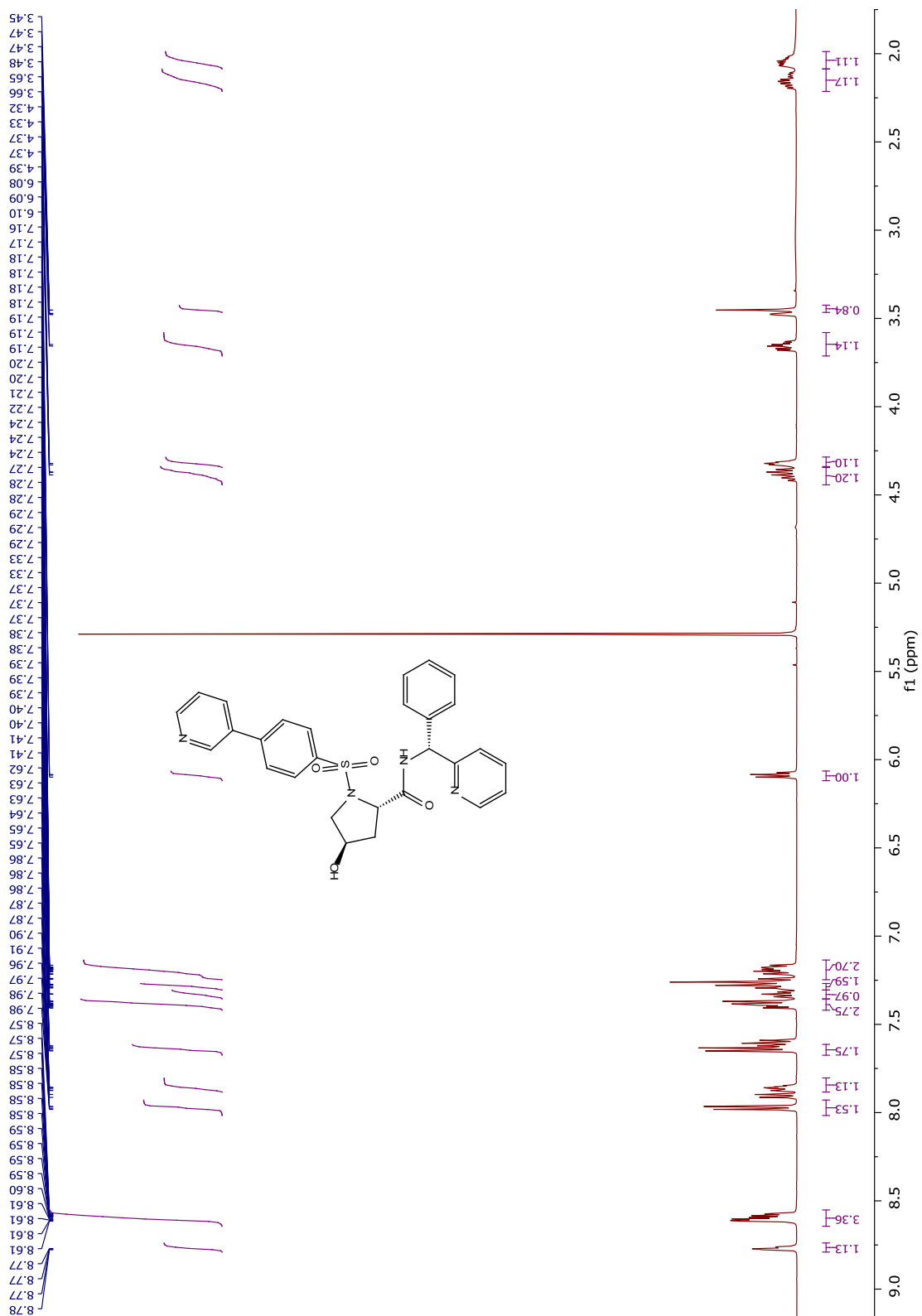
¹H NMR spectrum of compound 216



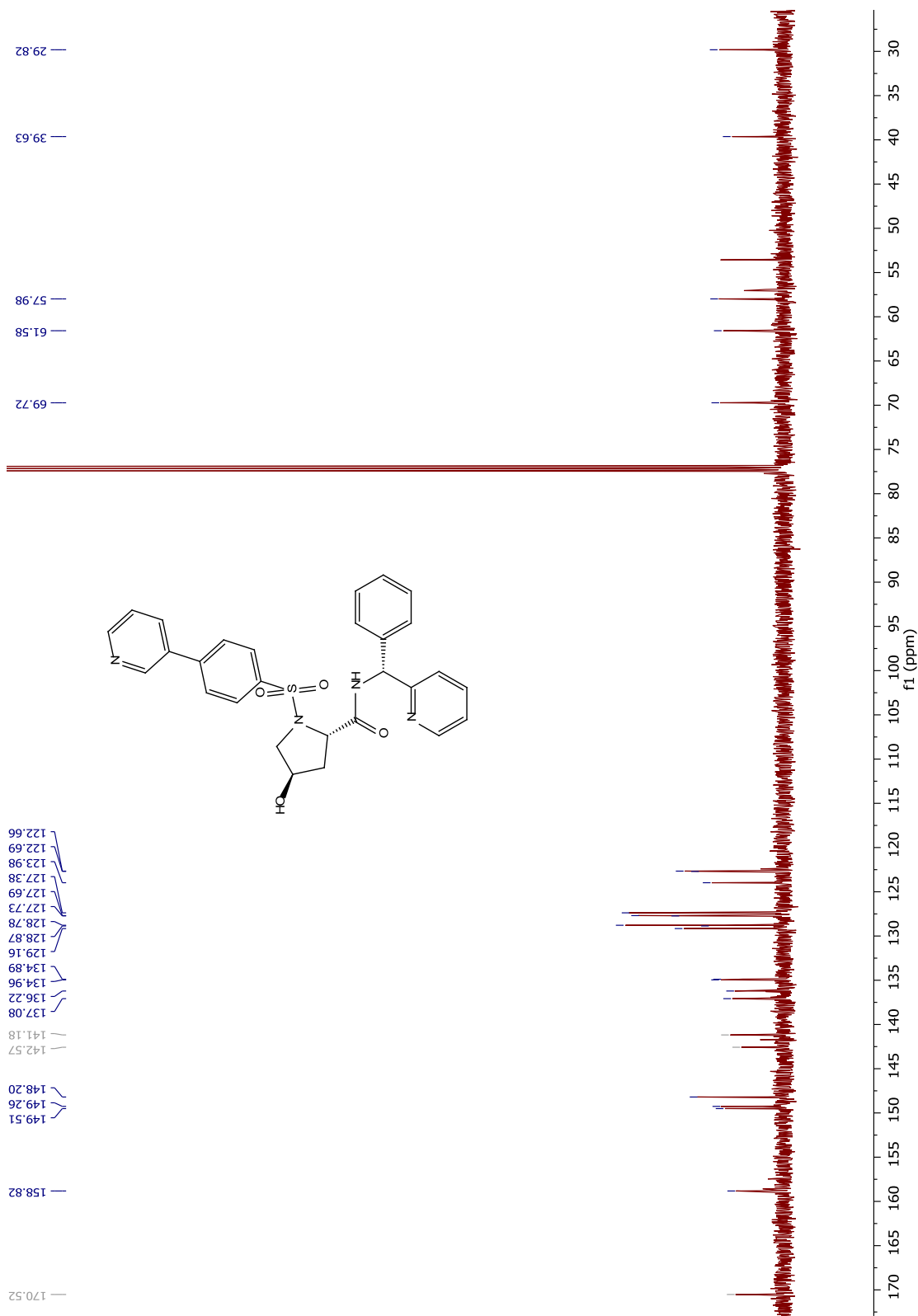
^{13}C NMR spectrum of compound 216



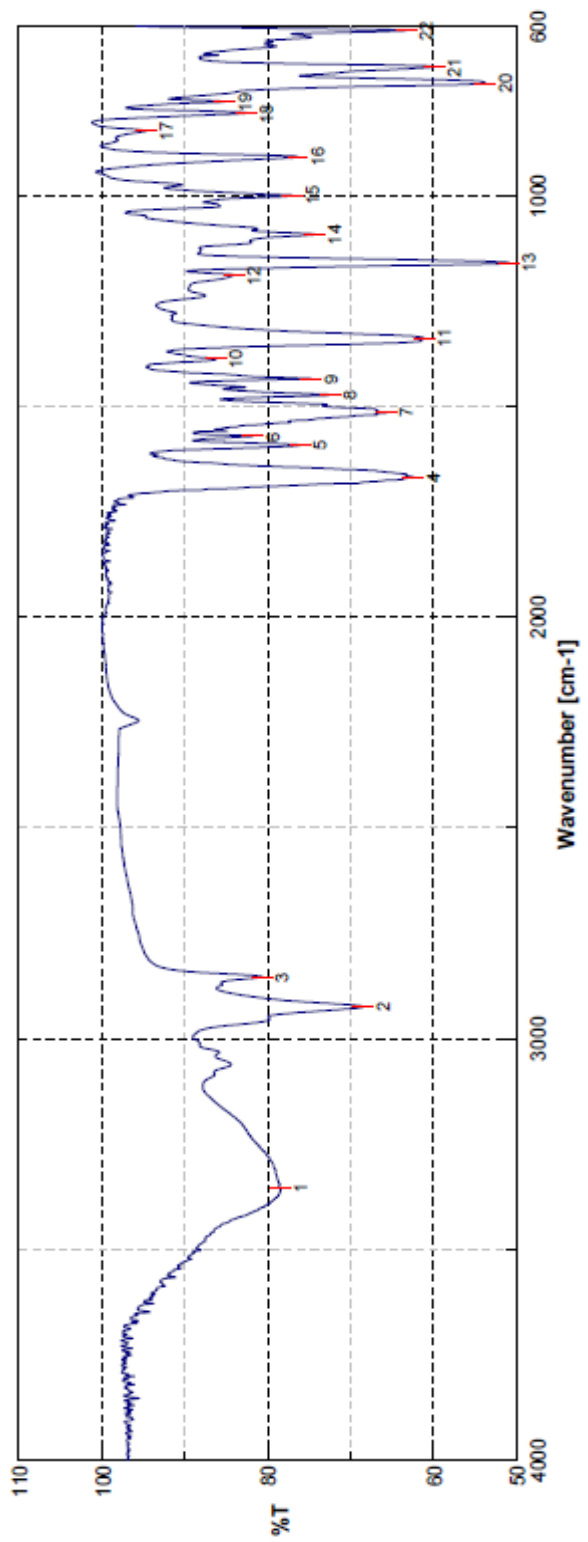
FTIR spectrum of compound **216**



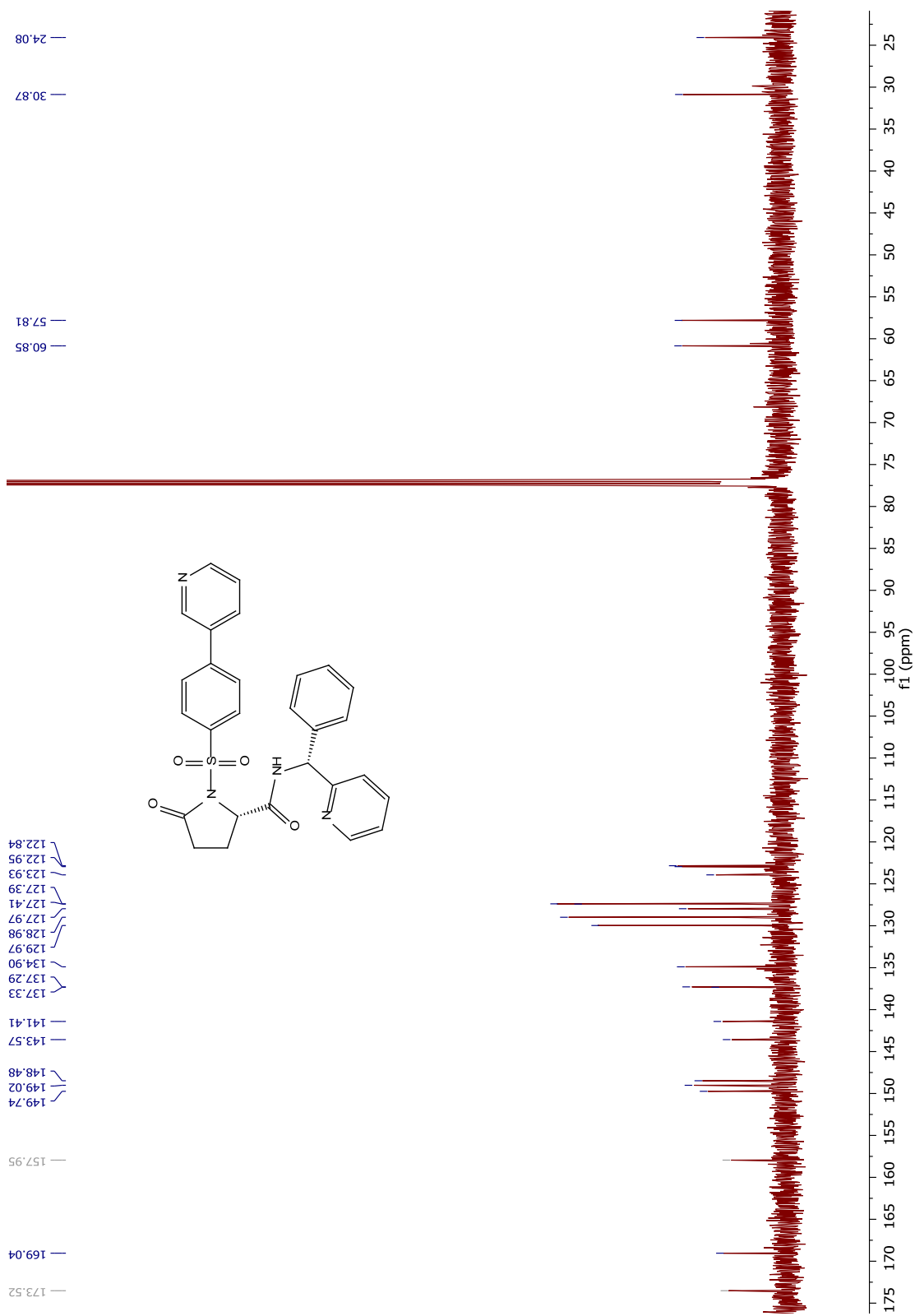
¹H NMR spectrum of compound 217



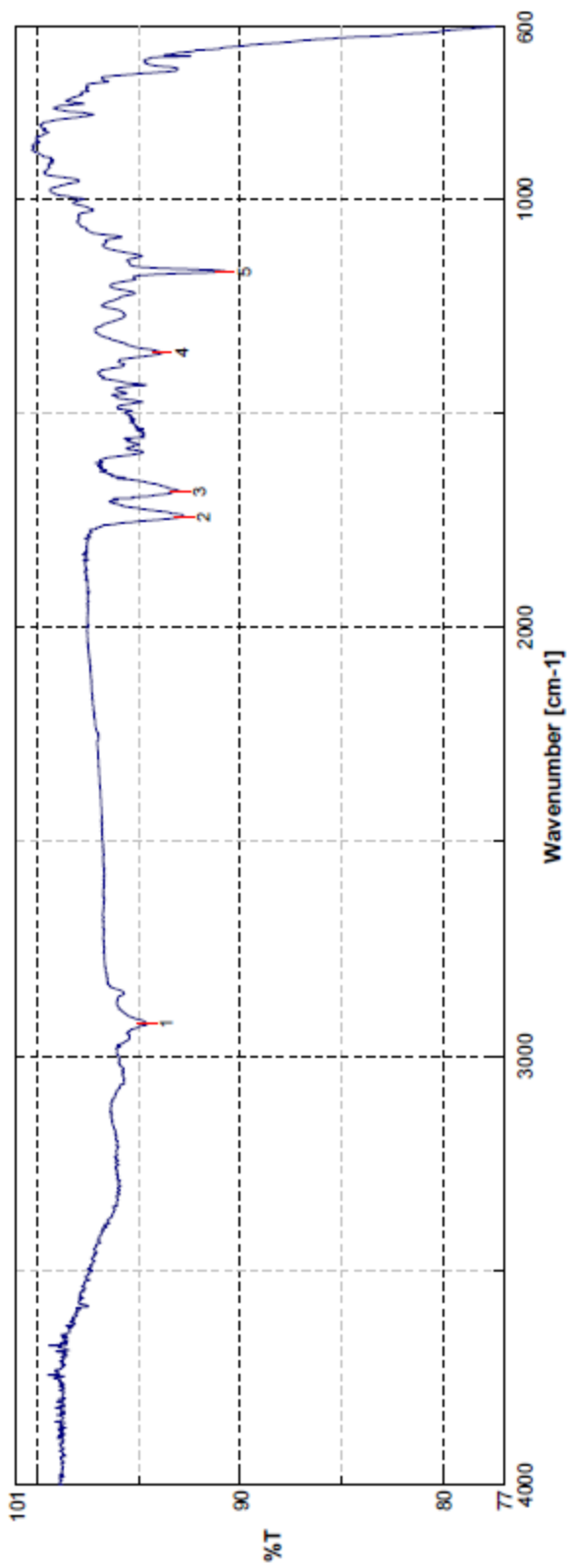
¹³C NMR spectrum of compound 217



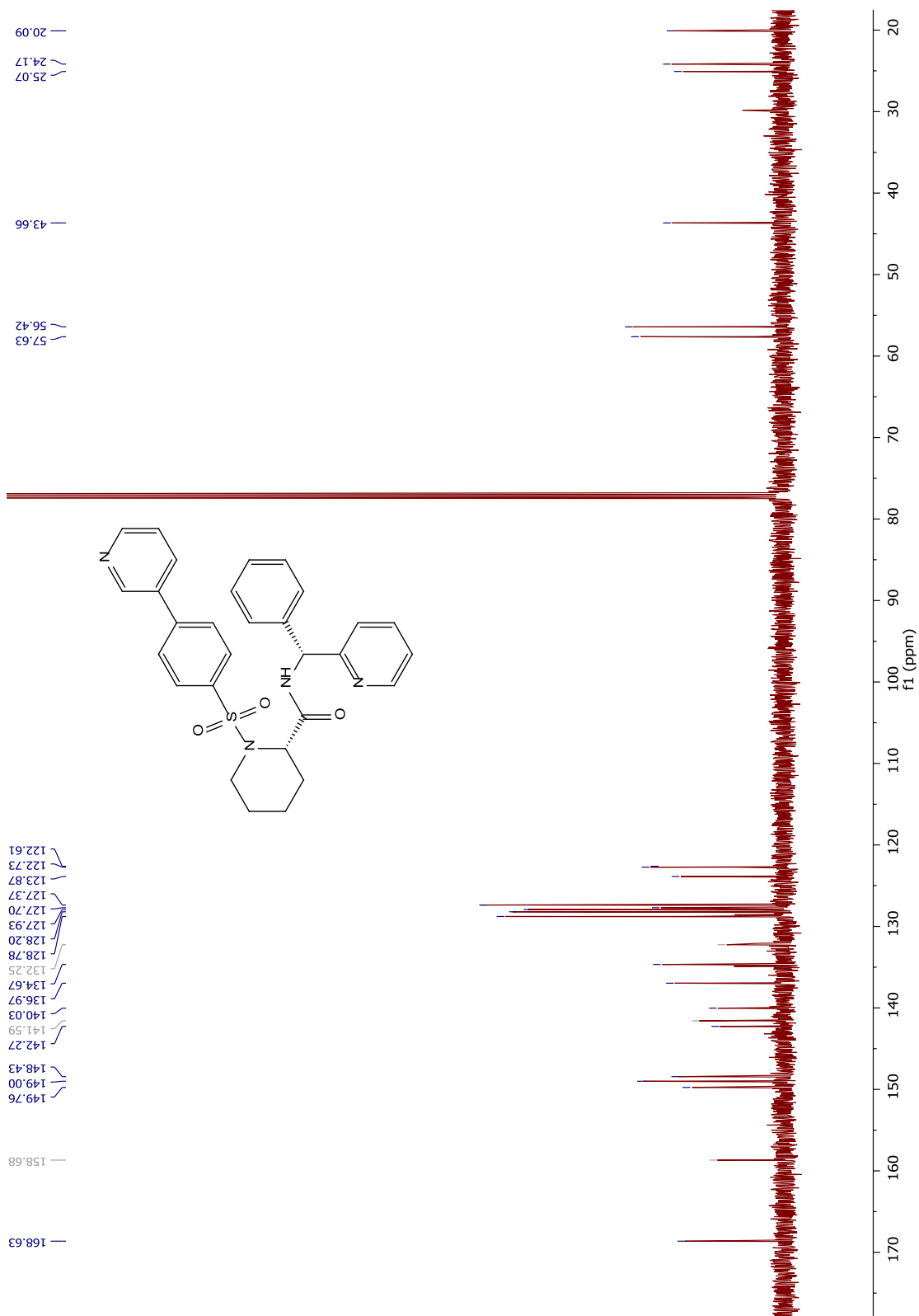
FTIR spectrum of compound 217



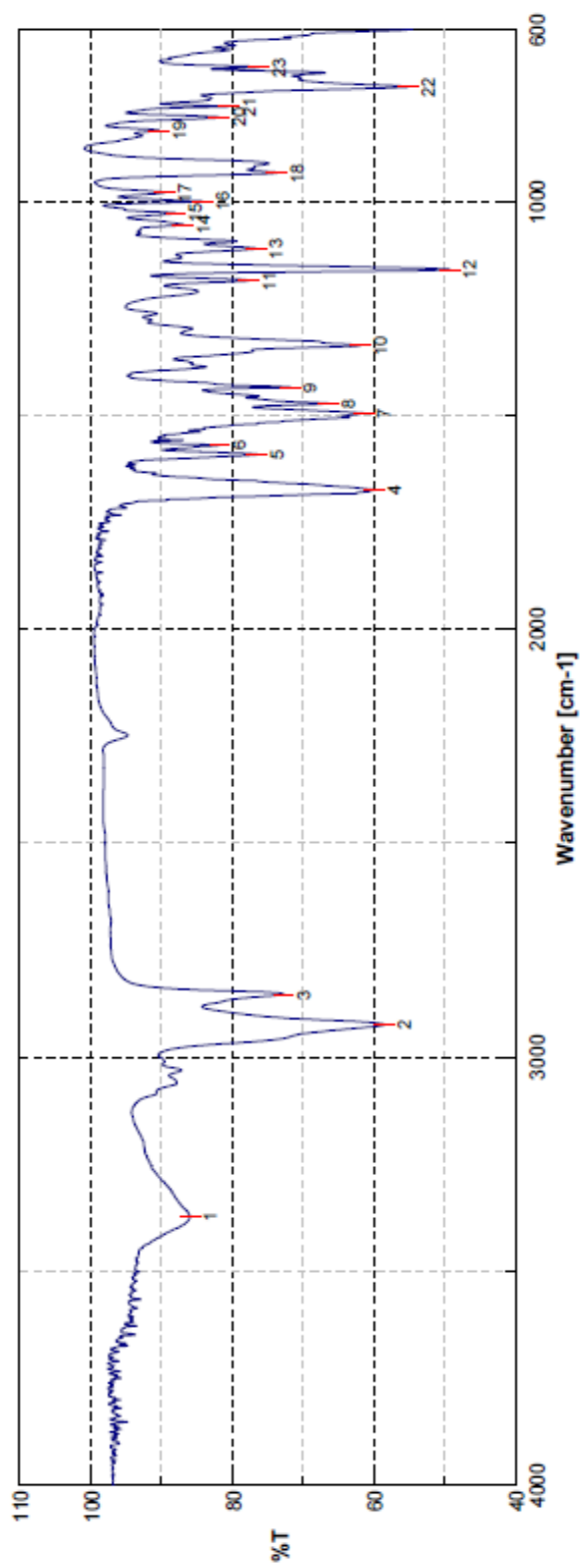
¹³C NMR spectrum of compound **218**



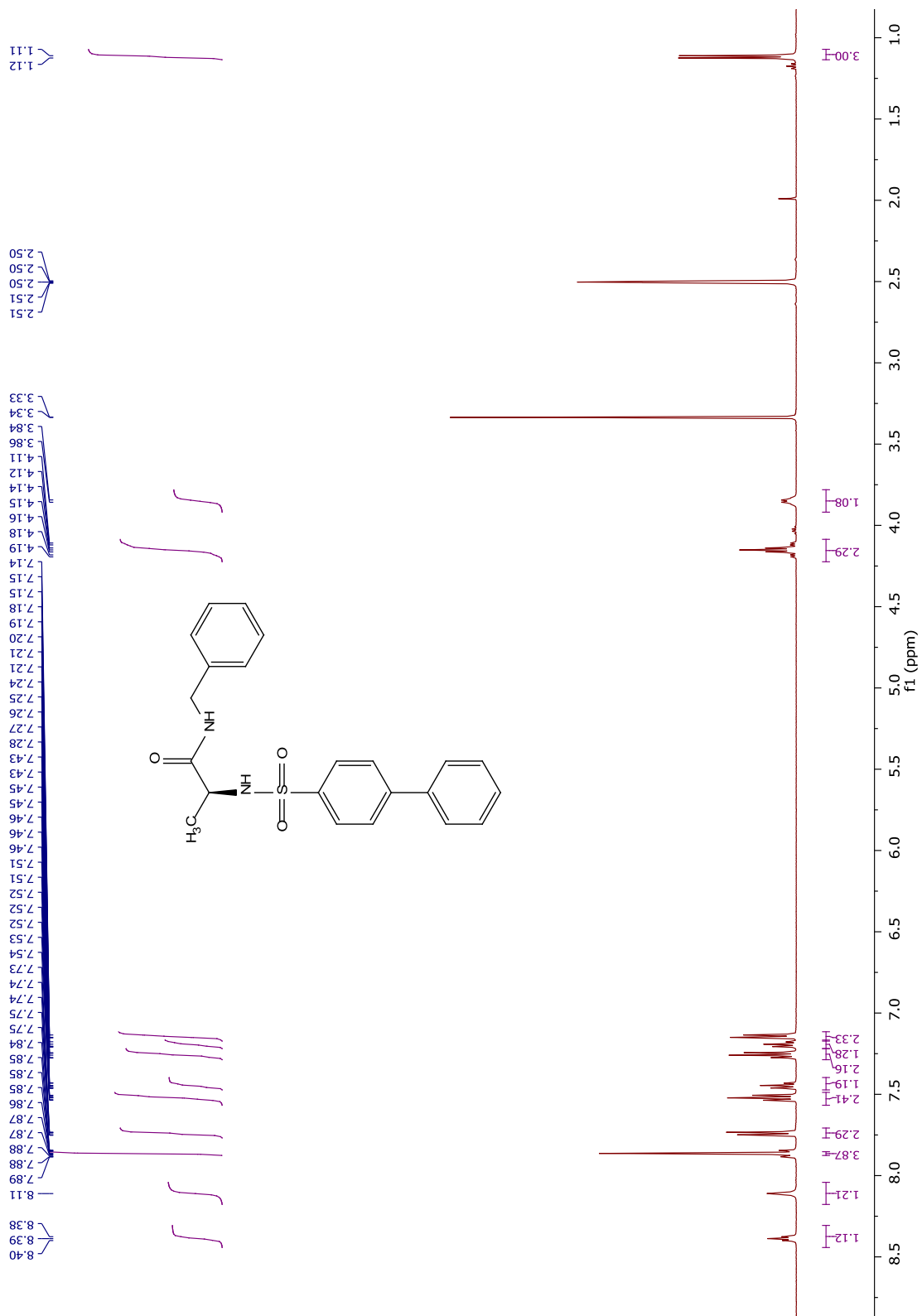
FTIR spectrum of compound **218**



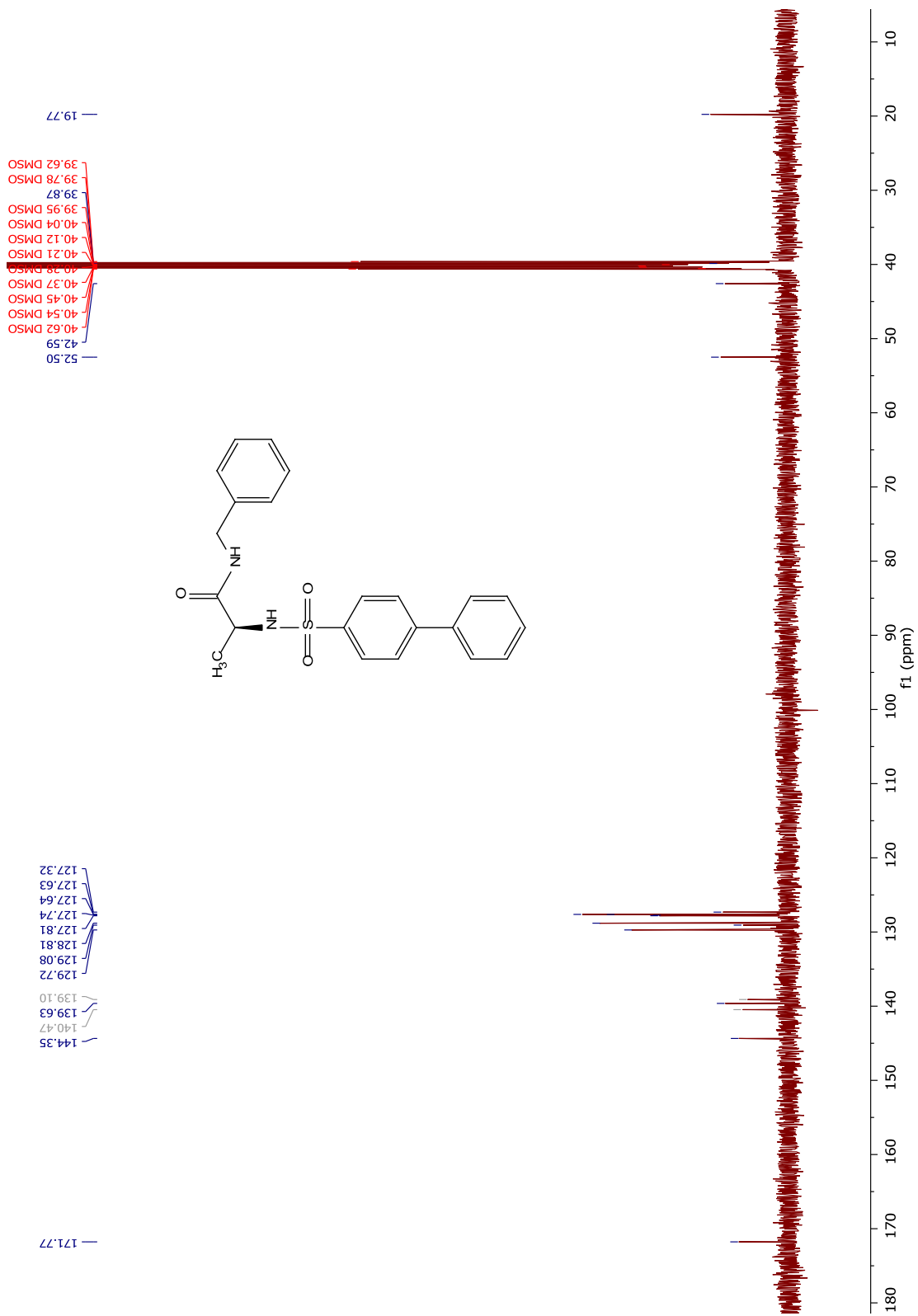
¹³C NMR spectrum of compound **219**



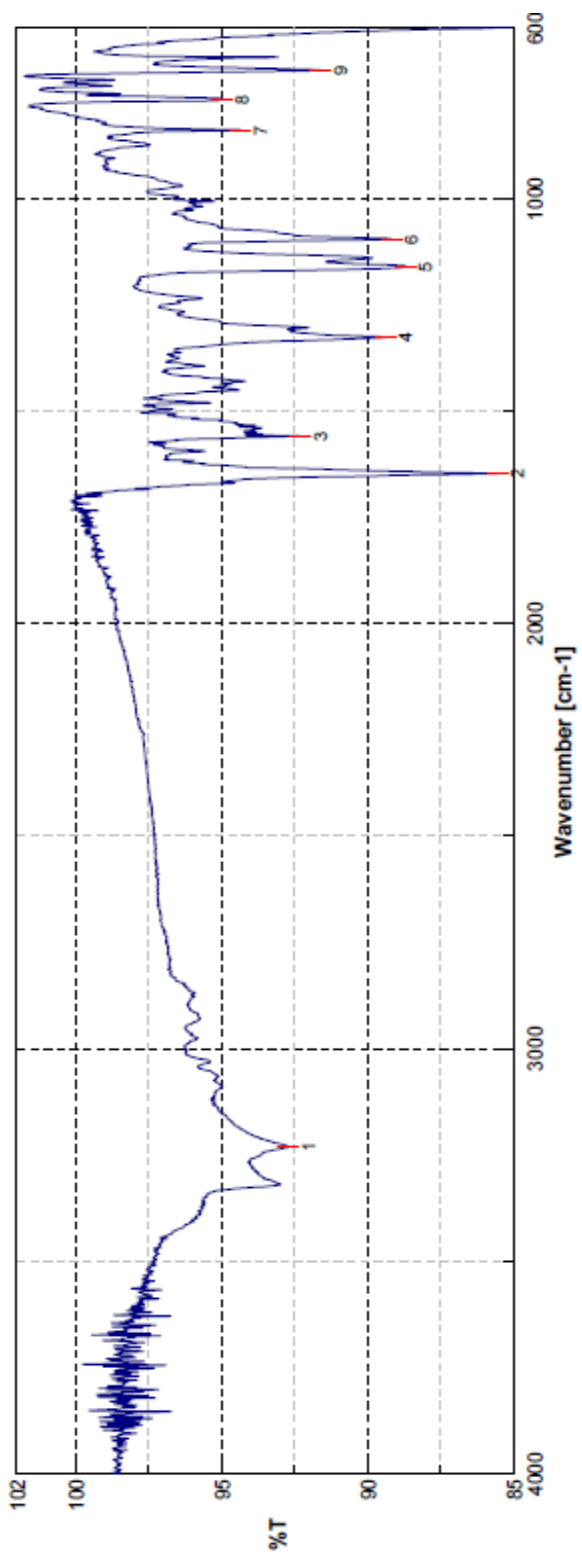
FTIR spectrum of compound 219



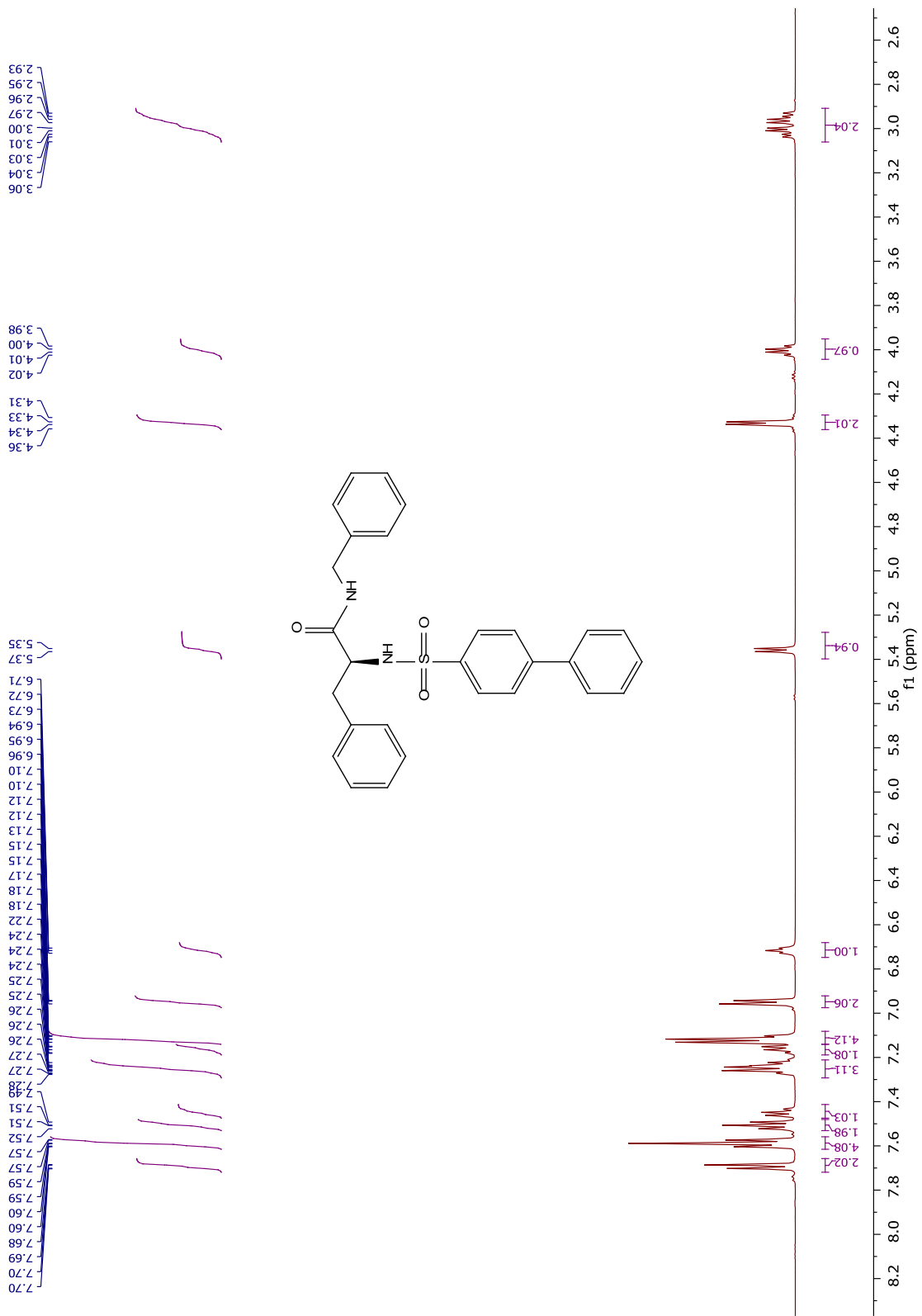
¹H NMR spectrum of compound **220**



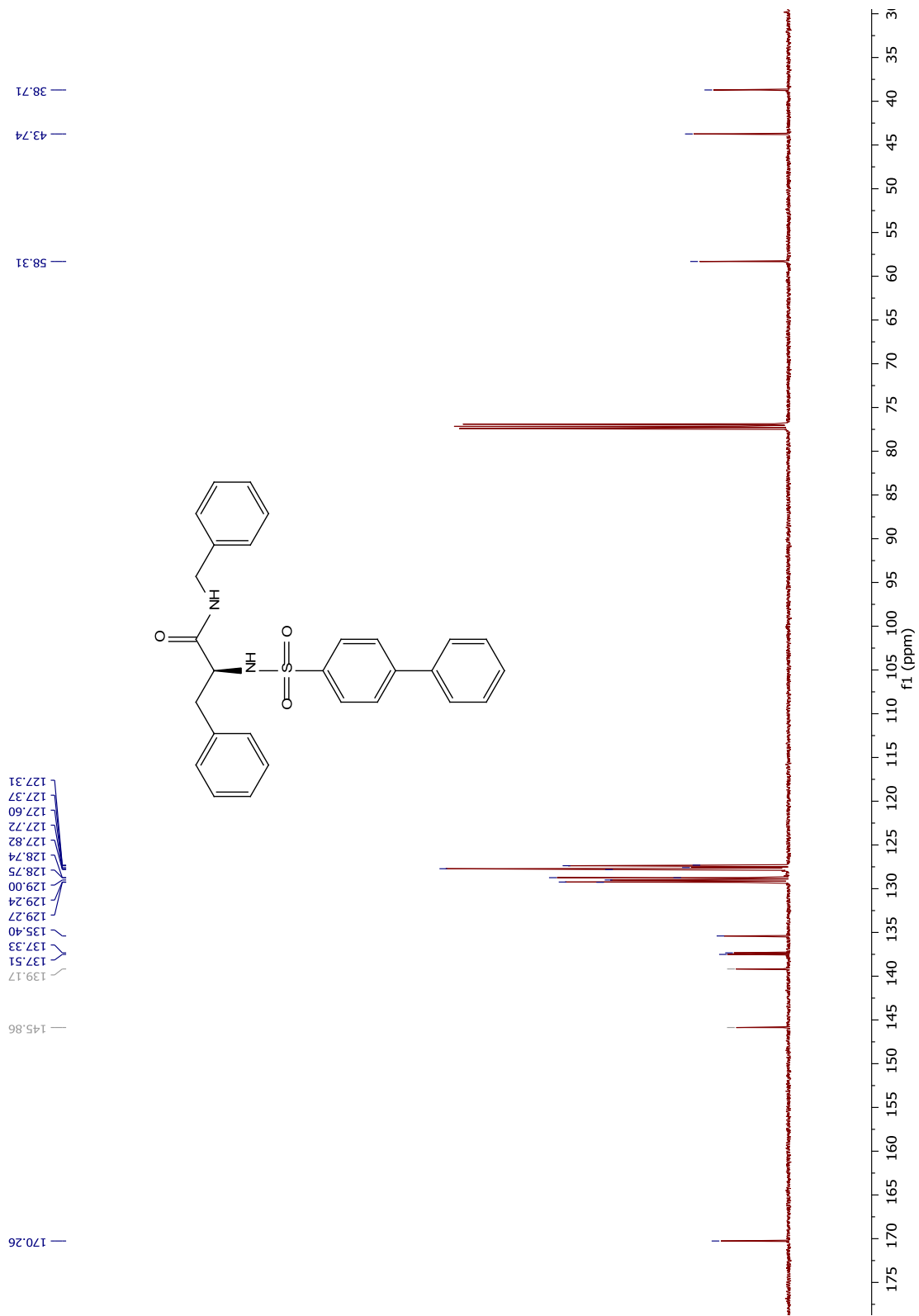
¹³C NMR spectrum of compound 220



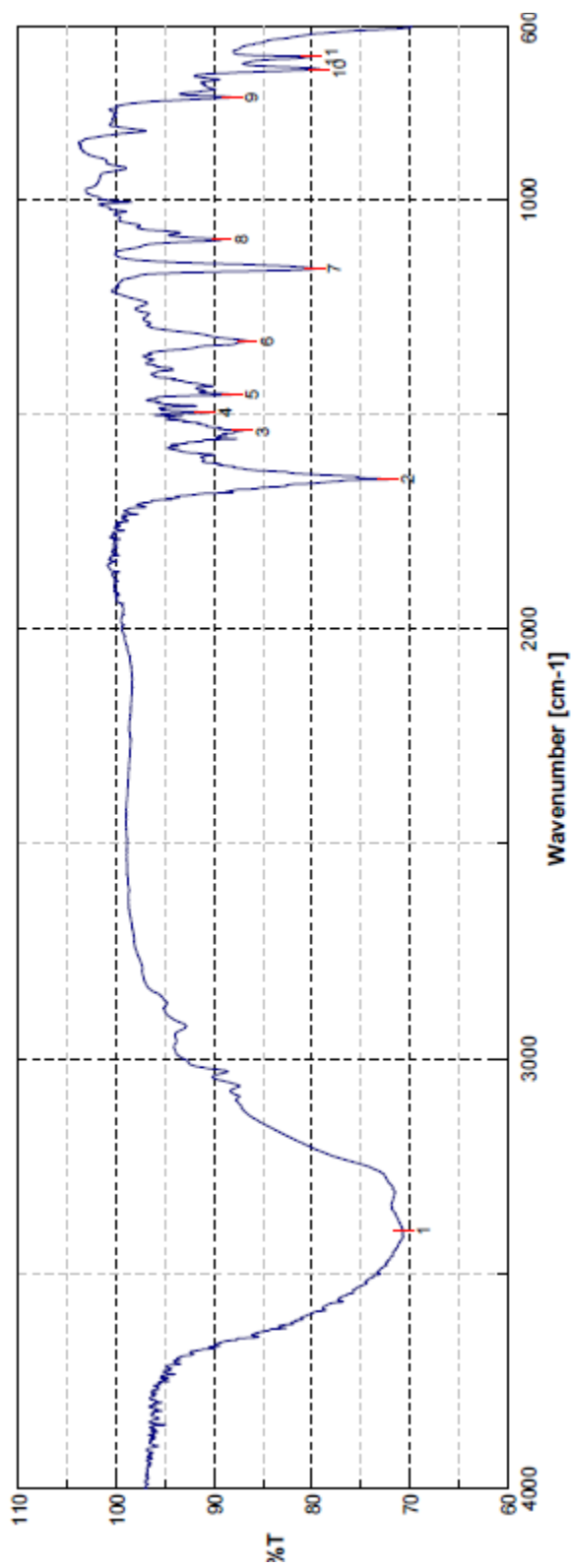
FTIR spectrum of compound **220**



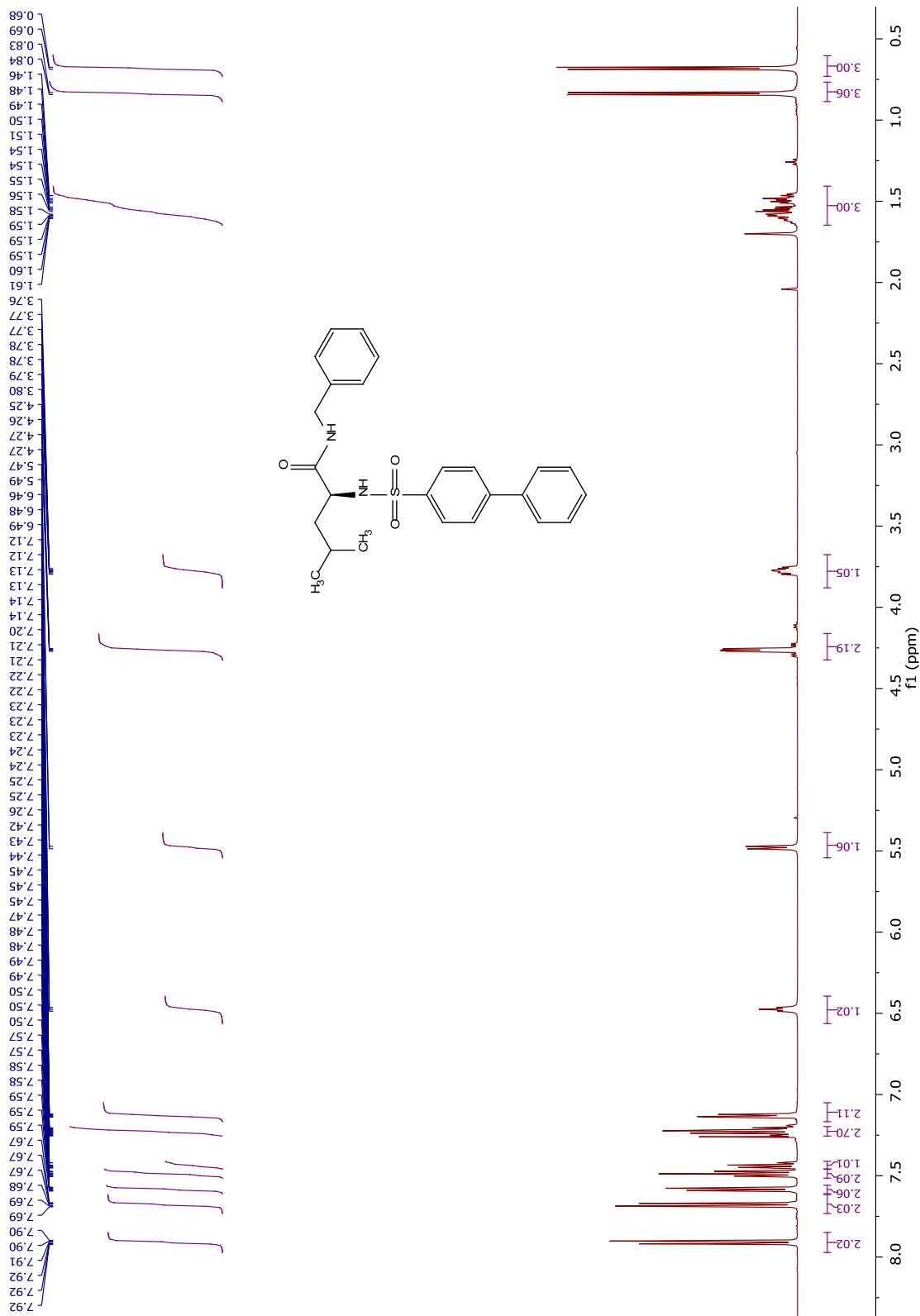
¹H NMR spectrum of compound 221



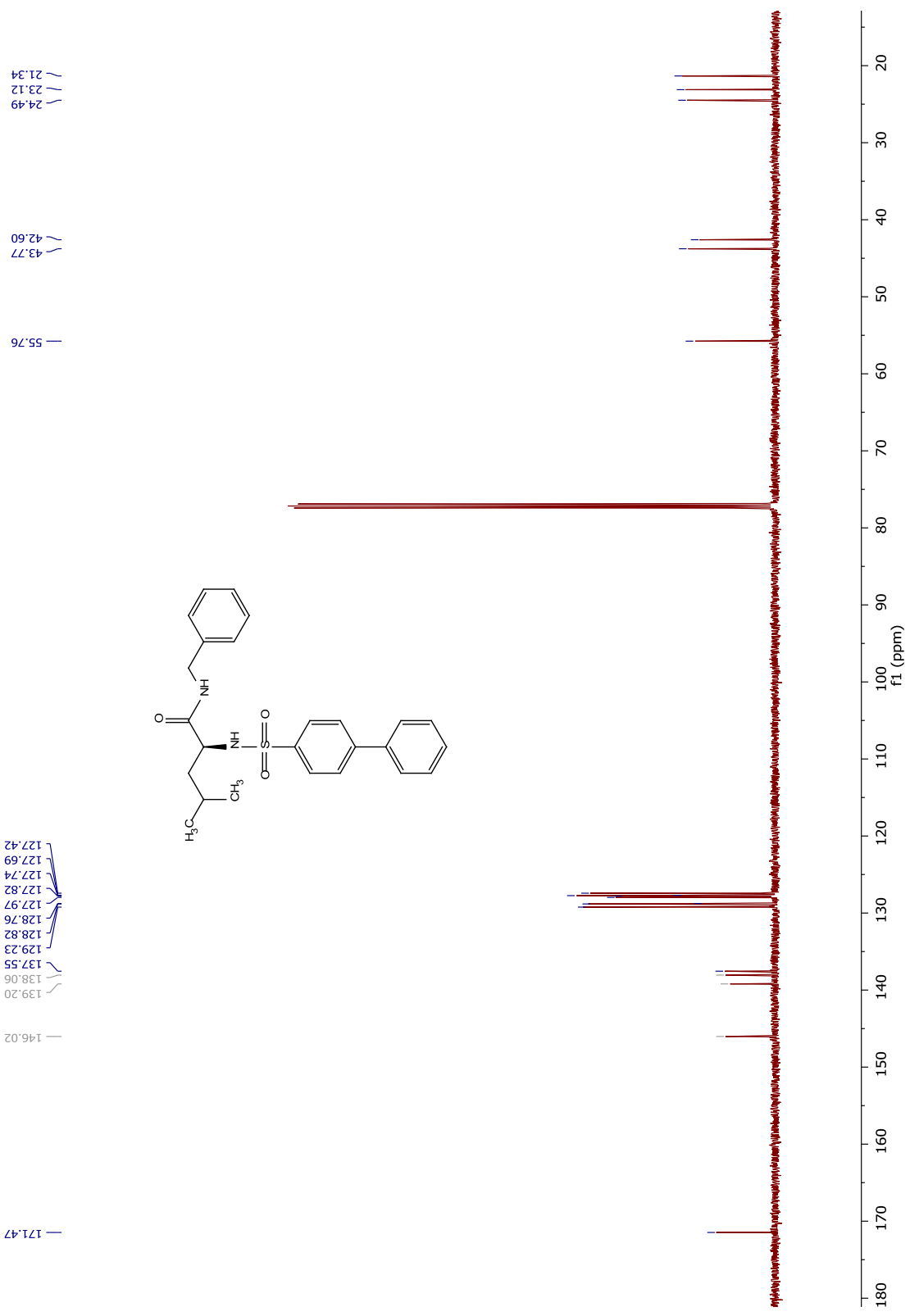
¹³C NMR spectrum of compound **221**



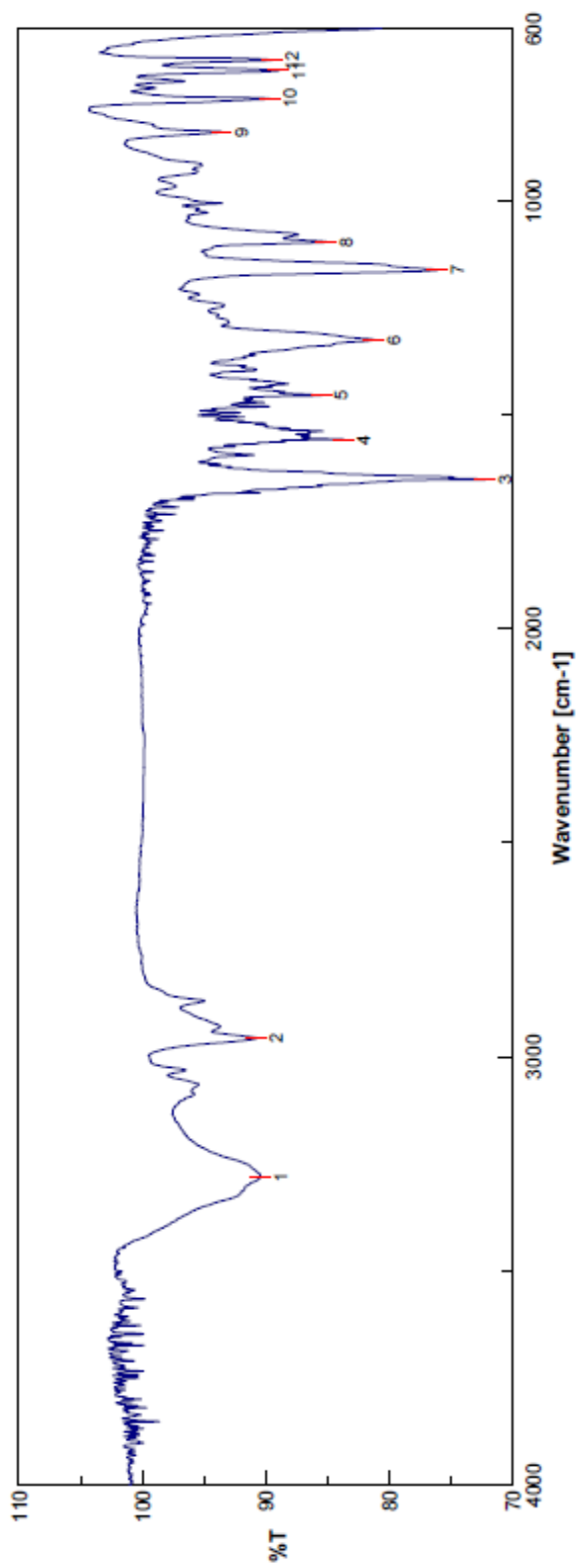
FTIR spectrum of compound 221



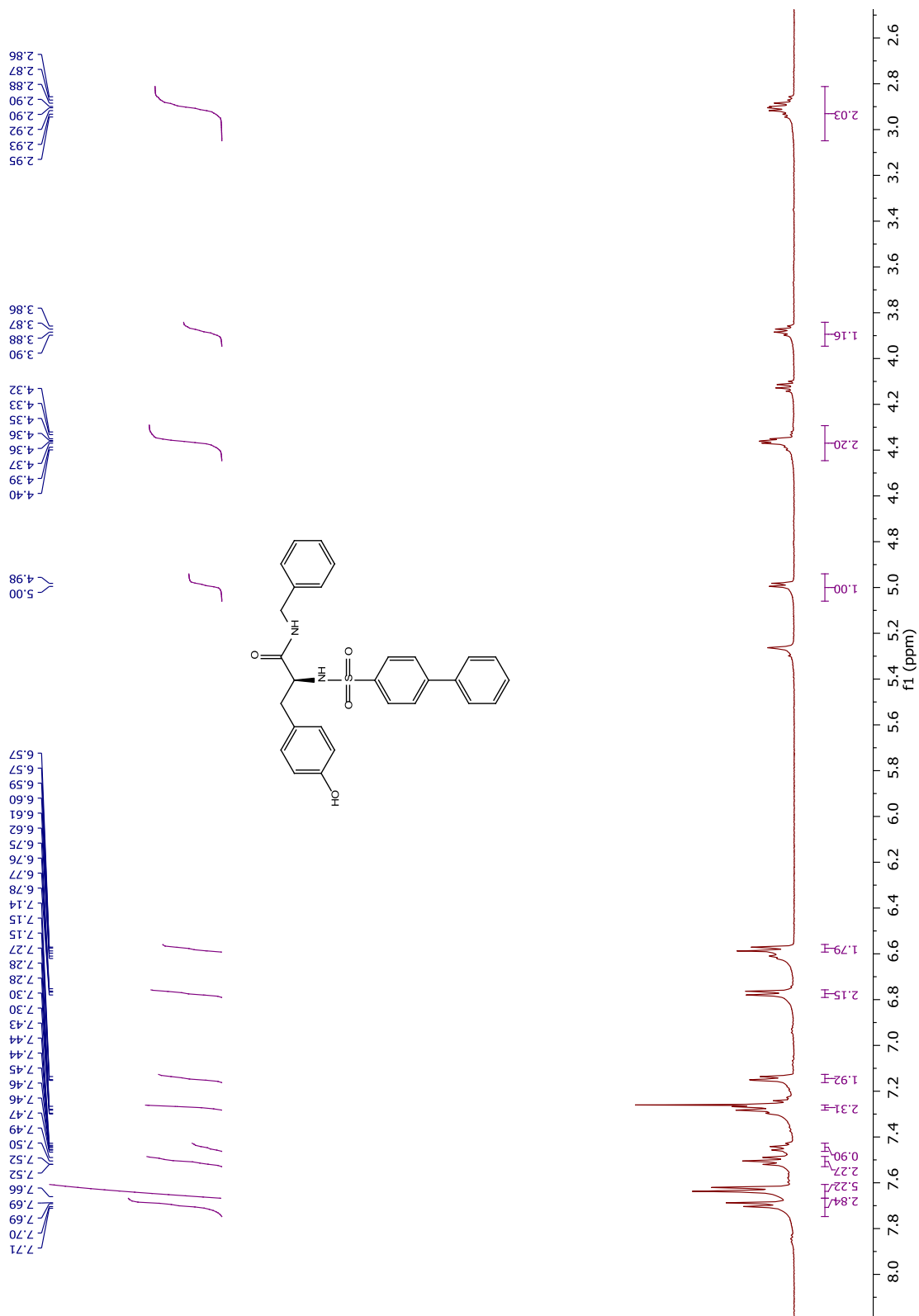
¹H NMR spectrum of compound 222



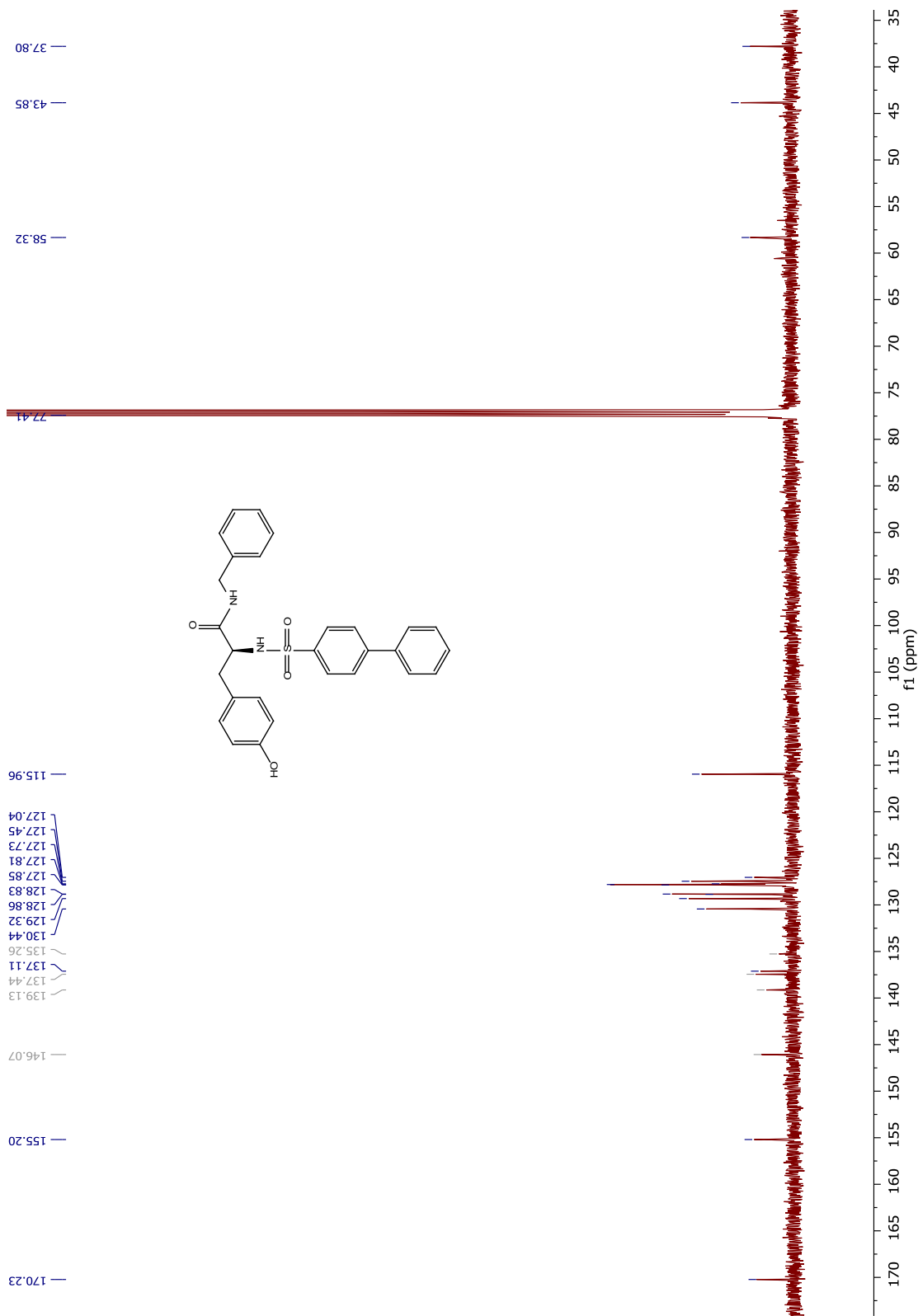
¹³C NMR spectrum of compound 222



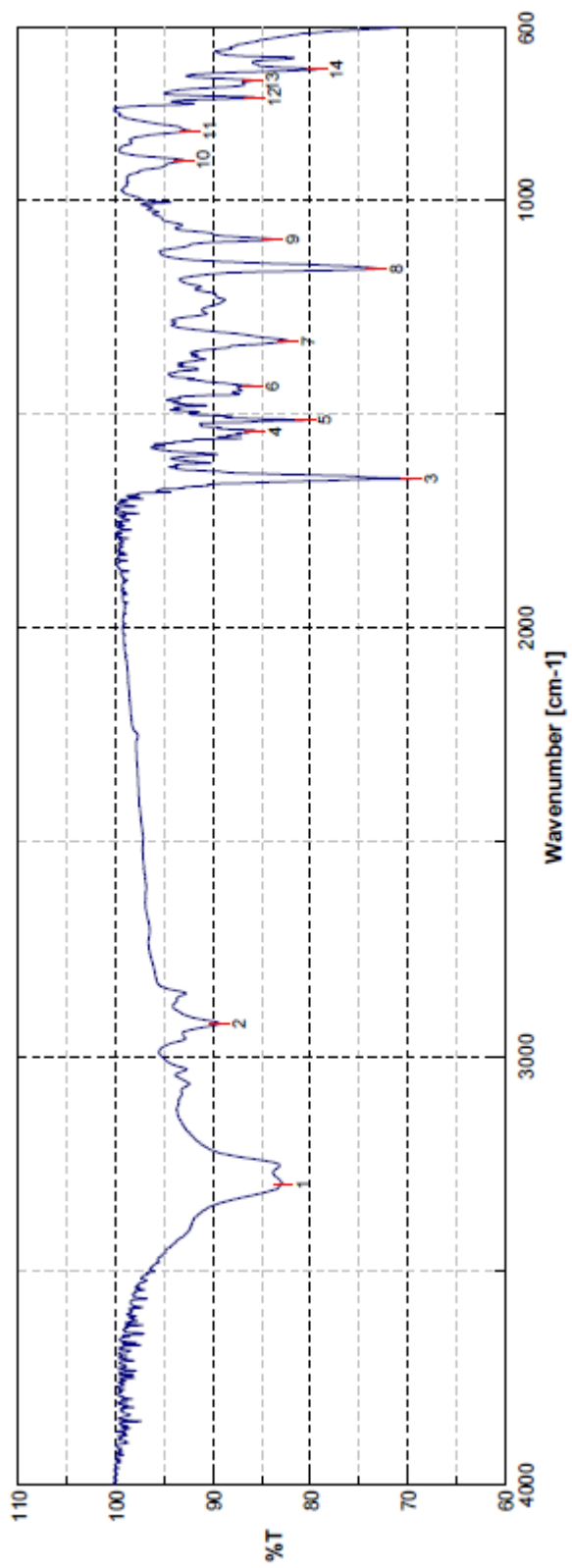
FTIR spectrum of compound **222**



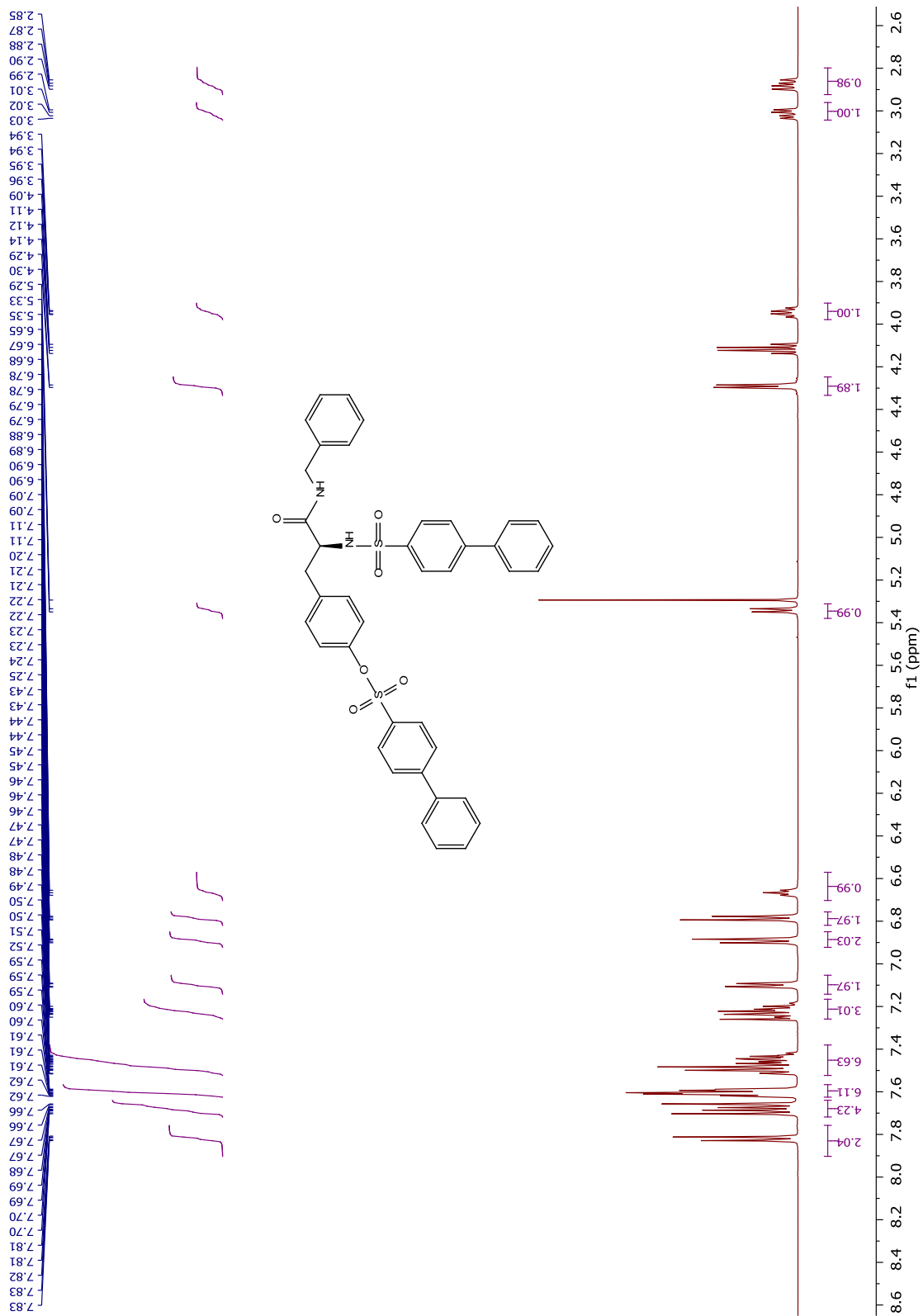
¹H NMR spectrum of compound **223**



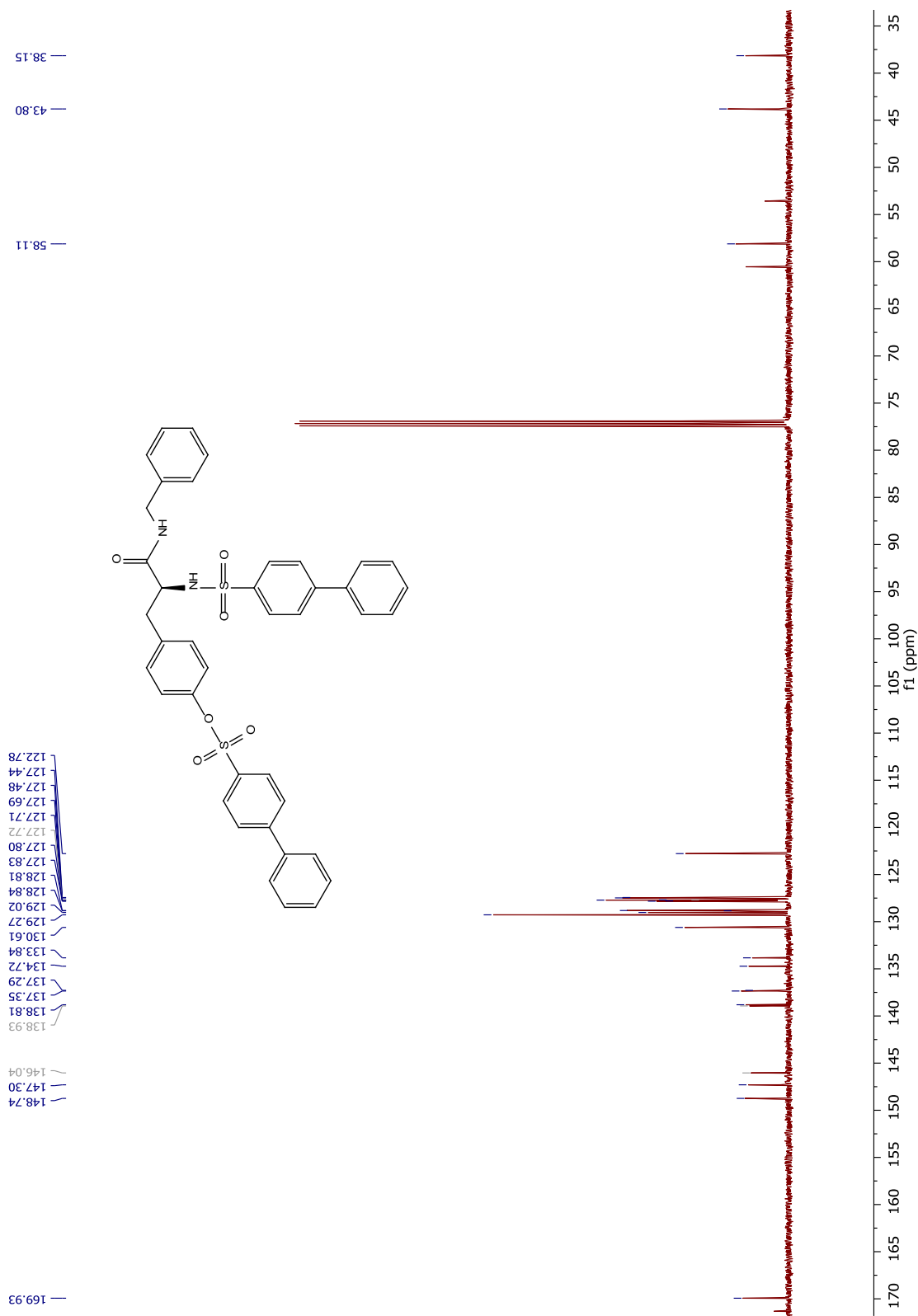
¹H NMR spectrum of compound 223



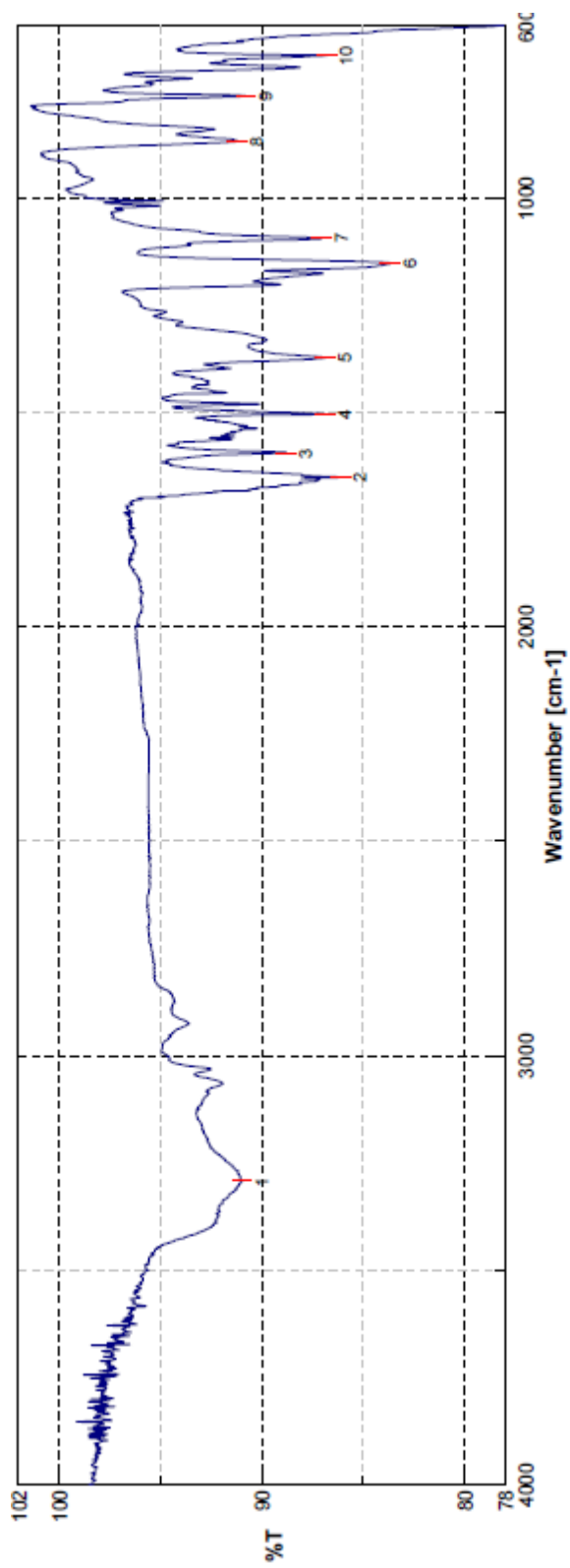
FTIR spectrum of compound **223**



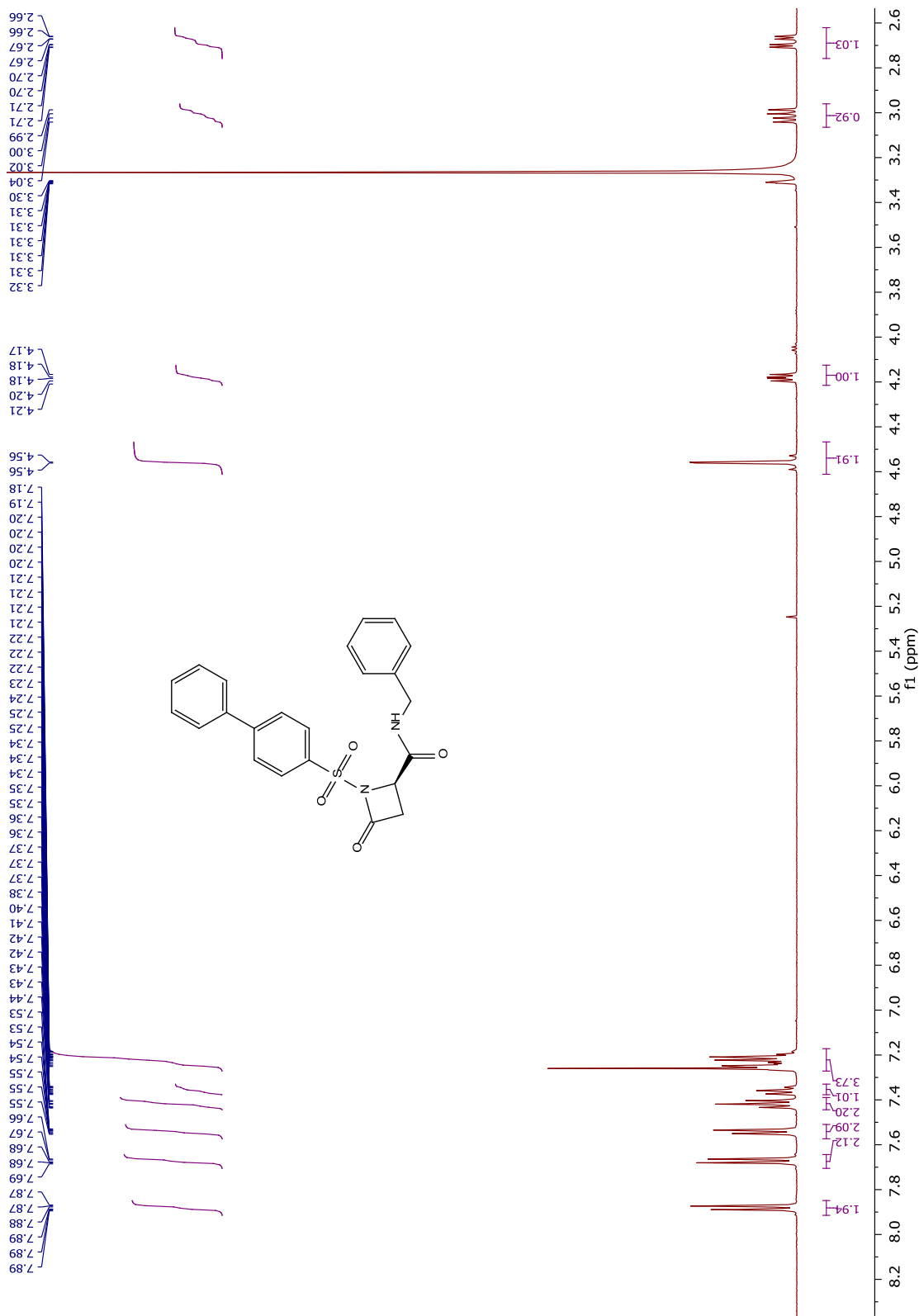
¹H NMR spectrum of compound 224



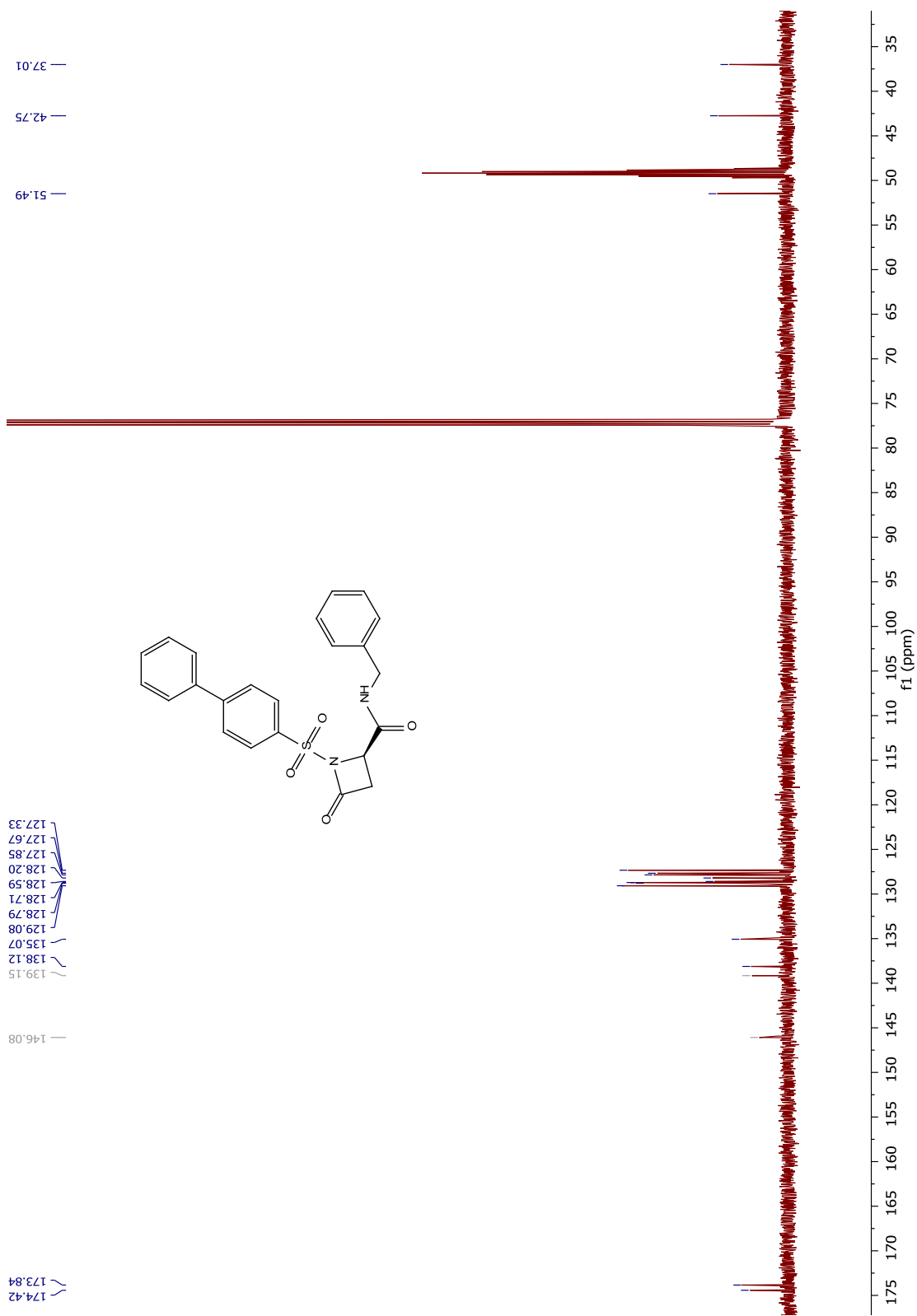
¹³C NMR spectrum of compound **224**



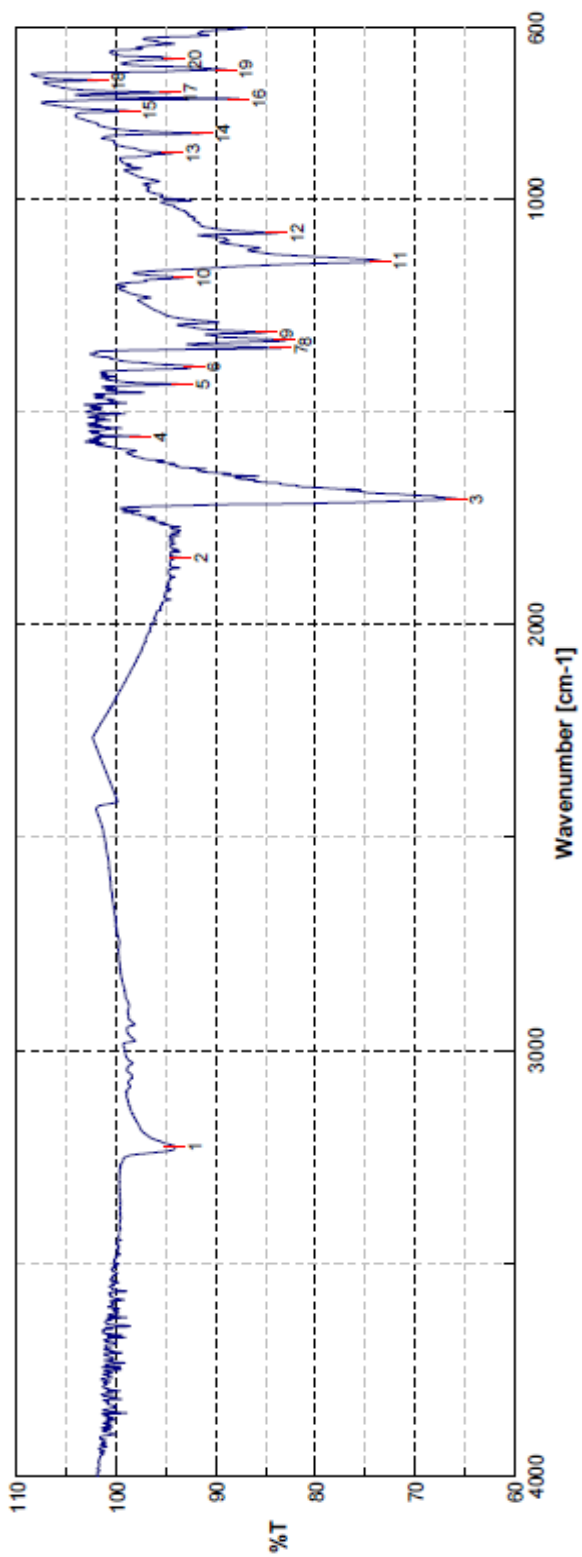
FTIR spectrum of compound **224**



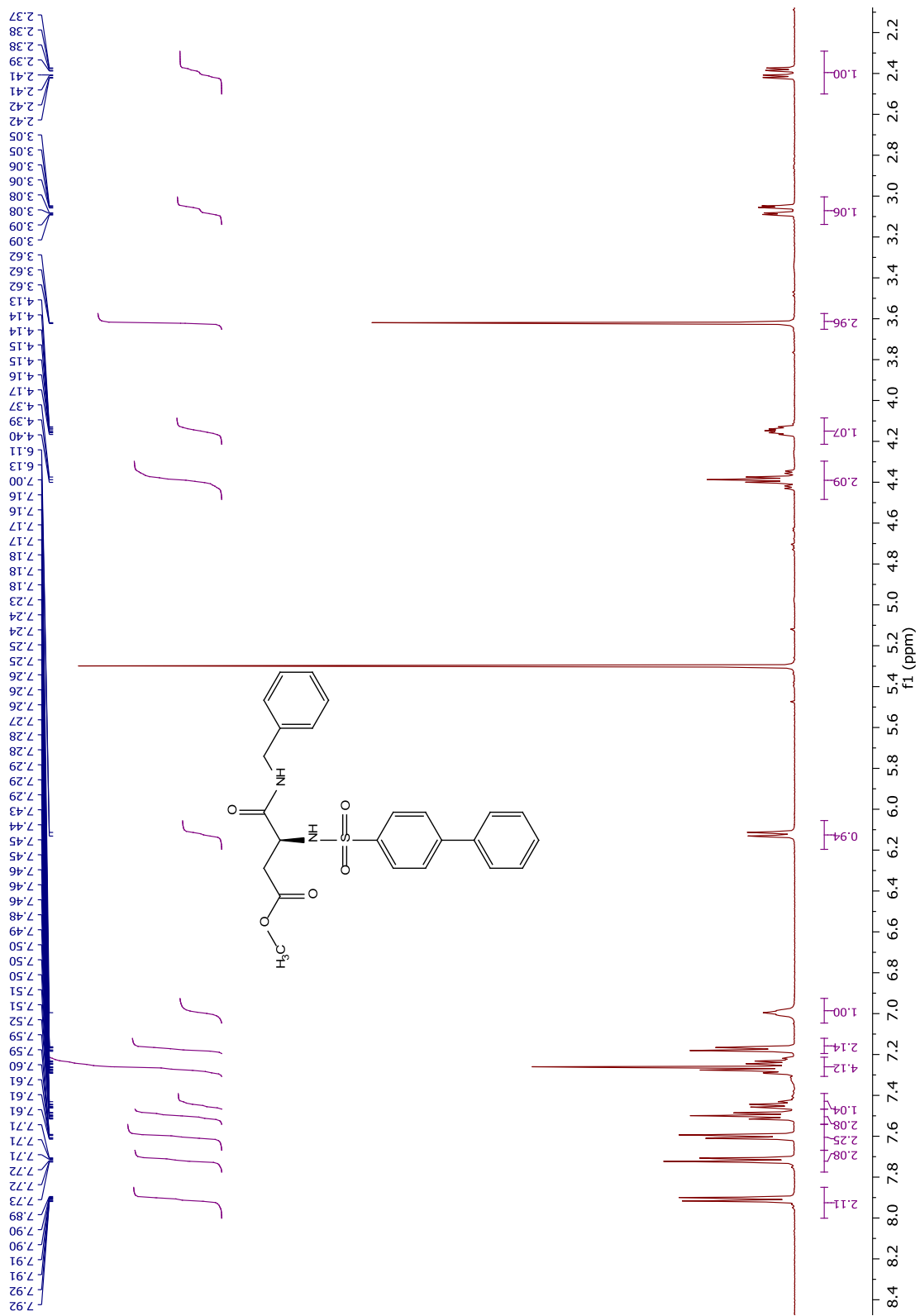
¹H NMR spectrum of compound 225



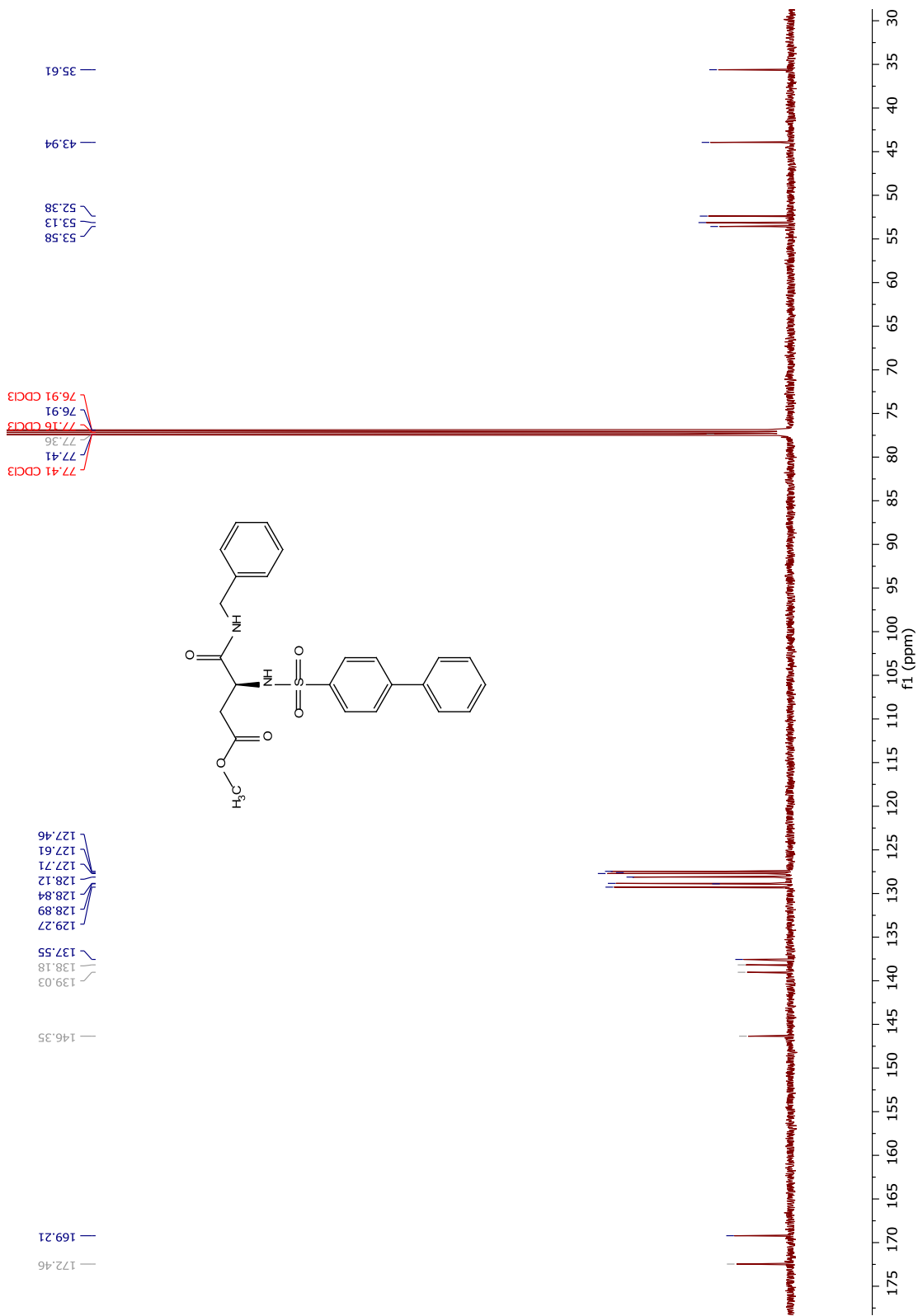
¹³C NMR spectrum of compound **225**



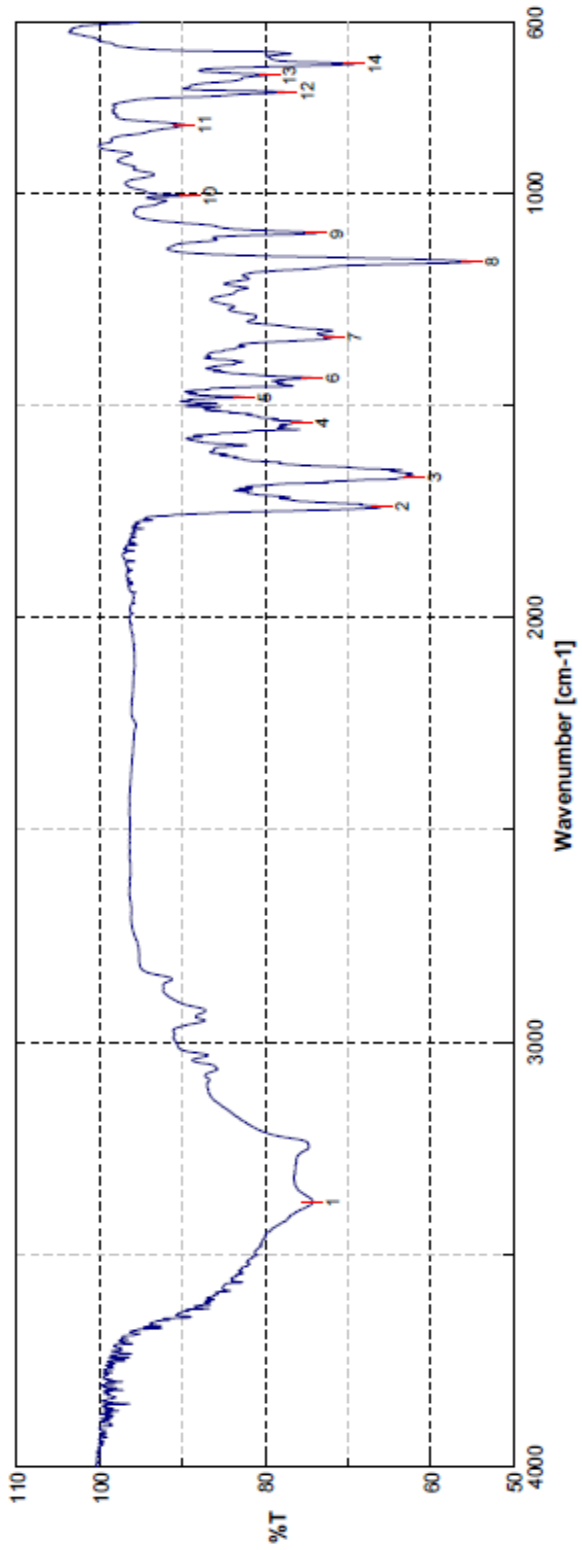
FTIR spectrum of compound 225



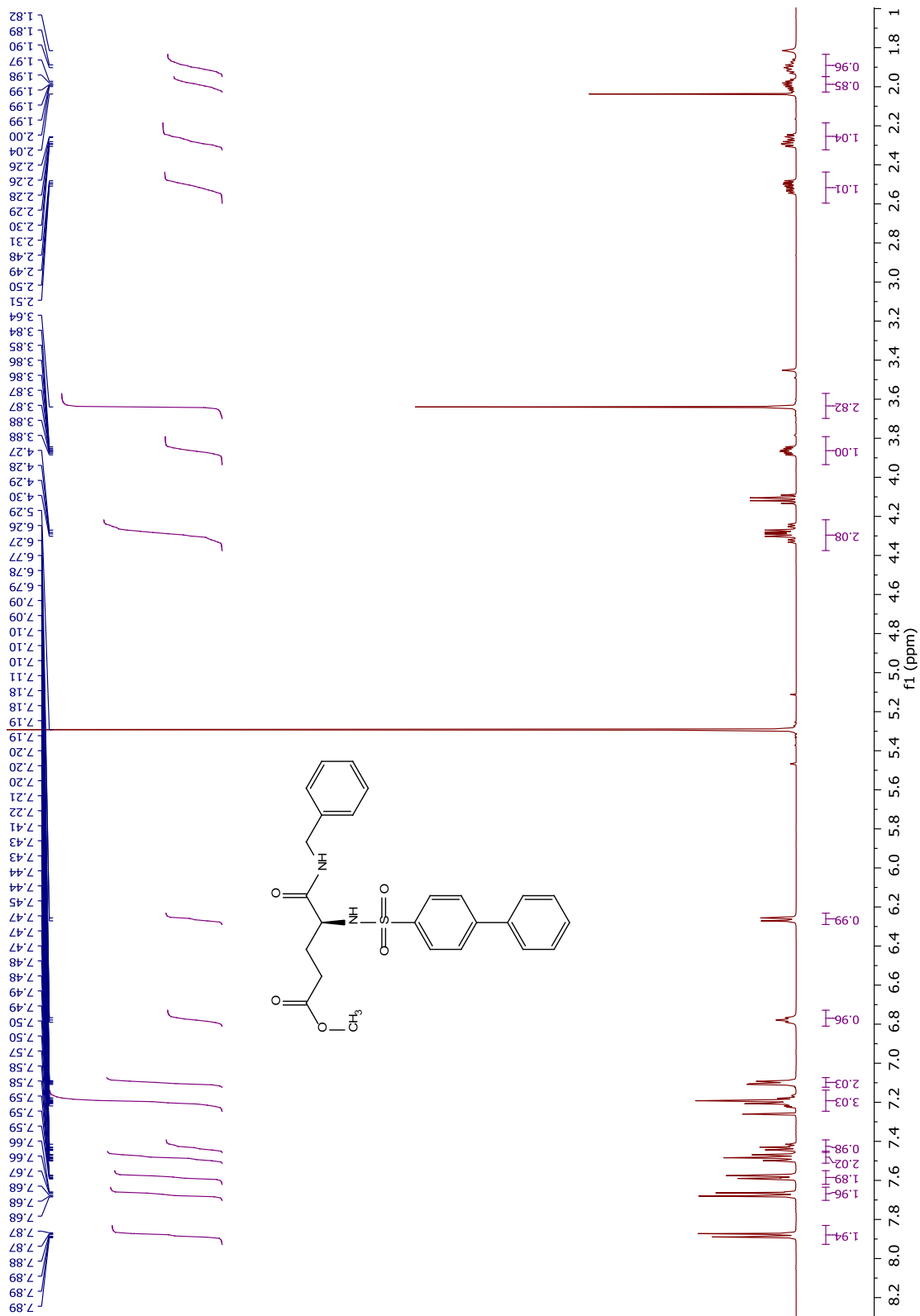
¹H NMR spectrum of compound **226**



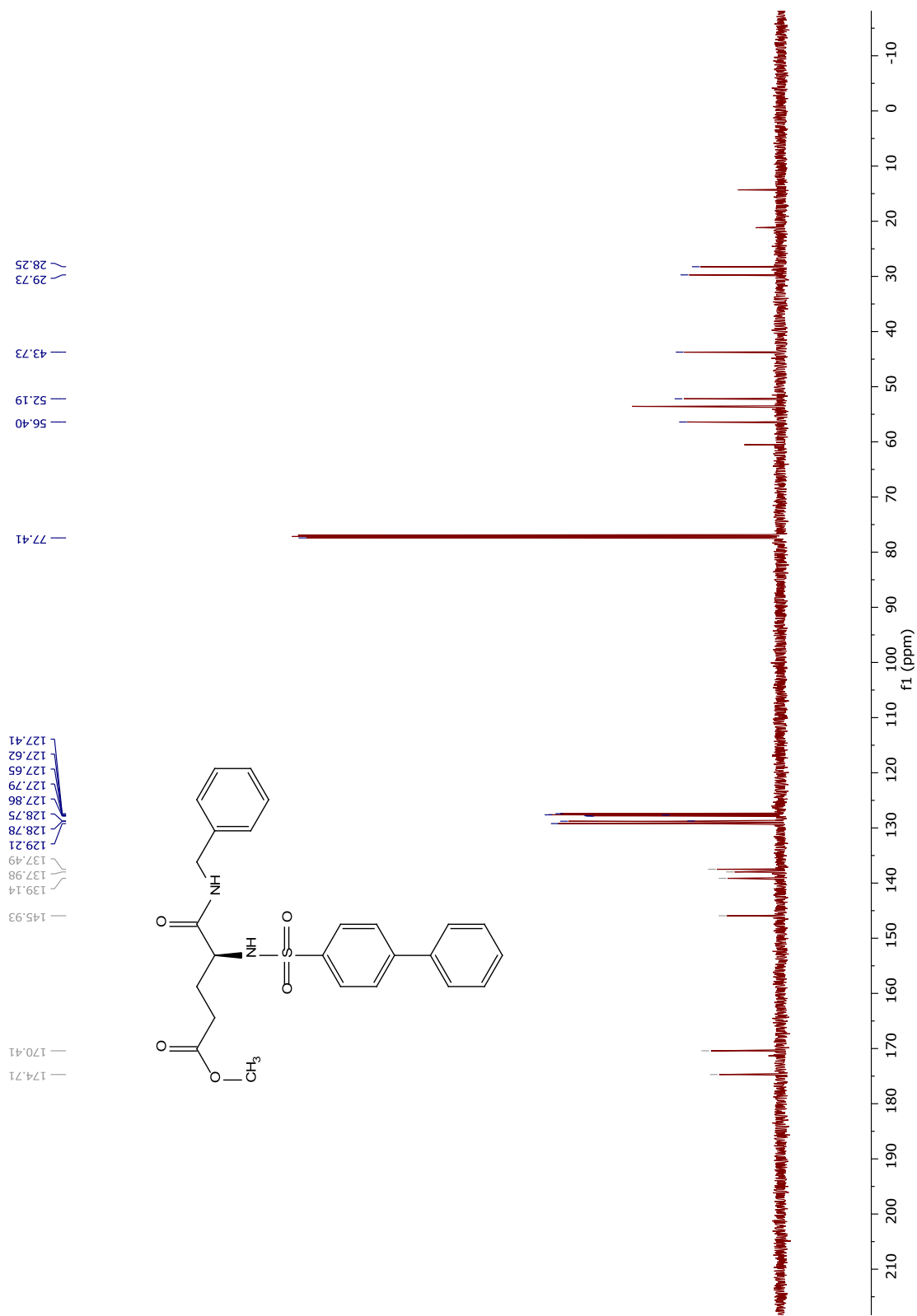
¹³C NMR spectrum of compound 226



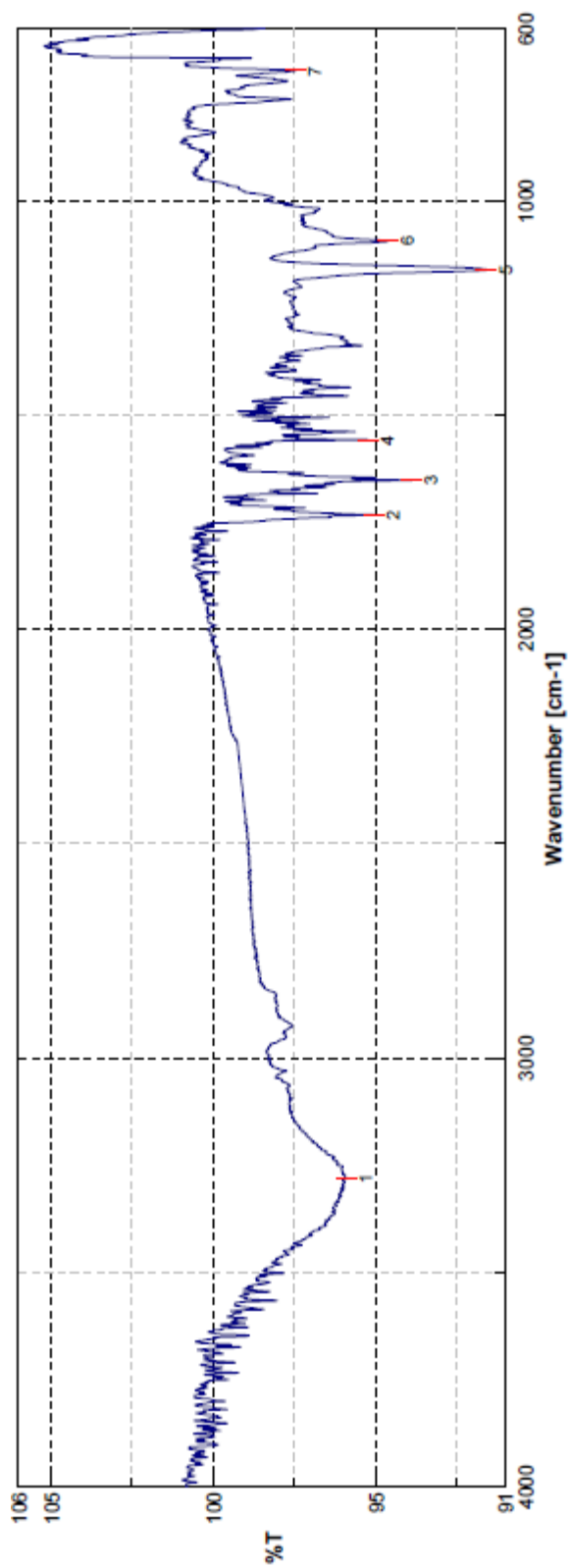
FTIR spectrum of compound **226**



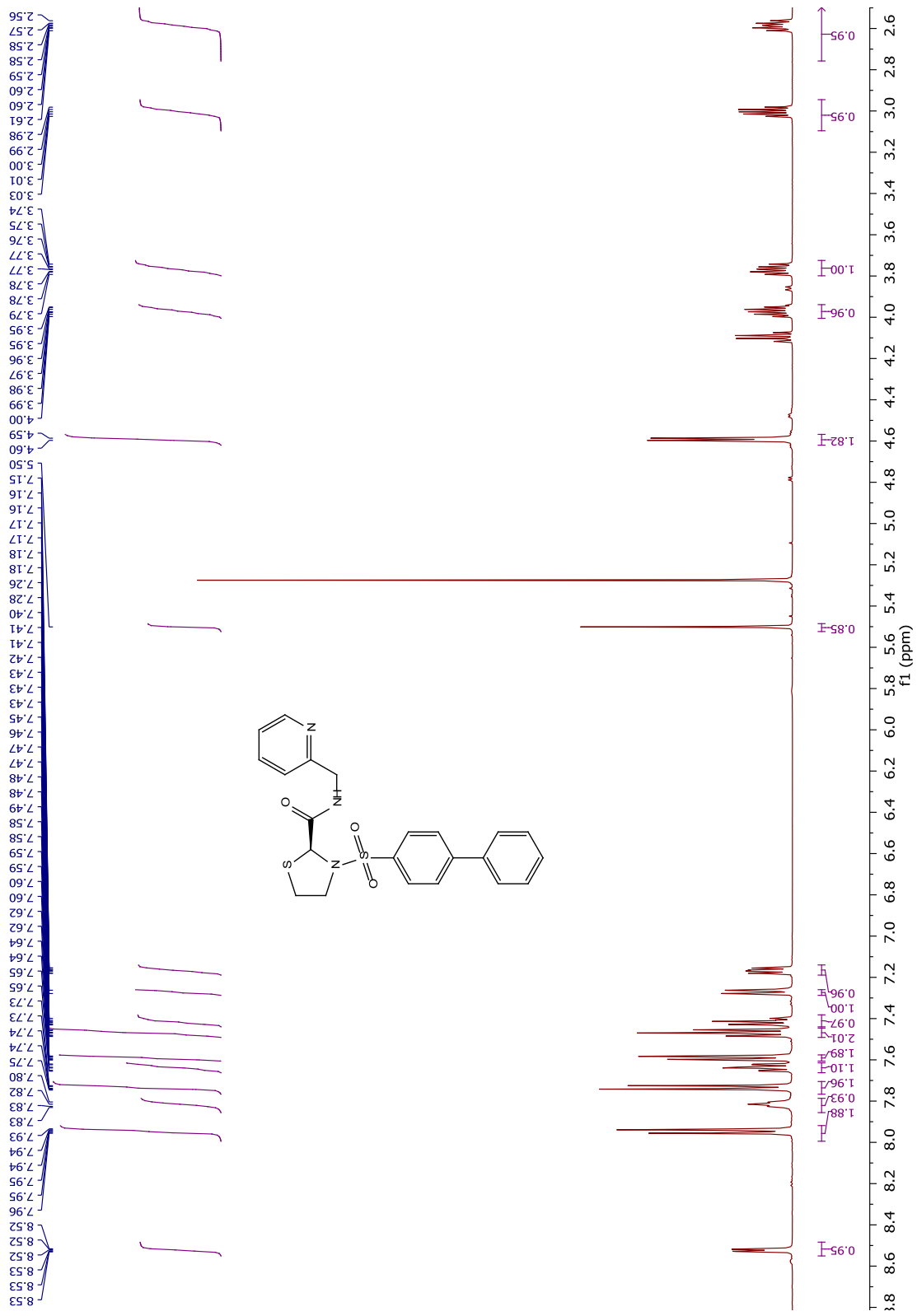
¹H NMR spectrum of compound 227



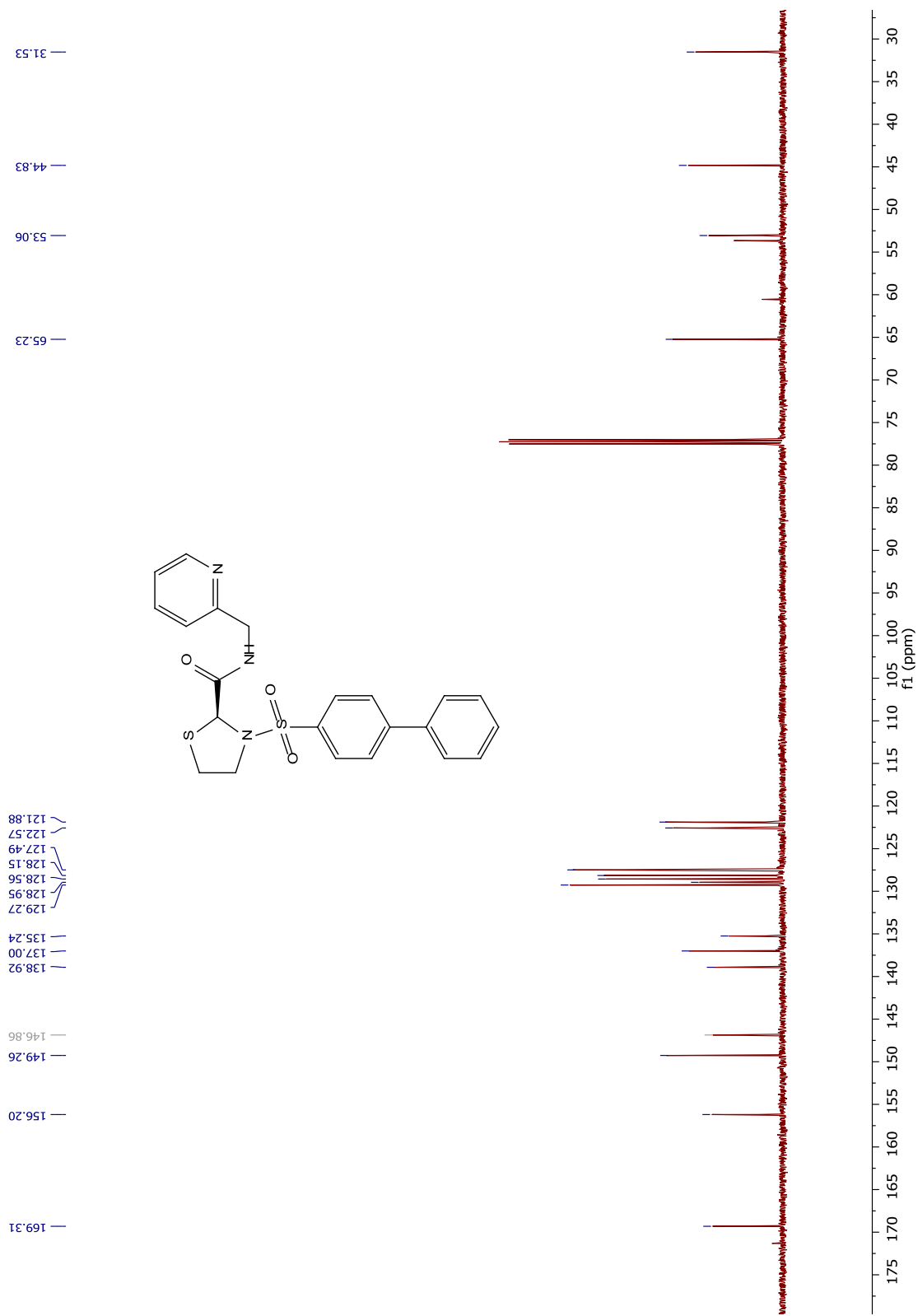
¹³C NMR spectrum of compound **227**



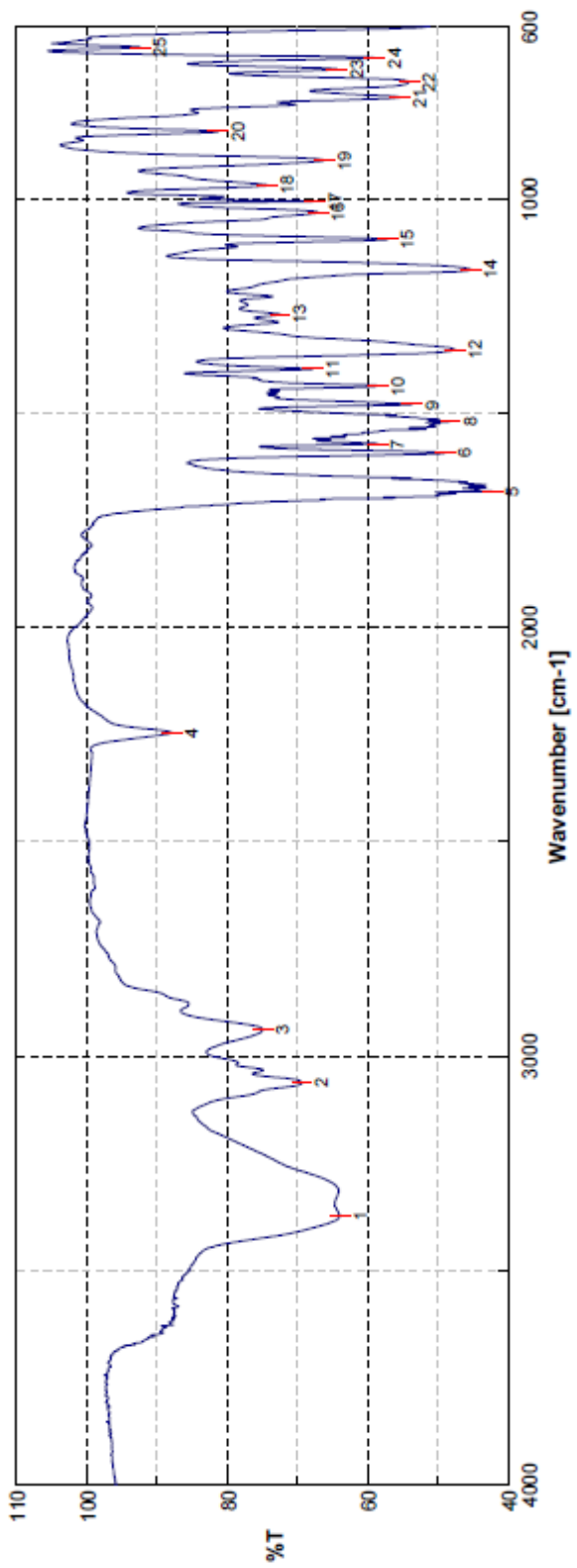
FTIR spectrum of compound **227**



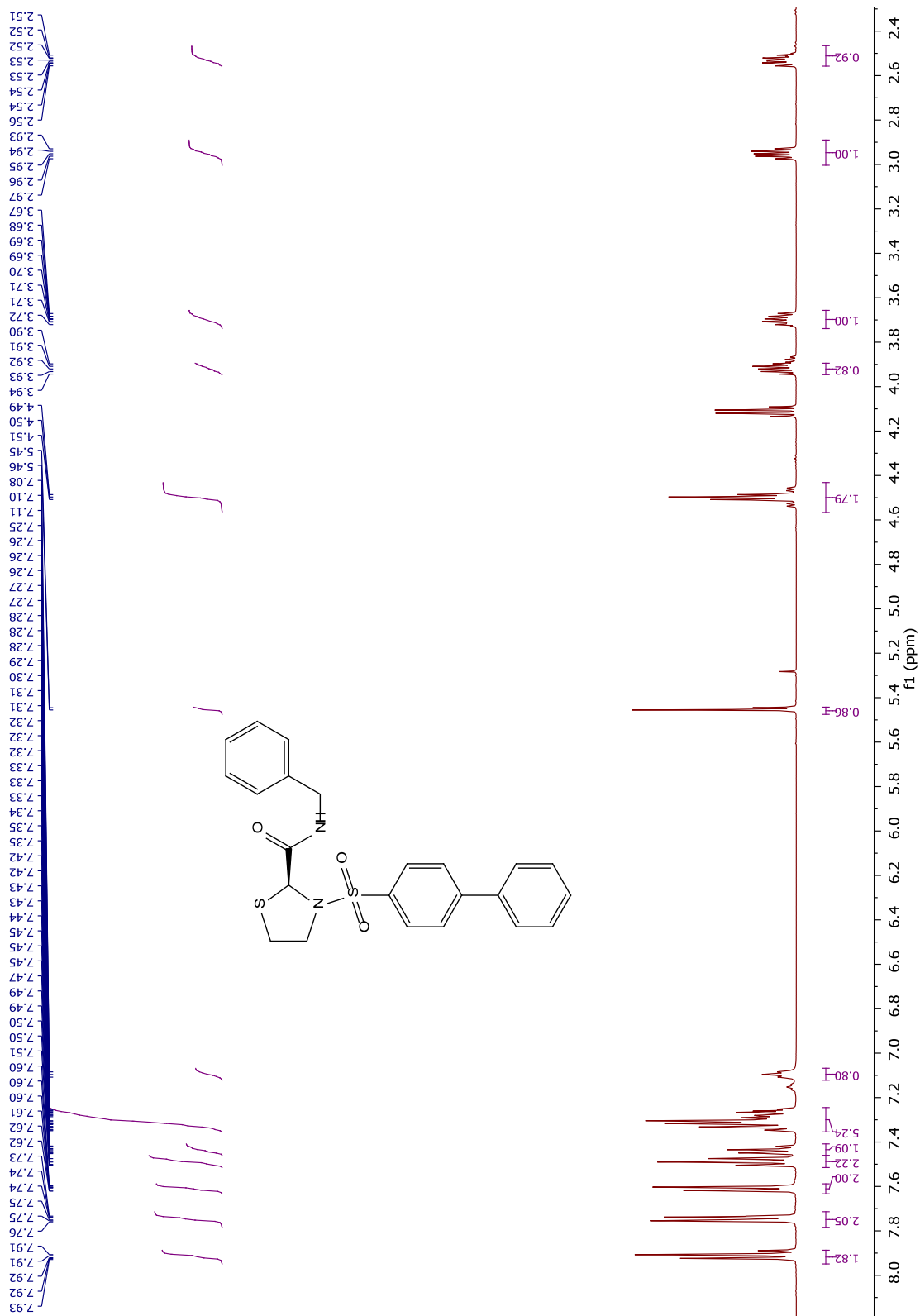
¹H NMR spectrum of compound **229**



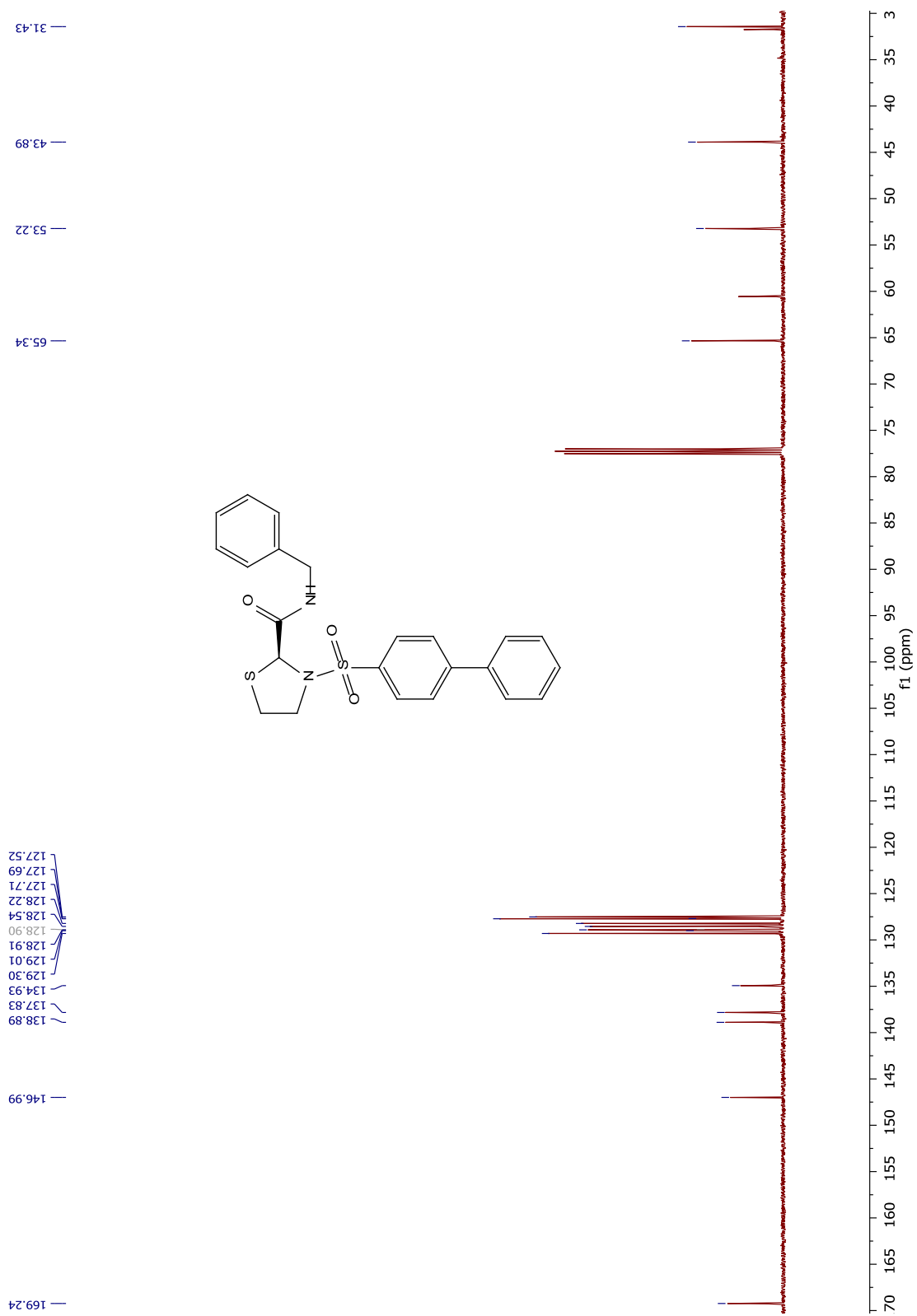
¹³C NMR spectrum of compound 229



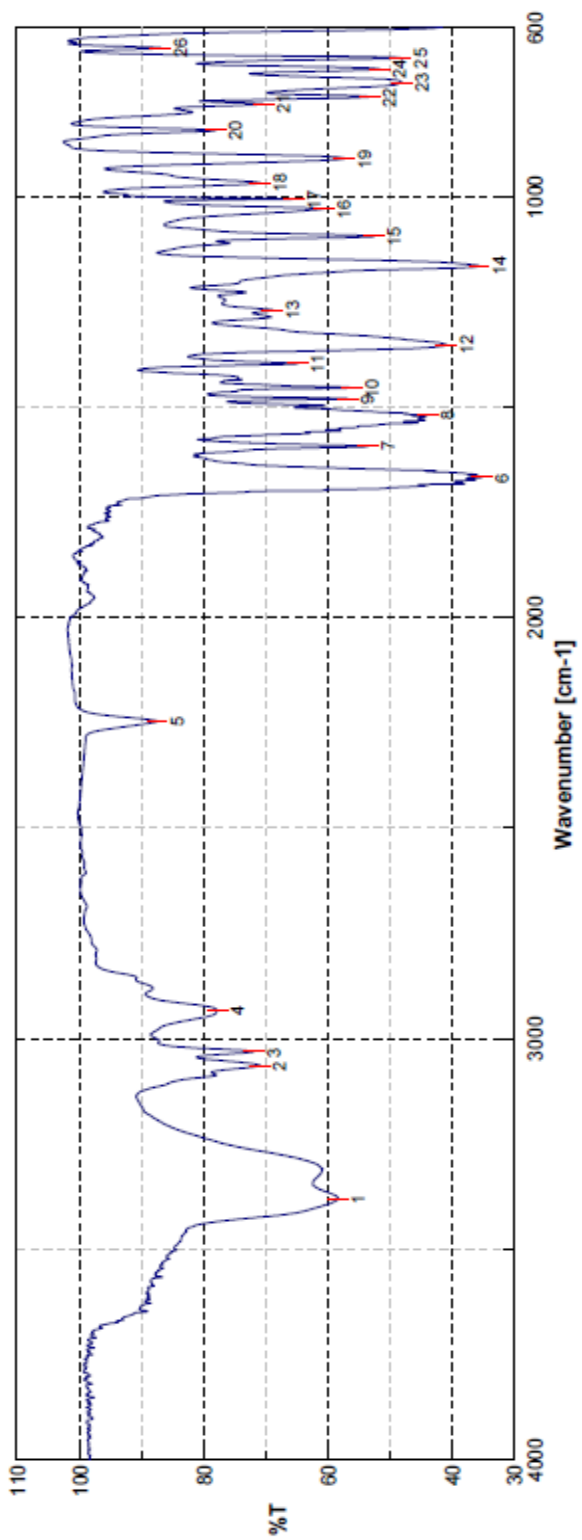
FTIR spectrum of compound **229**



¹H NMR spectrum of compound 230



¹³C NMR spectrum of compound 230



FTIR spectrum of compound 230

BIBLIOGRAPHY

- Baldwin, J. E. & Whitehead, R. C. On the biosynthesis of Manzamines. *Tetrahedron Lett.* **33**, 2059–2062 (1992).
- Boya, P. *et al.* Inhibition of Macroautophagy Triggers Apoptosis Inhibition of Macroautophagy Triggers Apoptosis. *Mol. Cell. Biol.* **25**, 1025–1040 (2005).
- Cao, R., Peng, W., Wang, Z. & Xu, A. β -Carboline alkaloids : Biochemical and pharmacological functions -Carboline Alkaloids : Biochemical and Pharmacological Functions. *Curr. Med. Chem.* **14**, 479–500 (2007).
- Cirillo, R. *et al.* Arrest of preterm labor in rat and mouse by an oral and selective nonprostanoid antagonist of the prostaglandin F₂alpha receptor (FP). *Am. J. Obstet. Gynecol.* **197**, 54.e1–9 (2007).
- El-Desoky, A. H. *et al.* Acantholactam and pre- neo -kauluamine, manzamine-related alkaloids from the indonesian marine sponge *Acanthostrongylophora ingens*. *J. Nat. Prod.* **77**, 1536–1540 (2014).
- El Sayed, K. A. *et al.* New Manzamine Alkaloids with Potent Activity against Infectious Diseases. *J. Am. Chem. Soc.* **123**, 1804–1808 (2001).
- Glick, D., Barth, S. & Macleod, K. F. Autophagy: cellular and molecular mechanisms. *J. Pathol.* **221**, 3–12 (2010).
- Kallifatidis, G., Hoepfner, D., Jaeg, T., Guzmán, E. A. & Wright, A. E. The marine natural product manzamine a targets vacuolar atpases and inhibits autophagy in pancreatic cancer cells. *Mar. Drugs* **11**, 3500–3516 (2013).
- Lakhter, A. J. *et al.* Chloroquine Promotes Apoptosis in Melanoma Cells by Inhibiting BH3 Domain – Mediated PUMA Degradation. *J. Invest. Dermatol.* **133**, 2247–2254 (2013).

- Marino, G., Niso-Santano, M., Baehrecke, E. H. & Kroemer, G. Self-consumption: the interplay of autophagy and apoptosis. *Nat Rev Mol Cell Biol* **15**, 81–94 (2014).
- Nishida, K., Yamaguchi, O. & Otsu, K. Crosstalk between autophagy and apoptosis in heart disease. *Circ. Res.* **103**, 343–351 (2008).
- Radwan, M., Hanora, A., Khalifa, S. & Abou-El-Ela, S. H. Manzamines: A potential for novel cures. *Cell Cycle* **11**, 1765–1772 (2012).
- Rebecca, V. W. & Amaravadi, R. K. Emerging strategies to effectively target autophagy in cancer. *Oncogene* **35**, 1–11 (2015).
- Sakai, R., Higa, T., Jefford, C. W. & Bernardinelli, G. Manzamine A, a Novel Antitumor Alkaloid from a Sponge. *J. Am. Chem. Soc.* **108**, 6404–6405 (1986).
- Thorburn, J. *et al.* Autophagy controls the kinetics and extent of mitochondrial apoptosis by regulating PUMA levels. *Cell Rep.* **7**, 45–52 (2014).
- Vance, D., Shah, M., Joshi, A. & Kane, R. S. Polyvalency: a promising strategy for drug design. *Biotechnol. Bioeng.* **101**, 429–34 (2008).
- Yee, K. S., Wilkinson, S., James, J., Ryan, K. M. & Vousden, K. H. PUMA- and Bax-induced autophagy contributes to apoptosis. *Cell Death Differ.* **16**, 1135–45 (2009).
- Yu, J. & Zhang, L. PUMA, a potent killer with or without p53. *Oncogene* **27**, S71–S83 (2008).
- Yu, Y. *et al.* Prostaglandin F₂α elevates blood pressure and promotes atherosclerosis. *Proc. Natl. Acad. Sci. U. S. A.* **106**, 7985–7990 (2009).